Diatom-based reconstruction of Late Glacial and Early Holocene environment in the Pyrenees

Reconstrucción ambiental del Tardiglaciar y el Holoceno Temprano en los Pirineos utilizando el registro sedimentario de diatomeas

Carlos Alberto Rivera Rondón

Diatom-based reconstruction of Late Glacial and Early Holocene environment in the Pyrenees

Reconstrucción ambiental del Tardiglaciar y el Holoceno Temprano en los Pirineos utilizando el registro sedimentario de diatomeas

Carlos A. Rivera Rondón

Ph.D. Thesis
2013

Tesi Doctoral
Universitat the Barcelona
Facultad de Biologia - Departament d`Ecologia
Programa de Doctorat: Ecologia Fonamental i Aplicada

Diatom-based reconstruction of Late Glacial and Early Holocene environment in the Pyrenees

Reconstrucción ambiental del Tardiglaciar y el Holoceno Temprano en los Pirineos utilizando el registro sedimentario de diatomeas

Memòria presentada per *Carlos Alberto Rivera Rondón* per a optar al grau de *Doctor per la Universitat de Barcelona*

Carlos Alberto Rivera Rondón
Centre d´Estudis Avançats de Blanes
Barcelona, novembre de 2013

Director de Tesi:
Dr. Jordi Catalan Aguilà
Centre de Recerca Ecològica i Aplicacions Forestals

Tutora de la tesi:
Dra. Isabel Muñoz Gracia
Universitat de Barcelona

Ph.D. Thesis

Diatom-based reconstruction of Late Glacial and Early Holocene environment in the Pyrenees

Carlos A. Rivera Rondón

A Angela

A mi familia

"...Cambia el clima con los años
Cambia el pastor su rebaño
Y así como todo cambia
Que yo cambie no es extraño

...Cambia el sol en su carrera
Cuando la noche subsiste
Cambia la planta y se viste
De verde en la primavera

Pero no cambia mi amor
Por mas lejo que me encuentre
Ni el recuerdo ni el dolor
De mi pueblo y de mi gente

Lo que cambió ayer
Tendrá que cambiar mañana
Así como cambio yo
En esta tierra lejana..."

Julio Numhauser
(Mercedes Sosa)

Agradecimientos

Agradezco a mi director, Jordi Catalan, por abrirme las puertas al mundo de la paleo, por tomar el riesgo, por la paciencia y la visión positiva, incluso cuando navegábamos por las aguas oscuras de Burg, gracias por el método y la limnología.

También quiero agradecer a las entidades que financiaron mis estudios de doctorado: La Pontificia Universidad Javeriana (Acuerdo DJE-025-2007) y el Departamento Administrativo de Ciencia, Tecnología e Innovación a través de una beca de estudios de posgrado (COLCIENCIAS-ICETEX-LASPAU, Convenio 016-95, Convocatoria 362-2006, Contrato 070-2007).

Gracias a todos los Burgueros: Albert Pelàch, Joan Manuel Soriano, Ramon Pérez y Ramon Julià, por prestarme su lago para viajar en el tiempo; por las muestras, los datos, la memoria, el trabajo, las excursiones, las reuniones, y por estar siempre dispuestos a hacerlo todo fácil. Larga vida y prosperidad al estany de Burg.

A las entidades que financiaron diferentes proyectos que hicieron posible la obtención de los datos, muestras y análisis usados: "Multidisciplinary research consortium on gradual and abrupt climate changes, and their impacts on the environment (GRACCIE)". CSD2007-00067. Programa Consolider 2007. Ministerio de Educación y Ciencia. European mountain lake ecosystems: "Regionalisation, diagnostic & socio-economic evaluation (EMERGE)". ENVI - Living, environment and climate. ENVIRONMENT. Unión Europea. EVK1-CT-1999-00032. Grup d'Ecologia dels Canvis Ambientals, GECA. Ajuts a grups de recerca (SGR-DGR), Generalitat de Catalunya (Ref. 2009 SGR 361). "Arqueologia de l'Alta Muntanya Pirinenca. Ocupació humana i canvi climàtic al llarg de l'Holocè". Generalitat de Catalunya (2006EXCAVA00022) - Universitat Autònoma de Barcelona. Grup de Geografia Aplicada AGAUR – Generalitat de Catalunya (2009 SGR 106).

I would like to thank professor Horst Lange-Bertalot. Thank you Horst, for coming to Blanes to teach me and for the inspiration. I appreciate your valuable time and effort checking my diatoms.

I would like to thank my PhD advisory Committee: N. John Anderson, Roland Schmidt and Emilia Gutiérrez.

A Roser Farres y Montserrat Soler por ayudarme en muchas de las tareas del laboratorio. Por supuesto a todo el staff administrativo, técnico y científico del CEAB, por su amabilidad y colaboración.

También quiero agradecer a Anna Domínguez, Aranzazu Villuenda y Eva Prats de la Unitat de Microscòpia de Rastreig, CCiTUB, Universitat de Barcelona, por su ayuda durante las sesiones en el micro.

A Jaime Frigola y Patricia Povea de Castro, por su ayuda durante las sesiones en el Avaatech XRF-Core Escáner del Departamento de Estratigrafía, Paleontología y Geociencias Marinas de la Universitat de Barcelona.

Al TEAM Llebreta 2010: Jordi, Santi Giralt, Alberto Sáez, Albert Pelàch, Joan Manuel Soriano, Sergi Pla y Lluís Camarero, por la oportunidad de aprender durante esa semana que acampamos en medio del lago. Sepan que entrenaré muy duro para que cuando regresemos podamos ir por debajo de los 9 m.

Agradezco a la familia Bahamón-Seils: Nixon, Bianka, Coco, Miel y su pequeña hija, la Boya. Gracias por ser mi familia en Blanes. Gracias por las tartas, galletas, pelos, los 50 de Joselito, los sancochos, y muchas cosas más. Gracias Bianka por ayudarme pacientemente hasta el final a que me escritura fuese aceptable. Gracias Nixon por introducirme al mundo e**R**ratico y por la asesoría en múltiples análisis.

También quiero agradecer a todos aquellos que me ayudaron resolviendo dudas o haciendo mi estancia más amable: a Marisol Felip, Sergi Pla, Susana Bernal, Fede Bartumeus, Esperança Gacia, Marc Ventura, Teresa Buchaca, Maria Angels Puig, Rafael Coma, Dani Matin, Ramón Coma, Eugenia Marti, Carmela Bosca, Gemma Peña, Lluís Camarero. Gracias Lluís por la hospitalidad en la montaña.

Muchas gracias Sergi Pla, por las divertidas discusiones sobre cosas muy profundas y otras irrelevantes, por el punto de vista crítico de todo y por darme siempre una mano.

A mis compañeros: Mireia Bartrons, por el tiempo que compartimos y por enseñarme muchas de las mejores cosas de su país. Al Compañero, Guillermo de Mendoza, por las muchas cosas vividas en estos años y las discusiones sobre nuestros lagos. A Tina Chappuis por las maravillosas cenas y por las salidas a correr con Mireia y Guillem Roca. A Tatiana Caraballo (alias Tati), Miguel Ballen (alias Migue) y Pau Giménez (alias Pau) por pasarla chévere.

Agradezco mucho a todos los compañeros del CEAB, los que han pasado y los que vendrán. Gracias por la fiesta de la playa, los partidos en el Casino, las cenas y la vida blanenca. A los que hicieron el trabajo en el laboratorio más ameno; Romero, Miquel Ribot, Roser, Letzy Serrano, Chiara Romano, Francesco Pititto, Celia Sitjà, María López. Gracias Steffi Merbt, Boris Weitzmann, Daniel von Schiller y Kathrin Bacher por resolver muchos de mis problemas con el alemán. A Marc Terradas y los botánicos, por las excursiones a los arrecifes catalanes. A los que se me quedaron sin nombrar por la prisa (perdoneu, si us plau).

Un agradecimiento muy especial A João Gil. Gracias João por los cafés de las tardes, las conversaciones, la introducción al punk, los partidos con hamburguesa y por muchas más cosas.

También quiero dar un agradecimiento muy sentido a Jaime Ordoñez. Gracias hermano, por la acogida y la hospitalidad al llegar hace unos años durante un frío día de noviembre. Gracias también por compartir durante estos años recuedos y muchas vainas.

A Isabel Muñoz y Sergi Sabater por hacer más amable mí llegada a Barcelona. Gracias Isabel por tu ayuda al final de este proceso. Pilar López siempre estuvo muy atenta a facilitar todos los asuntos administrativos.

Muchas personas en Colombia facilitaron esta experiencia. A Jhon Donato por abrirme la puerta a la limnología. En la Universidad Javeriana: a Elizabeth Hodson de Jaramillo por arriesgarse conmigo. Ingrid Schuler, Nohora Urrego, Fabio Roldan, Diana Álvarez, Lula y Rosmine Penagos pusieron muchos granos de arena durante todo el proceso.

A Dora Solano, por la amistad y la confianza, y por supuesto, por prestarme su apartamento estos seis años.

Agradezco a mi gran familia Rivera-Rondón-Zapata, para quienes mis logros siempre han sido suyos. Gracias por estar siempre. A mi tío Arturo especialmente le agradezco su apoyo. A mi madre y mis hermanos.

A Angela Zapata, quien me espera, dedico todas las flores de la primavera.

Finalmente, quiero agradecer al estany de Burg, quien me enseñó algunos de sus más profundos secretos. Al Pireneo por sus lagos. A Blanes por los paseos por su playa y por dejarme ver con claridad la estrella polar.

Contents

Resumen

1. Resumen

Introducción

Los lagos son ecosistemas expuestos a la influencia combinada del clima y la entrada de materiales y nutrientes desde la cuenca. Los lagos recopilan y archivan información de estos procesos y de la dinámica interna del sistema en los sedimentos. Descifrar y extraer la información almacenada en los sedimentos es una tarea difícil, ya que, además de la interdependencia entre los agentes externos, la ontogenia del lago influye sobre la respuesta del sistema. El registro sedimentario de los lagos incluye una amalgama de materiales inorgánicos y orgánicos y restos identificables de diferentes tipos de organismos. Estos últimos pueden aportar valiosa información de las condiciones en las que se desarrollaron. Dentro de los materiales biológicos subfósiles, las diatomeas ocupan un lugar destacado. Debido a la composición silícea de sus valvas, los restos de las diatomeas pueden ser identificados con una alta exactitud a nivel de especie. Este hecho, sumado a la alta riqueza de especies que puede encontrarse, hace que las diatomeas sean un gran indicador cuando se realizan reconstrucciones ambientales. Este estudio se centró en primer lugar en el conocimiento de la taxonomía y ecología de las diatomeas de los lagos de los Pirineos y su potencial como indicadores de las condiciones ambientales. En segundo lugar, la información obtenida en el estudio ecológico se aplicó a una secuencia sedimentaria del paleolago Burg, reconstruyendo las condiciones ambientales del lago durante el Tardiglaciar y el Holoceno Temprano.

Las diatomeas son algas unicelulares que se caracterizan por tener cloroplastos de color amarillo - marrón y paredes celulares de sílice (Round et al. 1990). El número de género es de aproximadamente 350 y el número de especies descrito se estima en 15000 (Williams and Kociolek 2011). Las diatomeas son utilizadas con éxito como indicadores ecológicos de las condiciones ambientales de agua dulce. El alto número de especies y su respuesta especializada a una amplia gama de condiciones son las bases para desarrollar a partir de ellas modelos estadísticos que describen las características químicas y físicas de las masas de agua (Kitner and Poulíčková 2003; Pan et al. 1996), incluyendo nutrientes (Borchardt 1996; Carrick and Lowe 2007; Luoto et al. 2012), la transparencia del agua (Cantonati et al. 2009; Hill 1996), temperatura (DeNicola 1996), el pH

(Cameron et al. 1999), y la salinidad (Gasse 2002; Wilson et al. 1994), entre otros.

Las diatomeas aportan información limnológica de los ecosistemas de agua dulce que es difícil de obtener con otros indicadores. Así por ejemplo, el polen es muy útil para entender variables ambientales externas al lago, como la temperatura del aire y la precipitación pluvial rain (Davis et al. 2003; Lotter et al. 2000), pero proporcionan información limitada sobre los procesos internos del lago. Indicadores geoquímicos y sedimentólogicos, aportan información sobre procesos de la cuenca, cambios en el balance hídrico o precipitación química en los sedimentos del lago, pero en general aportan poca información sobre los procesos que ocurren en la columna de agua. Por el contrario, las diatomeas son excelentes para reconstruir variables de la columna de agua, tales como la conductividad, el pH, la temperatura y los nutrientes, aportando información complementaria de los procesos externos del sistemas y los que ocurren dentro de los sedimentos (Chen et al. 2008; Reavie and Smol 2001; Reid 2005; Werner and Smol 2005).

La sustitución del tiempo por el espacio es la principal aproximación metodológica utilizada para realizar reconstrucciones ambientales cuantitativas mediante la información obtenida de restos biológicos contenidos en los sedimentos (Smol 2008). El supuesto básico de esta aproximación, es que la variabilidad de una variable ambiental específica en el pasado en un lago, puede ser encontrada en la variabilidad regional de un número suficientemente grande de sitios en el presente (Catalan 2008). En otras palabras, que el gradiente espacial del medio ambiente actual contiene análogos de las condiciones del pasado. Esta suposición se cumple cuando las secuencias estudiadas son relativamente recientes, pero es difícil de garantizar cuando se intenta realizar la reconstrucción de períodos muy antiguos. Cambios en las preferencias ecológicas de las especies y cambios en las relaciones entre las variables ambientales estudiadas, pueden afectar a invalidar la suposición principal de esta aproximación. No obstante, la utilización del espacio para sustituir el tiempo ha demostrado excelentes resultados en un gran número de estudios (por ejemplo, Larocque-Tobler 2010; Luoto et al. 2012; Quillen et al. 2013). Consecuentemente, en este estudio se asume que las actuales características ecológicas de las diatomeas de los lagos pirenaicos incluyen la variabilidad esperada de las diatomeas en las secuencias sedimentarias del Tardiglaciar y el Holoceno. Por lo tanto, desde el análisis de las relaciones ecológicas de diatomeas en la actualidad es posible entender y reconstruir las condiciones

pasadas en cualquier lago de los Pirineos. La interpretación de la condición ambiental del pasado utilizando comunidades de organismos tales como las diatomeas, se puede realizar de diferentes formas. En este estudio se utilizan dos enfoques complementarios: la interpretación de especies indicadoras y reconstrucciones cuantitativas basadas en funciones de transferencia.

Los cambios en el clima tienen un efecto sobre algunos de los componentes estructurales y funcionales de los ecosistemas acuáticos, debido a la compleja interacción entre mecanismos directos e indirectos (Fritz and Anderson 2013). La dinámica térmica e hidrológica, son las principalmente afectadas por la variabilidad climática (Agusti-Panareda et al. 2000; Livingstone and Padisák 2007). De tal manera, que la variabilidad en la radiación incidente, el viento, las lluvias y la temperatura del aire, afecta directamente el balance térmico de los lagos (Margalef 1983), modificando la temperatura, la estabilidad térmica, el ciclo de nutrientes y el nivel de agua.

El clima también tiene un efecto indirecto en los lagos a través de su influencia en la cueca. El clima suele ser el principal responsable de cambios en el desarrollo del suelo, la erosión, la cubierta vegetal y el balance hídrico de la cuenca de captación del lago. El principal reto de la paleoecología es desarrollar reconstrucciones ambientales desde una visión integral del ecosistema, incluyendo los efectos de la cuenca, la atmósfera y la dinámica interna del lago, pero separando al mismo tiempo la influencia relativa de cada uno de los componentes. Un enfoque multi-proxy puede proporcionar herramientas para comprender los distintos factores que influyen en el entorno del lago (Birks and Birks 2006) y discriminar el efecto relativo de cada uno de los factores. Por ejemplo, proxies geoquímicos pueden proporcionar información cuantitativa directa sobre algunos de los procesos de captación, mientras que las diatomeas permiten al mismo tiempo la reconstrucción de variables directamente relacionadas con el clima y de variables relacionadas con los procesos del lago.

Objetivos

El objetivo principal de esta tesis es explorar el potencial de las diatomeas para realizar reconstrucciones ambientales multivariadas del pasado, con una aplicación a la secuencia sedimentaria del Holoceno temprano y el Tardiglaciar del lago Burg (Pirineos). La variabilidad regional de la distribución de diatomeas en zonas alpinas y templadas es generalmente

explicada por el gradiente de pH y alcalinidad (Chen et al. 2008; Koster et al. 2004; Siver 1999). Sin embargo, existe una gran variabilidad aun no explicada (90-70%) que está relacionada con otros factores ambientales y que podría también ser utilizada en el desarrollo de la reconstrucción del ambiente acuático. Algunos autores ponen en duda la viabilidad de realizar reconstrucciones ambientales independientes, utilizando un único registro de diatomeas, argumentando que la alta correlación entre algunas de las variables puede alterar las señales que son reconstruidas (Anderson 2000). Sin embargo, otros autores sostienen que es posible realizar reconstrucciones, incluso entre variables muy dependientes, como por ejemplo el pH y la alcalinidad, si existen conjuntos de especies con respuestas distintas (Catalan et al. 2009c). Las diatomeas incluyen especies que crecen en muchos hábitats y microambientes diferentes por lo que puede esperarse, que posean información independiente acerca de los procesos ambientales que afectan diferencialmente los microambientes de los lagos. De acuerdo con esto, los objetivos específicos de la tesis son:

1. Estudiar la flora de diatomeas de los lagos de montaña de los Pirineos. Una extensa revisión taxonómica y la comparación de los especímenes encontrados con otros de ecorregiones similares, se presenta en el capítulo 5 y en los apéndices.

2. Explorar los factores ambientales que, además de pH, explican la distribución de diatomeas en los lagos de los Pirineos, incluyendo factores próximos al lago y descriptores generales de características de la cuenca. La parte II de la sección de resultados describe las relaciones entre las diatomeas y los factores ambientales en los lagos pirenaicos. En esta sección se proporcionan datos sobre la autoecología de las diatomeas de montaña más comunes y se explora el valor del indicador de un gran número de taxones para diferentes condiciones químicas (capítulo 6), nutrientes (capítulo 7), variables físicas (capítulo 8), y para variables relacionadas con el hábitat (capítulo 9). Un resumen de las especies indicadoras se presenta en el capítulo 10.

3. Demostrar que es posible reconstruir diferentes variables independientes a partir de un mismo conjunto de datos de diatomeas. El desarrollo de las funciones de transferencia y el análisis de la fiabilidad e independencia de los modelos realizados se demuestra en la Parte III de la sección de resultados (capítulo 11). El análisis se realizó mediante la comparación de dos conjuntos de muestras distintas (sedimento superficial y muestras de epiliton). Adicionalmente, en el capítulo 12 se analiza el potencial como un indicador ambiental de la relación entre cistos de crisofíceas y diatomeas.

4. Aplicar las especies indicadoras y las funciones de transferencia en la secuencia sedimentaria del lago Burg cubriendo el Tardiglaciar y el Holoceno Temprano. Para resolver este objetivo, inicialmente se realizó un análisis de las asociaciones de diatomeas en todo el registro sedimentario, de los principales cambios en la composición de diatomeas, la diversidad y un análisis de las especies indicadoras encontradas (capítulo 15). También se realizó la reconstrucción cuantitativa de las variables seleccionadas utilizando las funciones de transferencia (capítulos 16 y 17). La reconstrucción ambiental se complementó con el análisis de diferentes proxies de la geoquímica y de pigmentos fotosintéticos subfósiles (capítulo 16).

5. Analizar las variables reconstruidas en términos de los procesos internos del lago y su eventual vinculación con procesos relacionados con el clima y la cuenca. En la discusión se presenta un análisis de la fiabilidad de las reconstrucciones implementadas (capítulo 18). En el capítulo 19 se analiza la influencia de los cambios del clima y la ontogenia del lago sobre las comunidades de diatomeas y la productividad del lago. Por último, una interpretación de la reconstrucción climática del Tardiglaciar y el Holoceno se presenta en el capítulo 20.

Materiales y métodos

Área de estudio y muestreo

El estudio de la distribución de las especies de diatomeas y la ecología se basó en un muestreo de 83 lagos de los Pirineos realizado entre el 9/7/2000 y el 23/8/2000. Los lagos estudiados fueron escogidos tratando de capturar un amplio rango de condiciones geológicas, altitudinales, y de morfología de la cubeta. En general, los lagos de los Pirineos se encuentran en cuencas de litología plutónica y metamórfica con suelos escasamente desarrollados. Las cuencas son predominantemente desnudas o están cubiertas con prados; menos del 20% de los lagos estudiados tienen bosques de coníferas. Las cubetas de los lagos estudiados son relativamente pequeñas pero con una profundidad relativa alta.

Durante el muestreo se consideraron variables que describen el entorno físico, tales como la temperatura, la duración de la cubierta de hielo, el ambiente lumínico y el tipo de sustrato dominante. La temperatura del agua se midió en la superficie, en la parte central de cada lago. Duración de la cubierta de hielo por los lagos se estimó de acuerdo con Thompson et al. (2009). El ambiente lumínico se caracterizó utilizando dos indicadores diferentes: El porcentaje de la radiación en el fondo del lago y una estimación de la radiación media que llega al fondo del lago durante el verano.

Adicionalmente se registró información de las características de la zona litoral de cada lago. Así, se cuantificó la cobertura relativa de lecho de roca, arena, sustratos orgánicos y macrófitos. La diversidad de hábitat se caracterizó usando el número de diferentes tipos de sustrato y e^H, donde H es el índice de Shannon - Wiener (Magurran 2004) calculado con la abundancia relativa de sustratos. El contenido de materia orgánica en el sedimento se estimó mediante el método de pérdida por calcinación (LOI) siguiendo los procedimientos y recomendaciones de (Heiri et al. 2001).

Las muestras destinadas al análisis químico se recogieron en las salidas de agua de cada lago. Los métodos utilizados se describen con mayor detalle en Camarero et al. (2009). Las variables cuantificadas fueron pH, capacidad de neutralización de ácido (ANC), la conductividad, calcio, magnesio, sodio, potasio, sulfato, cloruro, fósforo total (TP), nitrato, amonio, nitrógeno total (TN) y carbono orgánico total (COT). La concentración de CO_2 se calculó utilizando los valores de pH, ANC, conductividad y la temperatura del agua (Mackereth et al. 1978).

El muestreo de las diatomeas se realizó simultáneamente a la colecta de las muestras para el análisis químico en dos tipos de sustrato: en el sedimento superficial y en el epiliton. Las muestras del sedimento fueron colectadas en la parte más profunda de cada lago usando un core de gravedad y cortando los primeros 0.5 cm del núcleo de sedimentos. El epiliton se muestreó en rocas de la zona litoral en áreas entre 0.3 y 1 m de profundidad. Las muestras fueron preservadas usando formaldehido.

Muestreo de lago de Burg

El lago de Burg se encuentra localizados en los Pirineos a 1821 m, 42 º 30'18 "N, 1º 18 '22" E. El lago es de origen glacial y actualmente es un humedal superficial que se seca casi en su totalidad durante el verano. Características fisionómicas y geológicas del terreno sugieren que el lago de Burg perdía agua a través de la morrena frontal que lo contiene.

La extracción del núcleo de sedimentos de lago se realizó utilizando una máquina de perforación RL Rolatec 48-L de 10 cm de diámetro. Se colectaron dos muestras de sedimentos con una gran continuidad lateral de la litología (CMB9: 0 a 215 cm y CMB8: desde 215 hasta 1.441 cm). El núcleo de sedimentos fue cortado cada centímetro. En este estudio se analizan 624 muestras, que corresponden a una sección entre 1330 y 642 cm en donde las diatomeas se conservaron de manera adecuada.

Análisis de otros proxies

La composición porcentual de los minerales dominantes en los sedimentos se estimó por difracción de rayos X (DRX) utilizando un difractometro de rayos X automático Siemens D - 500 en las siguientes condiciones : radiación K alfa de Cu , 40 kV , 30 mA , y monocromador de grafito. Para identificar y estimar la proporción de las diferentes especies mineralógicas presentes en la fracción cristalina un procedimiento estándar fue seguida Chung (1974). Los datos de este análisis fueron proporcionados por el doctor Ramón Julià (Institut Jaume Almera, CSIC).

Análisis de Fluorescencia de Rayos X (XRF) se llevaron a cabo utilizando el Avaatech XRF -Core Escáner del Departamento de Estratigrafía, Paleontología y Geociencias Marinas de la Universidad de Barcelona. Las mediciones realizaron cada 3 mm y cada sección se analizó a 10 kV, 1800 μA 10 s, y a 30 kV, 2000 μA y 35 s. Información acerca de la presencia de grietas, irregularidades y característicos morfológicos relevantes del núcleo fueron anotados para seleccionar las secciones útiles.

El análisis de los pigmentos fotosintéticos subfósiles se realizó mediante cromatografía líquida UPLC, usando un sistema de UPLC (Acquity, Waters, Milford, MA, E.U.) equipado con una columna Acquity UPLC HSS SB C18 (dimensiones: 100 x 2,1 mm, tamaño de partícula: 1,8 micras), una matriz de

fotodiodos (λ 300-800 nm) y con detectores de fluorescencia (λ excitación 440 nm, emisión 660 nm). Un gramo de peso seco de cada muestra fue utilizado para la extracción de los pigmentos en acetona.

Estudio de las diatomeas

La composición y abundancia de diatomeas fue estudiada en 76 muestras del sedimento y 78 muestras epiliticas del muestreo regional de los Pirineos y en 624 muestras del núcleo de sedimentos de Burg. Las muestras fueron digeridas mediante un procedimiento oxidativo utilizando HCl y H_2O_2. Después de la digestión, en el caso de las muestras de Burg, se añadió un volumen conocido de una solución de microesferas de látex. Una vez se retiró toda la materia orgánica de las muestras y el excedente de los reactivos, se montaron en portaobjetos permanentes utilizando Naphrax.

La determinación taxonómica de diatomeas y el conteo se realizó en un microscopio de contrate interferencial Zeiss Axio Imager A.1 a 1000x. La identificación se complementó mediante la observación de algunos especímenes en un microscopio electrónico de barrido Hitachi S - 4100 – FE. La identificación de las diatomeas se realizó utilizando estudios taxonómicos generales de la diatomoflora de los Pirineos, de Europa y un gran número de trabajos existentes sobre grupos taxonómicos más específicos e iconografías regionales. Dos índices cuantitativos se aplicaron para caracterizar la preservación de diatomeas en el registro de Burg: un índice de disolución y un índice de fragmentación.

Estudio de la ecología de las diatomeas en muestreo regional

La exploración de la relación entre el medio ambiente y la distribución de diatomeas en los lagos muestreados se realizó en diferentes niveles de complejidad con el objetivo final de entender los cambios en las diatomeas del registro de Burg. En primer lugar, se evaluaron los rasgos autoecológicos simples y el valor como indicadores de las especies. En segundo lugar, se desarrollaron funciones de transferencia para algunas variables.

La relación entre las especies de diatomeas y las variables ambientales se analizó a través de diferentes enfoques complementarios: especies indicadoras, optimo

ecológico de las especies y patrones de diversidad. Inicialmente los lagos fueron clasificados de acuerdo con sus características químicas; posteriormente, la presencia de especies indicadoras de estos grupos fue evaluada utilizando el índice de valor del indicador (IndVal) según Dufrêne and Legendre (1997) y De Cáceres et al. (2010). Un análisis de redundancia (RDA) utilizando la distancia Hellinger se aplicó para estudiar las relaciones especies-ambiente y determinar qué variables explicar significativamente la distribución de las especies de diatomeas. La diversidad de diatomeas se caracterizó con el total de taxones por muestra y mediante el desarrollo de curvas colector y de rarefacción. La relación entre la riqueza de taxones y las posibles variables explicativas fue examinada utilizando modelos aditivos generalizados (GAM).

Análisis de redundancia (RDA) utilizando la distancia Hellinger se realizaron para examinar la relación especies-medio ambiente y determinar variables candidatas para la reconstrucción. Las funciones de transferencia se desarrollaron utilizando el modelo Weighted Averaging - Partial Least Squares (WA-PLS) y bootstrapping como método de validación cruzada. La selección del número de componentes se llevaron a cabo siguiendo las recomendaciones de Juggins and Birks (2012). El efecto de la correlación espacial de las funciones de transferencia se analizó mediante el test de Telford y Birks Telford and Birks (2009).

La abundancia relativa de los cistes de crisofíceas con respecto a las valvas de diatomeas proporciona una indicación de la importancia de los procesos planctónicos en un lago poco profundo. De acuerdo con esto, se contó el total de cistes con respecto a 500 valvas de diatomeas. La importancia de la relación entre la relación cistes:diatomeas y el ambiente se exploró mediante un análisis de correspondencia canónica (CCA). Posteriormente, la relación entre la relación cistes:diatomas y las posibles variables explicativas fue examinada utilizando modelos aditivos generalizados (GAM).

Comunidades de diatomeas en el tiempo (Sequencia de Burg)

Los cambios temporales de las comunidades de diatomeas registrados en el lago Burg fueron estudiados por medio de la diversidad de diatomeas, la zonificación, la tasa de cambio de los ensamblajes, y un análisis de componentes principales. La zonificación se llevó a cabo por Constrained Incremental Sum-of-Squares Cluster Analysis – CONISS (Birks 2012; Grimm 1987), utilizando la distancia

euclidiana y datos transformados con raíz cuadrada. La tasa de cambio de las comunidades de diatomeas se estimó calculando distancias Hellinger entre muestras consecutivas y entre muestras separadas cada 50 años.

Las funciones de transferencia desarrollados con el estudio regional se aplicaron a la secuencia de diatomeas del lago Burg. La fiabilidad de las reconstrucciones se evaluó a partir de tres procedimientos complementarios: especies indicativas, confiabilidad estadística y mediante un análisis de la coherencia limnológica de las reconstrucciones.

Suavizado de datos

El registro Burg fue cortada en secciones de igual espesor que causaron una resolución temporal distinta ya que las tasas de acumulación variaron a lo largo del núcleo. Esta diferente resolución temporal hace incomparables los patrones de variabilidad entre zonas. Con el fin de minimizar esta restricción se aplicó un procedimiento de remuestreo, suavizando los datos en ventanas de tiempo de 50 años.

Resultados

Estudio de la flora de diatomeas de los lagos estudiados

La diversidad de diatomeas es particularmente alta en ambientes oligotróficos como lo son los lagos del Pirineo. De los 1.088 taxones registrados en la Península Ibérica, unos 300 están registrados en las provincias del Pirineo español y Andorra (Aboal et al. 2003). Sin embargo, estudios monográficos dedicados a conocer la flora de diatomeas de los Pirineos son escasos y se espera que el número real de taxones sea mucho mayor que lo reportado hasta el momento. La progresión en la descripción de nuevas especies en ecosistemas de agua dulce europeos durante los últimos 20 años sugiere que todavía existe una gran diversidad de formas sin describir en ecosistemas remotos y oligotróficos. Incluso, en ecosistemas de agua dulce de Europa Central que se han estudiado ampliamente, se siguen reportando un importante número de nuevos taxones.

Teniendo en cuenta una buena calidad de las identificaciones taxonómicas es uno de los factores que más influye en la calidad de la formulación e implementación de funciones de transferencia (Birks 1994), el objetivo de esta sección fue revisar, actualizar y ampliar la identificación de los taxones de diatomeas que se encuentra en los lagos pirenaicos. El detalle del trabajo taxonómico realizado se presenta en el Apéndice 1.

Un total de 73 géneros fueron encontrados en los lagos estudiados: 70 en los lagos del estudio regional y 58 en el registro sedimentario del lago Burg. Los géneros más diversos fueron *Pinnularia*, *Gomphonema*, *Eunotia*, *Nitzschia*, *Navicula*, *Naviculadicta*, *Encyonema* y *Fragilaria*.

El total de taxones registrados (especies y taxones infraespecíificos) fue de 549. En el estudio regional fueron encontrados 477 taxones, mientras que en el registro de Burg se encontraron 244 taxones. En el estudio regional, las muestras del sedimento presentaron un mayor número de taxones (417) con respecto al estudio del epiliton (355). La alta diversidad de los lagos estudiados también se refleja en el número de taxones exclusivos de cada tipo de sustrato: 121 exclusivamente encontrados en el sedimento y 59 del epiliton. La secuencia del lago Burg presentó un 23% de taxones (57) que no fueron encontrados en el estudio regional, sugiriendo un carácter inusual de este lago en el contexto actual de los lagos pirenaicos.

Los géneros con mayor riqueza de taxones no coincidieron con los géneros con mayor número de taxones dominantes. El género *Achnanthidium* fue frecuentemente el más dominante, tanto en los sedimentos como en el epiliton. Sin embargo, las muestras de sedimento presentaron una mayor variabilidad en el género dominante de muestras. Cuatro especies fueron el taxón dominante más frecuente en las muestras de sedimentos: *Achnanthidium minutissimum* (Kützing) Czarnecki, *Discostella stelligera* (Cleve y Grunow) Houk y Klee, *Denticula tenuis* Kützing y *Pseudostaurosira microstriata* (Marciniak) Flores Los taxones dominantes más frecuente en las muestras de epiliton fueron: *Achnanthidium minutissimum*, *Brachysira intermedia* (Østrup) Lange-Bertalot, *Encyonema minutum* (Hilse) Mann y *Psammothidium acidoclinatum* (Lange-Bertalot) Lange-Bertalot.

Las especies raras (frecuencia <3% y máxima abundancia <3%) mostraron un comportamiento similar tanto en el sedimento como en el epiliton. El total de taxones raros fue de 93 (22%) en el sedimento y 113 (32%) en el epiliton. Los géneros con mayor número de especies raras corresponden con los de la más alta

diversidad de especies en el sedimento (*Eunotia*, *Gomphonema*, *Encyonema* y *Pinnularia*) y en el epiliton (*Gomphonema*, *Naviculadicta*, *Nitzschia*, *Pinnularia* y *Eunotia*).

Curvas de acumulación de especies mostraron un rápido incremento en el número de taxones en el intervalo de 20-30 lagos, en los dos grupos de muestras. Diferentes estimadores de riqueza Índices de riqueza, sugieren que el número de taxones esperado para el sedimento podría estar entre 445 y 479 y el del epiliton entre 387-432. De acuerdo con esto, el procedimiento de muestreo y conteo subestima entre el 7 y el 15% de la riqueza de taxones del sedimento y entre el 8 y el 21% de la riqueza de taxones del epiliton.

En el estudio intensivo de la flora de diatomeas de los lagos estudiados se encontraron un 25% de taxones que no pudieron ser identificados como especies conocidas. Esto significa que 140 taxones requieren un esfuerzo taxonómico adicional y podría ser especies o variedades aún no descritas.

Ambiente y distribución de las diatomeas

Gradiente de pH y alcalinidad

La distribución regional de las diatomeas en zonas alpinas y templadas se explica principalmente por el gradiente de pH y la alcalinidad -ANC. El objetivo de esta sección fue identificar especies indicadoras del gradiente pH-ANC dentro de la variabilidad química de los lagos pirenaicos.

Una forma simple de comprobar si algunas especies de diatomeas muestran cierta tendencia dentro de un gradiente ambiental es comparar el valor medio de la variable en los lagos en los que la especie parece contra el valor esperado de una selección aleatoria de la misma serie de lagos. El resultado de este procedimiento indica que existe un alto número de especies que se distribuyen fuera de los valores medios esperados de pH y ANC en el Pirineo, sugiriendo que estas especies no distribuyen aleatoriamente respetar el gradiente ANC-pH en los lagos pirenaicos. La comparación de los óptimos ecológicos de las especies con las medias de su distribución indica que el rango de distribución de

la especie fue generalmente amplio, incluso para las especies con óptimos en los extremos de pH. Esto puede ser debido a una alta tolerancia de las especies, y a que las especies pueden crecer en determinados microambientes dentro del lago, que difieren sustancialmente de las condiciones en las aguas abiertas, donde se midieron las variables químicas. Por ejemplo, especies con óptimo en el rago ácido mostraron una gama de distribución que cubre desde los lagos más ácido hasta un pH de 7.2.

El gradiente de ANC-pH en los Pirineos se puede clasificar teniendo en cuenta las concentraciones de Ca^{2+} y SO_4^{2-} del agua. En este sentido, siguiendo la clasificación de Camarero et al. (2009) se construyeron 7 tipos distintos de ambientes, a partir de los cuales se estudiaron las características químicas de los lagos y la respuesta de las diatomeas al gradiente pH-ANC. El análisis de esta clasificación indicó que los lagos del Pirineo se caracterizan por aguas con tendencia neutra. Un 67% de los lagos estudiados presentó concentraciones de SO_4^{2-} <50 µeq/L y un 88% pH> 6,5. La ausencia de lagos con pH por debajo de 5,5 y SO_4^{2-} <50 µeq/L indica que la acidez es siempre causada por la oxidación de los sulfuros, mientras que la acidez orgánica es irrelevante.

El análisis de indicadores (IndVal) para los grupos de pH-ANC mostró que con excepción del grupo 2 (SO_4^{2-} <50 µeq/L, pH 6,5-7,25), todos los demás grupos tuvieron especies significativamente indicadoras. La utilización del procedimiento de combinación de los grupos del IndVal aumentó el número de especies indicadoras de 43 a 67 especies. Los grupos 1 (SO_4^{2-} <50 µeq/L, pH >5,5-6,5), 7 (SO_4^{2-} >50 µeq/L, pH <5,5) y 6 (SO_4^{2-} >50 µeq/L, pH >7,25), presentaron el mayor número de especies indicadoras, correspondiendo con las condiciones más extremas: lagos con pH muy alto o muy bajo, con la más alta concentración de SO_4^{2-}, y lagos ácidos escasamente mineralizados con baja concentración de SO_4^{2-}. Hubo un gran número de especies indicadoras de diferentes combinaciones de las clases 1, 4 (SO_4^{2-} >50 µeq/L, pH <5,5), 7, es decir especies indicadoras de condiciones ácidas sin estar afectadas por la concentración de SO_4^{2-}.

La clase 5 (SO_4^{2-} >50 µeq/L, pH 6,5-7,25) solo presentó dos especies indicadoras, pero hubo un más especies indicadores para diferentes combinaciones de clases que incluyen la clase 5. Así mismo, la clase 3 (SO_4^{2-} <50 µeq/L, pH >7,25) también presentó un bajo número de especies indicadoras, mientras la clase 6 y la combinación 3+6 presentó más especies que corresponde a especies de condiciones alcalinas.

Gradientes de nutrientes

Después de la luz y el carbono, los macronutrientes son los principales reguladores del crecimiento de las algas (Reynolds 2006). La relación de las diatomeas con la concentración de nutrientes del medio se ha utilizado para desarrollar función de transferencia, principalmente para el fósforo total (TP), al ser un indicador trófico general (Chen et al. 2008; Reavie and Smol 2001; Reid 2005; Werner and Smol 2005). La fiabilidad de algunas de estas funciones de transferencia han sido cuestionados por Juggins et al. (2013). Estos autores señalan algunas debilidades de estas funciones de transferencia relacionadas con la influencia de variables secundarias y el número de taxones estadísticamente relacionado con el TP. A pesar del relativo gran número de modelos de este tipo utilizados para reconstruir nutrientes utilizando las diatomeas (Buczkó et al. 2012; Cremer et al. 2009; Quillen et al. 2013) la relación ecológica de una gran cantidad de taxones con los nutrientes sigue siendo desconocida. En este capítulo, se exploran las relaciones entre los nutrientes y las diatomeas en los lagos de los Pirineos con el objeto de reconocer taxones de diatomeas indicativos de los cambios en nutrientes, que eventualmente, podrían aportan información de las condiciones ambientales pasadas del lago de Burg.

El patrón de la distribución de la especie a través del gradiente de nutrientes en los lagos pirenaicos difiere entre TN, TP y Si. En el caso de TN, las especies presentaron amplios intervalos; casi cualquier especie podría ocurrir en un amplio rango de valores de TN. Para el TP, el patrón fue ligeramente más asimétrico, particularmente en el extremo oligotrófico del gradiente de TP en el que algunos taxones aparecen restringidos a valores por debajo de 0.1 mmol/L.

La respuesta de los organismos ante los nutrientes no es lineal, ya sea a nivel celular o en el ecosistema. Por lo tanto, los lagos estudiados se clasificaron según algunos valores límites característicos conocidos, con el objeto establecer especies indicadoras de estas agrupaciones. La agrupación de los lagos según los valores de N y P se realizó siguiendo dos enfoques, utilizando las relación N:P y utilizando valores críticos de los dos nutrientes. La clasificación de los lagos con respecto al Si se realizó utilizando tres criterios: la concentración de sílice, la relación Si:TP y la concentración Si:TN. A partir de estas agrupaciones se pudo establecer un importante número de especies indicadoras de diferentes rangos de nutrientes.

El análisis mostró un importante número de especies indicadoras de baja relación TN:TP. Entre las especies más representativas se encuentran:

Asterionella formosa, *Aulacoseira perglabra*, *Aulacoseira* cf. *valida*, *Brachysira intermedia*, *Neidium longiceps*, *Nitzschia* sp. No. 11 Burg, *Navicula* cf. *submuralis* and *Psammothidium rossii*.

Factores físicos

El objetivo de esta sección fue identificar especies de diatomeas estadísticamente relacionadas con los principales gradientes físicos. Para esto, se exploró la distribución de las especies a través de los gradientes ambientales y se identificaron especies indicadoras de la duración de la cubierta de hielo, la temperatura superficial del agua durante el verano y del ambiente lumínico de los lagos.

La comparación del rango de distribución de las especies para una variable dada, contra su óptima ecológico proporcionó resultados contradictorios para los distintos gradientes físicos estudiados. Con respecto a la cobertura de hielo, no hubo una gran diferencia ente los valores medios de distribución y el óptimo ecológico. No obstante, en los extremos de la distribución si existe una diferenciación, sugiriendo que en condiciones extremas de duración de la cubierta de hielo existe una mayor influencia sobre el crecimiento diferencial de las especies. La distribución de las especies con respecto a la temperatura sigue el mismo modelo de la duración de la cubierta de hielo, pero muestra una diferenciación más pronunciada en el extremo de valores bajos que sugiere la existencia de especies más selectivas a valores bajos de temperatura.

Para identificas especies indicadoras asociadas a la temperatura, los lagos se agruparon en tres categorías: el primer grupo incluyó los lagos más fríos (<10 ºC), el segundo grupo los lagos con temperaturas entre 10 y 15 ºC, y el tercer grupo incluyó a los más cálidos lagos (> 15 ºC). Para la discriminación de los indicadores de la duración de la cubierta de hielo se utilizaron las categorías <160 días, 160-180 días, 180-195 días y >195 días.

Para la identificación de especies indicadores del ambiente lumínico se utilizaron tres sistemas de clasificación diferentes y complementarios: un agrupamiento de los lagos de acuerdo a la cantidad de luz que llega al fondo (1:<10 $\mu E/m^2/s$, 2: 10-120 $\mu E/m^2/s$, 3: >120 $\mu E/m^2/s$), la pertenencia a un grupo de lagos con biofilm de diatomeas activas (según Buchaca and Catalan 2008), y una clasificación béntica basada en la profundidad y la similitud entre las

muestras epilíticas y las del sedimento. El análisis de indicadores para todos estos grupos permitió encontrar especies indicadoras para cada una de estas clasificaciones. El detalle de estos indicadores se presenta en las tablas del capítulo 9.

Distribución de diatomeas y hábitats de los lagos

El crecimiento de algas bentónicas está relacionada principalmente con la disponibilidad de recursos y las condiciones ambientales (Borchardt 1996; DeNicola 1996), pero el tiempo disponible para la colonización del sustrato y las características de este último también son muy importantes (Burkholder 1996b). A escala microscópica, la microtopografía, la porosidad, la composición y la estabilidad del sustrato puede afectar el crecimiento de las algas. En una escala mayor, estas propiedades del sustrato se relacionan con descriptores de los meso-hábitat como son la presencia de macrófitas, macroalgas, rocas, arena, limo, etc. Se han realizado un gran número de estudios ecológicos y reconstrucciones ambientales utilizando organismos que crecen sobre las rocas (e.g. Cameron et al. 1999; DeNicola et al. 2004) y los sedimentos (e.g. Clarke et al. 2005; Puusepp and Punning 2011). Sin embargo, existen pocos estudios que cuantifiquen la relación entre los meso-hábitat y la composición de algas. Los macrófitos acuáticos pueden proporcionar información sobre los cambios en el clima, el estado trófico y el nivel de agua (Birks et al. 2012; Bos et al. 2006; Rooney et al. 2003; Sayer et al. 2010) y al mismo tiempo las macrófitas sumergidas tienen una influencia significativa en la comunidad de diatomeas. Por lo tanto, se puede esperar que las asociaciones de diatomeas en las secuencias sedimentarias puedan proporcionar indicios sobre la abundancia de macrófitas en el pasado y su relación con los factores ambientales. El objetivo de este capítulo fue identificar especies de diatomeas relacionados con características del meso-hábitat, centrándose especialmente en la presencia de macrófitas en los lagos pirenaicos.

A partir de esto se evaluó la evaluación de las especies indicadoras se realizó agrupando los lagos por su presencia o no de macrófitas y por la presencia o no de especies asociadas al *Potamogeton* (e.g., *Potamogeton*, *Rannunculus* and *Myriophyllum*). Este tipo de plantas ofrecen condiciones adecuadas para la fijación de las diatomeas y aunque tienen algún grado de solapamiento con los Isoetes, tienden a crecer en condiciones muy distintas. Los lagos incluidos en el

análisis fueron seleccionados mediante el límite de la distribución de los macrófitos con respecto al pH del agua en el Pirineo.

Síntesis del análisis de indicadores ecológicos

Además de su gran diversidad de diatomeas, los lagos del Pirineo se caracterizaron por un gran número de especies significativamente indicadoras de la química del agua, nutrientes, variables físicas y de las condiciones del hábitat.

Así por ejemplo, de un total de 368 taxones encontrados en las muestras de sedimento, 205 fueron indicadores de alguna clasificación medioambiental, registrándose 381 valores de indicación significativos. En el epiliton se encontraron 131 especies indicadoras (de 334 taxones posibles) y 202 valores de indicación significativos. Este elevado número de especies indicadoras es una herramienta útil para la reconstrucción ambiental del lago Burg Lake, ya que se presentaron 104 indicadores significativos (51 taxones) en el registro sedimentario. El resultado más destacado del estudio de indicadores, es el escaso número de especies indicadoras compartidas entre las diferentes clasificaciones usadas. Así, de las 112 especies más representativas de todo el estudio, 62 fueron indicadoras de una solo categoría y 33 fueron indicador de dos categorías.

Desarrollo de las funciones de transferencia

Actualmente se discute la validez de las reconstrucciones ambientales debido a la interferencia que puede causar sobre ellas la correlación espacial y la influencia de variables secundarias (Anderson 2000; Juggins 2013). De acuerdo con esto, en este capítulo se desarrollan funciones de transferencia para diferentes variables, analizando el efecto de correlación espacial y la correlación entre algunas de las variables. El análisis se realizó comparando las muestras colectadas de los sedimentos superficiales de los lagos y las muestras colectadas en el epiliton.

Los resultados muestran que las diatomeas almacenadas en los sedimentos de los lagos son explicadas por un mayor conjunto de variables, como son el gradiente de pH-ANC, el TP, la luz incidente en el fondo (I_{Zmax}) y la temperatura. Las diatomeas del epiliton son explicadas principalmente por el gradiente de pH. A

partir de esto se escogió el set de muestras del sedimento para la construcción de las funciones de transferencia. Las variables seleccionadas para la reconstrucción fueron pH, ANC, temperatura, I_{Zmax} y TP.

El análisis mostró que con excepción de la temperatura, la mayoría de las variables no están afectadas por la correlación espacial. Los valores reconstruidos de temperatura pueden ser afectados por el espacio en una distancia de 20 km. No obstante, este resultado está relacionado con un efecto de la altitud, en donde lagos más cercanos tienen una temperatura más parecida al estar a altitudes más parecidas, debido a aspectos geográficos del Pirineo.

Con el objeto de descartar la influencia de la correlación entre las variables seleccionadas, sobre el poder de predicción de los funciones, se compararon las varianzas de las especies explicadas por cada variable. Este análisis muestra que cada una de las variables seleccionadas está explicando un conjunto distinto de especies sugiriendo que estos modelos pueden ser usados para producir reconstrucciones independientes.

Relación entre cistos de crisóficeas y diatomeas

Chrysophyceae y Synurophyceae son algas unicelulares o coloniales que se encuentran en una amplia gama de condiciones ambientales, las cuales producen fases latentes silíceas que se acumulan en los sedimentos de los lagos, almacenando información sobre las condiciones ambientales del pasado (Pla and Catalan 2005; Zeeb and Smol 2001). A pesar de que la identidad de la especie de la mayoría de los cistos es desconocida, la riqueza y la posibilidad de distinguirlos por morfotipos, se ha utilizado para reconstruir condiciones ambientales del pasado (Pla and Anderson 2005; Pla and Catalan 2005). La relación entre el total de cistos y las valvas diatomeas acumulados en los sedimentos, se ha utilizado como un indicador de diferentes condiciones ambientales (Cumming et al. 1993; Smol 1983, 1985). En este sentido, con el objeto de aplicar la relación cistos:diatomeas en la reconstrucción ambiental de los lagos del Pirineo, en esta sección se analizan los factores ambientales relacionados con la variabilidad de índice.

El resultado más relevante de esta sección es que la relación cistos: diatomeas es explicada principalmente por la profundidad del lago y secundariamente por el gradiente de pH-ANC. Otras variables con las cuáles ha sido asociada la

relación, tales como la temperatura o el TP, tienen una explicación muy baja en los ambientes estudiados.

El comportamiento de la relación con respecto a la profundidad sugiere que lagos con una profundidad inferior a 6 m mostraron una alta probabilidad de presentar abundancias de cistos <5% (media de 2,3%) mientras lagos con profundidad entre 6 y 10 m mostraron abundancias <10%. Por el contrario, lagos con una profundidad superior a 35 m mostraron abundancia de cistos >20%. De acuerdo con esto resultados, la relación cistos:diatomeas puede ser usada como un índice de la profundidad en los lagos pirenaicos.

Composición y zonación del registro de diatomeas en el lago Burg

Diatomeas del lago Burg y zonación de la secuencia

El registros de diatomeas del lago Burg incluye 244 taxa, de los cuales 55 estuvieron presentes en más de un 10% de las muestras y 17 tuvieron una abundancia máxima> 5%. *Staurosira construens* Ehrenberg, *Staurosirella pinnata* (Ehrenberg) Williams & Round, *Punctastriata* cf. *lancettula* (Schumann) Hamilton & Siver M1, *Achnanthidium minutissimum* (Kützing) Czarnecki, *P. lancettula* (Schumann) Hamilton & Siver y *Encyonopsis subminuta* Krammer y Reichardt fueron las especies con mayor frecuencia y dominancia.

El registro fue dividido en ocho zonas a partir de la composición y abundancia de las especies de diatomeas. Una descripción de las especies de cada zona, así como su significado ambiental se presenta en el capítulo 15.

El primer eje de un Análisis de Componentes Principales explicó el 28,8% de la variabilidad de diatomeas a lo largo de todo el registro. *E. subminuta*, *A. minutissimum* y *P. lancettula* fueron las especies con una correlación positiva más alta con el primer componente del modelo. *S. construens*, *S. pinnata*, y *P. lancettula* M1 fueron las especies con una correlación negativa.

En esta sección también se incluye el análisis diagnóstico de la aplicación de algunos de los indicadores desarrollados en las secciones anteriores. Para esto, la

abundancia de especies indicadoras de una determinada clasificación se sumó por cada una de las categorías. Posteriormente se seleccionaron los indicadores que mostraran cambios importantes a través del registro. Los resultados muestran un sentido ecológico entre algunos de los indicadores, como es el caso de la abundancia de indicadores relaciones N:TP <50:1 y los diferentes indicadores de Si. Así mismo, los indicadores de presencia de macrófitos y macrófitos asociados a *Potamogeton* sugieren que las plantas acuáticas empezaron a ser importante en el entorno de lago desde ~ 15.300 años cal AP y mantuvieron una presencia relativamente alta en todo el registro.

Reconstrucción biogeoquímica

Minerales de talco, mostraron valores elevados en 16.500-13.600 yr cal BP y 12.500-10.500 años cal BP. Desde 11.000 yr cal BP, el talco disminuyó progresivamente hasta llegar a ser no detectable alrededor de 9000 yr cal BP. El talco es un mineral metamórfico resultante del metamorfismo de minerales de magnesio. Se forma en la cuenca y su disminución puede estar relacionada con el desarrollo de una cuenca con más vegetación, con suelos más profundos y por lo tanto, con una menor disponibilidad de minerales primarios.

Minerales de aluminosilicatos presentaron una tasa de sedimentación constante a través del registro, con una reducción progresiva durante el Holoceno, en particular alrededor de 9500-9000 yr cal BP. Este comportamiento puede estar relacionado con la formación del suelo y un aumento de la cobertura vegetal.

El titanio puede ser considerado un elemento indicativo de la erosión física de la cuenca debido a su alta insolubilidad. Entre 12.700 y 11.500 yr cal AP, periodo que corresponde con el Younger Dryas hubo un marcado aumento en la erosión física de la cuenca. Antes y después de este período ocurren varias oscilaciones con una tendencia general de disminución desde la base del registro hasta el Holoceno. La tendencia marcada y sostenida en la disminución de Al/Ti, K/Ti, y K/Al probablemente indica un aumento en la selección de las partículas que son transportadas. De tal manera que progresivamente, con el transcurso del tiempo, solo la partículas más pequeñas pueden llegar al lago. Mientras que el Ti permanece unido a las partículas más pequeñas, el Al y el K son en su mayoría parte de los minerales que forman partículas más grandes. Esta tendencia refleja los cambios ontogénicos relacionados con aspectos geomorfológicos; el

desarrollo de una pendiente más suave, y un aumento progresivo de la zona litoral que impide la llegada de partículas grandes al centro del lago.

Como se ha mencionado previamente, el lago Burg sufrió un proceso de relleno progresivo, que convirtió el lago en un pantano. Este proceso queda reflejado en la tendencia temporal del LOI. Además de esta tendencia temporal, el lago presentó varios eventos durante los cuales se presentó un input alto de materia orgánica hacia los sedimentos. Estos valores más altos corresponden en general con un aumento en la concentración de valvas de los sedimentos y un aumento en la relación Br/Ti. Valores más altos de materia orgánica estuvieron asociados con un aumento de las condiciones reductoras de los sedimentos, como lo reflejan diferentes proxies (S/Fe, Cr/V). En general, en los sedimentos del lago prevalecieron estas condiciones, con excepción de algunos periodos como el YD, cuando los valores de reducción y LOI fueron bajos, y ocurrió una notoria acumulación de P en los sedimentos.

El TP, que es un indicador de productividad plantónica, mostró un comportamiento diferente al registrado por el LOI y los otros indicadores de materia orgánica. El lago presentó valores altos de TP durante su fase temprana y después de esto los valores se redujeron progresivamente hasta el 12400 yr cal BP. A partir de ese momento el sistema muestra un cambio en la tendencia del TP, presentando un patrón creciente durante el Holoceno. La I_{Zmax} presentó una variabilidad semejante a la registrada por el TP.

Los pigmentos fotosintéticos subfósiles aportaron información adicional sobre la productividad del ecosistema. Las clorofilas no se conservaron bien en el registro sedimentario, pero se encontraron otros pigmentos que aportan información sobre la organización del componente béntico. Así, los pigmentos más abundantes en el sedimento fueron: luteina, diatoxantina, zeaxantina, e isoreniareteno. Aunque la zeaxantina, está presente en varios grupos algales, es más abundante en las cianobacterias. Este pigmento mostró una alta variabilidad en el registro y se correlacionó con el isoreniareteno, un indicador de carotenoides de Clorobiáceas marrones (bacterias fotosintéticas que requieren condiciones de luz y anóxicas) y equinenona, otro pigmento de las cianobacterias.

El lago presentó una ANC que se puede considerar alta para los lagos del Pirineo. El lago se caracterizó por estar bien tamponado y presentó una progresiva alcalinización a través de todo el registro. El pH y ANC presentan un patrón semejante, aunque el pH presentó una mayor variabilidad. Estas variables

no se relacionaron con la presencia de carbonatos, ni con la relación Ca/Ti, pero si con la relación S/Fe y con el LOI.

Reconstrucción de la temperatura y del nivel del agua

Burg fue un lago pequeño con filtración antes de convertirse en un pantano. Una gran parte de los lagos de origen glacial se alimentan del deshielo de los glaciares. Por lo tanto, la conexión entre la temperatura del agua y la temperatura del aire no es sencilla, además lagos pequeños pueden experimentar cambios de volumen debido a los cambios en la precipitación y el flujo de los glaciares. En este capítulo, se realiza una reconstrucción de las variables más directamente relacionadas con el clima, como son la temperatura superficial del agua, los indicadores del periodo libre de hielo y el índice de profundidad.

Discusión

Confiabilidad de las reconstrucciones cuantitativas

En este estudio se han utilizado dos procedimientos complementarios para reconstruir el medio ambiente acuático utilizando las diatomeas. El valor del indicador de las especies, que se basa en una clasificación previa de la variabilidad ambiental para las cuáles se buscan especies indicativas y la reconstrucción cuantitativa utilizando funciones de transferencia. La fiabilidad de la primera aproximación depende de la correcta clasificación medioambiental. En este estudio, las clasificaciones seleccionadas se basaron en estudios previos realizados en los lagos de montaña y en clasificaciones limnológicas generales. Este no es el caso de las funciones de transferencia que, a pesar de su amplia aplicación en las últimas décadas con excelentes resultados, en algunos casos han sido cuestionadas recientemente desde varios puntos de vista (Juggins 2013). De acuerdo con esto, la confiabilidad de las reconstrucciones cuantitativas se analizó mediante tres perspectivas: a) La representatividad de taxones modernos en el registro de especies de Burg que se utiliza para desarrollar las reconstrucciones, b) La significación estadística de

las variabilidad reconstruida, y c) los efectos de la covariabilidad entre las diferentes variables ambientales reconstruidas.

La representatividad en el lago de Burg de los taxones presentes en el set de muestras de referencia fue alta. En los periodos en los que hubo menos representatividad, las especies dominantes correspondieron a especies presentes en el estudio regional. El número N2 de Hill mostró valores altos y en los casos en que el valor fue bajo, su reducción correspondió a la reducción en la riqueza de la muestra mientras que una alta proporción de especies pertenece a las encontradas en el estudio regional.

En el registro se presentaron algunos episodios con una marcada reducción en la abundancia de las especies mejor representadas (>5% de lagos) en el estudio regional (~16300, 15400 13600-13300, 12700, 12300 yr cal BP). Por lo tanto, las especies menos representadas en el estudio regional tuvieron un mayor peso en las reconstruccione durante esos eventos. Sin embargo, sólo dos eventos (~ 16.300, 12.700, yr cal BP) se relacionaron con un marcado cambio en alguna de las variables reconstruidas (SSWT). El evento ~ 16.300 yr cal BP fue posiblemente el único en donde la reducción en la abundancia de especies análogas están influyendo la reconstrucción de la temperatura, dado que el cambio en la temperatura no se refleja en ningún otro indicador. En contraste, el evento ~ 12.700 yr cal BP corresponde con un evento frío que fue bien registrado por otros indicadores.

La validación de las reconstrucciones ambientales requiere la comparación entre las mediciones históricas y los valores reconstruidos (Birks 1998). Sin embargo, los datos históricos rara vez están disponibles debido a que los registros sedimentarios se extienden mucho más allá de los tiempos en que comenzaron las mediciones instrumentales. Por consiguiente, se utilizan enfoques indirectos para evaluar la fiabilidad de la reconstrucción. Recientemente, Telford y Birks (Telford and Birks 2011b) propusieron una prueba para evaluar la importancia de las reconstrucciones cuantitativas. El método utiliza un set de variables ambientales generadas al azar y luego la varianza explicada por estas variables aleatorias se compara con la varianza explicada por la variable reconstruida. De acuerdo con este método, se probó las significancia de las reconstrucciones cuantitativas del lago Burg.

El primer eje de un análisis de componentes principales (ACP) realizado con las diatomeas del registro de Burg indica tres periodos diferentes en la secuencia donde se produce un cambio en la especie dominante. Estos periodos

corresponden con la fase temprana del lago, el Tardiglaciar y el Holoceno. Ninguna de las variables reconstruidas reprodujo la variabilidad observada en el primer componente. Las variables reconstruidas aparecen como una combinación compleja de diferentes ejes de ACP de diatomeas y las correlaciones entre los PCs de diatomeas y las variables reconstruidas cambian a través del tiempo. Esto puede suceder debido a que el período de tiempo considerado es bastante largo, por la alta resolución temporal del estudio y por grandes cambios ambientales ocurridos dentro de la secuencia estudiada.

El TP fue la única variable que mostró una reconstrucción significativa de acuerdo con la prueba de Telford and Birks (2011b). Sin embargo, un análisis del comportamiento del test usando secuencias que progresivamente acumulan las muestras del registro y usando ventanas móviles de 100 y 200 muestras, mostraron resultados contradictorios. El análisis indicó que la ventana de tiempo seleccionada influye en los valores de la prueba.

El análisis de la covariación de las variables reconstruidas mostró que la mayor parte de las variables reconstruidas presentan una covariación completamente distinta a la que se detecta en el set de muestra del estudio regional. Así por ejemplo, el TP que es una de las variables que podrían estar muy condicionada por otras variables como la ANC y la temperatura (Juggins et al. 2013), mostró un patrón completamente opuesto al registrado en el estudio regional. El set de referencia mostró una correlación positiva entre el TP y el ANC, mientras que los valores reconstruidos estuvieron correlacionados negativamente. Por lo tanto, no puede afirmarse que la dependencia entre las variables se traduce en las reconstrucciones ambientales a través de las funciones de transferencia aplicadas. La relación entre el TP y la temperatura reconstruida también mostró un resultado semejante. Mientras existe una correlación positiva en el set de referencia, la relación entre las dos variables va cambiando a lo largo del registro sedimentario. Estos resultados sugieren más un cambio en los procesos internos del lago, que un problema de interdependencia de las dos variables. La I_{Zmax} fue la única variable que mostró una covariación con el TP en el registro sedimentario, semejante a la observada en el set de referencia. Sin embargo, una mayor correlación entre I_{Zmax} y el índice de profundidad que entre el TP y el índice de profundidad sugieren una coherencia limnológica en la reconstrucción de I_{Zmax}. En lagos relativamente oligotróficos como Burg, la luz que llega al fondo del lago depende más de la profundidad que de la transparencia del agua. Así mismo, las especies que son explicadas por I_{Zmax} difieren de las que son

explicadas por el TP. No obstante, las interpretaciones derivadas de la I_{Zmax} reconstruida fueron analizadas con precaución.

Desarrollo del ecosistema

La secuencia sedimentaria del Lago Burg colectó información sobre el clima, la ontogenia y los principales procesos internos del lago. Una alta tasa de acumulación de sedimentos, baja profundidad, el desarrollo de plantas acuáticas, y cambios en la cuenca, producen un escenario complejo que fue interpretado usando las diatomeas y la información de otras variables cuantificadas.

Durante el periodo estudiado, el lago sufrió una reducción en su profundidad máxima, correspondiente a la mitad del valor que presentaba al inicio del periodo estudiado. Este cambio dramático en profundidad fue probablemente responsable de las tendencias observadas a largo plazo en diferentes proxies como el LOI, el pH, y parcialmente el TP.

La tendencia observada en estas variables puede reflejar la conversión progresiva del sistema, desde un lago con filtración a un humedal. La transición entre estos dos sistemas se produjo después del período aquí estudiado (Pèlachs et al 2011.); sin embargo, algunos rasgos de esta transición como una mayor acumulación de materia orgánica y la alcalinización son observados durante la progresiva reducción de profundidad.

La disminución de la profundidad del lago no es independiente de otros cambios geomorfológicos en los alrededores del lago. El alisamiento de las laderas de la cuenca y la disminución de la energía de los flujos de agua se observa en varios de los indicadores geoquímicos.

El TP reconstruido es probable la variable que mejor describe la complejidad de la influencia del clima, de la cuenca y las interacciones de los procesos internos del lago. El TP puede ser entendido como una medida de la productividad de la columna de agua del lago. En ese sentido, la productividad del lago mostró una tendencia de descenso durante la mayor parte del Tardigalciar y desde el 12.200 yr cal BP, la tendencia se revirtió. El punto de inflexión coincidió con un aumento en la velocidad de sedimentación. El cambio en la tendencia TP se puede atribuir a las diferencias de las condiciones climáticas entre Tardiglaciar y el Holoceno. Sin embargo, la comparación entre dos períodos con condiciones

de temperatura y nivel de agua semejante mostró que la causa principal del cambio en la productividad fue la ontogenia del lago.

Por otro lado, ocurrió un periodo con alta concentración de TP durante las fases tempranas del lago que está probablemente relacionado con altas cargas de P desde la cuenca al haber un menor desarrollo del suelo y al estar las rocas más expuestas a la meteorización. Durante este periodo el TP mostró una disminución progresiva que es coherente con la formación del suelo y por lo tanto, con la disminución de la entrada externa de P. El período de valores altos de TP finalizó bruscamente, probablemente debido a una mejoría en el clima. La ontogenia del lago y de la cuenca, no están necesariamente relacionadas, pero durante el desarrollo de la cuenca se produce un control de los nutrientes que se exportan al lago, mientras que la evolución del lago hacia un humedal provoca un aumento progresivo en el estado trófico.

El TP y el LOI no están muy acoplados en el registro. El LOI muestra más concordancia con los indicadores de la productividad del bentos. Las condiciones del lago durante finales de Estadial 2a (GS -2a) y durante el Interestadial 1 (GI-1) ejemplifican la mayor importancia del compartimento béntico del lago. Los altos valores de indicadores de macrófitos y pigmentos de cianobacterias y bacterias fotosintéticas anóxicas, indican el desarrollo de una biopelícula compleja en el fondo de un lago rodeado de macrófitos. En este tipo de entorno existe un fuerte control de las condiciones redox del sedimento y del reciclaje de nutrientes. Las condiciones anóxicas deberían movilizar P pero difícilmente pueden difundirse a la columna de agua debido a la presencia de una biopelícula bien desarrollada. Mientras en la parte alta de este tapete hay un crecimiento, la materia orgánica se va acumulando por debajo de la biopelícula microbiana en condiciones anóxicas. Por otro lado, durante el GI-1 los macrófitos y el LOI tienen una tendencia desacoplada que sugiere que el componente bentónico y los macrófitos alternan el control de la productividad del lago mientras fitoplancton depende más de las entradas externas de nutrientes.

Para entender algunos de los efectos del clima sobre la productividad del lago se analizaron dos periodos en los que se espera un fuerte cambio en la temperatura: la transición de la fases tempranas del lago del GS - 2a al GI- 1 y la transición del GI-1a al Dryas Reciente (YD). Durante el primer periodo estudiado, el calentamiento repentino de temperatura acompañado de un aumento de los niveles por la probable fusión de glaciales de la cuenca, desencadenan un cambio en la organización interna de lago. La consecuencia más fundamental de

este cambio es la reorganización en un ecosistema más grande, con gran volumen de agua, en el que un mayor número de especies de diatomeas pueden crecer y en donde se pueden desarrollar comunidades litorales y bentónicas.

Durante el segundo periodo, el lago presentó una reducción abrupta de temperatura mientras las condiciones de nivel de agua se mantuvieron relativamente altas. Estas circunstancias causaron una reducción de la acumulación de la materia orgánica y en las condiciones reductoras del sedimento. El aumento en la columna de agua y la reducción en el reciclaje de nutrientes conducen a una reducción del estado trófico del sistema.

De acuerdo con la anterior, el lago Burg presenta cambios en la productividad causados por la influencia combinada del clima, y la ontogenia de la cuenca y el lago. La ontogénesis de lago se traduce en un cambio hacia condiciones más productivas, mientras que el clima provoca cambios más drásticos. La ontogenia de la cuenca juega un papel más importante durante las fases iniciales del lago y durante los periodos más fríos.

Reconstrucción del paleoclima usando la secuencia sedimentaria del lago Burg

El análisis de la secuencia sedimentaria del lago Burg indica que los principales eventos climáticos presentes en los registros de Groenlandia fueron identificados en los valores reconstruidos de temperatura. Solo existieron dos discrepancias con respecto a los registros de Groenlandia, la primera de ellas durante la última parte del GS-2a, cuando el lago presentó un rápido calentamiento acompañado de un aumento súbito del índice de profundidad. La segunda corresponde al YD, en el cual se detectan dos fases distintas en el lago Burg.

La terminación de GS-2a ocurre en Burg con una alta variabilidad en los valores de temperatura y de nivel de agua. Los valores registrados en el lago Burg son en general altos cuando se comparan con otros registros de Europa, los Pirineos y la península ibérica (Millet et al. 2012; Muñoz Sobrino et al. 2013).

En ~ 15.400 yr cal BP, el lago presentó un repentino aumento de temperatura que coincidió con un aumento del nivel del agua, de los valores de LOI y de la abundancia de indicadores de la presencia de macrófitos. Estas evidencias sugieren un punto de inflexión en el ecosistema, a partir del cual se presentan veranos más cálidos, se reduce la extensión del invierno y hay un balance

hídrico positivo en la cuenca, o al menos un alto punto de fusión de los glaciares remanentes. Después de este periodo ocurre un periodo frío en 14800 yr cal BP que se extiende hasta el 14500 yr cal BP.

Después del 14300 yr cal BP, durante el GI-1, la temperatura fue relativamente alta y constante, coincidiendo con la tendencia general reportada para este periodo. Así mismo, los principales eventos fríos del GI-1 son observados en la reconstrucción de temperatura realizada con las diatomeas. Durante todo este periodo la tendencia general del lago fue de presentar valores bajos de nivel de agua, especialmente durante el periodo que parece coincidir con el evento frío del 14100 yr cal BP (GI-1d). El final de GI (GI-1a) fue un periodo con valores altos de temperatura y con sorprendentemente valores altos de nivel del lago.

El YD comenzó en el lago con una rápida reducción en la temperatura superficial del agua, cambiando de 17.4 a 15.4 ºC en un periodo de tiempo que probablemente corresponde a un siglo. Después de esto el lago mantiene una baja temperatura del agua hasta el año 12370 yr cal BP. Con excepción de algunos episodios cortos, durante esta primera fase del YD en Burg, el nivel de agua fue relativamente alto. Esta diferencia con el registro de Groenlandia concuerda aparentemente con algunos registros del nivel de agua de lagos de Europa Central (Magny 2001; Magny et al. 2001; von Grafenstein et al. 2000) y sugiere un balance positivo de agua que es coherente con algunas de las hipótesis sobre las causas del Estadial (Broecker et al. 2010; Carlson and Clark 2012).

Después del 12300 yr cal BP el lago presenta valores de temperatura más altos y varios eventos en los cuales los niveles del agua se redujeron drásticamente. No obstante, indicadores de erosión de la cuenca indican que se mantuvieron condiciones frías durante todo el YD. El patrón de temperatura detectado durante el YD con las diatomeas, es más cercano al comportamiento de la temperatura registrada en el Atlántico y el Este del Mediterráneo (Cacho et al. 2001; Clark et al. 2012; Muñoz Sobrino et al. 2013; Rodrigues et al. 2010).

El final del YD estuvo marcado por una reducción de temperatura, seguida de un rápido incremento. Después de este incremento ocurre una nueva reducción en temperatura que cronológicamente corresponde con la Oscilación Preboreal (OP).

Conclusiones

• **Los lagos pirenaicos contienen una alta diversidad de diatomeas**. Existe gran proporción de taxones de diatomeas que no han sido aún descritos adecuadamente.

• **Muchas de las especies diatomeas encontradas tiene valor como indicadoras de diferentes clasificaciones de variables químicas, físicas, nutrientes y del hábitat de los lagos del Pirineo.** Tiene especial interés que cada especie sean indicadora de un número reducido de condiciones.

• **El conjunto de diatomeas de los sedimentos contiene mayor cantidad de información que las comunidades epilíticas.** Esto es debido al carácter tafonómico del fondo del lago que incorpora diatomeas de diferentes hábitats del lago y microambientes, mientras que las asociaciones de diatomeas epilíticas responden a las características generales epilimnéticas.

• **El pH, la capacidad de neutralización de ácidos, el fósforo total, la radiación incidente en el fondo y la temperatura superficial del agua durante el verano, pueden ser reconstruidas cuantitativamente en los lagos del Pirineo utilizando el registro de diatomeas de los sedimentos superficiales.** La fiabilidad de las reconstrucciones independientes de estas variables se basa en el hecho de que una cantidad suficiente de especies responde a cada variable, mientras las demás contribuyen neutralmente.

• **La relación entre el número total de cistos de crisofíceas y diatomeas es un indicador de la profundidad de la columna de agua en los lagos pirenaicos.** A partir de esta relación se pueden reconstruir las fluctuaciones pasadas del nivel del lago en ecosistemas de similares características.

• **La reconstrucción ambiental usando las diatomeas permite inferir las fluctuaciones en las variables químicas y físicas del agua durante el Tardiglaciar y el Holoceno Temprano, que difícilmente son registradas por otros proxies.**

• **Los cambios ontogénicos de los lagos durante largos períodos de tiempo pueden modificar la respuesta del ecosistema ante influencias climáticas**

similares (como se muestra en el lago Burg). Esto es particularmente pertinente para la productividad primaria y el flujo de la materia orgánica en sistemas menos profundos, en donde las distancias de transporte (reciclaje) son más cortas.

• En lagos de montaña relativamente poco profundos (como el lago Burg), la totalidad de la cubeta del lago desarrolla un biofilm productivo, haciendo que en la secuencia sedimentaria predomine la señal del bentos. Únicamente durante las primeras etapas, cuando hay una alta carga externa de nutrientes, la producción planctónica es más relevante en el sistema.

• Las principales oscilaciones climáticas del hemisferio norte registrados en los testigos de hielo de Groenlandia para el Holoceno Temprano y el Tardiglaciar se detectan en la secuencia sedimentaria del lago Burg a través de la reconstrucción de la temperatura de la superficie del agua del verano, el análisis de especies indicadoras y el índice de profundidad. Los cambios en la temperatura y la composición de diatomeas registrados a través de la secuencia sedimentaria, coinciden con eventos como el Interestadial (GI-1, 14.700-12.700 años cal BP), el GI 1-d (~ 14.100 años cal BP), el Dryas Reciente (12.800 a 11.700 años cal BP) y la Oscilación Preboreal (~ 11.400 años cal BP).

• La tendencia temporal de la temperatura superficial del agua durante el verano en el lago Burg y lago oscilaciones de profundidad no se observan acopladas a lo largo del Tardiglaciar y el Holoceno Temprano. Esto fue causado probablemente por las pérdidas por infiltración del lago y a la variable contribución de los glaciares y neveros de la cuenca a lo largo del tiempo.

• El Interestadial de Groenlandia (14.700-12.700 años cal BP) en los Pirineos se caracterizó por veranos cálidos e inviernos cortos. Una reducción de la influencia de masas de aire más frías del norte y el debilitamiento progresivo de los inviernos causa condiciones más cálidas que las observadas durante el Holoceno Temprano.

• Dentro del Younger Dryas (12.700 a 11.650 años cal BP), dos periodos diferentes fueron identificados en el Pirineo basado en los valores de temperatura superficial del agua del verano y profundidad de la columna de agua reconstruidos en el lago Burg: un primer período con condiciones frías y nivel alto de agua, seguido de un segundo período gradualmente más cálido y seco.

Introduction

2. Introduction

Lakes are ecosystems exposed to the combined influence of climate and catchment processes. Lakes collect and archive evidence of these forcings in their sediments through of a complex interaction with internal processes. Deciphering and extracting information from the sediments is a challenging task because, in addition to the inter-dependence between the forcing agents, the lake ontogeny affects the way in which the system responds to them. The sediment record includes an amalgam of inorganic and organic materials, and some recognizable remains of organisms. The latter can be extremely informative about the conditions in which they grew. Among the sub-fossil material, diatoms occupy an outstanding position. The remains can be identified to the species level, due to the siliceous composition of their valves. This fact, added to the rich community that at any instant exists in the lake, make diatoms an excellent proxy for environmental reconstructions. In this study, the focus is placed on the diatom assemblages of the lakes of the Pyrenees and their potential as indicators of environmental conditions. The findings are applied to the sedimentary sequence of the former Burg Lake to reconstruct the lake conditions during Late Glacial and early Holocene periods.

Diatom biology and ecology

Diatoms are unicellular algae characterised by yellow-brown chloroplasts and siliceous cell walls (Round et al. 1990). The number of genus is approximately 350, and the number of described species is estimated in 15,000 (Williams and Kociolek 2011). Diatoms can grow in a wide variety of freshwater and marine environments throughout the world (Battarbee et al. 2001). Diatoms are divided into two principal groups: Coscinodiscophytina and Bacillariophytina, the latter subdivided into the classes Mediophyceae and Bacillariophyceae (Medlin 2011; Sims et al. 2006).

Diatoms are successfully used as ecological indicators of freshwater environmental conditions. The high number of species and their specialized response to a wide range of water conditions are the basis of statistical models describing the chemical and physical characteristics of water bodies (Kitner and Poulíčková 2003; Pan et al. 1996) including nutrients (Borchardt 1996; Carrick and Lowe 2007; Luoto et al. 2012), water transparency (Cantonati et al. 2009;

Hill 1996), temperature (DeNicola 1996), pH (Cameron et al. 1999), and salinity (Gasse 2002; Wilson et al. 1994), among others.

Diatoms grow in a wide range of aquatic habitats, both planktonic and benthic, and segregate along the physical and chemical gradient that depth foster in a lake (Reynolds 1998). Some diatom species have their growing habitat in the plankton (euplanktonic); others can occasionally switch between plankton and benthic habitats (meroplanktonic), sometimes experiencing blooming conditions in the open water, and other are purely accidental (tychoplanktonic) carried by currents or suspended by strong mixing. The combination of depth, mixing regime, and seasonality control the importance of euplanktonic diatoms in the water column as they require some mixing to avoid the tendency to sink due to their heavy valves. Meroplanktonic species are usually even more dependent on mixing as they usually include large filamentous colonies.

Benthic habitats for diatoms include rocks (epilithon), sediment (epipsammon, epipelon) and vegetation (epiphyton) (Battarbee et al. 2001). Benthic diatoms generally distribute around the littoral of the lakes, though they may occupy the whole basin of the lake in shallow or highly transparent systems. Benthic algae respond to the same chemical and physical factors that affect planktonic diatoms; however, the strong selective influence of hydrodynamics on plankton is replaced by others constraints: space availability, physical stability and chemical composition of the substrate and the surrounding microenvironment.

The presence of siliceous valves wrapping the cell is the main advantage of diatoms for their use in palaeoecological studies. Valves accumulate in the lake sediments holding information about the past chemical, and physical lake conditions (Battarbee et al. 2004; Halland and Smol 2004). Usually, sediment cores are retrieved from the deepest part of a lake; place that collects a taphonomic diatom assemblage with valves coming from plankton and the diverse littoral habitats. The recording of the different habitats is not equal nor proportional to their abundance as there may be a differential transport of species (or morphotypes) to the deepest part according to the morphology of the lake (Yang and Flower 2012). Therefore, the whole diatom composition of an ecosystem is hardly preserved in a sediment sample and thus some environmental processes may be better recorded than others. Deep lakes probably are better direct sensors of out-lake factors such climate and catchment loadings, while in shallow lakes store this variation mediated by a stronger influence of in-lake processes and relative changes in littoral microhabitats.

Diatom valves are extremely resistant and preserve well in the sediments of lakes, only in some exceptional conditions they undergo partial or complete dissolution and the initial information of the sedimentary record results affected (Ryves et al. 2009). High alkalinity and some ionic ratios are the main cause of valve dissolution (Barker 1992; Barker et al. 1994; Flower 1993; Ryves et al. 2001). The dissolution can be quantified using different indexes (Flower and Ryves 2009; Ryves et al. 2001) that provide information about the lake environment.

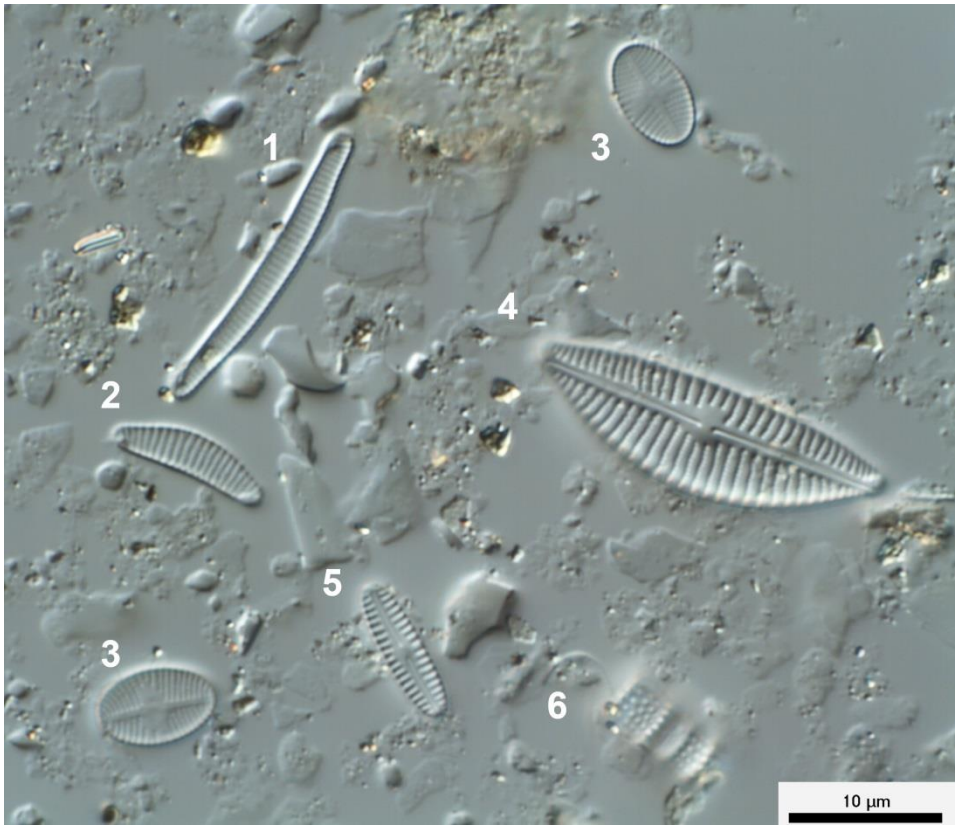

Figure 2.1. General aspect of a surface sediment sample collected from the bottom of a Pyrenean lake (Lake Negre). The image illustrates the high diversity of diatoms accumulated in the sedimentary record: eight valves belong to five different genus and six species. 1. *Eunotia* sp, 2. *Eunotia subarcuatoides* Alles, Norpel & Lange-Bertalot, 3. *Psammothidium helveticum* (Hustedt) Bukhtiyarova et Round, 4. *Encyonema* cf. *hebridicum* Grunow ex Cleve, 5. *Chamaepinnularia* sp, 6. *Aulacoseira* cf. *alpigena* (Grunow) Krammer.

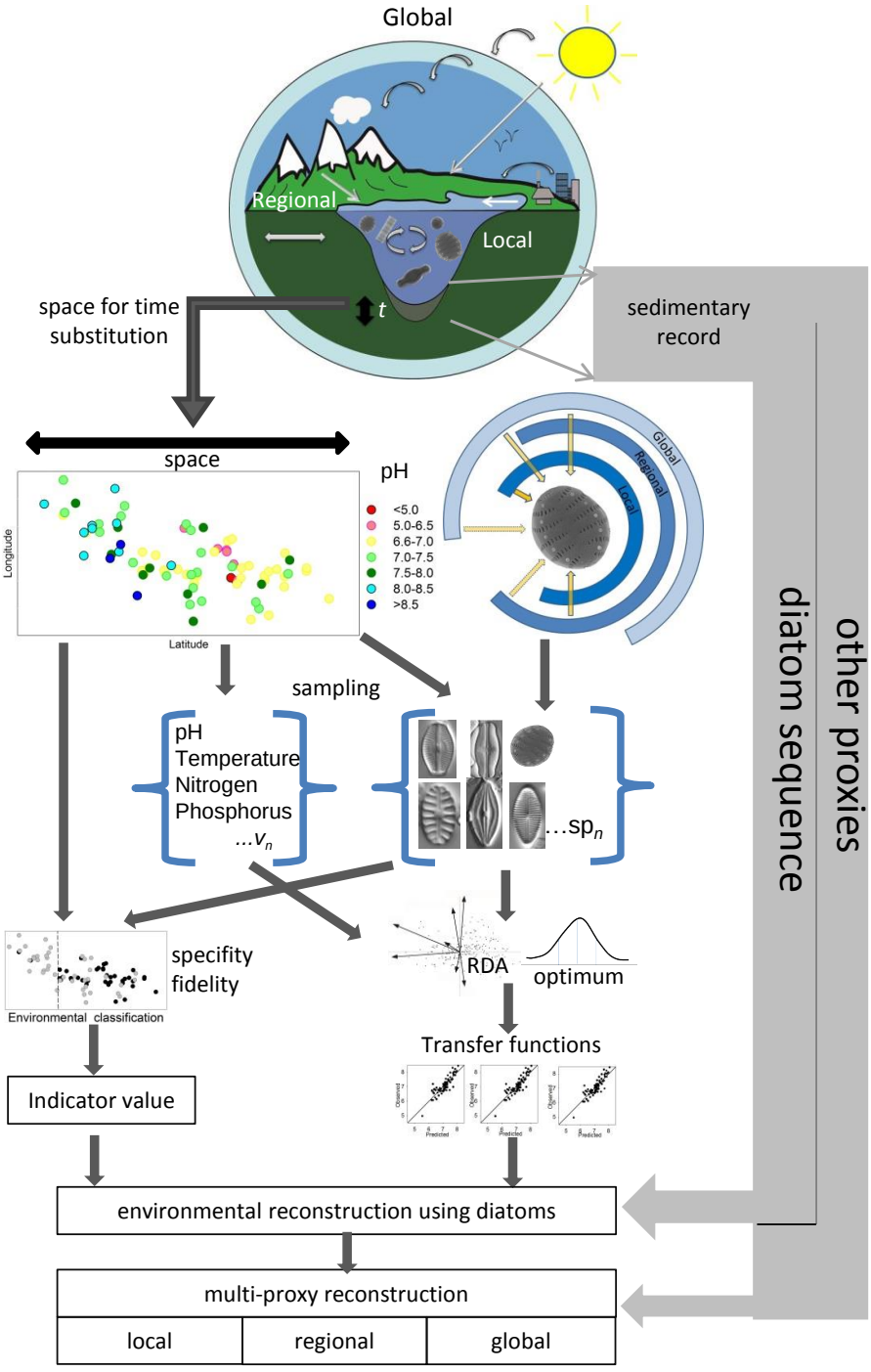

Figure 2.2. Schematic representation of the palaeolimnological approach used in this thesis.

Diatoms provide limnological information about freshwater ecosystems, which is difficult to obtain using other proxies (Figure 2.1). Pollen is useful for approaching out-lake variables such as air-temperature and rain (Davis et al. 2003; Lotter et al. 2000), but can provide limited information about the lake processes. Geochemical and sedimentological proxies supply information about catchment processes, changes in the basin water balance or chemical precipitation in the lake sediments, but they are limited in bringing information about processes occurring in the water column: nutrient changes, for instance. On the contrary, diatoms are excellent for reconstructing water column variables such as conductivity, pH, temperature and nutrients; therefore, they become complementary to proxies informative on out-lake (e.g., pollen) or within-sediment processes (e.g., geochemistry) (Chen et al. 2008; Reavie and Smol 2001; Reid 2005; Werner and Smol 2005).

The palaeolimnological approach

Global, regional, and local environmental changes can be studied by means of the sedimentary sequences accumulated in lakes. The lake basin divides into three parts: an erosion zone, a transportation zone, and an accumulation zone (Smol 2008). The latter zone is the most interesting for environmental reconstructions as it has the higher probability to content a continual sequence of lake sedimentation. Energy and matter fluxes mediated by climate forcing and catchment and in-lake processes are determining the sediment composition and its rate of accumulation (Leavitt et al. 2009).

Space for time substitution is the most common approach to quantitative environmental reconstructions using biological remains (Smol 2008). The basic assumption is that the past variability of an environmental variable in a specific lake is currently within the regional variability of a sufficiently large number of sites (Catalan 2008). In other words, that current environmental spatial gradient contains analogues for the past conditions. This assumption is fulfilled when the sequences studied are not relatively recent, but it is difficult to guarantee when the reconstruction of older periods is attempted. Changes in the ecological preferences of species and changes in the relationships between the environmental variables studied can affect invalidate the main assumption. All in all, use of space for time substitution has shown excellent results in a large number of studies (e.g. Larocque-Tobler 2010; Luoto et al. 2012; Quillen et al. 2013). Accordingly, here it is assumed that the present ecological traits of the

diatoms of the Pyrenean lakes include the expected variability of the diatoms in the sedimentary sequences of the Late Glacial and the Holocene. Thus, analysing the ecological relationships of diatoms at present is possible to understand and reconstruct the past conditions in any lake of the Pyrenees (Figure 2.2).

The interpretation of past environmental condition using assemblages of organisms, such as diatom, can be performed in different ways. Here, two complementary approaches are used: indicator species and quantitative reconstructions based on transfer functions.

The indicator value of diatoms

The strong segregation of diatom species along some environmental gradients and among different habitats is the base for developing reconstruction tools. There are different options, some of them pursuit quantitative reconstructions (see below) others may look for qualitative indications of the prevalence of some habitat types or environmental conditions. Whereas the first may be more valuable for addressing certain specific environmental issues (e.g., acid rain problems), in which quantification is extremely relevant in the context of the problem; the second are less constrained methodologically and may provide a more diverse overview on how lake conditions have been evolving across time. The indicator species approach is based in identifying the strength of the species association with certain groups of lakes classified according habitat or environmental properties. The indicator species analysis (Dufrêne and Legendre 1997) consists in the identification of the "specificity" and the "fidelity" of species to a lake group, and from them, an indicator value is calculated and the significance assessed by bootstrapping methods (Dufrêne and Legendre 1997). Despite this approach uses the abundance and distribution of species across the environment, it does not use the relation of species with expected environmental gradients, and then the subordinate distribution is not relevant to perform the model.

The selection of indicator species is useful when there is an interest in lake classifications rather than gradients (Legendre and Birks 2012). Therefore, the selection of the groups (lake classification) to be tested is the most crucial aspect but, at the same time, the main problem of the approach. Sometimes, the selection of the group is performed by clustering sites using the same matrix of biological data. This procedure helps to identify indicator species of

assemblages (communities) but they do not have necessarily an environmental simple meaning. Thus, in order to select environmentally-informative indicators, the groups should be selected clustering the environment in an independent way to the biological indicator. In this study, this second approach is followed as a complementary tool for quantitative reconstructions based on transfer functions.

Quantitative environmental reconstruction using diatoms

The usual high species richness of the diatom assemblages and their relationship with the environment are the basis for developing models to perform quantitative environmental reconstructions. The mathematical relationship between diatom species and an environmental variable can be modelled in different ways, but when an environmental gradient is long enough, it is expected that the species response to that environmental factor will follow a Gaussian curve (Battarbee 2000). The Gaussian curve corresponds to the general idea of the niche of an organism for that environmental variable. This approach facilitates the quantification of the ecological responses from a statistical viewpoint. The weighted average of the species response at different sites represents the ecological optimum, and its standard deviation is a measure of tolerance to the environmental variable (ter Braak and Looman 1986).

The Gaussian response is applied also to resources such as nutrients. Despite that the expected response to nutrients should be close to the Liebig's law of the minimum (de Baar 1994), the use of a Gaussian approach seems to work quite well (Bennion et al. 1996a; Chen et al. 2008). This suggests that, at the temporal and spatial scale of regional studies, the observed relationship between diatoms and some nutrients is closer to a complex environmental (trophic) gradient, along which species segregate, than a mere indication of the resource availability and use.

Based on the optimum of the species, the value of an environmental variable could be inferred using simple weighted average (WA) calibrations (ter Braak and Looman 1986). However, the organisms are exposed simultaneously to a set of variables, which are likely causing multivariate influence on the species distributions. Thus, the influence of other variables cannot be ignored in the reconstructions (Juggins and Birks 2012). The weighted average partial least square method (WA-PLS) was developed to solve this problem as it combines the advantages of WA and the extraction in different components of interferences from other variables (ter Braak and Juggins 1993). The technique

has become quite popular in palaeolimnology, although recently other approaches have been suggested as appropriate under certain circumstances (Birks and Simpson 2013).

The reliability of environmental reconstructions is permanently scrutinized (Birks 1998; Juggins 2013; Racca and Prairie 2004; Telford and Birks 2005, 2011a). At present, there is an open discussion about the statistical and conceptual assumptions under the numerical methods and how violation (or failure) of these assumptions may compromise the reconstructions. Different ways to check for potential statistical problems have been made available, which are worth to consider during the development and application of quantitative reconstructions. In addition, a more conceptual questioning asks to what extent the causal links can be overlooked by statistical procedures without creating artefacts (Anderson 2000). For instance, sometimes, the intermediate processes connecting climate and diatom assemblages are ignored and statistical links between general meteorological variables (e.g., air July temperature) and diatoms are established straightforward. This association, without considering causal links through catchment and in-lake processes, could cause spurious reconstructions, apparently correct from a statistical point of view, if the causal connections are changing through time. In summary, palaeolimnological reconstructions request, more and more, an integral understanding of the catchment and lake process. The quantitative reconstruction of some variables using biological proxies is a piece more to add to the plethora of other sources of information that exist in the sedimentary record. The understanding of the causal mechanisms of the fluctuations in a lake and the agents forcing its dynamics will arise from a comprehensive view of the system.

Climate and in-lake processes

Changes in the climatic conditions have an effect on some structural and functional components of aquatic ecosystems by a complex interaction between direct and indirect mechanisms (Fritz and Anderson 2013). Thermal and hydrologic dynamics of lakes are primarily affected by climate variability (Agusti-Panareda et al. 2000; Livingstone and Padisák 2007). The variability of incident radiation, wind, precipitation and air-temperature directly affect the thermal budget of lakes (Margalef 1983), modifying temperature, thermal stability, nutrients cycling and water level.

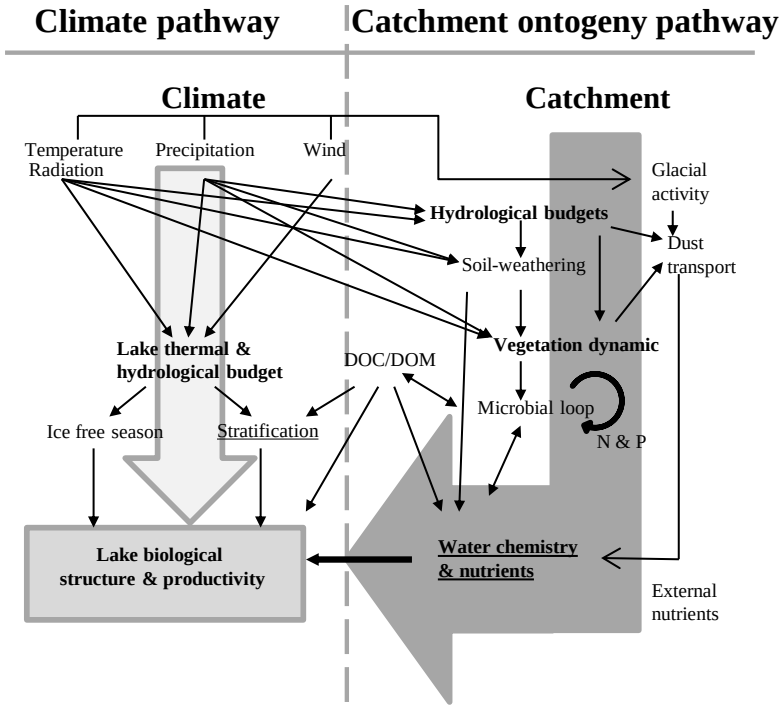

Figure 2.3. Conceptual model from Fritz and Anderson (2013) showing the direct climate forcings and catchment-mediated processes that affect the biological community structure and productivity.

Indirect climatic mechanisms are acting through the catchment (Figure 2.3). Climate is usually the main responsible for changes in the catchment (in places without human intervention): soil development, erosion, vegetation cover, and basin water balance, for instance, depend on it. In lakes of glacial origin, the effects of climate can be less prominent in the early phases of lakes (Anderson et al. 2008). After deglaciation, a lake is scarcely productive but quickly undergoes an increase in nutrient concentrations due to the poor development of soils and vegetation that retain nutrients from rock weathering (Norton et al. 2011).

The main challenge of the environmental reconstruction is to develop a comprehensive view of the ecosystems, including their water- and airsheds, and be able to decompose the sediment signature of the climatic, catchment, and in-lake processes. A multi-proxy approach can provide tools to understand the different factors affecting the lake environment (Birks and Birks 2006) and discriminate the relative effect of each of the factors. For instance, geochemical proxies can provide direct quantitative information about some of the catchment

process while diatoms sequences enable the reconstruction of variables directly related to climate (temperature, solar irradiance) and variables related to in-lake processes (e.g. nutrients, pH).

Objectives

3. Aims and contents

The main objective of this thesis was **to explore the diatom potential for past multivariate environmental reconstructions, with an application to the Late Glacial and Early Holocene sedimentary sequence of Burg Lake (Pyrenees).**

The regional variability of diatom distributions is usually explained by pH or acid neutralising capacity gradients in alpine and temperate areas (Chen et al. 2008; Koster et al. 2004; Siver 1999). However, there is a large remaining unexplained variability (90-70%), which is related to other environmental factors, and could be also used in environmental reconstructions. Some researchers question the feasibility of independent reconstructions of several variables from a single diatom record; they argue that the high temporal autocorrelation of the local assemblages might obscure secondary influences (Anderson 2000). However, some others sustain that it is possible to perform reconstructions, even of particularly dependent variables such as pH and alkalinity, if they present contrasting trends at some sites (Catalan et al. 2009c). The diatom assemblages found in sediments are taphonomic communities; they include species growing in many different habitats and microenvironments; therefore, it can be expected that they hold independent information about environmental processes that impinge differentially in the lake microhabitats. According to this viewpoint, the specific objectives of the thesis were:

1. **To study the diatom flora of the mountain lakes of the Pyrenees.** An extensive taxonomical assessment and comparison with similar ecoregions are shown in the **chapter 5** and the **appendix 1**.

2. **To explore the environmental factors that, besides pH, explains the diatom distribution in the lakes of the Pyrenees, including in-lake proximal factors as well as general descriptors of catchment characteristics.** The part II of the result section shows the relationships between diatoms and environmental factors in the Pyrenean lakes. This section provide data about the autoecology of the most common mountain diatoms exploring the indicator value of a large number of

taxa for chemistry (**chapters 6**), nutrients (**chapter 7**), physical (**chapter 8**), and habitat variables (**chapter 9**). A summary of indicator species is finally shown in **chapter 10**.

3. **To demonstrate that it is possible to reconstruct different independent variables from a unique diatom data set.** The development of transfer functions and analysis of reliability and the independence of models performed are shown in Part III of the results section (**chapter 11**). The analysis is carried out by comparing the performance of two sample data-sets (bottom surface sediment and epilithon samples). In **chapter 12,** the ratio between Chrysophycean cysts and diatoms is analysed as a potential environmental indicator.

4. **To apply the indicator species and the transfer functions developed to the diatoms of the sedimentary sequence of Burg Lake covering Late Glacial and Early Holocene.** An analysis of the diatom assemblages throughout the sedimentary record was performed analysing the main changes in diatom composition, diversity and relevant indicator species (**chapter 15**). The environmental reconstruction of selected variables using the diatom transfer functions was also performed (**chapters 16 and 17**), and the environmental reconstruction was supplemented by the analysis of different geochemical proxies and subfossil photosynthetic pigments **(chapter 16**).

5. **To analyse the reconstructed variables in terms of in-lake processes and their eventual link with climate and catchment processes.** The discussion section presents an analysis of the reliability of the quantitative reconstruction implemented (**chapter 18**). The influence of the past climate changes and the lake ontogeny on the changes in diatom assemblages and lake productivity is described in **chapter 19**. Finally, an interpretation of the reconstruction of climate during Late Glacial and Early Holocene is presented in **chapter 20**.

Materials and methods

4. Materials and methods

Lake survey

The study of the diatom species distribution and ecology was based on a survey of 83 lakes of the Pyrenees performed from 9/7/2000 to 23/8/2000 (Catalan et al. 2009b). Lakes were distributed across wide environmental gradients determined by bedrock type, altitudinal range and lake morphology (Table 1). They were selected to have a stratified representation of the environmental variability and cover the geographical extremes (Figure 4.1).

In general, the lakes of the Pyrenees are located on basins of plutonic and metamorphic lithology with scarcely developed soils (Table 1). Bare rock and meadows are the dominant land cover, and less than 20% of the lakes studied have coniferous woodlands in their respective catchments. The lakes are relatively small but with a high relative depth (Table 1, Table 2).

Table 1. Geographic, morphological, lithological and land cover characteristic of the lakes studied.

Variable	Median (range)
Altitude (m.a.s.l.)	2305 (1620-2990)
Lake area (ha)	5.5 (0.2-53.2)
Catchment area (ha)	114.6 (7-5437.9)
Depth (m)	17 (0.7-123)
Relative depth (%)	6.5 (0.8-18)
Ice-cover duration (days)	186 (115-215)
Lithology (>30% lake catchment area)	
Metamorphic (%)	27.1 (0-100)
Plutonic (%)	48.2 (0-100)
Detrital (%)	17.7 (0-100)
Carbonate (%)	17.5 (0-90)
Land cover	
Glacier presence (%)	0 (0-15)
Bare rock (%)	30 (0-90)
Meadows (%)	15 (0-90)
Shrubs (%)	0 (0-60)
Coniferous (%)	0 (0-40)

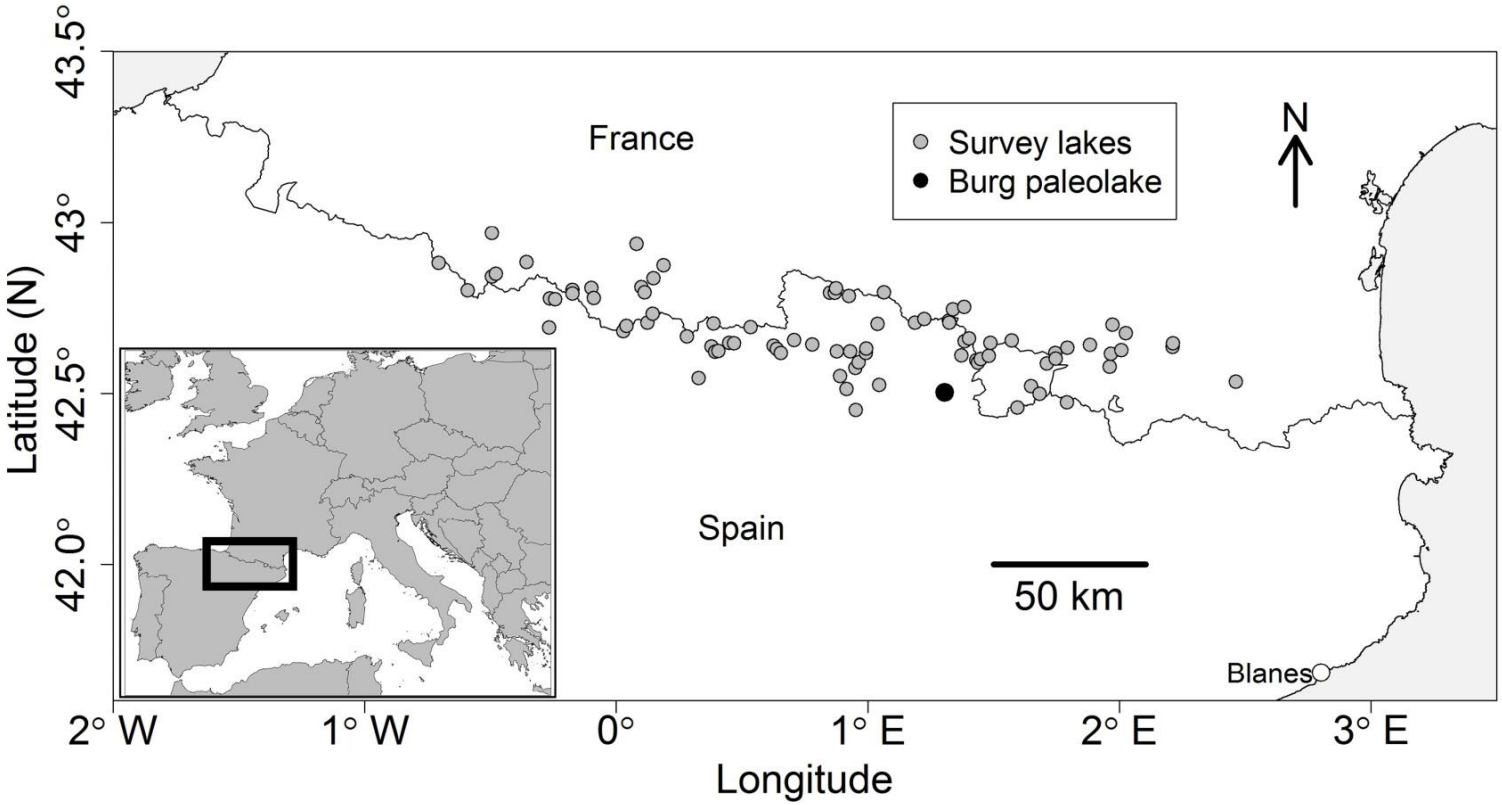

Figure 4.1. Map showing the location of the lakes included in the survey and Burg Lake.

Table 2. List of the lakes studied.

Lake code	Sample code	Lake	Latitude (º N)	Longitude (º E)	Altitude (m.a.s.l.)	Catchment area (ha)	Lake area (ha)	Depth (m)
PY0001	PYR01	Acherito	42.88089	-0.70608	1875	56.9	5.7	20
PY0008	PYR03	Bersau	42.84062	-0.49454	2077	61.4	12.3	35
PY0019	PYR04	Roumassot	42.84925	-0.47815	1845	268.2	5.0	22
PY0044	PYR05	Ormiélas	42.8838	-0.35562	1974	110.7	2.8	9
PY0080	PYR08	Pondiellos sup.	42.77699	-0.26312	2745	63.1	4.7	10
PY0089	PYR09	Arnales	42.77503	-0.24231	2305	93.5	2.7	6.5
PY0154	PYR11	Arratille	42.80158	-0.17364	2247	296.4	5.8	9
PY0155	PYR12	Col d'Arratille	42.79104	-0.17274	2501	33.3	2.3	17
PY0074	PYR14	Asnos	42.6918	-0.26629	2060	121.6	6.8	6.8
PY0165	PYR15	Estom	42.80752	-0.09853	1804	1145.0	6.2	20
PY0172	PYR17	Glacé	42.7783	-0.08845	2571	77.6	6.2	23
PY0194	PYR18	Helado de Marboré	42.69659	0.04104	2592	95.7	14.6	31
PY0192	PYR19	Helado del Monte Perdido	42.68213	0.02771	2990	11.0	0.2	4.8
PY0228	PYR20	La Munia Sup.	42.70615	0.12499	2537	109.0	2.3	8.5
PY0201	PYR22	Bleu	42.93705	0.08174	1950	389.2	53.2	123
PY0209	PYR23	Tourrat	42.80998	0.09966	2636	116.1	9.0	23
PY0223	PYR24	Cap Long	42.7951	0.11305	2845	46.8	1.6	2.1
PY0243	PYR27	Les Laquettes 1	42.83592	0.14806	2085	139.0	6.6	10
PY0265	PYR28	Port Bielh	42.87417	0.18846	2290	172.4	15.6	14
PY0237	PYR29	Barroude Inf.	42.73264	0.14478	2377	97.8	9.7	9.5
PY0291	PYR30	Urdiceto	42.66672	0.2816	2378	105.1	30.2	24
PY0304	PYR31	Bachimala Sup.	42.7044	0.38761	2630	131.3	2.8	12
PY0294	PYR32	Basa de la Mora	42.54526	0.32771	1908	461.8	5.5	2.4
PY0363	PYR33	Lliterola	42.69367	0.5338	2734	174.3	10.6	44
PY0305	PYR40	Sen	42.62148	0.39312	2360	104.3	8.5	39
PY0309	PYR41	Chelau Sup.	42.62419	0.40667	2805	11.8	0.9	16
PY0323	PYR42	Posets	42.64681	0.4494	2550	97.7	5.9	33
PY0338	PYR43	Eriste	42.64646	0.46808	2411	539.8	3.8	21

Lake code	Sample code	Lake	Latitude (º N)	Longitude (º E)	Altitude (m.a.s.l.)	Catchment area (ha)	Lake area (ha)	Depth (m)
PY0299	PYR44	Pixón	42.63682	0.37986	2199	169.1	2.3	13.5
PY0413	PYR45	Puis	42.65542	0.7076	2056	151.3	3.9	19.5
PY0390	PYR46	Llosás	42.61766	0.65483	2480	334.2	4.2	32
PY0383	PYR47	Coronas	42.62997	0.63848	2740	194.4	5.1	12.5
PY0378	PYR49	Cregüeña	42.63867	0.6253	2640	340.3	44.7	100
PY0461	PYR52	Pica Palòmera	42.79377	0.86878	2308	68.9	4.9	10
PY0449	PYR53	Nere de Güèrri	42.79334	0.85029	2280	76.6	4.0	24
PY0520	PYR54	Montoliu	42.78467	0.92614	2375	122.7	11.2	16.5
PY0469	PYR55	Long de Liat	42.80655	0.87398	2140	176.8	27.1	32
PY0499	PYR56	Gran del Pessó	42.51264	0.91563	2493	114.6	9.2	38
PY0463	PYR57	Monges	42.62301	0.87701	2418	110.4	14.7	51
PY0477	PYR58	Llebreta	42.55083	0.89031	1620	5437.9	8.0	11.5
PY0553	PYR59	Llong	42.57431	0.95063	2000	1111.3	7.1	12.5
PY0609	PYR63	Gerber	42.63065	0.99471	2170	388.4	14.9	63
PY0569	PYR65	Gelat Bergús	42.59106	0.96331	2493	23.8	1.4	8.5
PY0605	PYR66	Illa	42.61836	0.99348	2452	32.3	2.1	18
PY0519	PYR69	Plan	42.62248	0.9307	2188	23.0	5.0	11
PY0665	PYR70	Gran de Mainera	42.52516	1.04585	2450	95.4	5.4	21
PY0549	PYR71	Filià	42.45122	0.95328	2140	147.6	1.4	5.5
PY0672	PYR72	Rond	42.7944	1.0645	1929	97.8	7.4	34
PY0663	PYR73	Airoto	42.70281	1.03922	2210	175.4	18.9	42
PY0779	PYR76	Baiau Superior	42.59627	1.43188	2480	111.6	7.9	22
PY0790	PYR77	Forcat Inf.	42.60074	1.44883	2631	38.6	1.9	28
PY0800	PYR78	Angonella de Mes Amunt	42.61015	1.48138	2440	107.4	1.9	5.6
PY0785	PYR79	Negre	42.58913	1.43826	2627	44.2	1.6	16
PY0705	PYR80	Mariola	42.71737	1.22434	2276	121.6	17.8	46
PY0752	PYR81	Garbet	42.7526	1.38299	1683	424.9	15.1	28
PY0730	PYR82	Aubé	42.74549	1.33801	2094	71.9	8.2	48
PY0722	PYR84	Senó	42.71203	1.32291	2130	200.8	5.9	12
PY0723	PYR85	Romedo de Dalt	42.70601	1.32465	2110	259.8	11.9	40
PY0805	PYR86	Mes amunt de Tristaina	42.64685	1.48741	2300	158.2	12.3	24

Lake code	Sample code	Lake	Latitude (º N)	Longitude (º E)	Altitude (m.a.s.l.)	Catchment area (ha)	Lake area (ha)	Depth (m)
PY0695	PYR87	Inferior de la Gallina	42.70618	1.18763	2270	249.4	4.6	19
PY0751	PYR89	Sotllo	42.652	1.38445	2346	463.4	5.7	10
PY0743	PYR92	Aixeus	42.61098	1.3718	2370	82.3	3.4	15.5
PY0831	PYR94	Blaou	42.655	1.57264	2350	100.7	16.8	60
PY0929	PYR96	Albe	42.61835	1.74514	2355	74.3	6.9	19
PY0956	PYR97	Compte	42.63366	1.79306	1726	1047.0	3.4	4.6
PY0759	PYR100	Pica	42.66079	1.4024	2880	19.1	0.6	8.6
PY0953	PYR101	Malniu	42.47378	1.79238	2250	128.2	5.5	13.5
PY0839	PYR102	Gran de la Pera	42.45818	1.59509	2350	137.3	2.6	6.3
PY0893	PYR103	Montmalús	42.49832	1.68263	2440	181.2	10.7	21
PY0867	PYR106	Ensangents Sup.	42.52134	1.64923	2550	71.5	2.6	7.8
PY1058	PYR108	Negre	42.63592	2.21141	2083	79.8	4.5	17.5
PY1039	PYR110	Gros de Camporrells	42.62583	2.00788	2255	361.7	4.8	17
PY1047	PYR111	Laurenti	42.67525	2.02582	1936	264.0	6.6	18.5
PY1012	PYR112	Bleu de Rabassoles	42.70038	1.97274	1920	45.8	4.4	7
PY1005	PYR113	Blau	42.61554	1.96708	2531	30.6	4.4	29
PY1002	PYR114	Trebens	42.5778	1.96255	2306	285.1	5.8	14
PY0968	PYR116	Aygue Longue	42.64189	1.88263	2076	56.1	6.6	13.5
PY1062	PYR119	L'Estagnol	42.53361	2.46276	2164	7.0	0.5	0.7
PY1059	PYR120	Estelat	42.64632	2.21351	2021	149.7	4.6	3.8
PY0013	PYR121	Montagnon	42.96846	-0.49387	2003	12.6	1.2	4.8
PY0910	PYR124	Canals Roges	42.58673	1.7118	2410	96.1	1.5	6.2
PY0931	PYR126	Siscar	42.6014	1.74718	2187	358.0	4.2	3.9
PY0423	REDOM	Redon	42.64208	0.77951	2235	152.8	24.1	73

The physical environment

Variables describing the physical environment such as temperature, ice cover duration, light environment and habitat substrate were considered. Water surface temperature was measured at the central part of each lake. Ice cover duration for the lakes was estimated according to Thompson et al. (2009).

The light environment was characterised using two different indicators of relative and absolute irradiance: the percentage of irradiance at the bottom of the lake and an estimation of the average irradiance during summer at the bottom (I_{Sb}).

The irradiance percentage at the bottom respect surface and the average intensity during summer were estimated using the equation:

$$I_{Zmax}=I_0 e^{-k\ Zmax} \qquad \text{E. 4.1}$$

where I_{zmax} is the intensity (or percentage) of light at the lake maximum depth (Z_{max}) and I_0 the intensity (or percentage) of light at the water surface. Average intensity of light at the water surface was taken as 690 µE/m^2/s, which is the average of PAR radiation incident in the Pyrenees during July (Catalan 1988). The light attenuation coefficient (k) was estimated as $1.7/Z_{SD}$ (Margalef 1983), where Z_{SD} is the Secchi disk depth .

Littoral substrate was characterised based on the relative cover of bedrock, rocks, sand, organic detritus and macrophytes. The habitat diversity was characterized using both the number of different substrates and e^H, where H is the Shannon-Wiener index (Magurran 2004) calculated using the relative abundance of substrates. The content of organic matter in the sediment was estimated by loss on ignition (LOI) according to Heiri et al. (2001).

Water chemistry

Water samples for chemical analyses were collected at the outflow of each lake. The analytical methods are described in Camarero et al. (2009). Measurements include pH, acid neutralizing capacity (ANC), conductivity, calcium, magnesium, sodium, potassium, sulphate, chloride, total phosphorus (TP), nitrate, ammonium, total nitrogen (TN) and total organic carbon (TOC). CO_2

concentration was calculated using pH, ANC, conductivity and temperature (Mackereth et al. 1978).

Diatom sampling

Two types of samples were collected at each lake simultaneously with the water chemistry survey: top sediment and epilithon. Top samples were collected in the deepest part of each lake using a gravity corer and slicing the upper 0.5 cm. Epilithon samples were collected by brushing five stones in the shoreline area. Stones were selected in areas between 0.3 and 1.0 meter depth. The samples were preserved using formaldehyde.

Burg Lake core

Burg Lake is located on the Southern Pyrenees at 1821 m, 42º 30´18" N, 1º 18´ 22" E (Figure 4.1). The lake is currently a shallow wetland that often dries out in summer (Figure 1.2). It originated during deglaciation behind a frontal moraine (Figure 4.3). The geomorphology, geology, and the presence of small spring and wet vegetation in the other site of the moraine, suggest that Burg Lake was a seepage lake before becoming a seasonal fen. The Burg valley bedrock includes Cambro-Ordovician black slates, limestone, sandstones and conglomerates covered by Silurian to Devonian slates, schists and limestone (Pèlachs et al. 2011).

Figure 4.2. Panoramic view of the Burg Lake (13/08/2009). Photo pointing W-E.

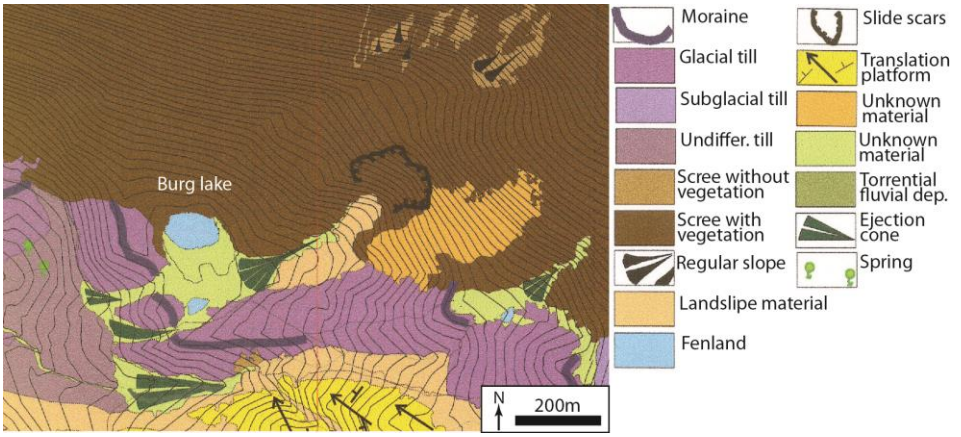

Figure 4.3. Geomorphological map of the Burg basin. Altitudinal isolines are plotted every 5 m. Adapted from Vizcaino (2003).

A geo-electrical prospection of the basin indicates that the maximum length and width of the former lake were 90 m and 75 m, respectively. The maximum lacustrine depth was around 15-16 m (Figure 4.4).

The lake is located in an area of both Mediterranean and Atlantic climatic influence. The current mean annual precipitation ranges from 700 to 1100 l m^{-2} yr^{-1} (Pèlachs et al. 2011). Mean annual temperature is 10.1 ºC at the base of the valley (900 m.a.s.l.) and -2.3 ºC at the highest point (2500 m.a.s.l.) (Ninyerola et al. 2000).

The present vegetation in the Burg valley includes *Pinus sylvestris* forest with patches of *Betula pendula*; shrublands of *Cytisus oromediterraneus* and *Juniperus communis* ssp. *alpina* and grasslands (Figure 4.2). The upper basin is mostly covered by *Pinus uncinata* forest (Pèlachs et al. 2011). The vegetation around the lake is distributed asymmetrically, forested in the northern part and with open vegetation southward.

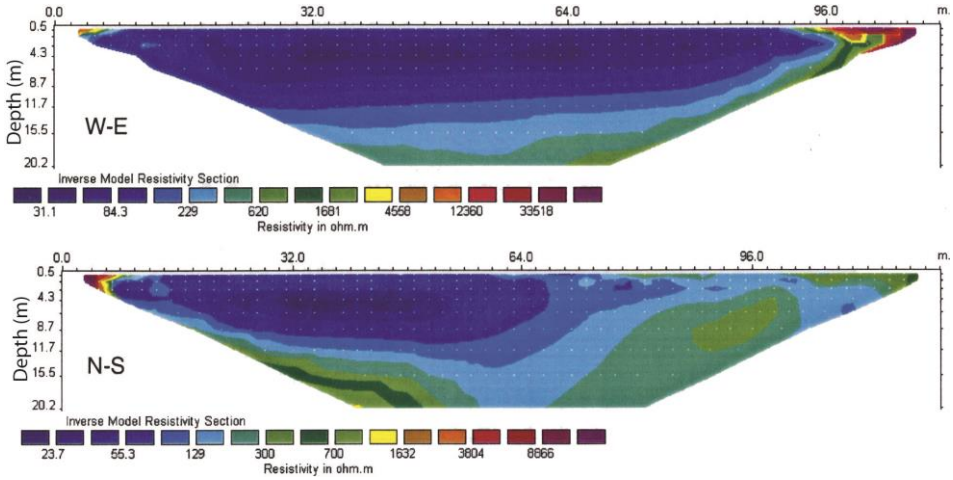

Figure 4.4. Geo-electrical prospection of the Burg Lake basin in two perpendicular sections (IGEOTEST 2001).

Burg Lake drilling

Drilling of the Burg Lake sediments was carried out using a Rolatec RL 48-L drill machine with 10 cm in diameter (Figure 4.5). Two sediment cores with a great lateral continuity of lithology were collected (CMB9: 0-215 cm and CMB8: 215-1441 cm). The record was sliced every centimetre. A set of 624 samples were analysed for this study. They correspond to those with preserved diatoms, mostly corresponding to the lake phase before the accumulation of peat to become a shallow wetland. The record showed five stratigraphic levels (Figure 4.6): from bottom to 1300 cm sediment was a heterometric gravel full of mud with high clay content; from 1300 to 525 cm a lacustrine silt; from 525 to 405 cm an organic silt; from 405 to 121 cm sediments corresponds to a peat, and from 121 to the top is a hydromorphic soil (Pèlachs et al. 2011). In this study, the section from 1330 cm to 642 cm was analysed.

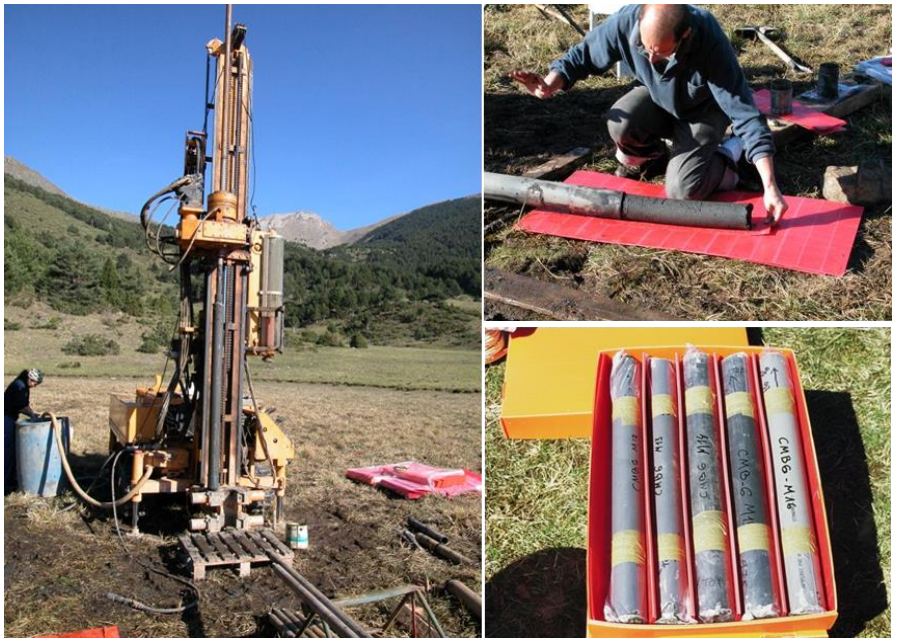

Figure 4.5. Drilling of Burg Lake (29/09/2006) and some examples of the cores recovered. Photographs provided by Albert Pèlachs.

Core age-depth modelling

Fifteen samples of the sequence were dated by NOSAMS and Beta-Analytic laboratories using the AMS radiocarbon method. The bottom of the sequence (1404 cm) was date at 19907 yr cal BP but the sequence was studied from the stratigraphic level 1330 cm (16,590 yr cal BP) to 642 cm (8694 yr cal BP) because it was the section with sufficient diatom density as indicated above.

The age-depth model was built applying a Bayesian approach using the Bacon software (Blaauw and Christeny 2011). The advantage of the model is that uses prior information of accumulation rates and their variability and autocorrelation over time (Blaauw and Christeny 2011). The core was divided into 282 contiguous segments (~5 cm). The age model was developed based on more than 30 million iterations. The shape parameter used was 1.3 and the initial mean of sedimentation was 20 yr cm^{-1}. A prior beta distribution with strength 5 and mean 0.4 was used. The model was built assuming a t-student distribution with wider tails for the ^{14}C dates (Christen and Pérez 2009). The model estimated the age for every centimetre between the bottom and the surface.

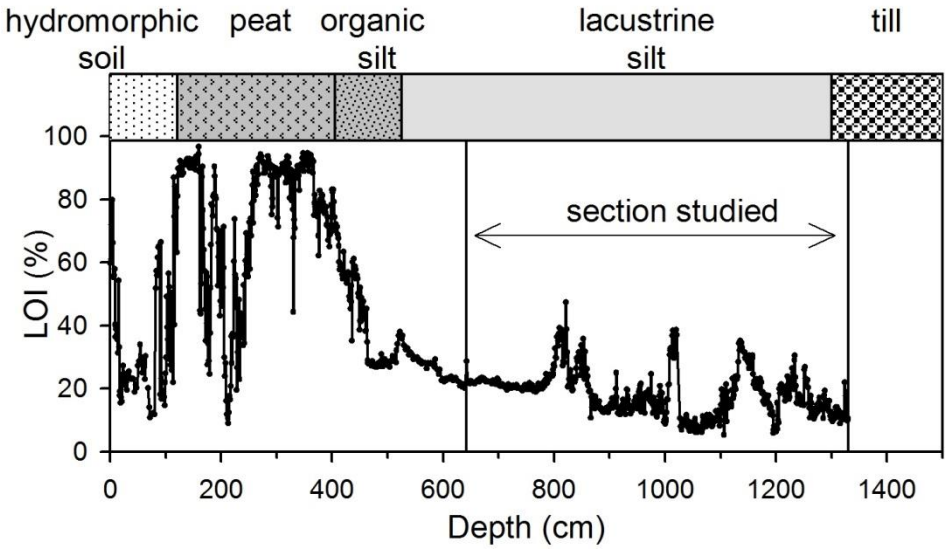

Figure 4.6. Stratigraphic levels and loss on ignition (LOI) of the Burg Lake record (CMB9: 0-215 cm and CMB8: 215-1441 cm). Adapted from Pèlachs et al. (2011).

Loss on ignition measurements

In addition to the study of diatoms some complementary measurements were made for a better interpretation of the record. The dry weight percentage of organic matter and carbonate content in the sediments of the Burg Lake was determined by means of loss on ignition (LOI) method following Heiri et al. (2001).

Approximately one gram of each sample was cold dried during 72 h in a lyophilizer. Samples were maintained in an oven during 24 h at 65 ºC and then organic matter was combusted at 550 ºC during four hours in a preheated furnace. The LOI at 550ºC (organic matter content) was calculated as:

$$LOI_{550} = \frac{W_I - W_{550}}{W_I} * 100 \qquad \text{E. 4.2}$$

Where LOI_{550} is the LOI at 550 ºC, W_I the dry weight of the sample before combustion and W_{550} the dry weight after heating to 550 ºC.

After this, samples were combusted at 950 ºC during two hours in a preheated furnace. The LOI at 950ºC (carbonate content) was calculated as:

$$LOI_{950} = \frac{W_{550} - W_{950}}{W_I} * 100 \qquad \text{E. 4.3}$$

Where LOI_{950} is the LOI at 950 ºC and W_{950} is the dry weight after heating to 950ºC.

In all cases the samples were equilibrated to the environmental temperature in a desiccator before weighing them in a Sartorius ME235s balance.

Specific density measurements

The specific density of each sample was estimated with a Gay-Lussac pycnometre using the following equation:

$$\rho_s = \frac{M_s}{M_s + M_a - M_b} * \rho_w \qquad \text{E. 4.4}$$

where ρ_s represent the density of the sample in g cm^{-3}, M_s is the weight of sample, M_a is the weight of the pycnometre filled with water only, M_b is the weight of pycnometre with the sample and filled with water, and ρ_w is the water density.

DRX analysis

Percentage composition of dominant minerals in the sediments was estimated by X-ray diffraction, which was performed using an automatic Siemens D-500 X-ray diffractometre in the following conditions: Cu kα, 40 kV, 30 mA, and graphite monochromator. To identify and estimate the proportion of the different mineralogical species present in the crystalline fraction a standard procedure was followed (Chung 1974). Data from this analysis were provided by Dr. Ramon Julià (Institut Jaume Almera, CSIC).

X-Ray Fluorescence analysis

X-Ray Fluorescence (XRF) measurements were carried out using the Avaatech XRF-Core Scanner of the Department of Stratigraphy, Paleontology and Marine Geosciences, University of Barcelona. XRF measurements were carried out every 3 mm and every section was passed twice: first with settings at 10 kV, 1800 µA 10 s, and secondly, at 30 kV, 2000 µA and 35 s.

Information about the presence of crevices, irregularities and relevant morphological characteristic of the core were annotated to discard problematic sections. Results are expressed as relative element intensities in counts per second (cps).

Subfossil photosynthetic pigments

The sediment samples were freeze dried and the pigments extracted from about 1 g sediment dry weight in 4 ml 90% acetone with a probe sonicator (Sonopuls GM70 Delft, The Netherlands) (50W, 2 min). The extract was centrifuged (4 min at 3000 rpm, 4 ^{o}C) and filtered through Whatman Anodisc 25 (0.1 µm) and analysed by ultraperformance liquid chromatography (UPLC). The UPLC system (Acquity, Waters, Milford, MA, U.S.A.) was equipped with an Acquity UPLC HSS C18 SB column (dimensions: 100 x 2.1 mm, particle size: 1.8 µm) and photodiode array (λ 300-800 nm) and fluorescence (λ excitation 440 nm, emission 660 nm) detectors. The detector was set at 440 and 660 nm for carotenoid and phorbin peak integration, respectively. After sample injection (4.5 µl), pigments were eluted by linear gradient from 100% solvent B (51 : 36 : 13 methanol : acetonitrile : MilliQ water, v/v/v 0.3 M ammonium acetate) to 75% B and 25% A (70 : 30 ethyl acetate : acetonitrile, v/v) for 3 min, followed by 0.45 min of isocratic hold at 75% B and 2 min of linear gradient to 99.9% solvent A. Initial conditions (100% B) were linearly recovered in 0.65 min. The flow rate was 0.7 ml min^{-1}. Pigments were identified checking retention times and absorption spectra against a library made based on commercial standard mixtures (DHI, PPS-MiX-1) and extracts from pure cultures of algae and bacteria.

Diatom analysis

Slide preparation

A total of 76 sediment and 78 epilithon samples from the lake survey, and 624 samples of the Burg Lake core were processed. Formaldehyde was removed from the lake survey samples before further processing: the sample was allowed to settle out during 48 hours by gravity, the supernatant liquid was decanted off and fresh Milli-Q water was added, the process was repeated four times. In the case of the Burg Lake samples, sediment lyophilised (15-25 mg) was placed directly in borosilicate tubes and rehydrated with one millilitre of Milli-Q water.

Thereafter, the samples were digested following an oxidative procedure that started by adding 0.3 ml 1N HCl and 5 ml 30% H_2O_2. The oxidation was initially performed in a water bath at room temperature to avoid out of control exothermic reactions in samples with high metal content. The temperature of the bath was gradually increased to 70-80ºC and the level of H_2O_2 was maintained until all the organic material was removed. In order to open the diatoms valves and make transparent some non-digested material, 1 ml 1N HCL were added. After digestion, residual dissolved chemicals were removed by the washing process described above until the sample pH reached 6.

In the case of Burg Lake samples, a known volume of microsphere solution was added (SERADYN® Uniform Latex Particle, diameter = 6.4 ±1.9 µm). The solution of microspheres was prepared with 3M concentration of KCl in order to obtain a homogeneous distribution of the microspheres. The concentration of microspheres was estimated using a Coulter® Multisizer II, counting the fraction of particles between 2.5 and 10 µm in diameter. The added solution volume to the samples was variable; it was adjusted trying to reach a proportion between diatom valves and microspheres as close as possible to 1:1. KCl was eventually removed washing as previously described.

Once the samples were cleaned, they were mounted in permanent slides. Samples were kept in an ultrasonic bath during five minutes in order to disperse diatoms. Thereafter, the diatom suspension was diluted to obtain a suitable solution. Afterwards, the solution was carefully dropped on a round glass cover slip. A big drop was added to assured that the cover slip margin was reached. The cover slips were kept undisturbed in dust-free conditions until they were completely dry (24-48 hours). Then, a drop of Naphrax (Brunel Microscopes LTD, refractive index = 1.74) was placed on glass slide set on a hotplate at 130

ºC and immediately the cover slip with the sample was inverted and put on the Naphrax drop. The slide was heated on a hotplate for 15 min to remove toluene.

Diatom counting

Diatom taxonomic determination and counting was made using a Zeiss Axio Imager A.1 differential interference contrast microscopy with a plan-apochromatic 100x objective. In some cases, diagnostic morphologic traits were studied using a field emission scanning electron microscopy Hitachi S-4100-FE. The determination was based firstly on general taxonomical studies of the diatoms of the Pyrenees (Carter 1970; Hustedt 1939) and European freshwater ecosystems (Hofmann et al. 2011; Krammer 2000, 2002, 2003; Krammer and Lange-Bertalot 1986, 1988, 1991a, b, 2004; Lange-Bertalot 2001; Lange-Bertalot et al. 2011; Lange-Bertalot et al. 2003; Lange-Bertalot and Metzeltin 1996; Levkov 2009; Werum and Lange-Bertalot 2004a), and, secondly, on a large number of papers and books on specific taxonomical updates and regional iconographies (Bukhtiyarova and Round 1996; Håkansson 2002; Houk 2003; Houk and Klee 2004; Houk et al. 2010; Krammer 1997a, b; Lange-Bertalot 1993, 1997; Lange-Bertalot and Krammer 1987, 1989; Reichardt 1997, 1999, 2007; Reichardt and Lange-Bertalot 1991; Van De Vijver et al. 2004). Professor Dr. Horst Lange-Bertalot kindly checked the species determination.

Specimens which resemble some known species but have differences in diagnostic traits were distinguished with "cf." Specimens with traits markedly different from the most similar species were operatively named using a combination of the name of the lake where they were found the first time and consecutive numbers, if necessary. They are likely new species or varieties.

A minimum of 1000 and 500 valves were counted from the survey lakes and Burg Lake samples, respectively. In the latter case, the microspheres were counted simultaneously. The ecological analyses were performed grouping some of the intraspecific varieties when they were difficult to distinguish, infrequent or the varieties showed a similar distribution.

Valve preservation analysis

Two quantitative indexes were applied to characterise the diatom preservation in the Burg Lake record: a dissolution index and a fragmentation index. Valve

dissolution was estimate using the Ryves et al. (2009) diatom dissolution index (DDI):

$$DDI = \frac{\sum_{s=1}^{4} n_s(S-1)}{N(S_{max}-1)} \quad \text{E. 4.5}$$

where *n* is the number of valves in state *S*, *N* is the total number of valves and S_{max} is the highest dissolution state that valves show in the assemblage. The index varies from 0 to 1, and 1 is obtained when all the valves in the sample show the highest dissolution state. Dissolution states vary from 1 to 4, being pristine valves assigned to state 1. In the state 2 are included those valves with an incipient dissolution that affect spines and a clear vision of the areolae at light microscopy. In the state 3 are included valves that show evident alteration of striae, e.g. areolae or alveoli look fused under light microscopy. Finally, the state 4 includes valves with a strong alteration of the valves; e.g., altered raphe may be present in addition to the damage of the striae structure (Figure 4.7). Examples of specimens with different stage of dissolution are shown in Figure 4.8.

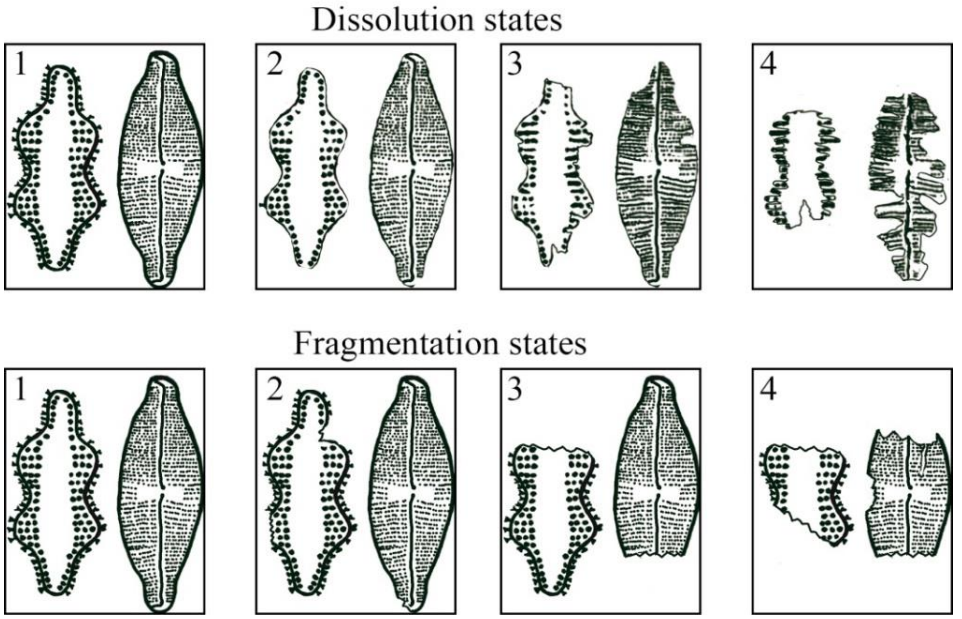

Figure 4.7. Classification states used to estimate the degree of the dissolution and fragmentation of the diatom valves.

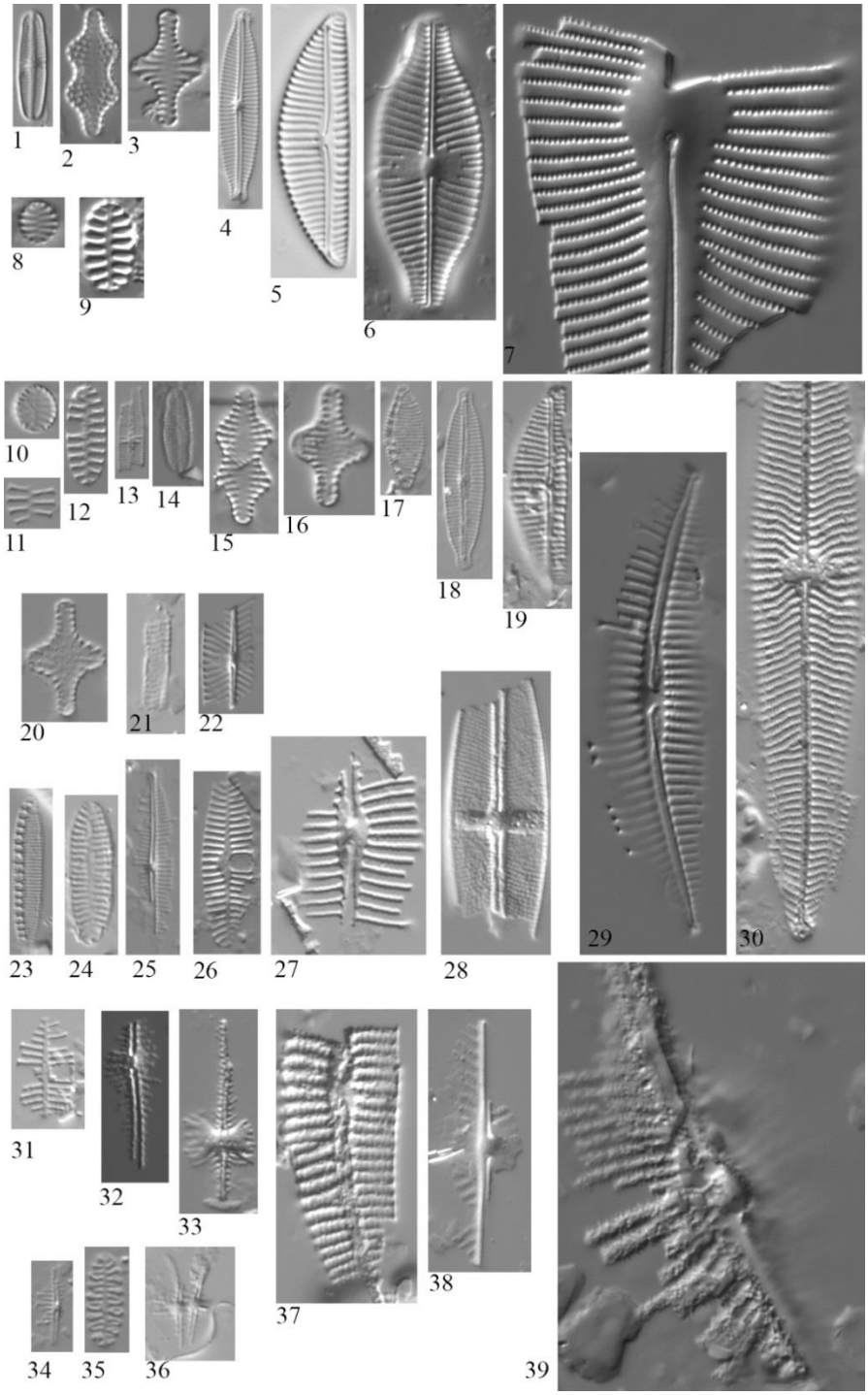

Figure 4.8. Specimens with different state of dissolution. 1-9: pristine valves (State 1), 10-19: State 2, 20-30: State 3, 31-39: State 4.

The fragmentation index (DFI) was quantified using the same equation than for DDI but changing the meaning of the states. In this case, intact valves were assigned to state 1; valves with only small breakage were assigned to state 2; valves with a unique large breakage were included in state 3; and valves with multiple damage were included in state 4 (Figure 4.7). The index varies from 0 to 1, and 1 is obtained when all valves show the highest fragmentation state.

Diatom assemblages in space (survey)

The exploration of the relationship between environment and diatom distribution in the survey lakes was performed at different levels of complexity with the ultimate goal of understanding the diatom assemblage change in the Burg Lake record. First, simple autoecological traits and indicative values of the individual species were evaluated. Second, transfer functions for some variables were developed.

Diatom assemblages and environment in the lake survey

The relationship between diatom assemblages and environmental variables was analysed through different complementary approaches: indicator species (IndVal), species ecological optima and tolerance, and species diversity patterns.

The survey lakes were classified according to their chemical characteristics. The lake classification was carried out using environmental groups and threshold values affecting algal distribution in freshwater ecosystems. Values and criteria used are supported by relevant literature and are described in the result section.

The occurrence of indicator species for these groups were assessed using the indicator value index (IndVal) calculated according to Dufrêne and Legendre (1997). Diatoms response to environment may not be completely captured by the lake grouping because the classification could not adequately represent the environmental preferences of the taxa. Therefore, the method of indicator species were complemented by calculating group-equalized indices for combinations of the initial groups (De Cáceres et al. 2010). The combination procedure creates new groups testing every possible combination of the initial groups. Group-equalized indices avoid the potential problem of unbalanced sampling as they give equal weights to all initial groups.

Bootstrap tests with 1000 permutation were used to test the statistical significance of the association between taxa and site-group or site-group

combinations. IndVal were calculated using the R language (R Development Core Team 2013) and package indicspecies v. 1.6.7 (De Cáceres and Legendre 2009).

Redundancy analyses (RDA) using the Hellinger distance were applied to examine species-environment relationships and determine which variables were relevant in explain the diatom distribution. Distribution optima and tolerances with respect to environmental variables were estimated using weighted averaging and weighted standard deviation (Oksanen et al. 1988).

Diatom diversity was characterised using taxa richness by sample and taxa-accumulation and sample-based rarefaction curves. Diversity indexes were calculated using the R language package vegan 2.0-8 (Oksanen et al. 2009). The relationship between taxa richness and potential explanatory variables were examined using generalized additive models (GAM). The more appropriate models were identified using Akaike`s information criterion (AIC) and deviation explained. Models were performed using the R language package mgcv 1.7-22 (Wood 2011).

Transfer function development

Redundancy analyses (RDA) using the Hellinger distance were applied to examine the species-environment relationship and determine which variables were candidates for reconstruction. The analysis was performed removing species with frequency <3% (Juggins and Birks 2012), transforming data to percentage, and removing variables with an inflation factor higher than 20%. Environmental variables were transformed (logarithmic or square root) to obtain a central distribution. Forward selection method with Monte-Carlo test (999 permutations) was used to select the environmental variables statistically explaining the composition and abundance of diatoms. The results of the model were analysed to recognize the principal environmental gradients explaining the distribution of diatom species and identify independent variables representing these gradients. Variation partitioning was carried out following Lepš and Šmilauer (2003) procedure.

Transfer functions were developed for the RDA selected variables using weighted averaging - partial least squares models (WA-PLS) and bootstrapping as cross-validation method (1000 permutations). WA-PLS was carried out deleting taxa in the training set with frequency lower than 3% and with taxa data

transformed using the square root of the percentage of abundance. Selection of the number of components were carried out following the recommendations of Juggins and Birks (2012) and using the van der Voet (1994) randomization t-test. The effect of spatial correlation on transfer functions was analysed using the Telford and Birks (2009) test.

Chrysophycean cyst- diatom ratio

Despite that some diatoms grow in the planktonic habitat and there are some rare benthonic chrysophyceae, in general, an assessment of the relative abundance of Chrysophycean cyst respect to diatom valves provides an indication of the relevance of planktonic processes in a shallow lake. To obtain some further insight into the meaning of the Chrysophycean cyst-diatom ratio (CD ratio) in mountain lakes, the ratio was estimated counting the cysts during the diatom counting until 500 diatom valves were achieved. The environmental significance of the CD ratio was explored by a canonical correspondence analysis (CCA) where environmental variables were constrained to be linearly related to the CD ratio. Then, the CD ratio relations with explanatory variables was further characterised using generalized additive models (GAM).

Diatom assemblages in time (Burg Lake record)

Temporal change characterization

The temporal changes of the diatom assemblages of Burg record were studied by means of diatom diversity, assemblage zonation, rate of change, and principal component analysis. Diatom diversity was characterised using species richness by sample and species-accumulation curves across the record. The zonation was carried out by a constrained incremental sum-of-squares cluster analysis technique – CONISS (Birks 2012; Grimm 1987), using the Euclidian distance and square root transformed data. The identification of species related to each CONISS zones was performed testing the association of each species to each zone using the indicator analysis describe above (De Cáceres et al. 2010).

The rate of change of the diatom assemblages was estimated calculating the Hellinger distance between consecutive samples and between samples separate every 50 yr. Principal component analysis (PCA) were performed using square root transformed data of the percentages, which result in applying an ordination based on a Hellinger distance instead of the common Euclidean distance. The number of likely significant components was assessed by comparing the variance explained by the axes and a broken stick model (Borcard et al. 2011). Analysis were carried out using R language packages vegan 2.0-8 (Oksanen et al. 2009) and rioja 0.8-4 (Juggins 2012).

Environmental reconstruction

The transfer functions developed were applied to the diatom sequence of Burg Lake. The reliability of the reconstructions was evaluated from three complementary perspectives: indicative species, statistical reliability, and functional sense. First, the reconstructions were compared with the fluctuations of the indicative species. Second, the reconstructions were compared with the principal components of the diatom assemblages and with randomly-generated environmental variables (using the test of Telford and Birks 2011b), and using cross-correlations at different time windows. Calculations were based on square root transformed abundances. Finally, the reconstructions were evaluated at the light of their functional coherence with independent indicators (e.g., elemental composition, pigments, etc.) of the biogeochemical processes.

Data smoothing and resampling

The Burg Lake sequence was sliced in sections of equal thickness (1 cm) that caused a different temporal resolution as accumulation rates varied along the core. This different temporal resolution compromises the comparisons of variability among zones. In order to minimise this constraint, a smoothing and resampling procedure was applied that approximated a time window of 50 yr throughout the core. Specifically, it was applied a temporally weighted average smoothing procedure (TWAS), which in the case of the diatoms and CD ratio data consisted in: 1) assigning an age to every sample according to age-model; 2) calculating the age difference between successive samples (Δt); 3) creating new samples repeating Δt times the diatom abundances of the youngest sample; 4) assigning an age to the new samples using a lineal interpolation between samples *n* and *n+1*; 5) smoothing the data recalculating the diatom abundance

for a centred window of size *w;* 6) moving the window every *k* units through the record repeating the step 5 every time; 7) calculating the environmental reconstruction (indicators, index, etc.) using the new diatom matrix.

In the case of other variables quantified (XRF, LOI) steps 1 and 2 were the same described above, followed by: 3) creating Δt new samples using a lineal interpolation of the respective variable between samples *n* and *n+1;* 4) assigning the age of new samples using a lineal interpolation between samples *n* and *n+1;* 5) smoothing the data calculating the mean of the variable for a centred window of size *w;* 6) moving the window every *k* units through the record repeating the step 5 every time.

In the age-model, the average Δt was 12.6±11 yr, consequently, 50 year was used as *w* and 1 year as *k*. Calculations were carried out using the age model with a resolution of 0.1 yr.

Results

Results

Part I

Diatom flora of the Pyrenean lakes

"El mundo era tan reciente, que muchas cosas carecían de nombre, y para mencionarlas había que señalarlas con el dedo"

Cien Años de Soledad, Gabriel García Márquez

"The world was so recent that many things lacked names, and in order to indicate them it was necessary to point"

5. Diatom composition

Diatom diversity is particularly high in oligotrophic environments similar to those of the Pyrenean lakes (Lange-Bertalot and Metzeltin 1996). Of the 1088 taxa recorded for the Iberian Peninsula, approximately 300 are registered in the Spanish Pyrenean provinces and Andorra (Aboal et al. 2003). However, monographic works about the diatoms of the Pyrenees are scarce and outdated (Carter 1970; Hustedt 1939). The actual number of taxa is expected to be much higher than up to now reported and taxa not yet described are likely to be found. The progression in the description of new species in European freshwater ecosystems (Table 3) suggests a large unknown diversity in remote and oligotrophic environments. Even for Central European freshwater ecosystems that have been studied extensively, recent taxonomical investigations continue describing new taxa. The taxonomical revision of some genera in Europa has followed the same pattern (Table 3).

Table 3. New taxa described in recent taxonomical monographs using type specimens of European localities.

Taxa	Group/genera/Geographical emphasis	Reference
11	Centrales, Fragilariaceae, Eunotiaceae	Krammer and Lange-Bertalot (1991b)
19	Achnanthaceae	Krammer and Lange-Bertalot (1991a)
55	Oligotrophic lakes	Lange-Bertalot and Metzeltin (1996)
61	*Encyonema*, *Encyonopsis*, *Cymbellopsis*	Krammer (1997a, b)
23	Central Europe	Lange-Bertalot (1993)
23	*Gomphonema*	Reichardt (1999)
30	*Navicula*	Lange-Bertalot (2001)
59	*Cymbella*	Krammer (2002)
76	Sardinia	Lange-Bertalot et al. (2003)
53	*Cymbopleura* and others	Krammer (2003)
36	Springs of Central Europe	Werum and Lange-Bertalot (2004b)
79	*Amphora*	Levkov (2009)
54	*Eunotia*	Lange-Bertalot et al. (2011)

Some authors argue that the most important limitation in quantitative palaeo-environmental reconstructions is the taxonomic quality and accuracy of environmental variables measurements in modern training sets (Birks 1994), despite that generally discussion tends to focus in statistical aspects (Anderson 2000; Juggins 2013). In fact, models used to reconstruct nutrients and major-ions content show a better performance the higher the taxonomical resolution is (Rimet and Bouchez 2012). Consequently, the aim of this part of the study was to revise, update and enlarge the identification of the diatom taxa found in the Pyrenean lakes. In appendix 1 there is an exhaustive documentation of the taxa considered, in this chapter.

General description of the diatom flora

A total of 73 genera were found in the lakes studied: 70 in the survey lakes and 58 in the Burg core, respectively. The most diverse genera included *Pinnularia* (40 taxa), *Gomphonema* (39), *Eunotia* (35), *Nitzschia* (32), *Navicula* (27), *Naviculadicta* (24), *Encyonema* (22) and *Fragilaria* (19). Considering exclusively the survey lakes, the ranking was similar: *Eunotia* (34 taxa), *Gomphonema* (31), *Pinnularia* (31), *Nitzschia* (30), *Navicula* (23), *Naviculadicta* (22), *Encyonema* (20) and *Fragilaria* (18).

Diatoms were grouped by shape into 11 artificial (not strictly evolutionary) types (Figure 5.1). The morphological types with the highest number of taxa were Naviculoid, Monoraphid and Cymbelloid, respectively. The types with the lowest number were Epithemioid, Surirelloid and Centric. This pattern was the same for the epilithon, sediment and Burg Lake sample sets.

The total taxa (species and infraspecies taxa) distinguished were 549: 477 in the lake survey and 244 in the Burg Lake (Figure 5.2). In the lake survey, the sediment samples showed higher number of taxa (417) than the epilithon samples (355). 121 and 59 taxa were exclusive of the sediment and epilithon samples, respectively. The Burg Lake sequence had 23% (57) taxa not present in the survey, which indicate the unusual character of this lake within the present context of the Pyrenean lakes.

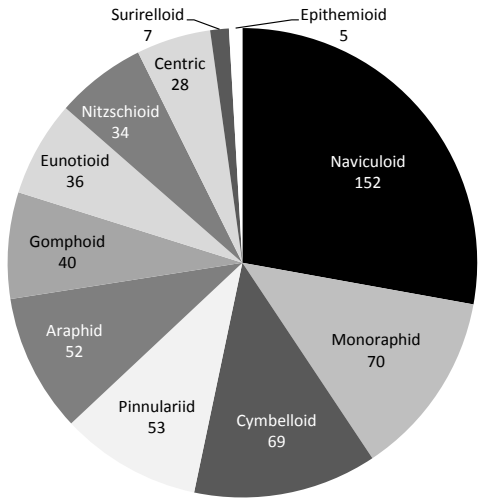

Figure 5.1. Taxa distribution into morphological types.

There were a 12% of taxa with frequency >10%, which were exclusive of epilithon samples, among them: *Encyonema* sp. No. 10 Burg, *Achnanthes* sp. No. 8 Angonella, *Krasskella kriegerana* (Krasske) Ross & Sims, *Eunotia tenella* (Grunow) Hustedt, *Nitzschia* cf. *inconspicua* Grunow, *Nitzschia* sp. No. 15 Burg and *Sellaphora stroemii* (Hustedt) Kobayasi. Sediment samples showed a 20% of exclusive taxa, among them: *Sellaphora pseudopupula* (Krasske) Lange-Bertalot, *Fragilaria* sp. No. 1 Airoto, *Navicula venerablis* Hohn & Hellerman, *Encyonema* sp. No. 1 Mora, *Navicula cryptocephala* Kützing, *Pinnularia* cf. *rumrichae* Krammer, *Geissleria similis* (Krasske) Lange-Bertalot & Metzeltin, *Cymbopleura subaequalis* (Grunow) Krammer, *Navicula trophicatrix* Lange-Bertalot, *Surirella angusta* Kützing, *Meridion circulare* var. *constrictum* (Ralfs) Van Heurck and *Stauroneis gracilis* Ehrenberg.

There were many taxa more frequent in epilithon samples than in sediment. The most frequent species in the epilithon were: *Encyonopsis* cf. *krammeri* Reichardt, *Navicula notha* Wallace, *Pinnularia subinterrupta* Krammer & Schroeter, *Nitzschia* cf. *alpina* Hustedt, *Encyonopsis minuta* Krammer et Reichardt, *Eunotia glacialis* Meister, *Encyonema reichardtii* (Krammer) Mann, *Cymbella* cf. *neocistula* Krammer, *Cymbella* cf. *cymbiformis* Agardh, *Eunotia novaisiae* var. *altopyrenaica* Lange-Bertalot & Rivera-Rondón, *Gomphonema capitatum* Ehrenberg, *Delicata delicatula* (Kützing) Krammer, *Reimeria sinuata* (Gregory) Kociolek & Stoermer, and *Cymbella parva* (Smith) Kirchner.

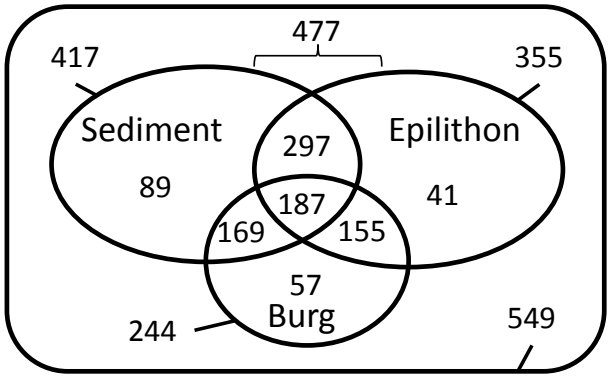

Figure 5.2. Total, coincident and exclusive taxa found in the lake survey set (sediment and epilithon) and Burg Lake samples.

Representative taxa of the sediment samples with low presence in the epilithon samples were: *Navicula opportuna* Hustedt, *Nitzschia garrensis* Hustedt, *Caloneis* sp. No. 2 Posets, *Sellaphora disjuncta* (Hustedt) Mann, *Diploneis* cf. *puella* (Schumann) Cleve, *Nitzschia pura* Hustedt, *Cymbella excisa* Kützing, *Sellaphora laevissima* (Kützing) Mann, *Surirella* cf. *roba* Leclercq, *Stauroneis neohyalina* Lange-Bertalot & Krammer, *Pinnularia* cf. *brebissonii* var. *minuta* Krammer.

Commonness, dominance and richness

Genera with the highest richness of taxa did not correspond with those with the highest number of dominant taxa. The genus *Achnanthidium* was the most frequently dominant taxon both in sediment and epilithon samples (Figure 5.3), yet the sediment samples showed a higher variability in the dominant genus than epilithon samples.

Four species were the most frequently dominant in sediment samples: *Achnanthidium minutissimum* (Kützing) Czarnecki (13 lakes), *Discostella stelligera* (Cleve & Grunow) Houk & Klee (11 lakes), *Denticula tenuis* Kützing (4 lakes) and *Pseudostaurosira microstriata* (Marciniak) Flower (4 lakes). On the other hand, the most frequently dominant in epilithon samples were: *Achnanthidium minutissimum* (Kützing) Czarnecki (54 lakes), *Brachysira*

intermedia (Östrup) Lange-Bertalot (4 lakes), *Encyonema minutum* (Hilse) Mann (3 lakes) and *Psammothidium acidoclinatum* (Lange-Bertalot) Lange-Bertalot (3 lakes).

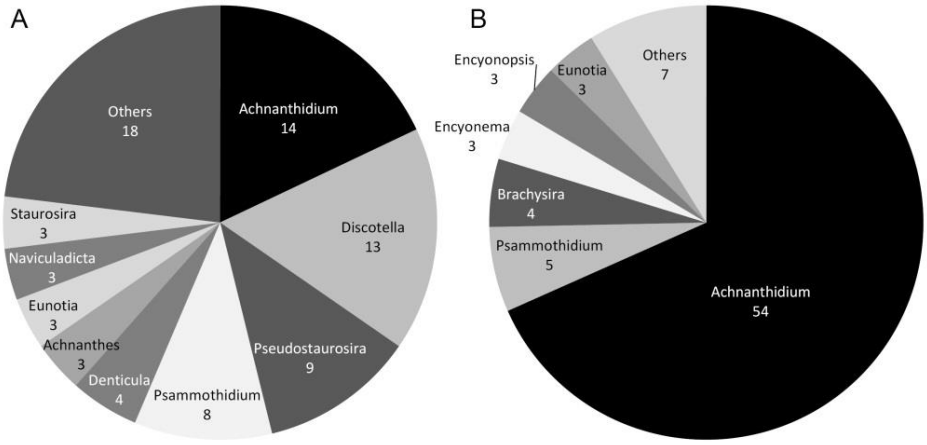

Figure 5.3. Dominant genera in sediment (A) and epilithon samples (B) of the survey lakes.

Rare species (frequency <3% and maximum abundance <3%) showed similar patterns in sediment and epilithon samples (Figure 5.4). The total of rare taxa was 93 (22%) in sediment samples and 113 (32%) in epilithon samples. Genera with the highest number of rare species approximately correspond with those with the highest species number: *Eunotia*, *Gomphonema*, *Encyonema* and *Pinnularia* in the sediment samples and *Gomphonema*, *Naviculadicta*, *Nitzschia*, *Pinnularia* and *Eunotia* in the epilithon samples.

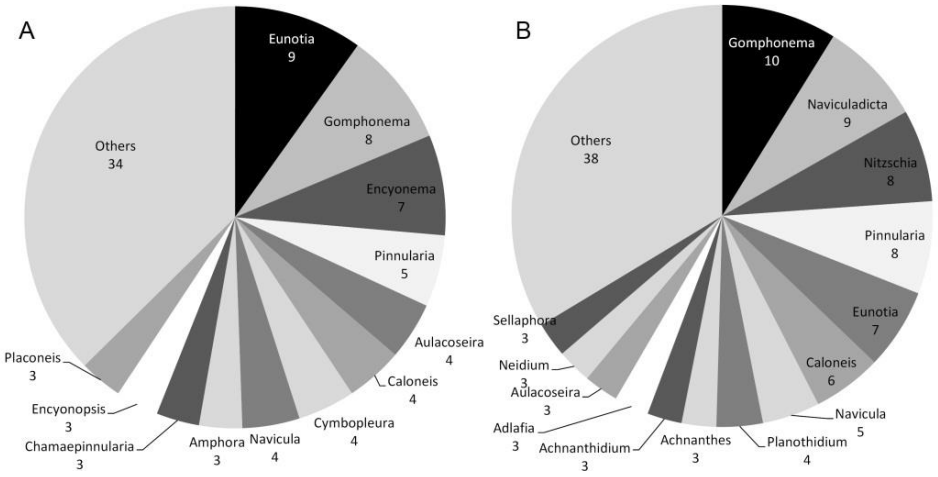

Figure 5.4. Rare taxa (frequency <3% and maximum abundance <3%) per genus in the sediment (A) and epilithon (B) samples.

The frequency of the diatom abundance in the whole training set followed a logarithmic decay and in most cases the species abundance was <2% (Figure 5.5). This pattern reflects the high number of rare species in both samples sets and suggests that there are many rare diatom taxa that persist in the Pyrenean lakes.

The relative abundance of the most dominant taxon in each sample showed a mean value of 33% in the sediment samples and 51% in the epilithon samples (Figure 5.6). There was a rapid change in the abundance of second dominant taxon in epilithon samples with respect to sediment samples, but the third most abundant taxon showed similar abundance both in sediment (9%) and epilithon samples (8%).

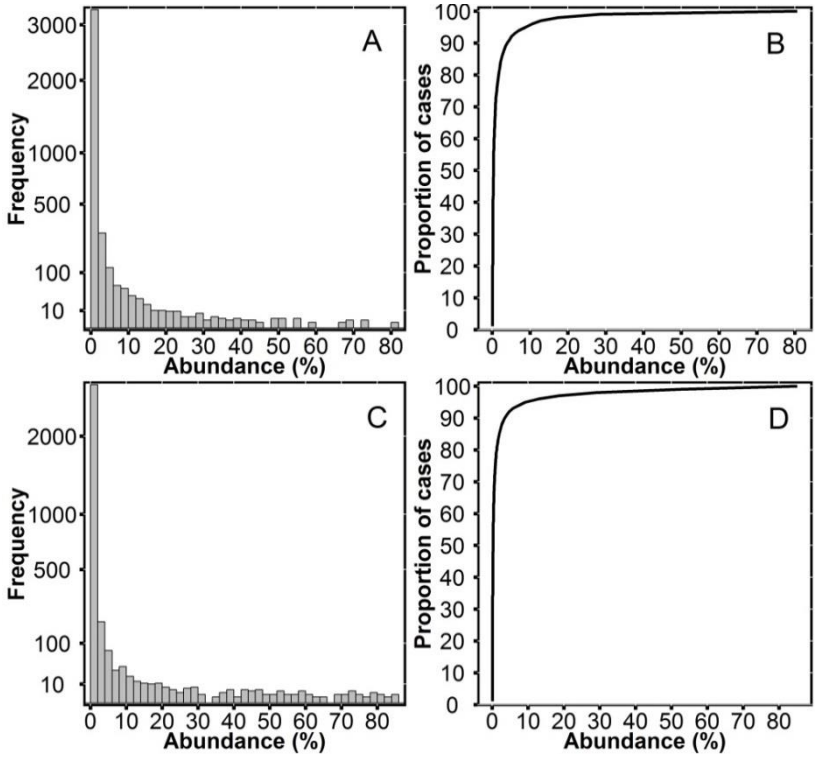

Figure 5.5. A. Frequency of the diatom abundance in whole training set and cumulative distribution of abundance for sediment (A, B) and epilithon (C, D) samples.

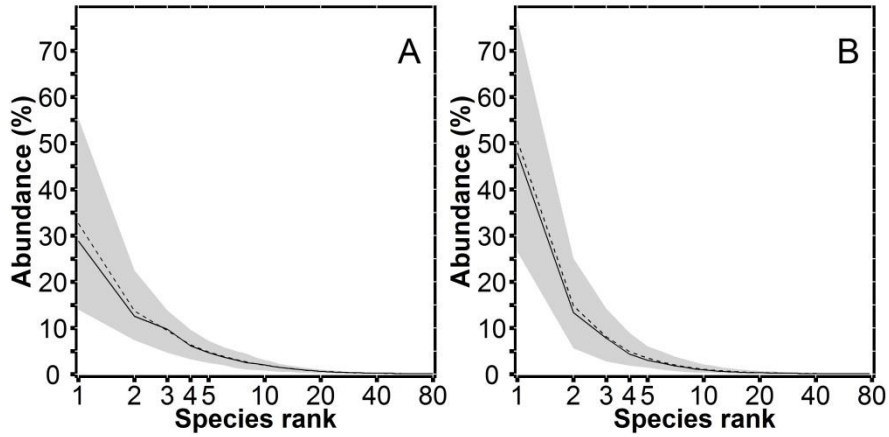

Figure 5.6. Rank-abundace plot for the raining-sets. Median (black line), mean (dashed line) and interval between 10 and 90 percentiles (shade area) of rank curves for the A) sediment (n=76) and B) epilithon (n=78) samples.

The species-accumulation curves showed a similar behaviour in both sample sets. The curves showed a rapid increase in the number of taxa in the range of 20-30 lakes (Figure 5.7). Richness estimators, such as Chao, Jack-knife, and Bootstrapping (Colwell and Coddington 1995) indicated that expected taxa richness could be between 445 and 479 in sediments and 387-432 in the epilithon. Taking into account that sediment and epilithon taxa richness were 417 and 355, respectively, the sampling and counting procedure may have underestimated between 7 and 15% of taxa richness in the sediment and between 8 and 21% in the epilithon.

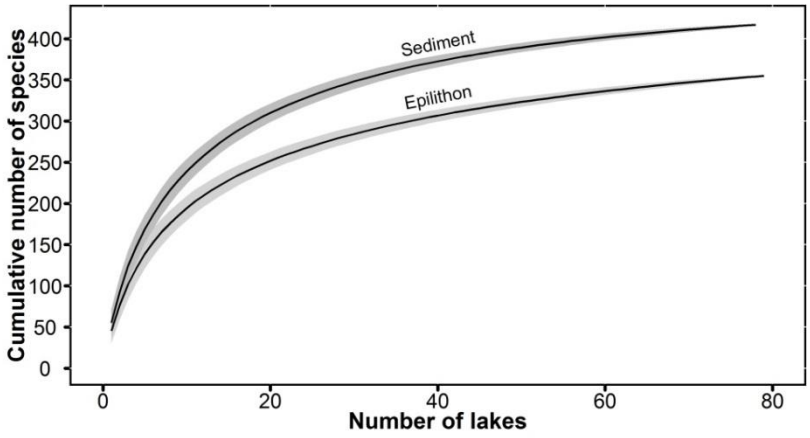

Figure 5.7. Comparison of the species-accumulation curves between sediment and epilithon samples. Shade areas correspond to one standard deviation.

Taxonomical remarks

The full list and images of the diatom taxa found in this study are compiled in the appendix at the end of the main text. 25% of taxa found were not determined as known species, which means that 140 taxa require an additional taxonomic effort and could be species or varieties not described yet. Among the most diverse genera, those with less species determined were *Pinnularia* (44%) *Gomphonema* (39%), *Nitzschia* (38%) and non-*Navicula* naviculoid diatoms (36%). Genera with low diversity but also with low species identification were *Stauroneis* (60%) and *Caloneis* (41%). Therefore, there is a large potential for diatom taxonomic studies in the Pyrenees. In fact, some of the species determined have not described until recently (Cantonati and Lange-Bertalot

2011; Lange-Bertalot et al. 2011) and correspond to intensely studied genus such as *Eunotia*, which represents 20% of the diatom European flora: *Eunotia neocompacta* var. *vixcompacta* Lange-Bertalot (Plate 33, figs.15-19), *Eunotia catalana* Lange-Bertalot & Rivera-Rondón (Plate 24, figs.1-12), *Eunotia novaisiae* Lange-Bertalot & Luc Ector (Plate 30, figs.1-10), *Eunotia novaisiae* var. *altopyrenaica* Lange-Bertalot & Rivera-Rondón (Plate 30, figs.12-39), *Eunotia fallacoides* Lange-Bertalot & Cantonati (Plate 35, fig.11). Another recently described taxa *Fragilaria* cf. *pararumpens* Lange-Bertalot, Hofmann & Werum, is common in the Pyrenean lakes and Central Europe (Hofmann et al. 2011).

Despite that some genera were studied thoroughly, there were many cases of problematic identification. For example, some *Eunotia* specimens of a strongly acid lake showed morphological traits between *E. pseudogroenlandica* Lange-Bertalot & Tagliaventi and *E. botuliformis* Wild, Nörpel & Lange-Bertalot (Plate 31). Similarly, there were common widespread morphotypes showing mixed traits, this is the case for an *Encyonema* showing traits of *E. minutum* (Hilse) Mann and *E. ventricosum* (Kützing) Grunow (Plate 105, figs. 14-31). Some small *Nitzschia* specimens presented the same problems (Plate 117, figs. 7-15), even when SEM images were compared.

Results

Part II

Environment and diatom distribution

6. ANC-pH gradient

The regional distribution of diatoms is mostly explained by pH and acid neutralising capacity (ANC) gradients in alpine and temperate areas (Chen et al. 2008; Koster et al. 2004; Siver 1999). Diatoms show a segregation of the species distribution through the pH gradient also in the Pyrenees (Catalan et al. 2009c). The primary influence of pH on diatom growth relates to the availability of CO_2 (Reynolds 2006). However, a variety of species can use HCO_3^- as carbon source (Wilhelm et al. 2006) and there is an large number of diatom species able to grow in alkaline conditions (Cremer et al. 2004; Reavie and Smol 2001; Schmidt et al. 2004).

Silification is another process in which pH can affect diatoms. Valve formation occurs under acid conditions in the silicon deposition vesicle (Vrieling et al. 1999). Silicon biomineralization in diatom depends on environmental pH; external pH controls intracellular diatom pH affecting the grade of the silica deposition, the morphogenesis process and the valve pattern (Hervé et al. 2012). On the other hand, high dissolution of diatom valves is expected at high pH as a consequence of ionic dissociation. Diatom species show different resistance to dissolution depending on form, size and valve silification (Barker et al. 1994; Ryves et al. 2006; Ryves et al. 2001).

The strong connection of the diatom distributions with pH has been applied to the study of regional and temporal acidification processes (Battarbee and Charles 1986; Birks and Simpson 2013; Charles et al. 1986). Despite evidences supporting that most of the diatoms have a statistically significant relationship with pH and that most of the diatoms are pH specialist (Telford et al. 2006), the actual ecological response of species seems to change regionally (Juggins and Birks 2012). Developing training sets for the same types of lakes and geographical region where fossil material has to be analysed increases the reliability of the transfer functions. In this section, the aim was to identify indicator species of the ANC-pH gradient within the chemical variability of the Pyrenean lakes. This gradient is largely non-linear and a detailed investigation of the species distribution throughout it may be useful for understanding changes in the diatom palaeo-sequences in the Pyrenees beyond quantitative reconstructions.

Diatom distribution in the ANC–pH gradient

A simple way to check whether diatom species show some tendency within an environmental gradient is to compare the mean value of the variable (e.g. pH) in the lakes in which the species appears against the expected value of a random selection of the same number of lakes (Figure 6.1). This procedure do not considers abundance, but is a first indication of a non-random distribution of the species across a gradient. In the Pyrenean lakes, the diatom distribution with respect to pH differ for many species from that expected from a random normal distribution: 26% of species were outside of the range mean±2SD and 55.6% species were outside of mean±1SD (Figure 6.1A). For ANC, the result was similar: 25.4% of species out of the mean±2SD and 60.4% out of the mean±1SD (Figure 6.1B). The results were different for other variables relate with the ionic composition such as SO_4^{2-} and Mg^{2+}, Na^{+}. For SO_4^{2-}, a 6.5% of species were outside of the mean±2SD and 25% were out of the mean±1SD. For Mg^{2+} an 8.4% of species were outside of the mean±2SD and 30.7% were out of the mean±1SD. Therefore, there is fundamental evidence that diatom species do not distribute randomly respect the ANC-pH gradient in the Pyrenean lakes.

For the most common species, which by definition are present in a large number of lakes, deviation from random distribution is better shown when considering not only occurrence but also abundance. The comparison of the optima of the species (calculated as the species abundance weighted average of the variable) respect the distribution (e.g. boxplot) of the variable in the sites where the species occur provides an indication of the preference (or competitive ability) of the species for certain subsets of its occurrence range (Figure 6.2). There were many species with optima outside of its 50% of pH distribution (Figure 6.2A). These species were found principally at both ends of pH gradient but also occurred along the gradient.

Some species of broad distribution show a well-defined unimodal distribution around the optimum (*Achnanthidium minutissimum*, Figure 6.3A; *Psammothidium helveticum* Figure 6.3C). However, in other cases, rather than a unimodal distribution the species showed a threshold value beyond which the abundance is always low, either towards low pH values (e.g., *Staurosirella pinnata*, Figure 6.3D) or towards high ones (*Neidium alpinum*, Figure 6.3B).

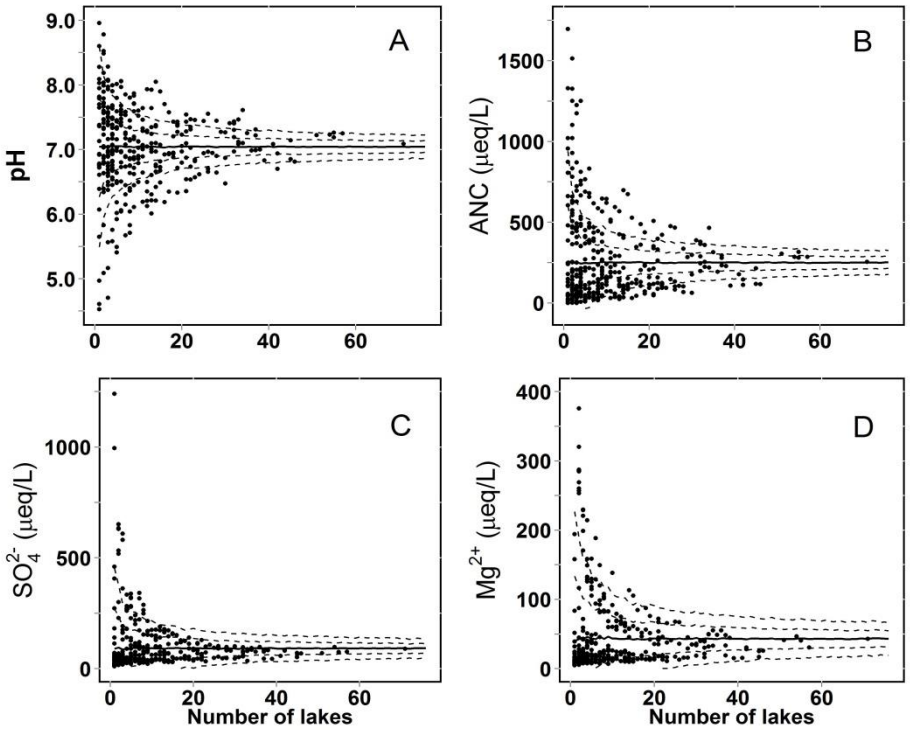

Figure 6.1. Average pH (A), acid-neutralising capacity-ANC (B), SO_4^{2-} (C), and Mg^{2+} (D) of the lakes in which a diatom species was present (dots) with respect to the mean for a random number of lakes of the survey lake (solid line). Dashed lines correspond to one and two standard deviation of the mean. Species n=381.

The range of species distribution is generally broad, even for species at the extremes of the pH range. This may be due to a high tolerance, but also to the taphonomic character that the top sediment has. The species may grow in certain microenvironments within the lake, which substantially differ from the conditions in open waters in which the chemicals were measured. For instance, species with an acidic optimum showed a range of distribution covering from the more acid lakes to pH 7.2 (e.g. *Stenopterobia delicatissima* (Lewis) Van Heurck, *Eunotia novaisiae* Lange-Bertalot & Luc Ector, *Psammothidium acidoclinatum*, *Neidium alpinum*, Figure 6.3B). Likewise, there were species which preferred lakes with pH >6.0, but which were found also in highly acid lakes (e.g. *Gomphonema auritum* Braun, *Psammothidium helveticum* Figure 6.3C). And there were species with circum-neutral or high pH optima appearing from pH >8.0 to weakly acid environments (e.g. *Amphora pediculus* (Kützing) Grunow, *Nitzschia* sp. No. 1 Sen, *Staurosirella pinnata*, Figure 6.3D). The broad

occurrence of many species combined with its well-defined optimum provides the basis for fine-tuning pH reconstructions.

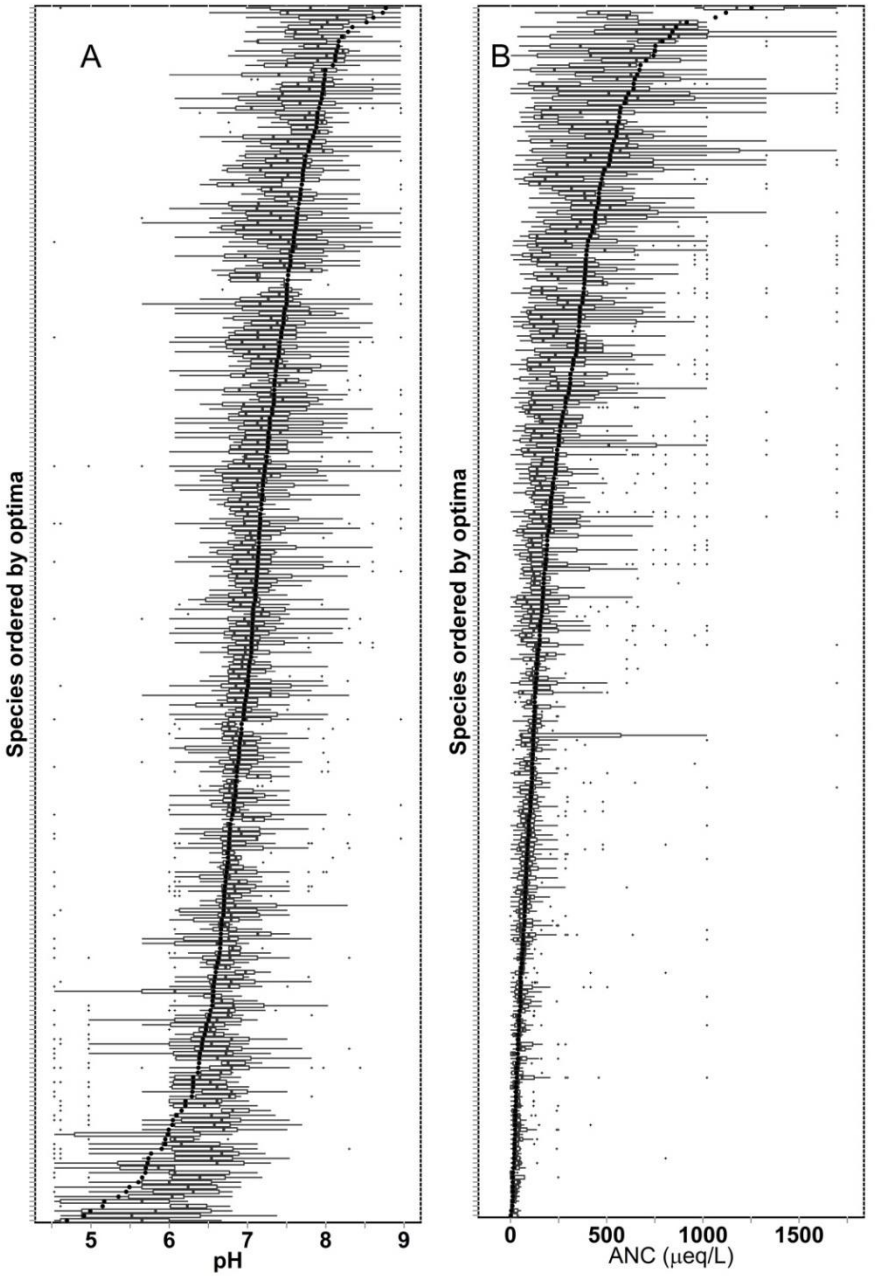

Figure 6.2. Optimum (dark points) and range distribution (boxplot) of the diatom species of the Pyrenean lakes (frequency >3 lakes) for pH (A) and acid-neutralizing capacity-ANC (B) based on top sediment samples. Small crosses indicate isolated extreme values.

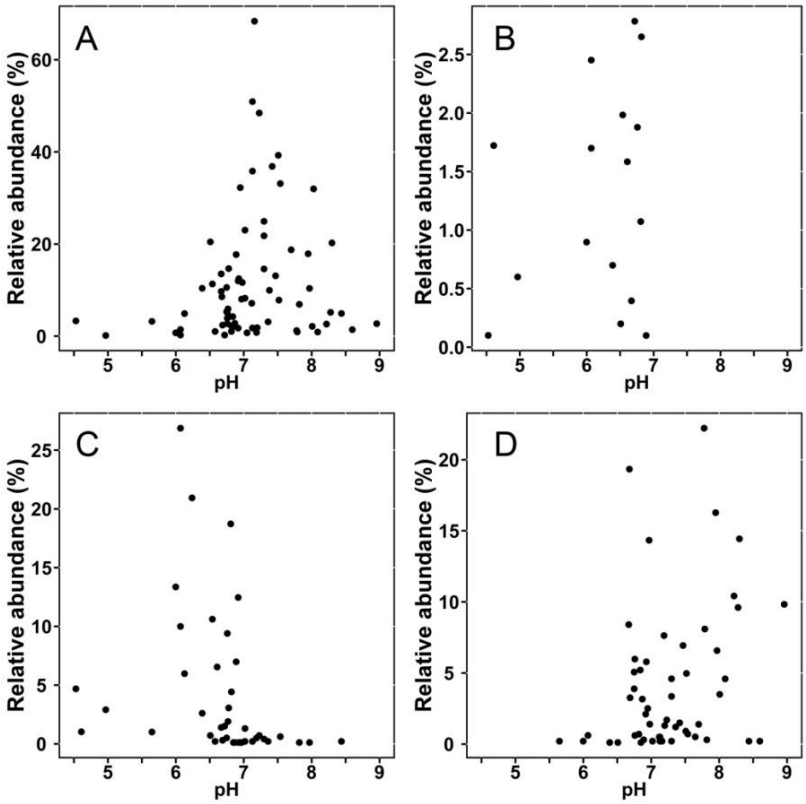

Figure 6.3. Relative abundance of *Achnanthidium minutissimum* (A), *Neidium alpinum* (B), *Psammothidium helveticum* (C) and *Staurosirella pinnata* (D) across the pH gradient.

The distribution patterns along the ANC gradient differ from those observed for pH (Figure 6.2B). In the lower end, the range of the distributions where narrow around the optimum (e.g. *Navicula schmassmanni* Figure 6.4A), whereas species with the optimum in the alkaline range tend to present a broad ANC distribution (e.g. *Cymbella parva* (Smith) Kirchner, *Encyonopsis microcephala* (Grunow) Krammer, Figure 6.4B). This implies some survival restriction for the species in the low ANC that are not present in those with optimum in alkaline conditions. The differential response respect pH and ANC has been suggested as the basis for a complementary reconstruction of pH and ANC from the same diatom palaeo-sequence (Catalan et al. 2009c).

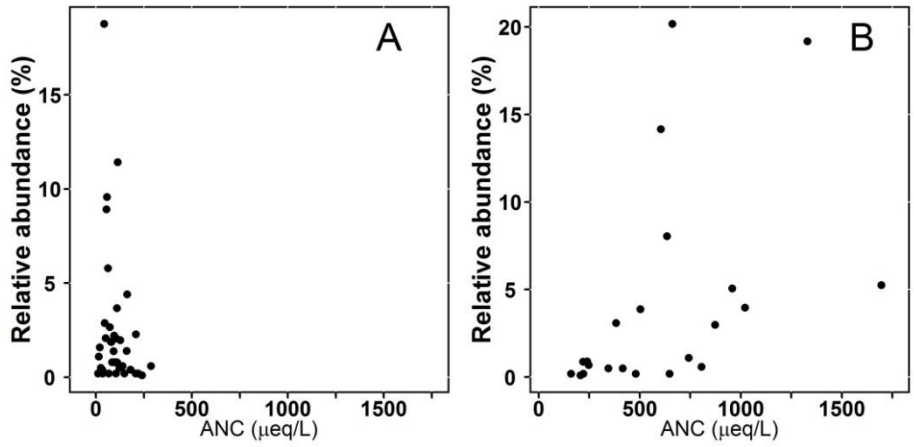

Figure 6.4. Relative abundance of *Navicula schmassmanni* (A), *Encyonopsis microcephala* (Grunow) Krammer (B) in the acid neutralizing capacity range.

ANC-pH classification of the Pyrenean lakes

The ANC-pH conditions of the Pyrenean lakes largely respond to the bedrock nature (Catalan et al. 1993). Fundamentally, there is an interplay between rocks scarcely weatherable (e.g., granodiorite), rocks rich in sulphides (e.g., some slates and schists), which afford acidity (SO_4^{2-}), and carbonate rocks (limestone), which supply buffering capacity (Ca^{2+}). Therefore, the variability in ANC-pH conditions in the Pyrenees can be classified taking into account the Ca^{2+} and SO_4^{2-} content (Camarero et al. 2009). Here, another class has been added to the six classes defined by Camarero et al. (2009), pH<5.5 and SO_4^{2-} >50 μeq/L, in order to further distinguish the highly acidic lakes (Table 4). A plot of SO_4^{2-} and pH shows the distribution of the studied lakes into the classes (Figure 6.5).

The circumneutral condition is the most common among the Pyrenean lakes. A 67% of the studied lakes presented a SO_4^{2-} <50 μeq/L and 88% presented a pH >6.5. A lack of lakes with pH below 5.5 and SO_4^{2-} <50 μeq/L indicates that acidity is always due to sulphide oxidation and organic acidity is irrelevant in these mountains lakes, in contrast to Nordic and Scottish lakes, for instance (Catalan et al. 2009b).

Table 4. Classification of Pyrenean lakes from concentration of SO_4^{2-} and Ca^{2+}. Modified from Camarero et al. (2009).

Class	SO_4^{2-} (µeq/L)	Ca^{2+} (µeq/L)	pH
1	<50	<50	5.50-6.50
2		50-200	6.50-7.25
3		>200	>7.25
4	>50	<50	5.50-6.50
5		50-200	6.50-7.25
6		>200	>7.25
7	>50	---	<5.50

The Pyrenean lakes show a broad ANC range (Figure 6.6A). The relation between log-transformed ANC and pH shows a lineal trend with a higher dispersion when values increase, lakes with pH between 7.5 and 8.9 show ANC between 500 and 1000 µeq/L.

The concentration of CO_2 was higher in circumneutral lakes and presented the lowest values in the lakes at both ends of the pH gradient (Figure 6.6B). Accordingly, lakes in class 2 and 3 showed the highest variability of CO_2 concentration, while lakes in class 7 showed the lowest free carbon concentration.

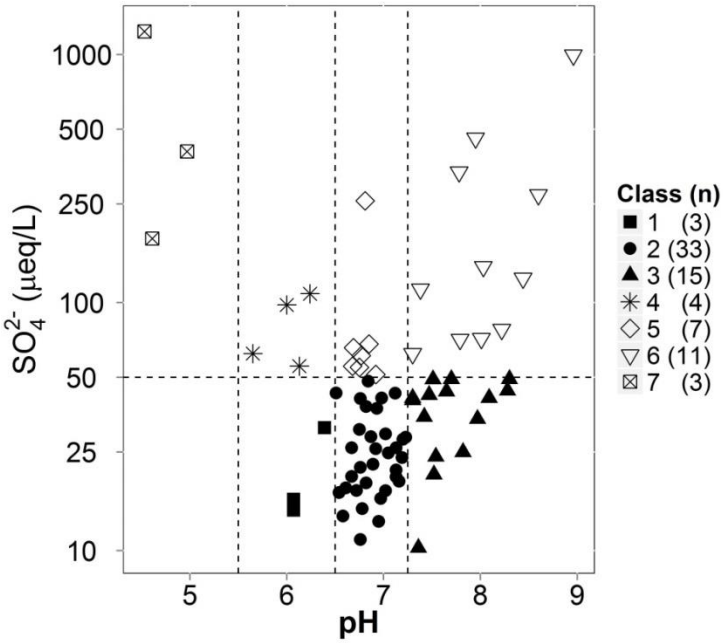

Figure 6.5. Classification of the Pyrenean lakes according to pH and SO_4^{2-}.

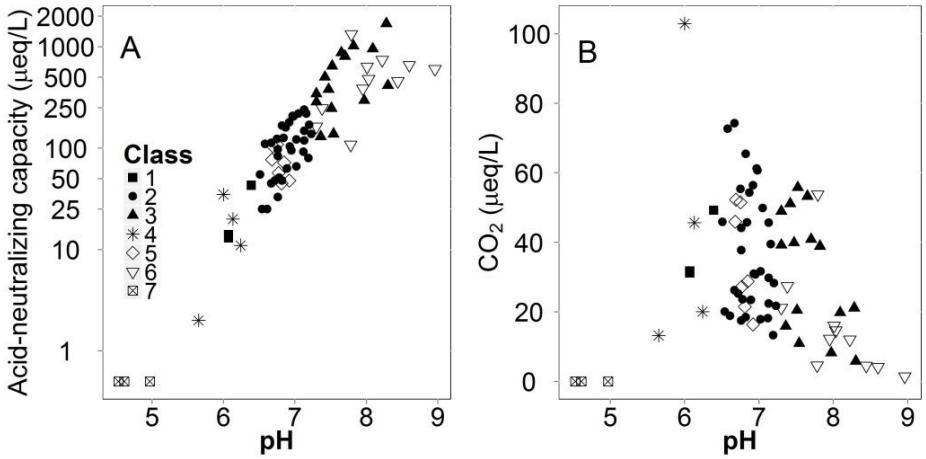

Figure 6.6. Relationship between pH and acid-neutralizing capacity (A), and CO_2 (B).

The ANC-pH gradient and major chemical composition

The relative ion composition showed the importance of lithology in the water chemistry (Figure 6.7). Generally, Ca^{2+} is the dominant cation (37-96%) and Mg^{2+} (2-49%) and $Na^+ + K^+$ (0.1-38%) contribute in a more variable proportion. Ca^{2+} concentration was particularly high in lakes of classes 3 and 6 and low in class 1 (Figure 6.8A). Mg^{2+} was high in lakes of classes 6 and 7, at both extremes of the acidity gradient, and presented the lowest values in class 1. $Na^+ + K^+$ presented a highly variable concentration, without any particular distribution among classes. These two cations are those more influenced by atmospheric deposition.

Anions showed a higher variability than cations, mostly due to SO_4^{2-} variability. Cl^- and NO_3^- had low contribution to acidity. Carbonate anions have higher relative importance in classes 3 and 6, in parallel with Ca^{2+} and reflecting the limestone influence (Figure 6.8F).

SO_4^{2-} was the dominant anion in lakes of classes 4, 7, and in some of the lakes of classes 5 and 6. SO_4^{2-} was closely related to the Mg^{2+} gradient ($r=0.73$, $p<0.01$, $n=76$) than to the Ca^{2+} gradient ($r=0.32$, $p<0.01$, $n=76$). Cl^- and NO_3^- did not show any association with the main cations.

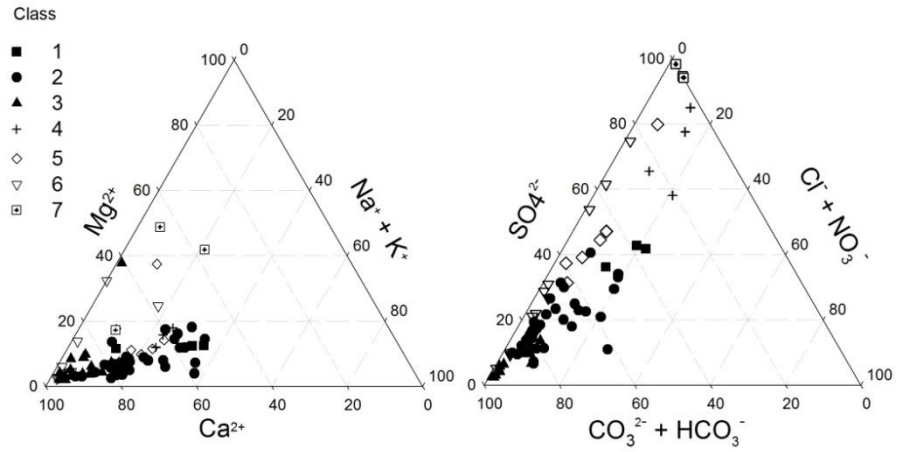

Figure 6.7. Ternary diagrams of the water ionic composition of the Pyrenean lakes.

There was no significant relationship between morphometric characteristics of the lakes and the ionic composition. For example, lakes did not show differences in pH, ANC and SO_4^{2-} concentration between depth classes (Figure 6.9).

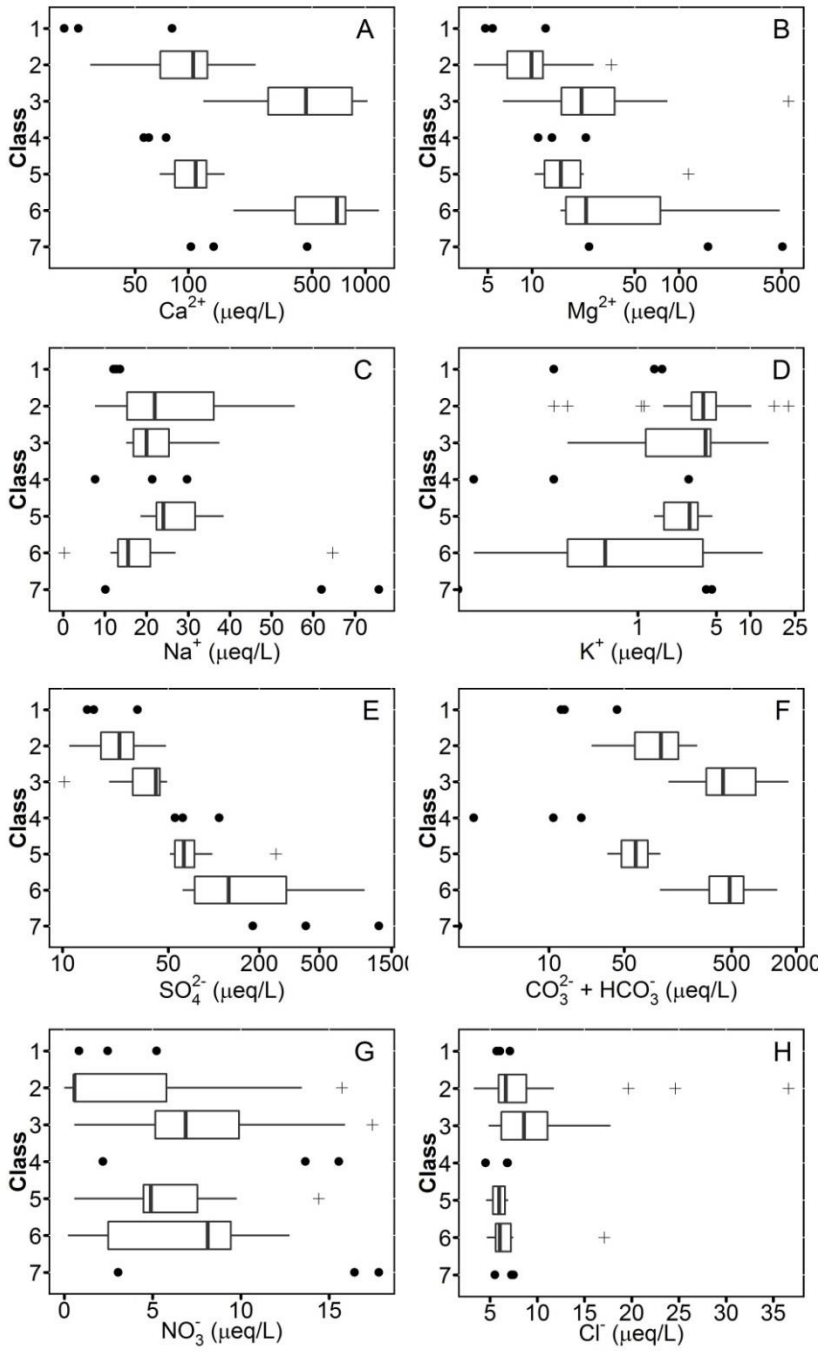

Figure 6.8. Cation and anion distribution in the lake classes described in Table 4. Boxplots are only drawn when n>7 lakes. Outliers are indicated with a cross.

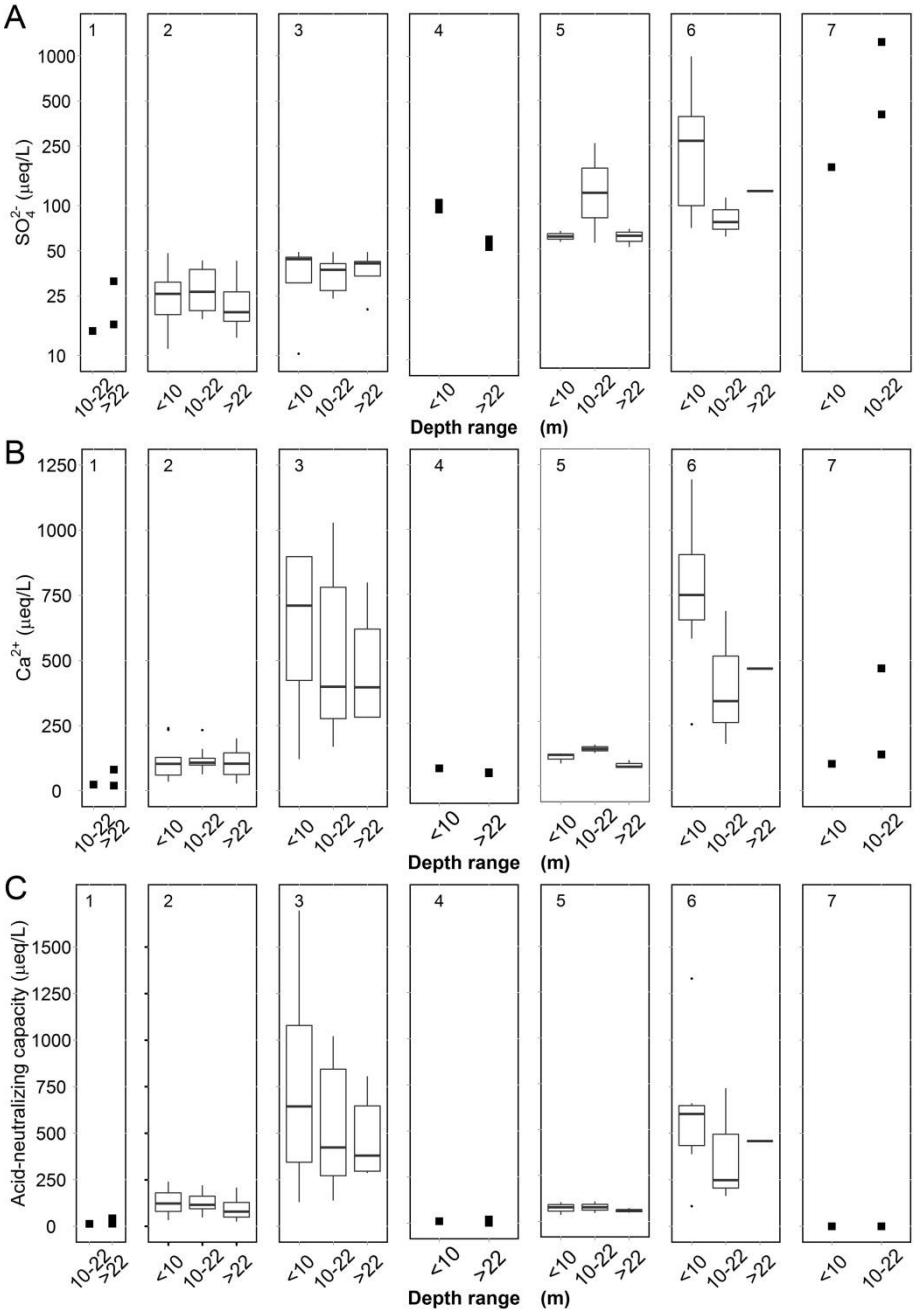

Figure 6.9. Relationships between depth and SO_4^{2+} (A), Ca^{2+} (B) and ANC (C). The numbers correspond with the lake classes described in Table 4.

Indicator species of ANC-pH lake classes

All ANC-pH lake classes had statistical indicator species (IndVal analysis) with the exception of class 2. The analysis combining groups increased the number of statistically indicator species from 43 to 67 species. Groups 1, 7 and 6 showed the highest number of indicator species, which corresponded to the more extreme conditions: lakes with very high or very low pH with the highest SO_4^{2-} concentration, and poorly mineralised acid lakes with low SO_4^{2-} concentration (Table 5).

There are two types of indicator species: 1) species indicative of a unique group of lakes, and 2) species indicative of a set of groups with a distribution bounded by a certain range of pH or SO_4^{2-}. The indicator species of lakes class 1 correspond with species typically present in environments with low ionic concentration: *Eunotia boreoalpina* Lange-Bertalot & Nörpel-Schempp (Figure 6.10), *Eunotia incisa* Gregory, *Eunotia mucophila* (Lange-Bertalot & Nörpel-Schempp) Lange-Bertalot, and *Peronia fibula* (Brébisson in Kützing) Ross.

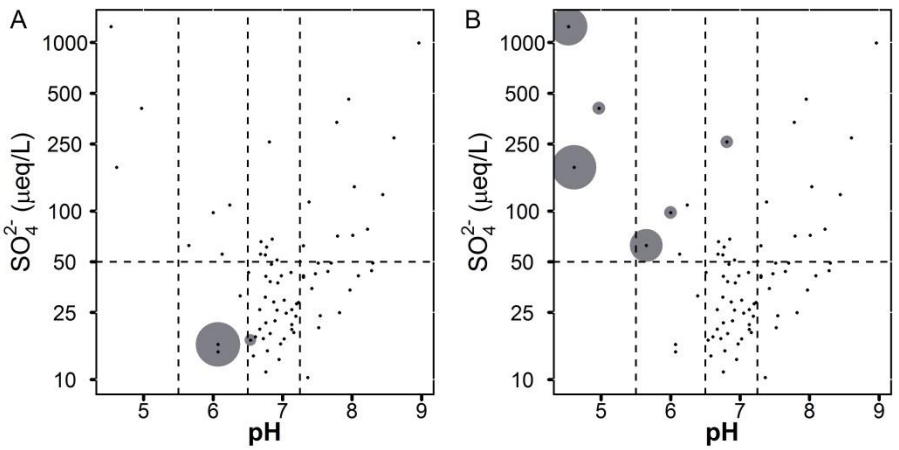

Figure 6.10. Relative abundance of A) *Eunotia boreoalpina* and B) *Eunotia catalana* with respect to pH and SO_4^{2-} concentration. Points correspond to the lakes studied and the shaded circle size indicates the specie abundance relative to the highest value in the data set.

Similarly, indicator species of lake class 7 were mainly Eunotiaceae such as *Eunotia catalana* Lange-Bertalot & Rivera-Rondón (Figure 6.10), *Eunotia* cf. *meridionalis* Lange-Bertalot & Tagliaventi, *Eunotia nymanniana* Grunow, *Eunotia* cf. *pseudogroenlandica* Lange-Bertalot & Tagliaventi and *Eunotia glacialis* Meister; and included some Pinnulariaceae such as *Caloneis* cf. *vasileyevae* Lange-Bertalot, Genkal & Vekhov, *Pinnularia* cf. *laucensis* Lange-Bertalot, Rumrich & Krammer, and *Pinnularia* No.10 Pica Palomera.

There is an important number of species indicative of the combination of lake classes 1, 4 and 7, that is, acidophilic diatoms without constrictions by SO_4^{2-} concentration: class 1+7 had as indicator species *Brachysira brebissonii* Ross (Figure 6.11), *Eunotia bilunaris* (Ehrenberg) Schaarschmidt, *Eunotia* cf. *soleirolii* (Kützing) Rabenhorst, and Surireraceae such as *Stenopterobia delicatissima* (Lewis) Van Heurck and *Surirella* cf. *robusta* Ehrenberg. The combination 1+4+7 classes had *Encyonopsis aequalis* (Smith) Krammer, *Frustulia* cf. *saxonica* Rabenhorst (Figure 6.11), *Eunotia exigua* (Brébisson Kützing) Rabenhorst, *Eunotia intermedia* (Krasske) Nörpel & Lange-Bertalot, *Neidium* No.1 Illa and *Pinnularia microstauron* var. *nonfasciata* Krammer as indicative species.

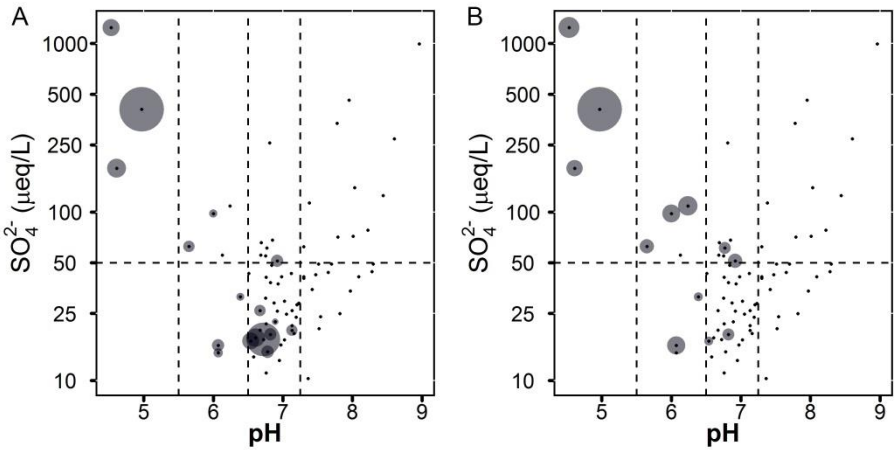

Figure 6.11. Relative abundance of A) *Brachysira brebissonii* and B) *Frustulia* cf. *saxonica* with respect to pH and SO_4^{2-} concentration. Points correspond to the lakes studied and the shaded circle size indicates the specie abundance relative to the highest value in the data set.

Table 5. Diatom species and its indicative value (IndVal, 1-0) for lake classes described in the Table 4. The statistical significance of association (p) is indicated. Analysis was carried out following Dufrêne and Legendre (1997) and combining classes (De Cáceres et al. 2010). T: sediment top samples, E: epilithon samples.

Species	Analysis with single classes						Analysis combining classes						Species frequency (*f*) and abundance (n)					
	Class		IndVal		p		Comb.		IndVal		p		*f*		Mean n		Max n	
	T	E	T	E	T	E	T	E	T	E	T	E	T	E	T	E	T	E
Kobayasiella subtilissima (Cleve) Lange-Bertalot	1		0.88		0.001								6		0.35		1.1	
Stauroforma cf. *exiguiformis* (Lange-Bertalot) Flower, Jones & Round	1	1	0.73	0.93	0.007	0.003							15	15	0.81	0.86	2.3	4.74
Peronia fibula (Brébisson in Kützing) Ross	1	1	0.66	0.65	0.031	0.030							9	12	1.88	0.87	9.07	3.29
Kobayasiella parasubtilissima (Kobayasi & Nagumo) Lange-Bertalot	1	1	0.64	0.76	0.031	0.004							7	6	0.55	0.25	1.77	0.70
Naviculadicta sp. No. 1 Ensangents	1		0.61		0.022								5		0.34		0.7	
Neidium longiceps (Gregory) Ross	1	1	0.6	0.82	0.049	0.002							8	2	0.15	0.10	0.2	0.10
Eunotia boreoalpina Lange-Bertalot & Nörpel-Schempp	1		0.57		0.031								3		0.83		2	
Brachysira intermedia (Østrup) Lange-Bertalot		1		0.73		0.008								14		20.42		61.5
Craticula submolesta (Hustedt) Lange-Bertalot		1		0.71		0.015								9		0.32		1
Encyonema perpusillum (Cleve) Mann		1		0.97		0.001								13		0.98		7.28
Luticola sp No. 5 Coronas		1		0.8		0.005								3		0.1		0.1
Neidium cf. *ampliatum* (Ehrenberg) Krammer		1		0.74		0.007								11		0.24		0.8
Stenopterobia densestriata (Hustedt) Krammer		1		0.81		0.001								4		0.35		0.99
Pinnularia subcapitata Gregory	1	1	0.7	0.69	0.013	0.016		1+4		0.81		0.002	15	24	0.51	0.45	1.47	2.19
Aulacoseira cf. *alpigena* (Grunow) Krammer		1		0.88		0.003	1+4+5		0.78		0.011		23	17	4.5	1.29	50.7	11.07
Eunotia mucophila (Lange-Bertalot & Nörpel-Schempp) Lange-Bertalot	1	1	0.74	0.83	0.022	0.003		1+4+7		0.89		0.001	8	15	1.62	2.86	6.18	19.48
Eunotia incisa Gregory	1		0.68		0.017			1+4+7		0.77		0.009	4	11	0.47	0.95	0.9	5.38
Eunotia subarcuatoides Alles, Norpel & Lange-Bertalot	1	7	0.66	0.74	0.048	0.028	1+4	4+7	0.76	0.91	0.009	0.006	14	15	2.62	10.01	13.33	68.71
Navicula angusta Grunow	1		0.7		0.009		1+5		0.73		0.015		14		0.54		1.58	
Psammothidium marginulatum (Grunow) Bukhtiyarova et Round	1		0.79		0.011		1+5	1+4	0.78	0.79	0.014	0.006	26	21	0.94	0.55	8.19	2.30
Aulacoseira pfaffiana (Reinsch) Krammer	1		0.69		0.036		1+7	1+7	0.74	0.69	0.047	0.018	14	6	4.81	2.29	33.69	9.17
Encyonema gaeumannii (Meister) Krammer	1	1	0.7	0.83	0.011	0.006	1+7		0.73		0.048		26		1.94		9.33	
Neidium alpinum Hustedt	1		0.73		0.008		1+7	4+7	0.9	0.74	0.001	0.010	16	13	1.3	0.26	2.78	1.00

Species	Analysis with single classes						Analysis combining classes						Species frequency (*f*) and abundance (n)					
	Class		IndVal		p		Comb.		IndVal		p		*f*		Mean n		Max n	
	T	E	T	E	T	E	T	E	T	E	T	E	T	E	T	E	T	E
Surirella cf. *roba* Leclercq	1		0.74		0.009		1+7		0.79		0.01		24		0.41		1.48	
Stenopterobia delicatissima (Lewis) Van Heurck	1	1	0.67	0.67	0.032	0.018	1+7	1+7	0.88	0.76	0.003	0.004	11	10	1.26	0.33	7.19	1.19
Pinnularia sp No. 5 Mora							1+7		0.54		0.041		4		0.6		1	
Brachysira brebissonii Ross							1+7	1+4+7	0.94	0.83	0.001	0.014	21	35	5	2.32	39.72	28.43
Chamaepinnularia mediocris (Krasske) Lange-Bertalot		1		0.86		0.001	1+7		0.85		0.003		12	12	1.15	1.32	3.99	4.26
Chamaepinnularia sp No. 1 Negre		1		0.72		0.021	1+7	1+7	0.8	0.87	0.003	0.003	8	15	1.68	0.84	7.58	4.67
Eunotia cf. *soleirolii* (Kützing) Rabenhorst							1+7		0.69		0.015		6		0.84		3.44	
Neidium affine (Ehrenberg) Pfitzer sensu lato							1+7	1+4	0.7	0.63	0.035	0.016	23	7	0.37	0.20	1.4	0.50
Surirella cf. robusta Ehrenberg							1+7	1+7	0.75	0.57	0.01	0.013	9	3	0.51	0.20	1.7	0.40
Pinnularia subinterrupta Krammer & Schroeter								1+7		0.72		0.008		7		0.14		0.3
Encyonema sp No. 5 Pica Palomera	7		0.63		0.05		1+7		0.9		0.002		19		1.7		7.2	
Aulacoseira cf. *nygaardii* (Camburn) Camburn & Charles	7		0.72		0.009								3		3		5.9	
Caloneis cf. *vasileyevae* Lange-Bertalot, Genkal & Vekhov	7		0.77		0.007								4		0.5		1.6	
Eunotia catalana Lange-Bertalot & Rivera-Rondón	7		0.88		0.001			1+4+7		0.77		0.003	8	6	1	0.53	3.1	0.99
Eunotia cf. *meridionalis* Lange-Bertalot & Tagliaventi	7		0.71		0.02								7		0.3		0.8	
Eunotia nymanniana Grunow	7	7	1	0.82	0.001	0.005							3	2	16.9	0.20	40.6	0.30
Pinnularia cf. *laucensis* Lange-Bertalot, Rumrich & Krammer	7		0.66		0.020								7		0.4		0.9	
Pinnularia sp No. 10 Pica Palomera	7	7	0.8	0.61	0.011	0.036		1+7		0.76		0.004	5	6	2.6	0.63	11.9	1.50
Eunotia cf. *pseudogroenlandica* Lange-Bertalot & Tagliaventi	7	7	0.65	0.90	0.019	0.002	4+7		0.74		0.011		5	4	17	13.98	37.2	29.96
Eunotia implicata Nörpel, Alles & Lange-Bertalot							4+7		0.62		0.035		5		0.39		0.99	
Encyonopsis aequalis (Smith) Krammer	7		0.66		0.026		1+4+7	1+4+7	0.75	0.77	0.012	0.007	8	9	1.6	1.66	4.8	7.08
Frustulia cf. *saxonica* Rabenhorst	7	1	0.82	0.74	0.002	0.010	1+4+7		0.87		0.007		13	7	0.7	0.54	3.6	1.79
Eunotia exigua (Brébisson Kützing) Rabenhorst							1+4+7	4+7	0.8	0.80	0.002	0.006	17	15	0.8	0.55	3.8	1.99
Eunotia fallax A. Cleve		1		0.64		0.024		1+4+7		0.77		0.006		6		0.25		0.7
Eunotia novaisiae Lange-Bertalot & Luc Ector		1		0.76		0.008		1+4+7		0.79		0.008		24		0.93		4.37
Eunotia intermedia (Krasske) Nörpel & Lange-Bertalot		7		0.75		0.009	1+4+7	1+4+7	0.81	0.88	0.005	0.002	12	12	0.9	2.20	2.5	8.20
Neidium sp No. 1 Illa							1+4+7		0.58		0.009		3		0.2		0.5	
Tabellaria flocculosa (Roth) Kützing		4		0.8		0.028		1+4		0.91		0.014		27		2.16		42.61

Species	Analysis with single classes						Analysis combining classes						Species frequency (*f*) and abundance (n)					
	Class		IndVal		p		Comb.		IndVal		p		*f*		Mean n		Max n	
	T	E	T	E	T	E	T	E	T	E	T	E	T	E	T	E	T	E
Eunotia bilunaris (Ehrenberg) Schaarschmidt		4		0.71		0.017	1+7		0.76		0.015		22	11	0.43	0.23	2.1	1.20
Naviculadicta cf. *difficillima* Hustedt		4		0.69		0.014								3		0.13		0.2
Eunotia paludosa Grunow		4		0.64		0.043		4+7		0.74		0.013		8		0.93		3.76
Pinnularia cf. *brebissonii* var. *minuta* Krammer		4		0.63		0.027								7		0.16		0.3
Eunotia cf. *islandica* Østrup		4		0.62		0.045		1+4		0.72		0.01		11		0.27		0.8
Pinnularia microstauron var. *nonfasciata* Krammer	4		0.85		0.015		1+4+7	1+4+7	0.96	0.79	0.002	0.003	30	17	5.2	0.41	73.2	2.19
Psammothidium acidoclinatum (Lange-Bertalot) Lange-Bertalot							1+4+7	1+4+7	0.72	0.89	0.012	0.004	13	16	4.7	8.37	12.8	64.54
Aulacoseira cf. *distans* (Ehrenberg) Simonsen								1+4+7		0.76		0.008		11		2.46		11.73
Encyonema hebridicum Grunow ex Cleve								1+4+7		0.82		0.004		10		0.6		2.08
Eunotia glacialis Meister								1+4+7		0.63		0.036		12		0.12		0.2
Eunotia neocompacta var. *vixcompacta* Lange-Bertalot								1+4+7		0.63		0.036		12		0.12		0.2
Neidium bisulcatum (Lagerstedt) Cleve sensu Krammer								1+4+7		0.67		0.019		7		0.24		0.8
Psammothidium helveticum (Hustedt) Bukhtiyarova et Round							1+4+5+7	1+4+7	0.92	0.96	0.001	0.001	42	50	4.1	2.03	26.9	13.27
Surirella cf. *linearis* Smith							1+4+5+7		0.67		0.031		15		0.2		0.5	
Psammothidium scoticum (Flower et Jones) Bukhtiyarova & Round							1+4+5	1+4	0.82	0.74	0.019	0.020	28	21	5	2.55	25	17.00
Achnanthes cf. *microscopica* (Cholnoky) Lange-Bertalot & Krammer							1+2+4+5	1+2+4+5	0.84	0.84	0.006	0.015	45	39	5.2	2.77	28.7	27.05
Navicula schmassmanni Hustedt							1+2+4+5		0.84		0.019		39		2.5		18.8	
Psammothidium subatomoides (Hustedt) Bukhtiyarova et Round							1+2+4+5	1+2+4+5	0.88	0.92	0.003	0.003	46	45	2.5	1.42	23.3	18.53
Achnanthidium pyrenaicum (Hustedt) Kobayasi	3		0.7		0.017			3+6			0.70	0.048	32	20	1.1	0.87	8.4	5.74
Gomphonema cf. *subclavatum* (Grunow) Grunow	5		0.69		0.011								4		0.1		0.2	
P. didymum (Hustedt) Bukhtiyarova & Round	5		0.65		0.048								6		0.15		0.19	
Geissleria similis (Krasske) Lange-Bertalot & Metzeltin	3		0.61		0.046								9		0.5		1.8	
Nitzschia sp No. 6 Sen	3		0.6		0.048								22		0.43		1.4	
Planothidium distinctum (Messikommer) Lange-Bertalot		5		0.6		0.044		4+5		0.61		0.039		8		0.19		0.4
Cymbella parva (Smith) Kirchner								3+5+6		0.9		0.002		58		3.79		28.12
Amphora neglecta f. *densestriata* Foged							3+6		0.81		0.014		31		1.2		10	

Species	Analysis with single classes						Analysis combining classes						Species frequency (*f*) and abundance (n)					
	Class		IndVal		p		Comb.		IndVal		p		*f*		Mean n		Max n	
	T	E	T	E	T	E	T	E	T	E	T	E	T	E	T	E	T	E
Amphora copulata (Kützing) Schoeman & Archibald							3+6		0.78		0.024		32		0.98		7.07	
Nitzschia sp No. 1 Sen							3+6		0.75		0.02		33		0.9		3.3	
Encyonopsis subminuta Krammer & Reichardt							3+6		0.74		0.023		26		0.9		6.4	
Amphora cf. *eximia* Carter							3+6		0.73		0.027		22		1.5		6.9	
Diploneis cf. *petersenii* Hustedt							3+6		0.67		0.044		13		0.51		2.98	
Encyonopsis microcephala (Grunow) Krammer								3+6		0.76		0.017		23		4		20.18
Gomphonema lateripunctatum Reichardt & Lange-Bertalot								3+6		0.72		0.02		22		1.8		7.94
Encyonema reichardtii (Krammer) Mann								3+6		0.69		0.038		16		0.66		3.4
Navicula cryptotenella Lange-Bertalot	6	6	0.75	0.75	0.021	0.030							15	19	1.6	0.58	13.2	5.76
Navicula cf. *antonii* Lange-Bertalot & Rumrich	6		0.72		0.03		3+6		0.73		0.023		14		2		11	
Denticula tenuis Kützing	6	3	0.7	0.69	0.04	0.029	3+6	3+6	0.93	0.92	0.002	0.001	34	48	5.6	6.35	48.6	44.54
Punctastriata cf. *lancettula* (Schumann) Hamilton & Siver	6		0.66		0.029								9		1.85		11.25	
Delicata delicatula (Kützing) Krammer	6	3+6	0.59	0.70	0.043	0.030							6	20	0.5	3.19	1.6	11.12
Encyonema ventricosum (Kützing) Grunow	6		0.78		0.003		1+2+3+5+6		0.89		0.028		57		2		17.4	
Encyonema minutum (Hilse) Mann								2+3+5+6		0.96		0.002		68		8.75		73.62
Nitzschia cf. *alpina* Hustedt								2+6		0.74		0.023		32		0.86		3.24
Eucocconeis laevis Østrup								1+3+6		0.67		0.047		19		0.47		1.89
Encyonema lange-bertalotii Krammer							1+2+3+5+6		0.87		0.007		54		0.6		3.1	
Staurosirella pinnata (Ehrenberg) Williams & Round							1+2+3+5+6		0.87		0.031		55		4.2		22.2	
Pseudostaurosira microstriata (Marciniak) Flower							1+2+3+5+6		0.86		0.001		51		5.7		39	

Lake class 5 only had the species *Achnanthes* No.7 Pixon and *Gomphonema* cf. *subclavatum* (Grunow) Grunow as indicators, but there were indicators for different combinations of classes that include class 5. Thus, *Psammothidium acidoclinatum* (Lange-Bertalot) Lange-Bertalot and *Psammothidium helveticum* (Hustedt) Bukhtiyarova et Round (Figure 6.12) were indicators of acid to circum-neutral condition regardless of SO_4^{2-} concentrations (group 1+4+5+7). *Psammothidium scoticum* (Flower et Jones) Bukhtiyarova & Round, *Aulacoseira* cf. *alpigena* (Grunow) Krammer, *Navicula schmassmanni* Hustedt and *Psammothidium subatomoides* (Hustedt) Bukhtiyarova et Round (Figure 6.12) were indicators of group 1+2+4+5.

There were few indicators species of class 3 (*Achnanthidium pyrenaicum* and *Geissleria similis* (Krasske) Lange-Bertalot & Metzeltin), with respect to species indicators of groups 6 and 3+6: *Navicula* cf. *antonii* Lange-Bertalot & Rumrich, *Delicata delicatula* (Kützing) Krammer, *Encyonema ventricosum* (Kützing) Grunow and *Navicula cryptotenella* Lange-Bertalot (Figure 6.13), *Amphora* cf. *eximia* Carter, *Amphora neglecta* f. *densestriata*, and *Encyonopsis subminuta* (Figure 6.13).

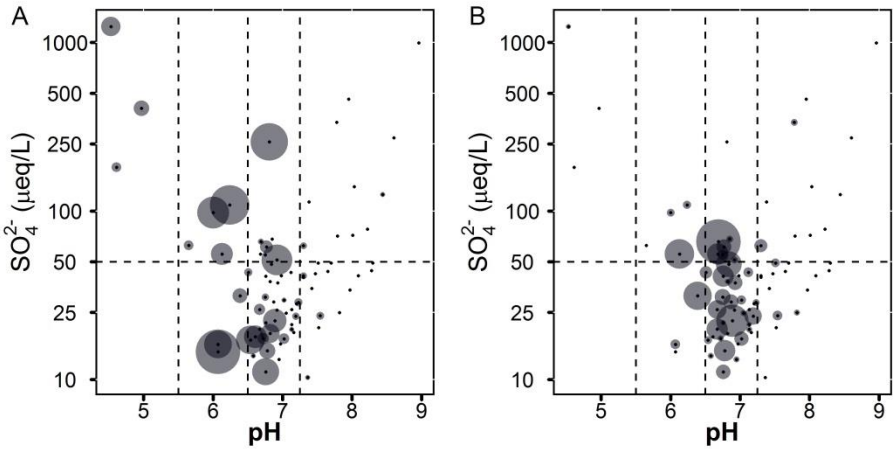

Figure 6.12. Relative abundance of A) *Psammothidium helveticum* and B) *Psammothidium subatomoides* with respect to pH and SO_4^{2-} concentration. Points correspond to the lakes studied and the shaded circle size indicates the specie abundance relative to the highest value in the data set.

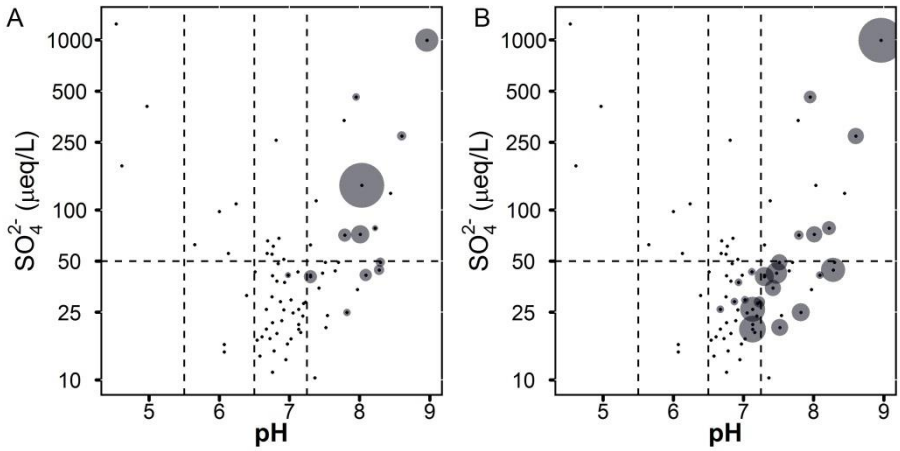

Figure 6.13. Relative abundance of A) *Navicula cryptotenella* and B) *Encyonopsis subminuta* with respect to pH and SO_4^{2-} concentration. Points correspond to the lakes studied and the shaded circle size indicates the specie abundance relative to the highest value in the data set.

7. Nutrient gradients

After light and carbon, macro-nutrients are the main factors regulating algal growth (Reynolds 2006). Nutrient availability and rate of uptake are the principal factors determining changes in algae dominances in freshwater ecosystems (Brauer et al. 2012; Tilman 1990). The limitation of algal productivity is related to changes in the ratio between N and P (Margalef 1983), and silicon, when we consider diatoms (Carrick and Lowe 2007; Martin-Jézéquel et al. 2000). Currently, atmospheric deposition can change the N:P ratio resulting in significant changes in the biogeochemical cycling and lake trophic dynamics (Camarero and Catalan 2012; Elser et al. 2009). Changes in the ratio between these nutrients produce a shift in the limiting factor and provoke changes in algal biomass (Bergström et al. 2008) and composition (Dong et al. 2012). In the past, although one cannot disregard the atmospheric influence, lake water N:P fluctuations were likely influenced by the P availability due to soil development and other changes in the catchments. In any case, the lake trophic state oscillations have been recorded in the sediments in different ways, including changes in the diatom assemblages (Hobæk et al. 2012; Kirilova et al. 2009; Lake et al. 2011; Reuss et al. 2010).

The response to eutrophication may differ between planktonic and benthic algae, and diatoms in particular (Hall and Smol 1999). For example, benthic algae are exposed to higher P concentrations because of the supply by diffusion from the sediment, therefore, they are more resilient to changes in P loadings than planktonic algae directly reacting to water column concentrations (Davidson and Jeppesen 2013). On the other hand, the benthic algae are more sensitive to littoral habitat changes, which occasionally may mask the ecological response to P (Sayer 2001).

All in all, the response of diatom assemblages to nutrients has been used for developing transfer function for nutrients, mainly for total phosphorus (TP) as a general trophic indicator (Chen et al. 2008; Reavie and Smol 2001; Reid 2005; Werner and Smol 2005). The reliability of some of this transfer functions have been questioned by Juggins et al. (2013). These authors point to some weakeness of these transfer function related to the influence of secondary variables and the number of taxa statistically related with TP. Despite the relatively large number of transfer function models used to reconstruct past nutrients conditions using

diatoms (Buczkó et al. 2012; Cremer et al. 2009; Quillen et al. 2013), the ecological relation of a large amount of taxa with nutrients remains unknown. On the other hand, when the interest is in N, non-experimental approaches to the taxa optima appear inconsistent (e.g. Arnett et al. 2012).

In this chapter, the relationships between nutrients and diatoms in the lakes of the Pyrenees is explored to identified diatom taxa indicative of nutrient changes that, eventually, could provide some light to the reconstruction of nutrient conditions in the Burg Lake.

Diatom distributions in the nutrient gradients

The pattern of the species range distribution across the nutrient gradient differs among TN, TP and Si (Figure 6.1). In the case of TN, species showed broad ranges; nearly any species can occur anywhere. For TP, the pattern was slightly more asymmetric, particularly in the oligotrophic extreme of the TP gradient in which some taxa appeared restricted to values <0.1 µmol/L. Finally, for Si the length of the species range was much more divers; the range generally increased with the Si optima. Several species had distributions restricted to <40-50 µmol/L.

In the case of nitrogen, because of the range of each species was generally broad; the optimum differentiation was determined by the relative abundance across this distribution. In general, there was not much difference between the median of the distribution and the optimum values, indicating scarce influence of TN on species segregation. Only for optima >15 µmol/L, the difference between median and optimum begins to increase markedly. This indicates the existence of a group of species with apparent preference (advantage) for markedly high TN conditions (e.g. *Amphora copulata (*Kützing) Schoeman & Archibald, Figure 7.2B). Species with optima >40 µmol/L include *Encyonema* sp. No. 1 Mora, *Cymbopleura* cf. *hercynica* (Schmidt) Krammer, *Gomphonema* cf. *parvulum* (Kützing) Kützing, *Navicula catalanogermanica* Lange-Bertalot & Hofmann, *Diploneis* cf. *modica* Hustedt, *Diploneis* cf. *peterseni* (petersenii) Hustedt, *Encyonopsis* cf. *falaisensis* (Grunow) Krammer.

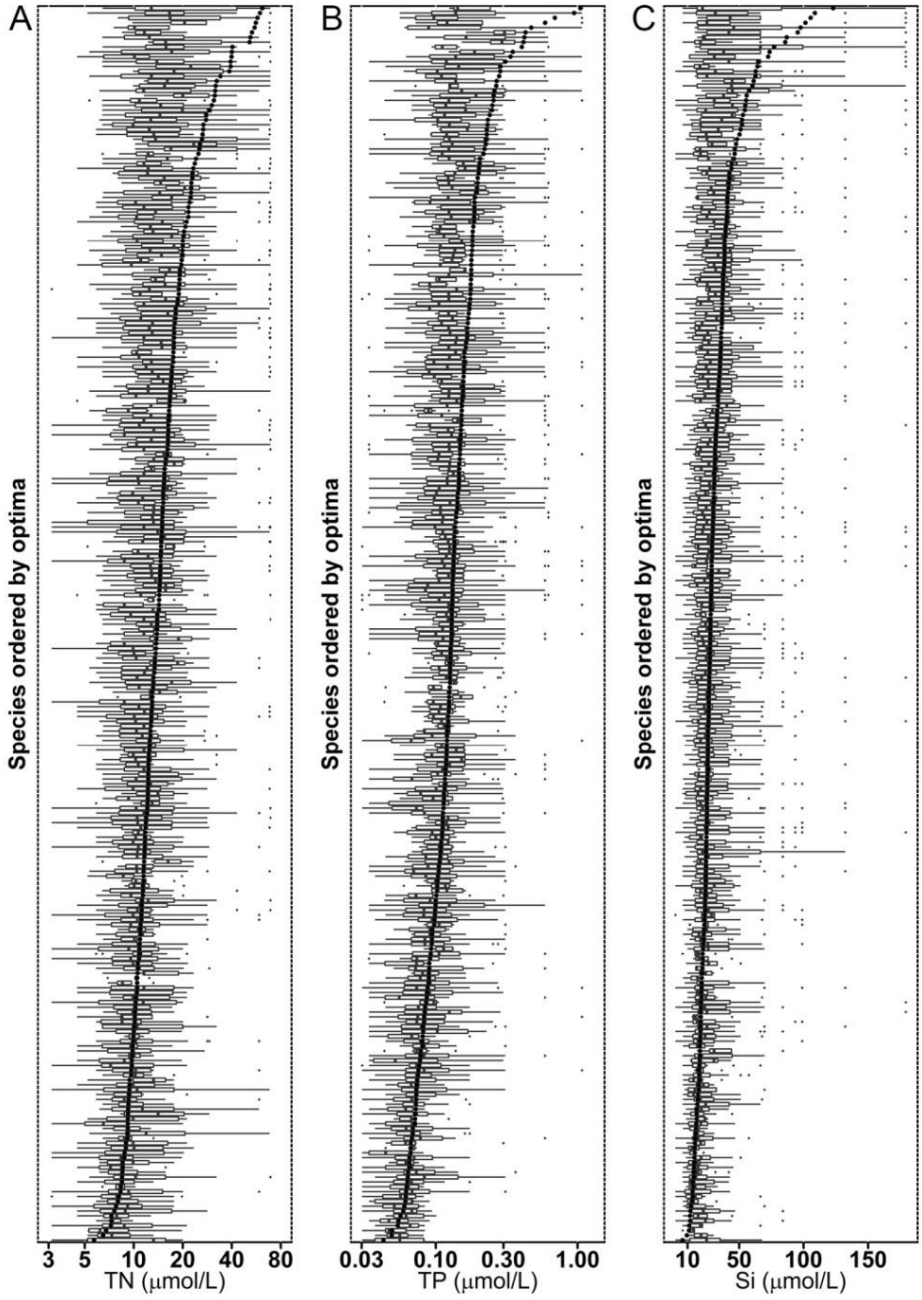

Figure 7.1. Optima (dark points) and range distribution (boxplot) of the diatom species (frequency >3 lakes) for total nitrogen (A), total phosphorous (B) and Si concentrations (C) based on sediment samples of the lake survey. Outliers of variable distribution are represented with small crosses.

There were species with a widespread distribution but showing a TN threshold above which they always show relative low abundances (e.g. *Navicula* spp. aff. N. *minima*, Figure 7.2A). The value of this threshold tended to be between 10 and 15 µmol/L. A further indication that only at very high TN values this nutrient starts to be relevant in the context of species segregation. Perhaps more related to toxicity than trophic issues. Most common species, such as *Encyonema silesiacum* (Bleisch) Mann, *Achnanthidium minutissimum* (Kützing) Czarnecki and *Karayevia suchlandtii* (Hustedt) Bukhtiyarova, did not show any optimum within the nitrogen gradient (Figure 7.2C). However, some of them such as *A. pyrenaicum* and *Cymbella parva* (Smith) Kirchner (Figure 7.2D) did show a unimodal distribution centred at intermediate values of nitrogen (ca. 15 µmol/L).

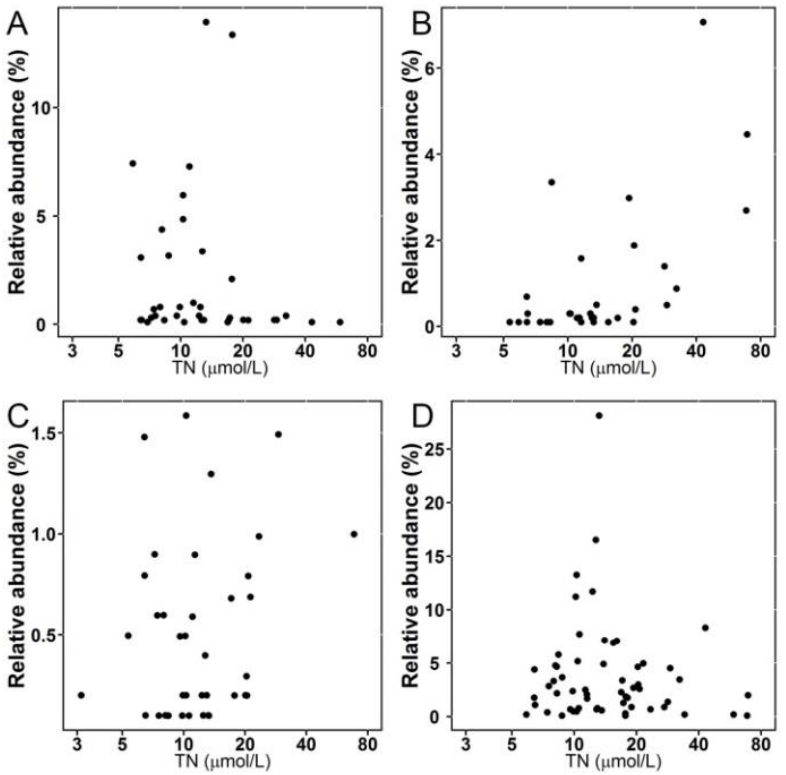

Figure 7.2. Relative abundance of *Navicula* spp. aff. *N. minima* (A), *Amphora copulata* (B), *Karayevia suchlandtii* (C) and *Cymbella parva* (D) across the total nitrogen gradient.

In the TP gradient, a key value appears to be 0.1 µmol/L. As mentioned, some species restrict their distribution below this value, some show a narrow distribution centred on it, and, finally, the differentiation between the species optimum and the median of the distribution is usually different above this value. When considering particular species, there are all kind of distributions: species with a threshold-like limitation below certain value (e.g. *Psammothidium helveticum* (Hustedt) Bukhtiyarova et Round, Figure 7.3A) or above it (e.g., *S. pinnata* (Figure 7.3D); species with a limited distribution with a unimodal optimum, for instance, at low TP concentration (e.g. *Encyonema hebridicum* Grunow ex Cleve) or at intermediate values (e.g., *Sellaphora laevissima* (Kützing) Mann (Figure 7.3C); and species, such as *Psammothidium levanderi* (Hustedt) Bukhtiyarova & Round (Figure 7.3B), that showed a widespread distribution through the TP gradient with a preference for high or medium TP concentrations.

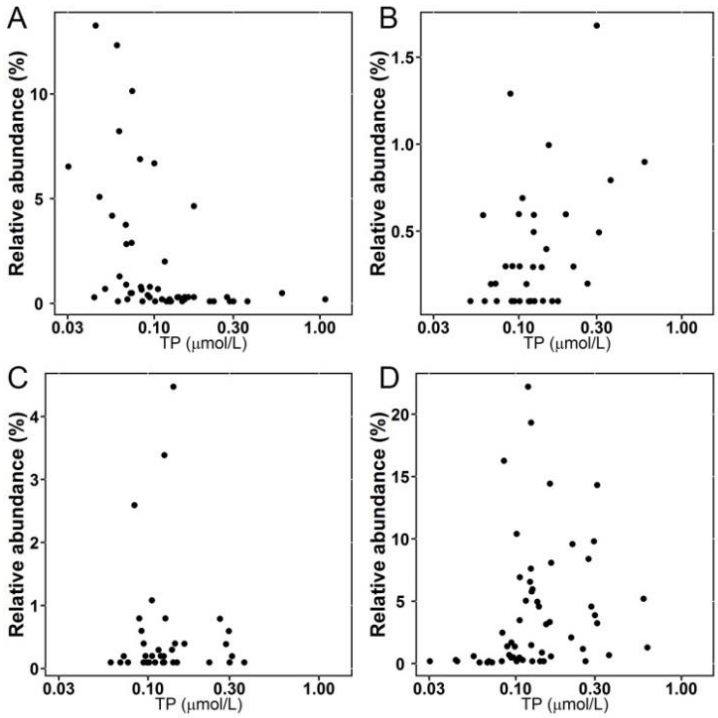

Figure 7.3. Relative abundance of *Psammothidium helveticum* (A), *Psammothidium levanderi* (B), *Sellaphora laevissima* (C) and *Staurosirella pinnata* (D) across the total phosphorus gradient.

In general, the species optimum for the TN:TP ratio was similar to the average value of the training-set TN:TP ratio. However, some pairs of species from the genus did show different TN:TP optimum. *Amphora neglecta* f. *densestriata* Foged (Figure 7.4A) showed a higher abundance close to 100:1 ratio while *Amphora copulata* (Kützing) Schoeman & Archibald Figure 7.4C) was dominant at higher TN:TP ratio (about 200:1). *Brachysira intermedia* (Østrup) Lange-Bertalot and *Brachysira brebissonii* Ross, morphologically similar species, showed a different environmental range (Figure 7.4 B and D).

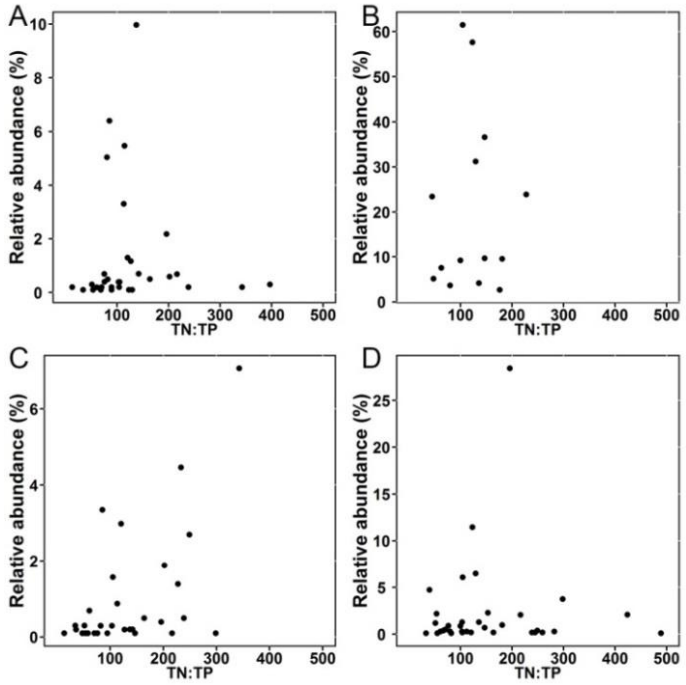

Figure 7.4. Relative abundance of *Amphora neglecta* f. *densestriata* (A), *Brachysira intermedia* (B), *Amphora copulata* (C) and *Brachysira brebissonii* (D) across the TN:TP gradient.

In the case of Si, the optimum, and the median of the distribution were close, probably due to the fact that the length of the ranges was short. In fact, both values differed for species with optima >40 µmol/L, which show the broader ranges. There were species such as *Achnanthes microscopica* (Cholnoky) Lange-Bertalot & Krammer (Figure 7.5A) with a widespread distribution but with dominance showing a marked threshold. Other species with broad distribution,

such as *E. silesiacum* and *Discostella stelligera* (Cleve & Grunow) Houk & Klee (Figure 7.5B), showed an optimum at intermediate concentration. Species showing large or very thick valves, such as *Diatoma mesodon* Kützing, *Surirella* cf. *linearis* Smith (Figure 7.5C), *Pseudostaurosira pseudoconstruens* (Marciniak) Williams & Round (Figure 7.5D) and *Fragilaria* cf. *opacolineata* Lange-Bertalot, showed a higher abundance in lakes with high Si concentration.

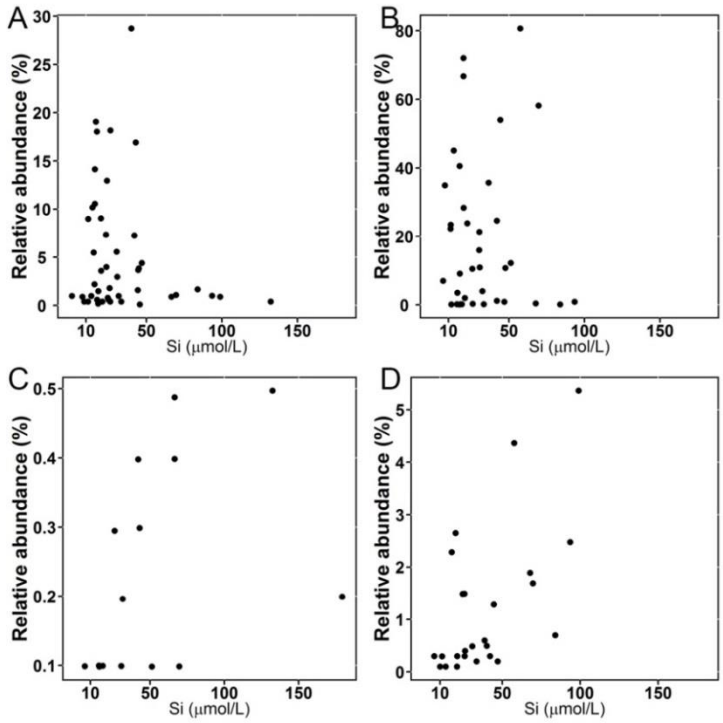

Figure 7.5. Relative abundance of *Achnanthes microscopica* (A), *Discostella stelligera* (B), *Surirella* cf. *linearis* (C) and *Pseudostaurosira pseudoconstruens* (D) across the total nitrogen gradient.

Nutrient classification of the Pyrenean lakes

The response to nutrients is non-linear, either at the cellular level or at the ecosystem. Therefore, it is also convenient to try to classified the lakes of the Pyrenees in groups defined according some known characteristic boundaries. Lakes were grouped using two different approaches: first, lakes were grouped into three classes (Figure 7.6) following the N:P ratios reported by Elser et al.

(2009) for which lakes are nitrogen or phosphorous limited. Lakes with N:P ratio <50:1 are assumed N-limited and were grouped into class 1; lakes with ratio >110:1 are assumed P-limited and were grouped into class 3; and lakes from 110:1 to 50:1 were grouped into class 2. Second, lakes were grouped using Camarero and Catalan (2012) DIN limiting threshold (7 µmol/L) for the Pyrenean lakes and Wetzel (2001) TP trophic categories. Seven lake classes were considered in this way (Figure 7.6B): TP <0.13 µmol/L and DIN <7 µmol/L (class 1), TP from 0.13 to 0.33 µmol/L - DIN <7 µmol/L (class 2), TP >0.33 µmol/L - DIN <7 µmol/L (class 3), TP <0.13 µmol/L - DIN >7 µmol/L (class 4), and TP <0.33 µmol/L - DIN >7 µmol/L (class 5).

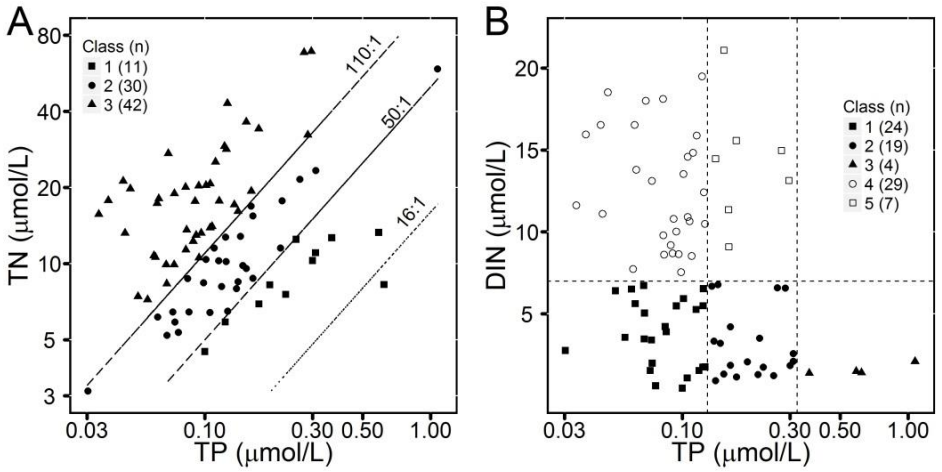

Figure 7.6. A. Total nitrogen (TN) and total phosphorous (TP) in the Pyrenean lakes. Dotted line TN:TP ratio = 16:1. Dashed lines indicating the boundaries of nitrogen algal limitation (TN:TP <50:1) and phosphorous (TN:TP >110:1) according to Elser et al. (2009). B. Lake classification according to TP trophic categories (Wetzel 2001) and DIN threshold (Camarero and Catalan 2012).

The classification using N:P values shows a great number of P-limited lakes and a few N-limited lakes. The only lake with a N:P below Redfield planktonic ratio (Redfield 1958) was lake Airoto, which showed the second highest P concentration. The N:P ratio calculated by using the mean N and P concentrations of the lake survey was 106:1.

The values of TN:TP did not respond to any marked pattern either in TN or TP; within a certain ratio range the scattering was high, although TN and TP where

not completely independent. Class 1 showed a TN average (9.2 µmol/L) lower than the whole training-set (16 µmol/L) whereas it showed a TP average higher (0.29 µmol/L) than the whole training-set (0.15 µmol/L). Class 3 presented an opposed pattern, showing a TN average of 20.7 µmol/L and a TP average of 0.1 µmol/L.

The second classification approach showed that a 44% of analysed lakes were limited by nitrogen and that a 64% of lake showed ultra-oligotrophic conditions (TP<0.13 µmol/L, which is <4 µg/L). There were only four mesotrophic lakes which are nitrogen limited and none with high nitrogen and phosphorous concentration.

The higher chlorophyll concentration, the lower TN:TP ratio (Figure 7.7), although variation was high within each class. The chlorophyll range in the survey was 0.03 to 19 µg/L and showed the highest variability in class 3 (0.05-19 µg/L). The lakes that tended to show the lowest chlorophyll values were those with high DIN and relatively high TP, which may indicate a limitation by another factor.

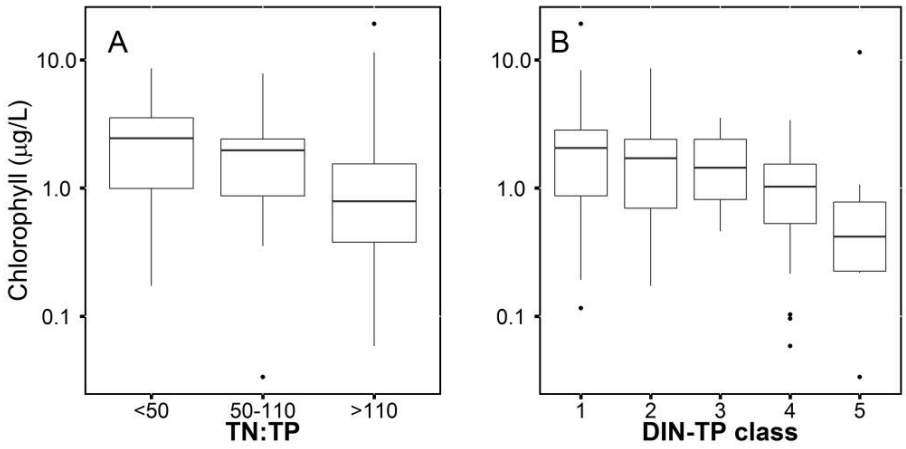

Figure 7.7. The chlorophyll concentration distribution according TN:TP ratio (A) and (DIN) –TP classes showed in Figure 7.6B (B).

The Pyrenean lakes showed a high silicate concentration that conditioned the ratio with other nutrients (Figure 7.8). Montagnon and L`Estagnol lakes were the

only ones with Si:TP ratios below 16:1. Si:TN ratio was highly variable but only 23% of the lake were below the 16:1 ratio.

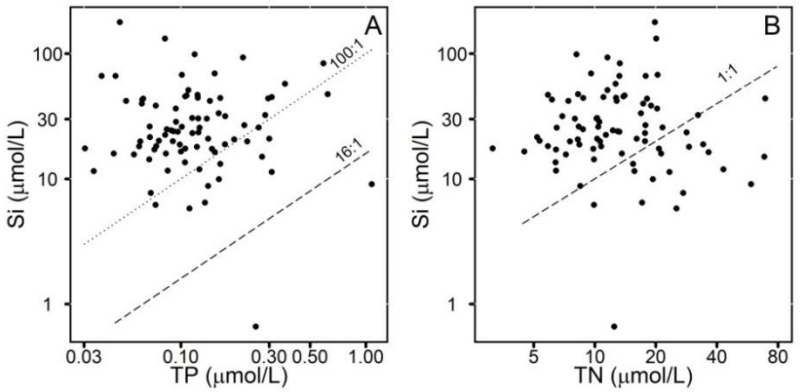

Figure 7.8. Silicate vs. total phosphorous (A) and total nitrogen (B) in the Pyrenean lakes. Dashed lines represented TP:Si and TN:Si reference ratios (Brzezinski 1985; Reynolds 2006; Teubner 2003).

There were no significant relationships between morphometric characteristics of the lakes and the nutrient concentration, although there was a tendency for shallow lakes to show higher nitrogen, phosphorous (Figure 7.9) and silicate concentration (Figure 7.10).

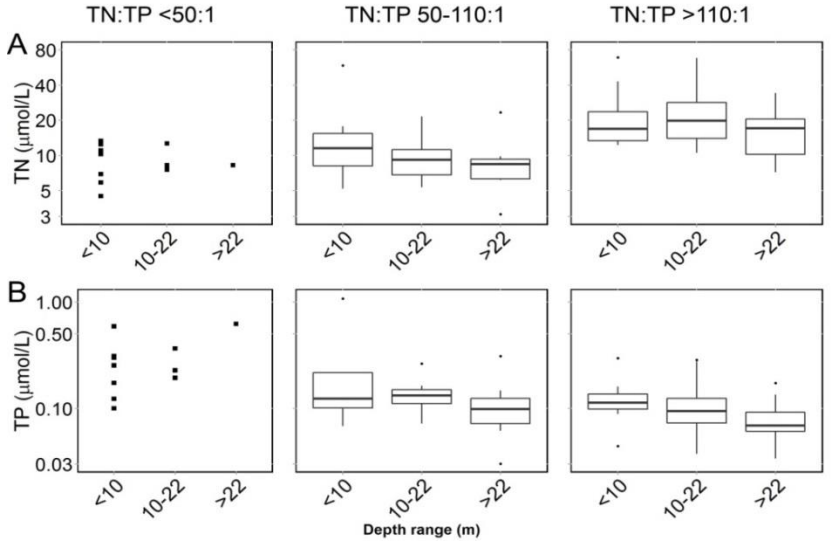

Figure 7.9. Relationships between depth and total nitrogen (A) and total phosphorous (B).

Very high values of Si were only found in relatively shallow lakes (<30 m depth) (Figure 7.10), which also showed a higher variability in the Si:N ratio, whereas deep lakes tended to a 1:1 ratio.

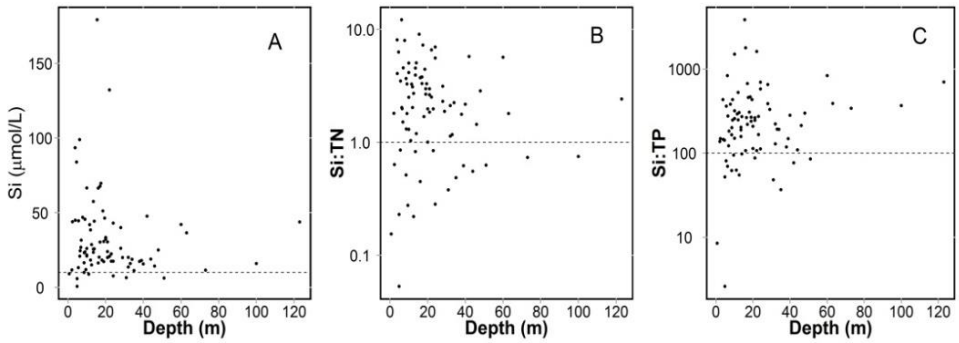

Figure 7.10. Relationships between depth and silicon (A), Si:TN ratio (B) and Si:TP ratio (C). Dashed lines represent reference values for Si limitation.

Indicator species of major nutrients

The analysis for TN:TP lake classes showed indicator species for all groups with a greater number of species in class 1 (nitrogen limited lakes, Table 6). Class 1 indicator species class included both species of limited distribution and widespread species but with high abundance in lakes with low TN:TP.

The sediment samples showed a large number of indicative species for class 1 with low frequency such as *Asterionella formosa*, *Aulacoseira perglabra*, *Aulacoseira* cf. *valida*, *Brachysira intermedia*, *Neidium longiceps*, *Nitzschia* sp. No. 11 Burg, *Navicula* cf. *submuralis* and *Psammothidium rossii* (Figure 7.11A). In contrast, the class 1 indicative species in epilithon samples were mainly species with high occurrence, such as *Navicula radiosa*, *Nitzschia acidoclinata*, *Psammothidium levanderi*, *Pseudostaurosira* sp. No. 2 Acherito, and *Staurosirella pinnata*. Other significant species in sediment samples were *Fragilaria* sp. No.8 Redon, *Navicula* cf. *seminulum*, and *Psammothidium subatomoides*. Indicator species for the combination 1+2 were *Navicula* spp. aff. *N. minima*, *Pseudostaurosira* cf. *brevistriata*, *Gomphonema auritum*, *Meridion circulare*, *Pseudostaurosira pseudoconstruens* and *Ulnaria biceps*.

Classes 2 and 3 showed a small number of indicator species suggesting a low specialization for equilibrate and high TN:TP ratio environments. Indicator

species for class 2 were *Achnanthidium minutissimum*, *Encyonopsis microcephala*, *Gomphonema lateripunctatum*, *Rossithidium pusillum*, and *Cyclotella* sp. No. 1 (Figure 7.11B and C).

Planothidium distinctum was the only species with a significant association with high TN:TP ratio (Figure 7.11D). *Nitzschia* sp. No. 1 Sen and *Denticula tenuis* were the only species with a significant association with TN:TP ratio >50:1 (group of classes 2+3).

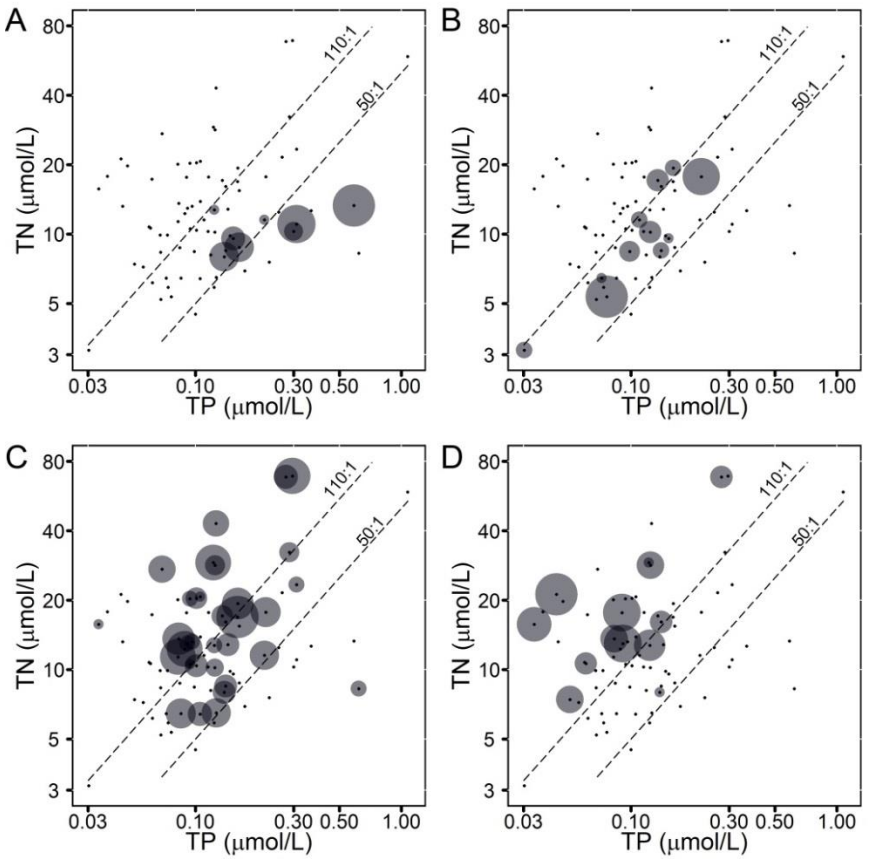

Figure 7.11. Relative abundance of A) *Psammothidium rossii*, B) *Encyonopsis microcephala*, C) *Nitzschia* sp. No. 1 Sen, and D) *Planothidium distinctum* with respect to total nitrogen (TN) and total phosphorous (TP). Points correspond to the lakes studied and the shaded circle size indicates the specie abundance relative to the highest value in the data set.

Table 6. Indicator species (IndVal) and statistical significance of association (p) with the TN:TP lake classes described in Figure 7.6. The analysis was carried out following Dufrêne and Legendre (1997) and combining classes (De Cáceres et al. 2010). T: sediment top samples, E: epilithon samples.

Species	Analysis with single classes						Analysis combining classes						Species frequency (*f*) and abundance (n)					
	Group		IndVal		p		Comb.		IndVal		p		*f*		Mean n		Max n	
	T	E	T	E	T	E	T	E	T	E	T	E	T	E	T	E	T	E
Navicula spp. aff. *N. minima*	1	1	0.76	0.68	0.001	0.014	1+2		0.77		0.003		37	31	2.1	0.95	13.9	9.2
Fragilaria sp. No. 8 Redon	1		0.71		0.01								33		2.77		22.8	
Psammothidium subatomoides (Hustedt) Bukhtiyarova et Round	1		0.71		0.023								46		2.53		23.3	
Fragilaria cf. *opacolineata* Lange-Bertalot	1		0.69		0.001								18		1.8		6.5	
Navicula sp No. 7 Bergus	1	1	0.68	0.51	0.007	0.020							30		1.24		4.9	2.4
Navicula venerablis Hohn & Hellerman	1		0.67		0.003								14		0.45		3.7	
Aulacoseira cf. *valida* (Grunow) Krammer	1		0.61		0.004								9		0.68		2.5	
Navicula cf. *seminulum* Grunow	1		0.61		0.049								28		1.41		11.5	
Navicula sp No. 4 Laquettes	1		0.58		0.009								11		0.66		2.9	
Navicula sp No. 3 Laurenti	1		0.56		0.015								12		0.77		2.0	
Adlafia cf. *minuscula* (Grunow) H. Lange-Bertalot	1		0.54		0.001								4		0.2		0.4	
Navicula heimansioides Lange-Bertalot	1	1	0.51	0.56	0.013	0.013							10		0.72		3.0	0.5
Asterionella formosa Hassall	1	1	0.5	0.42	0.035	0.045							9	4	6.17	0.10	29.3	0.1
Stauroforma cf. *exiguiformis* (Lange-Bertalot) Flower, Jones & Round	1		0.5		0.044								15		0.81		2.3	
Psammothidium rossii (Hustedt) Bukhtiyarova et Round	1	1	0.5	0.64	0.013	0.002							8	8	1.04	0.31	2.8	1.7
Aulacoseira perglabra (Østrup) Haworth	1		0.48		0.012								5		0.8		1.7	
Neidium longiceps (Gregory) Ross	1		0.46		0.023								8		0.15		0.2	
Nitzschia sp No. 11 Burg	1		0.44		0.014								3		1.54		2.9	
Brachysira intermedia (Østrup) Lange-Bertalot	1		0.42		0.028								6		0.92		3.5	
Navicula cf. *submuralis* Hustedt	1		0.42		0.025								4		0.17		0.3	

Species	Analysis with single classes						Analysis combining classes						Species frequency (*f*) and abundance (n)					
	Group		IndVal		p		Comb.		IndVal		p		*f*		Mean n		Max n	
	T	E	T	E	T	E	T	E	T	E	T	E	T	E	T	E	T	E
Pseudostaurosira pseudoconstruens (Marciniak) Williams & Round							1+2	1+2	0.7	0.61	0.025	0.039	32	25	4.87	1.19	68.7	5.4
Gomphonema auritum Braun							1+2		0.58		0.038		20		0.47		2.5	
Meridion circulare (Greville) Agardh							1+2		0.49		0.029		11		0.21		0.4	
Ulnaria biceps (Kützing) Compère sensu lato		1		0.47		0.050	1+2		0.46		0.041		10	11	0.12	0.11	0.2	0.2
Psammothidium levanderi (Hustedt) Bukhtiyarova & Round		1		0.73		0.001								35		0.4		1.7
Staurosirella pinnata (Ehrenberg) Williams & Round		1		0.68		0.049								42		1.15		14.8
Nitzschia acidoclinata Lange-Bertalot		1		0.66		0.05								41		0.96		7.4
Psammothidium didymum (Hustedt) Bukhtiyarova & Round		1		0.66		0.001								10		0.38		1.1
Navicula radiosa Kützing		1		0.62		0.01								21		0.19		0.5
cf. *Achnanthidium atomus* (Hustedt) Monnier, Lange-Bertalot & Ector		1		0.59		0.01								18		0.81		2.6
Nitzschia sp. No. 5 Arratille		1		0.59		0.008								11		0.26		0.7
Cavinula pseudoscutiformis (Hustedt) Mann & Stickle		1		0.58		0.015								14		0.22		1.1
Navicula pseudoventralis Hustedt *sensu* Krammer & Lange-Bertalot		1		0.57		0.001								4		0.45		0.8
Pseudostaurosira sp No. 2 Acherito		1		0.57		0.02								21		0.76		3.1
Gomphonema sp. No. 9 Posets		1		0.45		0.022								7		0.43		1.9
Cocconeis neothumensis Krammer		1		0.44		0.046								6		0.28		1.1
Pseudostaurosira cf. *brevistriata* (Grunow) Williams & Round								1+2		0.63		0.015		21		1.24		15.4
Achnanthidium minutissimum (Kützing) Czarnecki	2		0.7		0.038								71		11.63		68.3	
Encyonopsis microcephala (Grunow) Krammer	2		0.53		0.018								11		0.67		2.9	
Rossithidium pusillum (Grunow) Round et Bukhtiyarova	2		0.49		0.043								14		0.36		2.0	

Species	Analysis with single classes						Analysis combining classes						Species frequency (*f*) and abundance (n)					
	Group		IndVal		p		Comb.		IndVal		p		*f*		Mean n		Max n	
	T	E	T	E	T	E	T	E	T	E	T	E	T	E	T	E	T	E
Gomphonema lateripunctatum Reichardt & Lange-Bertalot	2		0.46		0.05								10		2.64		9.6	
Cyclotella sp No. 1 Llebreta	2		0.4		0.044								6		0.28		0.5	
Planothidium distinctum (Messikommer) Lange-Bertalot	3		0.52		0.029								13		0.35		0.8	
Denticula tenuis Kützing							2+3	2+3	0.71	0.79	0.015	0.019	34	48	5.58	6.35	48.6	44.5
Nitzschia sp No. 1 Sen							2+3		0.69		0.027		33		0.88		3.2	

The analyses of indicator species using tropic classes found a higher number in the epilithon samples than in the sediments. A few species were indicator of combined classes. There was a high number of indicator species for classes 3 and 5, particularly concerning to epilithon samples and sediment samples, respectively.

Indicator species of environment with low DIN and low TP were *Encyonema hebridicum*, *Eunotia exigua*, *Eunotia subarcuatoides*, *Pinnularia microstauron* var. *nonfasciata*, *Brachysira intermedia* (Figure 7.12A), *Eunotia mucophila*, *Eunotia novaisiae*, *Peronia fibula*, *Pinnularia subcapitata* and *Psammothidium scoticum*. *Psammothidium helveticum* was the only species indicative of an environment with a low phosphorous concentration (Figure 7.12B).

Epilithon indicators of high TP were *Asterionella formosa*, *Diatoma mesodon*, *Gomphonema* cf. *acidoclinatum* and *Gomphonema montanum*. Species with high occurrence in sediment samples and indicators of high TP were *Cavinula pseudoscutiformis*, *Navicula radiosa*, *Nitzschia* cf. *perminuta* M2, *Pseudostaurosira* sp. No. 2 Acherito, *Staurosira construens* var. *venter*, and *Ulnaria biceps*. *Navicula* aff. *minima* (Figure 7.12C), *Encyonema neogracile*, *Meridion circulare* (Figure 7.12D) were the only taxa indicative of low TN.

Species with a high occurrence in sediment samples and indicator of class 5 were *Cymbopleura subaequalis*, *Diploneis* cf. *peterseni*, *Encyonema minutum*, *Encyonema silesiacum*, *Encyonopsis subminuta* (Figure 7.12E), *Gomphonema pumilum*, *Navicula catalanogermanica*, *Navicula cryptotenella* (Figure 7.12F), *Nitzschia* sp. No. 1 Sen and *Nitzschia acidoclinata*.

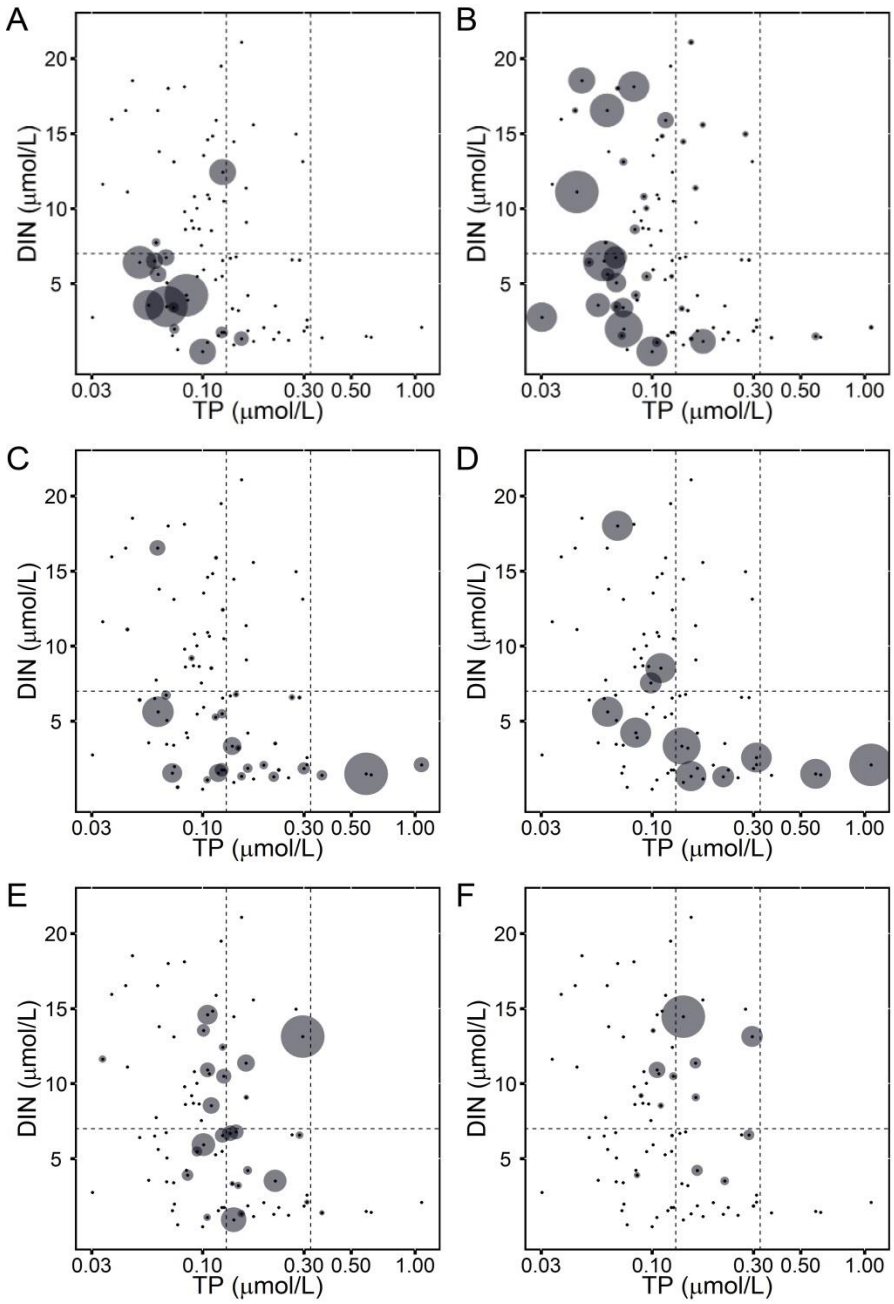

Figure 7.12. Relative abundance of A) *Brachysira intermedia*, B) *Psammothidium helveticum*, C) *Navicula aff. minima*, D) *Meridion circulare*, E. *Encyonopsis subminuta*, and F. *Navicula cryptotenella* across dissolved inorganic nitrogen (DIN) and total phosphorous (TP) gradients. Points correspond to the lakes studied and the shaded circle size indicates the specie abundance relative to the highest value in the data set.

Table 7. Diatom species indicative value (IndVal) and statistical significance of the association (p) with trophic classes described in Figure 7.6B The analysis was carried out following Dufrêne and Legendre (1997) and combining classes (De Cáceres et al. 2010). T: sediment top samples, E: epilithon samples.

	Analysis with single classes						Analysis combining classes						Species frequency (*f*) and abundance (n)					
	Group		IndVal		p		Comb.		IndVal		p		f		Mean n		Max n	
Species	T	E	T	E	T	E	T	E	T	E	T	E	T	E	T	E	T	E
Pinnularia microstauron var. *nonfasciata* Krammer	1		0.67		0.044								30		5.20		73.21	
Eunotia exigua (Brébisson Kützing) Rabenhorst	1		0.66		0.014								17		0.82		3.85	
Encyonema hebridicum Grunow ex Cleve	1		0.57		0.048								19		1.70		7.16	
Eunotia subarcuatoides Alles, Norpel & Lange-Bertalot	1	1	0.56	0.62	0.047	0.038							14	15	2.62	10.01	13.33	68.71
Eunotia novaisiae Lange-Bertalot & Luc Ector		1		0.68		0.013								24		0.93		4.37
Psammothidium helveticum (Hustedt) Bukhtiyarova et *Psammothidium scoticum* (Flower et Jones) Bukhtiyarova & Round		1		0.67		0.043	1+4		0.79		0.027			50		2.03		13.27
Brachysira intermedia (Østrup) Lange-Bertalot		1		0.65		0.028								21		2.55		17.00
Eunotia mucophila (Lange-Bertalot & Nörpel-*Pinnularia subcapitata* Gregory		1		0.63		0.012								14		20.42		61.50
Peronia fibula (Brébisson in Kützing) Ross		1		0.61		0.039								15		2.86		19.48
Rossithidium pusillum (Grunow) Round et Bukhtiyarova		1		0.61		0.03								24		0.45		2.19
Cymbella cf. *neocistula* Krammer		1		0.60		0.027								12		0.87		3.29
Encyonopsis microcephala (Grunow) Krammer		2		0.64		0.044								29		0.55		4.47
Discostella stelligera (Cleve & Grunow) Houk & Klee		2		0.51		0.043								9		0.18		0.30
Gomphonema spp. cf. *Gomphonema parvulum* (Kützing) Kützing							2+4		0.64		0.039			23		4		20.18
Asterionella formosa Hassall							2+3		0.74		0.033			37		19.52		80.65
Diatoma mesodon Kützing	3	3	0.70	0.66	0.024	0.014							13	15	2.60	0.25	28.91	1.89
Meridion circulare (Greville) Agardh	3		0.65		0.012								9		6.17		29.28	
Navicula sp. No. 1 Laurenti	3		0.64		0.028								32		0.39		1.70	
Gomphonema cf. *acidoclinatum* Lange-Bertalot &	3		0.57		0.043								11		0.21		0.39	
	3		0.49		0.032								2		0.64		0.98	
	3		0.46		0.037								4		0.64		1.28	

	Analysis with single classes						Analysis combining classes						Species frequency (*f*) and abundance (n)					
	Group		IndVal		p		Comb.		IndVal		p		f		Mean n		Max n	
Species	T	E	T	E	T	E	T	E	T	E	T	E	T	E	T	E	T	E
Gomphonema montanum Schumann	3		0.46		0.033								2		0.20		0.20	
Psammothidium rossii (Hustedt) Bukhtiyarova et Round		3		0.84		0.001								8		0.31		1.70
Navicula spp. aff. N. *minima*		3		0.76		0.009	1+2+3	2+3	0.74	0.8	0.043	0.007		31		0.95		9.18
Navicula absoluta Hustedt sensu lato		3		0.71		0.005								2		0.25		0.30
Pinnularia sp. 17 Cap Long		3		0.69		0.005								3		0.17		0.30
Staurosira construens var. *venter* (Ehrenberg) Hamilton		3		0.67		0.04								31		1.96		27.46
Planothidium frequentissimum (Lange-Bertalot) Lange-		3		0.64		0.008								7		0.20		0.70
Staurosirella oldenburgiana (Hustedt) Morales		3		0.64		0.005								6		0.30		0.70
Cavinula pseudoscutiformis (Hustedt) Mann & Stickle		3		0.62		0.02								14		0.22		1.10
Nitzschia cf. *perminuta* (Grunow) Peragallo M2		3		0.62		0.025								19		0.32		0.99
Psammothidium didymum (Hustedt) Bukhtiyarova & Round		3		0.62		0.016								10		0.38		1.09
Navicula radiosa Kützing		3		0.59		0.022		2+3		0.61		0.042		21		0.19		0.50
Pseudostaurosira sp. No. 2 Acherito		3		0.59		0.037								21		0.76		3.08
Cavinula cocconeiformis (Gregory ex Greville) Mann		3		0.58		0.024								5		0.28		0.69
Planothidium distinctum (Messikommer) Lange-Bertalot		3		0.57		0.045								8		0.19		0.40
Ulnaria biceps (Kützing) Compère sensu lato		3		0.57		0.026								11		0.11		0.20
Gomphonema sp. No. 9 Posets		3		0.51		0.04								7		0.43		1.90
Planothidium oestrupii (Cleve-Euler) Round & Bukhtiyarova		3		0.49		0.017								2		0.25		0.40
Caloneis sp. No. 2 Posets		3		0.48		0.037								2		0.15		0.20
Eunotia cf. *circumborealis* Lange-Bertalot & Nörpel		3		0.47		0.03								2		0.10		0.10
Encyonema neogracile Krammer								1+2+3		0.7		0.029		26		1.23		14.23
Amphora cf. *eximia* Carter								2+5		0.5		0.042		6		0.18		0.4
Psammothidium chlidanos (Hohn & Hellerman) Lange-								2+5		0.58		0.025		5		0.14		0.2
Staurosirella pinnata (Ehrenberg) Williams & Round								2+3+5		0.77		0.044		42		1.15		14.77
Rossithidium pusillum (Grunow) Round et								2+3+5		0.73		0.011		29		0.55		4.47

	Analysis with single classes						Analysis combining classes						Species frequency (*f*) and abundance (n)					
	Group		IndVal		p		Comb.		IndVal		p		f		Mean n		Max n	
Species	T	E	T	E	T	E	T	E	T	E	T	E	T	E	T	E	T	E
Denticula tenuis Kützing							2+4+5	2+4+5	0.73	0.85	0.041	0.001	34	48	5.58	6.35	48.62	44.54
Navicula cryptotenella Lange-Bertalot	5		0.86		0.001								15		1.61		13.23	
Nitzschia acidoclinata Lange-Bertalot	5		0.73		0.032								34		0.76		8.06	
Surirella angusta Kützing	5		0.72		0.005								8		0.24		0.80	
Encyonema silesiacum (Bleisch) Mann	5		0.71		0.006								54		0.63		3.05	
Nitzschia sp. No. 1 Sen	5		0.70		0.011								33		0.88		3.25	
Encyonema minutum (Hilse) Mann	5		0.68		0.047								57		2.02		17.37	
Gomphonema pumilum (Grunow) Reichardt & Lange-	5		0.68		0.016								20		0.44		3.18	
Navicula catalanogermanica Lange-Bertalot & Hofmann	5		0.66		0.017								14		1.99		11.04	
Encyonema obscurum var. *alpina* Krammer	5		0.63		0.003								3		0.43		1.09	
Encyonopsis subminuta Krammer & Reichardt	5		0.63		0.038								26		0.89		6.35	
Encyonema sp. No. 1 Mora	5		0.61		0.025								10		1.92		13.99	
Diploneis cf. *peterseni* (petersenii) Hustedt	5		0.58		0.031								13		0.51		2.98	
Encyonopsis cesatii (Rabenhorst) Krammer	5		0.57		0.036								9		0.36		1.09	
Gomphonema sp. No. 4 Posets	5		0.57		0.029								8		0.33		1.19	
Cymbopleura subaequalis (Grunow) Krammer	5		0.54		0.046								11		0.29		0.99	
Psammothidium chlidanos (Hohn & Hellerman) Lange-		5		0.52		0.025								5		0.14		0.20
Luticola cf. *mutica* (Kützing) Mann		5		0.50		0.007								3		0.10		0.10

The analysis of indicator species for the three criteria of Si limitation (described in Figure 7.10) showed a higher number of indicator species when Si:TN ratio was lower than 1:1 (Table 8). Frequent species related with low Si concentration (Si≤10µmol) were *Encyonema neogracile* Krammer, *Nitzschia acidoclinata* Lange-Bertalot, and *Achnanthidium pyrenaicum* (Hustedt) Kobayasi. Common species related with Si:N ratio ≤ 1:1 were *Encyonema minutum* (Hilse) Mann, *Encyonopsis subminuta* Krammer & Reichardt, *Denticula tenuis* Kützing, *Fragilaria* sp. No. 8 Redon and *Naviculadicta* cf. *digitulus* (Hustedt) Lange-Bertalot.

Some common species indicator for environment with Si:TP ratio ≤ 100:1 included *Encyonopsis microcephala* (Grunow) Krammer and *Rossithidium pusillum* (Grunow) Round et Bukhtiyarova. Species related with environments of low Si concentration and low Si:TN, and Si:TP ratio were *Achnanthidium pyrenaicum* (Hustedt) Kobayasi, *Encyonema reichardtii* (Krammer) Mann, *Gomphoneis* cf. *olivaceoides* (Hustedt) Carter and, *Sellaphora pupula* (Kützing) Mereschkowsky sensu lato.

Diatoma mesodon Kützing was the only indicator species of both environments with high Si:N and Si:P ratios (Figure 7.13C and D). *Navicula* sp. No. 7 Bergus, was associated with higher Si:N ratio and *Psammothidium marginulatum* (Grunow) was an indicator for environment with Si:TP ratio higher than 100:1.

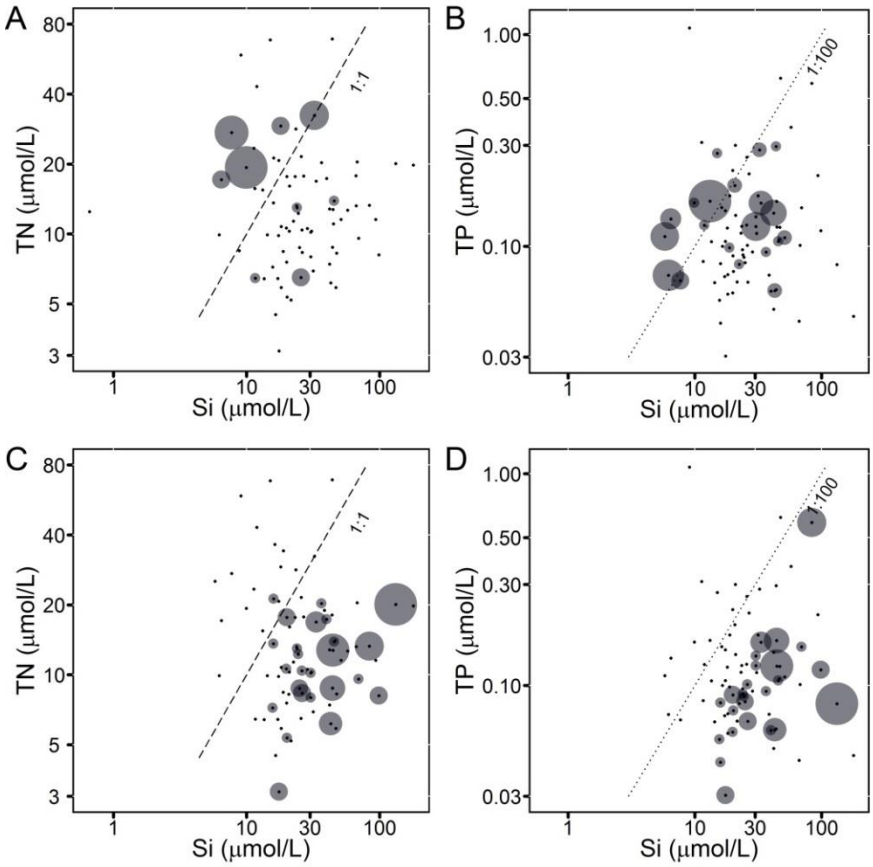

Figure 7.13. Relative abundance of A) *Geissleria similis*, B) *Achnanthidium pyrenaicum*, and C) and D) *Diatoma mesodon* with respect to Si and total nitrogen (TN) and total phosphorous (TP), respectively. Points correspond to the lakes studied and the shaded circle size indicates the specie abundance relative to the highest value in the data set.

Table 8. Diatom species indicative value (IndVal) and statistical significance of the association (p) with three criteria of Si limitation: Si≤10µmol, Si≤ N 1:1, and Si:TP≤ 100:1. The analysis was carried out following Dufrêne and Legendre (1997) and combining classes (De Cáceres et al. 2010). T: sediment top samples, E: epilithon samples.

	Si≤10µmol				Si≤ N 1:1				Si:TP ≤ 100:1				Species frequency (*f*) and abundance (n)					
	IndVal		p		IndVal		p		IndVal		p		*f*		Mean n		Max n	
Species	T	E	T	E	T	E	T	E	T	E	T	E	T	E	T	E	T	E
Achnanthidium cf. *atomus* (Hustedt) Monnier, Lange-Bertalot & Ector					0.75		0.016						21		1.19		6	
Fragilaria sp. No. 8 Redon					0.74		0.040						33		2.77		22.8	
Nitzschia cf. *bryophila* (Hustedt) Hustedt					0.73		0.014						22		0.48		2.4	
Naviculadicta digituloides Lange-Bertalot					0.67		0.043						27		1.37		9.5	
Naviculadicta cf. *difficillima* Hustedt					0.66		0.022						18		0.28		1.0	
Amphora cf. *eximia* Carter					0.65		0.048						22		1.52		6.9	
Geissleria similis (Krasske) Lange-Bertalot & Metzeltin	0.64		0.007		0.65		0.011						9		0.48		1.8	
Planothidium distinctum (Messikommer) Lange-Bertalot					0.65		0.020						13		0.35		0.8	
Navicula sp No. 2 Liat	0.62		0.014		0.64		0.026						12		0.48		1.2	
Achnanthes sp No. 3 Posets	0.51		0.032		0.63		0.013						7		0.59		1.7	
Navicula medioconvexa Hustedt					0.61		0.045						16		0.48		2.4	
Aulacoseira cf. *ambigua* (Grunow) Simonsen					0.58		0.012						2		1.28		1.4	
Stauroneis smithii Grunow	0.53		0.008		0.58		0.010						2		0.10		0.1	
Psammothidium chlidanos (Hohn & Hellerman) Lange-Bertalot					0.57		0.007						4		0.20		0.4	
Navicula venerablis Hohn & Hellerman	0.64		0.023		0.56		0.030						14		0.45		1.2	
Psammothidium bioretii (Germain) Bukhtiyarova & Round					0.55		0.020						9		0.14		2.1	
Fragilaria spp					0.55		0.026						7		0.81		2.0	
Nupela cf. *gracillima* (Hustedt) Lange-Bertalot	0.50		0.037		0.55		0.036						7		1.26		3.3	
Naviculadicta vitabunda (Hustedt) Lange-Bertalot					0.54		0.031						10		0.23		0.4	
Stauroneis sp No. 3 Negre					0.53		0.036						5		0.12		0.2	
Nitzschia gracilis Hantzsch	0.64		0.002		0.53		0.041						6		0.26		0.6	
Hippodonta costulata (Grunow) Lange-Bertalot, Metzeltin & Witkowski					0.47		0.039						6		1.23		5.7	
Rossithidium pusillum (Grunow) Round et Bukhtiyarova									0.71		0.008		29		0.56		1.9	
Sellaphora pupula (Kützing) Mereschkowsky sensu lato	0.64		0.014						0.59		0.019		16		4.44		51.1	

Species	Si≤10µmol IndVal T	Si≤10µmol IndVal E	Si≤10µmol p T	Si≤10µmol p E	Si≤ N 1:1 IndVal T	Si≤ N 1:1 IndVal E	Si≤ N 1:1 p T	Si≤ N 1:1 p E	Si:TP ≤ 100:1 IndVal T	Si:TP ≤ 100:1 IndVal E	Si:TP ≤ 100:1 p T	Si:TP ≤ 100:1 p E	Species frequency (*f*) and abundance (n) *f* T	*f* E	Mean n T	Mean n E	Max n T	Max n E
Asterionella formosa Hassall									0.45		0.042		9		6.17		29.2	
Surirella angusta Kützing									0.44		0.038		8		0.24			
Hippodonta cf. *neglecta* Lange-Bertalot, Metzeltin & Witkowski		0.58		0.006					0.44	0.39	0.025	0.027	6	2	2.78	0.50		0.6
Hantzschia cf. *amphioxys* (Ehrenberg) Grunow									0.42		0.034		5		0.12			
Gomphonema acuminatum Ehrenberg									0.38		0.037		2		0.30			
Gomphonema sp No. 15 Coronas		0.58		0.037					0.38		0.031		3	14	3.21	3.01		
Naviculadicta cf. *stauroneioides* Lange-Bertalot									0.37		0.038		4		0.45			
Luticola sp No. 5 Coronas									0.36		0.045		4		0.17			
Achnanthidium pyrenaicum (Hustedt) Kobayasi		0.84		0.002						0.70		0.001		20		0.87		5.7
Cavinula cocconeiformis (Gregory ex Greville) Mann & Stickle		0.47		0.041										5		0.28		0.7
Cymbopleura naviculiformis (Auerswald) Krammer	0.60		0.025										10		0.27		0.7	
Cymbopleura subaequalis (Grunow) Krammer	0.58		0.026										11		0.29		1.0	
Diadesmis perpusilla (Grunow) Mann						0.81		0.001						13		0.53		4.2
Encyonema reichardtii (Krammer) Mann		0.70		0.008						0.57		0.018		16		0.66		3.4
Encyonema neogracile Krammer	0.71		0.017										23		0.65		4.6	
Encyonopsis microcephala (Grunow) Krammer										0.61		0.043		23		4.00		20.2
Eucocconeis laevis Østrup		0.64		0.036		0.64		0.032						19		0.47		1.9
Gomphonema cf. *parvulum* (Kützing) Kützing	0.65		0.011										13		2.60		28.9	
Gomphoneis cf. *olivaceoides* (Hustedt) Carter		0.70		0.002						0.47		0.010		5		0.58		2.0
Krasskella kriegerana (Krasske) Ross & Sims										0.51		0.023		11		0.33		0.9
Navicula catalanogermanica Lange-Bertalot & Hofmann		0.52		0.026						0.41		0.035		5		0.22		0.6
Navicula cryptocephala Kützing		0.55		0.033						0.51		0.021		11		0.21		0.5
Nitzschia acidoclinata Lange-Bertalot	0.74	0.78	0.029	0.038									34	41	0.76	0.96	9.1	7.4
Nitzschia sp No. 5 Arratille	0.54		0.026										9		0.25		0.4	
Pinnularia acuminata Smith	0.49		0.039										6		0.28		0.8	
Stauroneis acidoclinata Lange-Bertalot & Werum		0.55		0.022						0.44		0.040		7		0.27		0.8

8. Physical factors

Physical factors such as temperature and light have a strong influence on algae in benthic and planktonic environments (Lowe 1996; Reynolds 2006). Water transparency, as measured using Secchi disk depth, for instance, is a surrogate for the light environment that the algae can be experiencing in a lake (Margalef 1983). Both abiotic and biological factors determine water transparency. The input of materials from the catchment through tributaries and the resuspension of sediments from the bottom caused by the wind increase the turbidity and thus reduce the light availability. Changes in algal biomass related with the eutrophication and the accumulation of organic dissolved compounds also affect the quantity and quality of the energy in the water column (Wetzel 2001).

Besides the fundamental role of light in photosynthesis, its influence on freshwater algae assemblages have not been studied as much as the role of nutrients (Hill 1996). In fact, in practice, nutrient, light and micro-habitat can present a high correlation in a lake. The study of diatom composition through the depth gradient in a set of oligotrophic lakes showed that light influenced benthic diatom abundance but composition was principally related to the substrate type (Yang and Flower 2012). Other studies indicate that the light gradient not only changes diatom biomass but also the community structure and physiological parameters (Cantonati et al. 2009; Kingsbury et al. 2012). The dominance of the main groups of algae growing on substrate may vary through the depth gradient. In some lakes, chlorophytes and diatoms are more common in shallow waters, whereas deep substrates are dominated by cyanobacteria (Sánchez et al. 2013).

Temperature is a key factor for any biological process and has an obvious connection to climate; therefore, it has been the focus of many environmental reconstructions. Planktonic and benthic algal growth is strongly related with temperature if nutrients and light are available and, as a consequence, maximum biomass usually is found in spring to late summer (DeNicola 1996; Reynolds 1984). Diatoms have been used to reconstruct the past water temperature of lakes (Schmidt et al. 2012; Thies et al. 2012; Von Gunten et al. 2008). However, there are also arguments against the adequacy of its use based on the strong seasonality of many diatoms species (Anderson 2000; Köster and Pienitz 2006) and the overall confounding influence of pH (Larocque and Bigler 2004). This

criticism could also be applied to the reconstruction of any other variable with the exception of pH.

The lakes of the Pyrenees are ice covered on average around half of the year. The duration of the ice and snow cover determines the growth period (light limitation) for the photosynthetic organisms and influences lake temperature throughout a long period of the year. It could be expected some influence on the diatom assemblages, with potential for reconstruction, although previous broad European surveys have not found diatom assemblage patterns related to ice duration (Catalan et al. 2009a), a transfer function of the ice-free period duration have been developed based on species individual response (Curtis et al. 2009).

The aim of this section was to identify diatom species statistically related with physical gradients. Distributions across gradients and potential indicator species were explored concerning ice cover duration, summer surface water temperature and the light environment of the lakes.

Diatom response to physical gradients

The comparison of the species range distribution with the optima evaluated considering their relative abundance provided contrasting results for distinct physical gradients (Figure 8.1). There was not much differentiation in the length of the range across the ice cover duration and the optima mostly matched with the median of the distribution, particularly at intermediate values between 160 and 180 days. However, at the extremes, these two parameters differentiate; thus extreme conditions in ice cover seem to have more influence in differential species growth. The length of the range across temperature was also broad but in this case the differentiation between optimum and median was stronger than for the ice cover duration, from about 12 ^{o}C downwards the difference between the two parameters increased progressively. Low temperatures appears more species selective than warmer conditions.

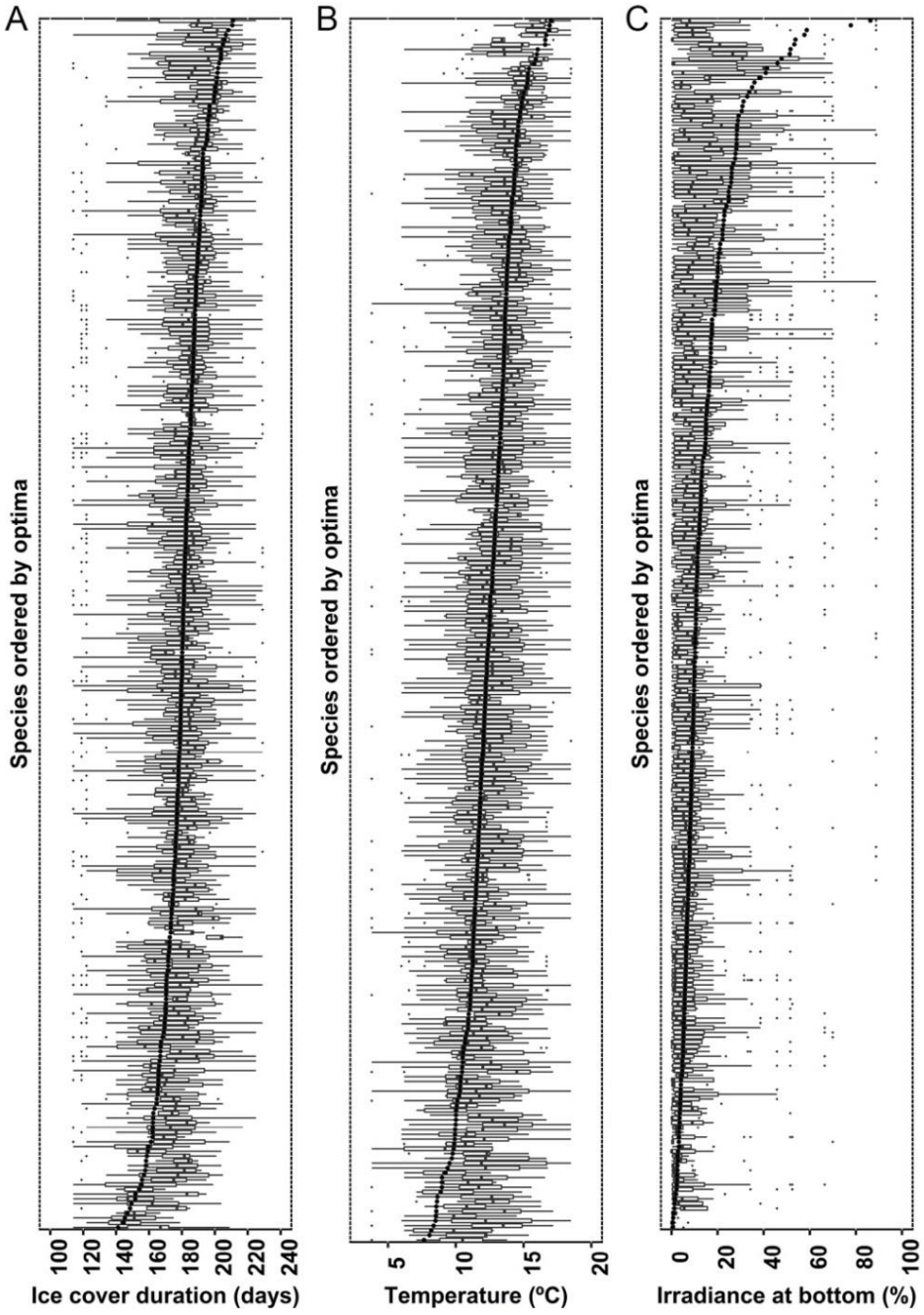

Figure 8.1. Optima (dark points) and environmental range distribution (boxplot) of diatom species (frequency>3 lakes) for ice cover duration (A), temperature (B) and irradiance at the bottom (C) of sediment samples. Outliers are represented with small crosses.

Mountain lakes are highly transparent; enough irradiance usually arrives to the bottom to sustain net productivity. In shallow lakes and in very high transparent ones, littoral conditions may extent to the bottom forming a differentiated biofilm compared to more light-limited bottoms (Buchaca and Catalan 2008). The estimation of the surface irradiance remaining at the bottom (see methods section for details) provides a way to figure out the possible influence on diatom assemblages (Figure 8.1). The length of the range increases following the optimum. Lakes well illuminated at the bottom may hold a broader diversity of species. In this case, optimum differentiates from the median of the distribution, the higher the percentage from about 20% upwards. As in the case of other factors, these patterns do not indicate any causal link between species and physical factors, but they do confirm that species statistical responses are quite different among these three factors that at first may seem quite related. In the following sections, the details of the association between species and factor are further analysed.

Diatom response to ice cover duration

The ice cover duration in the Pyrenean lakes was markedly related to altitude, as occur in other mountain lakes (Catalan et al. 2009b), and was independent of lake depth (Figure 8.2). Lakes were grouped in four classes of ice cover duration to analyse the species association with this factor: class 1 included lakes with ice cover duration <160 days; class 2, from 160 to 180 days; class 3 from 180 to 195 days; and class 4 lakes >195 days. Lakes of groups 2 and 3 are in the middle altitudinal range and consequently they include more morphological variety (e.g., lake depth) than classes 1 and 4.

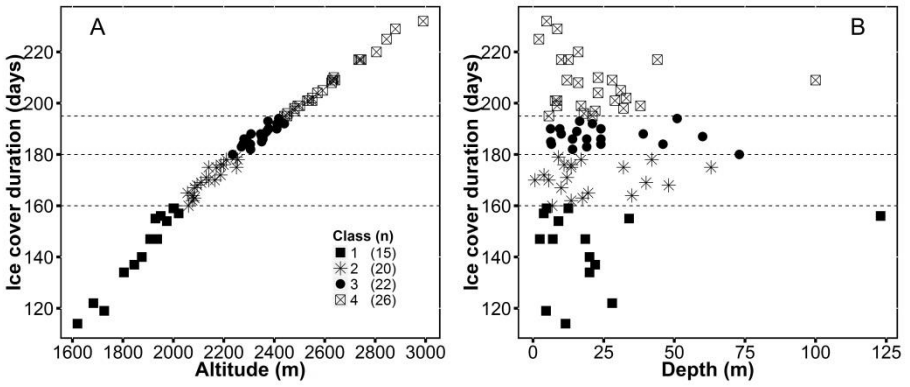

Figure 8.2. Relationships between ice cover duration and altitude (A), and depth (B).

The analysis of indicator species showed that the common epilithon species *Gomphonema lateripunctatum* (Figure 8.3A) and *Encyonopsis* cf. *krammeri* Reichardt are significant indicators of the lowest ice cover duration class (Table 9). Sediment samples showed indicator species for combined classes 1+2; e.g., *Encyonopsis subminuta*, *Navicula wildii* (Figure 8.3B), *Meridion circulare* and *Ulnaria biceps*.

Group 3 was represented principally by *Eunotia* such as *E. subarcuatoides* (Figure 8.3C), *E. intermedia*, *E. implicata*, and *E. catalana*. The species *Staurosira construens* var. *venter* (Figure 8.3D), *Navicula* spp. aff. N. *minima*, *Fragilaria* sp 9 Redon and *Cyclotella praetermissa* Lund, showed significant relation with ice cover duration <195 days (group of classes 1+2+3). Moreover, the species *Pinnularia* cf. *brebissonii* var. *minuta* and *Karayevia suchlandtii* (Figure 8.4A) showed a preference of lakes with ice cover duration <160 days (group of classes 2+3+4). Thus, there are many species that fundamentally avoid the extremes of the ice cover gradient (or one of them).

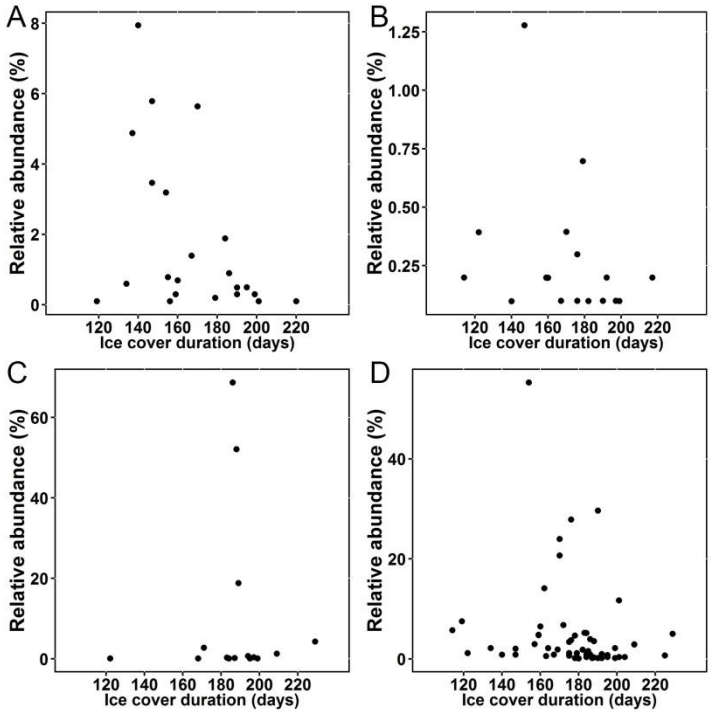

Figure 8.3. *Gomphonema lateripunctatum* (A), *Navicula wildii* (B), *Eunotia subarcuatoides* (C) and *Staurosira construens* var. *venter* (D) across the gradient of ice cover duration.

Table 9. Diatom species indicative value (IndVal) and statistical significance of association (p) with classes of ice cover duration. The analysis was carried out following Dufrêne and Legendre (1997) and combining classes (De Cáceres et al. 2010). T: sediment top samples, E: epilithon samples. Classes are ice cover duration <160 days (1), 160-180 days (2), 180-195 days (3), and >195 days (4).

Species	Indicator analysis						Species frequency (*f*) and abundance (n)					
	Class		IndVal		p		*f*		Mean n		Max n	
	T	E	T	E	T	E	T	E	T	E	T	E
Gomphonema lateripunctatum Reichardt & Lange-Bertalot		1		0.73		0.001		22		1.8		7.9
Encyonopsis cf. *krammeri* Reichardt		1		0.67		0.012		26		7.2		48.2
Encyonopsis descripta (Hustedt) Krammer	1		0.54		0.005		7		0.1		0.2	
P. parasitica var. *subconstricta* (Grunow) Morales	1		0.53		0.024		14		0.3		1.6	
Achnanthidium cf. *minutissimum* (Kützing) Czarnecki M1	1		0.5		0.015		9		1.2		4.4	
Cyclotella sp. No. 1 Llebreta	1		0.49		0.008		6		0.3		0.5	
Cyclotella sp. No. 3 Laurenti	1		0.48		0.003		4		12.8		20.8	
P. frequentissimum (Lange-Bertalot) Lange-Bertalot	1		0.46		0.007		4		0.8		1.4	
Navicula cf. *oligotraphenta* Lange-Bertalot & Hofmann	1	1	0.46	0.38	0.008	0.03	4	2	0.4	0.1	0.6	0.2
Navicula trophicatrix Lange-Bertalot	1		0.46		0.025		8		0.7		1.9	
Fragilaria cf. *nanana* Lange-Bertalot	1		0.39		0.038		3		1.5		3.5	
Nitzschia sp. No. 11 Burg	1		0.38		0.04		3		1.5		2.9	
Stenopterobia densestriata (Hustedt) Krammer		2		0.47		0.001		4		0.3		1
Rossithidium linearis (Smith) Round et Bukhtiyarova	2		0.4		0.041		4		2.5		9.8	
Aulacoseira sp. No. 1 Gerber	2		0.39		0.028		4		5.0		14.6	
Punctastriata cf. *lancettula* (Schumann) Hamilton & Siver	1+2		0.68		0.009		25		4.1		43.5	
Encyonopsis subminuta Krammer & Reichardt	1+2		0.66		0.008		26		0.9		6.3	
Navicula wildii Lange-Bertalot	1+2		0.58		0.019		18		0.3		1.3	
Fragilaria cf. *vaucheriae* (Kützing) Petersen	1+2		0.49		0.018		9		0.3		1.4	
Meridion circulare (Greville) Agardh	1+2		0.49		0.024		11		0.2		0.4	
Ulnaria biceps (Kützing) Compère sensu lato	1+2		0.45		0.045		10		0.1		0.2	
Neidium cf. *ampliatum* (Ehrenberg) Krammer		1+2		0.4		0.035		5		0.1		0.2
Eunotia subarcuatoides Alles, Nörpel & Lange-Bertalot		3		0.56		0.037		15		10.0		68.7
Eunotia intermedia (Krasske) Nörpel & Lange-Bertalot		3		0.49		0.046		12		2.2		8.2
Pinnularia sp. No. 10 Pica Palomera	3		0.42		0.049		5		2.6		11.9	
Eunotia implicata Nörpel, Alles & Lange-Bertalot	3		0.4		0.045		5		0.4		1	
Eunotia catalana Lange-Bertalot & Rivera-Rondón		3		0.4		0.048		6		0.5		1
Gomphonema montanum Schumann		3		0.38		0.034		3		0.2		0.3
Sellaphora disjuncta (Hustedt) Mann		3		0.38		0.03		3		0.1		0.2
Staurosira construens var. *venter* (Ehrenberg) Hamilton	1+2+3		0.87		0.008		55		5.3		55.3	
Navicula spp. aff. N. *minima*		1+2+3		0.67		0.033		31		0.9		9.2
Fragilaria sp. No. 9 Redon		1+2+3		0.66		0.022		25		1.1		13.6
Cyclotella praetermissa Lund	1+2+3		0.62		0.017		23		5.0		18.3	
Sellaphora pseudopupula (Krasske) Lange-Bertalot	1+3		0.72		0.044		33		1.4		28.9	
Eunotia novaisiae Lange-Bertalot & Luc Ector		2+3		0.61		0.031		24		0.9		4.4
Achnanthidium cf. *minutissimum* (Kützing) Czarnecki M3		2+3		0.56		0.036		19		0.3		0.7
Craticula cf. *vixnegligenda* Lange-Bertalot		4		0.45		0.006		5		0.1		0.2
Achnanthidium pyrenaicum (Hustedt) Kobayasi	1+4		0.71		0.007		32		1.1		8.8	
Pinnularia cf. *brebissonii* var. *minuta* Krammer	2+3+4		0.76		0.046		42		1.7		9.6	
Karayevia suchlandtii (Hustedt) Bukhtiyarova	2+3+4		0.72		0.027		38		0.5		1.6	

The type of diatom species distribution across the gradient of ice cover duration was diverse. In addition to significant indicator species for the classes summarised in table 6, there were species such as *Encyonema hebridicum*

Grunow ex Cleve (Figure 8.4B) and *Pinnularia* cf. *subanglica* Krammer that were present along the whole gradient but showed higher abundance in lakes with intermediate values of ice cover duration. Other species, such as *Staurosirella pinnata*, *Encyonema minutum* (Figure 8.4C), *Naviculadicta digituloides* and *Pinnularia* cf. *brebissonii* var. *minuta*, were also widespread but showed higher abundance in lakes with long ice cover duration. Finally, there were some common species, such as *Encyonema silesiacum* and *Psammothidium levanderi* (Figure 8.4D), with random abundance throughout the gradient.

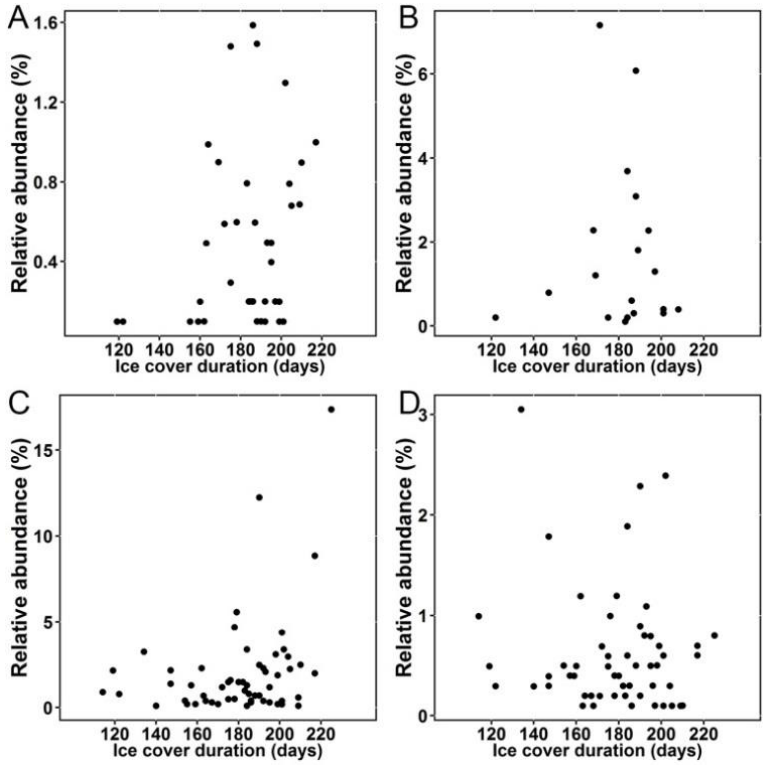

Figure 8.4. *Karayevia suchlandtii* (A), *Encyonema hebridicum* (B), *Encyonema minutum* (C) and *Encyonema silesiacum* (D) across the ice cover duration gradient.

Diatoms and summer surface water temperature

Summer surface water temperature (SSWT) showed a significant correlation with altitude, as it could be expected ($r = -0.64$, $p<0.001$, $n=83$, Figure 8.5). However, a regression partitioning analysis (carried out using the Package 'party'v.1.0-10 in R Development Core Team 2013) showed that the relationship changes at two possible threshold: 2550 m.a.s.l. ($p<0.001$) and 2270 m.a.s.l.

(p=0.003). When the data set is divided at the threshold 2270 m.a.s.l. lakes above 2270 m.a.s.l. had a significant correlation (r= -0.66, p=0.013, n=19) whereas lakes below 2270 m.a.s.l. were not significantly correlated (r= 0.15, p=0.38, n=58). The relationship between altitude and SSWT weakens at low altitude (water is colder than should be according the relationship at higher altitudes) because the lower is a lake, the higher the influence of streams bringing water from higher altitude. Temperature apparently did not show any relation with the bathymetric characteristics of the lakes.

In order to identify indicator species associated to temperature, lakes were grouped in three classes: the first group included the coldest lakes (< 10 ºC); the second group, lakes with temperatures between 10 and 15 ºC; and the third group included the warmest lakes (>15 ºC) (Figure 8.5A).

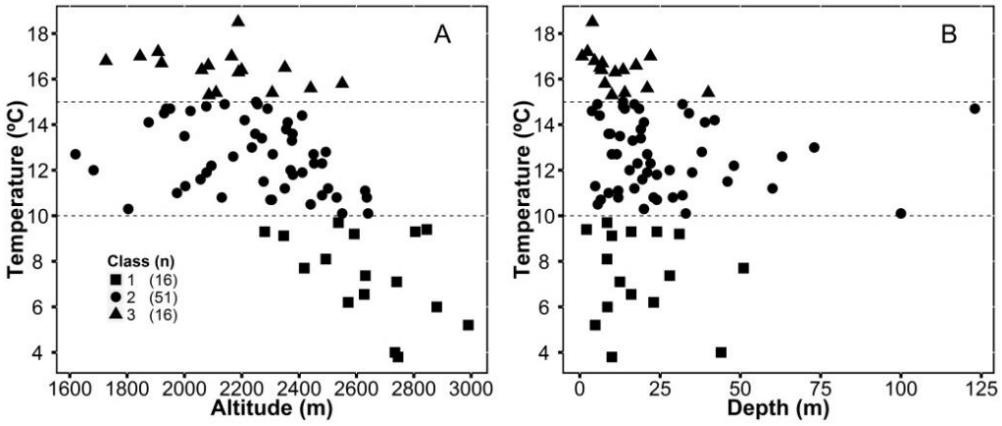

Figure 8.5. Relationships between summer surface water temperature and altitude (A), and depth (B).

Indicator analysis showed a few species significantly related with low temperatures, most of them from the sediment samples (Table 10). The common *Pinnularia microstauron var. nonfasciata* showed the highest indicator for class 1. Less frequent species such as *Surirella angusta* (Figure 8.6A), *Gomphonema* cf. *minusculum*, *Encyonema reichardtii*, *Hantzschia* cf. *amphioxys*, and *Geissleria acceptata* were also as indicators of <10 ºC SSWT.

Another common diatom, *Amphora cf. eximia*, was indicative of <15 ºC SSWT (group 1+2). However, no indicator species of class 2 was recorded. Probably as a consequence that the range of temperature corresponds to the most common conditions in the Pyrenean lakes.

Class 3 was represented by some frequent diatoms in sediment samples such as *Navicula* spp. aff. *N. minima* (Figure 8.6C), *Navicula* cf. *seminulum* and *Fragilaria* cf. *opacolineata*. Frequent species in epilithon samples such as *Encyonema neogracile*, *Navicula* spp. aff. *N. minima*, and *Cavinula pseudoscutiformis* were also significantly related with the warmest lakes (class 3, >15 ^{o}C).

Staurosira construens var. *venter* (Figure 8.6C), *Psammothidium levanderi*, *Sellaphora laevissima*, *Discostella stelligera*, *Pseudostaurosira* cf. *brevistriata*, and *Navicula radiosa*, common taxa in sediment samples, were indicators of environments with temperature >10ºC (classes 2+3).

The species with a wide thermal distribution could show some preference for intermediate values of temperature (e.g. *Cyclotella radiosa* (Figure 8.6C), *Cyclotella bodanica* var. i*ntermedia*, and *Fragilaria pararumpens*) or high temperature (e.g. *Navicula catalanogermanica*, *Navicula cryptocephala*). Some others were randomly distributed across the thermal gradient (e.g. *Karayevia suchlandtii*, *Achnanthidium minutissimum*).

Table 10. Diatom species indicative values (IndVal) and statistical significance of association (p) with classes of temperature. The analysis was carried out following Dufrêne and Legendre (1997) and combining classes (De Cáceres et al. 2010). T: sediment top samples, E: epilithon samples. Classes are: <10 ºC (1), 10-15 ºC (2), and >15 ºC (3).

Species	Indicator analysis						Species frequency (*f*) and abundance (n)					
	Class		IndVal		p		*f*		Mean n		Max n	
	T	E	T	E	T	E	T	E	T	E	T	E
P. microstauron var. *nonfasciata* Krammer	1		0.70		0.038		30		5.20		73.2	
Surirella angusta Kützing	1		0.53		0.007		8		0.24		0.8	
Gomphonema cf. *minusculum* Krasske	1		0.48		0.018		8		0.43		0.8	
Encyonema reichardtii (Krammer) Mann	1		0.48		0.004		3		2.08		4.1	
Hantzschia cf. *amphioxys* (Ehrenberg) Grunow		1		0.47		0.013		7		0.17		0.3
Geissleria acceptata (Hustedt) Lange-Bertalot & Metzeltin	1		0.45		0.03		7		0.47		1.7	
Diadesmis contenta (Grunow) Mann		1		0.45		0.018		3		0.23		0.3
P. cf. *brebissonii* var. *minuta* Krammer		1		0.44		0.034		7		0.16		0.3

Species	Indicator analysis						Species frequency (*f*) and abundance (n)					
	Class		IndVal		p		*f*		Mean n		Max n	
	T	E	T	E	T	E	T	E	T	E	T	E
A. cf. *minutissimum* (Kützing) Czarnecki M4	1		0.41		0.046		5		0.71		1.2	
Eunotia cf. *pseudogroenlandica* Lange-Bertalot & Tagliaventi	1		0.41		0.042		5		17		37.1	
Sellaphora cf. *nanoides* Lange-Bertalot, Cavacini, Tagliaventi & Alfinito	1		0.39		0.02		2		0.75		1.1	
Achnanthidium pfisteri Lange-Bertalot	1		0.39		0.046		4		3.43		7.4	
Nitzschia palea var. *debilis* (Kützing) Grunow	1		0.38		0.044		3		0.26		0.6	
Luticola sp. No. 5 Coronas	1		0.37		0.046		4		0.17		0.3	
Nitzschia sp No. 8 Bergus	1		0.35		0.049		4		0.20		0.20	
Amphora cf. *eximia* Carter	1+2		0.60		0.035		22		1.52		6.9	
Navicula spp. aff. *N. minima*	3	3	0.85	0.72	0.001	0.003	37	31	2.10	0.95	13.9	9.2
Stauroforma cf. *exiguiformis* (Lange-Bertalot) Flower, Jones & Round	3	3	0.72	0.58	0.002	0.024	15	15	0.81	0.86	2.29	4.7
Aulacoseira cf. *valida* (Grunow) Krammer	3		0.67		0.001		9		0.68		2.5	
Navicula cf. *seminulum* Grunow	3		0.66		0.035		28		1.41		11.5	
Encyonema neogracile Krammer		3		0.65		0.031		26		1.23		14.2
Navicula sp. No. 4 Laquettes	3		0.65		0.002		11		0.66		2.9	
Gomphonema aff. *Gomphonema* parvulum	3		0.62		0.004		13		2.60		28.9	
Fragilaria cf. *opacolineata* Lange-Bertalot	3		0.61		0.012		18		1.80		6.5	
C. pseudoscutiformis (Hustedt) Mann & Stickle		3		0.56		0.017		14		0.22		1.1
P. rossii (Hustedt) Bukhtiyarova et Round	3		0.56		0.005		8		1.04		2.8	
S. oldenburgiana (Hustedt) Morales	3		0.54		0.019		11		0.49		2.4	
Adlafia aff. *minuscula* (Grunow) Lange-Bertalot	3		0.52		0.003		4		0.20		0.4	
P. didymum (Hustedt) Bukhtiyarova & Round		3		0.51		0.009		10		0.38		1.1
Stauroneis gracilis Ehrenberg	3		0.48		0.017		7		0.20		0.5	
Navicula notha Wallace		3		0.47		0.044		11		0.78		2.7
Fragilaria cf. *nanana* Lange-Bertalot		3		0.46		0.009		3		0.43		1.0
Navicula pseudoventralis Hustedt sensu Krammer & Lange-Bertalot 1986		3		0.45		0.012		4		0.45		0.8
Nitzschia sp. No. 9 Mora	3		0.44		0.015		4		0.22		0.4	
Neidium cf. *ampliatum* (Ehrenberg) Krammer		3		0.44		0.006		5		0.14		0.2
Achnanthes spp.		3		0.38		0.033		2		0.25		0.3
Pinnularia cf. *viridis* (Nitzsch) Ehrenberg		3		0.38		0.024		2		0.25		0.4
R. linearis (Smith) Round et Bukhtiyarova		3		0.38		0.037		2		1.04		1.8
Nitzschia acidoclinata Lange-Bertalot	1+3		0.72		0.019		34		0.76		8.1	
Aulacoseira cf. *alpigena* (Grunow) Krammer	1+3		0.67		0.011		23		4.48		50.6	
Staurosira construens var. *venter* (Ehrenberg)	2+3	3	0.85	0.74	0.011	0.009	55	31	5.31	1.96	55.3	27.5
P. levanderi (Hustedt) Bukhtiyarova & Round	2+3		0.77		0.018		45		0.89		2.9	
Sellaphora laevissima (Kützing) Mann	2+3		0.75		0.007		37		0.54		4.5	
D. stelligera (Cleve & Grunow) Houk & Klee	2+3		0.73		0.018		37		19.52		80.7	
Pseudostaurosira cf. *brevistriata* (Grunow) Williams & Round	2+3		0.72		0.014		35		2.57		20.8	
Nitzschia cf. *alpina* Hustedt		2+3		0.68		0.019		32		0.86		3.2
Navicula radiosa Kützing	2+3	3	0.58	0.58	0.048	0.029	21	21	0.31	0.19	1.9	0.5

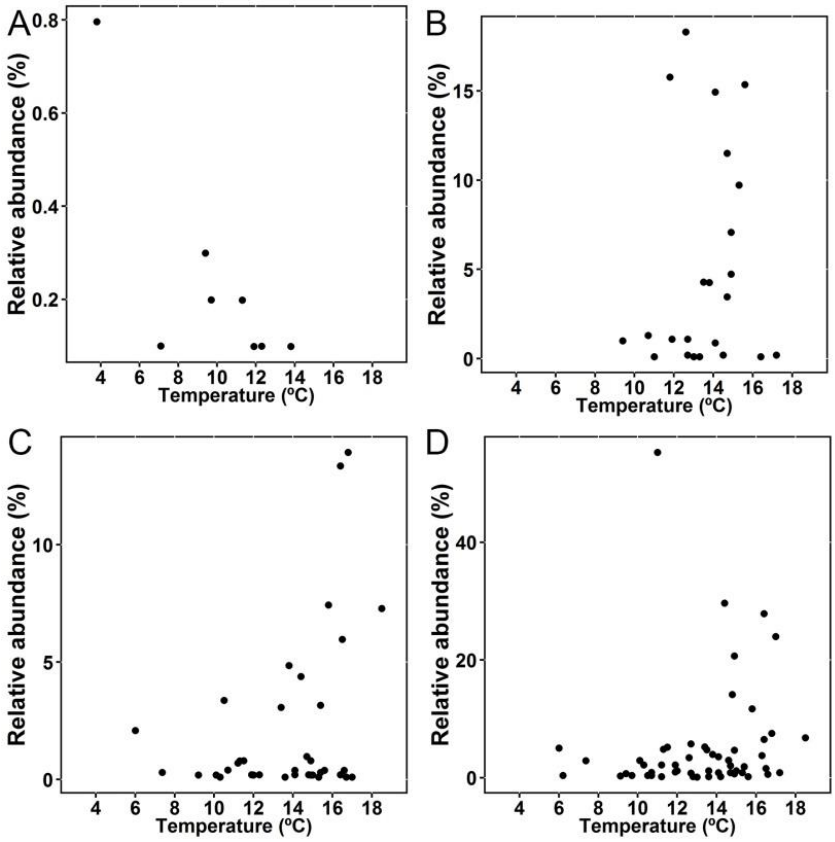

Figure 8.6. *Surirella angusta* (A), *Cyclotella radiosa* (B), *Navicula* spp. aff. *N. minima* (C) and *Staurosira construens* var. *venter* (D) across the summer surface water temperature (SSWT).

Light environment and diatom distribution

The Pyrenean lakes show a high water transparency. Irradiance at the bottom followed an asymptotic relation with depth, lakes between 5 and 40 m depth showing a higher variability in the percentage of irradiance (Figure 8.7).

In order to identify species of sediment samples related with the light environment, three different and complementary classification systems were used, respectively based on: irradiance at the bottom, lakes with an active diatom biofilm according to Buchaca and Catalan (2008), and a benthic classification which is describe later.

In the classification based on the irradiance at the bottom, lakes were grouped in three classes (Figure 8.7): class 1 included lakes with a summer irradiance at the bottom <10 µE/m^2/s (assumed to be limiting conditions for net photosynthesis); class 2 grouped lakes with irradiance from 10 to 120 µE/m^2/s; and class 3 included lakes with irradiance at the bottom >120 µE as commonly algae become saturated at 90-120 µE/m^2/s (Reynolds 2006).

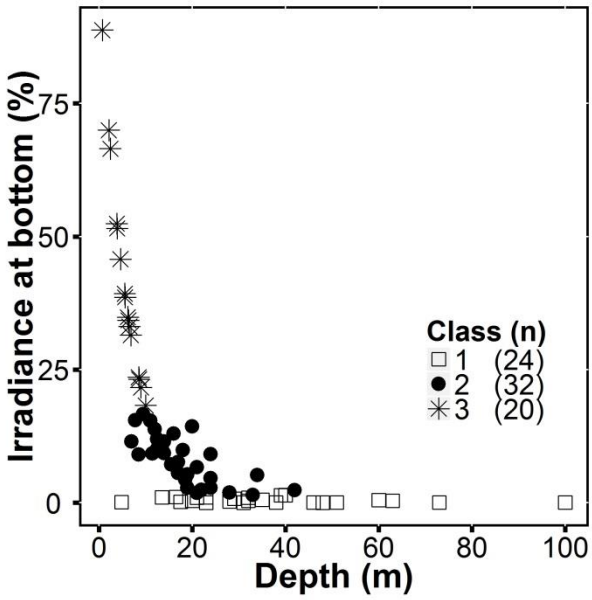

Figure 8.7. Relationship between depth and irradiance at the bottom. Plot shows the three classes distinguished for incident light at bottom (see the text for an explanation).

The assignation of lakes to classes of irradiance at the bottom provides information about the light environment without distinguishing between benthonic or planktonic species. In order to identify true benthic species, the significance of indicator species to lakes with active diatoms in the biofilm of the bottom (ADBB) were tested. Lakes with ADBB were identified according to data reported by Buchaca and Catalan (2008), which use as an indicator the algal pigments. Lakes with ADBB were grouped in the class 1 and lakes without ADBB were assigned to class 2.

Bray-Curtis coefficient between epilithon and sediment samples showed that lakes with ADBB were shallower than 20 m depth, showing dissimilarities >66%. Hence, lakes were also grouped accordingly to benthic conditions using three classes (Figure 8.8, benthic classes): class 1 included lakes expected to be

similar to ADBB lakes (<20m, Bray-Curtis coef. <0.33); class 2 included the deepest lakes with lower similarity between epilithon and sediment samples (Bray Curtis coef. <0.33, depth>20 m), and class 3 included lakes with the highest similarity between epilithon and sediment samples. The results of the three classification systems are shown in Table 11.

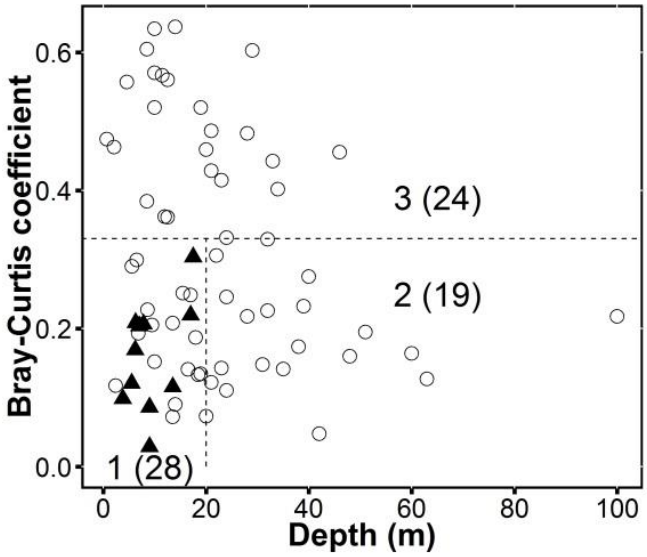

Figure 8.8. Relationship between sediment and epilithon samples similarity (Bray-Curtis coefficient) and depth. The numbers shown are the classification of lakes by benthic conditions (Benthic classes), in parentheses are shown the number of lakes. Triangles are the samples with an active diatom biofilm at the bottom (ADBB) according to Buchaca and Catalan (2008).

The indicator analysis using the ADBB classification showed that common *Fragilaria*-like species such as *Punctastriata* cf. *lancettula*, *Staurosirella oldenburgiana*, *Pseudostaurosira* sp. No. 2 Acherito, *Pseudostaurosira pseudoconstruens*, *Fragilaria* cf. *opacolineata*, and *Stauroforma* cf. *exiguiformis*, were significantly associated to lakes with ADBB. *Brachysira neoexilis* was the only species significantly related with class 2.

Indicator analysis of the classes built using the benthic classification showed a coincident indicator with the ADBB lake classification. Thus, *Punctastriata* cf. *lancettula*, *Navicula* sp. No. 4 Laquettes, *Staurosirella oldenburgiana* and *Delicata delicatula* were species significantly related with group 1. Class 3 of the benthic classification showed indicator species such as *Achnanthidium*

pyrenaicum, *Psammothidium ventrale*, and *Gomphonema lateripunctatum*. The highest similarity between sediment and epilithon samples in this group, suggests that these species could be an indicator of lakes where habitat conditions (related with depth and light), are relatively homogenous in the whole lake. Some indicator species of the class 1 (benthic classification), were *Fragilaria pararumpens*, *Navicula krasskei*, *Nupela* cf. *gracillima*, *Naviculadicta* sp. No. 1 Ensangents and *Gomphonema brebissonii*. Species related with non-light saturated environment were *Discostella stelligera* (Figure 8.9A), *Psammothidium marginulatum*, *Fragilaria* sp. No. 8 Redon, and *Encyonema gaeumannii*. On the other hand, *Pinnularia* cf. *subanglica*, *Navicula cryptotenella*, *Cymbella lange-bertalotii*, *Navicula pseudolanceolata*, were indicators of light saturated conditions (class 3).

The relationship of *Fragilaria pararumpens* (Figure 8.9B), *Navicula krasskei*, and *Karayevia laterostrata* with group 2 of the benthic classification and class 1 of irradiance indicates that these species are present in lakes with light limitation and, perhaps, deal particularly well with dim light conditions. *Staurosirella oldenburgiana* classifications suggests that it preferred benthic light saturation.

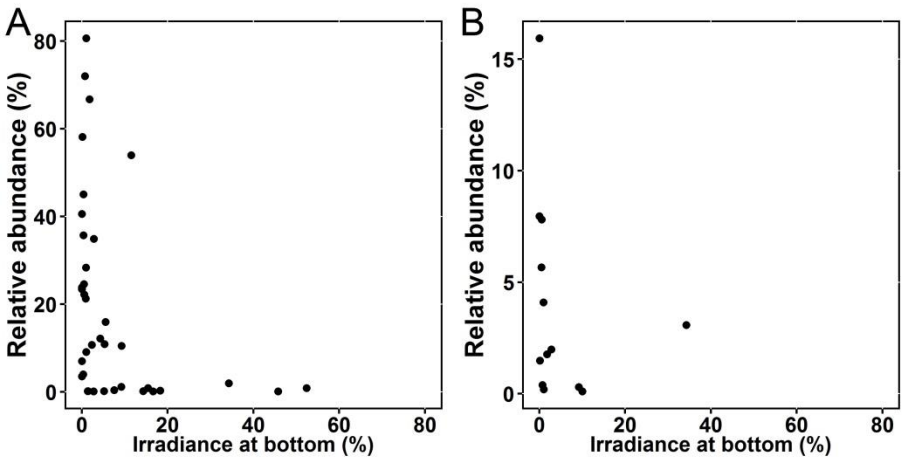

Figure 8.9. *Discostella stelligera* (A) and *Fragilaria pararumpens* (B) across the irradiance level at the bottom of lakes.

Table 11. Diatom specie indicative value (IndVal) and statistical significance of association (p) for classes of lakes with an active diatom biofilm (ADBB), classes shown in Figure 8.8 (benthic classes) and classes of irradiance level at bottom. Analysis was carried out following Dufrêne and Legendre (1997) and De Cáceres et al. (2010). ADBB classification: (1) lakes identified with ADDB sensu Buchaca and Catalan (2008) and (2) without ADBB. Benthic classification: (1) Lakes <20m and with Bray-Curtis coef. between epilithon and sediment samples<0.33, (2) lakes >20m and with Bray-Curtis coef.<0.33, and (3) lakes with Bray-Curtis coef.>0.3. Irradiance at the bottom classification: <10 µE/m^2/s (1), 10-120 µE/m^2/s (2), and >120 µE/m^2/s (3).

	ADBB classes (n= 71 lakes)			Benthic classes (n=71 lakes)			Classes of irradiance at the bottom (n=76 lales)			Species frequency (*f*) and abundance (n)		
Species	Class	IndVal	p	Class	IndVal	p	Class	IndVal	p	*f*	Mean	Max N
Pseudostaurosira cf. *brevistriata* (Grunow) Williams & Round				1	0.72	0.021				35	2.6	20.8
Punctastriata cf. *lancettula* (Schumann) Hamilton & Siver	1	0.77	0.001	1	0.65	0.025				25	4.1	43.5
Punctastriata cf. *lancettula* (Schumann) Hamilton & Siver M1	1	0.55	0.01	1	0.49	0.025				9	1.9	11.3
Navicula sp. No. 4 Laquettes	1	0.51	0.029	1	0.47	0.023				11	0.7	2.9
Staurosirella oldenburgiana (Hustedt) Morales	1	0.58	0.009	1	0.45	0.043	3	0.50	0.01	11	0.5	2.4
Delicata delicatula (Kützing) Krammer	1	0.55	0.002	1	0.41	0.041				6	0.5	1.6
Staurosirella leptostauron (Ehrenberg) Williams & Round				1	0.38	0.04				4	0.2	0.2
Encyonema perpusillum (Cleve) Mann				2	0.63	0.001				13	1.4	7.0
Fragilaria pararumpens Lange-Bertalot, Hofmann & Werum				2	0.53	0.006	1	0.54	0.007	13	3.9	15.9
Navicula krasskei Hustedt				2	0.50	0.002	1	0.53	0.003	8	0.4	1.8
Eunotia paludosa Grunow				2	0.46	0.007				5	1.0	4.1
Karayevia laterostrata (Hustedt) Bukhtiyarova				2	0.44	0.033	1	0.44	0.016	6	0.7	2.9
Pinnularia sinistra Krammer				2	0.44	0.019				8	0.6	2.0
Achnanthidium pyrenaicum (Hustedt) Kobayasi				3	0.72	0.005				32	1.1	8.8
Psammothidium ventrale (Krasske) Bukhtiyarova et Round				3	0.56	0.007	2	0.53	0.031	15	1.0	7.4
Psammothidium bioretii (Germain) Bukhtiyarova & Round				3	0.54	0.012				14	0.4	2.1
Gomphonema sp. No. 9 Posets				3	0.50	0.014				11	0.4	1.4
Gomphonema lateripunctatum Reichardt & Lange-Bertalot				3	0.52	0.011				10	2.6	9.6
Diatoma mesodon Kützing				2+3	0.68	0.027				32	0.4	1.7
Surirella cf. roba Leclercq				2+3	0.63	0.008	1+2	0.60	0.037	24	0.4	1.5
Eunotia bilunaris (Ehrenberg) Schaarschmidt				2+3	0.57	0.038				22	0.4	2.1
Nupela lapidosa (Krasske) Lange-Bertalot				2+3	0.53	0.017				15	0.3	1.1
Encyonema sp. No. 2 Sen				2+3	0.50	0.02				12	0.2	0.3
Pseudostaurosira sp. No. 2 Acherito	1	0.72	0.006							31	7.2	55.5
Brachysira neoexilis Lange-Bertalot	2	0.69	0.034							36	1.9	11.9

Pseudostaurosira pseudoconstruens (Marciniak) Williams & Round	1	0.68	0.048				32	4.9	68.7
Navicula sp. No. 3 Laurenti	1	0.65	0.001				12	0.8	2.0
Fragilaria cf. *opacolineata* Lange-Bertalot	1	0.60	0.021				18	1.8	6.5
Aulacoseira cf. *valida* (Grunow) Krammer	1	0.52	0.013				9	0.7	2.5
Nitzschia sp. No. 2 Posets	1	0.52	0.003	3	0.45	0.014	7	0.2	0.5
Stauroforma cf. *exiguiformis* (Lange-Bertalot) Flower, Jones & Round	1	0.51	0.048				15	0.8	2.3
Psammothidium rossii (Hustedt) Bukhtiyarova et Round	1	0.48	0.022	3	0.43	0.032	8	1.0	2.8
Fragilaria sp. No. 9 Redon				1	0.72	0.003	29	2.4	27.8
Nupela cf. *gracillima* (Hustedt) Lange-Bertalot				1	0.48	0.003	7	1.3	3.3
Naviculadicta sp. No. 1 Ensangents				1	0.37	0.047	5	0.3	0.7
Gomphonema brebissonii Kützing				1	0.35	0.048	3	0.1	0.1
Discostella stelligera (Cleve & Grunow) Houk & Klee				1+2	0.77	0.003	37	19.5	80.7
Psammothidium marginulatum (Grunow) Bukhtiyarova et Round				1+2	0.64	0.018	26	0.9	8.2
Fragilaria sp. No. 8 Redon				1+2	0.71	0.005	33	2.8	22.8
Encyonema gaeumannii (Meister) Krammer				1+2	0.65	0.007	26	1.9	9.3
Pinnularia cf. *subanglica* Krammer				2	0.59	0.01	20	0.9	4.5
Navicula cryptotenella Lange-Bertalot				3	0.64	0.001	15	1.6	13.2
Cymbella lange-bertalotii Krammer				3	0.43	0.003	5	0.2	0.3
Navicula pseudolanceolata Lange-Bertalot				3	0.43	0.014	6	0.3	1.3
Encyonema sp. No. 1 Mora				3	0.51	0.017	10	1.9	14.0
Adlafia cf. *minuscula* (Grunow) Lange-Bertalot				3	0.39	0.014	3	0.8	1.4
Encyonema obscurum var. *alpina* Krammer				3	0.39	0.023	3	0.4	1.1
Adlafia aff. *minuscula* (Grunow) Lange-Bertalot				3	0.37	0.019	4	0.2	0.4

9. Diatom distribution and lake habitats

Benthic algal growth is primarily related to the availability of resources and the environmental conditions (Borchardt 1996; DeNicola 1996) but the time available for the colonization of the substratum and the characteristics of the latter also matter (Burkholder 1996b). At the microscopic scale, microtopography, porosity, composition and stability of the substrate may affect algal growth. At a larger scale, these properties of the substrate are relate with meso-habitat descriptors such as macrophytes, macroalgae, rocks, sand, silt, and so on.

Many ecological studies and environmental reconstructions has been performed using organisms growing on rocks (e.g. Cameron et al. 1999; DeNicola et al. 2004) or sediment (e.g. Clarke et al. 2005; Puusepp and Punning 2011). However, there are few studies quantifying the relation between meso-habitats and algal composition, and performing quantitative models to reconstruct past habitats in lakes (Reavie and Smol 1997; Vermaire and Gregory-Eaves 2008).

Macrophytes can provide information about climate, trophic state and water level changes (Birks et al. 2012; Bos et al. 2006; Rooney et al. 2003; Sayer et al. 2010) and submerged macrophytes have a significant influence on diatom community. Therefore, one can expect that diatom assemblages in sedimentary sequences can provide indications about the macrophytes abundance in the past and their connection with environmental factors (Vermaire et al. 2011; Vermaire et al. 2012).

The aim of this chapter was to identify diatom species related with meso-habitat characteristics, particularly focusing on macrophytes presence in the Pyrenean lakes.

Meso-habitats in the Pyrenean lakes

The dominant substrate in the littoral of the Pyrenean lakes was rock (62%), which in the 10% of lakes covered more than 90% of the littoral. Despite this rock dominance, macrophytes are relevant in shallow lakes (Figure 9.1),

particularly for lake depth <20 m. Organic detritus were the least frequent substrate in the lakes surveyed.

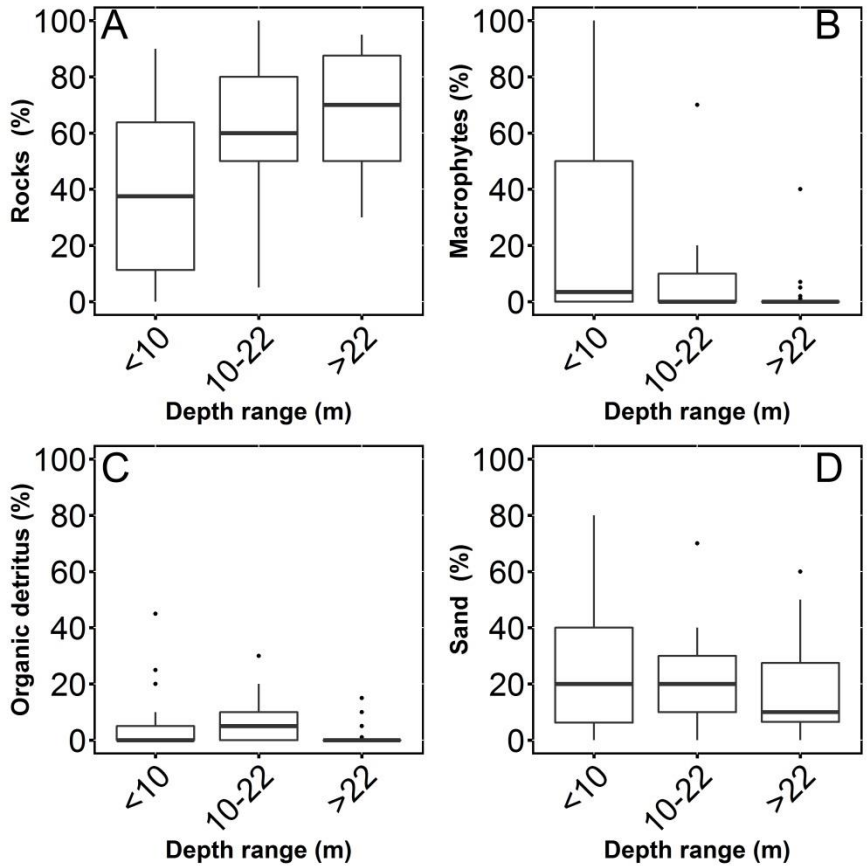

Figure 9.1. Substrate covered by rocks (A), macrophytes (B), organic detritus (C), and sand (D) across the depth gradient.

Diatom distribution and macrophytes

In order to find indicator species of macrophyte occurrence, the lakes were grouped into two classes taking into account the presence of any macrophyte, and, in a second classification, considering the specific presence of potamids (e.g., *Potamogeton*, *Rannunculus* and *Myriophyllum*), which offer a higher

standing biomass and area for the attachment of diatoms. Although there is some overlapping in their occurrence, potamids tend to grow in different lake conditions than isoetids (Gacia et al. 1994). Lakes included in the analysis were selected using the limit of the distribution of macrophytes in our data set with respect to water pH: ≥6, for the whole group and ≥6.76 for potamids.

There were many species related to lakes with macrophyte presence (Table 9). *Pseudostaurosira* sp. No. 2 Acherito, Psa*mmothidium scoticum*, *Encyonopsis subminuta*, *Naviculadicta digituloides*, and *Amphora* cf. *eximia* were the species with the highest indicative value. Analysis for potamids shared 9 indicator species with total macrophytes but showed additional species such as *Pseudostaurosira* cf. *brevistriata*, *Encyonopsis subminuta*, *Psammothidium helveticum*, and *Fragilaria pararumpens*.

Table 12. Diatom species indicative value (IndVal) and statistical significance of association (p) for macrophyte presence (n=33). Analysis was carried out following Dufrêne and Legendre (1997) and De Cáceres et al. (2010). The analysis includes only sediment samples with pH≥ 6.0, which is the limit of macrophytes distribution (n=71).

Species	IndVal	p	f	Mean	Max
Pseudostaurosira sp. No. 2 Acherito	0.68	0.009	31	7.22	55.48
Psammothidium scoticum Bukhtiyarova & Round	0.67	0.003	28	5.01	24.95
Encyonopsis subminuta Krammer & Reichardt	0.67	0.003	26	0.89	6.35
Naviculadicta digituloides Lange-Bertalot	0.63	0.02	27	1.37	9.49
Amphora cf. *eximia* Carter	0.58	0.041	22	1.52	6.88
Fragilaria cf. *opacolineata* Lange-Bertalot	0.58	0.004	18	1.8	6.48
Navicula sp. No. 4 Laquettes	0.58	0.001	11	0.66	2.93
Craticula submolesta (Hustedt) Lange-Bertalot	0.58	0.006	21	0.56	2.69
Nitzschia cf. *perminuta* (Grunow) Peragallo M2	0.57	0.022	21	0.67	3.98
Cocconeis euglyptoides (Geitler) Lange-Bertalot	0.57	0.003	18	0.32	0.79
Gomphonema auritum Braun	0.56	0.026	20	0.47	2.48
Planothidium distinctum (Messikommer) Lange-Bertalot	0.55	0.001	13	0.35	0.79
Neidium affine (Ehrenberg) Pfitzer sensu lato	0.55	0.021	23	0.37	1.4
Navicula wildii Lange-Bertalot	0.54	0.021	18	0.27	1.28
Staurosirella oldenburgiana (Hustedt) Morales	0.53	0.001	11	0.49	2.39
Gomphonema cf. *parvulum* (Kützing) Kützing	0.51	0.036	13	2.6	28.91
Punctastriata cf. *lancettula* (Schumann) Hamilton & Siver M1	0.49	0.002	9	1.86	11.25
Navicula sp. No. 2 Liat	0.48	0.015	12	0.48	1.19
Diadesmis perpusilla (Grunow) Mann	0.48	0.024	13	0.28	0.5
Gomphonema lateripunctatum Reichardt & Lange-Bertalot	0.48	0.013	10	2.64	9.6
Achnanthidium cf. *minutissimum* (Kützing) Czarnecki M3	0.47	0.049	13	0.41	1.09
Diploneis cf. *puella* (Schumann) Cleve	0.46	0.039	12	0.55	1.66
Surirella angusta Kützing	0.46	0.006	8	0.24	0.8
Ulnaria biceps (Kützing) Compère sensu lato	0.45	0.015	10	0.12	0.2

Species	IndVal	p	f	Mean	Max
Aulacoseira cf. *valida* (Grunow) Krammer	0.44	0.039	9	0.68	2.54
Delicata delicatula (Kützing) Krammer	0.43	0.008	6	0.51	1.59
Psammothidium rossii (Hustedt) Bukhtiyarova et Round	0.42	0.034	8	1.04	2.85
Gyrosigma sp. No. 1 Sen	0.41	0.048	9	0.25	0.6
Encyonopsis descripta (Hustedt) Krammer	0.41	0.029	7	0.13	0.2

Table 13. Diatom species indicative value (IndVal) and statistical significance of association (p) with potamid presence (n=19 lakes). Analysis was carried out following Dufrêne and Legendre (1997) and De Cáceres et al. (2010). The analysis includes only sediment samples with pH≥ 6.76, which is the limit of distribution for potamids in the Pyrenean lake data set analysed (n=55 lakes).

Species	IndVal	p	*f*	Mean	Max n
Pseudostaurosira cf. *brevistriata* (Grunow) Williams & Round	0.75	0.014	35	2.57	20.8
Encyonopsis subminuta Krammer & Reichardt	0.72	0.011	26	0.89	6.35
Cymbella parva (Smith) Kirchner	0.66	0.013	21	0.41	2.18
Gomphonema lateripunctatum Reichardt & Lange-Bertalot	0.61	0.005	10	2.64	9.6
Navicula sp. No. 4 Laquettes	0.6	0.001	11	0.66	2.93
Gomphonema auritum Braun	0.59	0.036	20	0.47	2.48
Delicata delicatula (Kützing) Krammer	0.58	0.002	6	0.51	1.59
Staurosirella oldenburgiana (Hustedt) Morales	0.53	0.019	11	0.49	2.39
Navicula pseudolanceolata Lange-Bertalot	0.52	0.005	6	0.33	1.29
Encyonema sp. No. 1 Mora	0.52	0.044	10	1.92	13.99
Encyonopsis cesatii (Rabenhorst) Krammer	0.48	0.047	9	0.36	1.09
Encyonopsis cf. *falaisensis* (Grunow) Krammer	0.47	0.02	5	1.19	5.06
Gomphonema truncatum Ehrenberg	0.47	0.014	4	0.42	0.59
Cymbopleura cf. *pyrenaica* Le Cohu & Lange-Bertalot	0.46	0.024	5	1.42	4.73
Psammothidium rossii (Hustedt) Bukhtiyarova et Round	0.4	0.047	8	1.04	2.85
Cymbella lange-bertalotii Krammer	0.39	0.035	5	0.18	0.3
Psammothidium helveticum (Hustedt) Bukhtiyarova et Round	0.74	0.004	42	4.12	26.86
Naviculadicta digituloides Lange-Bertalot	0.6	0.042	27	1.37	9.49
Neidium affine (Ehrenberg) Pfitzer sensu lato	0.55	0.043	23	0.37	1.4
Fragilaria pararumpens Lange-Bertalot, Hofmann & Werum	0.54	0.037	13	3.91	15.94

10. Synthesis of the indicator analyses

Besides the high diatom diversity, the Pyrenean lakes were characterised by a large number of statistically significant indicator species of water chemistry, nutrients, physical and habitat conditions (Table 14, Table 15, and Appendix 2). From 368 taxa found in the training-set, 205 were indicators of some environmental classification, being recorded 381 significant IndVal values. The epilithon training-set had 131 indicator species (of 334 taxa) and 202 significant IndVal values. These high number of indicator species is a useful tool for the environmental reconstruction of Burg Lake as there were 104 significant indicators (51 taxa) present in the sedimentary sequence.

The most outstanding result is the low number of indicator species shared by lake classifications made with different criteria analysed; from 112 species in Table 15, 62 were indicators of only one category and 33 were indicator of two categories.

Despite that naviculoids show a high number of diatom species (105); their proportion of indicator species is similar to less diverse types (Table 14) such as monoraphid, eunotioid, and centric types. As expected, eunotioid being strongly associated to acidic environments, showed a high number of pH indicator species and few of nutrient classifications. Surirelloids showed indicator species for six classifications despite the low number of species involved, indicating a high degree of environmental specialisation. Pinnulariids showed the lowest proportion of indicator species. Cymbelloid and monoraphid types showed at least one indicator case at each environmental classification. Monoraphid was the type with the most even distribution of indicators. Other types with an even distribution of indicator species were araphid and nitzschioid.

Table 14. Summary of the indicator analyses of the sediment survey-set. The number of significant indicator species of each morphological type for each classification are shown. I_{sb}: Irradiance at the bottom, ADBB: Active diatom biofilm at the bottom, ICD: Ice cover duration. The intensity of the colour is used to highlight from the maximum (black) to the minimum (white) values.

Classification		Araphid	Centric	Cymbelloid	Eunotioid	Gomphoid	Monoraphid	Naviculoid	Nitzschioid	Pinnulariid	Surirelloid
pH-ANC	pH-SO_4^{2-}	5	3	12	14	1	7	16	1	6	4
Nutrients	TN:TP	6	2	2		1	3	12	2		
	Trophic	4	2	6	1	4	3	4	1	1	1
	Si			3	2	1	2	5	3	1	
	Si:N			9		1	3	14	2	1	
	Si:TP	1		1		3	1	5	1		1
Physical	I_{sb}	4	1	4		1	5	7	1	1	1
	ADBB	7	2	2			2	3	1		
	Benthic	7		4	2	2	6	3	1	1	1
	Temperature	5	3	2	1	2	5	10	3	2	1
	ICD	6	4	3			6	9	1	1	
Habitat	Macrophytes	7	4	5	1	4	6	13	1	1	2
	Potamids	3		8		3	2	4			
Total indicator cases		55	21	61	21	23	51	105	18	15	11
Species recorded in sediment samples		32	23	46	28	19	55	102	25	32	6
Indicator species (%)		63.6	52.2	60.9	57.1	68.4	50.9	56.3	48.0	37.5	83.3

Table 15. Summary of the indicator analyses showing the most representative species of the sediment training-set (frequency >10 lakes) and the Burg Lake record. I_{sb}: irradiance at the bottom (µE/m^2/s), ADBB: active diatom biofilm at the bottom, ICD: ice cover duration (days), Temp.: temperature (ºC), TN: total nitrogen, TP: total phosphorous (µg/L), DIN: dissolved inorganic nitrogen (µg/L). SO_4^{2-} and Si units are µeq/L and mol/L, respectively. Details of the habitat indicators are explained in chapters 8 and 9. *Species present in Burg Lake record.

		Group of indicators			
Type	Species	pH-ANC	Nutrients	Physical	Habitat
Araphid	**Fragilaria delicatissima* (Smith) Lange-Bertalot		TN:TP <50:1, DIN <100 TP >4	Isb <120	
	Fragilaria sp. No. 9 Redon			Isb <10	
	**Fragilaria pararumpens* Lange-Bertalot, Hofmann & Werum			Isb <10	non-potamids, psam-deep
	**Meridion circulare* (Greville) Agardh		TN:TP <110:1, DIN<100 TP>	ICD <180 d	
	Fragilaria cf. *opacolineata* Lange-Bertalot		TN:TP <50:1, DIN <100 TP >4	Temp. >15	Macroph., ADBB
	Pseudostaurosira cf. *brevistriata* (Grunow) Williams & Round			Temp. >10	Macroph., potamids, psam-shallow
	Pseudostaurosira microstriata (Marciniak) Flower	pH >5.5			
	Pseudostaurosira parasitica var. *subconstricta* (Grunow) Morales			ICD <160 d	
	**Pseudostaurosira pseudoconstruens* (Marciniak) Williams & Round		TN:TP <110:1		ADBB
	**Pseudostaurosira* sp. No. 2 Acherito				Macroph., ADBB
	**Punctastriata* cf. *lancettula* (Schumann) Hamilton & Siver M1	SO_4^{2-} >50 pH >7.25			Macroph., psam-shallow, ADBB
	**Punctastriata lancettula* (Schumann) Hamilton & Siver			ICD <180 d	psam-shallow, ADBB
	**Stauroforma* cf. *exiguiformis* (Lange-Bertalot) Flower, Jones & Round	SO_4^{2-} <50 pH 5.5-6.5		Temp. >15	ADBB
	**Staurosira construens* Ehrenberg			ICD <195 d, Temp. >10	
	Staurosirella oldenburgiana (Hustedt) Morales			Isb >120 , Temp. >15	Macroph., potamids, psam-shallow, ADBB
	**Staurosirella pinnata* (Ehrenberg) Williams & Round	pH >5.5			
	**Ulnaria biceps* (Kützing) Compère sensu lato		TN:TP <110:1	ICD <180 d	Macroph.
Centric	*Aulacoseira* cf. *alpigena* (Grunow) Krammer	pH 5.5-7.25		Temp. bipolar	non-macroph.
	Aulacoseira pfaffiana (Reinsch) Krammer	pH <6.5			
	Cyclotella praetermissa Lund			ICD <195 d	

		Group of indicators			
Type	Species	pH-ANC	Nutrients	Physical	Habitat
	Discostella stelligera (Cleve & Grunow) Houk & Klee			Isb <120 , Temp. >10	
Cymbelloid	*Amphora* cf. *eximia* Carter	pH >7.25	Si:N<1	Temp. <15	
	**Amphora copulata* (Kützing) Schoeman & Archibald	pH >7.25	Si:N<1		
	Amphora neglecta f. *densestriata* Foged	pH >7.25			
	Cymbella parva (Smith) Kirchner				Macroph., potamids, psammon
	**Cymbopleura inaequalis* (Ehrenberg) Krammer				ADBB
	**Cymbopleura naviculiformis* (Auerswald) Krammer		Si<10, Si:N<1		
	**Cymbopleura subaequalis* (Grunow) Krammer		Si<10, Si:N<1		
	**Denticula tenuis* Kützing	pH >7.25	Si:N<1, TN:TP >50:1, TP< 10		
	**Encyonema gaeumannii* (Meister) Krammer	pH <6.5		Isb <120	
	**Encyonema hebridicum* Grunow ex Cleve	pH <6.5			
	**Encyonema minutum* (Hilse) Mann	pH >5.5			
	**Encyonema neogracile* Krammer		Si<10		
	Encyonema perpusillum (Cleve) Mann	pH <6.5	DIN<100 TP<4		psam-deep
	**Encyonema reichardtii* (Krammer) Mann			Temp. <10	
	**Encyonema silesiacum* (Bleisch) Mann	pH >5.5			
	Encyonema sp. No. 1 Mora		Si:N<1, DIN>100 TP4-10	Isb >120	Macroph., potamids
	Encyonema sp. No. 2 Sen				plankton
	**Encyonopsis microcephala* (Grunow) Krammer		TN:TP 50-110:1		
	**Encyonopsis subminuta* Krammer & Reichardt	pH >7.25	Si:N<1, TP 4-10	ICD <180 d	Macroph., potamids
Eunotioid	*Eunotia bilunaris* (Ehrenberg) Schaarschmidt	pH <6.5			plankton
	Eunotia exigua (Brébisson Kutzing) Rabenhorst	SO_4^{2-} >50 pH <6.5	DIN<100 TP<4		
	Eunotia intermedia (Krasske) Nörpel & Lange-Bertalot	SO_4^{2-} >50 pH <6.5			
	Eunotia subarcuatoides Alles, Norpel & Lange-Bertalot	pH 5.5-6.5			
Gomphoid	**Gomphonema acuminatum* Ehrenberg		Si:P <100:1		
	**Gomphonema auritum* Braun		TN:TP <110:1		Macroph., potamids
	**Gomphonema* cf. *parvulum* (Kützing) Kützing sensu lato		Si<10, Si:P <100:1,	Temp. >15	Macroph.

		Group of indicators			
Type	Species	pH-ANC	Nutrients	Physical	Habitat
			DIN<100 TP>10		
	Gomphonema lateripunctatum Reichardt & Lange-Bertalot				Macroph., potamids, non-psam
	Gomphonema pumilum (Grunow) Reichardt & Lange-Bertalot		DIN>100 TP4-10		
	**Gomphonema* sp. No. 15 Coronas		Si:N<1, Si:P <100:1		
	**Gomphonema* sp. No. 9 Posets				non-psam
	**Gomphonema truncatum* Ehrenberg				Macroph., potamids
Monoraphid	**Achnanthes microscopica* (Cholnoky) Lange-Bertalot & Krammer	pH 5.5-6.5			
	Achnanthidium atomus (Hustedt) Monnier, Lange-Bertalot & Ector		Si:N<1		
	**Achnanthidium pyrenaicum* (Hustedt) Kobayasi				non-psam
	**Cocconeis euglyptoides* (Geitler) Lange-Bertalot				Macroph.
	**Karayevia suchlandtii* (Hustedt) Bukhtiyarova			ICD >160 d	
	Nupela lapidosa (Krasske) Lange-Bertalot	SO_4^{2-} <50 pH 5.5-6.5			plankton
	Planothidium distinctum (Messikommer) Lange-Bertalot		TN:TP >110:1		non-macroph.
	**Planothidium frequentissimum* (Lange-Bertalot) Lange-Bertalot			ICD <160 d	
	Psammothidium acidoclinatum (Lange-Bertalot) Lange-Bertalot	SO_4^{2-} >50 pH <6.5			non-macroph.
	**Psammothidium bioretii* (Germain) Bukhtiyarova & Round				non-psam
	**Psammothidium helveticum* (Hustedt) Bukhtiyarova et Round	pH <7.25	TP <4		non-potamids
	**Psammothidium levanderi* (Hustedt) Bukhtiyarova & Round			Temp. >10	
	Psammothidium marginulatum (Grunow) Bukhtiyarova et Round	SO_4^{2-} <50 pH 5.5-6.5	Si:P >100:1	Isb <120	
	Psammothidium scoticum (Flower et Jones) Bukhtiyarova & Round	pH 5.5-7.25			non-macroph.
	Psammothidium subatomoides (Hustedt) Bukhtiyarova et Round	pH 5.5-6.5			
	Psammothidium ventrale (Krasske) Bukhtiyarova et Round			Isb 10-120	non-psam
	**Rossithidium pusillum* (Grunow) Round et Bukhtiyarova				Macroph.
Naviculoid	**Brachysira brebissonii* Ross	pH <6.5			
	Brachysira neoexilis Lange-Bertalot				non-ADBB
	**Chamaepinnularia mediocris* (Krasske) Lange-Bertalot	pH <6.5			
	Craticula submolesta (Hustedt) Lange-Bertalot				non-macroph.
	**Diploneis* cf. *peterseni* (petersenii) Hustedt	pH >7.25	Si:N<1, DIN>100 TP4-10		

Type	Species	Group of indicators: pH-ANC	Nutrients	Physical	Habitat
	**Diploneis* cf. *puella* (Schumann) Cleve		Si:N<1		Macroph.
	Navicula cf. *minima*		TN:TP <50:1	Temp. >15	Macroph.
	**Frustulia* cf. *saxonica* Rabenhorst	SO_4^{2-} >50 pH <6.5		ICD 180-195 d	non-macroph.
	Frustulia crassinervia (Brébisson) Lange-Bertalot et Krammer	pH <6.5			
	**Gyrosigma* sp. No. 1 Sen				Macroph.
	Navicula angusta Grunow	pH 5.5-7.25			
	**Navicula catalanogermanica* Lange-Bertalot & Hofmann	pH >7.25	Si:N<1, DIN>100 TP4-10		
	**Navicula* cf. *oligotraphenta* Lange-Bertalot & Hofmann		Si:N<1	ICD <160 d	
	**Navicula cryptotenella* Lange-Bertalot	SO_4^{2-} >50 pH >7.25	DIN>100 TP4-10	Isb >120	
	**Navicula heimansioides* Lange-Bertalot		TN:TP <50:1		
	**Navicula pseudolanceolata* Lange-Bertalot			Isb >120	Macroph., potamids
	**Navicula radiosa* Kützing			ICD <195 d	Macroph.
	Navicula venerablis Hohn & Hellerman		Si<10, TN:TP <50:1		
	**Navicula wildii* Lange-Bertalot			ICD <180 d	Macroph.
	**Navicula* cf. *seminulum* Grunow			Temp. >15	
	Navicula schmassmanni Hustedt	pH 5.5-6.5			
	Navicula sp. No. 2 Liat		Si<10, Si:N<1		non-macroph.
	Navicula sp. No. 3 Laurenti		TN:TP <50:1		ADBB
	Navicula sp. No. 4 Laquettes		TN:TP <50:1	Temp. >15	Macroph., potamids, psam-shallow, ADBB
	**Navicula* sp. No. 7 Bergus	pH 5.5-6.5	Si:N>1, TN:TP <50:1		
	**Naviculadicta digituloides* Lange-Bertalot		Si:N<1		non-potamids
	**Neidium affine* (Ehrenberg) Pfitzer sensu lato	pH <6.5			non-macroph., non-potamids
	Neidium alpinum Hustedt	pH <6.5			
	**Sellaphora laevissima* (Kützing) Mann			Temp. >10	
	**Sellaphora pupula* (Kützing) Mereschkowsky sensu lato		Si<10, Si:N<1, Si:P <100:1		
	**Stauroneis gracilis* Ehrenberg			Temp. >15	
	**Stauroneis smithii* Grunow		Si<10, Si:N<1		

		Group of indicators			
Type	Species	pH-ANC	Nutrients	Physical	Habitat
Nitzschioid	**Hantzschia* cf. *amphioxys* (Ehrenberg) Grunow		Si:P <100:1		
	**Nitzschia acidoclinata* Lange-Bertalot		Si<10, DIN>100 TP4-10		
	**Nitzschia* cf. *perminuta* (Grunow) Peragallo M2				non-macroph.
	Nitzschia sp. No. 1 Sen	pH >7.25	Si:N<1, TN:TP >50:1		
Pinnulariid	**Pinnularia* cf. *brebissonii* var. *minuta* Krammer			ICD >160 d	
	Pinnularia cf. *subanglica* Krammer			Isb 10-120	
	**Pinnularia microstauron* var. *nonfasciata* Krammer	SO_4^{2-} >50 pH <6.5	DIN<100	Temp. <10	non-macroph.
	**Pinnularia subcapitata* Gregory	SO_4^{2-} <50 pH 5.5-6.5			
Surirelloid	**Stenopterobia delicatissima* (Lewis) Van Heurck	pH <6.5			
	**Surirella* cf. *linearis* Smith	pH <7.25			non-macroph.
	Surirella cf. *roba* Leclercq	pH <6.5		Isb <120	plankton

Results

Part III

Diatom-based quantitative environmental reconstructions

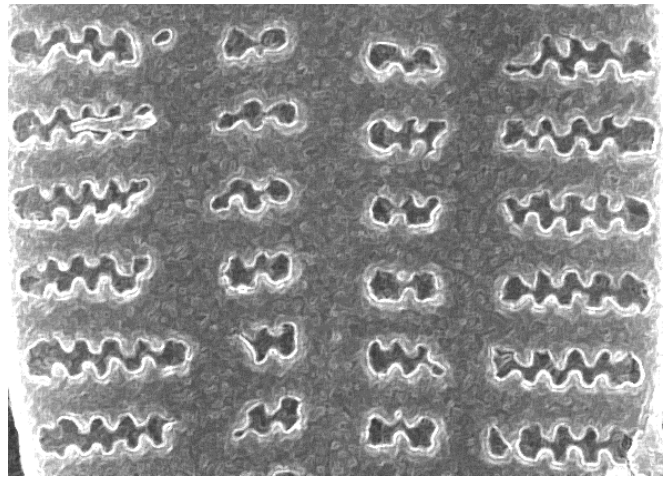

Karayevia suchlandtii (Hustedt) Bukhtiyarova

With the passing of time the code inscribes itself on all things

11. Transfer function development

The quantitative reconstruction of some environmental variables (e.g., pH, temperature, salinity, nutrients) using biological remains has been a major achievement of palaeolimnology during the last decades (Bennion et al. 1996b; Birks et al. 1990; Gasse et al. 1995; Larocque et al. 2001; Lotter et al. 1997; Terbraak and Juggins 1993) and palaeoceanography (de Vernal et al. 2000; Duplessy et al. 1991; Jiang et al. 2002; Kucera et al. 2005; Sikes and Keigwin 1994). Fundamentally, the quantitative reconstruction consists in a space for time substitution. The reconstruction of an environmental variable of interest (e.g., pH) based on a biological proxy (e.g., diatom assemblages) is calibrated using a training set for which both components are available and then applied to some sediment sequence of the proxy. For lake sediment sequences, diatoms have been one of the most used proxies in quantitative reconstruction, particularly for pH but also total phosphorus and salinity, among others (Birks 1998). The large number of species present in any sample and the high sensitivity of the diatom species to some environmental factors (i.e., pH) provided reliable reconstructions since early applications despite technical improvements throughout the years (Birks and Simpson 2013).

Nowadays, the limits of quantitative environmental reconstructions is being discussed in relation to the constraints imposed by the spatial correlation that may exist in the training sets and the influence of secondary variables on the statistical assumptions of the model used (Anderson 2000; Juggins 2013). Weighted average partial least squares (WA-PLS) emerged as a method that corrects edge effect and reduces the influence of additional variables (ter Braak and Juggins 1993) with respect to previous approaches based on simple weighted average-WA (ter Braak and Looman 1986). However, recent analyses have revealed that the explanatory power of transfer function developed using WA-PLS can be affected by different factors, including the spatial structure (Telford and Birks 2009). Nearby lakes could be more similar chemically to each other than more distant lakes. Consequently, cross-validation in the presence of spatial correlation violates the assumption of statistical independence of the data-set samples (Juggins and Birks 2012; Telford and Birks 2005).

The independence between the variables of interest and that their joint distribution does not change in the time are two basic assumptions of the reconstruction techniques (Birks et al. 2010). Simulations of diatom assemblages

in different scenarios of correlation between two environmental variables showed that secondary variables can produce an important spurious effect on the reconstruction when the correlation is higher than 0.4 (Juggins 2013). However, the experimental analysis of the effects of correlated variables on reconstructed variables is difficult to be performed because it is necessary to know historical values of the reconstructed variables, which are hardly available.

In any case, the development of new transfer functions requires checking (to the extent is possible) for these statistical weaknesses. An adequate sampling design may minimise transfer function biases and the comparison of the reconstruction with other indicative variables (e.g., geochemistry) may help to evaluate whether joint distributions are maintained throughout time.

Diatoms grow in a wide variety of substrates. Some require specific substrates, others show some preference for some of them and others are generalists (Krammer 2000, 2002; Lange-Bertalot et al. 2003). Epilithic assemblages have been largely used to develop transfer functions to reconstruct past changes in pH, water temperature and phosphorous concentration (DeNicola et al. 2004; Kitner and Poulíčková 2003). The sampling of the epilithon is easier than sampling other substrates. However, the assemblages used in the reconstructions are those accumulated on top of the sediment. The relationship between diatom assemblages and water chemistry is sensitive to the substrate considered (Burkholder 1996a; Carrick and Lowe 2007). In that respect, surface sediment samples collected at the bottom of the lake appear more adequate as training sets (Dixit et al. 1988; Hadley et al. 2013; Saunders et al. 2009). The main disadvantage of this procedure is that a few millimetres of surface sediment can be the result of year to decades of sedimentation (Cameron et al. 1999). Therefore, the information stored in these samples might contain diatom responses to chemical variability that do not correspond to the current chemistry of the lake water. On the other hand, sediment samples store information about the lake as a whole (Smol 2008); distinct processes that may be influencing the water column and the littoral area can be recorded simultaneously in the settling diatom assemblages. In this section, one of the aims is to compare to what extent transfer functions developed with epilithon samples or sediment samples may differ for the Pyrenean lakes.

The pH-ANC gradient is the main explanatory factor of diatom assemblage in crystalline lakes similar to the Pyrenean lakes (Cameron et al. 1999; Koster et al. 2004; Siver 1999). ANC and related variables can explain more than 20% of the species assemblage variability. Is there anything meaningful left than can be

(independently) reconstructed? The high richness of diatom species in the Pyrenean lakes and the contrasting indicative value of many of them (see chapter 10) suggests that several transfer functions can be developed. To evaluate this possibility is a second aim of this chapter.

Diatom composition and environmental factors

Redundancy analyses (RDAs) based on the Hellinger distance performed to examine the diatom ordination respect environmental gradients using, respectively, sediment and epilithon samples.

The sediment data-set

The first RDA axis was related to the pH-ANC gradient (Table 16, Table 17, Figure 11.1), in particular to Ca^{2+} (r_{axis1}=0.75) and ANC (r_{axis1}=0.65). The second axis was related to I_{Zmax} (r_{axis2}=0.44) and SO_4^{2-} (r_{axis2}=0.36) and the third axis to I_{Zmax} (r_{axis3}=0.51) and temperature (r_{axis3}=0.46). TP was correlated with the first (r=0.46) and third axis (r=0.39). Other nutrients such as nitrogen compounds and Si had no-significant explanatory value.

Table 16. Variance of the diatom assemblages in the sediment data-set explained by the environmental variables measured.

Variable	λ	p	F
Ca^{2+}	0.1	0.001	8.50
Acid-neutralizing capacity (ANC)	0.05	0.001	4.41
Irradiance at the bottom (I_{Zmax})	0.04	0.001	3.45
Na^{+}	0.04	0.001	3.37
Mg^{2+}	0.03	0.001	2.59
Temperature	0.02	0.001	2.38
Dissolved organic carbon (DOC)	0.02	0.003	1.82
SO_4^{2-}	0.02	0.022	1.59
Total phosphorous (TP)	0.01	0.042	1.51
Macrophyte occurrence	0.02	0.092	1.35
Catchment vegetation cover	0.01	0.087	1.33
K^{+}	0.01	0.127	1.29
pH	0.02	0.088	1.38
Si	0.01	0.342	1.08
Total nitrogen (TN)	0.01	0.5	0.95
Cl^{-}	0.01	0.464	0.98
NH_4^{+}	0	0.608	0.88
NO_3^{-}	0.01	0.877	0.71

Table 17. Summary of the minimal RDA model and lengths of the ordination gradients of the sediment diatom data-set. Minimal model included the significant variables shown in Table 16.

Axes	1	2	3	4	Total variance
Eigenvalues:	0.131	0.064	0.034	0.03	1
Species-environment correlations:	0.92	0.786	0.72	0.676	
Cumulative percentage variance					
of species data:	13.1	19.6	23	26	
of species-environment	39.6	59	69.3	78.4	
Sum of all eigenvalues					1
Sum of all canonical eigenvalues					0.332
DCA lengths of gradient:	4.892	2.209	2.327	1.486	

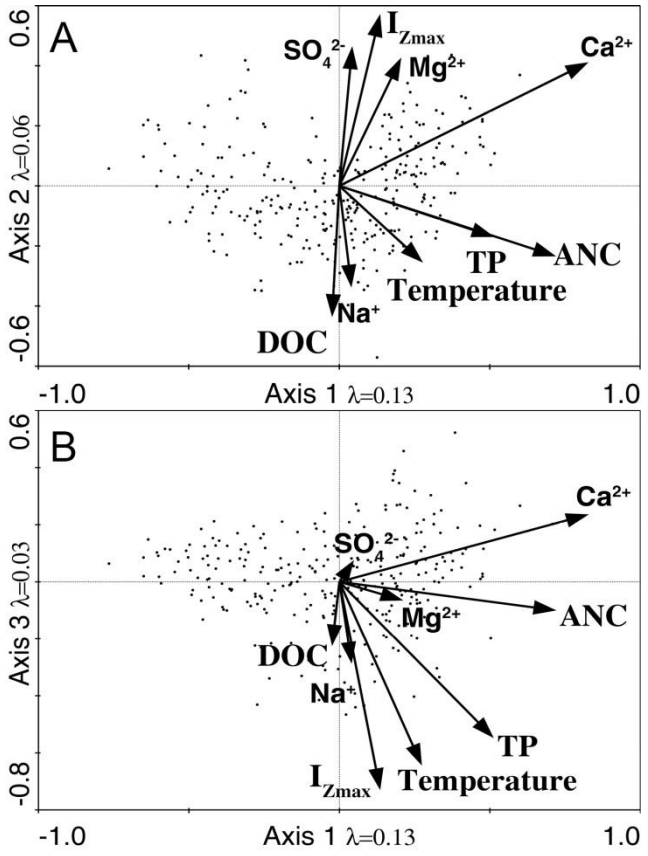

Figure 11.1. RDA ordination biplot showing the relationship between diatom assemblages of the sediment data-set and the environmental variables (n=76, taxa=287).

1 vs. 2 (A) and 1vs. 3 (B) axes showing significant variables. Black points indicate the taxa distribution.

Partitioning of the sediment data-set variation showed that trophic (TP and DOC) and physical (Temperature and I_{Zmax}) variables explained together less than water chemistry (Figure 11.2). Water chemistry shared about 1/3 of the trophic explicative capacity, whereas the overlapping with physical variables was quite low.

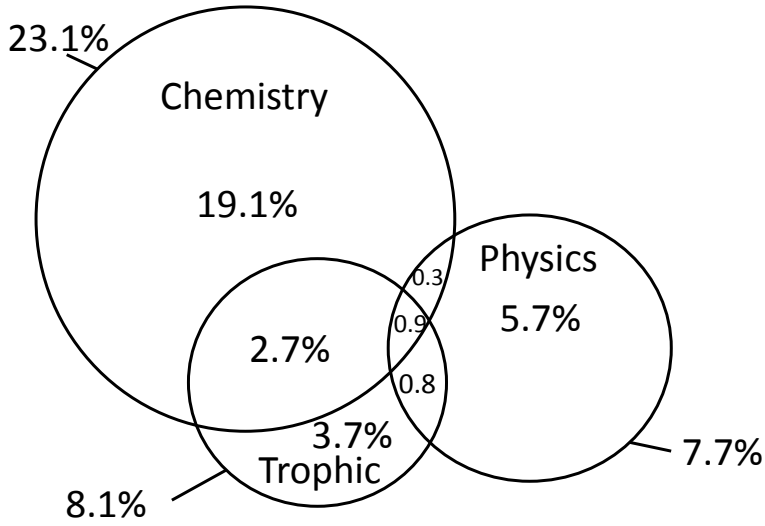

Figure 11.2. Partitioning of the diatom assemblage variance in the sediment data-set.

The epilithon data-set

Results of the RDA using the epilithon data-set were similar to the RDA using the sediment data-set. The model explained a 32% of total species variance and the first axis was related to the pH-ANC gradient (Table 18, Table 19, Figure 11.3): Ca^{2+} (r_{axis1}=0.74) and ANC (r_{axis1}=0.72). However, the second and third axes were related to variables different than in the sediment data-set RDA. The second axis was related to Mg^{2+} (r_{axis2}=0.54) and SO_4^{2-} (r_{axis2}=0.49) and the third to macrophyte coverture (r_{axis2}=0.45), temperature (r_{axis2}=0.36) and Na^{+} (r_{axis3}=0.27).

Table 18. Variance of the diatom assemblages in the epilithon data-set explained by the environmental variables measured.

Variable	λ	p	F
Ca^{2+}	0.14	0.001	12.16
Acid-neutralizing capacity (ANC)	0.08	0.001	8.07
Macrophytes coverture in the lake	0.03	0.004	2.6
Na^{+}	0.03	0.002	2.85
Temperature	0.02	0.011	1.98
Mg^{2+}	0.01	0.013	1.98
SO_4^{2-}	0.02	0.032	1.68
Basin cover with vegetation	0.02	0.089	1.45
Si	0.01	0.106	1.37
Total phosphorous	0.01	0.247	1.14
Cl^{-}	0.01	0.173	1.27
K^{+}	0.01	0.342	1.06
Total nitrogen	0.01	0.541	0.92
Dissolved organic carbon DOC	0.01	0.551	0.91
pH	0.01	0.597	0.88
Photic index	<0.01	0.665	0.83
NO_3^{-}	0.01	0.801	0.73
NH_4^{+}	0.01	0.837	0.7

Table 19. Summary of the minimal RDA model and lengths of the gradient of diatoms in the epilithon data-set.

Axes	1	2	3	4	Total variance
Eigenvalues:	0.173	0.065	0.028	0.023	1
Species-environment correlations:	0.893	0.75	0.669	0.694	
Cumulative percentage variance					
of species data:	17.3	23.8	26.6	28.9	
of species-environment relation:	53.8	73.9	82.7	89.8	
Sum of all eigenvalues					1
Sum of all canonical eigenvalues					0.322
DCCA lengths of gradient:	4.483	1.705	1.368	1.229	

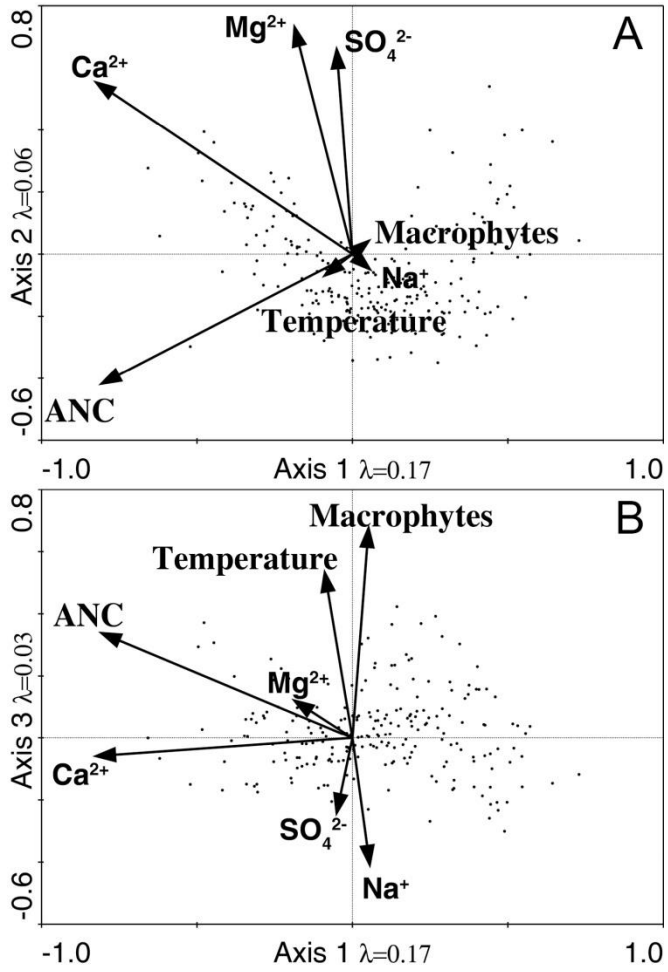

Figure 11.3. RDA ordination biplot showing relationships between diatom assemblages and environmental variables of epilithon data-set (n=78, taxa=227). 1 vs. 2 (A) and 1vs. 3 (B) axes showing significant variables. Black points represent the taxa.

Partitioning of the variation of the epilithon data-set indicated that chemistry variables explained most of the variance (Figure 11.4) and the influence of alternative variables (physics, habitat) had less explicative capacity than for the sediment data-set.

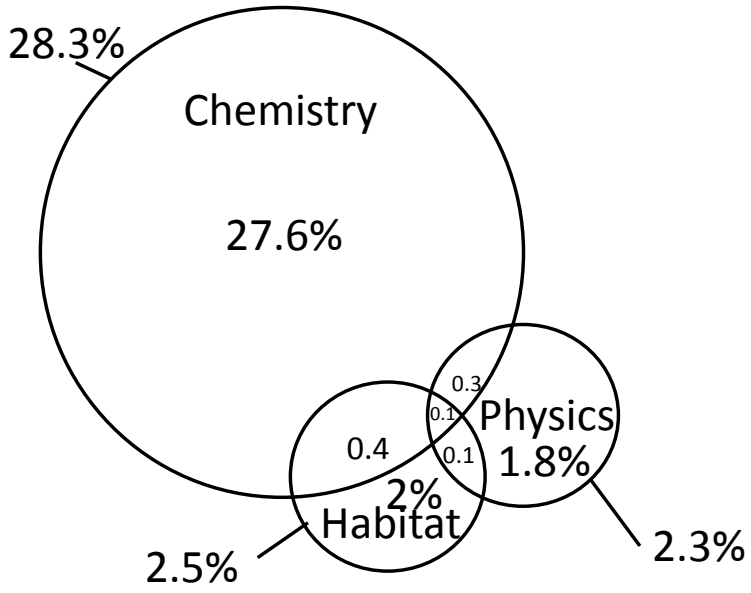

Figure 11.4. Partitioning of the diatom variation in the epilithon data-set.

Transfer function development

The variables suitable for developing transfer functions were selected using different approaches that included the significant explanation of species variation and the ecological meaning of these variables. Details about the procedure are described in methods (chapter 4).

The performance of the models of selected variables for sediment and epilithon data-sets is shown in Table 20 and Table 21. Other variables potentially suitable for developing transfer function such as nitrogen, Si, ice cover duration, basin cover with vegetation, did not presented an acceptable performance.

Transfer functions for pH and ANC showed the best performance using the sediment data-set. Bootstrapping for pH and ANC showed a small reduction in the explanation of the models and a small increase of RMSE. Data distribution and residuals of these two variables indicate that the predictability of the models could be more reliable to reconstruct log10(ANC+1) values between 1.1 and 3.1 (that is 10-1300 µeq/L) and pH between 6.5 and 8.2 (Figure 11.5).

Table 20. Summary of the transfer functions using the sediment data-set.

	pH	ANC	SSWT	TP	I_{Zmax}
Model					
Transformation	-	Log10(x+1)	-	Log10(x*1000)	$x^{0.5}$
r^2	0.92	0.94	0.82	0.78	0.79
RMSE	0.23	0.16	1.3	0.14	1.04
r^2 bootstrapping	0.79	0.83	0.38	0.35	0.36
RMSE bootstrapping	0.39	0.29	2.58	0.25	1.91
Number of samples	76	76	76	76	76
Number of species	287	287	287	287	287
WA-PLS component	2	2	3	2	2
Training-set					
Minimum	4.53	0	3.8	2.97	0.001
Maximum	8.96	3.23	18.5	4.55	9.42
Mean	6.98	2.05	12.5	3.52	2.72
Standard deviation	0.79	0.66	3.04	0.29	2.27
Range	4.43	3.23	14.7	1.58	9.42

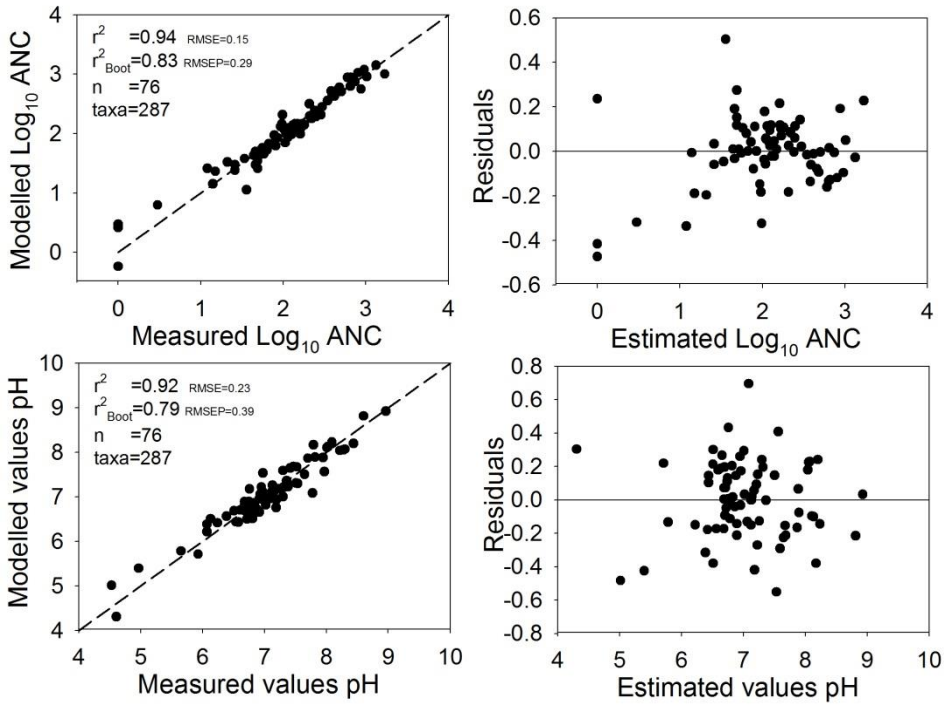

Figure 11.5. Observed versus predicted values and their residuals of pH and acid neutralising capacity (ANC) obtained using WA-PLS transfer functions based on diatom assemblages from the sediment data-set.

Model for TP, I_{Zmax} and temperature showed an important reduction in r^2 and an increase in the RMSE after bootstrapping (Table 20). However, the data distribution and residuals of the models suggest a high reliability of reconstruction at TP values from 3.1 to 4.1 (1.2-12.5 µeq/L), I_{Zmax} values from 0 to 7 (0-49%), and temperature from 7 to 17ºC (Figure 11.6).

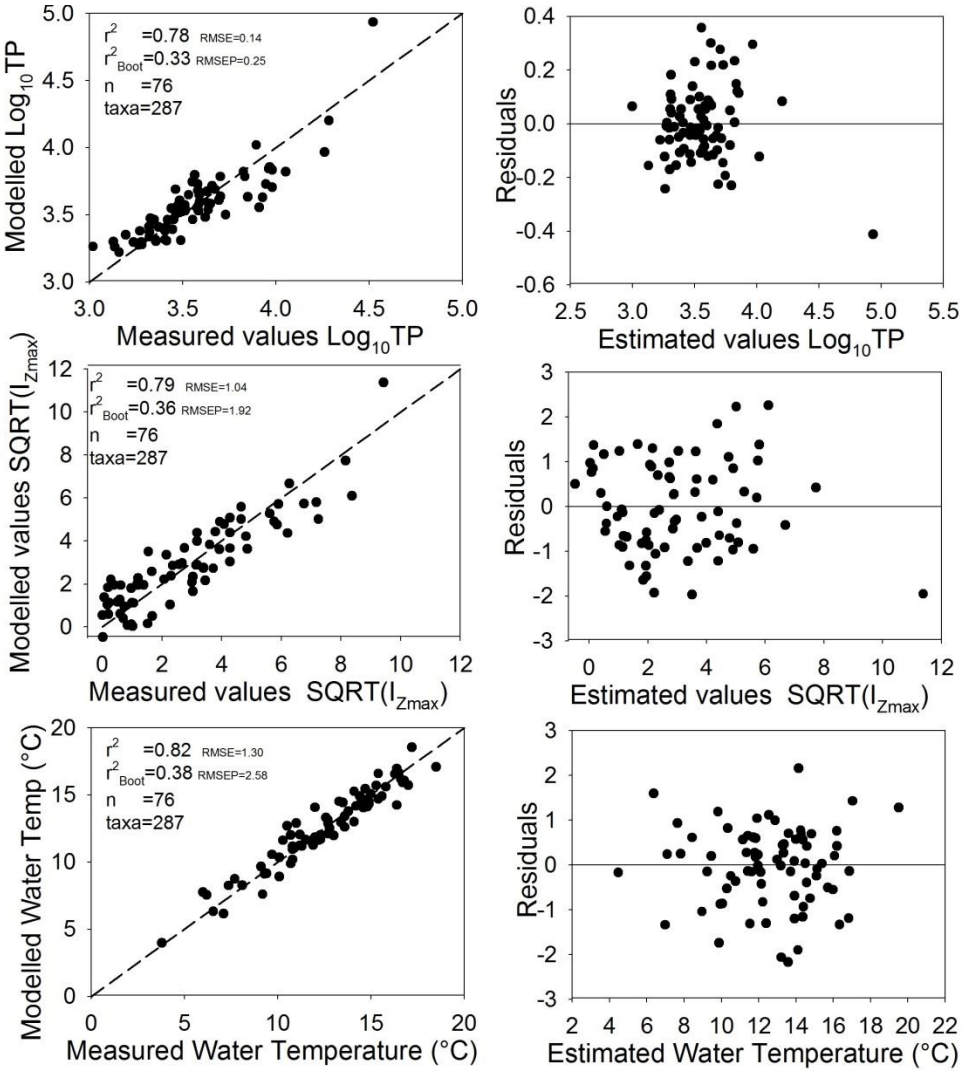

Figure 11.6. Observed versus predicted values and their residuals of total phosphorous, irradiance at the bottom (I_{Zmax}) and summer surface water temperature (SSWT) obtained using WA-PLS transfer functions based on the diatom assemblages from the sediment data-set.

The potentially reliable transfer functions from the epilithon data-set were less than those from the sediment data-set. pH and ANC models showed a similar performance in both data-sets. However, both variables presented a higher increase in RMSE after bootstrapping in the epilithon data-set (Table 16, Figure 11.7).

The transfer function for temperature using the epilithon samples showed lower r^2 and higher RMSE than the model using the sediment data-set. After bootstrapping, the function presented an important reduction in r^2 and an increase in the RMSE (Table 21). The data distribution and residuals of the model indicate that the range of temperature where the reliability of the transfer function is high is similar to that in the sediment data-set (Figure 11.7).

According to the transfer function performance, the sediment data-set appears more suitable for environmental reconstructions using the diatom sedimentary records of the Pyrenees. However, for pH, ANC and SSWT the results are acceptably similar.

Table 21. Summary of the transfer function models and reconstructed variables using epilithon data-set.

	pH	ANC	SSWT
Model			
Transformation	-	Log10(x+1)	-
r^2	0.88	0.93	0.77
RMSE	0.28	0.17	1.5
r^2 bootstrapping	0.74	0.83	0.35
RMSE bootstrapping	0.44	0.3	2.73
Number of samples	78	78	78
Number of species	227	227	227
WA-PLS component	2	2	3
Training-set			
Minimum	4.53	0	3.8
Maximum	8.96	3.23	17.2
Mean	7.00	2.09	12.3
Standard deviation	0.82	0.68	3.15
Range	4.43	3.23	13.4

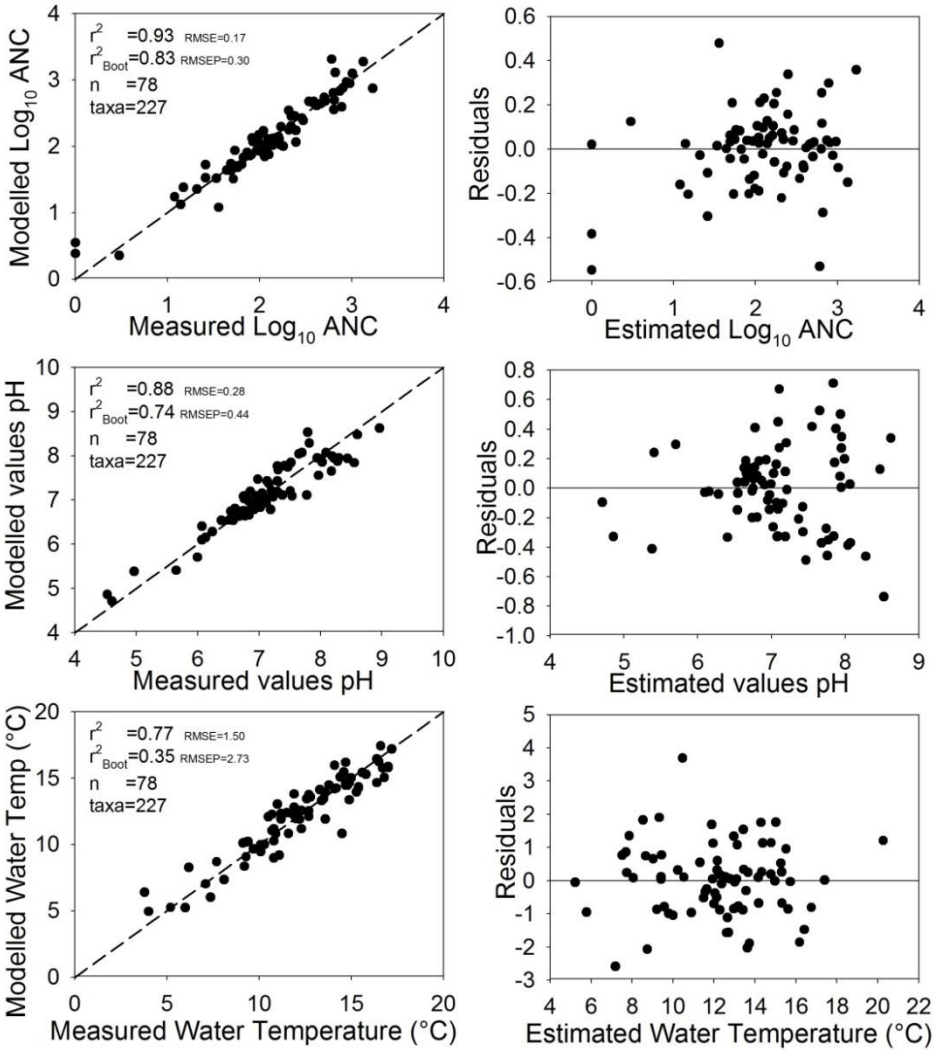

Figure 11.7. Observed vs. predicted values and their residuals for pH, acid neutralising capacity (ANC) and summer surface water temperature (SSWT) obtained using WA-PLS transfer functions based on diatom assemblages from the epilithon data-set.

The relationships between the species optimum and the mean of their occurrences (Figure 11.8) showed that relative abundance was most relevant in defining the optimum in the upper range of TP and I_{Zmax}. For the rest of variables and the lower range of the latter the most important feature is the occurrence of the species rather than its relative abundance. The species present in the Burg Lake sequence basically followed the same patterns.

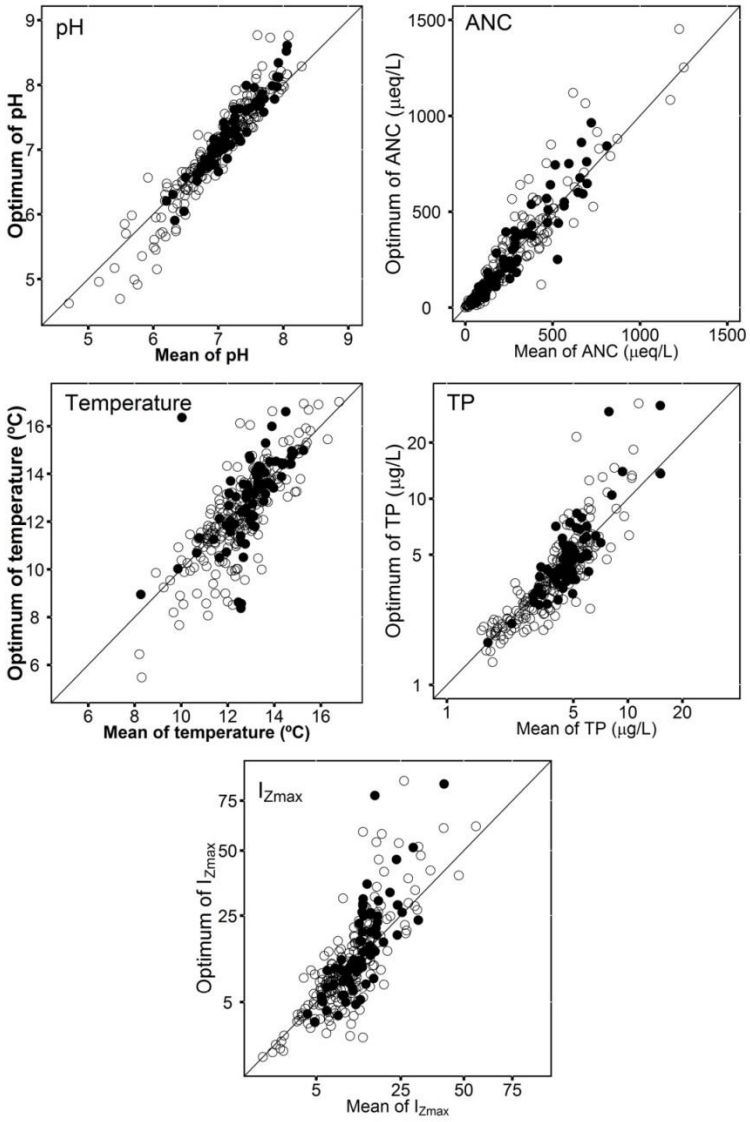

Figure 11.8. Relationship between the species optimum and the mean of their occurrences for the variables for which a transfer function was developed using the sediment data-set. Solid points indicate the species present in the Burg Lake sequence with frequency >1%.

Effect of the spatial correlation on the transfer functions

The effect of the spatial correlation on the transfer functions developed was analysed using the graphical test of Telford and Birks (2009). Transfer function for pH, ANC, TP and I_{Zmax} showed a small reduction in r^2 when the most

neighbourhood lakes are removed from the training set (Figure 11.9, Figure 11.10).

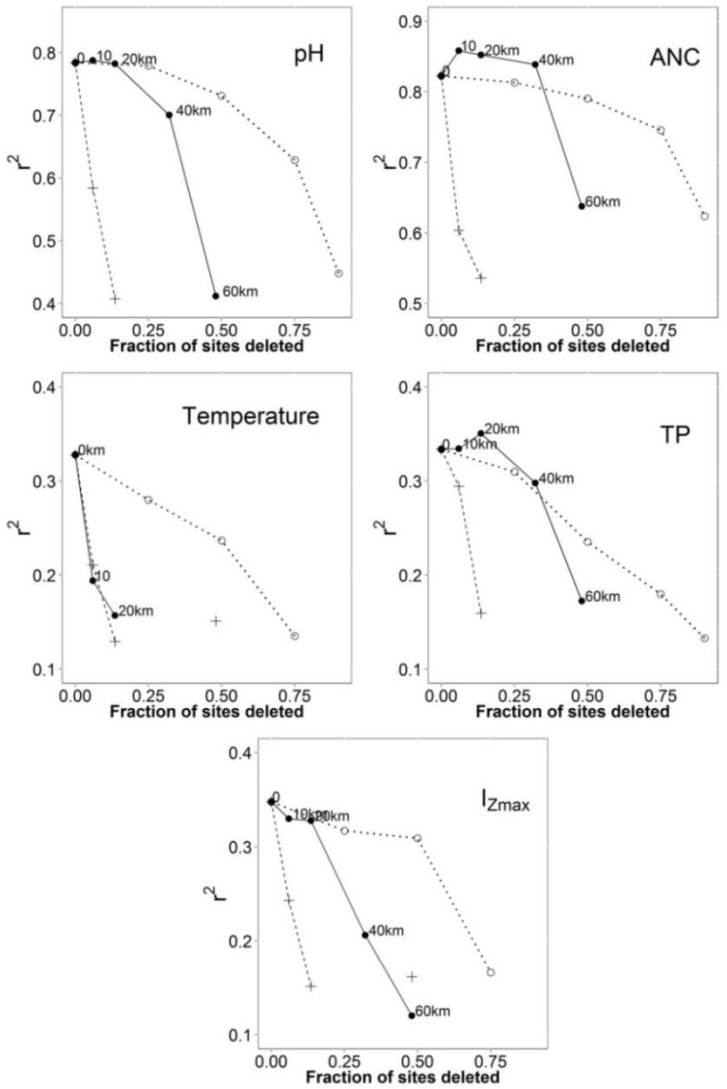

Figure 11.9. Effect of the spatial correlation on the transfer functions developed based on the sediment data-set. The dotted line is the change in r^2 when the lakes are deleted at random; the dashed line when the most similar lakes are successively deleted; and the solid line shows the change in r^2 when lakes are deleted using a neighbourhood distance from 0 to 60 km.

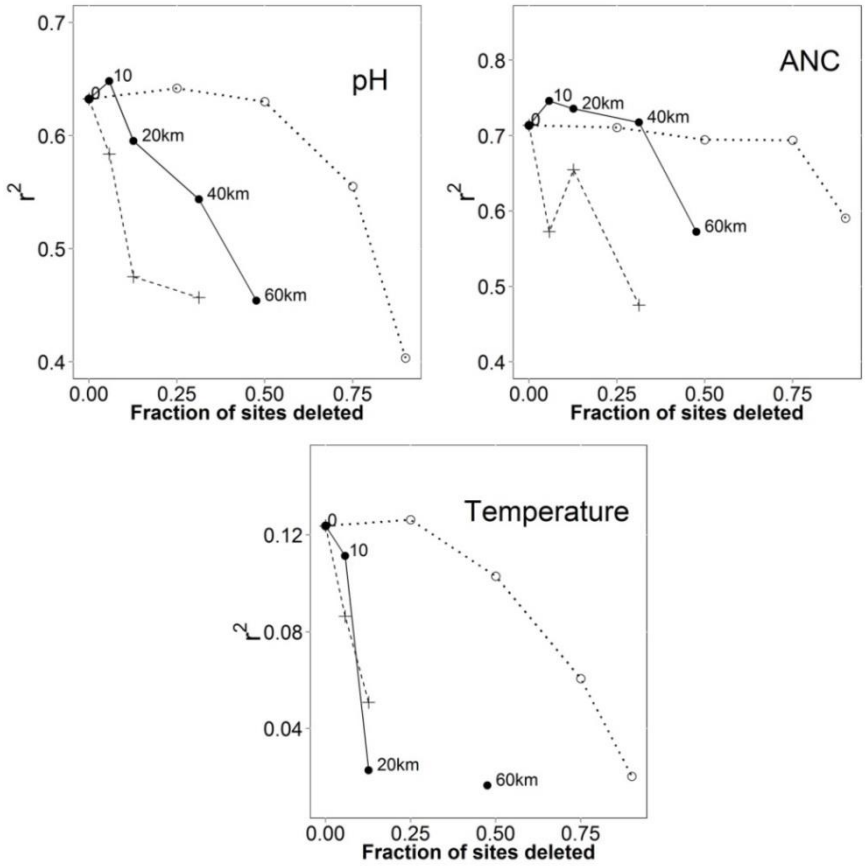

Figure 11.10. Effect of the spatial correlation on the transfer functions developed based on the epilithon data-set. The dotted line is the change in r^2 when the lakes are deleted at random; the dashed line when the most similar lakes are successively deleted; and the solid line shows the change in r^2 when lakes are deleted using a neighbourhood distance from 0 to 60 km.

On the other hand, SSWT presented a strong spatial structure. When neighbouring samples were deleted, r^2 declined similarly to the reduction occurring by deleting the samples more similar to each other. The spatial structure of temperature (SSWT) is due to the high correlation between temperature and the altitude of the lakes ($r = -0.58$, $p<0.001$, $n=76$) and the spatial distribution of high-altitude and low-altitude lakes in the Pyrenees (Figure 11.11A). Low-altitude lakes are located to the east and to both flanks of the Pyrenees; whereas high-altitude lakes are located in the middle part and usually they are grouped together. Consequently, lakes with more similar

temperature are distributed closer than lakes with contrasting temperature. The environmental spatial structure was not completely reflected on the spatial distribution of the diatom assemblages (Figure 11.11B). Only assemblages from lakes with a distance to each other less than 20 km where more similar than those from distant lakes ($p<0.01$, $n=2850$).

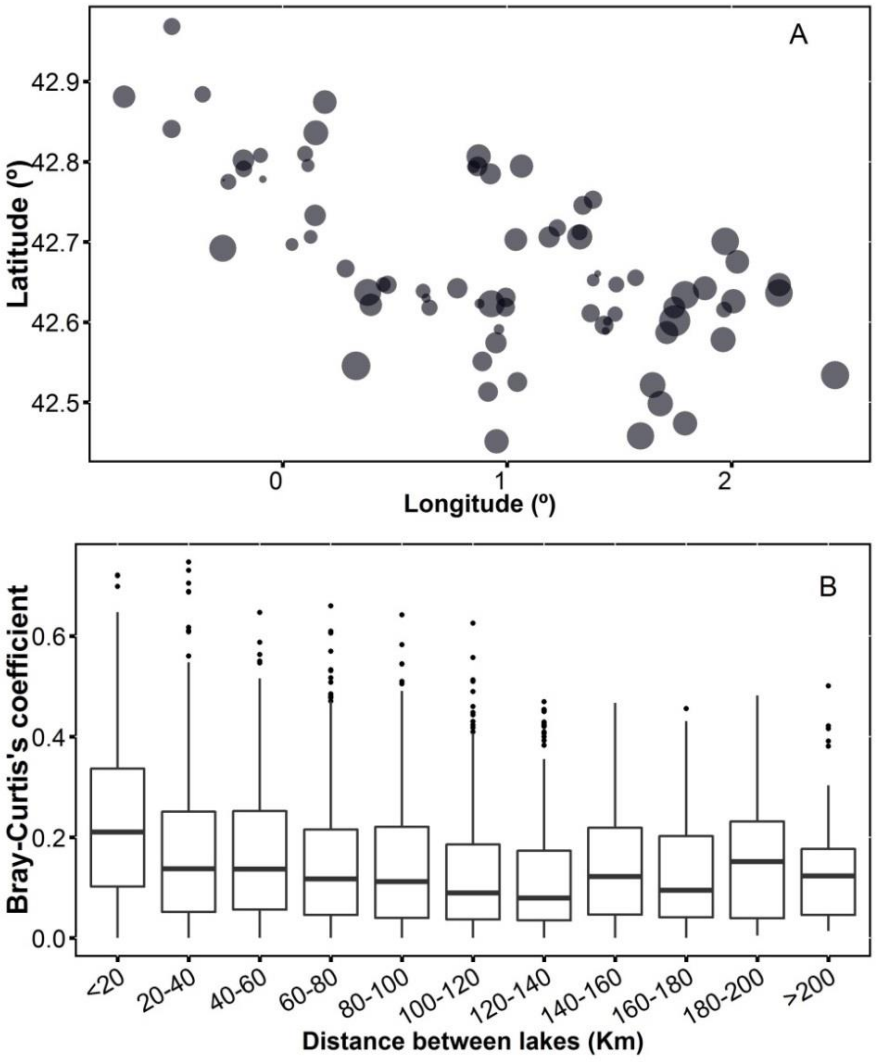

Figure 11.11. A) Spatial distribution of summer surface water temperature (SSWT) in the Pyrenean lakes. The size of the shade circles indicate SSWT relativized to the maximum and minimum survey values. B) Bray-Curtis´s coefficient of diatom assemblage similarity grouped by the distance between lakes.

Effect of the environmental covariance on transfer functions

The unique variance explained by the each environmental variable after removing the explicative capacity of the other variables included in the minimal RDA model (showed in Figure 11.1) was used to investigate whether the species were similarly sensitive to different variables (Figure 11.12). Comparing the 20 species with the highest variance explained by the respective environmental variable, only two were shared by two variables: *Nitzschia palea* var. *debilis* (TP and SSWT) and *Cymbella lange-bertalotii* (SSWT and I_{Zmax}).

Despite of the correlation between some of the environmental variables used to develop transfer functions, this was not translated into the individual species response to each of them (Figure 11.13 vand Figure 11.14). I_{Zmax} and temperature showed some correlation but there were many species with different response to each variable (Figure 11.13B). There were species present in the Burg Lake record such as *Fragilaria delicatissima*, *Karayevia suchlandtii*, *Navicula pseudolanceolata*, and *Staurosirella pinnata* that were highly explained by I_{Zmax} but slightly by SSWT. In contrast, *Stauroforma* cf. *exiguiformis*, *Navicula* cf. *seminulum*, *Pinnularia* cf. *brebissonii* var. *acuta*, and *Sellaphora laevissima* are more sensitive to SSWT than to I_{Zmax}.

TP aslo significantly correlates with I_{Zmax} and SSWT, the species response to the variables also differ (Figure 11.14). *Achnanthes microscopica*, *Encyonema hebridicum*, *Gomphonema* cf. *parvulum*, *Gomphonema* sp. No. 15 Coronas, *Meridion circulare*, *Pinnularia microstauron* var. *nonfasciata*, and *Pseudostaurosira pseudoconstruens* showed a relation with TP that is independent of temperature.

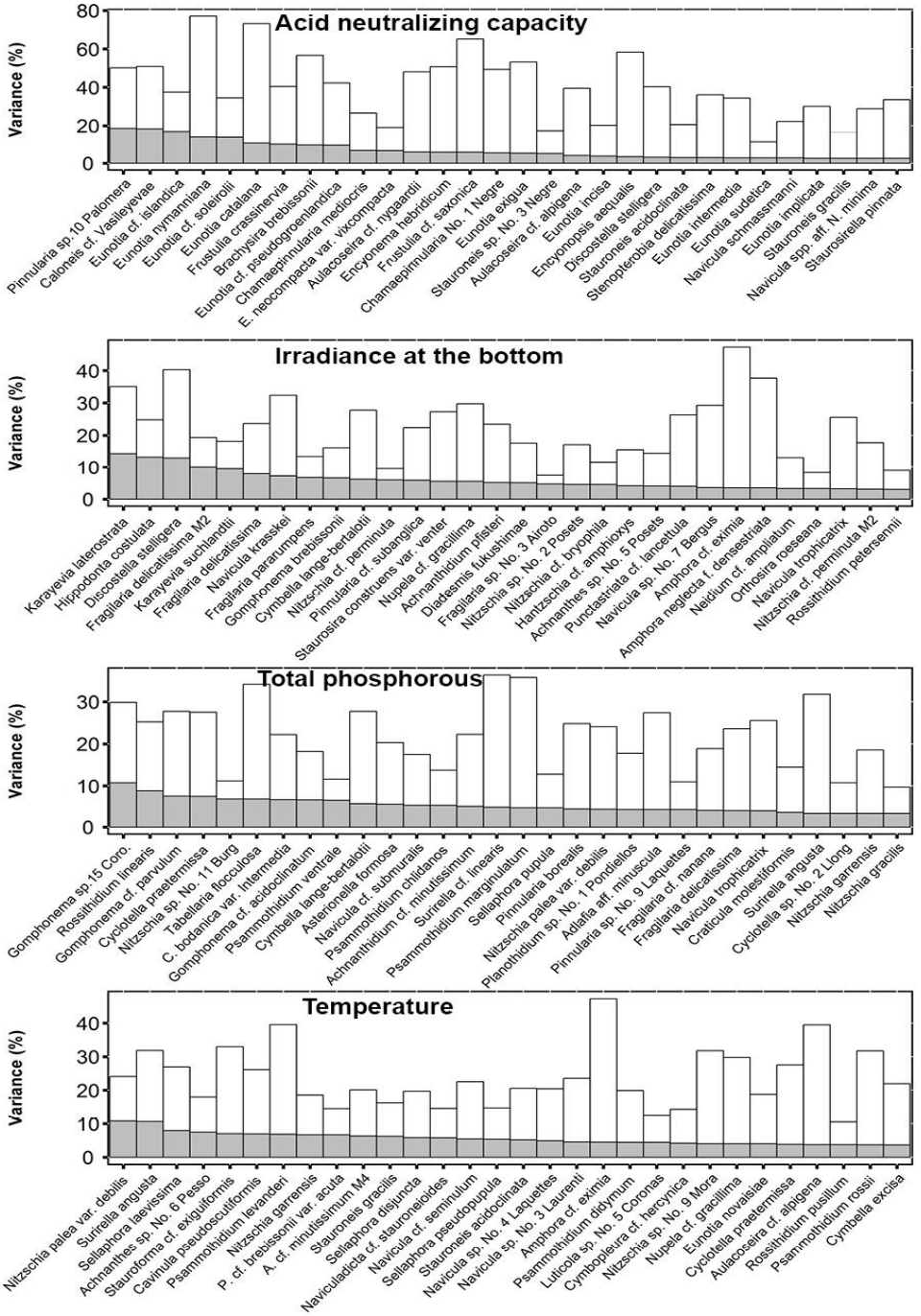

Figure 11.12. Variance of species (grey bars) explained by some selected variables after subtracting the influence of other variables included in the RDA shown in Table 17. White bars indicate the total species variance explained by the RDA of the sediment training-set.

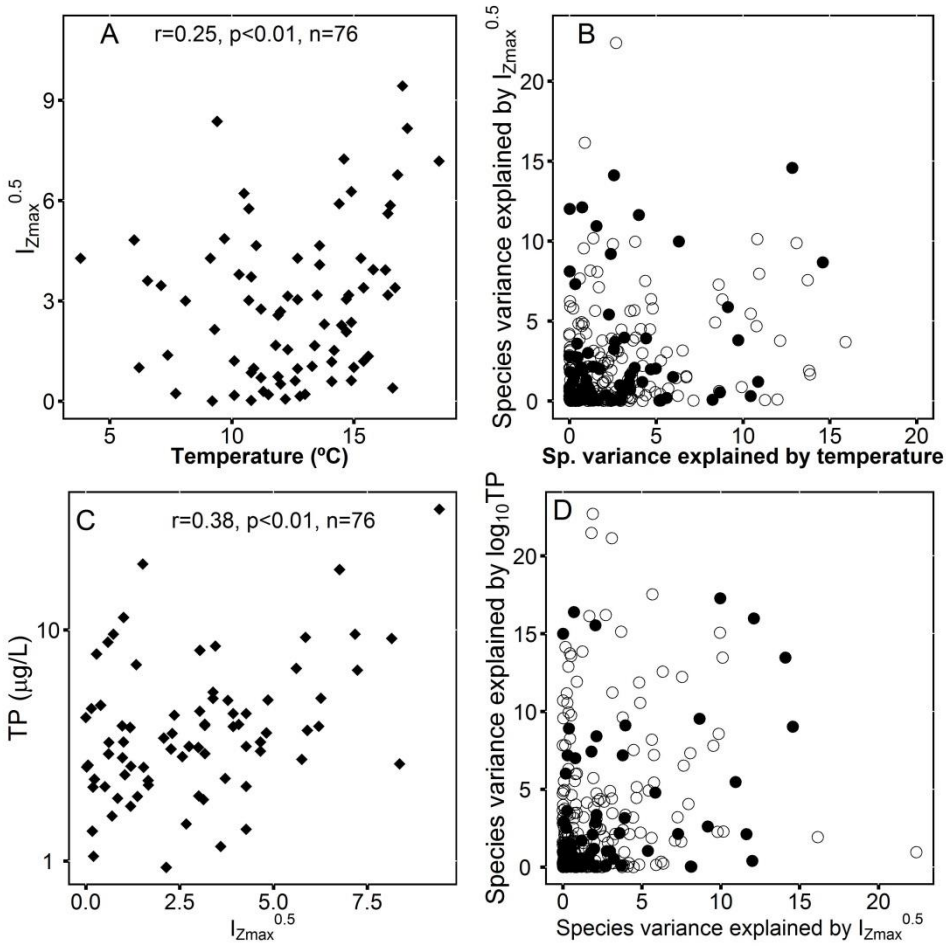

Figure 11.13. Comparison of the correlation between the variables (A, C) used to develop transfer functions and the variance of the species explained by the same variables (B,D). Solid points in B and D are the species of the sediment training-set occurring in the Burg Lake sequence with frequency >1%.

On the other hand, pH and ANC, the highest correlated variables used to develop transfer functions, showed more correlation between the species variance explained by each variable (Figure 11.14). However, the correlation declined for the species of more variance explained by each variable. That is, the species more sensitive to pH are not the same as the species more sensitive to ANC.

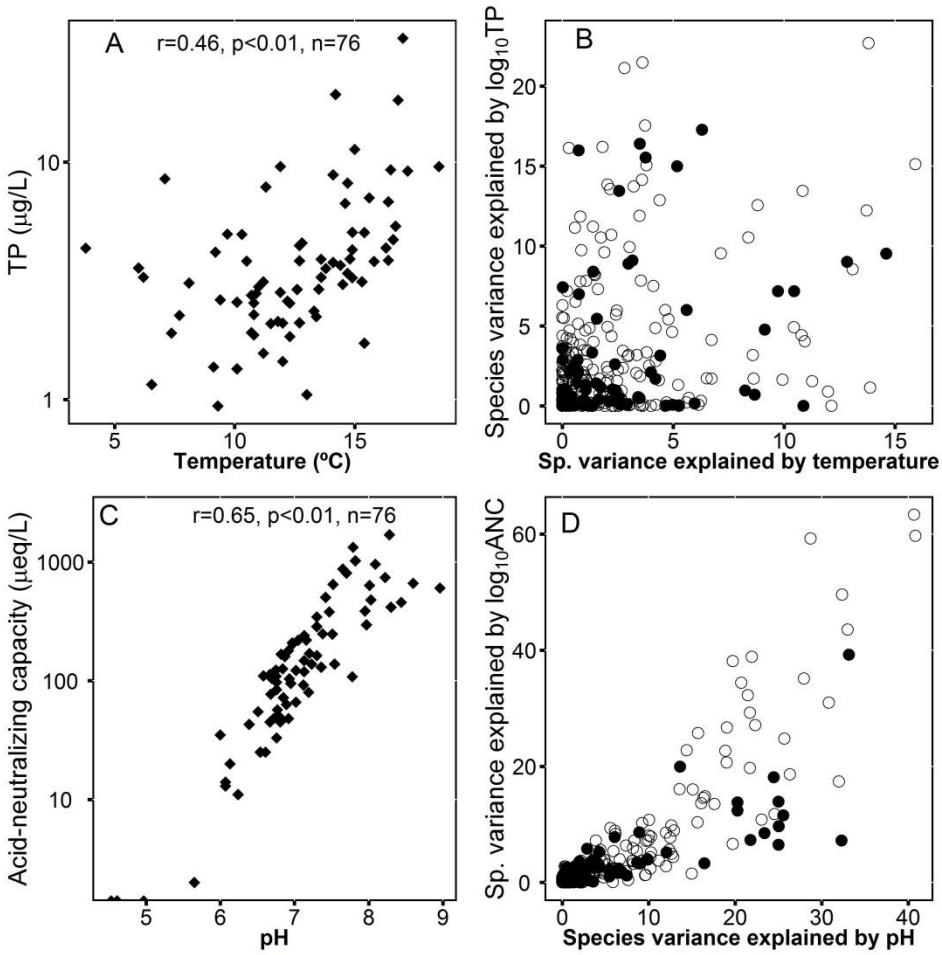

Figure 11.14. Comparison of the correlation between the variables (A, C) used to develop transfer functions and the variance of the species explained by the same variables (B,D). Solid points in B and D are the species of the sediment training-set occurring in the Burg Lake sequence with frequency>1%.

A RDA runned only with the variables selected to develop the transfer functions were used to further identify the species explained by each variable (Figure 11.15). The variation partitioning showed that pH, I_{Zmax} and acid-neutralizing capacity had more marginal explicative capacity. Highly related variables, such as pH and ANC, showed a different combination of species with a high variance explained. There were a representetative number of species occurring in the Burg record explained by a different environmental variable (underlined in Figure 11.15).

Total phosphorous

Species	Var. (%)
Gomphonema sp. No. 15 Coronas	15.99
Asterionella formosa	12.25
Psammothidium marginulatum	12.14
Rossithidium linearis	11.27
Gomphonema cf. *parvulum*	10.94
Navicula cf. *submuralis*	10.33
Stauroneis neohyalina	8.25
Tabellaria flocculosa	7.31
Nitzschia sp. No. 11 Burg	7.18
Nitzschia palea var. *debilis*	7
Pinnularia borealis	6.52
Fragilaria delicatissima	6.49
Pseudostaurosira pseudoconstruens	5.25
Neidium cf. *dubium*	5.23
Pinnularia microstauron var. *nonfasciata*	4.8
Achnanthes microscopica	4.78
Sellaphora pupula	4.09
Stauroneis acidoclinata	3.15
Staurosirella pinnata	2.93
Cavinula pseudoscutiformis	2.91

pH

Species	Var. (%)
Navicula catalanogermanica	40.76
Diploneis cf. *peterseni*	29.18
Encyonema sp. No. 1 Mora	27.47
Navicula pseudolanceolata	21.3
Diploneis cf. *puella*	20.89
Amphora copulata	19.48
Navicula cryptotenella	18.84
Navicula cryptocephala	18.47
Psammothidium subatomoides	17.66
Navicula schmassmanni	17.11
Encyonopsis subminuta	16.4
Achnanthes microscopica	11.55
Encyonema minutum	11.51
Navicula cf. *oligotraphenta*	8.53
Sellaphora pupula	8.51
Gyrosigma sp. No. 1 Sen	8.49
Encyonema silesiacum	7.57
Cymbella excisa	7.53
Punctastriata cf. *lancettula* M1	7.28
Pinnularia subcapitata	6.69

ANC

Species	Var. (%)
Eunotia nymanniana	36.4
Eunotia catalana	20.58
Caloneis cf. *Vasileyevae*	19.59
Frustulia cf. *saxonica*	16.32
Navicula catalanogermanica	15.92
Chamaepinnularia No. 1 Negre	15.82
Encyonema sp. No. 1 Mora	14.77
Brachysira brebissonii	14.5
Pinnularia sp. No.10 Pica Palom.	13.34
Navicula schmassmanni	11.81
Diploneis cf. *peterseni*	10.33
Navicula pseudolanceolata	8.64
Achnanthes microscopica	7.78
Chamaepinnularia mediocris	6.03
Diploneis cf. *puella*	5.82
Navicula sp. No. 7 Bergus	5.57
Stauroneis neohyalina	5.44
Navicula cryptotenella	5.35
Amphora copulata	4.66
Encyonema hebridicum	4.58

Temperature

Species	Var. (%)
Surirella angusta	23.39
Nitzschia palea var. *debilis*	18.35
Stauroforma cf. *exiguiformis*	15.23
Amphora cf. *eximia*	12.71
Pinnularia cf. *brebissonii* var. *acuta*	9.99
Achnanthes sp. No. 6 Pesso	9.82
Nitzschia garrensis	9.37
Psammothidium levanderi	8.39
Navicula cf. *seminulum*	8.15
Achnanthidium cf. *minutissimum* M4	7.76
Navicula cryptotenella	7.39
Sellaphora laevissima	7.38
Cymbella excisa	7.22
Stauroneis gracilis	6.56
Navicula spp. aff. *N. minima*	6.55
Cavinula pseudoscutiformis	6.21
Encyonema reichardtii	5.98
Cocconeis euglyptoides	5.43
Staurosira construens var. *venter*	5.4
Cymbopleura cf. hercynica	5.25

Variation partitioning

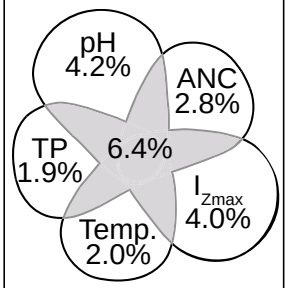

Irradiance at the bottom

Species	Var. (%)
Discostella stelligera	23.4
Karayevia laterostrata	18.89
Hippodonta costulata	14.22
Navicula krasskei	13.62
Fragilaria delicatissima F2	12.17
Karayevia suchlandtii	12.03
Fragilaria delicatissima	12
Nupela cf. gracillima	11.78
Fragilaria pararumpens	9.68
Gomphonema brebissonii	9.24
Staurosira construens var. *venter*	7.02
Navicula cryptotenella	5.87
Nitzschia cf. *bryophila*	5.84
Navicula sp. No. 7 Bergus	4.68
Punctastriata cf. *lancettula*	4.31
Hantzschia cf. *amphioxys*	4.13
Staurosirella pinnata	4.08
Achnanthidium cf. minutissimum M3	3.85
Navicula pseudolanceolata	3.75
Neidium cf. *ampliatum*	3.43

Figure 11.15. Variance of species explained by the environmental variables used to develop transfer functions. Underlined species are present in Burg Lake. The first 10 species for each variable are the species with the highest variance explained in the sediment training set. The next 10 species are the following species present in Burg Lake with high variance explained. The variance for species and variables were obtained with a RDA where the effect of other variables was subtracted. The shaded area is the variance that is share between two or more variables.

Results

Part IV

The ratio between chrysophycean stomatocysts and diatoms

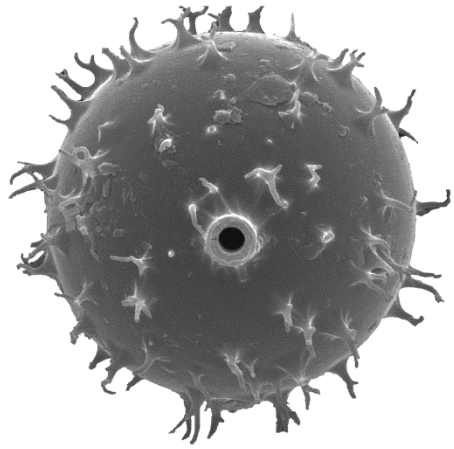

12. The ratio between chrysophycean stomatocysts and diatoms

Chrysophyceae and Synurophyceae are unicellular or colonial algae that are found in a broad range of environmental conditions (Pla et al. 2003; Pla et al. 2009; Zeeb et al. 1994). They produce siliceous resting stages that accumulate in lake sediments storing information about past environmental conditions (Pla and Catalan 2005; Zeeb and Smol 2001). Despite the species identity of most cysts is unknown, the richness and distinctiveness of cyst morphotypes has been used to reconstruct relevant environmental variables (Pla and Anderson 2005; Pla and Catalan 2005). The ratio between Chrysophycean cysts and diatom valve in the sediments indicate the relative importance of these algal groups in the lake ecosystem and may have an environmental meaning that may vary according to the lake type: between polymictic and dymictic lakes (Werner and Smol 2005) or ponds and lakes (Douglas and Smol 1995), for instance. The cyst:diatom ratio has been used as an indicator of past lake water salinity (Cumming et al. 1993), ice cover duration (Smol 1983) and tropic status in temperate lakes (Smol 1985). In order to apply the cysts:diatom ratio in past environment reconstruction of the Pyrenean lakes, in this section the ratio environmental meaning in these lakes was investigated.

The ratio was considered as the percentage of cyst with respect to the sum of cyst and diatom cells. Cyst showed a lower abundance with respect to diatom, only in 9% of the lakes the quantity of cyst counted was higher than the diatom cells. Cyst ratio ranged from zero to 73.3%, with a mean of 17.1% and a median of 10.5%. The only lakes without recorded cysts were Cap Long and Barroude Inferior; these lakes were very shallow (2.1 and 9.5 m depth, respectively) and had a high pH (7.95, 8.60, respectively).

A canonical correspondence analysis (CCA) showed that cysts abundance was related mainly with lake depth, Ca^{2+} and I_{Zmax} (Figure 12.1).

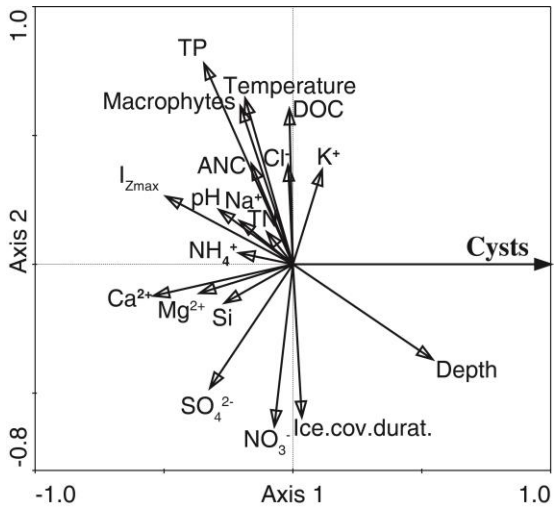

Figure 12.1. Biplot of a canonical correspondence analysis where environmental variables were constrained to be lineally related to the Chrysophycean cysts:diatom ratio.

Lakes with a depth lower than 6 m showed a high probability of presenting cyst abundances lower than 5% (mean of 2.3%) (Figure 12.2). Lakes with depth between 6 and 10 m showed abundances lower than 10%. On the contrary, lakes with depth higher than 35 m showed abundance of cyst higher than 20% with a median of 48%.

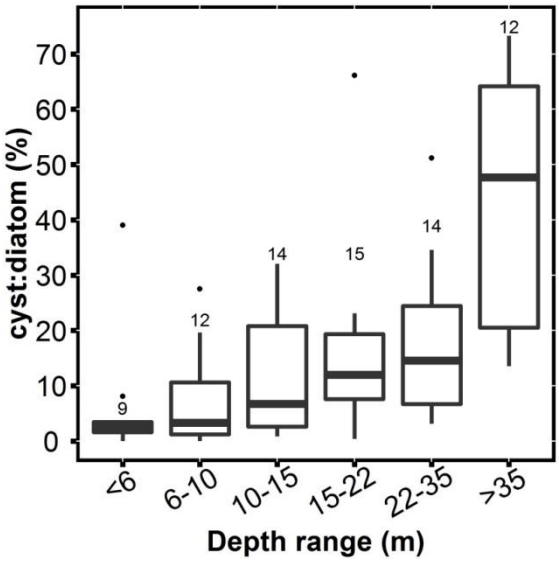

Figure 12.2. Relationship between cyst:diatom ratio in the sediment samples and depth of the Pyrenean lakes. The number of lakes included in each depth range is indicated.

The second explanatory variable of the cyst:diatom ratio was the Ca^{2+} concentration. The comparison between the ratio and classes of SO_4^{2-} and Ca^{2+} of the Pyrenean lakes (Figure 6.5) showed that cyst:diatom ratio was higher in the most acid lakes. The lower cyst:diatom ratio was quantified in lakes with pH >7.25 (Figure 12.3).

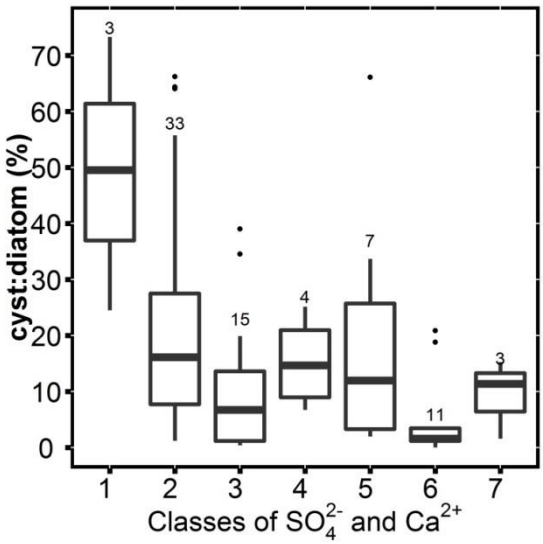

Figure 12.3. Relationship between cyst.diatom ratio of classes of SO_4^{2-} and Ca^{2+} as described in (Figure 6.5). Number indicated above every box is the number of lakes included in every depth range.

If the relationship between the cyst:diatom ratio is further analysed using generalized additive models (Table 22), similar results to the CCA are obtained. Lake depth, Ca^{2+}, Mg^{2+} and I_{Zmax} were the variables with higher relation with the ratio. TP was significantly related with cyst, but the variance explained was half of the depth. Models using two variables showed that TP was significant only in models in which depth and Ca^{2+} were not included. Models including three variables showed that TP was significant only in the model that included depth and I_{Zmax}. The analysis of multivariate models suggests that the best model to explain cyst:diatom ratio included only Depth + Ca^{2+}. Accordingly, the strong relation between the cyst abundance and the depth can be used as index of water level or depth in Pyrenean lakes (Figure 12.4).

Table 22. Generalized additive models to explain the cyst:diatom ratio. The best models were identified using Akaike`s information criterion (AIC) and deviation explained (Dev. Exp.).

Variable(s)	AIC	Dev. Exp. (%)
Univariate models		
Depth***	626	40.1
Ca^{2+}***	644	28
Mg^{2+}***	645	31.2
I_{Zmax}***	647	22.3
TP*	653	21.3
SO_4^{2-}*	658	18.5
Si*	660	7.0
Best models with two variables		
Depth*** + Ca^{2+} ***	610	55.1
Depth*** + Mg^{2+} *	616	54.6
Depth*** + TP	619	56.2
Depth*** + I_{Zmax}	626	44.5
Ca^{2+} * + Mg^{2+}	636	43.9
Best models with three variables		
Depth*** + Ca^{2+} *** + Mg^{2+}	610	56.1
Depth*** + Ca^{2+} *** + I_{Zmax}	611	55.6
Depth*** + Ca^{2+} *** + TP	611	55.1
Depth*** + I_{Zmax}* + TP*	615	59.7
Ca^{2+} ** + I_{Zmax}*** + Mg^{2+} *	616	59.3

*p<0.05, **p<0.01, ***p<0.001

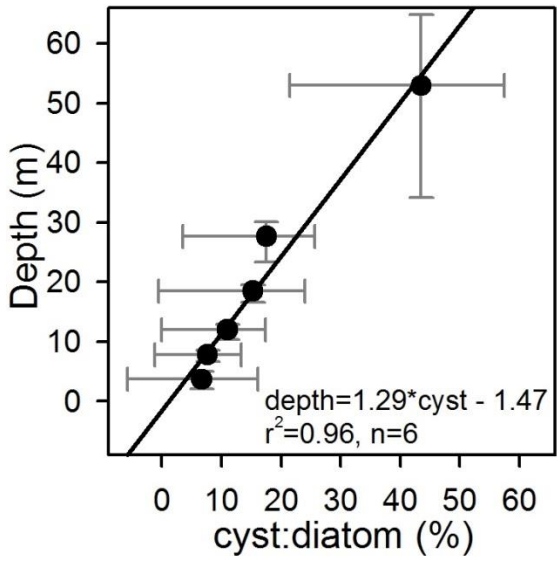

Figure 12.4. Lineal regression between the mean of depth and the mean cyst abundance of group of depths showed in Figure 12.2. Error bars at 95% of means are showed.

Results

Part V

The Burg Lake diatom sequence and Late Glacial and Early Holocene changes

Casa Batlló, Barcelona

The world seen through the silica

13. Late Glacial and Early Holocene in the Northern Hemisphere: context for the Burg Lake sequence study

Deglaciation (GS-2a,b, ~18000 -14600 yr cal BP)

After the Late Glacial maximum, the transition towards a more stable Holocene (ca., 11,000 yr cal BP) was a period with a high climatic variability showing changes in insolation, ice sheets, concentration of greenhouse gases, and other significant global processes (Clark et al. 2012); the complexity of the adjustments caused the insertion of cold periods (stadials) within the general warming trend. The early deglaciation period (17500-14500 yr cal BP) showed contrasting situations around the world and some authors refer to it as the "mystery interval" (Denton et al. 2006; Williams et al. 2012). During early deglaciation, the ice record of Greenland indicates cold conditions (Rasmussen et al. 2006) while the major recession of mountain glaciers in the two hemispheres, a drop in atmospheric ^{14}C, deglacial warming of Antarctica, maximum aridity in the African rift valley, and cold conditions in Mediterranean and North Atlantic Ocean were occurring (Denton et al. 2006). This spatial differences have been attributed to an increased in the seasonality, which consisted of hypercold winters and warmer summers (Denton et al. 2006). Hypercold winters were related to a reduction in the Meridional Overtuning Circulation (MOC) combined with a positive feedback associated with a high albedo (Williams et al. 2012). The high volume of North-Hemisphere ice accumulated during LGM and the rise in summer isolation produced large quantities of icebergs and meltwater that reduced the MOC and resulted in a North-Hemisphere stadial with severe winters (Denton et al. 2010).

The reduction in MOC has been explained by the massive melting of the Northern-Hemisphere Ice Sheets around 19000 yr BP, the Heinrich event 1 (Heinrich 1988), and routing events along the Ice Sheet margin (Clark et al. 2012; Stanford et al. 2011). There are evidences of a continuum melting that suggest the continuation of hypercold winters and warmer summers throughout the entire mystery interval (Williams et al. 2012).

Palaeolimnogical records of GS-2a in Europe show the complexity of this period. Thus, for example, melting process produced a high fluvial discharge that has been recorded in sedimentary sequences from the Black Sea (Bahr et al. 2006) to the Iberian Peninsula (González-Sampériz et al. 2005). Terrestrial records suggest dry conditions during this period. Pollen and chironomid records indicate precipitation around 200-300 mm and July temperatures between 9-13ºC in Jura Mountains (Magny et al. 2006; Peyron et al. 2005). Northern French Alps showed a dominance of steppe vegetation with a rapid change to arboreal vegetation around 14500 yr cal BP (David 2001). The Pyrenees had steppe vegetation, and high records of *Artemisia*, Poaceae, Chenopodiaceae and *Ephedra* pollen (González-Sampériz et al. 2005), indicating aridity. Chironomid records for the western Pyrenean foothill indicate cold conditions during GS-2a (Millet et al. 2012).

Marine records show contrasting evidence between the Iberian margin of the Atlantic Sea and the Mediterranean Sea. Foraminifera oxygen isotopic records from the Gulf of Cadiz show colder surface sea temperature during deglaciation time than during LGM (Cacho et al. 2001; Palumbo et al. 2013). In contrast, Western Mediterranean Sea surface temperature rose at approximately 16000 yr cal BP (Cacho et al. 2001; Frigola et al. 2008) while the pollen record in marine sediments of the Alboran Sea suggests dry and cold conditions during GS-2a (Fletcher et al. 2010).

Greenland Interstadial (GI-1, ~14600-12850 yr cal BP)

The GI-1 period, also known as Bølling –Allerød, showed a rapid increase in temperature at the onset (Björck et al. 1998). Western Europe underwent an increase in summer temperature of 3-5 ºC (Renssen and Isarin 2001). A chironomid record from the Jura mountains suggests a progressive increase of temperature of 2-3 ºC in Central Europe (Peyron et al. 2005) whereas other records suggest a rapid increase in temperature (Samartin et al. 2012; Tóth et al. 2012). Temperature reconstruction in North-western Pyrenees using a chironomids indicates a rapid rise in temperature around 14800 yr cal BP (Millet et al. 2012) in agreement with the most common pattern.

The warm phase was punctuated by three cold and short periods that also has been recorded in Europe (Friedrich et al. 2001; van Raden et al. in press). The

principal cold events recorded in GI-1 are GI-1d, ~14020-13900 yr cal BP, and GI-1b, ~13260-13050 yr cal BP (Lowe et al. 2008). The record of evidences of the cold periods in GI is variable (Fletcher et al. 2010; Millet et al. 2012; Mortensen et al. 2011; Peyron et al. 2005; Robinson et al. 2006; Shumilovskikh et al. 2012; Tóth et al. 2012), probably as a consequence of the sampling resolution, the regional variability and the idiosyncrasy of each register.

Younger Dryas stadial (YD, ~12800-11650 yr cal BP)

The Younger Dryas, also called GS-1 in INTIMATE terminology (Björck et al. 1998; Lowe et al. 2008) is recorded in Greenland as a period of very cold and dry winter (Rasmussen et al. 2006), which started with a rapid decrease in temperature and humidity. During the YD, the Northern Hemisphere and, principally, the Artic underwent a rapid increase in ice and glacial extension (Denton et al. 2005). However, some simulations suggest that YD was warmer than the reconstructed values in Greenland indicated because of the alteration of temperature-$\delta^{18}O$ relationship caused by deglacial atmospheric circulation (Liu et al. 2012).

The rapid change of temperature detected with different proxies in many sedimentary records around the North Hemisphere is a topic of debate (Fiedel 2011), there is no consensus about the specific cause that triggered the YD. The sudden change in temperature has been correlated with evidences of a meteoritic impact at 12,900 yr cal BP (Israde-Alcántara et al. 2012; Wittke et al. 2013). However, the age of the sedimentary record with meteoric impact cannot be established correctly (Blaauw et al. 2012) and chemical compositions of microspherules and other evidences on the corresponding stratigraphic level of the YD are not coherent with an extra-terrestrial mechanism (Pinter et al. 2011; Wu et al. 2013). Other hypothesis with a catastrophic triggering mechanism is the overflow of the glacial Lake Agassiz to the Atlantic, which caused a weakening of MOC (Broecker et al. 1989). However, geomorphological evidences of a flood of Agassiz are not completely accepted and it is suggested that a Heinrich event (H0) occurred at the onset of the YD (Andrews et al. 1995) as an integral part of global transition from glacial to interglacial climate (Broecker et al. 2010) or caused by the meltwater discharge from the Artic (Cronin et al. 2012). Recently, water budget reconstructions of Lake Agassiz during the onset of YD suggest a decline in lake level as a consequence of the opening of an outlet lower than the one at the southern end of the lake (Teller

2013). Clark et al. (2012) suggest that the YD was likely caused by a combination of the freshwater routing through the St. Lawrence River and the H0.

Recording of the YD stadial in Europe is variable according to the geographical position and the proxy used. The main consequence of temperature reduction during the YD was the development of steppe-grassland communities in the south of Europe and tundra in the north (Clark et al. 2012). Some records from Central Europe show cold conditions (Samartin et al. 2012) but other records suggest a moderate cooling and dry conditions during YD (Joannin et al. 2013; Peyron et al. 2005). Records from Western Europe indicate severe cold conditions (Ménot and Bard 2012) and records from the Alps cold but high lake level during the first centuries of the YD (Magny et al. 2003). In the Iberian Peninsula cold and dry conditions were recorded, but the severity of the YD was apparently highly variable both in latitude and altitude (González-Sampériz et al. 2006; Moreno et al. 2012; Muñoz Sobrino et al. 2013).

The end of the YD in Greenland and North European records are marked by a sudden increase of temperature and humidity (Rasmussen et al. 2006). The analysis of the end of YD suggest that there was a N-S gradient with less cold conditions near to the Mediterranean Sea (Davis et al. 2003). Sea surface temperature at the Alboran sea and the Iberian Margin recovered faster than Greenland temperatures when the YD was ending (Cacho et al. 2001; Palumbo et al. 2013).

Early Holocene (EH, ~11650-8000 yr cal BP)

The Holocene started with a rapid increased in Greenland temperature (Alley 2000; Björck et al. 1998). There are a lot synchronic evidences through Europe of the onset of the Holocene around 11600 yr cal BP. The most common evidence is a rapid reduction in steppe vegetation and an increase in the inferred temperature using different proxies (Dormoy et al. 2009; Samartin et al. 2012).

In the Iberian Peninsula there is a general correspondence with Greenland record, showing warm and wet conditions (Moreno et al. 2012) with a rapid regression of semiarid vegetation (Fletcher et al. 2010; González-Sampériz et al. 2006). However, a record of lake Estanya suggests dry conditions during the Holocene onset (Morellón et al. 2009).

Despite that the warming at the onset of the Holocene is faster than the cooling during YD onset in Artic records, the attention of EH has been focused on the coldest events and its consequences on different ecosystems. The 8.2, 9.3 (cal yr BP) and Preboreal oscillation (PBO) are the main cold events of the EH (Lowe et al. 2008; Rasmussen et al. 2007). The PBO oscillation is one of the events of most interest because occurred only 300 years after the Holocene onset and it was a rapid regression to cold conditions (Bohncke and Hoek 2007; Bos et al. 2007; Joannin et al. 2013).

In this section the Burg Lake diatom sequence corresponding to Late Glacial and Early Holocene will analysed from a limnological perspective in the general climatic context of these periods.

The Burg Lake diatom sedimentary sequence

Changes in composition and abundance of diatoms in a stratigraphic sequence are related with changes in past environmental conditions (Fritz and Anderson 2013). The main changes in diatom assemblages have been related to changes in pH, salinity, temperature (Battarbee 2000; Medeiros et al. 2012; Solovieva et al. 2005; Westover et al. 2006) and nutrients (Fritz et al. 2004). The environmental interpretation of the past changes in diatom assemblages only assumes that organisms responded in the past in the same way as they do with present conditions, which is an assumption that is reasonable within the Holocene and Lake glacial at a regional scale.

Diatoms, as any microorganism, respond to their immediate (proximal) environment. It makes sense to reconstruct average chemical and physical conditions of the lake but the cause of these changes has to be considered in a broader limnological context. Basically there are two drivers: lake ontogeny and climate change. The latter modify the physical atmospheric forcing and also the loadings from the catchment. Due to this complexity, it is desirable to add other elements of the stratigraphic record to the interpretation of the environmental changes that diatoms may indicate (Juggins and Birks 2012). In this study, geochemistry and subfossil pigments have been used as complementary information to the diatom assemblages.

In summary, using the interpretative tools that were developed in previous chapters, the aim of this chapter was to analyse the chronological changes of the diatom assemblages in the Burg Lake sequence and the limnological and

climatic contexts in which they may have occurred, with the aim to contribute to the understanding of lake ontogenic processes and palaeoenvironmental and palaeoclimatological reconstructions.

14. A chronological model of the Burg Lake sequence

The chronological model of the Burg Lake sequence was based on 15 radiocarbon data (Table 23). The most surficial section was dated using ^{210}Pb, which indicated 100 yr cal BP at 7.5 cm depth.

The age-depth model was built using the Bayesian approach described in the methods section. The distribution of the Markov Chain Monte Carlo iterations indicate that the output of the age-depth model was relatively stable (Figure 14.1B). The low correlation with respect to the prior value (Figure 14.1C) suggests a higher than expected sub-centennial sedimentary variability (Blaauw and Christeny 2011).

According to the model, the sedimentation rates ranged from 0.6 to 68 yr/cm (mean = 12.7, median = 9.2 yr/cm). During the early period (1348 cm to 1150 cm, ~17000-13000 yr cal BP) the lake presented the lowest sedimentation rate (mean = 20.2, median = 14.5 yr/cm). After this phase, between 1150 and 642 cm, sedimentation rate was higher (mean = 9.8, median = 7.5 yr/cm).

Table 23. Samples of the Burg Lake sequence used for radiocarbon dating (Pèlachs et al. 2011).

Sample (cm)	Lab. code	^{14}C age	Age (yr cal BP) used for the chronological model (CalPal2007_HULU)	Material dated
77-78	NOSAMS - 59778	600±30	602±37	Microcharcoals (*Betula* sp)
110-111	Beta-246362	2050±40	2024±60	Microcharcoals
121-122	NOSAMS-59779	1920±30	1871±32	Peat
211-212	NOSAMS-59781	2960±30	3142±54	Shrub remains (*Rosa* sp.)
343-344	Beta-246363	4360±40	4935±53	Macroplant remains
459-460	NOSAMS-59782	5230±30	5975±29	Macroplant remains
540-541	Beta-246364	7590±40	8399±19	Peat
618-619	Beta - 345421	7520±40	8075±64	Peat
786-787	Beta-246365	8800±40	9831±82	Wood-charcoal
914-915	NOSAMS-59784	9520±45	10888±15	Tree remains
1026-1027	NOSAMS-59785	10050±45	11582±16	Tree remains
1143-1144	NOSAMS-59786	10950±50	12883±94	Tree remains
1226-1227	Beta-246366	12420±60	14655±34	Peat
1251-1252	NOSAMS-59787	13350±60	16286±42	Peat
1346-1348	NOSAMS-59788	13750±60	16907±17	Seed from aquatic plants

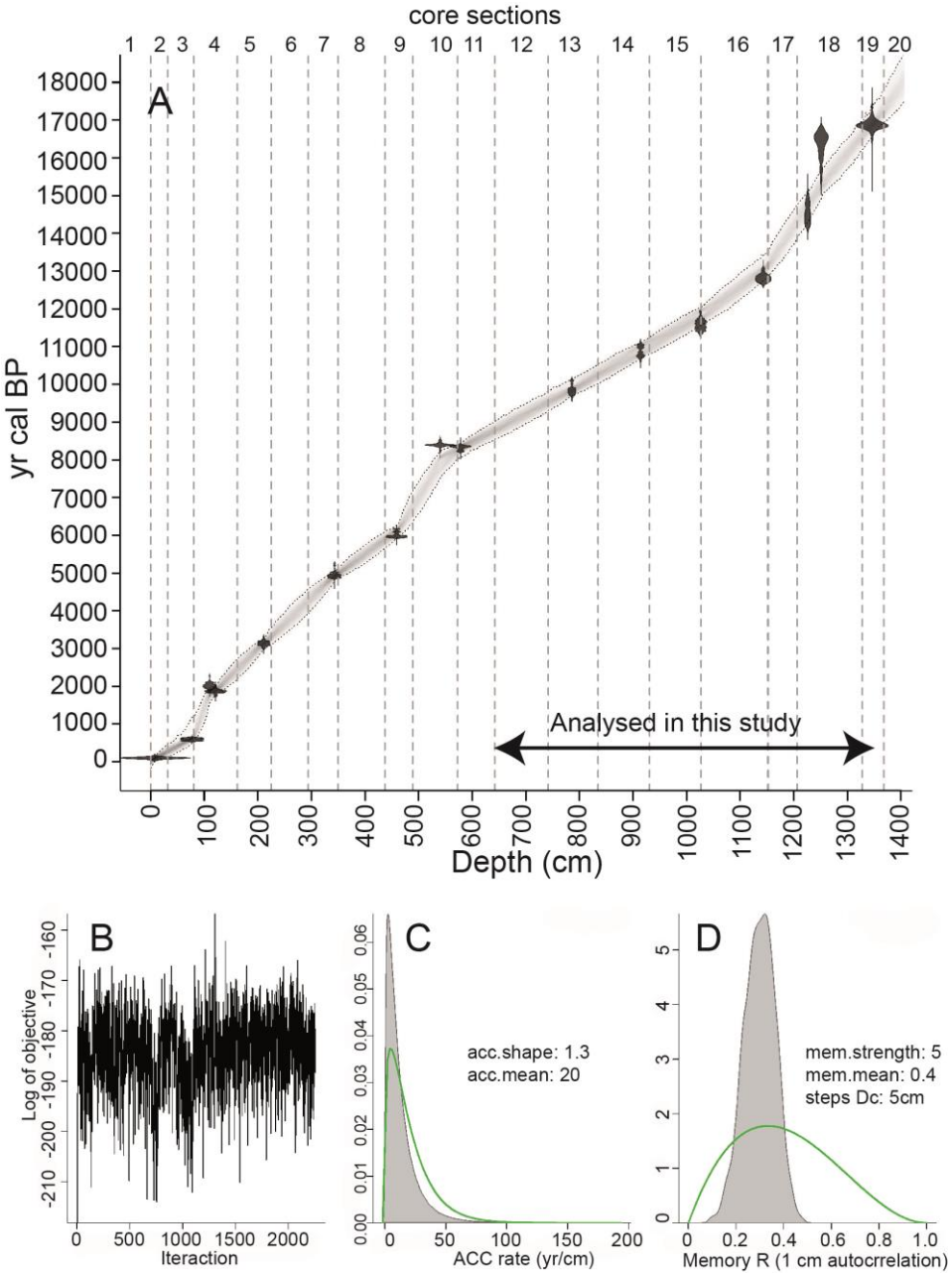

Figure 14.1. Age-depth model for the Burg Lake sequence built using Bacon program (Blaauw and Christeny 2011). A) Age-depth model and distributions of the calibrated ^{14}C dates (dark shaded area). The gray-shaded area limited by dotted lines indicate the 95% intreval. Numbers in the top legend and vertical lines indicate the core sections. B) Stability of itereactions using Markov chain Monte Carlo. C) Accumulation rates. D) Memory of the accumulation rate. Lines in C and D are the prior values and gray histograms are the estimation.

15. Diatom composition and sequence zonation

Diatom composition

The Burg Lake diatom record includes 244 taxa. 55 species were present in more than a 10% of samples and 17 species had a maximum abundance >5% (Figure 15.1, Figure 15.2). *Staurosira construens* Ehrenberg, *Staurosirella pinnata* (Ehrenberg) Williams & Round, *Punctastriata* cf. *lancettula* (Schumann) Hamilton & Siver M1, *Achnanthidium minutissimum* (Kützing) Czarnecki *P. lancettula* (Schumann) Hamilton & Siver, and *Encyonopsis subminuta* Krammer & Reichardt were the species with the highest frequency and dominance.

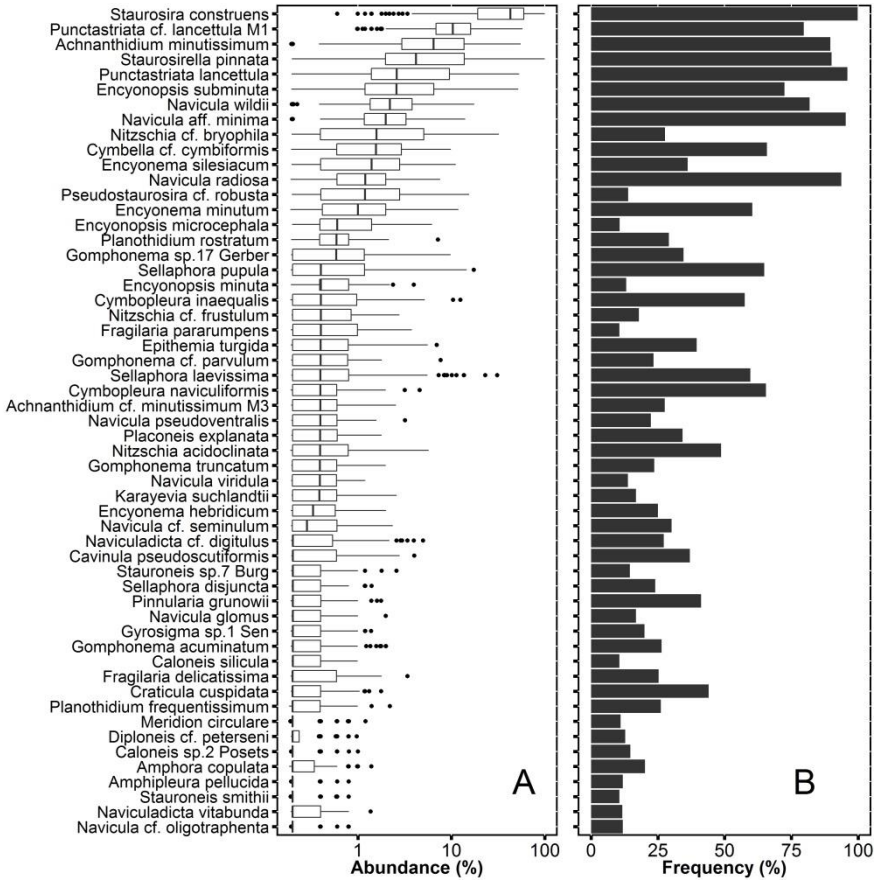

Figure 15.1. Relative abundance (A) and occurrence frequency (B) of the most common species (frequency >10%) in the Burg Lake sequence. Species are ordered by the abundance median.

Navicula radiosa Kützing, *Sellaphora laevissima* (Kützing) Mann, *Sellaphora pupula* (Kützing) Mereschkowsky sensu lato, *Nitzschia acidoclinata* Lange-Bertalot, *Cymbopleura inaequalis* (Ehrenberg) Krammer and *Cavinula pseudoscutiformis* (Hustedt) Mann & Stickle, presented an intermediate abundance and high frequency; whereas species such as *Nitzschia* cf. *bryophila* (Hustedt) Hustedt, *Encyonema silesiacum* (Bleisch) Mann, *Encyonopsis microcephala* (Grunow) Krammer, and *Fragilaria pararumpens* Lange-Bertalot, Hofmann & Werum showed also an intermediate abundance but a low frequency.

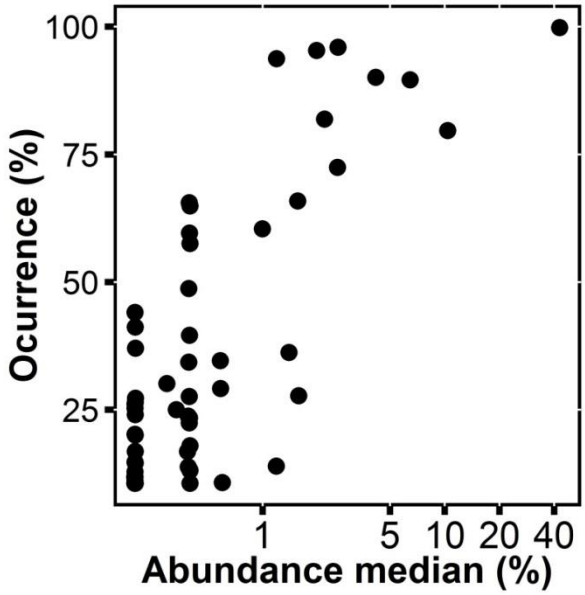

Figure 15.2. Relationship between the median of the abundance and occurrence frequency of the most common species (frequency >10%) in the Burg Lake sediment sequence.

Species richness per sample ranged from 1 to 44 species and the average number was 23.5. Species richness was lower than five in a few samples levels, at the base of the sequence studied (1330-1317 cm, 16700-16500 yr cal BP). *Staurosirella pinnata* (Ehrenberg) Williams & Round, *Staurosira construens* Ehrenberg, *Staurosirella leptostauron* (Ehrenberg) Williams & Round and *Encyonema reichardtii* (Krammer) Mann were the only species at the beginning of the diatom record. After that, species accumulation increased and richness

reached 50 accumulated species during the first six centuries (1287 cm, ~16000 yr cal BP, Figure 15.3A).

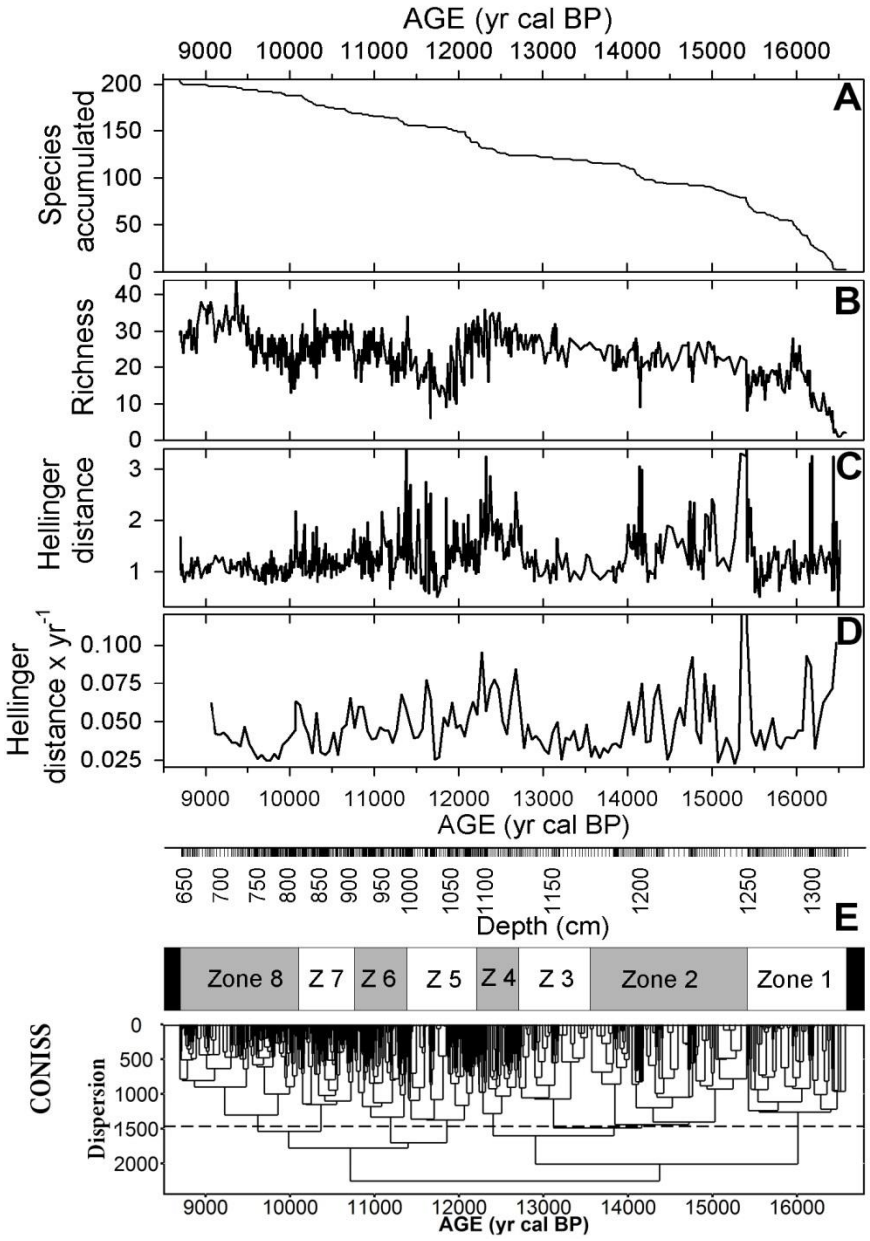

Figure 15.3. Descriptors of the diatom assemblage change across the Burg Lake record A) curve of species accumulation; B) species richness by sample); C) Hellinger distance between consecutive samples (after smoothing data using a three samples moving average); D) rate of change in units of Hellinger distance per calendar age every 50 yr (after TWAS procedure); and E) zonation using CONISS clustering.

Species accumulation showed a marked increase at levels: 1250 cm (~15300 yr cal BP), 1197 cm (~14000 yr cal BP), 1090 cm (~12200 yr cal BP), and 823 cm (~10080 yr cal BP). With the exception of sample 1090 cm, the increase in species accumulation rate occurred after a period of time when species richness per sample had experienced an important decline (Figure 15.3B).

Diatom assemblage change between consecutive samples showed a high variability throughout the core (Figure 15.3C, D). The highest variability occurred at 1256-1197 cm (~15400-14000 yr cal BP) and 1133-1004 cm (~12900-11370 yr cal BP) levels.

Zonation of the diatom sequence

Eight significant zones were obtained using a constrained incremental sum-of-squares cluster analysis (CONISS). The zones were related with the changes in accumulation rate, species richness, and rate of diatom change (Figure 15.3E). The characteristics of each zone are described below:

Pseudostaurosira pseudoconstruens (Marciniak) Williams & Round, *Cocconeis euglyptoides* (Geitler) Lange-Bertalot, *Caloneis* sp. No. 3 Posets, *Caloneis silicula* (Ehrenberg) Cleve sensu lato, *Diploneis* cf. *puella* (Schumann) Cleve, and *Navicula catalanogermanica* Lange-Bertalot & Hofmann, were exclusively significantly associated to **zone 1** (1330-1251 cm, 16700-15300 yr cal BP). Other characteristic species of the zone, *Amphora copulata* (Kützing) Schoeman & Archibald, *Planothidium frequentissimum* (Lange-Bertalot) Lange-Bertalot, and *Staurosirella pinnata* (Ehrenberg) Williams & Round were also related to other zones (4, 6 and 7).

S. pinnata was the dominant species in zone 1 (Figure 15.4). It was present in a wide range of environmental conditions in the training-set. It was only indicative of pH>5.5 but occurred preferentially at intermediate light and phosphorous concentration, depth <20 m, and was especially dominant (abundance >9%) in lakes with temperature of 12.3 ºC (±3.2).

N. catalanogermanica and *A. copulata* are indicative of environments with a pH higher than 7.25, independently of the SO_4^{2-} concentration, and *C. euglyptoides* and *D. puella* were indicators of lakes with macrophytes. *P. pseudoconstruens* was an indicator of training-set lakes with a TN:TP ratio lower than 110:1 and it is present in lakes with a bottom active diatom biofilm (BADB).

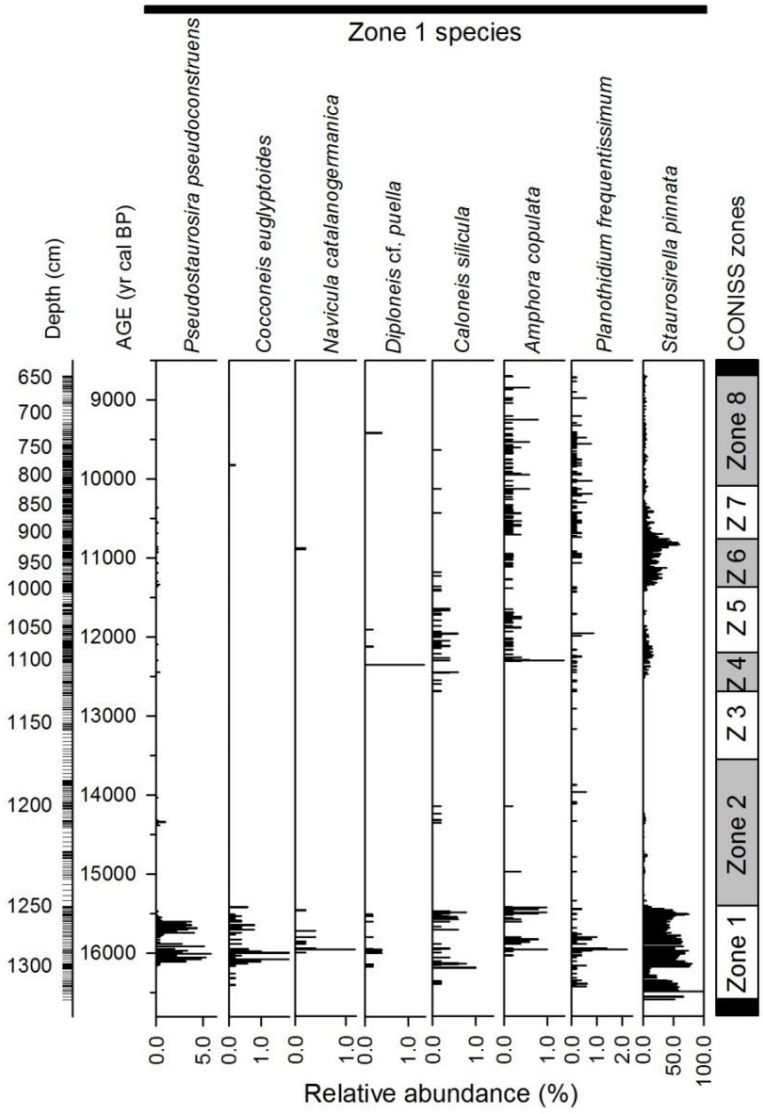

Figure 15.4. Stratigraphic diagram of the Burg sequence showing the relative abundance of diatom species significant as indicators of the zone 1 (Figure 15.3E).

Zone 2 (1250-1169 cm, 15300-13520 yr cal BP) was the longest phase and showed a high variability in diatom composition. Species significantly related to it were: *Cymbella excisa* Kützing, *Encyonema silesiacum* (Bleisch) Mann, *Encyonopsis minuta* Krammer et Reichardt, *Encyonopsis subminuta* Krammer & Reichardt, *Gomphonema acuminatum* Ehrenberg, *Meridion circulare* (Greville) Agardh, *Nitzschia acidoclinata* Lange-Bertalot (Figure 15.5). Some species

indicator of this zone, such as *E. silesiacum* and *N. acidoclinata* had also an important abundance in zone 4.

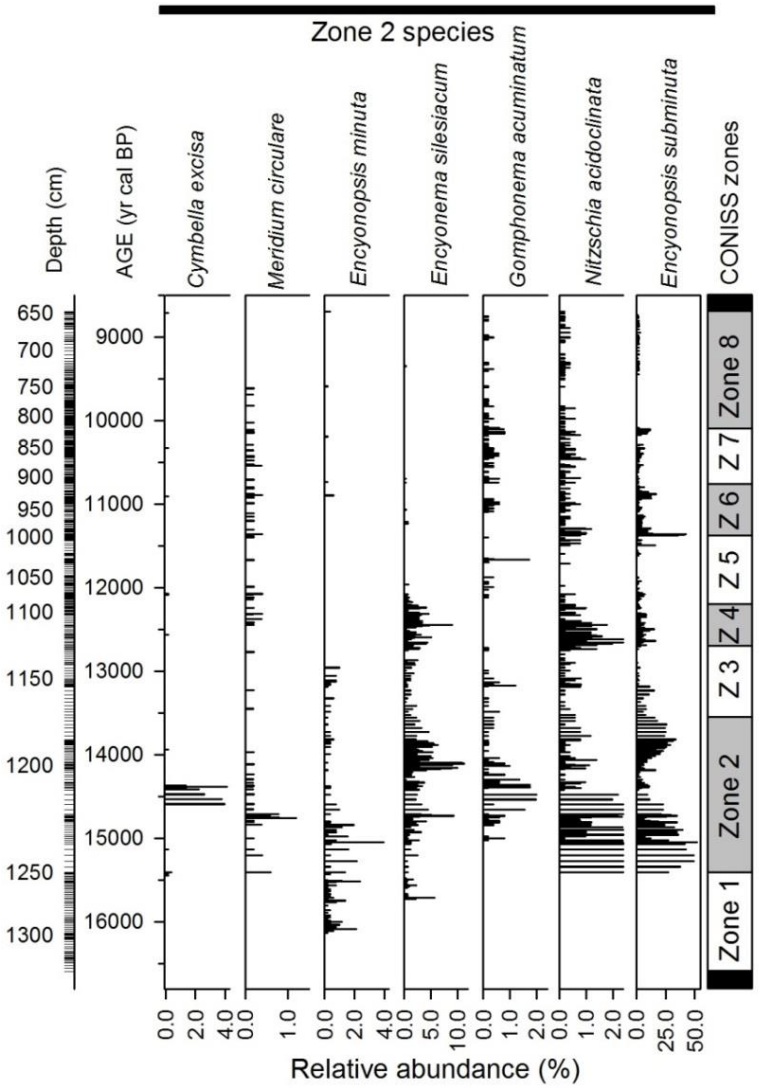

Figure 15.5. Stratigraphic diagram of the Burg sequence showing the relative abundance of diatom species significant as indicators of the zone 2 (Figure 15.3E).

E. subminuta was the species with the higher abundance during this period and is an indicator of macrophyte occurrence and, particularly, potamids, pH >7.25, and low Si concentration. *M. circulare*, *G. acuminatum* and *N. acidoclinata* are indicative of high phosphorous concentration and low Si concentration. *M.*

circulare was indicator of low DIN concentration and lakes with a well-defined water inlet (91% of the lakes where it was present), it is a species common in streams. *E. silesiacum* was indicator of pH >5.5.

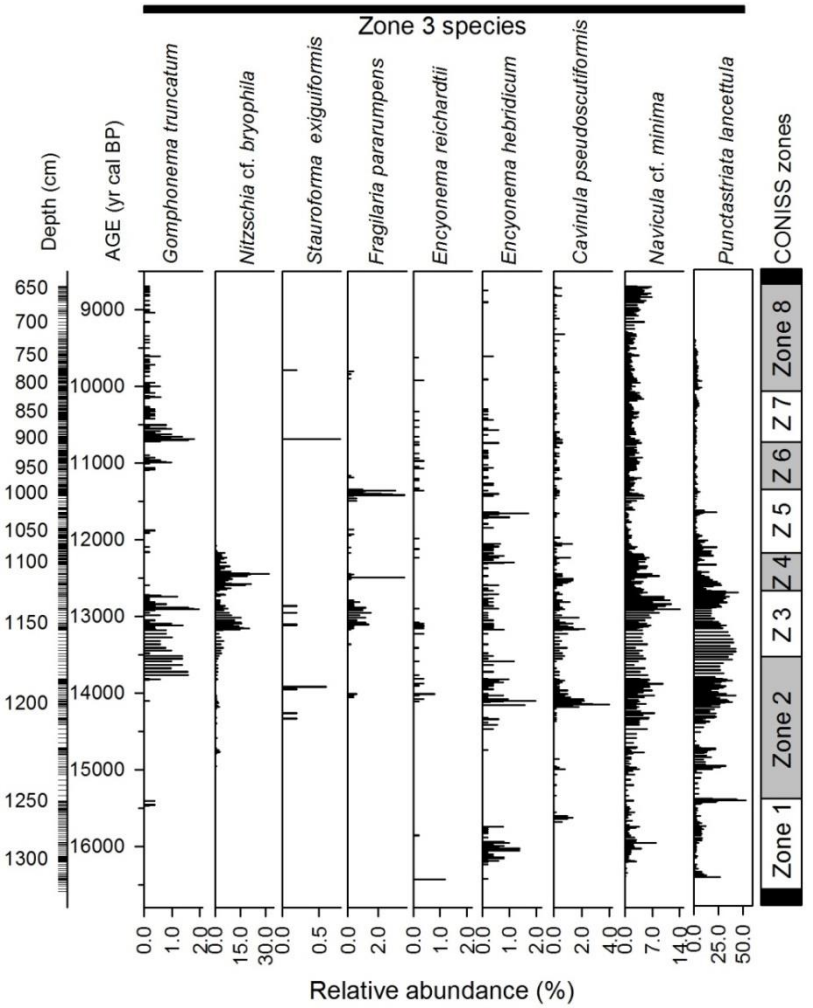

Figure 15.6. Stratigraphic diagram of the Burg sequence showing the relative abundance of diatom species significant as indicators of the zone 3 (Figure 15.3E).

Species associated to **zone 3** (1169-1131 cm, 13520-12930 yr cal BP) indicate high chemical and physical variability despite the short period comprised in this zone (Figure 15.6). *Punctastriata lancettula* (Schumann) Hamilton & Siver, *Gomphonema truncatum* Ehrenberg, and *Navicula* cf. *minima* sensu lato indicate

the presence of macrophytes or potamids in particular for the most part of the zone and pH >7.2. *N. minima* is an indicator of TN:TP ratio <50:1 and summer surface water temperature > 15ºC. In contrast, *Fragilaria pararumpens* Lange-Bertalot, Hofmann & Werum, only present during the end of this zone, indicates absence of macrophytes and low incident radiation on the sediment. *F. pararumpens* had an pH optimum of 6.9 and TN:TP optimum of 160:1 in the training-set.

Encyonema hebridicum Grunow ex Cleve and *Stauroforma* cf. *exiguiformis* (Lange-Bertalot) Flower, Jones & Round, are indicators of lower pH and temperature >15ºC in training-set lakes. *E. hebridicum* occurred also in the middle part of zone 1 and at the end of zone 2. It tends to change in a complementary way to the ones indicating higher pH listed above.

Nitzschia cf. *bryophila* (Hustedt) Hustedt and *Cavinula pseudoscutiformis* (Hustedt) Mann & Stickle also related with zone 3, showed circumneutral pH, higher TN:TP ratio, and occurred principally in deep lakes with temperatures between 12-13 ºC.

Zone 4 (1131-1087 cm, 12930-12350 yr cal BP) presented indicator species of equilibrated N and P concentrations with low availability of Si, such as *Encyonopsis microcephala* (Grunow) Krammer, *Naviculadicta digituloides* Lange-Bertalot, *Gomphonema* sp. No. 15 Coronas, and *Sellaphora pupula* (Kützing) Mereschkowsky sensu lato (Figure 15.7).

Karayevia suchlandtii (Hustedt) Bukhtiyarova and *Pinnularia* cf. *brebissonii* var. *minuta* Krammer indicate ice cover period >160 days, with optima of ice cover duration between 180-190 days and SSWT optima in training-set between 11-12 ºC. *Naviculadicta* cf. *digitulus* (Hustedt) Lange-Bertalot and *Nitzschia* cf. *frustulum* (Kützing) Grunow were other species with higher abundance at the beginning of this period; they have pH optima between 7.4 and 7.6.

Epithemia sorex Kützing appears together with *Epithemia turgida* (Ehrenberg) Kützing, both species have endosymbiotic spheroid bodies that very likely perform nitrogen fixation (Geitler 1977; Nakayama et al. 2011). This may indicate a period of strong N limitation at transition between zone 4 and 5.

Encyonema minutum (Hilse) Mann, also present in zones 6 and 7, and at the beginning of zone 2, is a common taxa in the Pyrenean lakes growing in a broadly range of environmental conditions, but with a low SSWT optimum (11.4±3.4 ºC) and present in lakes with weakly basic conditions (7.6±0.6).

Punctastriata cf. *lancettula* (Schumann) Hamilton & Siver M1 showed its maximum abundance at the end of this zone, this species is an indicator of macrophyte presence and prefers lakes with basic conditions (pH optimum 8.0±0.2) and relatively high temperature (13.5±0.9 ºC).

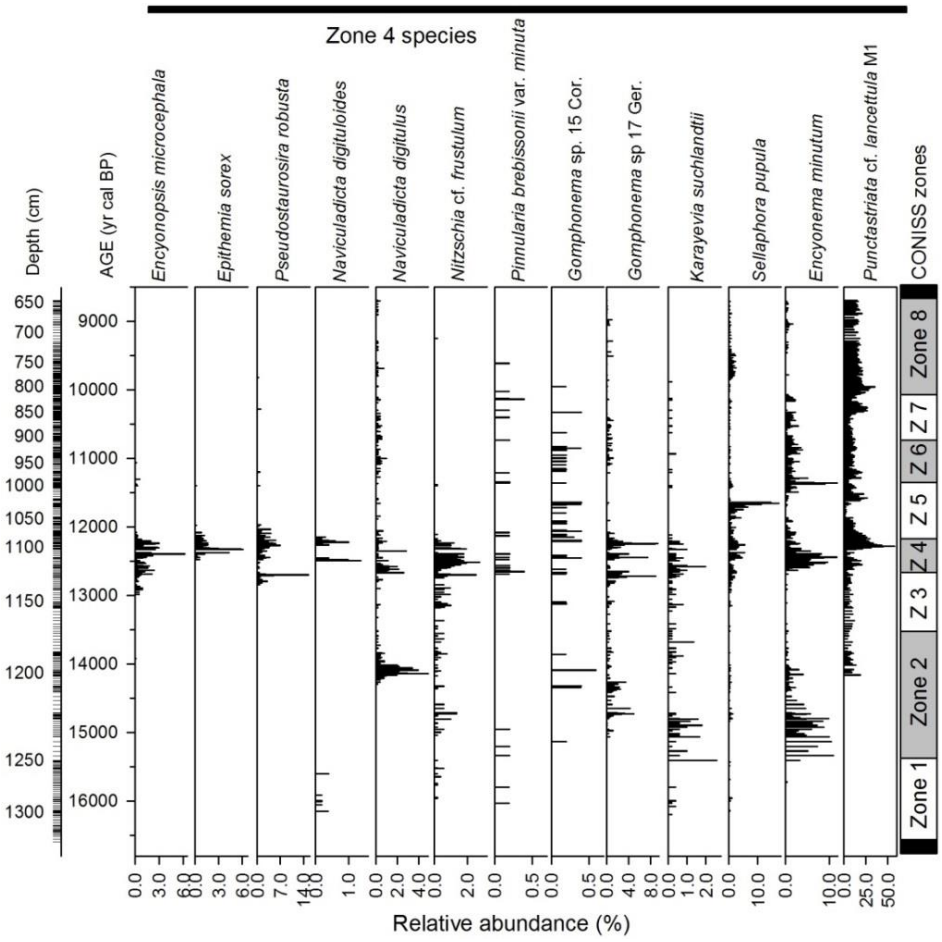

Figure 15.7. Stratigraphic diagram of the Burg sequence showing the relative abundance of diatom species as indicators of the zone 4 (Figure 15.3E).

Species associated to **zone 5** (1087-998 cm, 12350-11340 yr cal BP), were *Cymbopleura inaequalis* (Ehrenberg) Krammer, *Neidium* cf. *ampliatum* (Ehrenberg) Krammer, and *Sellaphora laevissima* (Kützing) Mann (Figure 15.8). *C. inaequalis* was only registered in two lakes of the training set, occurring in

lakes with lakes with active diatoms in the biofilm of the bottom (ADBB), pH between 7.6-7.8 and presence of macrophytes. *S. laevissima* is an indicator of SSWT >10 ºC.

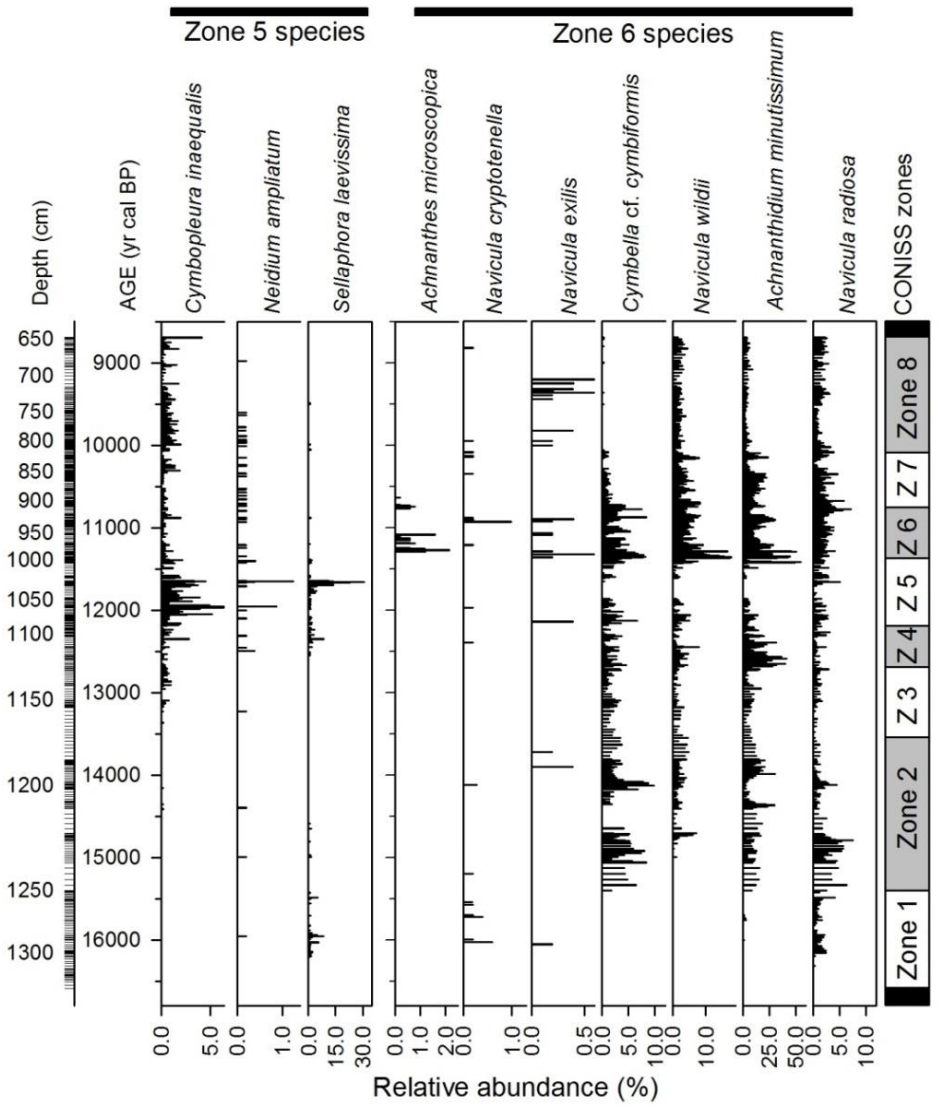

Figure 15.8. Stratigraphic diagram of the Burg sequence showing the relative abundance of diatom species as indicators of the zone 5 an 6 (Figure 15.3E).

Species associated to **zone 6** (998-911 cm, 11340-10720 yr cal BP), were *Achnanthes microscopica* (Cholnoky) Lange-Bertalot & Krammer, *Cymbella* cf. *cymbiformis* Agardh, *Navicula cryptotenella* Lange-Bertalot, *Navicula exilis* Kützing, *Navicula radiosa* Kützing, *Navicula wildii* Lange-Bertalot, *Pinnularia subinterrupta* Krammer & Schroeter, *Stauroneis acidoclinata* Lange-Bertalot & Werum, and *Achnanthidium minutissimum* (Kützing) Czarnecki (Figure 15.8). *S. pinnata* was also important during this period.

A. microscopica occurred during short periods starting and ending the zone. It is indicator for pH <7.25. *N. radiosa* and *N. wildii* were species indicators of macrophytes presence and short ice cover periods.

A. minutissimum had higher abundance at the beginning of zone 6. It is a species of a broad distribution, it shows higher abundance in Pyrenean lakes with circumneutral (pH 7.2 ±0.5) chemical conditions and temperature between 10 and 15 ºC. Basically, matching the most common conditions in the whole lake district.

Species associated to **zone 7** (911-823 cm, 10720-10080 yr cal BP) were *Navicula heimansioides* Lange-Bertalot, *Gyrosigma* sp. No. 1 Sen, *Ulnaria biceps* (Kützing) Compère sensu lato, *Gomphonema* cf. *parvulum* (Kützing) Kützing sensu lato, *Fragilaria delicatissima* (Smith) Lange-Bertalot, and *Achnanthidium* cf. *minutissimum* (Kützing) Czarnecki M3 (Figure 15.9).

N. heimansioides and *F. delicatissima* were indicators of TN:TP ratio lower than 50:1. *G. parvulum* and *F. delicatissima* were indicators of lower DIN concentration. All together indicate a situation of N limitation. *Gyrosigma* sp.1 and *G. parvulum* are indicators of macrophytes and the latter was also an indicator of low Si availability and temperature >15ºC.

Finally, species associated to **zone 8** (823-642 cm, 10080-8850 yr cal BP), were *Neidium bisulcatum* (Lagerstedt) Cleve sensu Krammer, *Naviculadicta vitabunda* (Hustedt) Lange-Bertalot, *Sellaphora pseudopupula* (Krasske) Lange-Bertalot, *Navicula* cf. *oligotraphenta* Lange-Bertalot & Hofmann, *Navicula* cf. *seminulum* Grunow, *Diploneis* cf. *petersenii* Hustedt, *Sellaphora disjuncta* (Hustedt) Mann, *Placoneis explanata* (Hustedt) Lange-Bertalot, *Staurosira construens* var. *venter* (Ehrenberg) Hamilton.

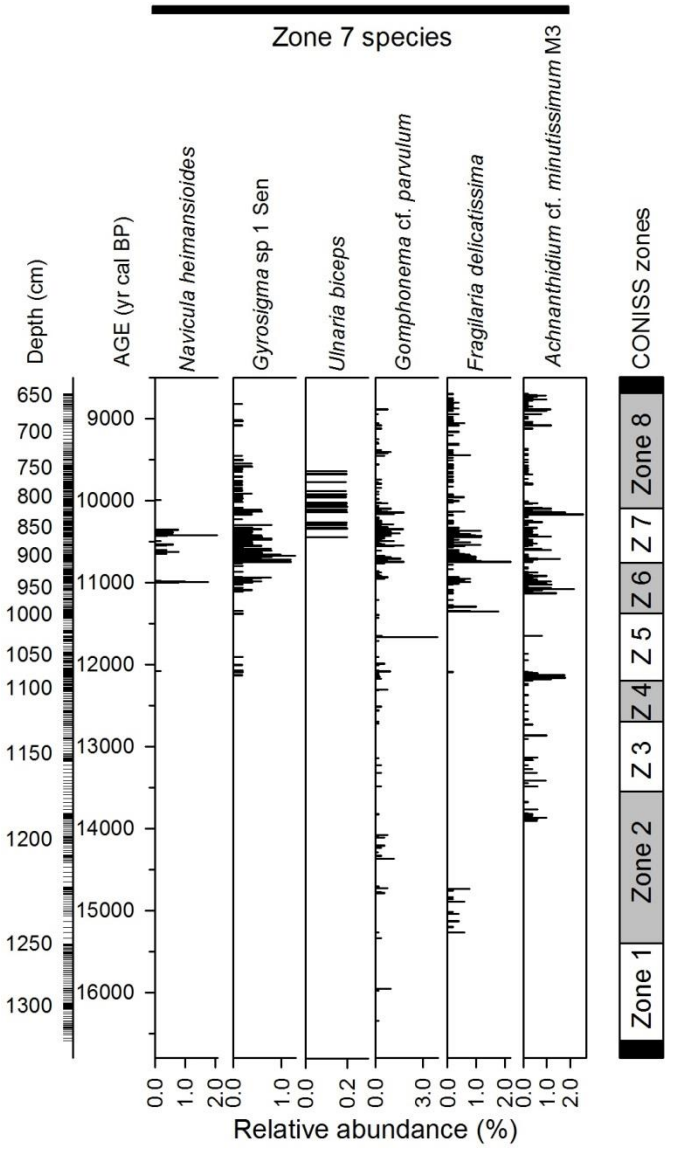

Figure 15.9. Stratigraphic diagram of the Burg sequence showing the relative abundance of diatom species as indicators of the zone 7 (Figure 15.3E).

N. oligotraphenta and *D. peterseni* were indicators of DIN concentration <100 µg/L, TP between 4 and 10 µg/L, and low Si:N ratio. *N. oligotraphenta* is indicator of short ice cover periods and *D. peterseni* was indicator of pH >7.25.

S. construens was the most abundant species throughout the sequence, but particularly in zones 7 and 8. It is an indicator of SSWT >10 ºC, which simply

indicates that summer water temperature was not very low in the early Holocene. *S. construens* complex is a common diatom in the Pyrenean lakes (55 lakes out of 76 studied).

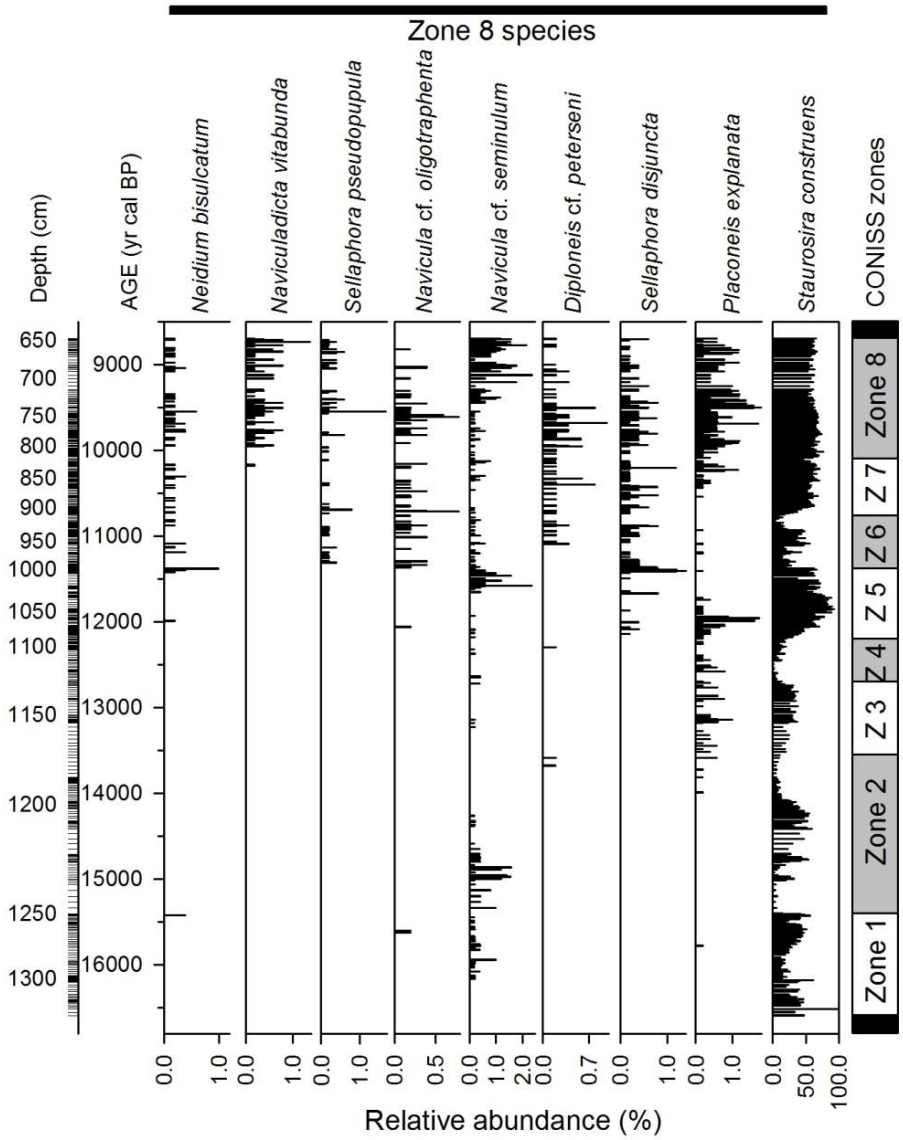

Figure 15.10. Stratigraphic diagram of the Burg sequence showing the relative abundance of diatom species as indicators of the zone 8 (Figure 15.3E).

Main variability components of the Burg diatom sequence

The **first axis** of a Principal Component Analysis explained the 28.8% of diatom variability throughout the whole record (Figure 15.11). *E. subminuta*, *A. minutissimum* and *P. lancettula* were the species with the highest positive correlation with the first component. *S. construens*, *S. pinnata*, *P. lancettula* M1 were the species with the highest negative loadings of the first component.

The first component showed three phases. The first (1330-1254 cm, 16700-15390 yr cal BP), correspond with the zone 1 defined by CONISS. This phase showed low variability in the first component that ended abruptly with the reduction in density of *S. pinnata*, the appearance of *E. subminuta* and the increase of *A. minutissimum*. Then, there was a period showing a higher variability until 1082 cm (15390 - 12330 yr cal BP) that included zones 2, 3 and 4.

The section between 1082-1021 cm (12330-11500 yr cal BP) showed low values of the first component, largely correspond to zone 5 and was characterized by a reduction in *E. subminuta* and *A. minutissimum* densities. The following period showed high variability and a progressive reduction in the values of the first component. The last part of the record (823-642 cm, 10080- 8850 yr cal BP), which correspond to zone 8, was characterized by a low variability in the scores of first component.

The second and third axes explained 21.8% and 13.7% of the diatom sequence variability, respectively. These axes explained the variability of secondary species with low loading in the first axis but also explained the variability of dominant species related with the first component: *S. pinnata, Staurosirella spp.*, *P. pseudoconstruens*, and *P. lancettula*. Therefore, second and third axes are related mostly to non-linear variability of the main species, but they do not compile much information about other species. They will not be considered further.

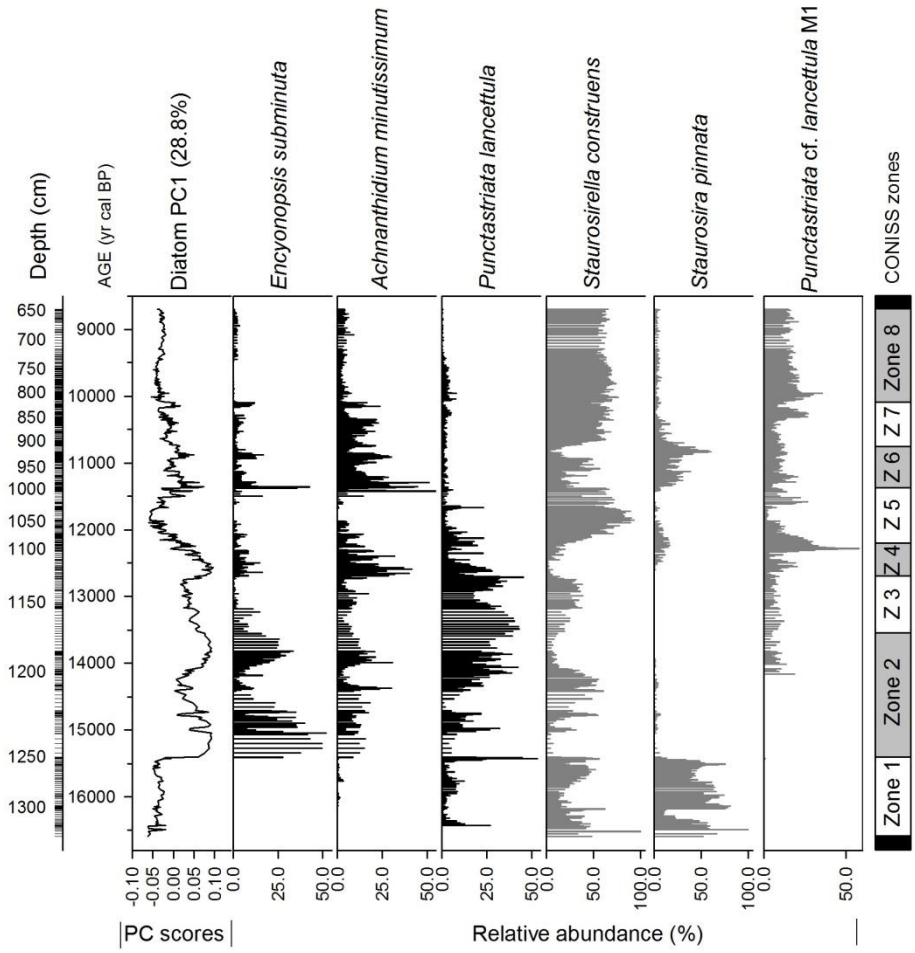

Figure 15.11. First principal component of the Burg Lake diatom sequence. Black and grey species plots correspond to positive and negative loadings in the first component, respectively.

Indicator diagnosis

In this section, the indicative value of the diatom species developed in chapter 10 is applied to the Burg Lake sequence. Indicators of macrophyte and potamid occurrence (Figure 15.12) suggest that aquatic plants started to be important in the lake environment since the beginning of zone 2 (~15300 yr cal BP) and have maintained a fluctuating constant presence with a deep valley between 12000-11600 yr cal BP. Potamids were much more relevant during zone 2. Zones 6, 7 and 8 were the phases with the lowest variability in macrophyte occurrence according to the diatom record.

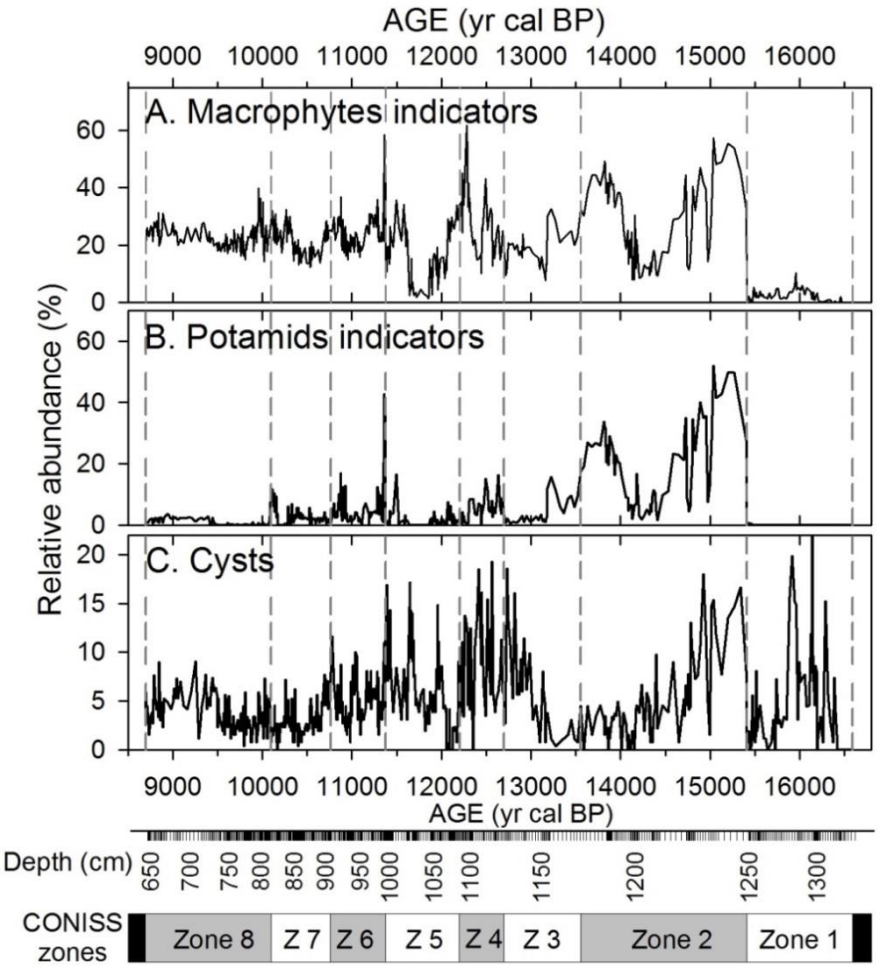

Figure 15.12. Diatom indicators of A) macrophytes in general and B) potamids. C) Relative abundance of Chrysophycean cyst with respect to the total of diatoms and cysts.

The Chrysophycean cysts abundance respect to diatoms was highly variable across the record, showing high values at zones 1, 2, 4 and 5, although the cyst fluctuations do not match the diatom zonation. For instance, within zone 2 there were about 700 yr of high values at the beginning and other 700 yr of low values at the end. Cyst abundance did not correlate also with macrophytes and potamids indicators. According to the environmental analysis performed in chapter 12, the relative abundance of cysts mainly indicated changes in the water column depth in the Pyrenean lakes. Following this interpretation, changes in macrophytes cannot simply be interpreted in terms of changes in the water column depth. This issue will be revisited later.

The species indicating summer surface water temperature >15 ºC can be used to identified the warmer periods in the lake (Figure 15.13). As this is a shallow seepage lake, the water column depth may fluctuate markedly according the changes in water inflow. The latter may be driven by precipitation but also glacier melting across parts of the period studied. Therefore, the relationship between water temperature and air temperature could have been changing according to the water column depth. High abundance of SSWT>15 ºC indicators occurred in zones 2, 3, 4 and at the end of zone 8. Low abundances of SSWT>15 ºC indicators occurred at the beginning and the end of the zone 1 and during the period of time included in zones 5, 6, 7. All in all, the most outstanding feature was the high values at end of zone 3 between 13000 and 12700 yr cal BP.

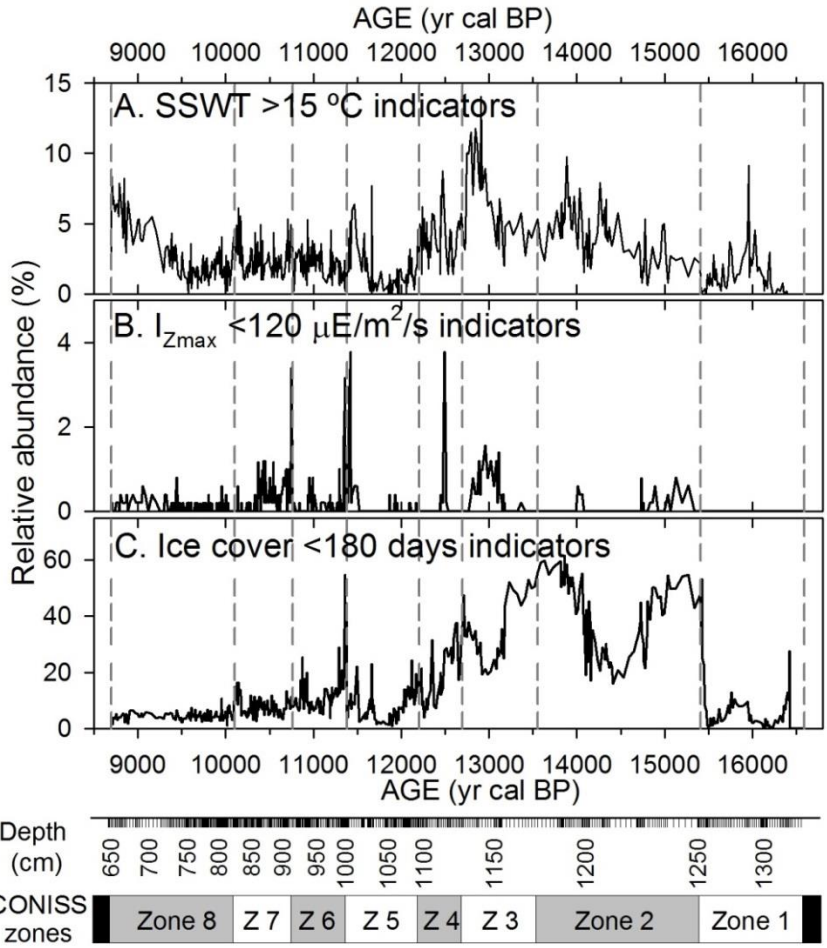

Figure 15.13. Abundance of indicator species of A) Summer surface water temperature >15 ºC (SSWT); B) Irradiance at the bottom (I_{Zmax}) and C) Ice cover duration.

Indicator species of low irradiance at the lake's bottom showed low abundances through the record. Therefore, the lake has been in the category of lakes with an extended littoral throughout its bottom during all its history. Episodes of certain increase in taxa of low irradiance occurred at the beginning of zone 2 and in zones 3, 6 and 7, without ever arriving to 4% of relative abundance (Figure 15.13B).

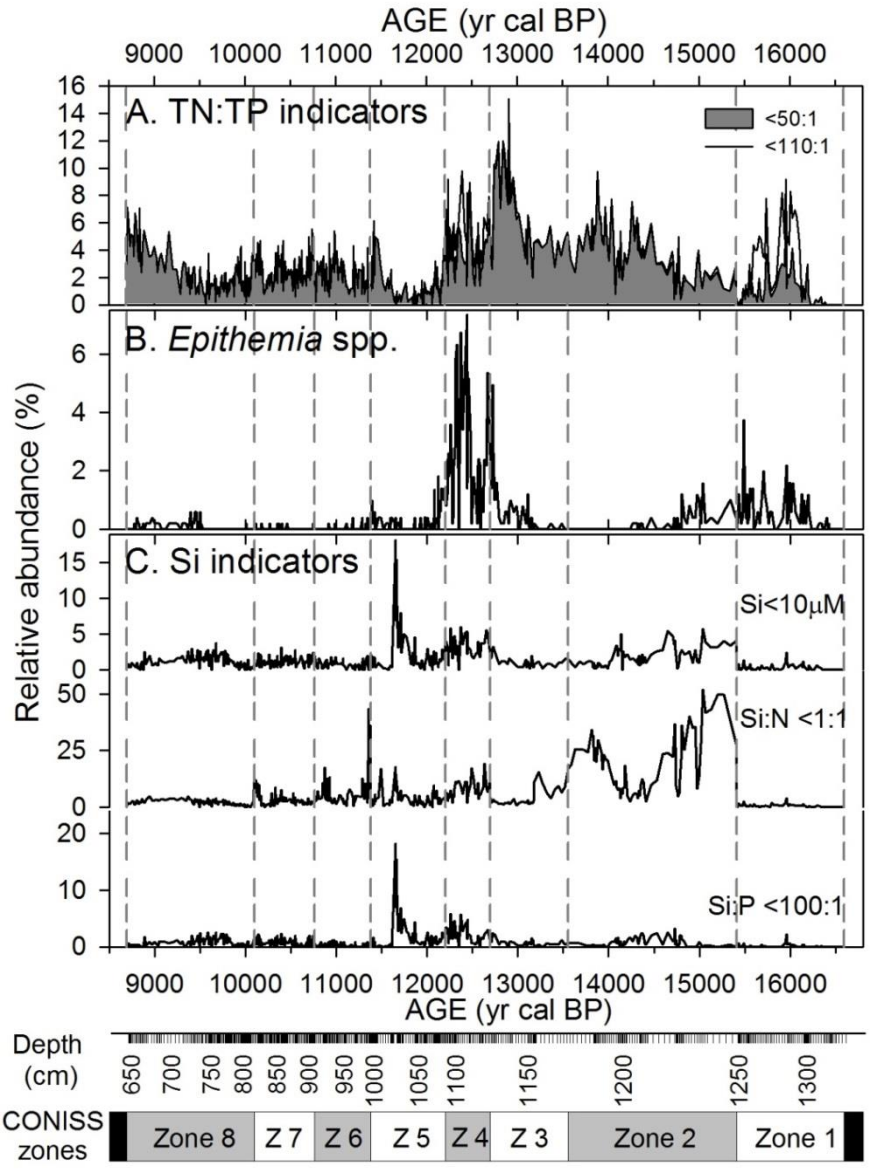

Figure 15.14. Burg Lake sequence of A) TN:TP diatom indicators, B) *Epithemia* species and C) distinct Si diatom indicators.

Indicators of ice cover suggest short ice cover duration (<180 days) in zone 2 and zone 3 (15300-12930 yr cal BP). Latter and before the ice cover duration was probably much longer with episodes similar to those in zone 2 and 3 of short duration.

Species indicator of TN:TP <50:1 (indicators of N limitation) ratio showed a low abundance but indicator of TN:TP ratio >110:1 (P limitation) were absent throughout the diatom record (Figure 15.14A). From the middle part of zone 2 to section 4 (14500-12350 yr cal BP) occurred the highest abundance of indicator of low TN:TP ratio. *Epithemia* species showed higher abundance during the major part of zone 1 and during zone 3 and 4 and the beginning of zone 5 (Figure 15.14B). If the two indications are combined periods of more N limitation appear clearly defined.

The three complementary indicators of Si limitation analysed in the training-set showed a slightly different pattern across the record (Figure 15.14C). The three had high values in zones 2, 4 and 5. However, indicators of Si:N ratio <1:1 showed distinctive higher values at the beginning and the ending of zone 2.

Synthesis of the diatom changes throughout the Burg Lake record and of their indicative value

The Burg Lake diatom sequence showed a rich variability that was summarized using CONISS and PCA analyses performed in the previous sections. Here, the environmental circumstances that the indicators suggest are summarized (Table 24). According to the principal component analysis three sections were more distinctive. The first, which only included zone 1, represented the early time of the lake after deglaciation. The second major section (zones 2, 3 and 4) was characterized by a high variability in the diatom assemblages. The third section, which included zones 5, 6, 7, and 8, showed a progressive dampening of the variability up to zone 8. A synthesis of each zone is described in Table 24 and Figure 15.15.

Table 24. Summary of diatom assemblages and the indicator information for each zone obtained by CONISS.

Zone	General description
1	1330-1251 cm (16,700-15,300 yr cal BP). Period corresponding with the beginning of diatom record and showing the early lake formation (e.g., pioneer species such as *S. pinnata*). Scarce macrophyte presence, pH >7.2 (e.g. *A. copulata*), relatively deep water column (high cysts abundance), low TN:TP ratio (*Epithemias* spp), relatively high TP (*P. pseudoconstruens*), and relatively cold water conditions (ice cover and SSWT indicators).
2	1250-1169 cm (15,300-13,520 yr cal BP). Started with a sudden increase in indications of macrophytes including potamids (e.g. *E. subminuta*). Period with warm conditions (shorter ice cover, and higher SSWT), high TP (e.g. *G. acuminatum*), low Si concentration. This period showed a high variability in the species richness, the rate of diatom change and indicators as a whole. It showed intervals of time with pH tending to circum-neutral conditions (*E. silesiacum*) and a progressive change towards shallower conditions (cyst abundance). During a short period around 14,000 yr cal BP the change in the diatom assemblage was particularly high.
3	1169-1131 cm (13520-12930 yr cal BP). Period with a low presence of potamids but warm conditions and low TN:TP ratio continued. At the end of this zone, there was a short period of low irradiance at the bottom (*F. pararumpens*) and a high variability of benthic-limnetic conditions and of TN:TP ratio; which may indicate unstable oscillating conditions.
4	1131-1087 cm (12,930-12,350 yr cal BP). Started with a sudden cooling that was maintained throughout the whole period Low TN:TP (*Ephitemia* spp), high diatom turnover rate and high pH (e.g. *N. frustulum, P. robusta*). This period had indications of an increase in macrophytes different to potamids and more prevalence of deep than shallow conditions (high cyst abundance).

Zone	General description
5	1087-998 cm (12,350-11,340 yr cal BP). Summer surface water temperature between 10-15ºC (e.g. *S. laevissima*, *S. construens*), low macrophyte presence, high probability of Si limitation. Macrophytes different to potamids started to be important at the end of the zone. A higher variability in the cysts abundance suggested change between periods with low depth (*C. inaequalis*) and higher water level (high cyst abundance). This zone showed a reduction in species richness dropping the mean from 29 (in zone 4) to 21 species.
6	998-911 cm (11,340-10,720 yr cal BP). SSWT, ice cover and pH indicators suggest low water temperature and circumneutral condition at the beginning and at the end of this period. Relative high abundance of macrophyte indicators and low cyst abundances suggest conditions of a shallow lake.
7	911-823 cm (10,720-10,080 yr cal BP). Period with low variability in diatom assemblage (*S. construens* and *P. lancettula* M1 had >75% of diatom abundance). Temperature and ice cover indicators suggest high summer water temperature. Relatively high abundance of macrophyte indicators and low cyst abundance suggest the maintenance of shallow lake conditions.
8	823-642 cm (10,080-8850 yr cal BP). This zone was similar to zone 7. It was scarcely variable in diatom assemblages and the indicators suggest warm conditions with a high macrophyte influence in a shallow system. The abundance of indicators of low TN:TP increased at the end of this period.

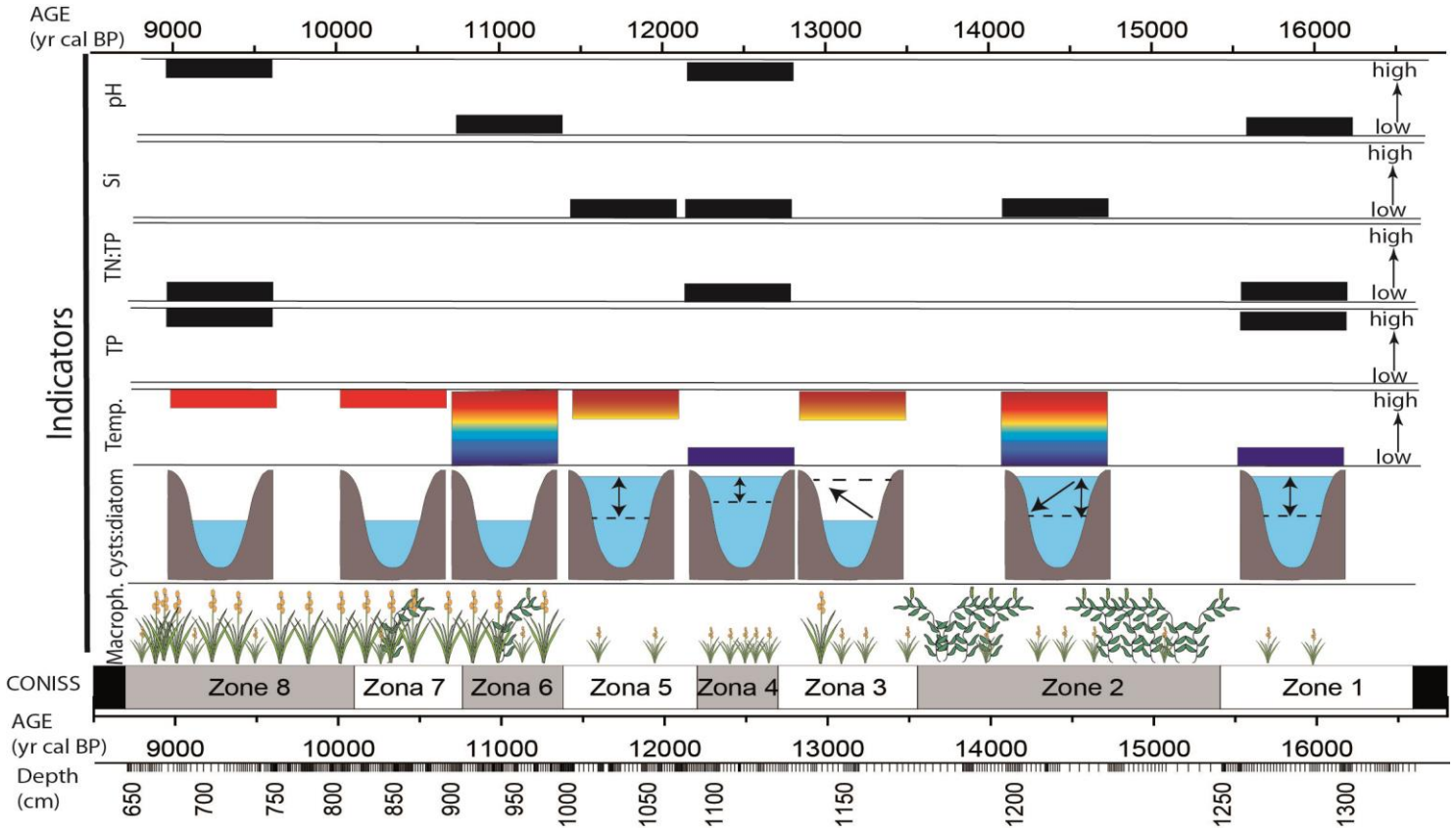

Figure 15.15. Scheme summarizing the indicator information of the diatom assemblages of the Burg Lake sedimentary sequence.

16. Biogeochemical reconstructions: a palaeoecosystem view

Mineral composition as indicator of catchment ontogeny

The main changes in mineral composition throughout the sedimentary sequence are indicated in Figure 16.1. It is worth to mention that a lower number of samples was analysed, thus the temporal resolution is coarser than for diatoms. Talc minerals ($Mg_3Si_4O_{10}(OH)_2$), showed high values from 16500 to 13600 yr cal BP and from 12500 to 10500 yr cal BP (Figure 16.1A). Since 11000 yr cal BP, talc progressively declined until become no detectable around 9000 yr cal BP. Talc is a metamorphic mineral resulting from the metamorphism of magnesium minerals. It forms in the catchment and the decline may be related to the development of a more vegetated catchment, thicker soils and thus lower availability of primary minerals.

Illite ($(K,H_3O)(Al,Mg,Fe)_2(Si,Al)_4O_{10}[(OH)_2,(H_2O)]$) showed a progressive reduction in abundance from 16500 to 12800 yr cal BP. It increased during the YD until 11600 yr cal BP, and then underwent progressive reduction again (Figure 16.1B). Quartz patterns (SiO_2) were opposed to illite variability, showing a progressive increase through the record and higher values from 14000 to 12700 yr cal BP, and from 11600 yr cal BP to the end of the studied sections (Figure 16.1C). The complementary change between illite and quartz may indicate the degree of chemical metamorphism. Illite is a clay size mineral that forms from incongruent weathering of feldspar and muscovite. Dominance of quartz, highly resistant to chemical decomposition, may indicate a more complete chemical weathering than the presence of intermediate clays such as illite. Wetter and warmer climate provide better conditions for chemical weathering of primary minerals.

Primary alumina-silicates minerals (e.g., orthoclase, $KAlSi_3O_8$, anorthite, $CaAl_2Si_2O_8$), showed a constant sedimentation rate through the record with a progressive reduction during the Holocene, particularly around 9500-9000 yr cal BP (Figure 16.1D). This may respond to the soil formation and forestation.

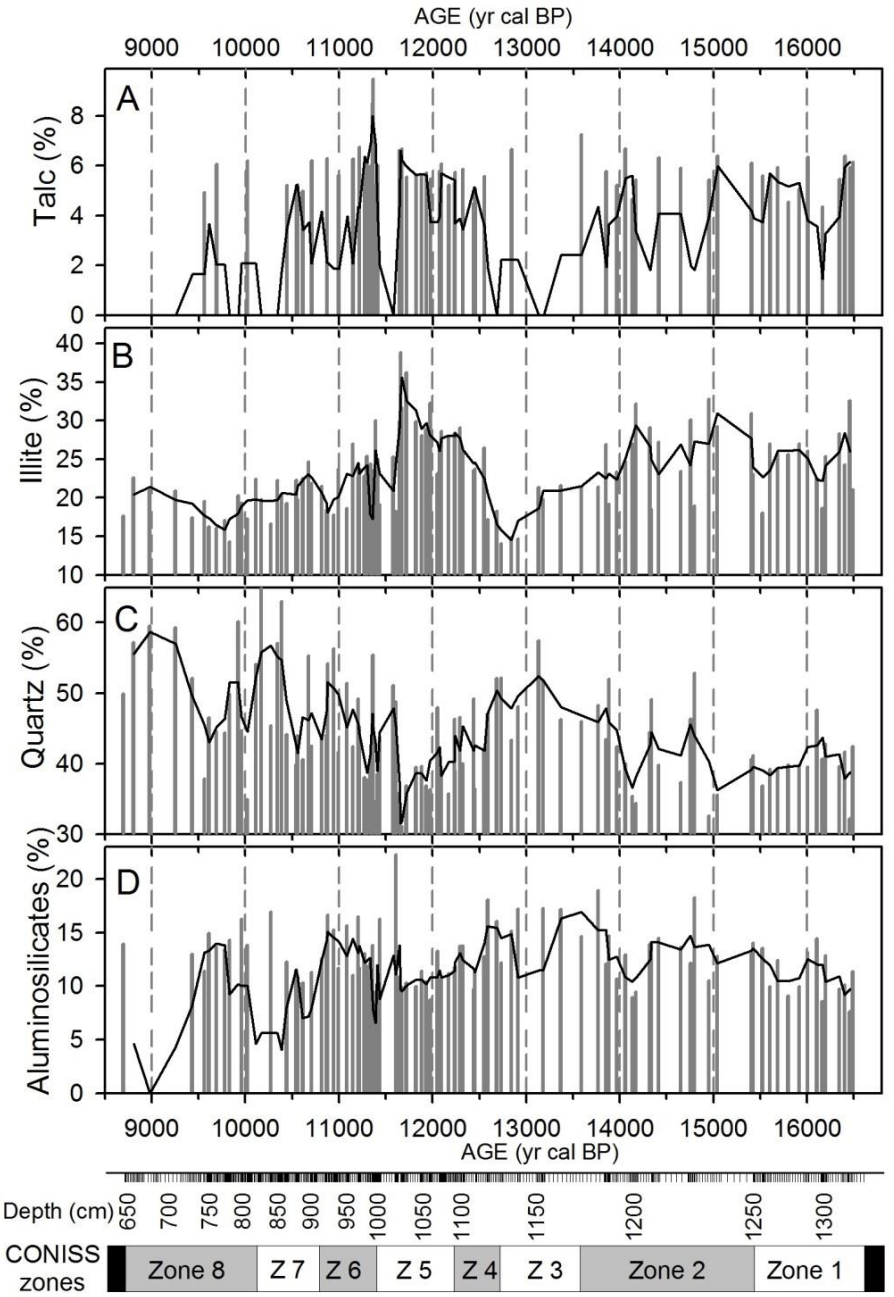

Figure 16.1. Selected minerals in the stratigraphic Burg Lake sequence: talc (A), illite (B), quartz (C) and primary alumina-silicates estimated by X-ray diffraction analysis. Black lines indicate data smoothing using three samples moving average and grey bars are the original measures.

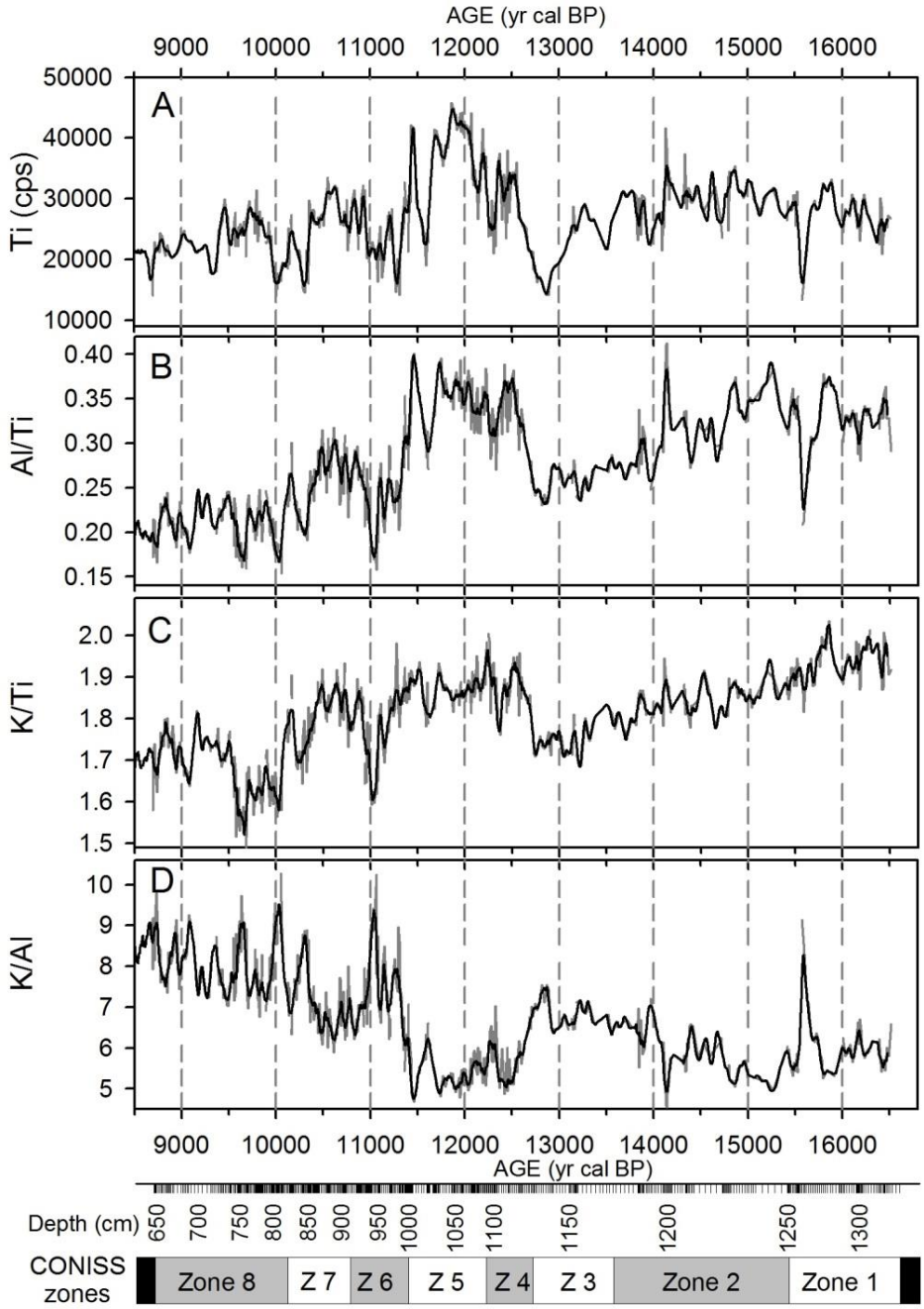

Figure 16.2. Changes in the sediment elemental composition estimated by X-ray fluorescence analysis (XRF). A) Ti, B) Al/Ti, C) K/Ti, and D) K/Al. Black lines are the smoothed data using the TWAS procedure (see methods).

Titanium (Ti) may be indicative of physical erosion in the catchment as is highly insoluble (Figure 16.2). Between 12700 and 11500 yr cal BP (YD) there was a marked increase in the physical erosion. Previously and after this period the oscillation were common with certain tendency to decrease progressively from LGM to Holocene. The marked and sustained trend to decline in Al/Ti, K/Ti, and K/Al probably indicates an increase in particle sorting; progressively only the smaller particles arrive to the lake. Ti remains attached to the smallest particles, whereas Al and K are mostly part of minerals that form larger particles. This tendency reflects the ontogenic lake changes related with geomorphological aspects; the development of a softer relieve, and increased littoral progressively prevents the arrival of large particles to the centre of the lake.

Lake infilling and diatom abundance

As mentioned in the introduction Burg Lake suffered a progressive infilling process that converted the lake into a fen. In this study, only the lake period is studied but, even in this situation, a progressive increase of organic matter accumulation in the sediments was observed (Figure 16.3). Loss on ignition (LOI) showed a lower correlation with age ($r=-0.28$, $p<0.001$, $n=624$) than Br/Ti ratio ($r=-0.37$, $p<0.001$, $n=552$), probably, because the latter corrects for the physical erosion that may dilute organic matter. Diatom density showed a gentle but significant trend to increase also ($r=-0.14$, $p<0.001$, $n=624$) and followed relatively accurately the oscillations of both LOY and Br/Ti. Thus, diatom abundance fluctuated accordingly with the organic character of the system. All these variables showed a high correlation among them (Br/Ti vs LOI ($r=0.66$, $p<0.001$, $n=552$, Figure 16.3); Br/Ti vs diatom density ($r=0.50$, $p<0.001$, $n=552$); diatom density vs LOI ($r=0.70$, $p<0.001$, $n=624$)).

Beyond the overall tendency, the temporal sequence showed six periods with higher organic inputs (Figure 16.3). The first, ~15900-15500 yr cal BP, was recorded by Br/Ti, and diatom density but not by LOI. The second, ~14800-14200 yr cal BP, was recorded by all of the proxies. The third, also recorded by all the proxies, occurred after a suddenly drop around 14100 yr cal BP and it extended to 12700 yr cal BP. After a long period of low organic matter accumulation in sediment (12700 -11600 yr cal BP), between 11600 and 11400 yr cal BP there was a short but intensive increase in organic matter accumulation. From 11300 to 11000 yr cal BP there was an increase of Br/Ti but

not of the other proxies. Finally, from 10300 to 9900 yr cal BP there was an increase in organic matter recorded with different intensity by each proxy. During some of these peaks, diatoms were a significant source of Si to the sediment as evidenced by the Si/Al ratio and diatom abundance similarities.

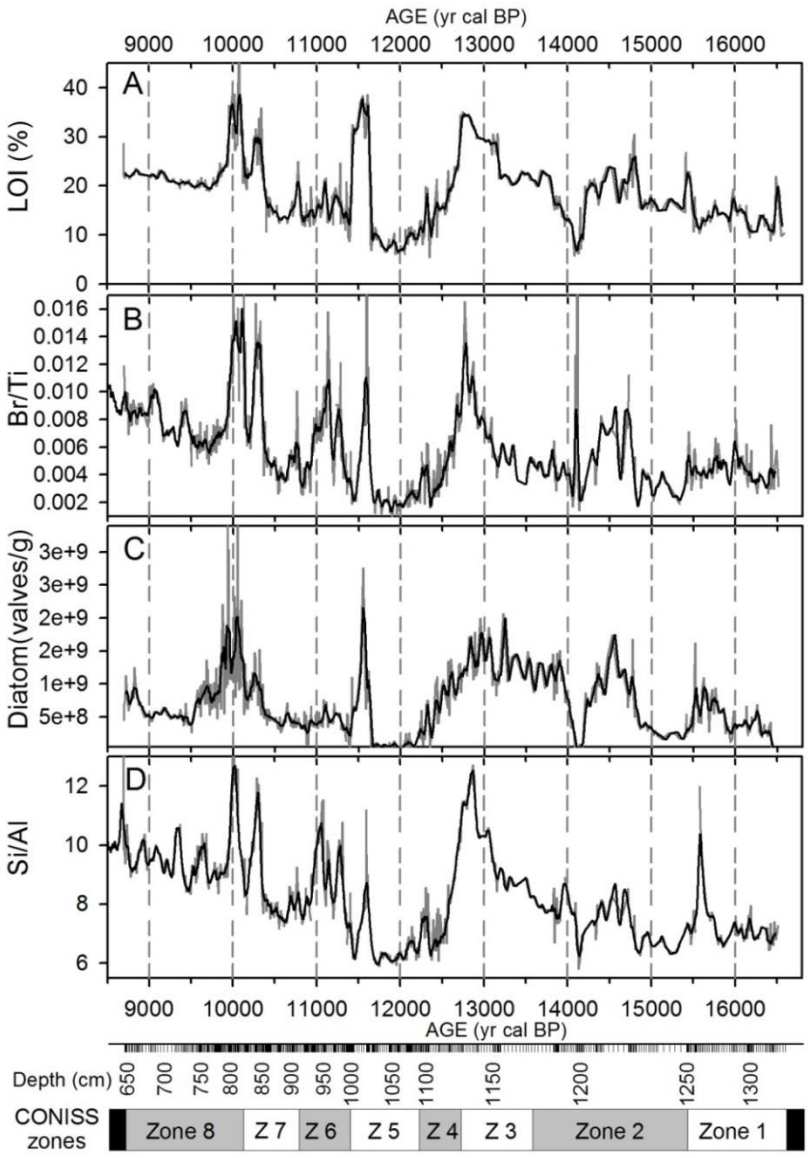

Figure 16.3. Sequence of proxies related with organic matter accumulation. A) Loss on ignition (LOI); B) BR/Ti ratio, C) diatom density; and D) Si/Al ratio. Black lines are the smoothed data after the TWAS procedure and grey lines are the original measurements.

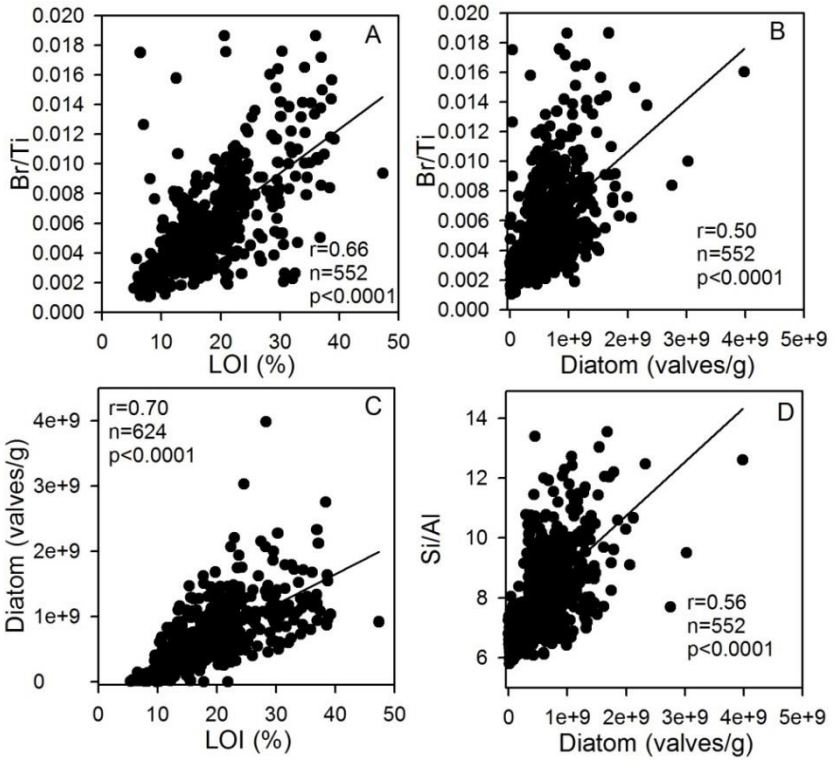

Figure 16.4. Relationship between A) LOI and Br/Ti ratio; B) Diatom density and Br/Ti ratio; C) Diatom valves and LOI; and D) Diatom valves and Si/Al ratio.

Redox indicators

The characteristics of the lake and organic content of the sediments indicate a system with a high demand of oxygen at the sediment surface despite that it could have been covered by a biofilm with a high autotrophic component. Internal nutrient loadings related to redox conditions in the sediments may be relevant in addition to external loads. Therefore, it is worth to look at proxies that indicate redox conditions (Figure 16.5). S/Fe ratio varied in parallel to pyrite, indicating that the S accumulation was mainly due to precipitation in anoxic conditions The lake showed an alternation between oxygenated and hypoxic phases. The latter statement can either be interpreted as average conditions through the period of time considered, or as longer periods of seasonal anoxia, as may happen in mountain lakes during winter, for instance. The S and Fe relationship suggest that precipitation of pyrites is a dominant process (Figure 16.6 A1) with respect to Fe-oxides precipitation (Figure 16.6 A2). Taking into account that vanadium prevails in oxygenated waters forming

surface complexes with iron hydroxides, and that in anoxic waters chromium form stronger surface complexes than V, the Cr/V ratio can be used as indicator of redox in bottom waters (Schaller et al. 1997). Accordingly, the Cr/V ratio showed positive correlation with the S values ($r=0.45$, $p<0.001$, $n=541$, Figure 16.6B) and the S/Fe ratio ($r=0.61$, $p<0.001$, $n=541$, Figure 16.6C). Proxies of redox condition were significantly related with the LOI of the sediment (Figure 16.6E), particularly S/Fe.

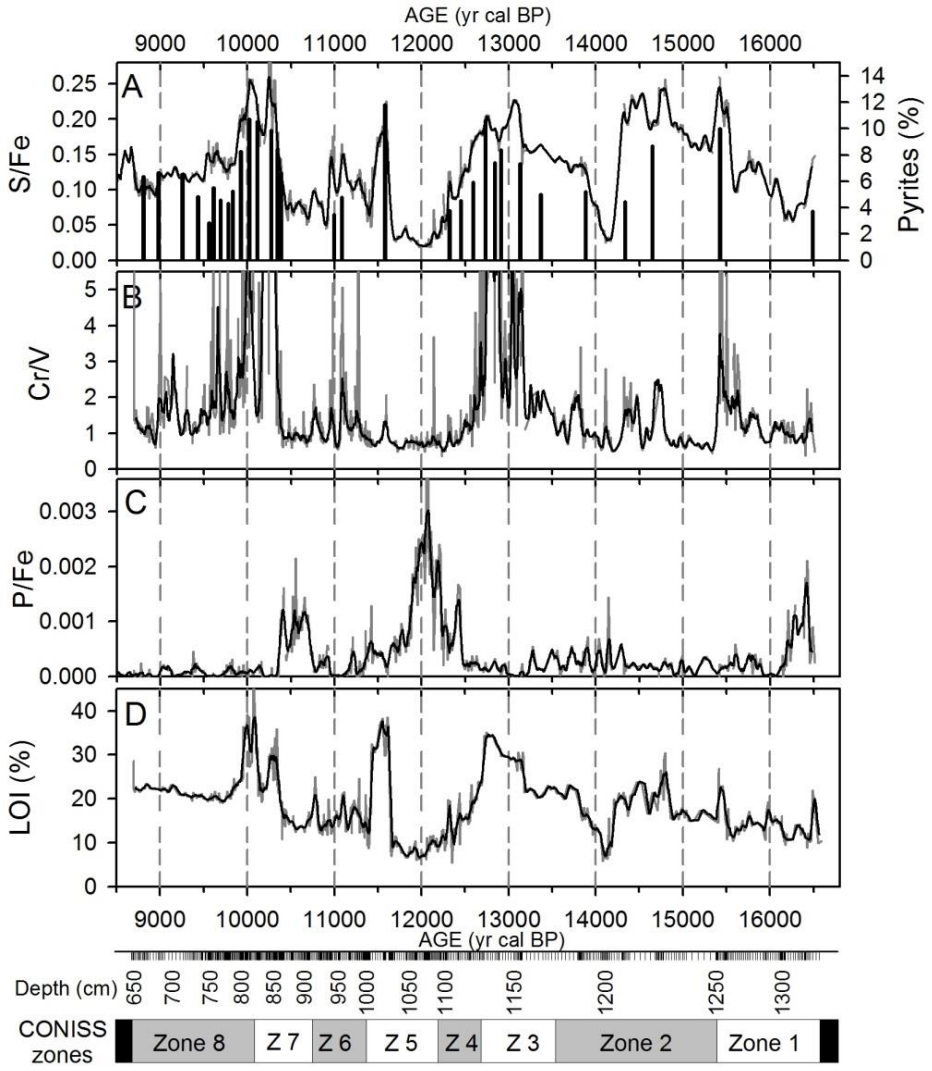

Figure 16.5. Sequence of proxies related with redox conditions. A) S/Fe ratio and percentage of pyrites among minerals (vertical bars); B) Cr/V ratio; C) P/Fe ratio, and D. loss on ignition (LOI). Black lines are the smoothed data after the TAS procedure and grey lines are the original measures.

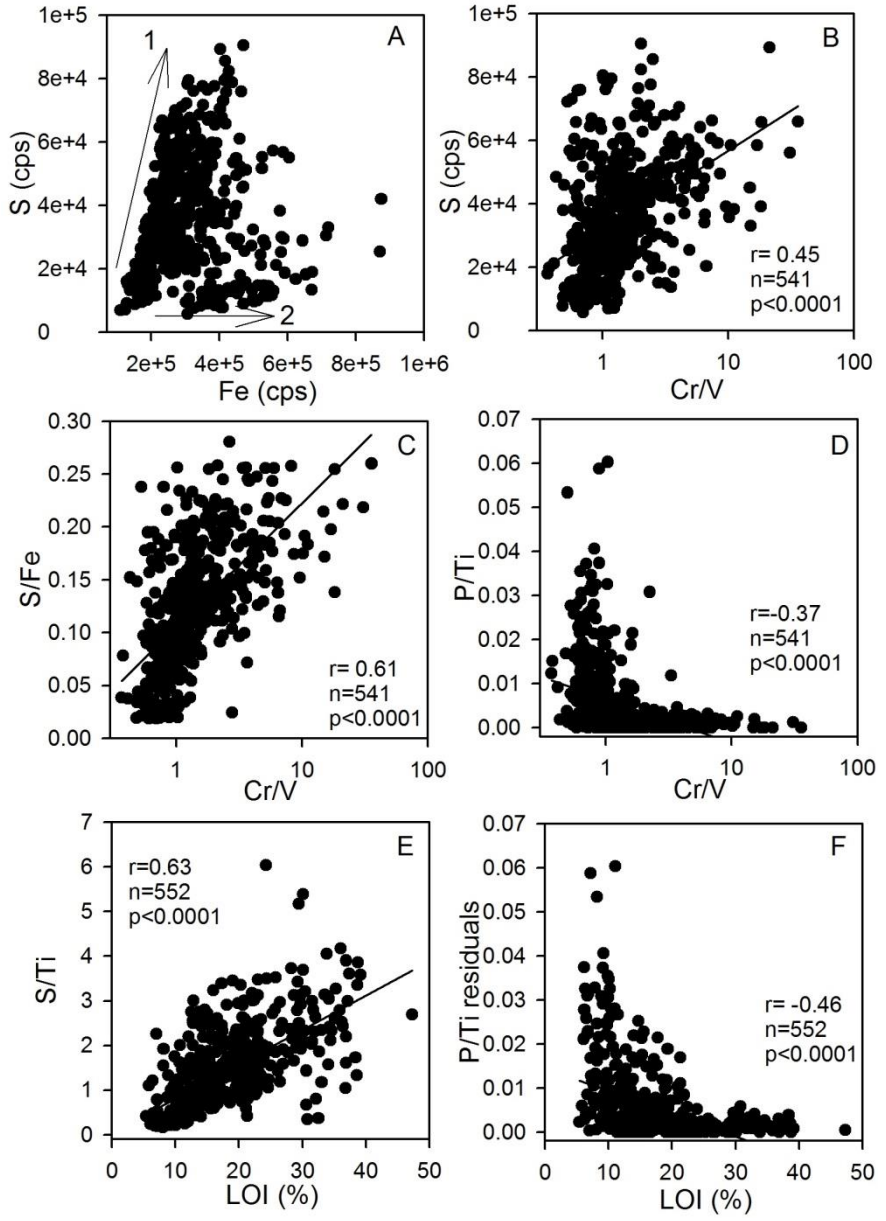

Figure 16.6. Relationship between indicators of redox conditions. A) S vs. Fe; B) S vs. Cr/V; C) Cr/V vs. S/Fe; D) Cr/V vs. P/Ti; E) Loss on ignition-LOI vs. S/Ti; and F) LOI vs. P/Ti. Numbers in plot A are the dominant processes of pyrite precipitation (1) and Fe-oxide precipitation (2).

Initially (16500-15500 yr cal BP), the lake bottom tended to be well oxygenated. From 15500 to 14100 yr cal BP, the Cr/V ratio was highly variable but S/Fe indicated anoxic conditions. Around 14100-13800 yr cal BP, the lake bottom appears to be well oxygenated again and then until ~12500 yr cal BP the sediment was anoxic. After this, from 12400 to 10300 yr cal BP, the oxygenation of bottom was variable and started to be predominant poorly oxygenated. As a consequence of the well oxygenated bottom conditions, P was trap in the sediment during the early phase of the lake (16500-16000 yr cal BP) and at 12400-11800 and 10700-10400 yr cal BP (Figure 16.5). Thus internal loading of nutrients to the water column was lower during these periods.

Lake productivity

Total phosphorus in the water column is an indicator of planktonic productivity, although in shallow and transparent lakes, as probably was Burg, benthic algal production could be more relevant. From 16500 to 12500 yr cal BP the lake showed a progressive decline in diatom-TP ($r = -0.35$, $p<0.001$, $n=205$) and two periods with high concentration (from 16500 to 15400 and from 14600 to 14100 yr cal BP) (Figure 16.7). From 12500 yr cal BP to the end of the record, the lake showed the opposed tendency, a significant trend to increase ($r = 0.87$, $p<0.001$, $n=419$) and high diatom-TP between 11800 and 11600 yr cal BP (Figure 16.7). Diatom-TP tended to increase when LOI was low ($r=-0.19$, $p<0.001$, $n=624$).

Abundances of TN:TP<50 diatom indicators (nitrogen limitation) varied mostly mirroring TP throughout the sedimentary record. During the early phase (16500 – 15400 yr cal BP) there was a high TP concentration with apparently low nitrogen limitation. From 15400 to 12500 yr cal BP, the TP concentration was variable and inversely related to nitrogen limitation. After this period, from 12500 to 11500 yr cal BP, the lake had a progressive increase in the TP and a reduction in nitrogen limitation. Since 11500 yr cal BP, during Holocene, there was a weak relationship between TP and TN:TP indicators. In general, it appears that during the Bølling-Allerød period TP and N limitation varied together, whereas outside this period the higher the TP, the lower the nitrogen limitation (Figure 16.8).

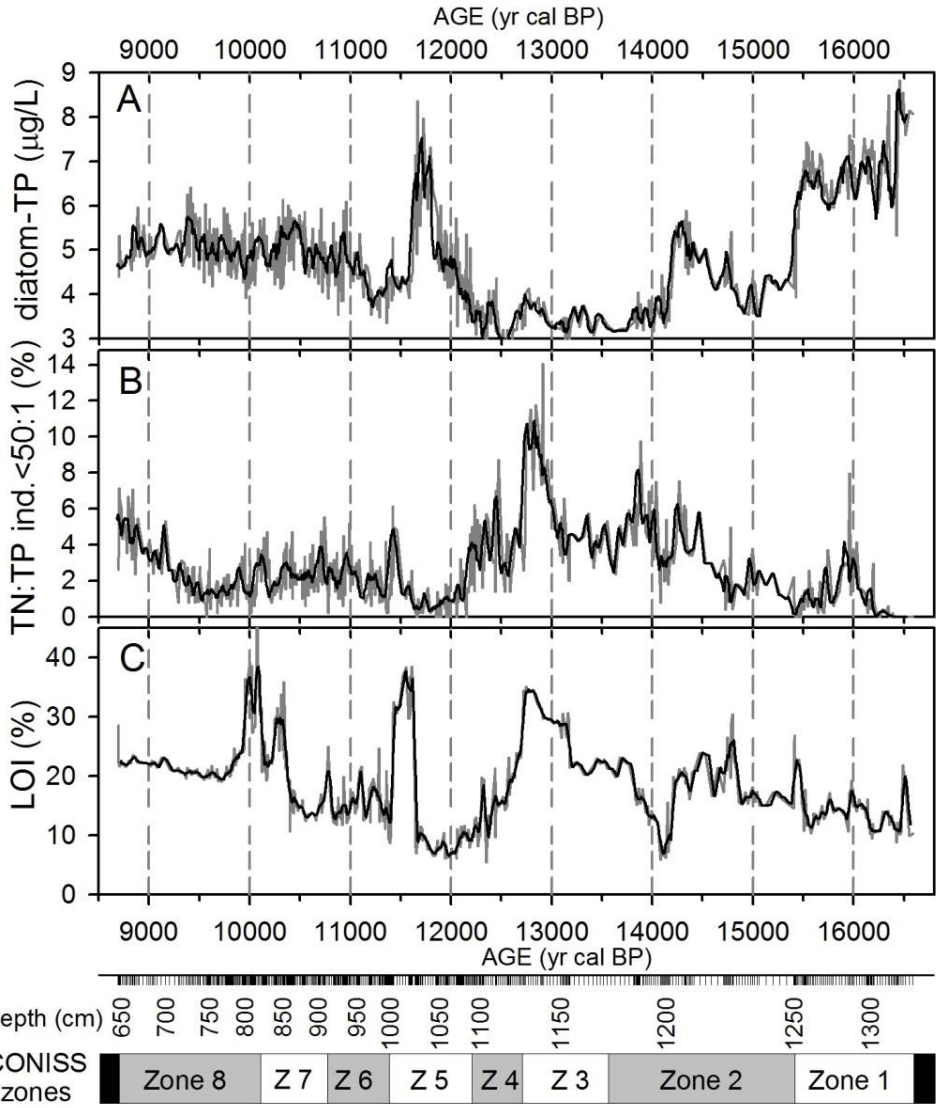

Figure 16.7. Sequence of proxies related with lake productivity. A) Reconstructed total phosphorous (diatom-TP); B) abundance of diatom indicators of TN:TP ratio <50:1; and C) LOI. Black lines are the smoothed data after the TWAS procedure and grey lines are the original data.

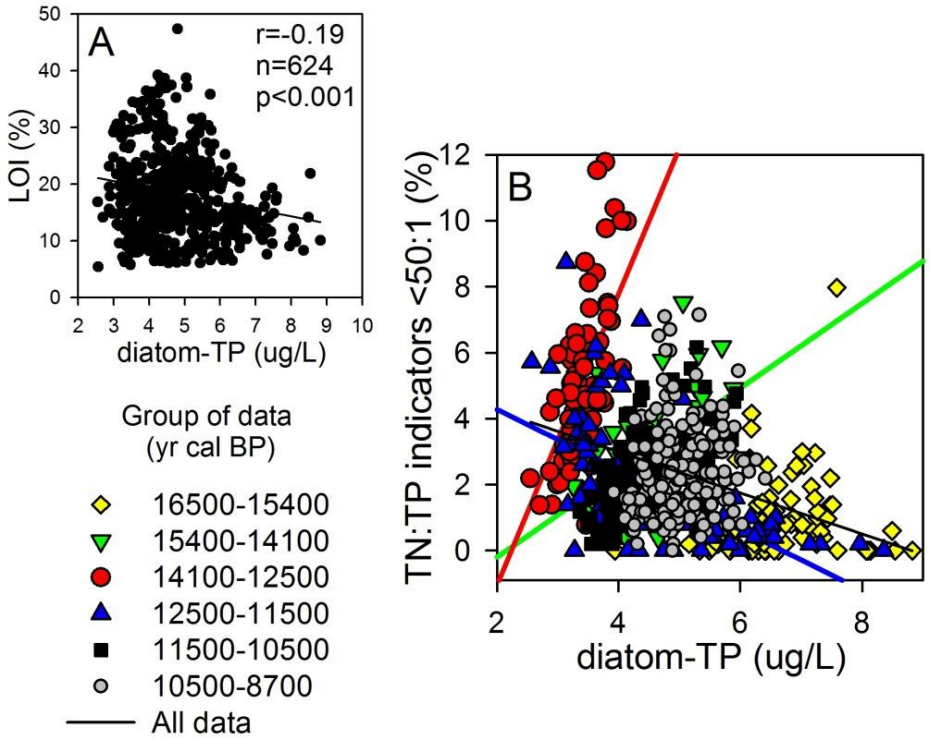

Figure 16.8. Relationship between A) reconstructed total phosphorus (diatom-TP) and loss on ignition-LOI, and B) reconstructed total phosphorous (diatom-TP) and abundance of indicators of TN:TP ratio <50 (nitrogen limitation). Lines drawn in plot B are the group of data with significant correlation. Group of data of plot B were selected according to diatom-TP phases throughout the sedimentary record.

Irradiance at the bottom of the lake (diatom-I_{Zmax}) showed a temporal trend (r= 0.36, p<0.001, n=624, Figure 16.9) and fluctuation patterns similar to diatom-TP (r=0.75, p<0.001, n=624). The diatom-I_{Zmax} also showed a significant negative correlation, but weaker than for TP, with the cyst-depth index (r=-0.23, p<0.001, n=624) and the abundance of macrophyte indicators (r=-0.51, p<0.001, n=624). Diatom-I_{Zmax} showed the highest values before 15500 yr BP, after this period, was declining progressively until 12600 yr cal BP, when it showed a minimum. There was a slightly increase between 12000 and 11500 yr cal BP followed by a sudden reduction around 11400 yr cal BB. From 11200 yr cal BP to the end of the record, the diatom-I_{Zmax} showed values between 20 and 30%.

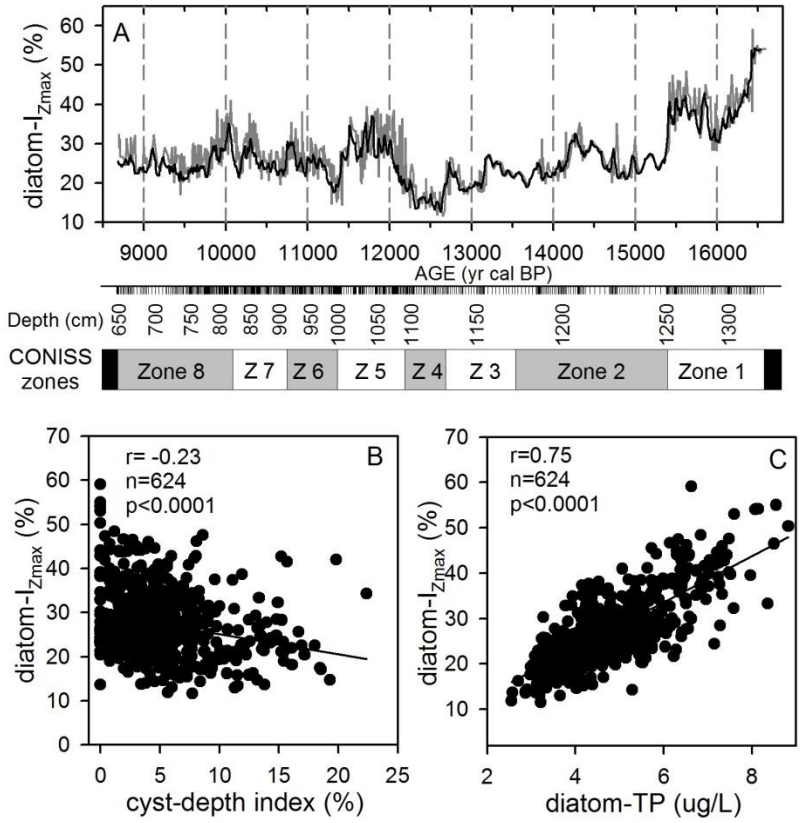

Figure 16.9. A) Sequence of reconstructed irradiance at the bottom (diatom-I_{Zmax}), B) relationship between the cyst-depth index vs. diatom-I_{Zmax}; and C) abundances of indicators of macrophytes presence vs. diatom-I_{Zmax}.

Sub-fossil photosynthetic pigments provide a complementary view of the productivity process. Chlorophylls were not well preserved in the sedimentary record; however some representative carotenoids from different groups were informative about the dominant phototrophic microorganisms. The pigments lutein, diatoxanthin, zeaxanthin, isoreniaretene and echinenone were the most abundant in the sediment (Figure 16.10). Lutein, an exclusive pigment of chlorophytes, showed the highest abundance between 13700 and 12700 yr cal BP and episodic peaks in other short periods. Diatoxanthin, indicative for diatoms, differed from the lutein pattern; it showed high values from 15300 to 14300 yr cal BP and from 11400 yr cal BP to the end of the record. The zeaxanthin, present in other groups but most abundant in cyanobacteria, showed a high variability across the record and was correlated with isoreniaretene, a carotenoid indicator of brown Chlorobiacea (photosynthetic bacteria that require

light and anoxic conditions), and echinenone, another cyanobacterial pigment. The correlation between pigments of aerobic cyanobacteria and anaerobic photosynthetic bacteria indicate that during these periods a photosynthetic microbial mat, with strong redox gradients between top and bottom, covered the bottom of the lake. In fact, the microbial biofilm probably included also diatoms and chlorophytes. The total concentration of the most abundant pigments (lutein + diatoxanthin + zeaxanthin + isoreniaretene + echinenone), was significantly correlated with LOI ($r=0.55$, $n=624$, $p<0.001$) and the S/Fe ratio ($r=0.53$, $n=624$, $p<0.001$). Likewise, each pigment was also individually correlated with LOI and S/Fe ratio. Thus it can be concluded that a biofilm with a strong redox gradient covered the lake bottom across the lake history.

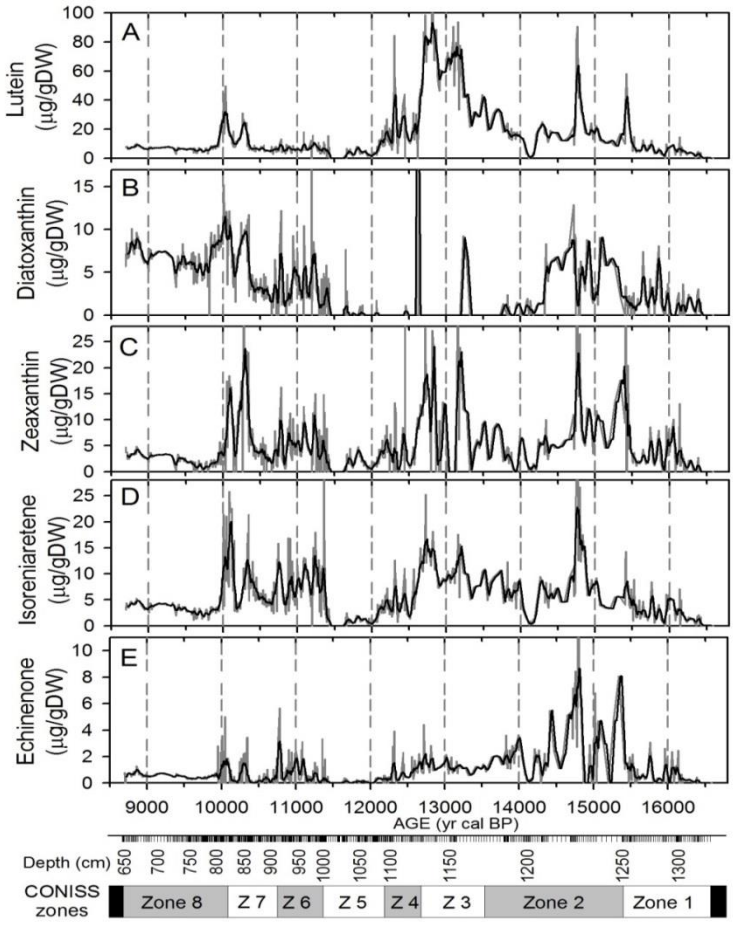

Figure 16.10. Burg Lake sequence of the most abundant photosynthetic pigments that preserved through time. A) lutein, B) diatoxanthin; C) zeaxanthin, D) isoreniaretene, and E) Echinenone. Black lines are the smoothed data after the TWAS procedure and grey lines are the original data.

The pH-ANC temporal evolution

Lake Burg acid neutralizing capacity was in the upper range of ANC for the Pyrenean lakes. It was a well-buffered system that showed a progressive alkalinisation throughout the lake history. Diatom reconstructed pH (diatom-pH) ranged from 7.1 to 7.9 and acid-neutralising capacity (diatom-ANC) from 195 to 500 µeq/L. Both variables were significantly correlated with the age ($r_{diatom\text{-}pH}$=-0.66, $r_{diatom\text{-}ANC}$=-0.35, p<0.001, n=624) and both variables showed a similar temporal pattern (Figure 16.11), although during the period between 14000 to 12000 yr cal BP the relative changes differed.

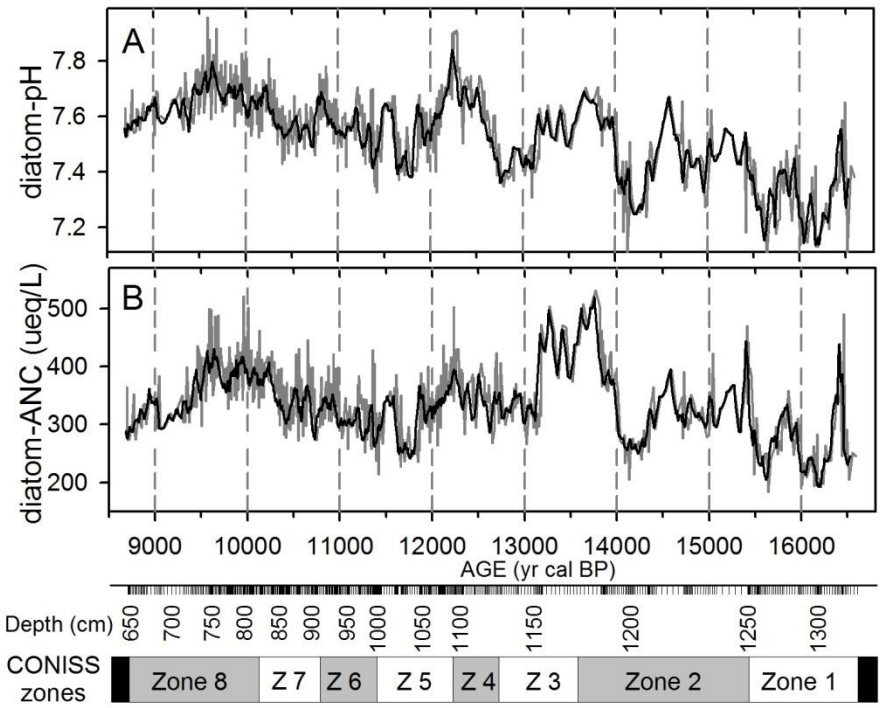

Figure 16.11. A) Diatom reconstructed pH (diatom-pH); B) Acid-neutralising capacity (diatom-ANC). Black lines are the smoothed data after the TWAS procedure and grey lines are the original data.

The highest values of ANC were achieved during the Bøling-Allerød period (i.e., 14000-13000 yr BP; whereas the highest pH were achieved at the onset of Younger Dryas (~12700-12800 yr BP) and during early Holocene. The ANC respond to the changes in rock weathering in the catchment and within lake ANC production by processes such as sulphate reduction. In fact, the diatom-ANC showed a positive correlation with the S/Fe ratio (r=0.27, p<0.001, n=541) (Figure 16.12). However, diatom-ANC were not significant correlated with

sediment carbonates neither to the Ca/Ti ratio. Carbonate precipitation in the sediments may be more related to episodic CO_2 under-saturation (e.g., high macrophytes CO_2 demand), whereas Ca/Ti depends on the hydrological sorting of mineral particles. On the other hand, ANC was highly related to organic matter accumulation in the sediment. There are alternative hypothesis to explain this fact. Higher anoxia decreases the organic matter decomposition and produces alkalinity; alternatively, a more vegetated catchment might export more organic matter and increase chemical weathering and, thus, water alkalinity. Both processes may be complementary.

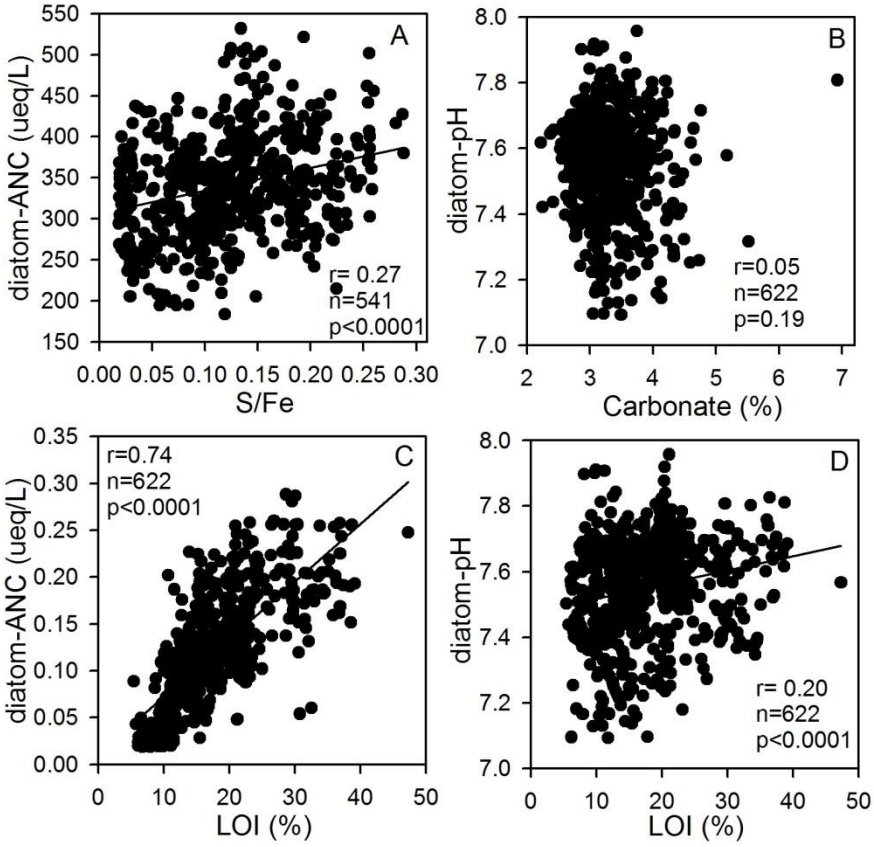

Figure 16.12. Relationship between A) S/Fe and reconstructed acid neutralising capacity (diatom-ANC), B. Carbonate and reconstructed pH (diatom-pH), C. LOI and diatom-ANC, and D. LOI and diatom-pH.

17. Thermal and hydric reconstructions: a palaeoclimatic view

The biogeochemical changes reconstructed in the last chapter were driven in great extent by climatic forcing acting upon a progressive ontogenic change of the lake that was varying the response to that forcing. In this chapter, a reconstruction of the variables more directly linked to climate is undertaken. Burg Lake was a small, shallow seepage lake before becoming a fen. During part (if not all) of the Lake Glacial the lake was fed by melting glaciers. Therefore, the connection between water temperature and air temperature is not straightforward because the water volume was likely changing across the period considered due to changes in precipitation and flow from the glaciers. The reconstruction of distinct physical features of the lake (i.e., summer surface water temperature, ice-free period duration and water column depth) will later allow for a discussion in palaeoclimatic terms.

Summer surface water temperature

Reconstructed summer surface water temperature (diatom-SSWT) ranged from 12.8 to 18.5 ºC showing a mean of 16.2 ºC and a median of 16.4 ºC (Figure 17.1A). Centennial variability changed across the record, with two periods of particular high variability: 15000-14000 yr cal BP and 13000-11500 yr cal BP (Figure 17.2A).

The SSWT were low during the first millennium of the record. Around 15400 yr cal BP, abruptly started a period of higher temperatures (~1.5^{o}C above previous ones), this warm period lasted until 14700 yr cal BP at ~17 ºC. Then a decline to ~15 ºC again occurred rapidly, and lasted a few centuries. Then, a long period of warm conditions started until 12750 yr cal BP, which was punctuated by short cold excursion at ~14000, 13400 and 13100 yr cal BP. From 12700 to 12100 yr cal BP (zone 4), there was a rapid decline in SSWT, showing a mean of 15.2 ºC and values ranging from 14.6 to 16.6 ºC. At the end of this period, the SSWT started to rise, reaching a mean of 16.5 from 12100 to 11400 yr cal BP (most of the zone 5). After this, between 11300 and 10800 yr cal BP, SSWT presented a

rapid decline reaching ~15.8 ºC. From 10800 yr cal BP to the end of the record, the diatom-SSWT showed a relatively low variability and a mean of 16.7 ºC. There was a cold episode at 9500 yr cal BP, with an excursion of ~1 ºC.

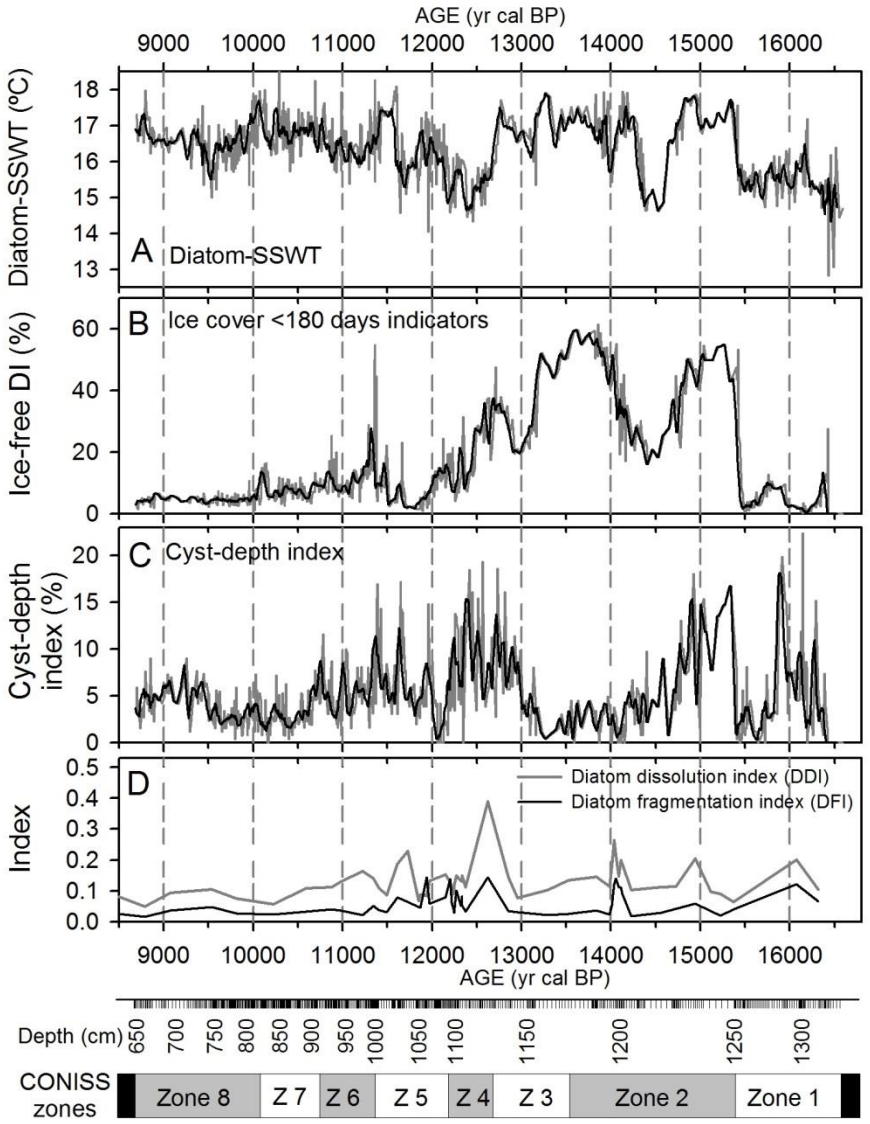

Figure 17.1. A) Diatom reconstructed summer surface water temperature (Diatom-SSWT); B) Ice-free period duration index (Ice-free DI, which is the abundance of indicator species of ice cover <180 days); C) Water column depth as indicated by the cyst-depth index (Chrysophycean cysts abundance with respect to cyst+diatom), and D) diatom dissolution and fragmentation indexes (DDI, DFI). In plots A, B, and C, black lines are the smoothed data using the TWAS procedure and grey lines are the original data.

Ice-free period duration

The abundance of species indicative of ice cover duration <180 days suggests that there were shorter winters between 15500 and 12700 yr cal BP (Figure 17.2B). The ice free period become progressively shorter reaching a minimum at about 11800 yr cal BP. The ice-free duration was relatively low during the rest of the sequence, with a peak of longer duration around 11,350 yr cal BP, the period 10000 to 9000 was particularly flat with sustained short ice-free periods.

Water column depth

The water column relative depth was approximated using the relative abundance of cysts respect to diatoms (cyst-depth index). Accordingly to analysis carried out in the chapter 12 (Figure 12.2), periods with cyst-depth index >6% are considered of higher depth. The sequence characterised by periods of relative high water depth and periods of shallower conditions, always with high variability within the main trend (Figure 17.1D). Centennial variability was particularly high before 14500 yr cal BP, and during the period 12500-12000 yr cal BP. (Figure 17.2C). From 15400 yr cal BP the lake showed a progressive reduction in water level until reaching the lower values around 13300 yr cal BP. From 13200 yr cal BP the lake showed a period of high water level, which extend to 12100 yr cal BP. After this, the cyst-depth index showed a high variability and from 10500 yr cal BP to the end of the period studied the lake was permanently shallow.

High values of valves dissolution and fragmentation were found at some depths: 1289 cm (~16000 yr cal BP), 1203-1197 cm (~14100-14000 yr cal BP), 1106 cm (~12600 yr cal BP), and 1061-1051 cm (~12200-11950 yr cal BP). Depths 1034-1028 (~11700-11600 yr cal BP) and 1203-1197 cm (~14100-14000 yr cal BP) presented higher fragmentation being related with the presence of plant rhizocretions in these levels. These two episodes are coherent with very low levels indicated by the cyst-depth index. High dissolution index (DDI) at 12700 is related with a short episod when the cyst-depth index was <6%.

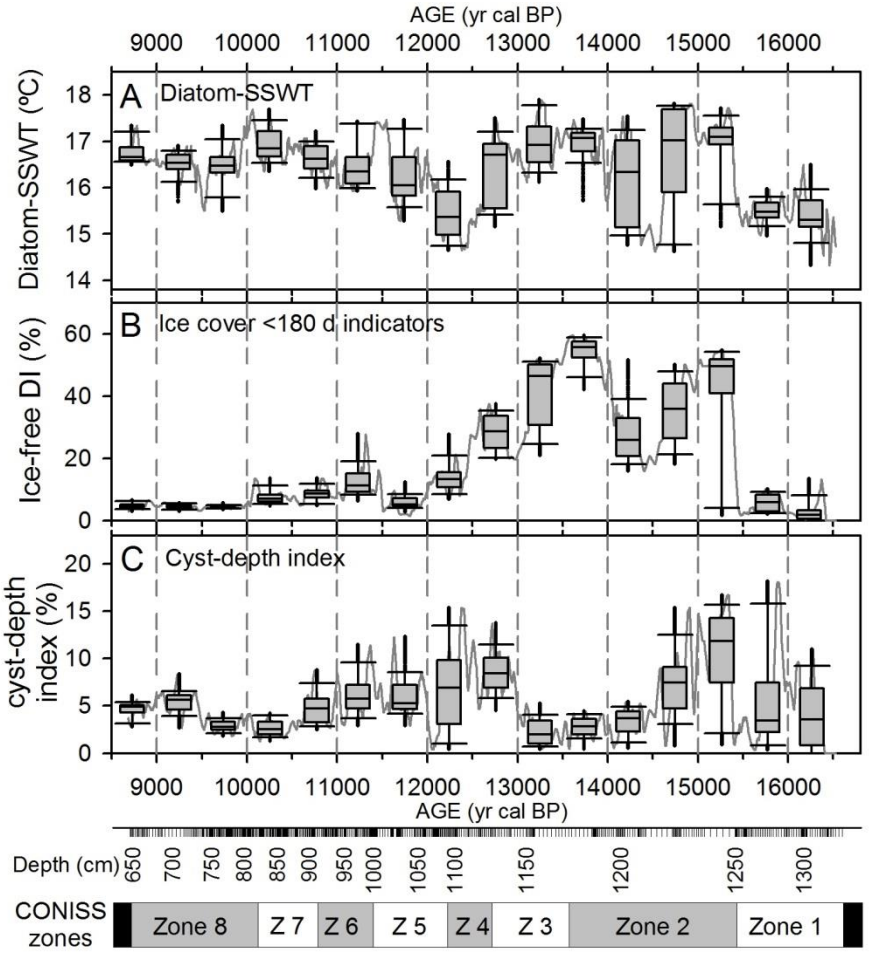

Figure 17.2. Boxplots indicating centennial variability at 500-year intervals. A) reconstructed summer surface water temperature (Diatom-SSWT); B) Ice-free duration index (Ice-free DI, which is the abundance of species indicator of ice cover <180d), and C) cyst-depth index (Chrysophycean cysts abundance with respect to cyst+diatom). Grey lines are the smoothed data using the TWAS procedure.

SSWT and water level

Diatom-SSWT and cyst-depth index showed high variability during different periods across the sequence (Figure 17.3). The comparison of the diatom-SSWT and cyst-depth index in different temporal windows showed a decoupling in their variability both at bicentennial and millennial time windows. Around 15400 yr cal BP was the only period when both variables underwent high and

synchronically bicentennial variability. Millennial analysis showed that the cyst-depth index underwent sudden increase in variability (15900 and 13400 yr cal BP), just some centuries before diatom-SSWT. Likewise, the first period with high millennial cyst-depth index variability last less time than high diatom-SSWT.

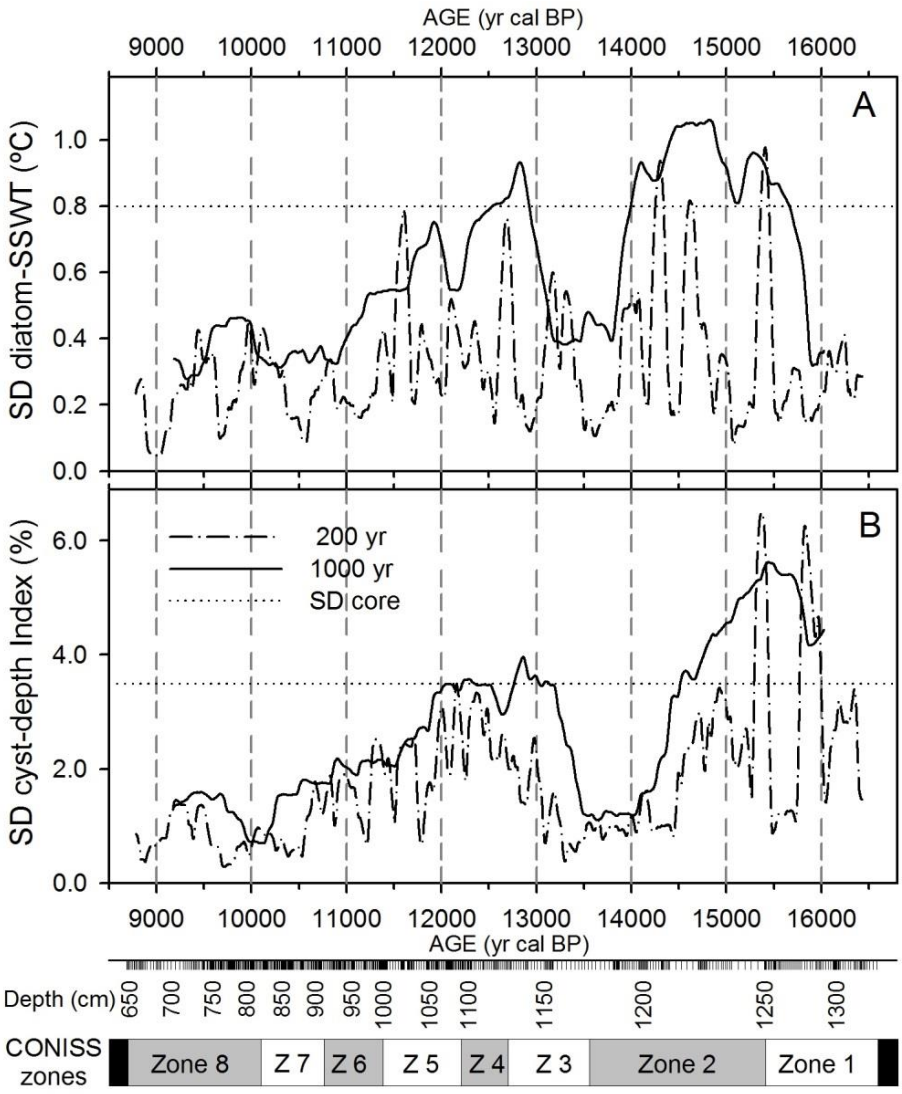

Figure 17.3. Variability at different temporal windows of A) the reconstructed summer surface water temperature (Diatom-SSWT), and B) cyst-depth index (Chrysophycean cysts abundance respect cyst+diatoms). SD is the standard deviation calculated with the smoothed data after TWAS procedure.

The diatom-SSWT and cyst-depth index were not correlated (r=-0.06, p=0.134, n=624) (Figure 17.4). Across the Burg Lake sequence all combinations of SSWT and cyst-depth index were found. The comparison of the diatom-SSWT values during periods with a similar cyst-depth index suggests a scarce effect of the water level on the reconstructed diatom-SSWT (Figure 17.5). Thus, when lakes had a high water level (cyst-depth Index >6%) the diatom-SSWT ranged from 14.6 to 17.8 ºC, periods of cyst-depth index between 4 and 6% had diatom-SSWT values from 14.6 to 17.7 ºC, and periods of lower water level (Depth Index <4%) showed diatom-SSWT values ranging from 14.3 to 17.9 ºC. Accordingly, reconstructed values did not show an easily appreciable effect of the lake level on the reconstructed SSWT.

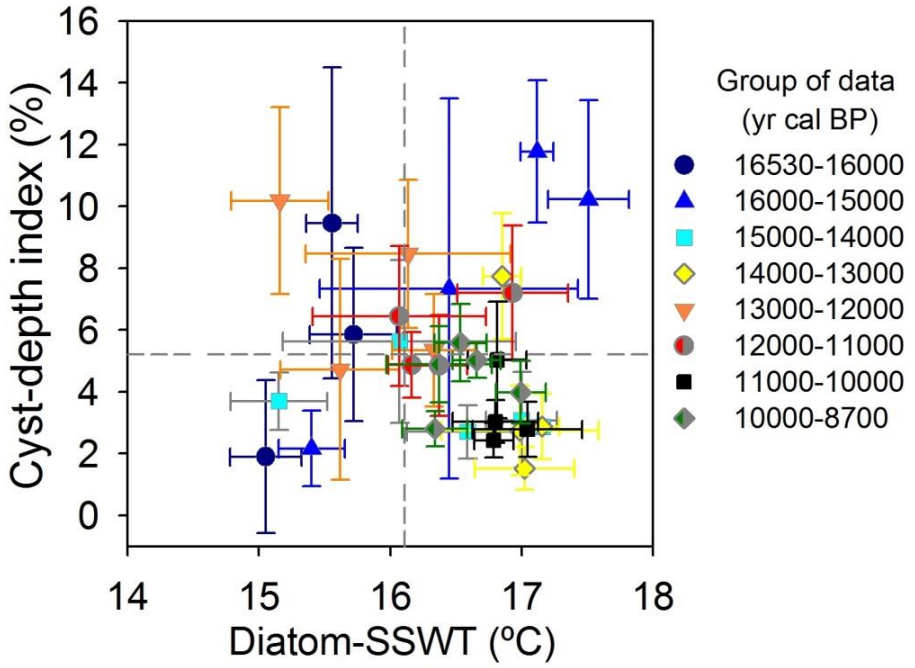

Figure 17.4. Relationship between the summer surface water temperature (diatom-SSWT) and cyst-depth Index in Burg Lake record. Data was smoothed using the TWAS procedure and then grouped every 250 yr.

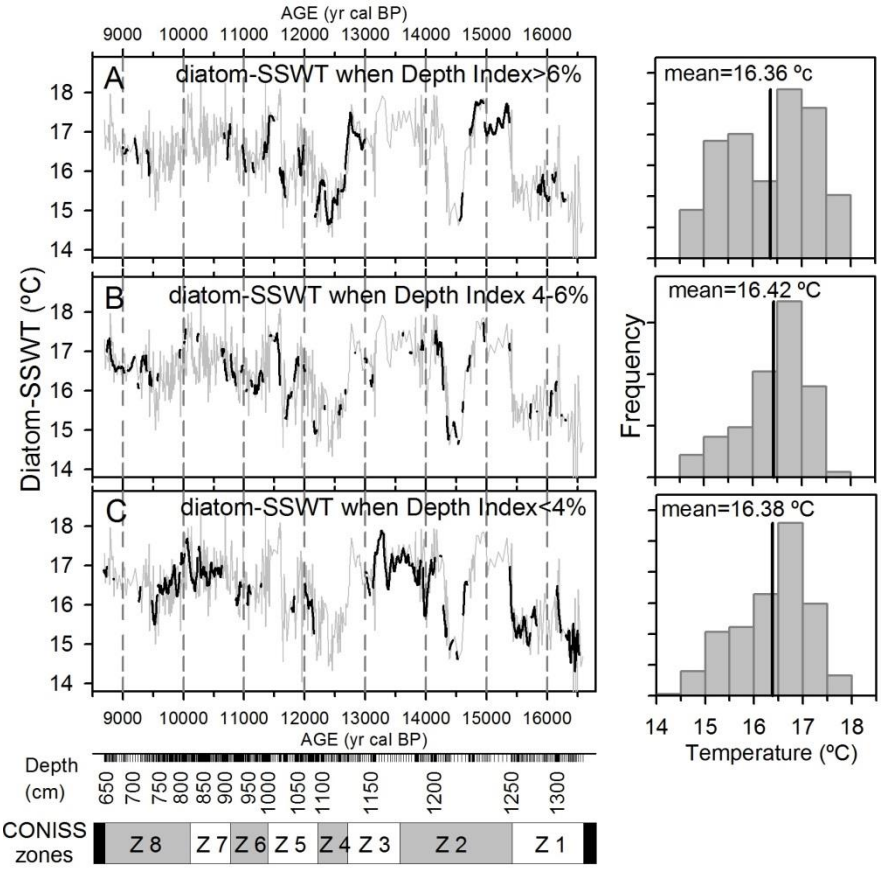

Figure 17.5. Values of summer surface water temperature (Diatom-SSWT) when cyst-depth index was A) >6%, B) between 4 and 6%, and C) <4%. The values 6% and 4% were selected according to the median (4.06%) and third quartile (6.3%) of whole record and 90 percentile of cyst abundance of training-set lakes <6m (5.6%). Black lines are the smoothed data using the TWAS procedure and grey line are the measured data.

Discussion

18. Reliability of the quantitative reconstructions

In this study two complementary procedures of environmental reconstruction using diatoms have been applied. The indicator value of the species, which is based on a previous classification of the environmental variability into archetypical situations for which indicative diatom species are searched, and the quantitative reconstructions using transfer functions, which are based on a continuous view of the environmental gradients and the distribution of the species optima across them. The reliability of the first approach depends on the adequacy of the environmental classifications. In this study, the classifications were based on previous studies on mountain lakes and/or general limnological classifications. Therefore, the significance of these classifications is outside the scope of this study. On the other hand, the statistical methods to look for indicator species are not subject to controversy at present. This is not the case for transfer functions that, despite of their broad application during the last decades with outstanding results in some cases, have been recently questioned from several points of view (Anderson 2000; Juggins 2013). In this study, transfer functions to reconstructed five different environmental variables have been developed and applied, therefore, before going into further discussion of what these reconstructions may indicated in limnological and climatic terms, some consideration of their reliability is necessary. Fundamentally, the issues to consider can be grouped into three categories: a) the representation of the Burg Lake diatom taxa in the modern data set used for calibration; b) the statistical significance of the fluctuations reconstructed; and c) the effects of co-variability among environmental variables.

Burg Lake taxa representation in the modern data-set

The quantitative reconstructions using WA-PLS are based on the ecological optima of the taxa in the modern training-set (ter Braak and Juggins 1993). Consequently, the reliability of the predicted values depends on the representation of taxa in the sedimentary sequence in the modern data-set used for calibration (Birks 1998). This was particularly relevant to consider in this case, because Burg Lake characteristics were not among the most common in the Pyrenean lakes (e.g., altitude, ANC) and underwent an ontogenic transition from a lake to a fen.

The representation of the Burg Lake diatom taxa in the training set was regularly high. Between 60 and 100% (mean=78%) of the recorded species per sample occur in the modern data (Figure 18.1). Taxa occurring in more than 5% of training-set samples range between 35 and 100 % (mean=54%). Therefore, for some specific periods, many of the taxa were not common species in the training set (i.e., low reliability of the optimum estimation). However, the species not present in the training set represented a very low percentage of the diatom abundance in each sample (Figure 18.1 C), although in a few cases the dominant species where relative rare in the training set, particularly at some short periods between 14000 and 12000 yr cal BP.

The richer the samples in species and the more balanced the proportions, the higher the reliability of the estimations as values are obtained by a weighted average of the optimum of each species present. Hill`s N2 values (Hill 1973), a measure of diversity, were low during the first three centuries (before 16200 yr cal BP) but increased to a value above 5 in the next centuries. The N2 highest values were recorded between 15500 and 12050 yr cal BP, contrasting with the low abundance of species well represented in training-set (Figure 18.1). From 12050 to 11500 yr cal BP, the N2 values dropped to a mean of 6.9, ranging from 2.7 to 10.4. The reduction in N2 values correspond with a reduction in the species richness but a high proportion of the taxa was represented in the training set.

There were some episodes with a marked reduction in the abundance of taxa occurring in more than 5% of the training-set samples (~16300, 15400 13600-13300, 12700, 12300 yr cal BP). Therefore, the poorest represented taxa in training-set had a higher weight in reconstructions during these events. However, only two events (~16300, 12700, yr cal BP) were related with a marked change in some reconstructed variable (SSWT). The event ~16300 yr cal BP, when there were a sudden increase in SSWT, could be the only where the reduction in the abundance of analogue species are influencing the temperature reconstruction. This temperature change is not reflected in any other proxy. In contrast, the event ~12700 yr cal BP corresponds with a cold event that was extensively supported by other proxies and which duration was not related with the period of time in which the analogue abundance was low.

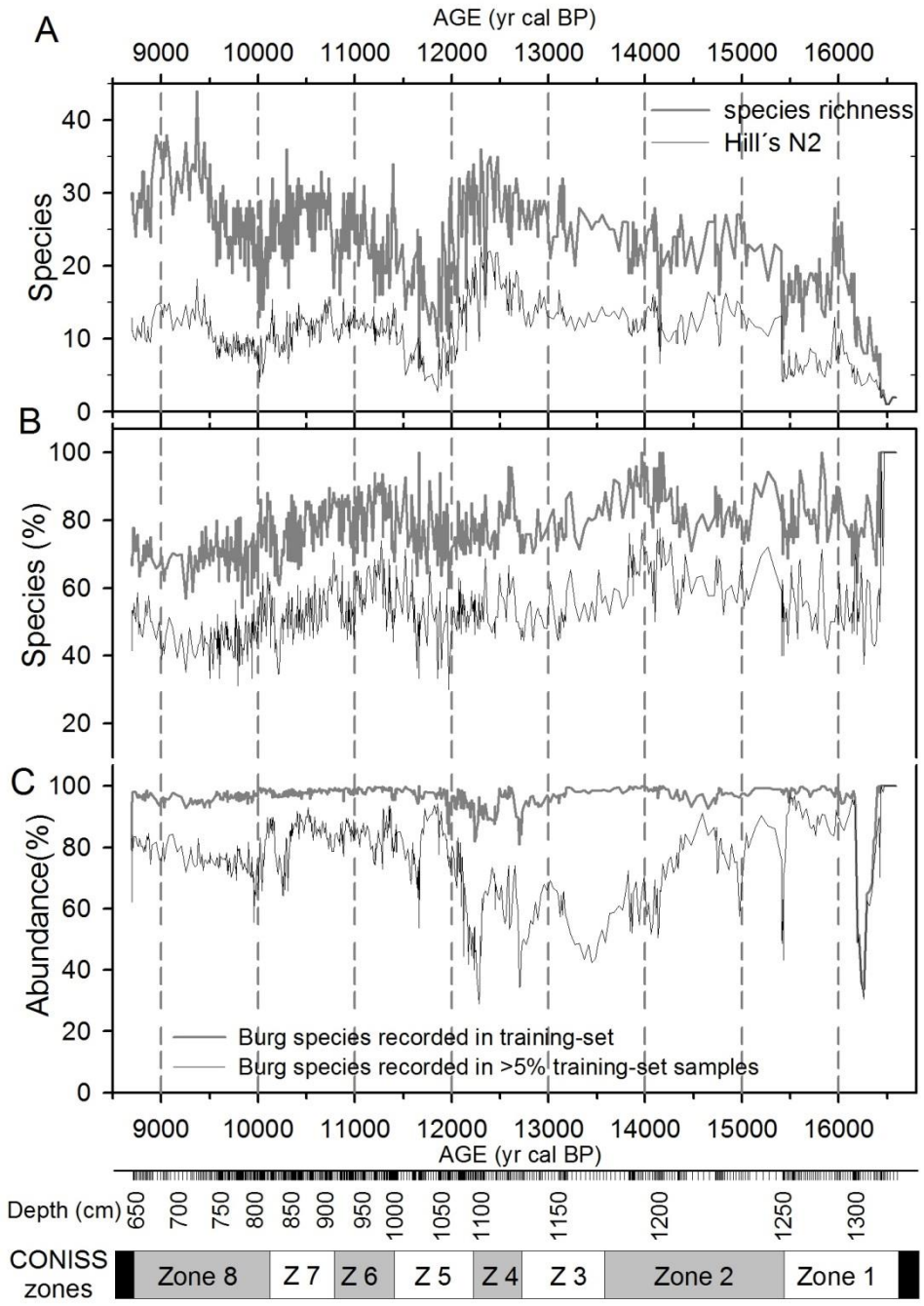

Figure 18.1. Diagnostic features of the Burg Lake diatom taxon representation in modern training set. A) Species richness the samples and Hill N2 diversity index, B) Sample species present in the modern training set C. Relative abundance of the Burg species occurring in the training-set.

Statistical significance of the variables reconstructed

Evaluation, validation and reliability of quantitative reconstructions are not simple and straightforward; some of them are subject to a similar heuristic nature than the development and model selection of the transfer functions. The validation process uses the comparison between historical measurements and the reconstructed values (Birks 1998). However, historical data are rarely available as sedimentary records extend far beyond the times when instrumental measurements started. Consequently, indirect approaches are used to assess the reliability of quantitative reconstruction (Juggins and Birks 2012). Recently, Telford and Birks (2011b) proposed a test to evaluated the significance of quantitative reconstruction. The method uses the modern training-set to generated random environmental variables. The variance explained by these random variables is compared against the variance explained by the reconstructed variable. The maximum variance that can be explained, linearly independent from other variables, is obtained by the first principal component (PC1) of the diatom record. Accordingly with this method, the significance of Burg Lake quantitative reconstruction was tested.

The first principal component (PC1) of diatom Burg Lake record (Figure 15.11) indicates three periods in the diatom sequence with a greater change in the dominant species, which corresponds approximately to the early lake phase, the Late Glacial and the Holocene periods. None of the reconstructed variables reproduce the PC1 pattern *per se*. The reconstructed variables appear as a complex combination of different diatom PC axes. Correlations between the diatom PCs and the reconstructed variables change through time (Figure 18.2). The correlation vary between negative, non-significant and positive, suggesting that PC axes has a more statistical character than environmental meaning. This may happen because the time period considered is quite long, the temporal resolution high and the environmental changes large and varied. As a consequence of this complexity, the statistical summary that PCA provides indicates the nature of the changes (diatom communities) rather than the drivers of the changes (environmental forcing). At long time scales, similar community changes may result from different forcing situations and, oppositely, similar forcing may result in different community changes.

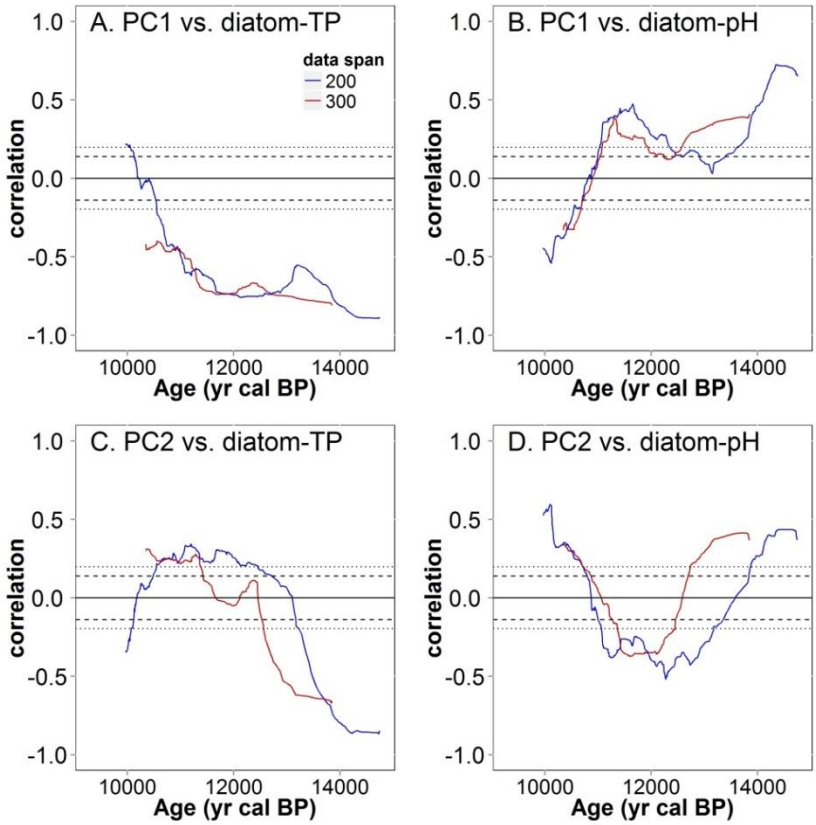

Figure 18.2. Correlation coefficient between principal components (PC1, PC2) of Burg Lake diatom assemblage and some diatom reconstructed variables: TP (A, C), and pH (B, D) using data spans of 200 and 300 samples, respectively. Limits of significance (p-value=0.05 are indicated by dotted (300 samples) and dashed (200 samples) lines.

Diatom-TP was the only variable with a significant reconstruction for the whole sequence according to the Telford and Birks (2011b) test (Figure 18.3 A). However, the behaviour of the accumulative sequence (Figure 18.3 A) and moving windows (Figure 18.3 A, B) showed contradictory results. With the exception of diatom-ANC, windows of time of 100 and 200 samples show some periods where the reconstructed variables are significant. Thus, for example, diatom-TP was a significant driving factor for diatom change in Late Glacial, and had scarce influence during Holocene when windows of 100 and 200 samples were selected. Nevertheless, the accumulative sequence suggests that reconstruction of diatom-TP was not significant in Late Glacial and started to be significant later. These results show that the time window selected influences the

values of the test. The same reconstructed values may turn significant or not according the temporal period considered as reference; this does not makes sense as the absolute value is exactly the same. Therefore, this test has to be applied with caution as an indicative tool.

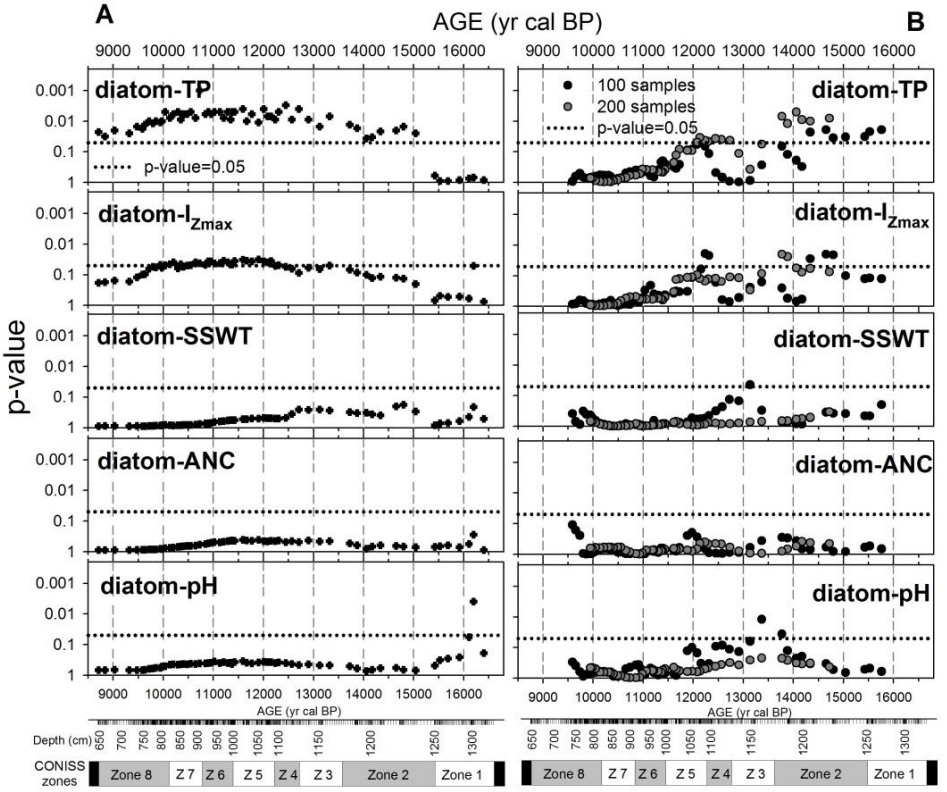

Figure 18.3. Test of the reliability of the reconstruction according Telford and Birks (2011b) for total phosphorous (diatom-TP), irradiance at the bottom (diatom-I_{Zmax}), summer surface water temperature (diatom-SSWT), acid-neutralising capacity (diatom-ANC) and pH (diatom-pH). A). Considering the whole sequence increasing size of the section 10 samples each time from the bottom to the top-end of the record (classical approach). B) Performing the test moving every 10 samples and considering sections of 100 (black) and 200 (grey) samples. Dotted horizontal lines indicate p-values = 0.05.

The Telford & Birks test should work better when the first axis of the diatom variability in the sedimentary sequence corresponds with the first axis of the diatom variability in the modern training-set. It can be assumed that this condition is fulfil when the first PC of the diatom sedimentary sequence correlates with the same explanatory (environmental) variable than the first axis

of the RDA of the training-set. In the case of the Pyrenean training set, this is the pH-ANC gradient. This situation happened during the first 2000 yr of the record (Figure 18.3 B), when the first PC of Burg diatoms was related with pH and ANC. During this period the test of pH reconstruction was not significant when considering the whole sequence (Figure 18.3) with the exception of the section in which the first 20 samples (16590-16300 yr cal BP) were included. Contradictorily, when time windows where considered, pH appears significant (~13500), precisely when the correlation of PC1 and pH is the weakest.

Overall, the assumption that the reliability of a reconstruction must be linked to its explanatory capacity of the diatom composition changes can be questioned. If an environmental variable is not particularly changing during periods in which other variables do change, it is reasonable that it does not explain changes in the diatom composition; however, this does not mean that the existing species (or new ones appearing) do not adjust to the stable value of that conditioning variable. Comparison with the explicative capacity of random variables has no other meaning that warning that the variable is not driven the changes, but not that the values reconstruct are incorrect.

In summary, from the test performed it can be concluded that trophic variables (e.g. TP) had more influence in driving diatom assemblages than thermal or pH-ANC oscillations. And, in general, that the environmental forcing was more significant during Late Glacial than Holocene.

Independence (or dependence) of reconstructed variables

The quantitative reconstruction of environmental variables is a topic of permanent discussion due to the difficulties to recognise causal relations and evaluate the statistical robustness of the models respect the violation of some assumptions (Birks 1998; DeNicola 1996; Telford and Birks 2005, 2011c; ter Braak and Juggins 1993). In fact, even conceptual ecological assumptions may be under discussion. The effect of secondary variables on the reliability of quantitative reconstruction has been evaluated by Juggins (2013) performing experimental simulations of training sets with different scenarios of correlations between the environmental variables. Despite the simulations suggest a significant effect of the secondary variables, the weakness of this approach is that it try to test the independence of reconstructions when the environmental variables are in fact correlated; the result cannot be other than to find a correlation between the reconstructed variables. The point should be to test

whether there are species responding differentially to environmentally correlated variables, such as in this study have been shown in the last section of chapter 11. On the other hand, causal relationships between variables external to the lake (e.g., climate components) and the organism assemblages (e.g., diatom composition) may be mediated by variables that change through time according to the changing characteristics of the lake and the catchment itself (Anderson 2000). Therefore, beyond pure statistics, it is worth to analyse case by case the possible spurious associations between reconstructed parameters.

Relationship between reconstructed values of TP and ANC

TP is one of the variables reconstructed using the Burg diatom record that could be highly conditioned by other variables such as ANC and temperature (Juggins et al. 2013). In Burg Lake, reconstructed TP shows a different temporal pattern than ANC. In fact, the training-set data shows a positive correlation between TP and ANC, while the reconstructed values are negatively correlated (Figure 18.4). Therefore, it cannot be argued that the training-set dependency is translated into the environmental reconstructions through the transfer functions applied. The relationship between reconstructed TP and ANC change at different periods, being most of the time non-significant: 15000-14000 yr cal BP ($r=0.10$, $p=0.45$, $n=51$), 14000-13000 ($r=0.09$, $p=0.55$, $n=43$), 13000-12000 ($r=0.04$, $p=0.70$, $n=85$), 11000-10000 ($r=-0.06$, $p=0.43$, $n=135$), and 10000-8700 yr cal BP ($r=-0.06$, $p=0.55$, $n=117$).

The independence between the reconstructed values of TP and pH-ANC is also supported by the species response to the environmental gradients and the significant indicator species found in the training-set. As it is shown in Figure 11.15, the species responding to the environmental gradient are different for each variable. Species such as *Gomphonema* sp. No. 15 Coronas, *Gomphonema* cf. *parvulum*, *Fragilaria delicatissima*, and *Pinnularia microstauron* var. *nonfasciata* are mainly explained by TP, whereas *Navicula catalanogermanica*, *Diploneis* cf. *peterseni*, *Navicula pseudolanceolata*, *Diploneis* cf. *puella*, and *Amphora copulate* are explained by pH. On the other hand, significant indicator species were different for TP and pH-ANC classifications (Table 15) and their abundance fluctuations across the sedimentary records agree with reconstructed values using transfer functions (Figure 16.7, Figure 16.11).

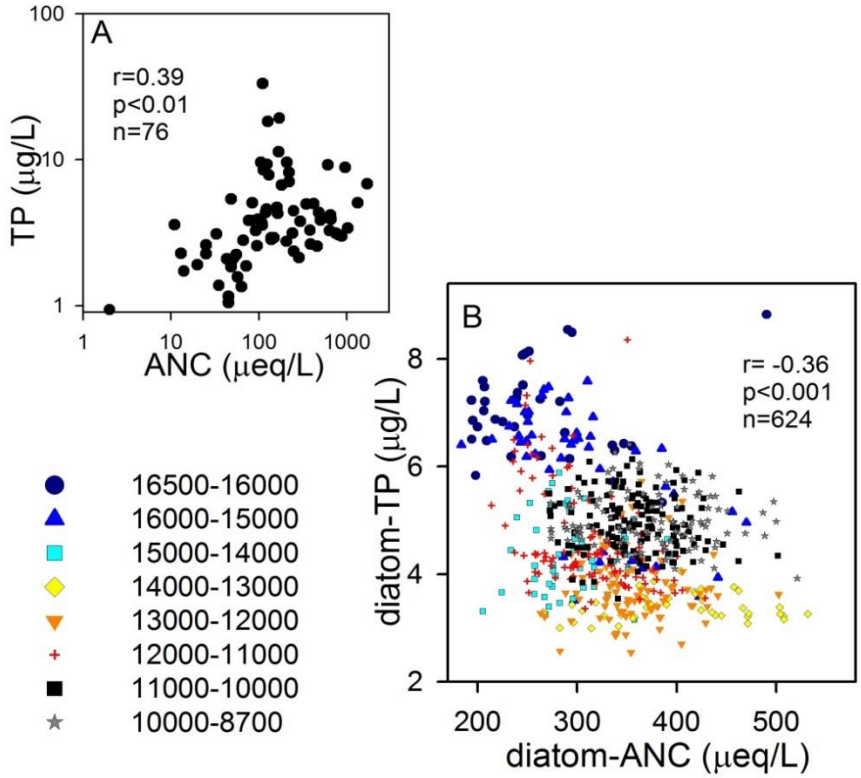

Figure 18.4. Relation between total phosphorous (TP) and acid-neutralising capacity (ANC) in the training set (A), and between reconstructed total phosphorous (diatom-TP) and ANC (diatom-ANC) in the Burg Lake record (B).

Relationship between reconstructed values of TP and SSWT

The positive correlation between TP and summer surface water temperature (SSWT) in the training-set is different to the trend observed in the reconstruction of both variables. There is a significant and negative correlation between both variables through the record (Figure 18.5). However, before 12800 yr cal BP, the correlation was negative ($r = -0.67$, $p<0.001$, $n=185$) in contrast to the positive correlation after 12800 yr cal BP ($r=0.19$, $p<0.001$, $n=439$). These results suggest a change in internal process of lake from Late Glacial to Early Holocene. Sedimentological proxies indicated that the catchment coverture was low during the early phase of the sedimentary record (before 15400 yr cal BP). However, even under these conditions there was no association between TP and SSWT ($r = -0.18$, $p=0.12$, $n=75$).

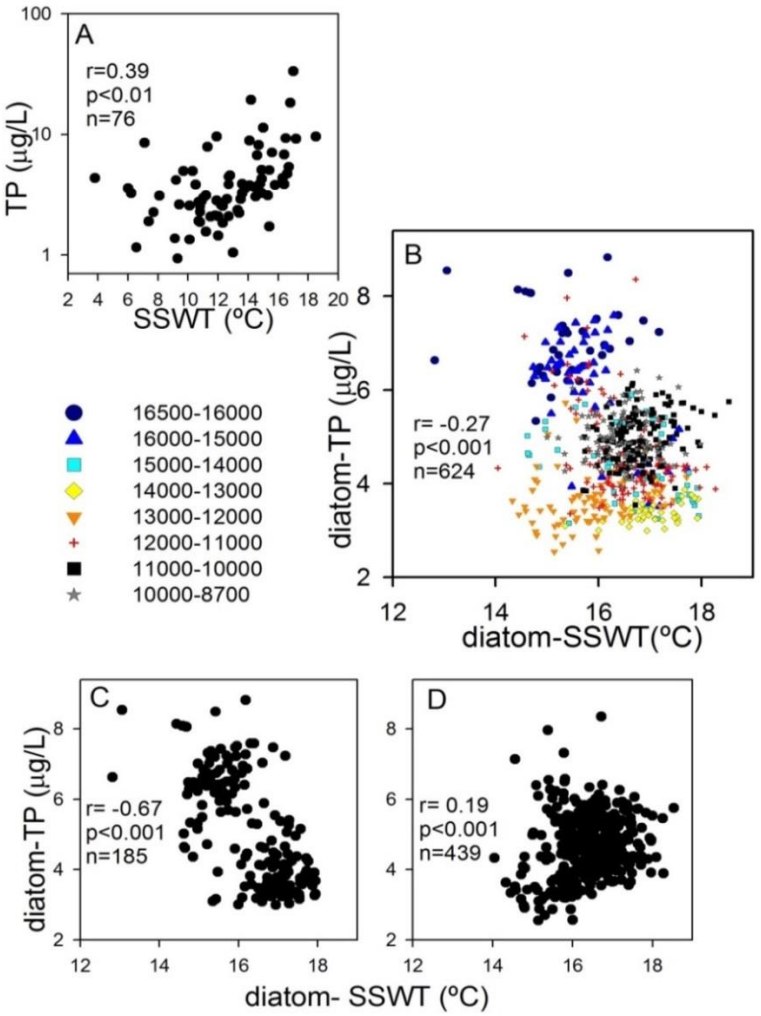

Figure 18.5. Relation between total phosphorous (TP) and summer surface water temperature (SSWT) in the training-set (A) and the Burg Lake record (B, C, D). B) Reconstructed values of TP (diatom-TP) vs. SSWT (diatom-SSWT) in the whole Burg Lake sequence. C) Diatom-TP vs. diatom-SSWT of samples before 12800 yr cal BP. D) Diatom-TP vs. diatom-SSWT of samples from 12800 to 8700 yr cal BP.

The SSWT also primarily explain the variation of a different set of species than TP in the training set. Species present in Bur Lake record, such as *Navicula* cf. *seminulum*, *Navicula cryptotenella*, and *Sellaphora laevissima* were mainly explained by the SSWT but not by TP (Figure 11.15). Likewise, the interpretation of the significant indicator species present in the Burg Lake

sequence showed the same temporal pattern than the SSWT values obtained by the transfer function.

Relationship between reconstructed values of TP and I_{Zmax}

TP and I_{Zmax} were correlated in the training-set and showed a similar correlation in sedimentary record (Figure 18.6). The correlation between both variables was maintained also throughout the sedimentary sequence. However, a higher correlation between I_{Zmax} and cyst-depth index (r=-0.24, p<0.001, n=624) than TP and cyst-depth index (r=-0.09, p<0.0025, n=624) suggest a limnological coherence in the reconstruction of I_{Zmax} as in relatively oligotrophic lakes irradiance to the bottom may depend more on the depth of the lake than on water transparency related to phytoplankton growth (i.e., TP). The set of species explained by I_{Zmax} differ also from those that are explained by TP (Figure 11.15). All in all, reconstructed I_{Zmax} has to be considered carefully in the limnological context where they occur.

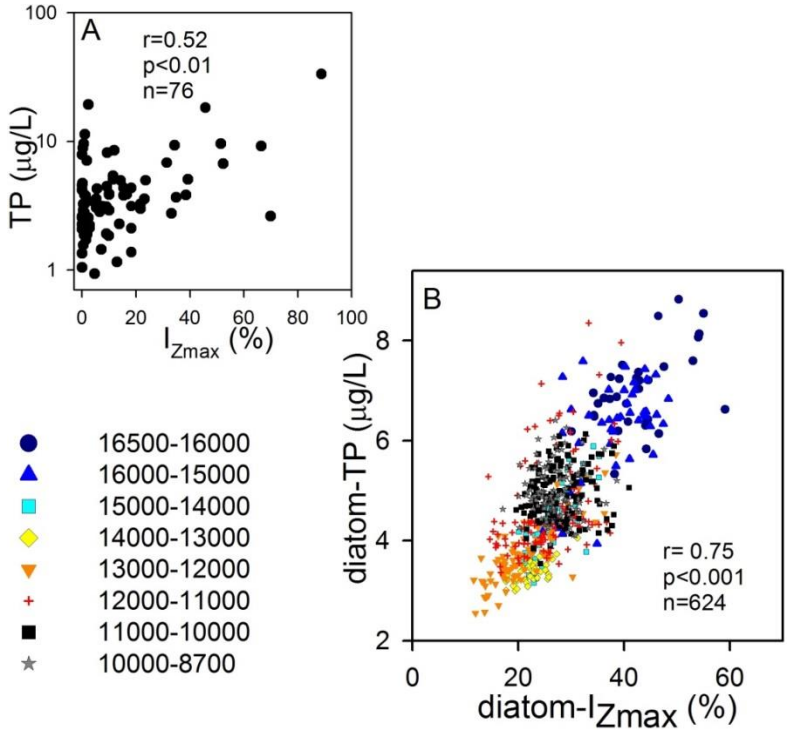

Figure 18.6. Relation between total phosphorous (TP) and irradiance at the bottom (I_{Zmax}) in A) the training set and B) the reconstructed values for Burg Lake.

19. Burg Lake ecosystem development

The sedimentary sequence of the Burg Lake collected information on climate, catchment ontogeny, and the main in-lake processes. The high sediment accumulation rate, shallow conditions, aquatic plant development, and changing catchment conditions produce a complex scenario to be interpreted based on the diatom composition and some auxiliary geochemical information (i.e., mineral composition, elemental composition and subfossil pigments).

Lake ontogeny

The lake underwent a reduction in the maximum depth achievable corresponding to half the initial value at the beginning of the time period considered (Late Glacial and Early Holocene). This dramatic change in depth was probably responsible of the long-term trend of different proxies such as LOI, pH, and, partially, TP (Figure 19.1, Figure 19.2), which base-line increased as depth declined across Late Glacial and the Holocene. As this is a seepage lake, the actual water column depth at any moment could have differed from the maximum depth achievable depending on the water mass balance.

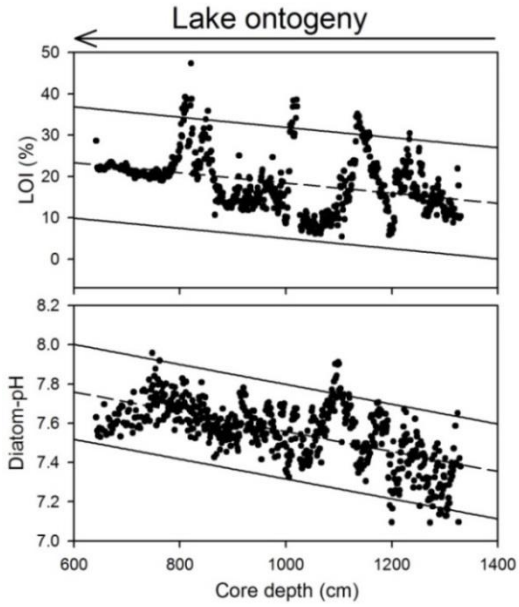

Figure 19.1. Temporal sequence of the organic matter accumulated in the sediment (as Loss on ignition (LOI)) and water column pH reconstructed using diatoms (diatom-pH) in the Burg Lake.

The trend may reflect the progressive conversion of the system to a wetland, a seepage shallow lake switched progressively to the current fen state. The transition between these two systems occurred later in time to the period here studied (Pèlachs et al. 2011); however, some traits of this transition such as increased accumulation of organic matter and alkalinisation were progressively taking place as depth declined. The pH trend is the opposite to the declining trend detected in boreal and some alpine regions with moderate concentrations of base cations and colder conditions (Fritz and Anderson 2013; Schmidt et al. 2006). In these cases, the infilling process brings to a dystrophic acidic peatbog, whereas here warmer and water-buffered conditions bring the system to a fen with alkaline water. The increase in pH may occur both because of the progressive slight increase in ANC (Figure 16.11) or for a higher CO_2 uptake by plants relative to the lake volume. In any case the system remains in a moderate alkalinity state without significant carbonate precipitation. Ultimately, the nature of the wetland formed is determined by the mineral composition of the catchment bedrock and climate, which respectively provide cations to the water and long-enough periods for decomposition of a large part of the organic matter produced in the system and allochthonous subsidies. Relative dry summers and/or warm autumns prevent from a podsolization of the catchment soils and high accumulation of dissolved organic carbon and refractory particulate carbon.

The decline in depth of the lake is not independent of other geomorphological changes in their lake surroundings. The smoothening of the watershed slopes and decrease in the energy of the water flows is illustrated by the changes in the elemental ratios between elements linked to minerals of relatively large particle-size and elements associated to fine particles (K/Ti) that indicate a progressive decline in the size of the particles that reach the lake (Figure 19.2).

Lake productivity

The reconstructed TP is likely the variable that describes better the complexity of the influence of climate, catchment and in-lake process interactions. Reconstructed TP can be assumed as a surrogate for water column (phytoplankton) productivity in the current context. TP showed a decline tendency during most of the Late Glacial and from 12200 yr cal BP (core depth: 1080 cm) the trend reverted. The tipping point coincided with an increase in the sedimentation rate (Figure 19.2).

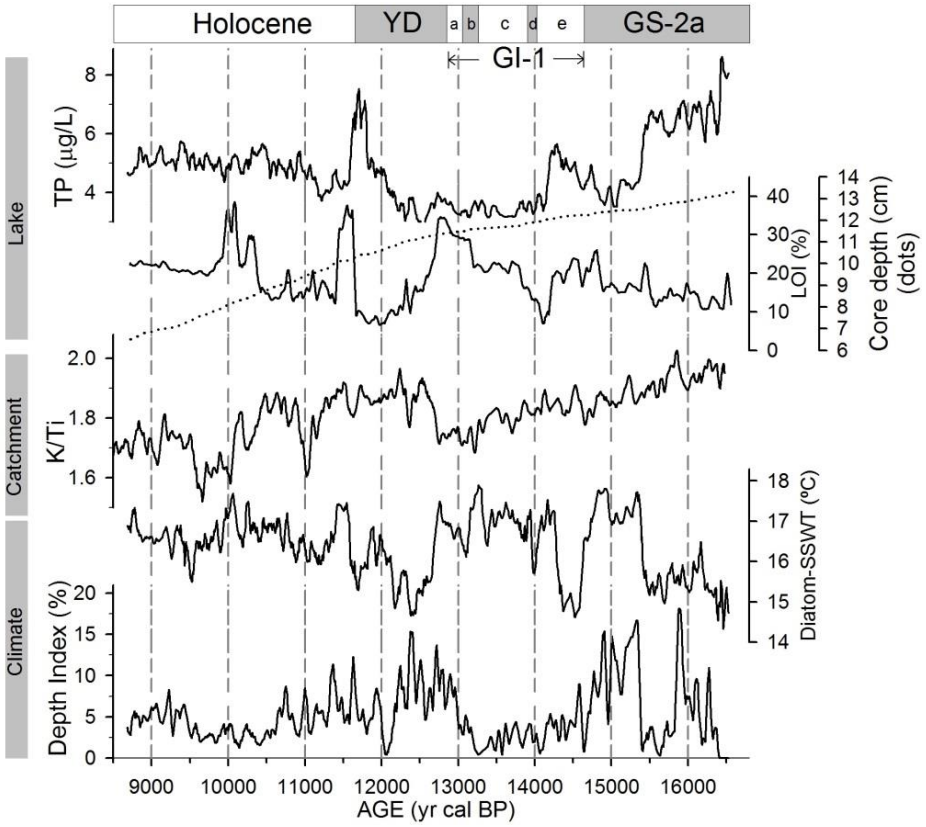

Figure 19.2. Sequence of proxies related with lake productivity (TP and loss on ignition - LOI), catchment erosion (K/Ti) and climate (summer surface water temperature (diatom-SSWT) and Cyst-depth Index).

The change in the TP tendency could be attributed to differences of climatic conditions between Late Glacial and Holocene. However, the comparison between periods with similar thermal and hydric conditions in the lake (SSWT and cyst-depth index at 14000-13000 in Late Glacial and 10300-9000 in the Holocene) shows that the main cause of change could be an effect of the lake ontogeny (Figure 19.3). During similar temperature and water level conditions, it is expected a similar lake productivity (i.e., TP), if this is climatically driven. However, the Burg Lake record shows contrasting TP distributions for the two periods, during the Holocene the values are about 50% higher, and the whole range of TP values scarcely overlap between the two periods. This ontogenic change is also evidenced by the increased LOI, pH and S/Fe ratio in the sediments. Everything points to a shallower lake with a higher biological activity

per unit of surface during the Holocene period considered respect the climatically similar period of the Late Glacial, when the lake was deeper.

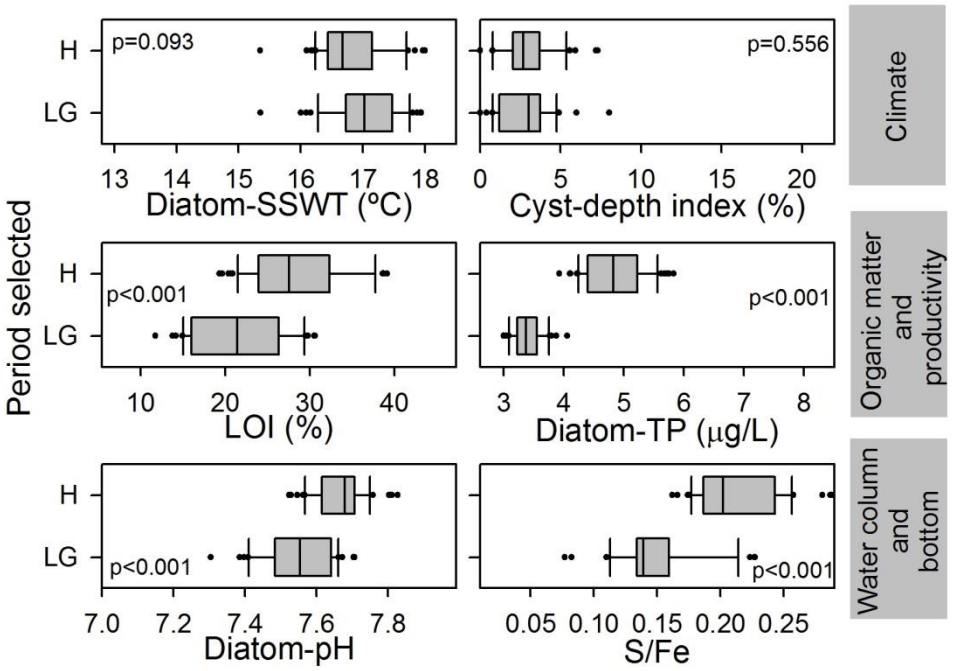

Figure 19.3. Comparison of selected variables between two periods with similar thermal and hydric conditions (summer surface water temperature (diatom-SSWT) and cyst-depth index). **LG**: 14000-13000 yr cal BP (n=43), **H**: 10300-9900 yr cal BP (n=56). The significance of a two-sample t-tests is indicated (p-value). X-axes scales are plotted according to the minimum and maximum value for each variable in the whole sedimentary sequence.

External nutrient loading

The first scenario of high TP concentration (up to ~15300 yr cal BP) was probably related with high external P loadings from a catchment with high amounts of exposed fresh rock and till debris as glaciers were shrinking and soil and weathered patina on rocks were scarcely developed. Even during this period, the lake TP showed some persistent decline coherent with the soil formation in the catchment (Figure 19.6) and consequent decline of external P loading. However, the period of high TP finished abruptly, probably due to further

climatic amelioration as indicated by SSWT. Interestingly, another TP high peak occurred at the end of the Younger Dryas cold phase.

The catchment ontogeny and lake ontogeny are necessarily correlated, but whereas the catchment development produces a control of nutrients (i.e., P) exported to the lake, the lake ecosystem development towards a wetland causes a progressive increase in the lake trophic state, probably due to shorter distances for internal nutrient recycling (Figure 19.4).

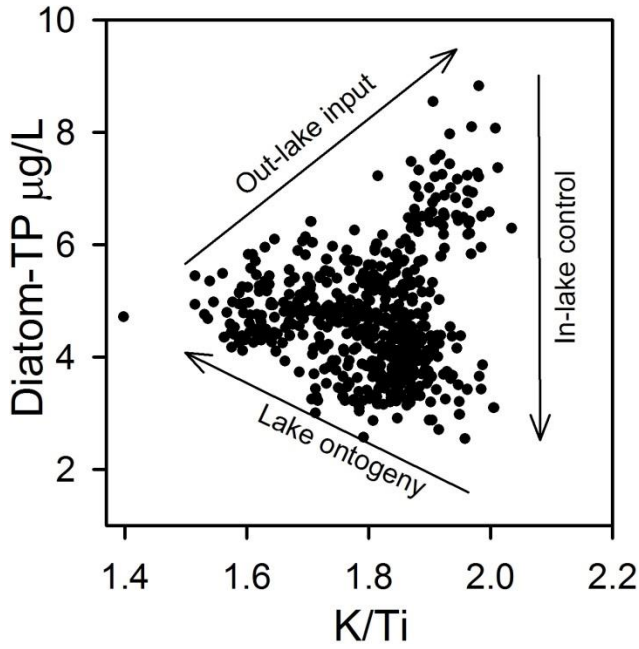

Figure 19.4. Scheme summarising the complex relationship between the ontogeny and the lake productivity. K/Ti is used as indicator of physical erosion in the catchment.

Benthos vs. plankton productivity

As mentioned above, LOI showed the trend of the lake ontogeny (Figure 19.4). Despite there are periods in which TP and LOI follow the same general trend, in general they are not highly coupled (Figure 19.2). LOI show more concordance with indicators of benthic productivity (i.e., pigments and benthic proxies), which in this kind of lake may probably be more relevant.

The lake conditions during late GS-2a and GI-1 exemplify the most important of the benthic compartment. Around 15400 yr cal BP the lake undergoes a change in the main source of production, extending throughout the GI-1. The high

values of macrophyte indicators and pigments of cyanobacteria (zeaxanthin, echinenone) and anoxic photosynthetic bacteria (Isoreniaretene) indicate the development of a complex biofilm in the bottom of the lake surrounded by macrophytes (Figure 19.5). In this type of environment there is a strong control of redox conditions of the sediment and nutrients recycling. Anoxic conditions mobilise P but they hardly can diffuse to the water column as the photosynthetic microbial mat cap uptake it. As the microbial mat growth upwards, organic matter can accumulate in the anoxic conditions below the microbial biofilm.

On the other hand, while during the late GS-2a macrophytes and pigments of benthic indicators start to increase synchronically; during the GI-1 they have a decoupled trend. This suggests that the benthic component and macrophytes alternate the control of lake productivity while phytoplankton depends more on external loads.

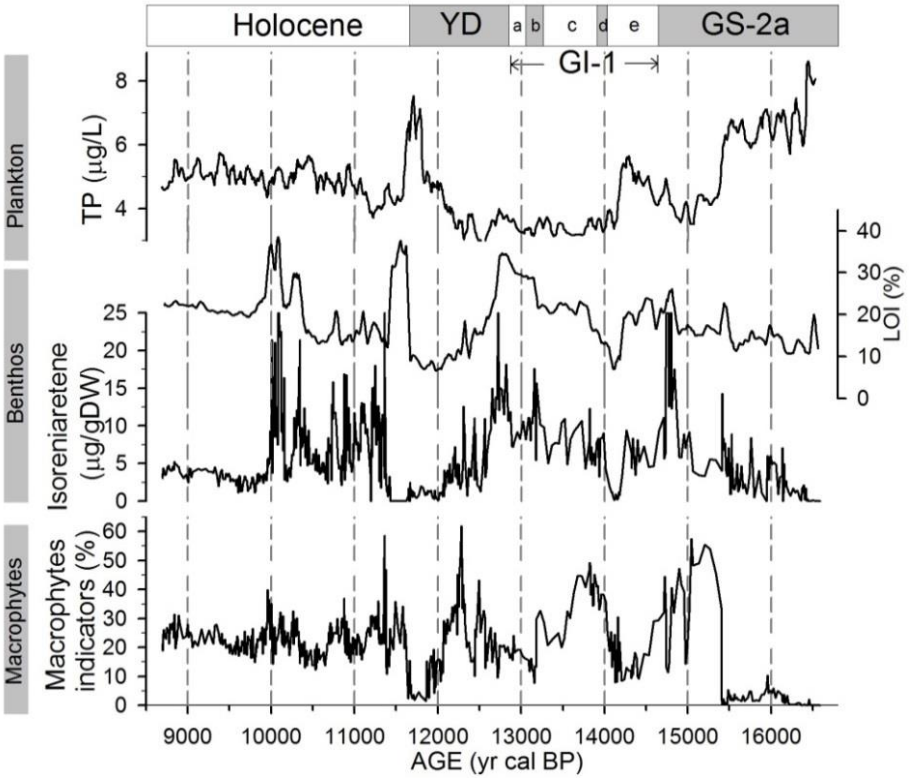

Figure 19.5. Sequence of proxies related with plankton productivity (TP9, Benthos productivity (LOI, Isoreniaretene pigments), and macrophytes presence (macrophytes indicators).

Influence of climate

The influence of past climatic variability on lake productivity processes is extensively recorded in the literature (Birks et al. 2012; Jones et al. 2013; Kirilova et al. 2009; Luoto et al. 2012). Climate affects the lake directly and indirectly through the influence in the catchment (Fritz and Anderson 2013). The identification of an independent climatic signal in productivity proxies of an ecosystem such as Burg Lake is complex. Therefore, it is adequate to focus in two periods in which a strong change in temperature was expected: the transition of early phases of the lake in GS-2a to the GI-1 and the transition of GI-1a to GS-1 (Younger Dryas, Figure 19.6).

The first millennium of the Burg Lake record shows high TP, and a progressive increase in diatom richness, LOI and reduced conditions. A sudden heating around 15400 yr cal BP triggered a shift in the internal lake organisation (E1 in Figure 19.6).

The rise in SSWT happened together with an increase in lake level, suggesting a regional warming that produced a massive melting of the catchment glaciers. Despite the Burg catchment indicators and the general knowledge of this period suggest dry conditions around Europe (Clark et al. 2012), the gradual melting of glaciers could have maintained a high water level during several centuries.

The most fundamental consequence of this shift is the reorganization into a larger ecosystem with large limnetic volume in which a higher number of diatom species could grow. As shown by the macrophytes and redox indicators, the new conditions foster the development of littoral and benthic communities reducing the importance of the planktonic compartment in the ecosystem (TP).

The second time slice (GI-1a to YD) was a warm period with high water level (E2 in Figure 19.6) during which the lake accumulated more organic matter (higher LOI) and the sediment at the bottom showed reduced conditions and microbial mats with strong redox gradients. This was followed by a cooling period (YD), in which the main characteristic, at the beginning, was a predominant high water level (E3 in Figure 19.6). As will be discussed later (chapter 20), this circumstance is coherent with the advance of the catchment glaciers. The new circumstances caused a reduction of the both the organic matter accumulated (lower LOI) and the reductive conditions at the bottom of the lake. The internal loading of nutrients probably decreased. The increase water column and the lower internal nutrient loading trigger the

oligotrophication of the system, which was evidenced in a decline in the TP concentration.

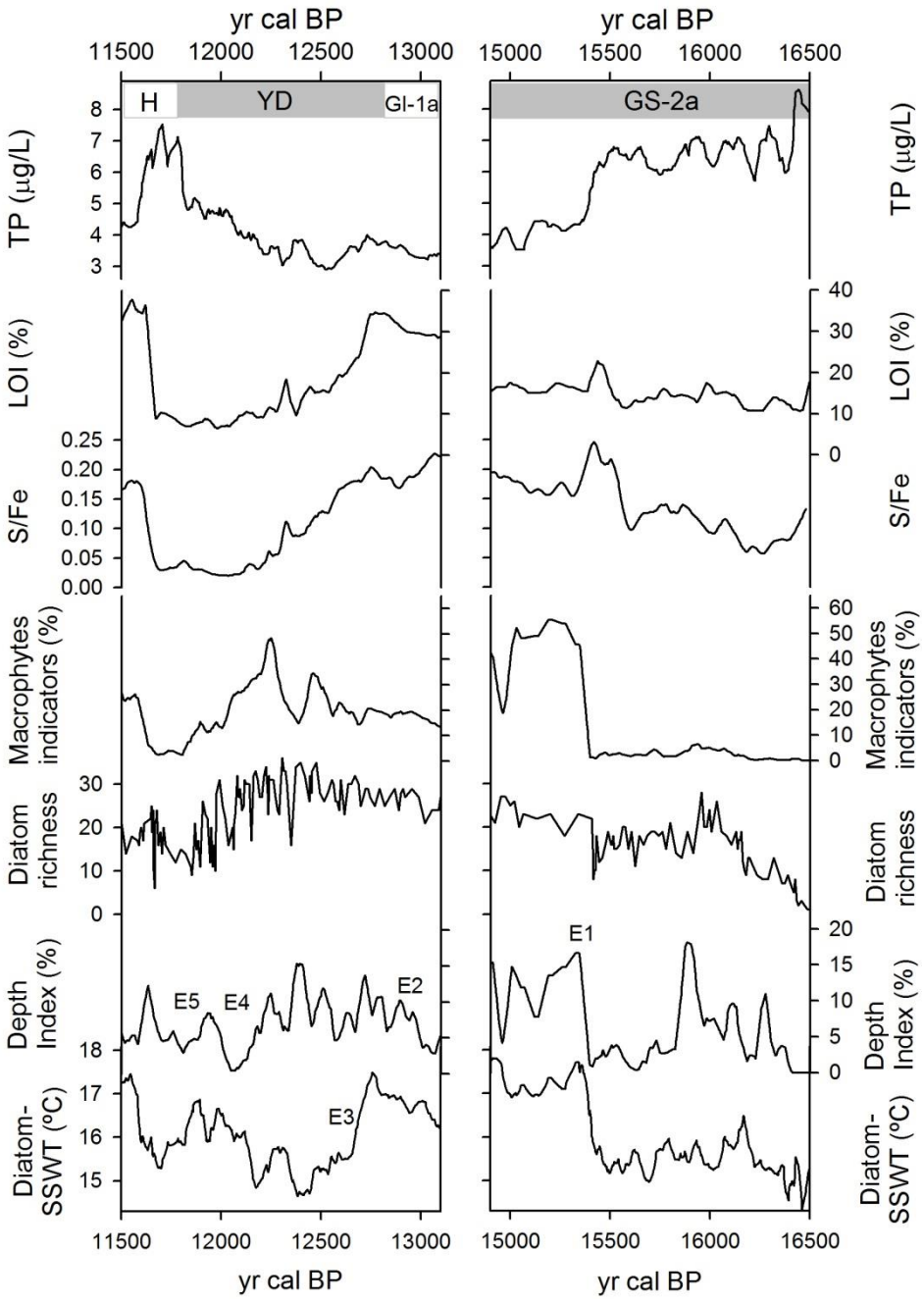

Figure 19.6. Comparison of selects proxies between two contrasting periods. Right panel shows the early phase of the lake and left panel shows mainly the Younger Dryas period.

At the middle of YD the system experienced another shift. The persistent dry conditions probably caused the decline in water column depth (cyst-depth index) and SSWT increase (E4, E5 in Figure 19.6). These events caused a reduction in the diatom richness and a shift in TP towards higher values as the lower depth facilitated that external nutrient inputs had a greater importance.

Summarising, Burg Lake underwent changes in productivity ought to the combined influence of climate, and catchment and lake ontogeny. Lake ontogenesis mainly determined a base-line shift towards more productive conditions, whereas climate drove more abrupt fluctuations. The catchment ontogeny plays an important role during the early phase and the main cold events, when periglacial processes gain relevance.

20. Burg Lake sedimentary sequence and palaeoclimate

The environmental variables reconstructed using the diatom record corresponded to lake features to which the diatom species may be directly responding. There were no direct climatic inferences (e.g., July mean air temperature). However, as shown in the last chapter, part of the changes in the lake was driven by climate. There are two variables, among the reconstructed, that link directly to atmospheric weather: summer surface water temperature and water column depth (cyst-depth index).

The temperature of lakes is controlled by the heat budget in which radiation, conductance and mass exchanges are involved mediated by weather conditions, topography and connection to other elements of the hydrological system (e.g., glaciers, groundwater, etc.) (Kettle et al. 2004; Livingstone and Padisák 2007; Novikmec et al. 2013; Sharma et al. 2008). Despite this complexity of interacting elements surface water temperature from many lakes are strongly correlated with the air temperature (Livingstone and Dokulil 2001) if water inflow do not contribute decisively to the heat budget and the water volume do not change considerably throughout time. In Burg Lake, water flowing from glaciers and changes in water volume are both likely during at least part of the period studied. Therefore, inferences to air temperature from summer surface water temperature reconstruction (SSWT) have to take into account the potential role of these two factors, which are also not independent among them.

The reconstruction of the lake depth is an important feature in palaeolimnological studies as the depth reflects changes in water balance of the catchments. There are many studies using ecological aspects or organism (Finkelstein et al. 2005; Gasse 2000) and different sedimentary proxies (Magny 2001; Shuman et al. 2001) from which the lake level has been inferred. Diatom and chironomids have been used to reconstruct the depth or the water level of lakes also (Luoto 2009; Shinneman et al. 2010; Wolin and Duthie 1999; Yang et al. 2003), which in some cases have been correlated with other sedimentological proxies indicative of lake level changes (Engels et al. 2012). Occasionally, the reconstructions using biological remains have been criticized because depth may represent a composite variable rather than a single environmental gradient (Juggins 2013). In this study, a novel approach is used that is based on the strong

relation between the cyst:diatom ratio and the lake depth found in the training-set of the Pyrenean mountain lakes. Beyond the statistical association, the interpretation of the index makes sense as chrysophyceae lives predominantly in the planktonic environment, whereas diatoms main contribution is benthic. In lake types in which water transparency varies substantially between water bodies, the connection between the ratio and depth would vanish, but the Pyrenean mountain lakes are all of them in a range of high water transparency. Therefore the cyst-depth index can be used as a surrogate of the relative changes in the water column depth.

The analysis of the diatom sequence shows that the main climatic events and periods recorded in the Greenland record GICC05 (Svensson et al. 2008) are also identified in the SSWT reconstructed for Burg Lake (Figure 20.1). There was only a major discrepancy for the period 15400-14200 yr cal BP respect the GICC05 and other records from the Northern Hemisphere (e.g. Frigola et al. 2008; Lotter et al. 2012; Lowe et al. 2008) and some other discrepancies in the details of the climatic patterns during the Younger Dryas respect to Greenland. Following, the climatic interpretation of the Burg Lake record is considered in more detail using the main Greenland periods as guidelines (Lowe et al. 2008).

The Greenland Stadial termination (GS-2a, ~16500-14700 yr cal BP)

The age of the bottom of the Burg lake sedimentary record indicated that the last glacial regression in the catchment could have happened ~20000 yr cal BP. However, the countable record of diatoms suggests stable lake conditions from 16590 yr cal BP. Temperature and water level showed a high variability during the first centuries with excursions from the lowest to relatively high values. The average diatom-SSWT value recorded (~15 ºC) until 15400 yr cal BP was in the lowest range for the lake. Lower reconstructed air temperatures were found in lake Ech (northern slope of the Pyrenean range, 710 m.s.a.l.), which were around 12 ºC for the same period (Millet et al. 2012), and in the La Roya lake (1608 m.a.s.l., Northwest Iberian Peninsula) July air temperatures ranged between 7.9 and 9.5ºC from 15550 to 15000 yr cal BP (Muñoz Sobrino et al. 2013). However, the Burg SSWT agrees with values of water-reconstructed temperature for lake Jeserzersee (Austria, 593 m.a.s.l.) using a diatom record (Schmidt et al. 2012). During this relatively cold period there was a warming

episode (~16200 yr cal BP), which is not coherent with the variability of other proxies of Burg Lake during the GS-2a.

At ~15400 yr cal BP, diatom-SSWT increased suddenly up to 17.6 ºC, and coincided with a rise in the water level, LOI and the abundance of indicators of macrophyte presence as well as a significant change in the diatom assemblage (starting CONISS zone 2). These evidences suggest a tipping point in the lake ecosystem, related with warmer summers and a reduction of the cool winter season and a positive water balance in the catchment, or at least a high melting of remaining glaciers. After the first warming, diatom-SSWT maintained values above 16.5 ºC until 15000 yr cal BP, and the lake water column depth kept high values. This warming period is not recorded in Greenland and regional records, which show a warming later in time. However, reconstructions of surface sea temperature from the Iberian margin show a heating from ~15400 yr cal BP (Rodrigues et al. 2010) and Western Mediterranean Sea records confirm that this heating started from ~16000-15100 yr cal BP (Cacho et al. 2001; Frigola et al. 2008). Burg SSWT shows a sudden cooling at 148000, which drop water temperature below 15^{o}C by 14500 BP. The chronology and characteristics of this warm phase at the end of GS-2a require further investigation and evidences, before more conclusive assessments can be made.

GS-2a termination and Greenland interstadial (GI-1, 14700- 12700 yr cal BP)

The GI-1 diatom-SSWT follows the general trend of Greenland records (Figure 20.1). However, the chronology of the transition from GS-2a to GI-1 differs slightly. This may be related with the warm period above discussed between 15400-14800 yr cal BP that the Burg SSWT shows, followed by the reduction in temperature from 14600 to 14350 yr cal BP. Thus, GI-1 warming started apparently some centuries later than in other records. The Burg Lake showed a progressive reduction in water level during GS-2a termination. After this, there was a rapid increase in temperature (~14350) which might correspond with the end of GS-2a recorded at 14600 yr cal BP in Greenland. The start of GI-1 in Europe is relatively variable depending on the record and its geographical position. An increase in temperature is recorded at 14900 yr cal BP in the lake Ech (Northwest Pyrenees, Millet et al. 2012) and in lake La Roya (Northwest Iberian Peninsula, Muñoz Sobrino et al. 2013) while pollen record of El Portalet lake (south-western Pyrenees) shows that steppe taxa started to decrease from

14700 yr cal BP (González-Sampériz et al. 2006). Likewise, the record of Gerzensee (Alps, 603 m.a.s.l., Lotter et al. 1992) and Brazi lake (Carpathians, 1740 m.a.s.l., Tóth et al. 2012) showed that the GI-1 start at ~14700-14600 yr cal BP. Pollen studies underway for Burg Lake might provide some additional light to the validity of Burg Lake chronology and development of the GS-2a to GI-1 transition.

At ~14300 yr cal BP, the high values of diatom-SSWT and high physical erosion correspond with conditions described in different proxies for the "Mystery Interval", when Northern Europe records show cold winters (Renssen and Isarin 2001) whereas mountain glaciers underwent major recessions (Williams et al. 2012). This situation could have been related to extensive sea-ice cover in the North Atlantic due to cold winters and the reduction in the temperature of mountain glacier caused by warm summers (Denton et al. 2006). Both conditions correspond with the sedimentary records of the Burg Lake and suggest an scenario with high insolation provoking warm summers and a progressive deglaciation, the latter also detected in other records of the Northern Hemisphere. The winters evolved towards mild conditions quickly, as indicated by the short ice-covered periods in the Burg Lake (Figure 17.2) in agreement with other reconstructions of the Bølling-Allerød period (Williams et al. 2012). Indicators of catchment evolution showed an increase on land covered by vegetation from 14900 to 12800 yr cal BP, in agreement with milder winters and warmer summers. This pattern agrees with other records of the Pyrenees (Millet et al. 2012).

Despite the reconstructed SSWT follows the general climatic patterns of GI-1, the warmest periods (GI-1e, GI-1c, GI-1a) were more similar between them in Burg than the ones recorded in Greenland. The differences may be attributed to real climatic regional difference or to the specificity of the diatom for reconstructing spring and summer temperature. Thus, for example, in a reconstruction of GI in Gerzensee, there were differences between chironomid and pollen air temperature reconstructions, which have been attributed to the response to different climatic constraints. Pollen would respond to the mean annual temperature whereas chironomids could be more influenced by the July temperature and the insolation (Lotter et al. 2012). This seems quite an *ad hoc* explanation and reality may involve more complex causes including technical issues.

Some cold events during GI-1 (~14100 and ~13200 yr cal BP) were detected also detected in the Burg record. Event at ~14100 yr cal BP was a short event

(<200 yr) characterized by an extremely low lake level and SSWT 1.5 ºC below GI-1e usual Burg Lake values. Different proxies indicate that the lake went through periods of drought and that the catchment suffered a regression in the vegetation cover. This event correspond with the GI-1d (Lowe et al. 2008), which have been detected in many different Northern Hemisphere sites of Europe, such as in the Jura Mountains (Peyron et al. 2005), the Alps (Lotter et al. 2012), the northern (Millet et al. 2012) and southern slopes of the Pyrenees (González-Sampériz et al. 2006). The cold event at ~13200 yr cal BP showed a drop in SSWT from 17.3 to 16.1 ºC and the water level suggests that it was not as dry as GI-1d in Greenland. This event corresponds to GI-1b (Lowe et al. 2008) and is equivalent to the Gerzensee oscillation (Lotter et al. 2012). After this short, cold and relatively wet period, the lake level rose suddenly reaching a water level similar to the end of GS-2a. Temperature followed the same increasing trend, until reaching 17.4 ºC at 12800 yr cal BP.

GS-1, The Younger Dryas (YD, ~12850-11650 yr cal BP)

The YD started with a rapid reduction in diatom-SSWT, declining from 17.4 to 15.4ºC, that is, 2 ºC in one century. After this, SSWT continued decreasing until 14.7 ºC at 12370 yr cal BP. This abrupt change in temperature coincides with an increase of catchment erosion (K/Ti, Al/Ti, Figure 16.2) and a reduction in the vegetation cover. This reduction is more abrupt than the one recorded in other records from the Iberian Peninsula and the Pyrenees. Thus, for example, a pollen record for lake Banyoles (Eastern Iberian Peninsula, 172 m.s.a.l.) showed a small increase in steppe taxa (Pèrez-Obiol and Julià 1994) and a chironomid record of Ech lake (northern slope of Pyrenees) showed a small reduction in air temperature (Millet et al. 2012). The apparent diffuse signal in some of the records of the Iberian Peninsula and the Pyrenees contrasts with records at higher latitudes and Central Europe (Birks et al. 2012; Lotter et al. 2000; Mortensen et al. 2011; Samartin et al. 2012) and the Northern Iberian record of Pindal Cave (Moreno et al. 2010) and La Roya lake (Muñoz Sobrino et al. 2013), where a rapid change was evident. Regional geographical differences, the temporal resolution, and the different sensitivity of proxies may cause the diffuse signal. But likely the geographical location of Iberian Peninsula is more relevant as its climate is highly affected by the latitudinal displacement of the North Atlantic Anticyclone, and therefore the signal recorded could include the noise caused by periods with extreme climatic variability.

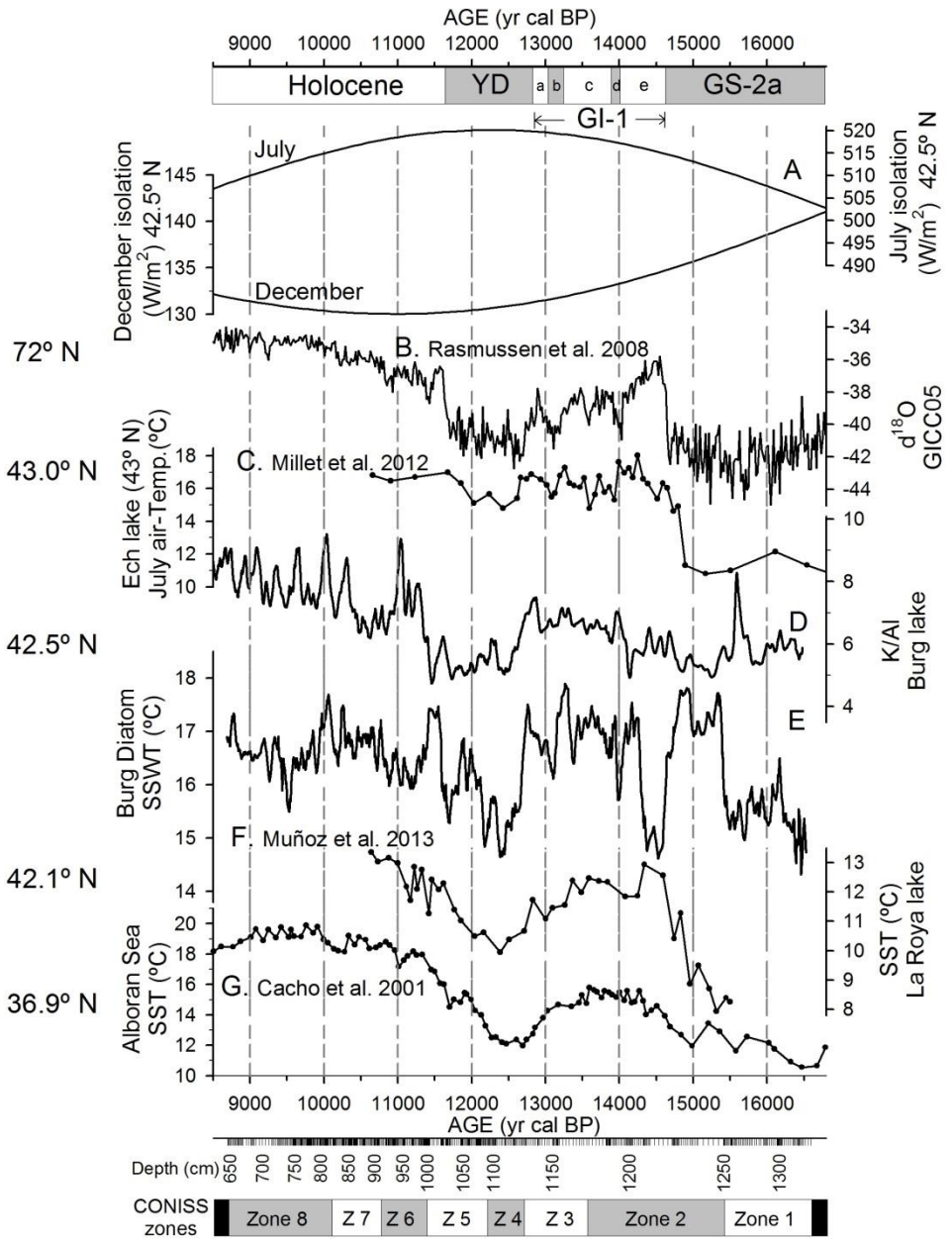

Figure 20.1 Comparison of the Burg Lake diatom-reconstructed summer surface water temperature (diatom-SSWT) with other proxies: A) insolation during July and December at 42.5º N estimated according to Laskar et al. (2004); B) NGRIP $\delta^{18}O$ Greenland Ice Core Chronology 2005 (GICC05, Rasmussen et al. 2008); C) July air-temperature inferred for Lake Ech (Northwestern Pyrenees, Millet et al. 2012); D) Burg Lake K/Al ratio. E) Burg Lake diatom-SSWT; F) July air-temperature inferred for Lake La Roya using chironomids (Muñoz Sobrino et al. 2013); G) Alboran sea surface temperature (SST, Cacho et al. 2001).

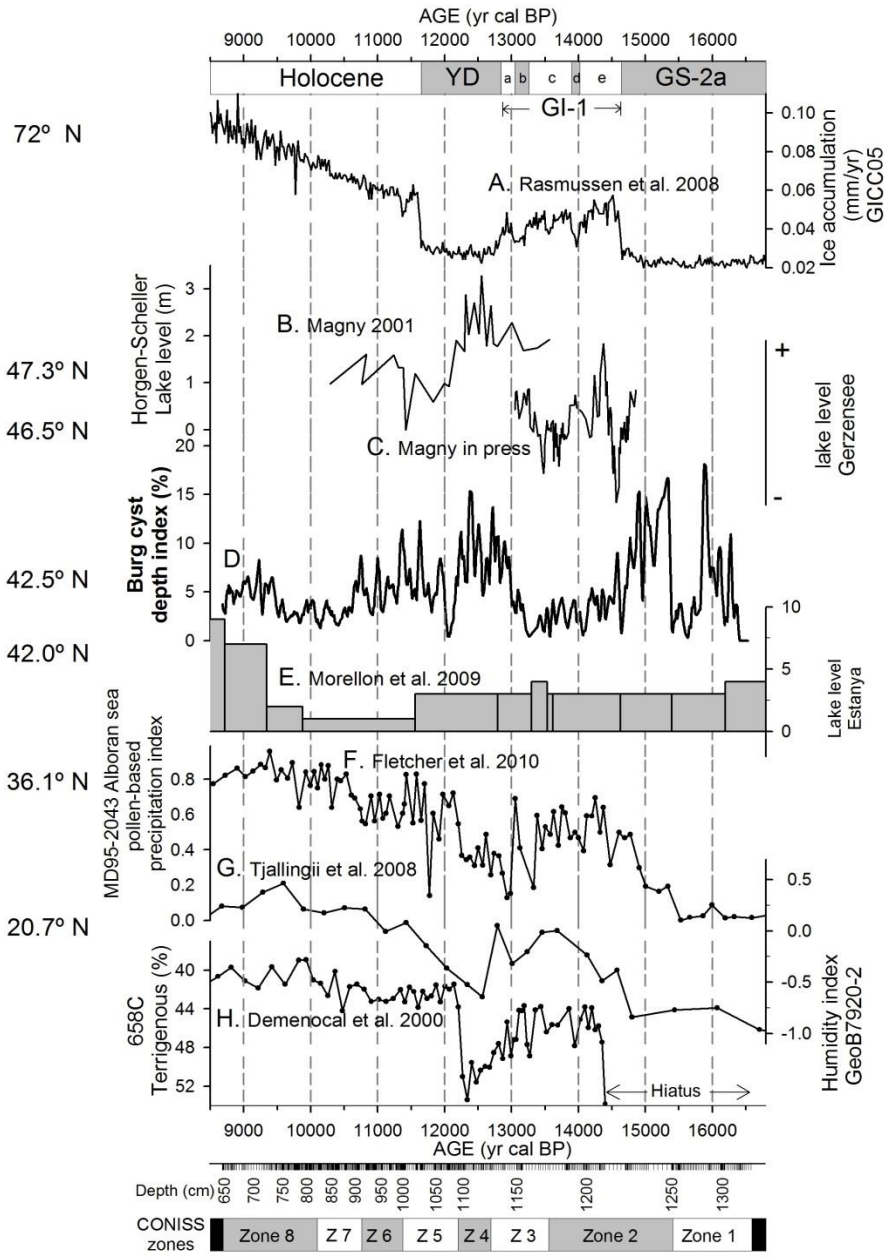

Figure 20.2. Comparison of records related with moisture in the Northern Hemisphere. A) Ice accumulation NGRIP-based Greenland Ice Core Chronology 2005 (GICC05, Rasmussen et al. 2008). B) Horgen-Schellen lake level (Magny 2001). C) Gerzensee lake level (Magny in press). D) Depth index of Burg lake. E) Lake Estanya level (Morellón et al. 2009). F) Pollen-based precipitation index of core MD95-2043 of the Alboran Sea (Fletcher et al. 2010). G) Humidity index of African margin core GeoB7920-2 (Tjallingii et al. 2008). H) Percentage of terrigenous material in the Western African Sea margin –site 658C (Demenocal et al. 2000).

The diatom-SSWT in Burg Lake showed two differentiated parts in the YD than contrasts with a more homogenous Greenland record. Indicators of catchment erosion, vegetation cover and LOI indicated that the cold conditions of YD in Burg Lake clearly extended until 11700 yr cal BP as in Greenland, but the whole period differentiated into a colder oscillation (centred around 12300 yr cal BP) and a warmer phase (centred around 12000 yr cal BP). The latter phase may refer exclusively to warm conditions during summers as in its shown mainly by SSTW and less by other proxies. This diatom-SSTW pattern in Burg Lake is closer to patterns in the Atlantic and Western Mediterranean Seas and the Iberian Peninsula than to Central European and Greenland palaeoclimatic patterns (Cacho et al. 2001; Clark et al. 2012; Muñoz Sobrino et al. 2013; Rodrigues et al. 2010). The end of YD was marked by a reduction in SSWT (15.4 ºC) followed by a rapid increase (17.2 ºC).

The depth index indicated that there was a positive water balance during the end of GI-1 and during the coldest phase of YD showing some short episodes of low lake level (e.g. 12700, 12350 yr cal BP. Figure 20.2). Around 12100 yr cal BP, Burg underwent a dramatic dry period. After this, the water level showed a high variability but tending to low values. This result is apparently contradictory with the Greenland records that indicate cold and dry conditions during the whole YD (Clark et al. 2012). However, some records from different sites of Central Europe do not show a change in the water balance when YD started but, instead, they indicate an increase in lake level from 12700 to ~12100 yr cal BP (Magny 2001; Magny et al. 2001; von Grafenstein et al. 2000). Records from the South-Western Mediterranean (Alboran Sea, Fletcher et al. 2010) suggest a moisture pattern during YD more similar to the Burg Lake SSWT than to the water level reconstructed. However, the positive water balance from the end of GI-1 to the initial part of YD is coherent with some of the hypothesis regarding the causes of the Stadial (Broecker et al. 2010; Carlson and Clark 2012). High wet condition in the Northern Hemisphere could cause an increase of freshwater input to the Atlantic and could be related with the weakening of the Meridional Overturning Circulation.

On the other hand, wet conditions during the first part of YD are opposed to the trend recorded in North-western African records (Figure 20.2). This could be related with a similar mechanism that explains the latitudinal gradient in wet conditions for Preboreal Oscillation, as is described by Magny et al. (2007) for lakes above 43º N. Thus, a southward displacement of the Atlantic Westerly Jet could produce wet condition in the middle latitudes of the North Hemisphere

while in the Arctic region and subtropical area there were dry conditions. From 12200 yr cal BP there was a rapid change suggesting a northward displacement of cyclonic activity.

The Early Holocene (EH, 11650-8700 yr cal BP)

The Holocene started with a sudden increase in the diatom-SSWT (17-17.3 ºC) that extended until 11400 yr cal BP. After this, diatom-SSWT dropped rapidly to 16 ºC (~11150 yr cal BP) maintaining low values until 10950 yr cal BP. Thereafter, SSWT oscillated throughout the period around 16.7 ºC, with a warm oscillation at ~10000 yr cal BP and a cold one at ~9500 yr cal BP of ~1 ºC, respectively. At the beginning of the Holocene, the depth of the lake was relatively high, but then it becomes highly variable and underwent a progressive reduction. After, 8700 yr cal BP peat accumulated and the lake become a wetland with an extremely poor diatom register that has not been possible to analyse.

The cold event at 11400 yr cal BP corresponds in age and pattern with the Preboreal Oscillation (PO, Björck et al. 1997). Despite the temperature reduction was not as strong as YD, the reconstructed values suggest that during PO the summer temperature could have been similar to the coldest events of GI-1 (GI-1b, GI-1d, Figure 20.1). The relatively high water level during PO indicates a positive water balance and corresponds with the hypothesis of the increase of cyclonic activity at mid-latitudes as a consequence of southward displacement of the Atlantic Westerly Jet (Magny et al. 2007). Therefore, the Pyrenees and probably the Northern part of the Iberian Peninsula may have experienced wet conditions during the PO. After this event, the lake shows a reduction in water level and a progressive increase in diatom-SSWT until 10000 yr cal BP, when it again started to drop. Dry conditions recorded during this period correspond with another record of the same latitude (Magny et al. 2013).

Conclusions

21. Conclusions

- **The Pyrenean lakes contain remarkable diatom diversity**. There is a high proportion of the diatom taxa that has not been properly described yet.

- **Many diatom species has indicative value for chemical, nutrient, physical and habitat classifications of the Pyrenean lakes.** The strength of this indicator character is that species are statistically significant for a reduced number (usually one) of the lake classification across the different environmental gradients.

- **Diatom assemblages from top sediments contain more information for environmental reconstruction than epilithic assemblages.** This is due to the taphonomic character of the lake bottom assemblages that incorporate diatoms from different lake habitats and microenvironments, whereas epilithic diatom assemblages respond to general epilimnetic features (e.g., water chemistry) filtered by the constraints of their specific habitat.

- **Using sediment diatom sequences, pH, acid-neutralising capacity, total phosphorous, irradiance at the lake-bottom, and summer surface water temperature can be reconstructed quantitatively in the Pyrenean lakes.** The reliability of independent reconstructions of these variables is based in the fact that a sufficient quantity of species (but much less than the total present) responds to each variable and the others contribute neutrally (i.e. pH-ANC).

- **The ratio between total numbers of chrysophycean stomatocysts and diatoms is an indicator of the water column depth in the Pyrenean lakes.** This allows for the reconstruction of lake level fluctuations in the past for lakes of similar characteristics.

- **Diatom-based reconstructions allow inferring fluctuations on chemical and physical water variables during Late Glacial and Early Holocene that are hardly recorded by any other proxy.** As

these variables are currently measured in biogeochemical and limnological studies, the reconstructed time series can be analysed at the light of current limnological paradigms.

- **The lake ontogenic changes over long periods of time may modify the response to similar climatic forcing (as shown for Burg Lake).** This is particularly pertinent to primary productivity and organic matter flux, which in shallower systems may become enhanced by shorter transport (recycling) distances.

- **In relatively shallow mountain lakes (such as Burg Lake), the entire lake basin becomes a productive biofilm making benthic signals predominant in the sedimentary sequence.** Only at early stages, when there is high external nutrient loading, the planktonic production is more relevant for the whole system.

- **The main climatic oscillations in the Northern Hemisphere recorded in the Greenland ice records during Late Glacial and Early Holocene are also reflected in Burg Lake sedimentary sequence through the diatom-based reconstruction of the summer surface water temperature, the indicator species analysis and the cyst-depth index.** Changes in temperature and diatom compositions recorded through the sedimentary sequence coincide with events such as Greenland interstadial 1 (GI-1, 14700- 12700 yr cal BP), GI-1d (~14100 yr cal BP), Younger Dryas (12800-11700 yr cal BP), and the Preboreal Oscillation (~11400 yr cal BP).

- **The temporal trend of summer surface water temperature in Burg Lake and lake depth oscillations were not coupled throughout the Late Glacial and Early Holocene.** This was probably due to the seepage character of the lake and changing contribution to the water budget of glaciers and snowfields during this period.

- **The Greenland interstadial (14700- 12700 yr cal BP) in the Pyrenees was characterised by warm summers and short winters.** A reduction in the influence of Northern colder air masses and the progressive weakening of winters caused warmer conditions than in the Early Holocene.

- **Two climatic phases were identified during the Younger Dryas (12700-11650 yr cal BP) in the Pyrenees based on the summer surface water temperature and the water column depth reconstructed at Burg Lake: a first period with cold conditions and high water level, followed by a second period gradually warmer and drier.**

References

References

Aboal M, Witkowski A, Cobelas MA, Cambra J and Ector L 2003. Diatoms Monographs: Floristic list of the non marine diatoms (bacillariophyceae) of Iberian Peninsula, Balearic Islands and Canary Islands: updated taxonomy and bibliographic. G (A.R.G. Gantner Verlag K.G.).

Agusti-Panareda A, Thompson R and Livingstone DM 2000. Reconstructing temperature variations at high elevation lake sites in Europe during the instrumental period. In: W. D. Williams (ed.), International Association of Theoretical and Applied Limnology, Vol 27, Pt 1, Proceedings, pp. 479-483.

Alley RB 2000. The Younger Dryas cold interval as viewed from central Greenland. Quaternary Science Reviews 19: 213-226.

Anderson NJ 2000. Miniview: Diatoms, temperature and climatic change. European Journal of Phycology 35: 307-314.

Anderson NJ, Brodersen KP, Ryves DB, McGowan S, Johansson LS, Jeppesen E and Leng MJ 2008. Climate versus in-lake processes as controls on the development of community structure in a low-arctic lake (South-West Greenland). Ecosystems 11: 307-324.

Andrews JT, Jennings AE, Kerwin M, Kirby M, Manley W, Miller GH, Bond G and MacLean B 1995. A Heinrich-like event, H-0 (DC-0): Source(s) for detrital carbonate in the North Atlantic during the Younger Dryas Chronozone. Paleoceanography 10: 943-952.

Arnett H, Saros J and Alisa Mast M 2012. A caveat regarding diatom-inferred nitrogen concentrations in oligotrophic lakes. Journal of Paleolimnology 47: 277-291.

Bahr A, Arz HW, Lamy F and Wefer G 2006. Late glacial to Holocene paleoenvironmental evolution of the Black Sea, reconstructed with stable oxygen isotope records obtained on ostracod shells. Earth and Planetary Science Letters 241: 863-875.

Barker P 1992. Differential diatom dissolution in Late Quaternary sediments from Lake Manyara, Tanzania: an experimental approach. Journal of Paleolimnology 7: 235-251.

Barker P, Fontes JC, Gasse F and Druart JC 1994. Experimental dissolution of diatom silica in concentrated salt solutions and implications for paleoenvironmental reconstruction. Limnology and Oceanography 39: 99-110.

Battarbee R, Charles D, Dixit SS and Renberg I 2004. Diatoms as indicators of surface water acidity. In: E. Stoermer and J. P. Smol (eds.), The Diatoms. Applications for the Environmental and Earth Sciences. Cambridge University Press, pp. 85-127.

Battarbee RW 2000. Palaeolimnological approaches to climate change, with special regard to the biological record. Quaternary Science Reviews 19: 107-124.

Battarbee RW and Charles DF 1986. Diatom-based pH reconstruction studies of acid lakes in Europe and North America: A synthesis. Water, Air, and Soil Pollution 30: 347-354.

Battarbee RW, Jones V, Flower R, Cameron N and Bennion H 2001. Diatoms. In: W. M. Last, J. P. Smol and H. J. Birks (eds.), Tracking Environmental Change Using Lake Sediments: Volume 3: Terrestrial, Algal, and Siliceous Indicators. Springer, pp. 155-202.

Bennion H, Juggins S and Anderson NJ 1996a. Predicting epilimnetic phosphorus concentrations using an improved diatom- based transfer function and its application to lake eutrophication management. Environmental Science and Technology 30: 2004-2007.

Bennion H, Juggins S and Anderson NJ 1996b. Predicting epilimnetic phosphorus concentrations using an improved diatom-based transfer function and its application to lake eutrophication management. Environmental Science & Technology 30: 2004-2007.

Bergström AK, Jonsson A and Jansson M 2008. Phytoplankton responses to nitrogen and phosphorus enrichment in unproductive Swedish lakes along a gradient of atmospheric nitrogen deposition. Aquatic Biology 4: 55-64.

Birks HH and Birks HJB 2006. Multi-proxy studies in palaeolimnology. Vegetation History and Archaeobotany 15: 235-251.

Birks HH, Jones VJ, Brooks SJ, Birks HJB, Telford RJ, Juggins S and Peglar SM 2012. From cold to cool in northernmost Norway: Lateglacial and early Holocene multi-proxy environmental and climate reconstructions from Jansvatnet, Hammerfest. Quaternary Science Reviews 33: 100-120.

Birks HJ 2012. Analysis of stratigraphical data. In: H. J. B. Birks, A. F. Lotter, S. Juggins and J. P. Smol (eds.), Tracking Environmental Change Using Lake Sediments. Springer Netherlands pp. 355-378.

Birks HJ and Simpson G 2013. 'Diatoms and pH reconstruction' (1990) revisited. Journal of Paleolimnology 49: 363-371.

Birks HJB 1994. The importance of pollen and diatom taxonomic precision in quantitative palaeoenvironmental reconstructions. Review of Palaeobotany and Palynology 83: 107-117.

Birks HJB 1998. D.G. Frey and E.S. Deevey review 1: Numerical tools in palaeolimnology - Progress, potentialities, and problems. Journal of Paleolimnology 20: 307-332.

Birks HJB, Heiri O, Seppä H and Bjune AE 2010. Strengths and weaknesses of quantitative climate reconstructions based on late-quaternary biological proxies. Open Ecology Journal 3: 68-110.

Birks HJB, Line JM, Juggins S, Stevenson AC and Ter Braak CJF 1990. Diatoms and pH reconstruction. Philosophical Transactions - Royal Society of London, B 327: 263-278.

Björck S, Rundgren M, Ingólfsson Ó and Funder S 1997. The Preboreal oscillation around the Nordic Seas: terrestrial and lacustrine responses. Journal of Quaternary Science 12: 455-465.

Björck S, Walker MJC, Cwynar LC, Johnsen S, Knudsen K-L, Lowe JJ and Wohlfarth B 1998. An event stratigraphy for the Last Termination in the North Atlantic region based on the Greenland ice-core record: a proposal by the INTIMATE group. Journal of Quaternary Science 13: 283-292.

Blaauw M and Christeny JA 2011. Flexible paleoclimate age-depth models using an autoregressive gamma process. Bayesian Analysis 6: 457-474.

Blaauw M, Holliday VT, Gill JL and Nicoll K 2012. Age models and the Younger Dryas Impact Hypothesis. Proceedings of the National Academy of Sciences of the United States of America 109.

Bohncke SJP and Hoek WZ 2007. Multiple oscillations during the Preboreal as recorded in a calcareous gyttja, Kingbeekdal, The Netherlands. Quaternary Science Reviews 26: 1965-1974.

Borcard D, Gillet F and Legendre P 2011. Numerical Ecology with R. Springer.

Borchardt MA 1996. Nutrients. In: R. J. Stevenson, L. B. Max and L. L. Rex (eds.), Algal Ecology. Academic Press, San Diego, pp. 183-227.

Bos JAA, Bohncke SP and Janssen CR 2006. Lake-Level Fluctuations and Small-Scale Vegetation Patterns During the Late Glacial in The Netherlands. Journal of Paleolimnology 35: 211-238.

Bos JAA, van Geel B, van der Plicht J and Bohncke SJP 2007. Preboreal climate oscillations in Europe: Wiggle-match dating and synthesis of Dutch high-resolution multi-proxy records. Quaternary Science Reviews 26: 1927-1950.

Brauer VS, Stomp M and Huisman J 2012. The nutrient-load hypothesis: Patterns of resource limitation and community structure driven by competition for nutrients and light. American Naturalist 179: 721-740.

Broecker WS, Denton GH, Edwards RL, Cheng H, Alley RB and Putnam AE 2010. Putting the Younger Dryas cold event into context. Quaternary Science Reviews 29: 1078-1081.

Broecker WS, Kennett JP, Flower BP, Teller JT, Trumbore S, Bonani G and Wolfli W 1989. Routing of meltwater from the Laurentide Ice Sheet during the Younger Dryas cold episode. Nature 341: 318-321.

Brzezinski MA 1985. The Si:C:N ratio of marine diatoms: Interspecific variability and the effect of some environmental variables. Journal of Phycology 21: 347-357.

Buczkó K, Magyari E, Hübener T, Braun M, Bálint M, Tóth M and Lotter A 2012. Responses of diatoms to the Younger Dryas climatic reversal in a South Carpathian mountain lake (Romania). Journal of Paleolimnology 48: 417-431.

Buchaca T and Catalan J 2008. On the contribution of phytoplankton and benthic biofilms to the sediment record of marker pigments in high mountain lakes. Journal of Paleolimnology 40: 369-383.

Bukhtiyarova L and Round FE 1996. Revision of the genus Achnanthes sensu lato. Psammothidium, a new genus based on A. marginulatum. Diatom Research 11: 1-30.

Burkholder JM 1996a. Interactions of benthic algae with their substrata. Algal Ecology: Freshwater Benthic Ecosystems, pp. 253-297.

Burkholder JM 1996b. Interactions of Benthic Algae with Their Substrata. In: R. J. Stevenson, L. B. Max and L. L. Rex (eds.), Algal Ecology. Academic Press, San Diego, pp. 253-297.

Cacho I, Grimalt JO, Canals M, Sbaffi L, Shackleton NJ, Schönfeld J and Zahn R 2001. Variability of the Western Mediterranean sea surface temperature during the last 25,000 years and its connection with the Northern Hemisphere climatic changes. Paleoceanography 16: 40-52.

Camarero L and Catalan J 2012. Atmospheric phosphorus deposition may cause lakes to revert from phosphorus limitation back to nitrogen limitation. Nat Commun 3: 1118.

Camarero L, Rogora M, Mosello R, Anderson NJ, Barbieri A, Botev I, Kernan M, Kopáček J, Korhola A, Lotter AF, Muri G, Postolache C, StuchlÍk E, Thies H and Wright RF 2009. Regionalisation of chemical variability in European mountain lakes. Freshwater Biology 54: 2452-2469.

Cameron NG, Birks HJB, Jones VJ, Berge F, Catalan J, Flower RJ, Garcia J, Kawecka B, Koinig KA, Marchetto A, Sánchez-Castillo P, Schmidt R, Šiško M, Solovieva N, Štefková E and Toro M 1999. Surface-sediment and epilithic diatom pH calibration sets for remote European mountain lakes (AL:PE project) and their comparison with the Surface Waters Acidification Programme (SWAP) calibration set. Journal of Paleolimnology 22: 291-317.

Cantonati M and Lange-Bertalot H 2011. Diatom monitors of close-to-pristine, very-low alkalinity habitats: Three new eunotia species from springs in nature parks of the south-eastern alps. Journal of Limnology 70: 209-221.

Cantonati M, Scola S, Angeli N, Guella G and Frassanito R 2009. Environmental controls of epilithic diatom depth-distribution in an oligotrophic lake characterized by marked water-level fluctuations. European Journal of Phycology 44: 15-29.

Carlson AE and Clark PU 2012. Ice sheet sources of sea level rise and freshwater discharge during the last deglaciation. Reviews of Geophysics 50: RG4007.

Carrick HJ and Lowe RL 2007. Nutrient limitation of benthic algae in Lake Michigan: The role of silica. Journal of Phycology 43: 228-234.

Carter JR 1970. Diatoms from Andorra. Nova Hedwigia Beihefte 31: pp. 605-633.

Catalan J 1988. Physical Properties of the Environment Relevant to the Pelagic Ecosystem of a Deep High-Mountain Lake (Estany Redo, Central Pyrenees). Oecologia aquatica 9: 89-123.

Catalan J 2008. The ecology of environmental changes: a palaeolimnological perspective. In: F. Valladers, A. Camacho, A. Elosegui, C. Gracia, M. Estrada, J. Senar and J. M. Gili (eds.), Unity in diversity: reflections on ecology after the legacy of Ramon Margalef. Fundación BBVA, pp. 95-118.

Catalan J, Ballesteros E, Gacia E, Palau A and Camarero L 1993. Chemical composition of disturbed and undisturbed high-mountain lakes in the Pyrenees - a reference for acidified sites. Water Research 27: 133-141.

Catalan J, Barbieri MG, Bartumeus F, BituŠÍk P, Botev I, Brancelj A, Cogalniceanu D, Manca M, Marchetto A, Ognjanova-Rumenova N, Pla S, Rieradevall M, Sorvari S, ŠtefkovÁ E, StuchlÍk E and Ventura M 2009a. Ecological thresholds in European alpine lakes. Freshwater Biology 54: 2494-2517.

Catalan J, Curtis CJ and Kernan M 2009b. Remote European mountain lake ecosystems: Regionalisation and ecological status. Freshwater Biology 54: 2419-2432.

Catalan J, Pla S, Garcia J and Camarero L 2009c. Climate and CO2 saturation in an alpine lake throughout the Holocene. Limnology and Oceanography 54: 2542-2552.

Clark PU, Shakun JD, Baker PA, Bartlein PJ, Brewer S, Brook E, Carlson AE, Cheng H, Kaufman DS, Liu Z, Marchitto TM, Mix AC, Morrill C, Otto-Bliesner BL, Pahnke K, Russell JM, Whitlock C, Adkins JF, Blois JL, Clark J, Colman SM, Curry WB, Flower BP, He F, Johnson TC, Lynch-Stieglitz J, Markgraf V, McManus J, Mitrovica JX, Moreno PI and Williams JW 2012. Global climate evolution during the last deglaciation. Proceedings of the National Academy of Sciences 109: E1134-E1142.

Clarke G, Kernan M, Marchetto A, Sorvari S and Catalan J 2005. Using diatoms to assess geographical patterns of change in high-altitude European lakes from pre-industrial times to the present day. Aquatic Sciences 67: 224-236.

Colwell RK and Coddington JA 1995. Estimating terrestrial biodiversity through extrapolation. In: D. L. Hawksworth (ed.), Biodiversity: measurement and estimation. Chapman & Hall, for Royal Society, pp. 101-118.

Cremer H, Bunnik FM, Kirilova E, Lammens ERR and Lotter A 2009. Diatom-inferred trophic history of IJsselmeer (The Netherlands). Hydrobiologia 631: 279-287.

Cremer H, Gore D, Hultzsch N, Melles M and Wagner B 2004. The diatom flora and limnology of lakes in the Amery Oasis, East Antarctica. Polar Biol 27: 513-531.

Cronin TM, Rayburn JA, Guilbault JP, Thunell R and Franzi DA 2012. Stable isotope evidence for glacial lake drainage through the St. Lawrence Estuary, eastern Canada, ~13.1–12.9 ka. Quaternary International 260: 55-65.

Cumming BF, Wilson SE and Smol JP 1993. Paleolimnological potential of chrysophyte cysts and scales and of sponge spicules as indicators of lake salinity. International Journal of Salt Lake Research 2: 87-92.

Curtis CJ, Juggins S, Clarke G, Battarbee RW, Kernan M, Catalan J, Thompson R and Posch M 2009. Regional influence of acid deposition and climate change in European mountain lakes assessed using diatom transfer functions. Freshwater Biology 54: 2555-2572.

Charles D, Whitehead D, Anderson D, Bienert R, Camburn K, Cook R, Crisman T, Davis R, Ford J, Fry B, Hites R, Kahl J, Kingston J, Kreis R, Jr., Mitchell M, Norton S, Roll L, Smol J, Sweets PR, Uutala A, White J, Whiting M and Wise R 1986. The PIRLA project (paleoecological investigation of recent lake acidification): Preliminary results for the Adirondacks, New England, N. Great Lakes states, and N. Florida. Water, Air, and Soil Pollution 30: 355-365.

Chen G, Dalton C, Leira M and Taylor D 2008. Diatom-based total phosphorus (TP) and pH transfer functions for the Irish Ecoregion. Journal of Paleolimnology 40: 143-163.

Christen AJ and Pérez EP 2009. A new robust statistical model for radiocarbon data. Radiocarbon 51: 1047-1059.

Chung F 1974. Quantitative interpretation of X-ray diffraction patterns of mixtures: II. Adiabatic principles of X-ray diffraction analysis of mixtures. Journal of Applied Crystallography 7: 526–531.

David F 2001. Le tardiglaciaire des Ételles (Alpes françaises du Nord) : instabilité climatique et dynamique de végétation. Comptes Rendus de l'Académie des Sciences - Series III - Sciences de la Vie 324: 373-380.

Davidson TA and Jeppesen E 2013. The role of palaeolimnology in assessing eutrophication and its impact on lakes. Journal of Paleolimnology 49: 391-410.

Davis BAS, Brewer S, Stevenson AC and Guiot J 2003. The temperature of Europe during the Holocene reconstructed from pollen data. Quaternary Science Reviews 22: 1701-1716.

de Baar HJW 1994. von Liebig's law of the minimum and plankton ecology (1899–1991). Progress in Oceanography 33: 347-386.

De Cáceres M and Legendre P 2009. Associations between species and groups of sites: Indices and statistical inference. Ecology 90: 3566-3574.

De Cáceres M, Legendre P and Moretti M 2010. Improving indicator species analysis by combining groups of sites. Oikos 119: 1674-1684.

de Vernal A, Hillaire-Marcel C, Turon JL and Matthiessen J 2000. Reconstruction of sea-surface temperature, salinity, and sea-ice cover in the northern North Atlantic during the last glacial maximum based on dinocyst assemblages. Canadian Journal of Earth Sciences 37: 725-750.

Demenocal P, Ortiz J, Guilderson T, Adkins J, Sarnthein M, Baker L and Yarusinsky M 2000. Abrupt onset and termination of the African Humid

Period: Rapid climate responses to gradual insolation forcing. Quaternary Science Reviews 19: 347-361.

DeNicola DM 1996. Periphyton Responses to Temperature at Different Ecological Levels. In: R. J. Stevenson, L. B. Max and L. L. Rex (eds.), Algal Ecology. Academic Press, San Diego, pp. 149-181.

DeNicola DM, De Eyto E, Wemaere A and Irvine K 2004. Using epilithic algal communities to assess trophic status in Irish lakes. Journal of Phycology 40: 481-495.

Denton GH, Alley RB, Comer GC and Broecker WS 2005. The role of seasonality in abrupt climate change. Quaternary Science Reviews 24: 1159-1182.

Denton GH, Anderson RF, Toggweiler JR, Edwards RL, Schaefer JM and Putnam AE 2010. The last glacial termination. Science 328: 1652-1656.

Denton GH, Broecker WS and Alley RB 2006. The mystery interval 17.5 to 14.5 kyrs ago. PAGES News 14: 14-16.

Dixit SS, Dixit AS and Evans RD 1988. Sedimentary diatom assemblages and their utility in computing diatom-inferred pH in Sudbury Ontario lakes. Hydrobiologia 169: 135-148.

Dong X, Bennion H, Maberly SC, Sayer CD, Simpson GL and Battarbee RW 2012. Nutrients exert a stronger control than climate on recent diatom communities in Esthwaite Water: evidence from monitoring and palaeolimnological records. Freshwater Biology 57: 2044-2056.

Dormoy I, Peyron O, Nebout NC, Goring S, Kotthoff U, Magny M and Pross J 2009. Terrestrial climate variability and seasonality changes in the Mediterranean region between 15000 and 4000 years BP deduced from marine pollen records. Climate of the Past 5: 615-632.

Douglas MSV and Smol JP 1995. Paleolimnological significance of observed distribution patterns of chrysophyte cysts in arctic pond environments. Journal of Paleolimnology 13: 79-83.

Dufrêne M and Legendre P 1997. Species assemblages and indicator species: The need for a flexible asymmetrical approach. Ecological Monographs 67: 345-366.

Duplessy JC, Labeyrie L, Juilletleclerc A, Maitre F, Duprat J and Sarnthein M 1991. Surface salinity reconstruction of the North-Atlantic ocean during the Last Glacial Maxium. Oceanologica Acta 14: 311-324.

Elser JJ, Andersen T, Baron JS, Bergström AK, Jansson M, Kyle M, Nydick KR, Steger L and Hessen DO 2009. Shifts in lake N: P stoichiometry and nutrient limitation driven by atmospheric nitrogen deposition. Science 326: 835-837.

Engels S, Cwynar L, Rees AH and Shuman B 2012. Chironomid-based water depth reconstructions: an independent evaluation of site-specific and local inference models. Journal of Paleolimnology 48: 693-709.

Fiedel SJ 2011. The mysterious onset of the Younger Dryas. Quaternary International 242: 262-266.

Finkelstein SA, Peros MC and Davis AM 2005. Late Holocene paleoenvironmental change in a Great Lakes coastal wetland: Integrating pollen and diatom datasets. Journal of Paleolimnology 33: 1-12.

Fletcher WJ, Goni MFS, Peyron O and Dormoy I 2010. Abrupt climate changes of the last deglaciation detected in a Western Mediterranean forest record. Climate of the Past 6: 245-264.

Flower RJ 1993. Diatom preservation: experiments and observations on dissolution and breakage in modern and fossil material. Hydrobiologia 269-270: 473-484.

Flower RJ and Ryves DB 2009. Diatom preservation: Differential preservation of sedimentary Diatoms in two saline lakes. Acta Botanica Croatica 68: 381-399.

Friedrich M, Kromer B, Kaiser KF, Spurk M, Hughen KA and Johnsen SJ 2001. High-resolution climate signals in the Bølling–Allerød Interstadial (Greenland Interstadial 1) as reflected in European tree-ring chronologies compared to marine varves and ice-core records. Quaternary Science Reviews 20: 1223-1232.

Frigola J, Moreno A, Cacho I, Canals M, Sierro FJ, Flores JA and Grimalt JO 2008. Evidence of abrupt changes in Western Mediterranean Deep Water circulation during the last 50 kyr: A high-resolution marine record from the Balearic Sea. Quaternary International 181: 88-104.

Fritz SC and Anderson NJ 2013. The relative influences of climate and catchment processes on Holocene lake development in glaciated regions. Journal of Paleolimnology 49: 349-362.

Fritz SC, Engstrom DR and Juggins S 2004. Patterns of early lake evolution in boreal landscapes: A comparison of stratigraphic inferences with a modern chronosequence in Glacier Bay, Alaska. Holocene 14: 828-840.

Gacia E, Ballesteros E, Camarero L, Delgado O, Palau A, Riera JL and Catalan J 1994. Macrophytes from lakes in the Eastern Pyrenees- community composition and ordination in relation to environmental factors. Freshwater Biology 32: 73-81.

Gasse F 2000. Hydrological changes in the African tropics since the Last Glacial Maximum. Quaternary Science Reviews 19: 189-211.

Gasse F 2002. Diatom-inferred salinity and carbonate oxygen isotopes in Holocene waterbodies of the western Sahara and Sahel (Africa). Quaternary Science Reviews 21: 737-767.

Gasse F, Juggins S and Khelifa LB 1995. Diatom-based transfer-functions for inferring past hydrochemical characteristics of African lakes. Paleogeogr. Paleoclimatol. Paleoecol. 117: 31-54.

Geitler L 1977. On the life history of the Epithemiaceae Epithemia, Rhopalodia and Denticula (Diatomophyceae) and their presumably symbiotic sphaeroid bodies. Plant Systematics and Evolution 128: 259-275.

González-Sampériz P, Valero-Garcés BL, Carrión JS, Peña-Monné JL, García-Ruiz JM and Martí-Bono C 2005. Glacial and Lateglacial vegetation in

northeastern Spain: New data and a review. Quaternary International 140–141: 4-20.

González-Sampériz P, Valero-Garcés BL, Moreno A, Jalut G, García-Ruiz JM, Martí-Bono C, Delgado-Huertas A, Navas A, Otto T and Dedoubat JJ 2006. Climate variability in the Spanish Pyrenees during the last 30,000 yr revealed by the El Portalet sequence. Quaternary Research 66: 38-52.

Grimm EC 1987. CONISS: a FORTRAN 77 program for stratigraphically constrained cluster analysis by the method of incremental sum of squares. Computers and Geosciences 13: 13-35.

Hadley KR, Douglas MSV, Lim D and Smol JP 2013. Diatom assemblages and limnological variables from 40 lakes and ponds on Bathurst Island and neighboring high Arctic islands. International Review of Hydrobiology 98: 44-59.

Håkansson H 2002. A compilation and evaluation of species in the general Stephanodiscus, Cyclostephanos and Cyclotella with a new genus in the family Stephanodiscaceae. Diatom Research 17: 1-139.

Hall RI and Smol JP 1999. Diatoms as indicators of lake eutrophication. The Diatoms. Cambridge University Press.

Halland R and Smol JP 2004. Diatoms as indicators of lake eutrophication. In: E. Stoermer and J. P. Smol (eds.), The Diatoms. Applications for the Environmental and Earth Sciences. Cambridge University Press, pp. 128-168.

Heinrich H 1988. Origin and consequences of cyclic ice rafting in the Northeast Atlantic Ocean during the past 130,000 years. Quaternary Research 29: 142-152.

Heiri O, Lotter AF and Lemcke G 2001. Loss on ignition as a method for estimating organic and carbonate content in sediments: Reproducibility and comparability of results. Journal of Paleolimnology 25: 101-110.

Hervé V, Derr J, Douady S, Quinet M, Moisan L and Lopez PJ 2012. Multiparametric Analyses Reveal the pH-Dependence of Silicon Biomineralization in Diatoms. PLoS ONE 7.

Hill MO 1973. Diversity and evenness: A unifying notation and its consequences. Ecology 54: 427-432.

Hill W 1996. Effects of Light. In: J. Stevenson, L. B. Max and R. L. Lowe (eds.), Algal Ecology. Academic Press, San Diego, pp. 121-148.

Hobæk A, Løvik JE, Rohrlack T, Moe SJ, Grung M, Bennion H, Clarke G and Piliposyan GT 2012. Eutrophication, recovery and temperature in Lake Mjøsa: detecting trends with monitoring data and sediment records. Freshwater Biology 57: 1998-2014.

Hofmann G, Werum M and Lange-Bertalot H 2011. Diatomeen im Süßwasser - Benthos von Mitteleuropa. Bestimmungsflora Kieselalgen für die ökologische Praxis. Über 700 der häufigsten Arten und ihre Ökologie. A.R.G. Gantner Verlag K.G., Ruggell, 908 pp.

Houk V 2003. Atlas of freshwater centric diatoms with a brief key and descriptions - Part I. Melosiraceae, Orthoseiraceae, Paraliaceae and Aulacoseiraceae. Czech Phycology Supplement 1: 1-111.

Houk V and Klee R 2004. The stelligeroid taxa of the genus cyclotella (Kützing) bré bisson (Bacillariophyceae) and their transfer into the new genus Discostella gen. nov. Diatom Research 19: 203-228.

Houk V, Klee R and Tanaka H 2010. Atlas of freshwater centric diatoms with a brief key and descriptions Part III. Stephanodiscaceae A Cyclotella, Tertiarius, Discostella. Fottea 10 (Supplement): 1-498.

Hustedt F 1939. Diatomeen aus den Pyrenäen. Bericht der Deutschen Botanischen Gessellschaft 56: 543-572.

IGEOTEST 2001. Informe de resultats relatiu a la campanya d`eextracció de mostra contínua i ampliació de la prospecció geolèctrica a l`estany de la coma de Burg de Farrera. IGEOTEST, p. 30.

Israde-Alcántara I, Bischoff JL, Domínguez-Vázquez G, Li H-C, DeCarli PS, Bunch TE, Wittke JH, Weaver JC, Firestone RB, West A, Kennett JP, Mercer C, Xie S, Richman EK, Kinzie CR and Wolbach WS 2012. Evidence from central Mexico supporting the Younger Dryas extraterrestrial impact hypothesis. Proceedings of the National Academy of Sciences.

Jiang H, Seidenkrantz MS, Knudsen KL and Eiriksson J 2002. Late-Holocene summer sea-surface temperatures based on a diatom record from the north Icelandic shelf. Holocene 12: 137-147.

Joannin S, Vannière B, Galop D, Peyron O, Haas JN, Gilli A, Chapron E, Wirth SB, Anselmetti F, Desmet M and Magny M 2013. Climate and vegetation changes during the Lateglacial and early–middle Holocene at Lake Ledro (southern Alps, Italy). Clim. Past 9: 913-933.

Jones TD, Lawson IT, Reed JM, Wilson GP, Leng MJ, Gierga M, Bernasconi SM, Smittenberg RH, Hajdas I, Bryant CL and Tzedakis PC 2013. Diatom-inferred late Pleistocene and Holocene palaeolimnological changes in the Ioannina basin, northwest Greece. Journal of Paleolimnology 49: 185-204.

Juggins S 2012. rioja: Analysis of Quaternary Science Data. R package. version (0.8-4).

Juggins S 2013. Quantitative reconstructions in palaeolimnology: New paradigm or sick science? Quaternary Science Reviews 64: 20-32.

Juggins S, Anderson NJ, Hobbs JR and Heathcote A 2013. Reconstructing epilimnetic total phosphorus using diatoms: statistical and ecological constraints. Journal of Paleolimnology 49: 373-390.

Juggins S and Birks JB 2012. Quantitative Environmental Reconstructions from Biological Data. In: H. J. B. Birks, A. F. Lotter, S. Juggins and J. P. Smol (eds.), Tracking Environmental Change Using Lake Sediments. Springer Netherlands, pp. 431-494.

Kettle H, Thompson R, Anderson NJ and Livingstone DM 2004. Empirical modeling of summer lake surface temperatures in southwest Greenland. Limnology and Oceanography 49: 271-282.

Kingsbury MV, Laird KR and Cumming BF 2012. Consistent patterns in diatom assemblages and diversity measures across water-depth gradients from eight Boreal lakes from north-western Ontario (Canada). Freshwater Biology 57: 1151-1165.

Kirilova E, Heiri O, Enters D, Cremer H, Lotter AF, Zolitschka B and Hübener T 2009. Climate-induced changes in the trophic status of a Central European lake. Journal of Limnology 68: 71-82.

Kitner M and Poulíčková A 2003. Littoral diatoms as indicators for the eutrophication of shallow lakes. Hydrobiologia 506-509: 519-524.

Köster D and Pienitz R 2006. Seasonal Diatom Variability and Paleolimnological Inferences – A Case Study. Journal of Paleolimnology 35: 395-416.

Koster D, Racca JMJ and Pienitz R 2004. Diatom-based inference models and reconstructions revisited: Methods and transformations. Journal of Paleolimnology 32: 233-245.

Krammer K 1997a. Die cymbelloiden Diatomeen - Eine Monographie der weltweit bekannten Taxa. Teil 1. Allgemeines und Encyonema Part. J. Cramer, Berlin.

Krammer K 1997b. Die cymbelloiden Diatomeen. Ein Monographie der weltweit bekannten Taxa. Teil 2. Encyonema part., Encyonopsis and Cymbellopsis. J. Cramer, Berlin.

Krammer K 2000. The genus Pinnularia. A.R.G. Gantner Verlag K.G, Ruggell, 703 pp.

Krammer K 2002. Cymbella. A.R.G. Gantner Verlag K.G, Ruggell, 584 pp.

Krammer K 2003. Cymbopleura, Delicata, Navicymbula, Gomphocymbellopsis, Afrocymbella Supplements to cymbelloid taxa. A.R.G. Gantner Verlag K.G, Ruggell, 530 pp.

Krammer K and Lange-Bertalot H 1986. Bacillariophyceae. 1. Teil: Naviculaceae. Gustav Fischer Verlag, Stuttgart, 876 pp.

Krammer K and Lange-Bertalot H 1988. Bacillariophyceae. 2. Teil: Bacillariaceae, Epithemiaceae, Surirellaceae. Gustav Fischer Verlag, Stuttgart, 596 pp.

Krammer K and Lange-Bertalot H 1991a. Bacillariophyceae 4. Teil: Achnanthaceae, Kritische Erganzungen zu Navicula (Lineolatae) und Gomphonema Gesamtliteraturverzeichnis Teil 1-4. Gustav Fischer Verlag, Stuttgart, 437 pp.

Krammer K and Lange-Bertalot H 1991b. Bacillariophyceae. 3. Teil: Centrales, Fragilariaceae, Eunotiaceae. Gustav Fischer Verlag, Stuttgart, 576 pp.

Krammer K and Lange-Bertalot H 2004. Bacillariophyceae 4. Teil: Achnanthaceae, Kritische Erganzungen zu Navicula (Lineolatae) und Gomphonema Gesamtliteraturverzeichnis Teil 1-4. Ssecond revised

edition with "Ergänzungen und Revisionen" by H. Lange-Bertalot. Spektrum Akademischer Verlag Heidelberg, Berlin, 468 pp.
Kucera M, Weinelt M, Kiefer T, Pflaumann U, Hayes A, Weinelt M, Chen MT, Mix AC, Barrows TT, Cortijo E, Duprat J, Juggins S and Waelbroeck C 2005. Reconstruction of sea-surface temperatures from assemblages of planktonic foraminifera: multi-technique approach based on geographically constrained calibration data sets and its application to glacial Atlantic and Pacific Oceans. Quaternary Science Reviews 24: 951-998.
Lake BA, Wigdahl CR, Strock KE, Saros JE and Amirbahman A 2011. Multi-proxy paleolimnological assessment of biogeochemical versus food web controls on the trophic states of two shallow, mesotrophic lakes. Journal of Paleolimnology 46: 45-57.
Lange-Bertalot H 1993. 85 neue taxa und über 100 weitere neu definierte Taxa ergänzend zur SüBwasserflora von Mitteleuropa, Vol. 2/1-4. J. Cramer, Berlin.
Lange-Bertalot H 1997. Revision of the genus achnanthes sensu lato (Bacillariophyceae): Achnantheiopsis, a new genus with the type species A. lanceolata. Zur revision der Gattung Achnanthes sensu lato (Bacillariophyceae): Achnantheiopsis, eine neue Gattung mit dem Typus generis A. lanceolata 148: 199-208.
Lange-Bertalot H 2001. Navicula sensu stricto, 10 Genera Separated from Navicula sensu stricto, Frustulia. A.R.G. Gantner Verlag K.G, Ruggell, 526 pp.
Lange-Bertalot H, Bak M, Witkowski A and Tagliaventi N 2011. Eunotia and some related genera. A.R.G. Gantner Verlag K.G, Ruggell, 747 pp.
Lange-Bertalot H, Cavacini P, Tagliaventi N and Alfinito S 2003. Diatoms of Sardinia. Rare and 76 new species in rock pools and other ephemeral waters. A.R.G. Gantner Verlag K.G, Ruggell, 438 pp.
Lange-Bertalot H and Krammer K 1987. Bacillariaceae Epithemiaceae Surirellaceae. Neae und wenig bekannte Taxa, neae Kombinationen und Synonyme sowie Bemerkungen und Erganzungen zu den Naviculaceae.
Lange-Bertalot H and Krammer K 1989. Achnanthes eine Monographie der Gattung mit Definition der Gattung Cocconeis und Nachtragen zu den Naviculaceae.
Lange-Bertalot H and Metzeltin D 1996. Indicators of oligotrophy - 800 taxa representative of three ecologically distinct lake types, Carbonate buffered - Oligodystrophic - Weakly buffered soft water. Koeltz Scientific Books, Königstein, 390 pp.
Larocque-Tobler I 2010. Reconstructing temperature at Egelsee, Switzerland, using North American and Swedish chironomid transfer functions: potential and pitfalls. Journal of Paleolimnology 44: 243-251.
Larocque I and Bigler C 2004. Similarities and discrepancies between chironomid- and diatom-inferred temperature reconstructions through the

Holocene at Lake 850, northern Sweden. Quaternary International 122: 109-121.

Larocque I, Hall RI and Grahn E 2001. Chironomids as indicators of climate change: a 100-lake training set from a subarctic region of northern Sweden (Lapland). Journal of Paleolimnology 26: 307-322.

Laskar J, Robutel P, Joutel F, Gastineau M, Correia ACM and Levrard B 2004. A long-term numerical solution for the insolation quantities of the Earth. Astronomy and Astrophysics 428: 261-285.

Leavitt PR, Fritz SC, Anderson NJ, Baker PA, Blenckner T, Bunting L, Catalan J, Conley DJ, Hobbs WO, Jeppesen E, Korhola A, McGowan S, Ruehland K, Rusak JA, Simpson GL, Solovieva N and Werne J 2009. Paleolimnological evidence of the effects on lakes of energy and mass transfer from climate and humans. Limnology and Oceanography 54: 2330-2348.

Legendre P and Birks HJ 2012. Clustering and Partitioning. In: H. J. B. Birks, A. F. Lotter, S. Juggins and J. P. Smol (eds.), Tracking Environmental Change Using Lake Sediments. Springer Netherlands, pp. 167-200.

Lepš J and Šmilauer P 2003. Multivariate Analysis of Ecological Data Using CANOCO. Cambridge University Press, Cambridge, United Kingdom.

Levkov Z 2009. Amphora sensu lato. A.R.G. Gantner Verlag K.G, Ruggell, 916 pp.

Liu Z, Carlson AE, He F, Brady EC, Otto-Bliesner BL, Briegleb BP, Wehrenberg M, Clark PU, Wu S, Cheng J, Zhang J, Noone D and Zhu J 2012. Younger Dryas cooling and the Greenland climate response to CO2. Proceedings of the National Academy of Sciences 109: 11101-11104.

Livingstone DM and Dokulil MT 2001. Eighty years of spatially coherent Austrian lake surface temperatures and their relationship to regional air temperature and the North Atlantic Oscillation. Limnology and Oceanography 46: 1220-1227.

Livingstone DM and Padisák J 2007. Large-Scale Coherence in the Response of Lake Surface-Water Temperatures to Synoptic-Scale Climate Forcing During Summer. Limnology and Oceanography 52: 896-902.

Lotter AF, Birks HJB, Eicher U, Hofmann W, Schwander J and Wick L 2000. Younger Dryas and Allerød summer temperatures at Gerzensee (Switzerland) inferred from fossil pollen and cladoceran assemblages. Palaeogeography, Palaeoclimatology, Palaeoecology 159: 349-361.

Lotter AF, Birks HJB, Hofmann W and Marchetto A 1997. Modern diatom, cladocera, chironomid, and chrysophyte cyst assemblages as quantitative indicators for the reconstruction of past environmental conditions in the Alps .1. Climate. Journal of Paleolimnology 18: 395-420.

Lotter AF, Eicher U, Siegenthaler U and Birks HJB 1992. Late-glacial climatic oscillations as recorded in Swiss lake sediments. Journal of Quaternary Science 7: 187-204.

Lotter AF, Heiri O, Brooks S, van Leeuwen JFN, Eicher U and Ammann B 2012. Rapid summer temperature changes during Termination 1a: High-resolution multi-proxy climate reconstructions from Gerzensee (Switzerland). Quaternary Science Reviews 36: 103-113.

Lowe JJ, Rasmussen SO, Björck S, Hoek WZ, Steffensen JP, Walker MJC and Yu ZC 2008. Synchronisation of palaeoenvironmental events in the North Atlantic region during the Last Termination: a revised protocol recommended by the INTIMATE group. Quaternary Science Reviews 27: 6-17.

Lowe RL 1996. Periphyton patterns in lakes. Algal Ecology: Freshwater Benthic Ecosystems, pp. 57-76.

Luoto TP 2009. A Finnish chironomid- and chaoborid-based inference model for reconstructing past lake levels. Quaternary Science Reviews 28: 1481-1489.

Luoto TP, Nevalainen L, Kauppila T, Tammelin M and Sarmaja-Korjonen K 2012. Diatom-inferred total phosphorus from dystrophic Lake Arapisto, Finland, in relation to Holocene paleoclimate. Quaternary Research 78: 248-255.

Mackereth FJH, Heron J and Talling JF 1978. Water analysis: some revised methods for limnologists. Titus Wilson & Sons Ltd, Kendal, 1-120 pp.

Magny M Climatic and environmental changes reflected by lake-level fluctuations at Gerzensee from 14,850 to 13,050 yr BP. Palaeogeography, Palaeoclimatology, Palaeoecology.

Magny M 2001. Palaeohydrological changes as reflected by lake-level fluctuations in the Swiss Plateau, the Jura Mountains and the northern French Pre-Alps during the Last Glacial–Holocene transition: a regional synthesis. Global and Planetary Change 30: 85-101.

Magny M, Aalbersberg G, Bégeot C, Benoit-Ruffaldi P, Bossuet G, Disnar J-R, Heiri O, Laggoun-Defarge F, Mazier F, Millet L, Peyron O, Vannière B and Walter-Simonnet A-V 2006. Environmental and climatic changes in the Jura mountains (eastern France) during the Lateglacial–Holocene transition: a multi-proxy record from Lake Lautrey. Quaternary Science Reviews 25: 414-445.

Magny M, Combourieu-Nebout N, de Beaulieu JL, Bout-Roumazeilles V, Colombaroli D, Desprat S, Francke A, Joannin S, Ortu E, Peyron O, Revel M, Sadori L, Siani G, Sicre MA, Samartin S, Simonneau A, Tinner W, Vannière B, Wagner B, Zanchetta G, Anselmetti F, Brugiapaglia E, Chapron E, Debret M, Desmet M, Didier J, Essallami L, Galop D, Gilli A, Haas JN, Kallel N, Millet L, Stock A, Turon JL and Wirth S 2013. North–south palaeohydrological palaeohydrological contrasts in the central Mediterranean during the Holocene: tentative synthesis and working hypotheses. Clim. Past 9: 2043-2071.

Magny M, Guiot J and Schoellammer P 2001. Quantitative Reconstruction of Younger Dryas to Mid-Holocene Paleoclimates at Le Locle, Swiss Jura, Using Pollen and Lake-Level Data. Quaternary Research 56: 170-180.

Magny M, Thew N and Hadorn P 2003. Late-glacial and early Holocene changes in vegetation and lake-level at Hauterive/Rouges-Terres, Lake Neuchâtel (Switzerland). Journal of Quaternary Science 18: 31-40.

Magny M, Vannière B, de Beaulieu J-L, Bégeot C, Heiri O, Millet L, Peyron O and Walter-Simonnet A-V 2007. Early-Holocene climatic oscillations recorded by lake-level fluctuations in west-central Europe and in central Italy. Quaternary Science Reviews 26: 1951-1964.

Magurran AE 2004. Measuring Biological Diversity. Blackwell Publishing, Malden, USA.

Margalef R 1983. Limnología. Ediciones Omega.

Martin-Jézéquel V, Hildebrand M and Brzezinski MA 2000. Silicon metabolism in diatoms: implications for growth Journal of Phycology 36: 821-840.

Medeiros AS, Friel CE, Finkelstein SA and Quinlan R 2012. A high resolution multi-proxy record of pronounced recent environmental change at Baker Lake, Nunavut. Journal of Paleolimnology 47: 661-676.

Medlin L 2011. A Review of the Evolution of the Diatoms from the Origin of the Lineage to Their Populations. In: J. Seckbach and P. Kociolek (eds.), The Diatom World. Springer Netherlands, pp. 93-118.

Ménot G and Bard E 2012. A precise search for drastic temperature shifts of the past 40,000 years in southeastern Europe. Paleoceanography 27: PA2210.

Millet L, Rius D, Galop D, Heiri O and Brooks SJ 2012. Chironomid-based reconstruction of Lateglacial summer temperatures from the Ech palaeolake record (French western Pyrenees). Palaeogeography, Palaeoclimatology, Palaeoecology 315-316: 86-99.

Morellón M, Valero-Garcés B, Vegas-Vilarrúbia T, González-Sampériz P, Romero Ó, Delgado-Huertas A, Mata P, Moreno A, Rico M and Corella JP 2009. Lateglacial and Holocene palaeohydrology in the western Mediterranean region: The Lake Estanya record (NE Spain). Quaternary Science Reviews 28: 2582-2599.

Moreno A, González-Sampériz P, Morellón M, Valero-Garcés BL and Fletcher WJ 2012. Northern Iberian abrupt climate change dynamics during the last glacial cycle: A view from lacustrine sediments. Quaternary Science Reviews 36: 139-153.

Moreno A, Stoll H, Jiménez-Sánchez M, Cacho I, Valero-Garcés B, Ito E and Edwards RL 2010. A speleothem record of glacial (25-11.6 kyr BP) rapid climatic changes from northern Iberian Peninsula. Global and Planetary Change 71: 218-231.

Mortensen MF, Birks HH, Christensen C, Holm J, Noe-Nygaard N, Odgaard BV, Olsen J and Rasmussen KL 2011. Lateglacial vegetation development in Denmark – New evidence based on macrofossils and

pollen from Slotseng, a small-scale site in southern Jutland. Quaternary Science Reviews 30: 2534-2550.
Muñoz Sobrino C, Heiri O, Hazekamp M, van der Velden D, Kirilova EP, García-Moreiras I and Lotter AF 2013. New data on the Lateglacial period of SW Europe: a high resolution multiproxy record from Laguna de la Roya (NW Iberia). Quaternary Science Reviews 80: 58-77.
Nakayama T, Ikegami Y, Ishida KI, Inagaki Y and Inouye I 2011. Spheroid bodies in rhopalodiacean diatoms were derived from a single endosymbiotic cyanobacterium. Journal of Plant Research 124: 93-97.
Ninyerola M, Pons X and Roure JM 2000. A methodological approach of climatological modelling of air temperature and precipitation through GIS techniques. International Journal of Climatology 20: 1823-1841.
Norton SA, Perry RH, Saros JE, Jacobson GJ, Fernandez IJ, Kopáček J, Wilson TA and SanClements MD 2011. The controls on phosphorus availability in a Boreal lake ecosystem since deglaciation. Journal of Paleolimnology 46: 107-122.
Novikmec M, Svitok M, Kočický D, Šporka F and Bitušík P 2013. Surface Water Temperature and Ice Cover of Tatra Mountains Lakes Depend on Altitude, Topographic Shading, and Bathymetry. Arctic, Antarctic, and Alpine Research 45: 77-87.
Oksanen J, Kindt R, Legendre P, O'Hara B, Simpson GL, Solymos P, Stevens MHH and Wagner H 2009. Vegan: Community ecology package. R package version 1.15-4. Vegan: Community Ecology Package.
Oksanen J, Läärä E, Huttunen P and Meriläinen J 1988. Estimation of pH optima and tolerances of diatoms in lake sediments by the methods of weighted averaging, least squares and maximum likelihood, and their use for the prediction of lake acidity. Journal of Paleolimnology 1: 39-49.
Palumbo E, Flores JA, Perugia C, Emanuele D, Petrillo Z, Rodrigues T, Voelker AHL and Amore FO 2013. Abrupt variability of the last 24 ka BP recorded by coccolithophore assemblages off the Iberian Margin (core MD03-2699). Journal of Quaternary Science 28: 320-328.
Pan Y, Stevenson RJ, Hill BH, Herlihy AT and Collins GB 1996. Using diatoms as indicators ecological conditions in lotic systems: a regional assessment, pp. 481-495. pp.
Pèlachs A, Julià R, Pérez-Obiol R, Soriano JM, Bal MC, Cunill R and Catalan J 2011. Potential influence of bond events on mid-holocene climate and vegetation in southern pyrenees as assessed from burg lake loi and pollen records. Holocene 21: 95-104.
Pèrez-Obiol R and Julià R 1994. Climatic Change on the Iberian Peninsula Recorded in a 30,000-Yr Pollen Record from Lake Banyoles. Quaternary Research 41: 91-98.
Peyron O, Bégeot C, Brewer S, Heiri O, Magny M, Millet L, Ruffaldi P, Van Campo E and Yu G 2005. Late-Glacial climatic changes in Eastern France

(Lake Lautrey) from pollen, lake-levels, and chironomids. Quaternary Research 64: 197-211.

Pinter N, Scott AC, Daulton TL, Podoll A, Koeberl C, Anderson RS and Ishman SE 2011. The Younger Dryas impact hypothesis: A requiem. Earth-Science Reviews 106: 247-264.

Pla S and Anderson NJ 2005. Environmental factors correlated with Chrysophyte cyst assemblages in low arctic lakes of southwest greenland. Journal of Phycology 41: 957-974.

Pla S, Camarero L and Catalan J 2003. Chrysophyte cyst relationships to water chemistry in Pyrenean lakes (NE Spain) and their potential for environmental reconstruction. Journal of Paleolimnology 30: 21-34.

Pla S and Catalan J 2005. Chrysophyte cysts from lake sediments reveal the submillennial winter/spring climate variability in the northwestern Mediterranean region throughout the Holocene. Climate Dynamics 24: 263-278.

Pla S, Monteith D, Flower R and Rose N 2009. The recent palaeolimnology of a remote Scottish loch with special reference to the relative impacts of regional warming and atmospheric contamination. Freshwater Biology 54: 505-523.

Puusepp L and Punning JM 2011. Spatio-temporal variability of diatom assemblages in surface sediments of Lake Peipsi. Journal of Great Lakes Research 37: 33-40.

Quillen AK, Gaiser EE and Grimm EC 2013. Diatom-based paleolimnological reconstruction of regional climate and local land-use change from a protected sinkhole lake in southern Florida, USA. Journal of Paleolimnology 49: 15-30.

R Development Core Team 2013. R: A Language and Environment for Statistical Computing. R: A Language and Environment for Statistical Computing. R Foundation for Statistical Computing, Vienna, Austria.

Racca JMJ and Prairie YT 2004. Apparent and real bias in numerical transfer functions in palaeolimnology. Journal of Paleolimnology 31: 117-124.

Rasmussen SO, Andersen KK, Svensson AM, Steffensen JP, Vinther BM, Clausen HB, Siggaard-Andersen ML, Johnsen SJ, Larsen LB, Dahl-Jensen D, Bigler M, Röthlisberger R, Fischer H, Goto-Azuma K, Hansson ME and Ruth U 2006. A new Greenland ice core chronology for the last glacial termination. Journal of Geophysical Research: Atmospheres 111: D06102.

Rasmussen SO, Seierstad IK, Andersen KK, Bigler M, Dahl-Jensen D and Johnsen SJ 2008. Synchronization of the NGRIP, GRIP, and GISP2 ice cores across MIS 2 and palaeoclimatic implications. Quaternary Science Reviews 27: 18-28.

Rasmussen SO, Vinther BM, Clausen HB and Andersen KK 2007. Early Holocene climate oscillations recorded in three Greenland ice cores. Quaternary Science Reviews 26: 1907-1914.

Reavie E and Smol J 2001. Diatom-environmental relationships in 64 alkaline southeastern Ontario (Canada) lakes: a diatom-based model for water quality reconstructions. Journal of Paleolimnology 25: 25-42.
Reavie ED and Smol JP 1997. Diatom-based model to infer past littoral habitat characteristics in the St. Lawrence River. Journal of Great Lakes Research 23: 339-348.
Redfield AC 1958. The biological control of chemical factors in the environment. American Scientist 46: 230A-221.
Reichardt E 1997. Taxonomische Revision des Artenkomplexes um Gomphonema pumilum (Bacillariophyceae). Nova Hedwigia 65: 99-129.
Reichardt E 1999. Zur Revision der Gattung Gomphonema. Die Arten um G. affine/insigne, G. angustatum/micropus, G. acuminatum sowie gomphonemoide Diatomeen aus dem Oberoligozan in Bohmen. A.R.G. Gantner Verlag K.G, Ruggell, 250 pp.
Reichardt E 2007. Neue und wenig bekannte Gomphonema-Arten (Bacillariophyceae) mit Areolen in Doppelreihen. Nova Hedwigia 85: 103-137.
Reichardt E and Lange-Bertalot H 1991. Taxonomische revision des artenkomplexes um Gomphonema angustatum- G. dichotomun- G. intricatum- G. vibrio und ähnliche taxa (Bacillariophyceae). Nova Hedwigia 53: 519-544.
Reid M 2005. Diatom-based models for reconstructing past water quality and productivity in New Zealand lakes. Journal of Paleolimnology 33: 13-38.
Renssen H and Isarin RFB 2001. The two major warming phases of the last deglaciation at ~14.7 and ~11.5 ka cal BP in Europe: climate reconstructions and AGCM experiments. Global and Planetary Change 30: 117-153.
Reuss N, Hammarlund D, Rundgren M, Segerström U, Eriksson L and Rosén P 2010. Lake Ecosystem Responses to Holocene Climate Change at the Subarctic Tree-Line in Northern Sweden. Ecosystems 13: 393-409.
Reynolds C 1998. The state of freshwater ecology, 741-753. pp.
Reynolds CS 1984. The ecology of freshwater phytoplankton. Cambridge University Press, Cambridge, UK, 384 pp.
Reynolds CS 2006. The Ecology of Phytoplankton (Ecology, Biodiversity and Conservation). Cambridge University Press, Cambridge, UK, 552 pp.
Rimet F and Bouchez A 2012. Biomonitoring river diatoms: Implications of taxonomic resolution. Ecological Indicators 15: 92-99.
Robinson SA, Black S, Sellwood BW and Valdes PJ 2006. A review of palaeoclimates and palaeoenvironments in the Levant and Eastern Mediterranean from 25,000 to 5000 years BP: setting the environmental background for the evolution of human civilisation. Quaternary Science Reviews 25: 1517-1541.
Rodrigues T, Grimalt JO, Abrantes F, Naughton F and Flores J-A 2010. The last glacial–interglacial transition (LGIT) in the western mid-latitudes of the

North Atlantic: Abrupt sea surface temperature change and sea level implications. Quaternary Science Reviews 29: 1853-1862.
Rooney N, Kalff J and Habel C 2003. The Role of Submerged Macrophyte Beds in Phosphorus and Sediment Accumulation in Lake Memphremagog, Quebec, Canada. Limnology and Oceanography 48: 1927-1937.
Round FE, Crawford RM and Mann DG 1990. The Diatoms: The Biology and Morphology of the Genera. Cambridge University Press.
Ryves DB, Battarbee RW and Fritz SC 2009. The dilemma of disappearing diatoms: Incorporating diatom dissolution data into palaeoenvironmental modelling and reconstruction. Quaternary Science Reviews 28: 120-136.
Ryves DB, Battarbee RW, Juggins S, Fritz SC and Anderson NJ 2006. Physical and chemical predictors of diatom dissolution in freshwater and saline lake sediments in North America and West Greenland. Limnology and Oceanography 51: 1355-1368.
Ryves DB, Juggins S, Fritz SC and Battarbee RW 2001. Experimental diatom dissolution and the quantification of microfossil preservation in sediments. Palaeogeography, Palaeoclimatology, Palaeoecology 172: 99-113.
Samartin S, Heiri O, Vescovi E, Brooks SJ and Tinner W 2012. Lateglacial and early Holocene summer temperatures in the southern Swiss Alps reconstructed using fossil chironomids. Journal of Quaternary Science 27: 279-289.
Sánchez ML, Pérez GL, Izaguirre I and Pizarro H 2013. Influence of underwater light climate on periphyton and phytoplankton communities in shallow lakes from the Pampa plain (Argentina) with contrasting steady states. Journal of Limnology 72: 62-78.
Saunders KM, Hodgson DA and McMinn A 2009. Quantitative relationships between benthic diatom assemblages and water chemistry in Macquarie Island lakes and their potential for reconstructing past environmental changes. Antarctic Science 21: 35-49.
Sayer CD 2001. Problems with the application of diatom-total phosphorus transfer functions: Examples from a shallow English lake. Freshwater Biology 46: 743-757.
Sayer CD, Burgess AMY, Kari K, Davidson TA, Peglar S, Yang H and Rose N 2010. Long-term dynamics of submerged macrophytes and algae in a small and shallow, eutrophic lake: implications for the stability of macrophyte-dominance. Freshwater Biology 55: 565-583.
Schaller T, Christoph Moor H and Wehrli B 1997. Sedimentary profiles of Fe, Mn, V, Cr, As and Mo as indicators of benthic redox conditions in Baldeggersee. Aquatic Sciences 59: 345-361.
Schmidt R, Kamenik C, Lange-Bertalot H and Klee R 2004. Fragilaria and Staurosira (Bacillariophyceae) from sediment surfaces of 40 lakes in the Austrian Alps in relation to environmental variables, and their potential for palaeoclimatology. Journal of Limnology 63: 171-189.

Schmidt R, Kamenik C, Tessadri R and Koinig KA 2006. Climatic changes from 12,000 to 4,000 years ago in the Austrian Central Alps tracked by sedimentological and biological proxies of a lake sediment core. Journal of Paleolimnology 35: 491-505.

Schmidt R, Weckström K, Lauterbach S, Tessadri R and Huber K 2012. North Atlantic climate impact on early late-glacial climate oscillations in the south-eastern Alps inferred from a multi-proxy lake sediment record. Journal of Quaternary Science 27: 40-50.

Sharma S, Walker SC and Jackson DA 2008. Empirical modelling of lake water-temperature relationships: A comparison of approaches. Freshwater Biology 53: 897-911.

Shinneman ALC, Bennett DM, Fritz SC, Schmieder J, Engstrom DR, Efting A and Holz J 2010. Inferring lake depth using diatom assemblages in the shallow, seasonally variable lakes of the Nebraska Sand Hills (USA): calibration, validation, and application of a 69-lake training set. Journal of Paleolimnology 44: 443-464.

Shuman B, Bravo J, Kaye J, Lynch JA, Newby P and Webb Iii T 2001. Late Quaternary Water-Level Variations and Vegetation History at Crooked Pond, Southeastern Massachusetts. Quaternary Research 56: 401-410.

Shumilovskikh LS, Tarasov P, Arz HW, Fleitmann D, Marret F, Nowaczyk N, Plessen B, Schlütz F and Behling H 2012. Vegetation and environmental dynamics in the southern Black Sea region since 18kyr BP derived from the marine core 22-GC3. Palaeogeography, Palaeoclimatology, Palaeoecology 337–338: 177-193.

Sikes EL and Keigwin LD 1994. Equatorial Atlantic sea-surface temperature for the last 30 kyr - a compariso of UK'37, delta-O-18 and foraminiferal assemblage temperature estimates. Paleoceanography 9: 31-45.

Sims PA, Mann DG and Medlin LK 2006. Evolution of the diatoms: Insights from fossil, biological and molecular data. Phycologia 45: 361-402.

Siver PA 1999. Development of paleolimnological inference models for pH, total nitrogen and specific conductivity based on planktonic diatoms. Journal of Paleolimnology 21: 45-59.

Smol JP 1983. Paleophycology of a high arctic lake near Cape Herschel, Ellesmere Island. Canadian Journal of Botany 61: 2195-2204.

Smol JP 1985. The ratio of diatom frustules to chrysophycean statospores: A useful paleolimnological index. Hydrobiologia 123: 199-208.

Smol JP 2008. Pollution of lakes and rivers. A paleoenvironmental perspective. Blackwell publishing, Singapore, 383 pp.

Solovieva N, Jones VJ, Nazarova L, Brooks SJ, Birks HJB, Grytnes JA, Appleby PG, Kauppila T, Kondratenok B, Renberg I and Ponomarev V 2005. Palaeolimnological evidence for recent climatic change in lakes from the northern Urals, arctic Russia. Journal of Paleolimnology 33: 463-482.

Stanford JD, Rohling EJ, Bacon S, Roberts AP, Grousset FE and Bolshaw M 2011. A new concept for the paleoceanographic evolution of Heinrich event 1 in the North Atlantic. Quaternary Science Reviews 30: 1047-1066.

Svensson A, Andersen KK, Bigler M, Clausen HB, Dahl-Jensen D, Davies SM, Johnsen SJ, Muscheler R, Parrenin F, Rasmussen SO, Röthlisberger R, Seierstad I, Steffensen JP and Vinther BM 2008. A 60 000 year Greenland stratigraphic ice core chronology. Climate of the Past 4: 47-57.

Telford RJ and Birks HJB 2005. The secret assumption of transfer functions: Problems with spatial autocorrelation in evaluating model performance. Quaternary Science Reviews 24: 2173-2179.

Telford RJ and Birks HJB 2009. Evaluation of transfer functions in spatially structured environments. Quaternary Science Reviews 28: 1309-1316.

Telford RJ and Birks HJB 2011a. Effect of uneven sampling along an environmental gradient on transfer-function performance. Journal of Paleolimnology 46: 99-106.

Telford RJ and Birks HJB 2011b. A novel method for assessing the statistical significance of quantitative reconstructions inferred from biotic assemblages. Quaternary Science Reviews 30: 1272-1278.

Telford RJ and Birks HJB 2011c. QSR Correspondence "Is spatial autocorrelation introducing biases in the apparent accuracy of palaeoclimatic reconstructions?". Quaternary Science Reviews 30: 3210-3213.

Telford RJ, Vandvik V and Birks HJB 2006. How many freshwater diatoms are pH specialists? A response to Pither & Aarssen (2005). Ecology Letters 9: E1-E5.

Teller JT 2013. Lake Agassiz during the Younger Dryas. Quaternary Research 80: 361-369.

ter Braak CJF and Juggins S 1993. Weighted averaging partial least squares regression (WA-PLS): an improved method for reconstructing environmental variables from species assemblages. Hydrobiologia 269-270: 485-502.

ter Braak CJF and Looman CWN 1986. Weighted averaging, logistic regression and the Gaussian response model. Vegetatio 65: 3-11.

Terbraak CJF and Juggins S 1993. Weighted averaging partial least-squares regression (WA-PLS) -an improved method for reconstructing environmental variables from species assemblages. Hydrobiologia 269: 485-502.

Teubner K 2003. Phytoplankton, pelagic community and nutrients in a deep oligotrophic alpine lake: Ratios as sensitive indicators of the use of P-resources (DRP:DOP:PP and TN:TP:SRSi). Water Research 37: 1583-1592.

Thies H, Tolotti M, Nickus U, Lami A, Musazzi S, Guilizzoni P, Rose NL and Yang H 2012. Interactions of temperature and nutrient changes: effects on

phytoplankton in the Piburger See (Tyrol, Austria). Freshwater Biology 57: 2057-2075.
Thompson R, Ventura M and Camarero L 2009. On the climate and weather of mountain and sub-arctic lakes in Europe and their susceptibility to future climate change. Freshwater Biology 54: 2433-2451.
Tilman D 1990. Constraints and tradeoffs: toward a predictive theory of competition and succession. Oikos 58: 3-15.
Tjallingii R, Claussen M, Stuut JBW, Fohlmeister J, Jahn A, Bickert T, Lamy F and Röhl U 2008. Coherent high- and low-latitude control of the northwest African hydrological balance. Nature Geoscience 1: 670-675.
Tóth M, Magyari EK, Brooks SJ, Braun M, Buczkó K, Bálint M and Heiri O 2012. A chironomid-based reconstruction of late glacial summer temperatures in the southern Carpathians (Romania). Quaternary Research 77: 122-131.
Van De Vijver B, Beyens L and Lange-Bertalot H 2004. The genus Stauroneis in the Arctic and (Sub-) Antartic Regions. J. Cramer, Berlin.
van der Voet H 1994. Comparing the predictive accuracy of models using a simple randomization test. Chemometrics and Intelligent Laboratory Systems 25: 313-323.
van Raden UJ, Colombaroli D, Gilli A, Schwander J, Bernasconi SM, van Leeuwen J, Leuenberger M and Eicher U in press. High-resolution late-glacial chronology for the Gerzensee lake record (Switzerland): δ 18O correlation between a Gerzensee-stack and NGRIP. Palaeogeography, Palaeoclimatology, Palaeoecology.
Vermaire J and Gregory-Eaves I 2008. Reconstructing changes in macrophyte cover in lakes across the northeastern United States based on sedimentary diatom assemblages. Journal of Paleolimnology 39: 477-490.
Vermaire JC, Prairie YT and Gregory-Eaves I 2011. The influence of submerged macrophytes on sedimentary diatom assemblages. Journal of Phycology 47: 1230-1240.
Vermaire JC, Prairie YT and Gregory-Eaves I 2012. Diatom-inferred decline of macrophyte abundance in lakes of southern Quebec, Canada. Canadian Journal of Fisheries and Aquatic Sciences 69: 511-524.
Vizcaino A 2003. Geologia glacial de la Coma de Burg (Pirineo Central). Treball de Final de Carrera. p. 33.
von Grafenstein U, Eicher U, Erlenkeuser H, Ruch P, Schwander J and Ammann B 2000. Isotope signature of the Younger Dryas and two minor oscillations at Gerzensee (Switzerland): palaeoclimatic and palaeolimnologic interpretation based on bulk and biogenic carbonates. Palaeogeography, Palaeoclimatology, Palaeoecology 159: 215-229.
Von Gunten L, Heiri O, Bigler C, Van Leeuwen J, Casty C, Lotter AF and Sturm M 2008. Seasonal temperatures for the past ~400 years reconstructed from diatom and chironomid assemblages in a high-altitude

lake (Lej da la Tscheppa, Switzerland). Journal of Paleolimnology 39: 283-299.

Vrieling EG, Gieskes WWC and Beelen TPM 1999. Silicon deposition in diatoms: Control by the pH inside the silicon deposition vesicle. Journal of Phycology 35: 548-559.

Werner P and Smol JP 2005. Diatom–environmental relationships and nutrient transfer functions from contrasting shallow and deep limestone lakes in Ontario, Canada. Hydrobiologia 533: 145-173.

Werum M and Lange-Bertalot H 2004a. Diatoms in Springs from Central Europe and elsewhere under the influence of hydrogeology and anthropogenic impacts. A.R.G. Gantner Verlag K.G, Ruggell, 480 pp.

Werum M and Lange-Bertalot H 2004b. Diatoms in Springs from Central Europe and elsewhere under the influence of hydrologeology and anthropogenic impacts. In: H. Lange-Bertalot (ed.), Iconographia Diatomologica. Annotated Diatom Micrographs. Vol. 13. Ecoloy-Hydrology-Taxonomy. A.R.G. Gantner Verlag K.G. , Ruggell, p. 417.

Westover KS, Fritz SC, Blyakharchuk TA and Wright HE 2006. Diatom paleolimnological record of Holocene climatic and environmental change in the Altai Mountains, Siberia. Journal of Paleolimnology 35: 519-541.

Wetzel RG 2001. Limnology: Lake and river ecosystems. Academic Press, San Diego. USA, 1006 pp.

Wilhelm C, Büchel C, Fisahn J, Goss R, Jakob T, LaRoche J, Lavaud J, Lohr M, Riebesell U, Stehfest K, Valentin K and Kroth PG 2006. The Regulation of Carbon and Nutrient Assimilation in Diatoms is Significantly Different from Green Algae. Protist 157: 91-124.

Wilson SE, Cumming BF and Smol JP 1994. Diatom-salinity relationships in 111 lakes from the Interior Plateau of British Columbia, Canada: the development of diatom-based models for paleosalinity reconstructions. Journal of Paleolimnology 12: 197-221.

Williams C, Flower BP and Hastings DW 2012. Seasonal Laurentide Ice Sheet melting during the "Mystery Interval" (17.5-14.5 ka). Geology 40: 955-958.

Williams D and Kociolek JP 2011. An Overview of Diatom Classification with Some Prospects for the Future. In: J. Seckbach and P. Kociolek (eds.), The Diatom World. Springer Netherlands, pp. 47-91.

Wittke JH, Weaver JC, Bunch TE, Kennett JP, Kennett DJ, Moore AMT, Hillman GC, Tankersley KB, Goodyear AC, Moore CR, Daniel IR, Ray JH, Lopinot NH, Ferraro D, Israde-Alcántara I, Bischoff JL, DeCarli PS, Hermes RE, Kloosterman JB, Revay Z, Howard GA, Kimbel DR, Kletetschka G, Nabelek L, Lipo CP, Sakai S, West A and Firestone RB 2013. Evidence for deposition of 10 million tonnes of impact spherules across four continents 12,800 y ago. Proceedings of the National Academy of Sciences.

Wolin JA and Duthie H 1999. 8-Diatoms as indicators of water level change in freshwater lakes. The Diatoms. Cambridge University Press.

Wood SN 2011. Fast stable restricted maximum likelihood and marginal likelihood estimation of semiparametric generalized linear models. Journal of the Royal Statistical Society. Series B: Statistical Methodology 73: 3-36.

Wu Y, Sharma M, LeCompte MA, Demitroff MN and Landis JD 2013. Origin and provenance of spherules and magnetic grains at the Younger Dryas boundary. Proceedings of the National Academy of Sciences 110: E3557-E3566.

Yang H and Flower RJ 2012. Effects of light and substrate on the benthic diatoms in an oligotrophic lake: A comparison between natural and artificial substrates. Journal of Phycology 48: 1166-1177.

Yang X, Kamenik C, Schmidt R and Wang S 2003. Diatom-based conductivity and water-level inference models from eastern Tibetan (Qinghai-Xizang) Plateau lakes. Journal of Paleolimnology 30: 1-19.

Zeeb BA, Christie CE, Smol JP, Findlay DL, Kling HJ and Birks HJ 1994. Responses of diatom and chrysophyte assemblages in Lake 227 sediments to experimental eutrophication. Canadian Journal of Fisheries and Aquatic Sciences 51: 2300-2311.

Zeeb BA and Smol JP 2001. Chrysophyte scales and cysts. In: J. P. Smol, H. H. Birks and W. M. Last (eds.), Tracking Environmental Change Using Lake Sediments, Terrestrial, Algal, and Siliceous Indicators. Kluwer Academic Publishers, pp. 203-223.

Appendices

Appendix 1

Diatom Iconography

[Rivera Rondón, C.A. 2013. Diatom-based reconstruction of Late Glacial and Early Holocene environment in the Pyrenees. Ph.D. Thesis, Universitat de Barcelona. 581pp]

Index

Genera	Plates
Hygropetra	88
Karayevia	36
Kobayasiella	70
Kraskella	67
Luticola	67
Meridion	12
Navicula (sensu stricto)	53-58
Navicula (sensu lato)	65, 67-70
Naviculadicta	67-71
Neidium	73-74
Nitzschia	117-121
Nupela	37
Orthoseira	5
Peronia	28
Pinnularia	86-92
Placoneis	64
Planothidium	38
Psammothidium	36, 40-41, 49-51
Pseudostaurosira	16-19
Punctastriata	20
Punticulata	2
Reimeria	108
Rhopalodia	124
Rosithidium	48
Sellaphora	59-62, 70
Stauroforma	16
Stauroneis	75-76
Staurosira	16, 22
Staurosirella	19-20
Stenopterobia	126
Surirella	125
Tabellaria	13
Tabularia	18
Ulnaria	21

Plates

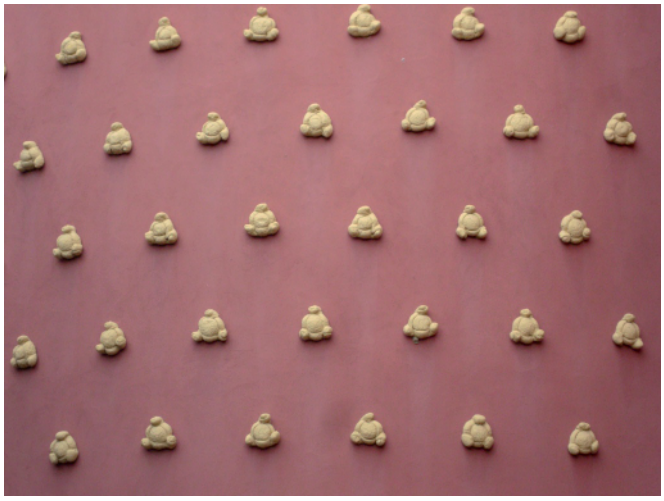

The Dalí Museum (Figueres, Catalonia)

Plate 1 LM: x1500
SEM: Figs. 15,18 x7000, Fig. 16 x810000, Fig. 17 x20000

Figs. 1-2 *Cyclotella* cf. *radiosa* (Grunow) Lemmermann

Figs. 3-18 *Cyclotella radiosa* (Grunow) Lemmermann

Fig. 1	Lake Estom, sediment PYR15
Figs. 2-12	Lake Sen, sediment PYR40
Figs. 13-14	Lake Llebreta, sediment PYR58
Figs. 15,17,18	Lake Laurenti, sediment PYR111
Fig. 16	Lake Gros de Camporrells, sediment PYR110


1


2

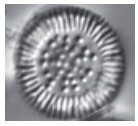
3


4

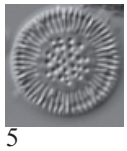
5


6

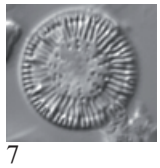
7


8

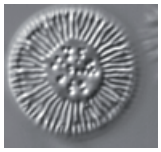
9


10


11

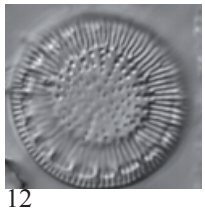
12

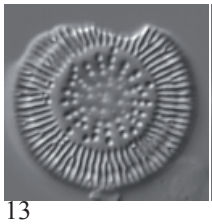
13

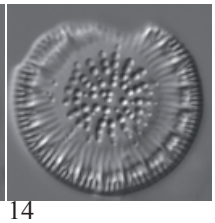
14

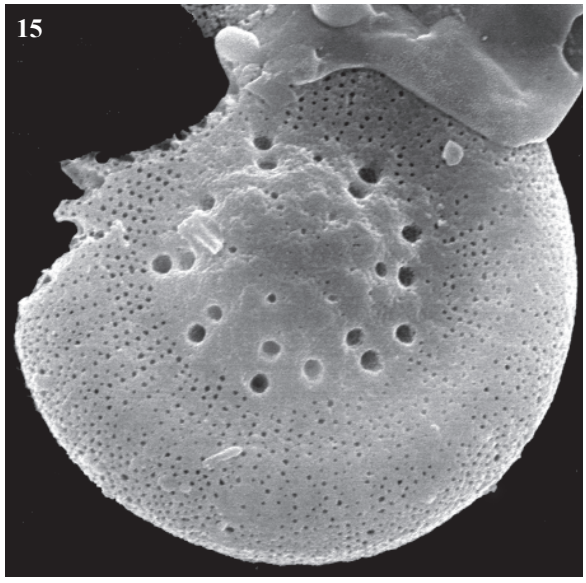
15

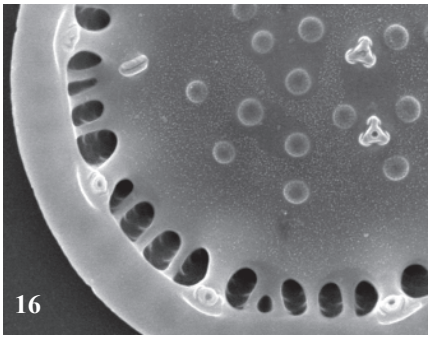
16

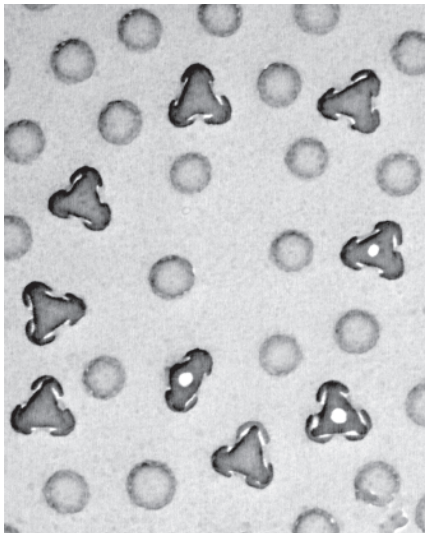
17

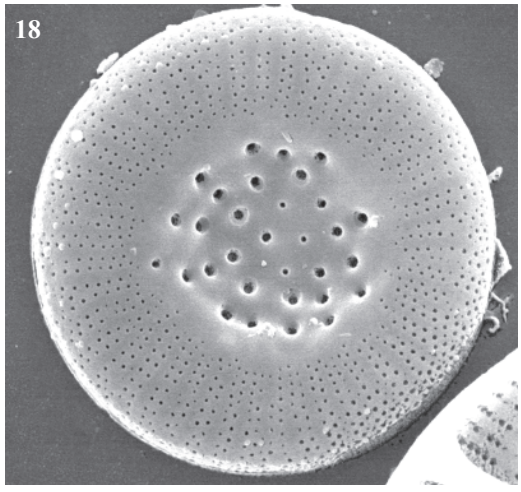
18

Plate 2 LM: x1500
SEM: Figs. 3,5 x4000, Fig. 4 x3000

Figs. 1-3,5 *Puncticulata praetermissa* (Lund) Håkansson

Figs. 4 *?Puncticulata praetermissa* (Lund) Håkansson

Figs. 1, 2 Lake Acherito, sediment PYR01

Figs. 3,5 Lake Laurenti, sediment PYR111

Fig. 4 Lake Arnales, sediment PYR09

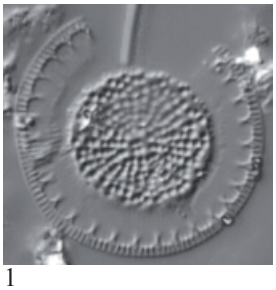

1

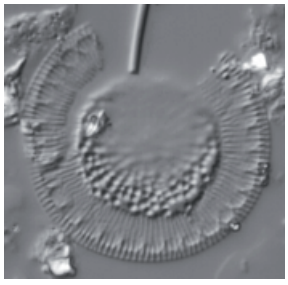

2

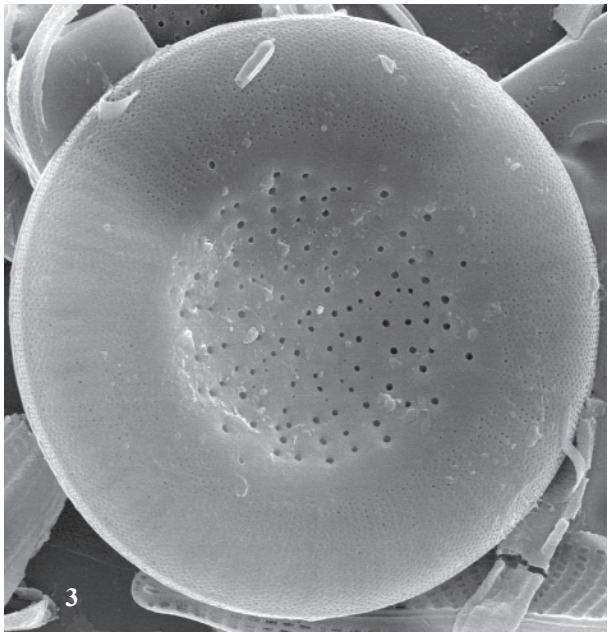

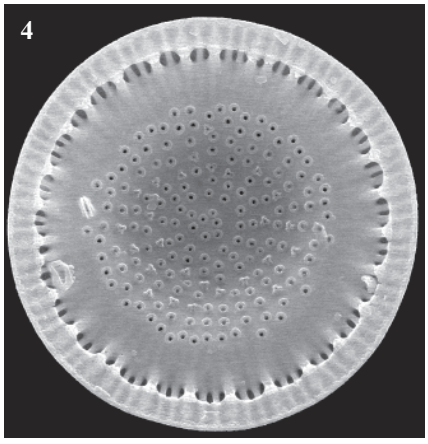

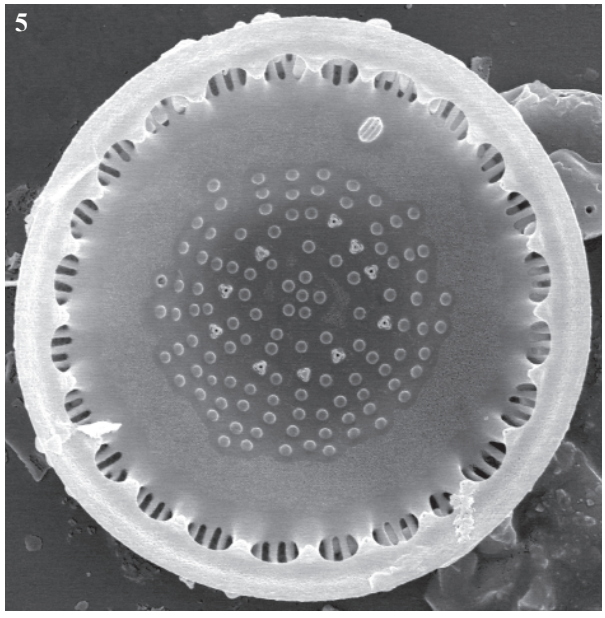

Plate 3 LM: x1500

Figs. 1-9 *Cyclotella* sp. No. 1 Llebreta

Figs. 1, 2, 8, 9 Lake Llebreta, sediment PYR58
Figs. 3-7 Lake Estom, sediment PYR15

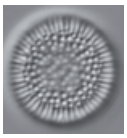
1


2

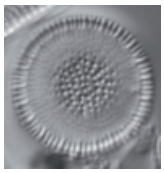
3

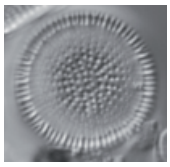
4

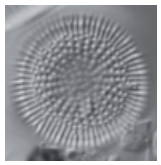
5

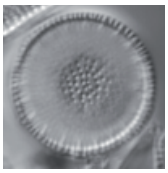
6

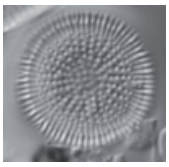
7

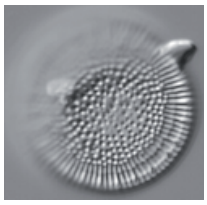
8

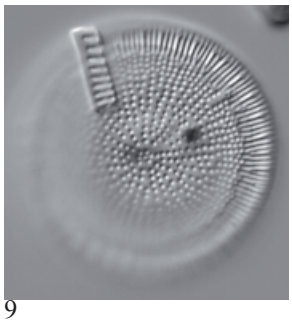
9

Plate 4 LM: x1500

Figs. 1-12 *Cyclotella intermedia* (Manguin) Houk, Klee & Tanaka

Figs. 1-7 Lake Airoto, sediment PYR73

Figs. 8-12 Lake Sen, sediment PYR40

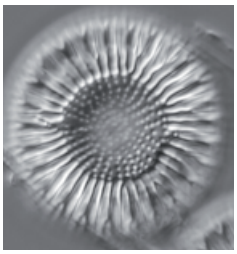

1

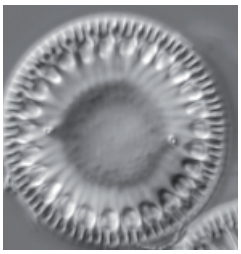

2

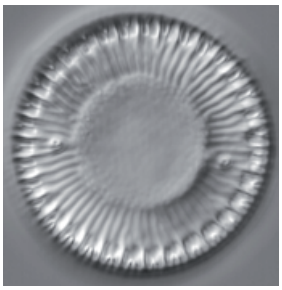

3

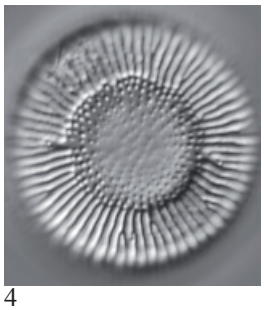

4

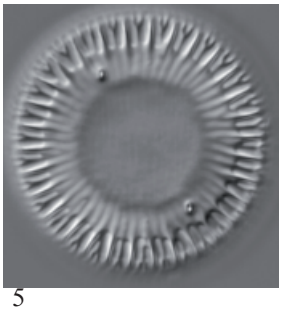

5

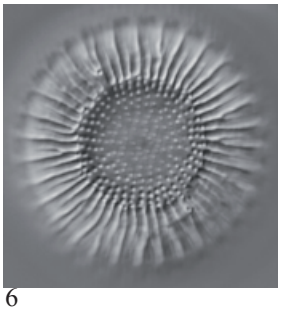

6

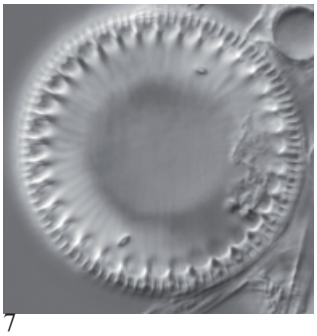

7

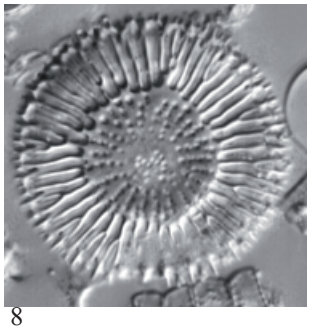

8

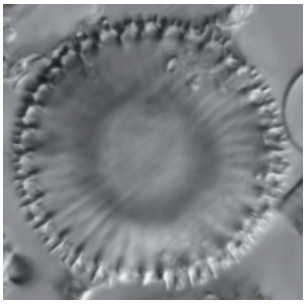

9

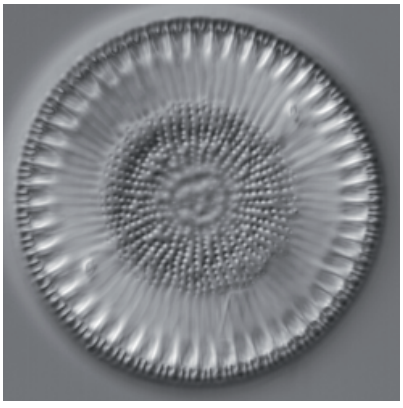

10

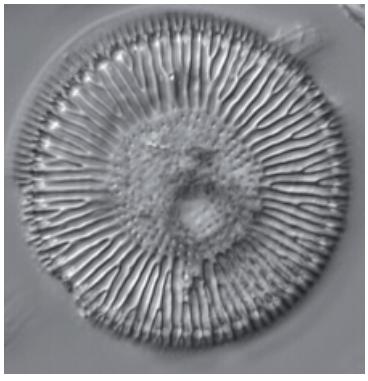

11

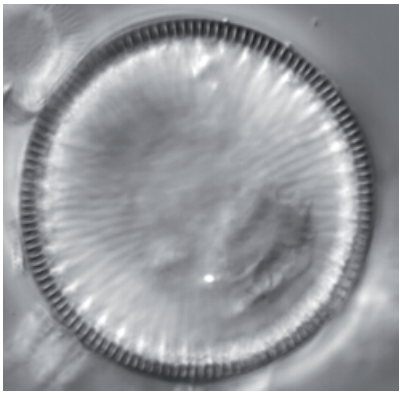

12

Plate 5 LM: x1500
SEM: Fig. 16 x15000

Figs. 1-4	*Cyclotella antiqua* Smith
Figs. 5-16	*Cyclotella* sp. No. 3 laurenti, aff. *cyclopuncta* Håkansson & Carter
Fig. 17	*Cyclotella ocellata* Pantocsek
Fig. 18	*Cyclotella* cf. *polymorpha* Meyer & Håkansson
Fig. 19	*Cyclotella* cf. *comensis* Grunow
Fig. 20-22	*Orthosira roeseana* (Rabenhorst) O'Meara

Figs. 1-2	Lake Sen, sediment PYR40
Figs. 3,4,19,20	Lake Estom, sediment PYR15
Figs. 5-11,16	Lake Laurenti, sediment PYR111
Figs. 12, 14, 15	Lake Acherito, sediment PYR27
Fig. 13	Lake Les Laquettes 1, sediment PYR27
Fig. 17	Lake Glacé, sediment PYR42
Fig. 18	Lake Puis, epilithic EpiPYR45
Figs. 21-22	Lake Monges, sediment PYR57

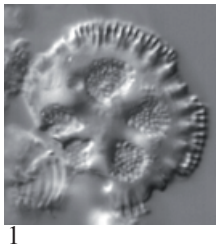
1


2


3


4


5


6


7


8


9


10


11


12


13


14


15

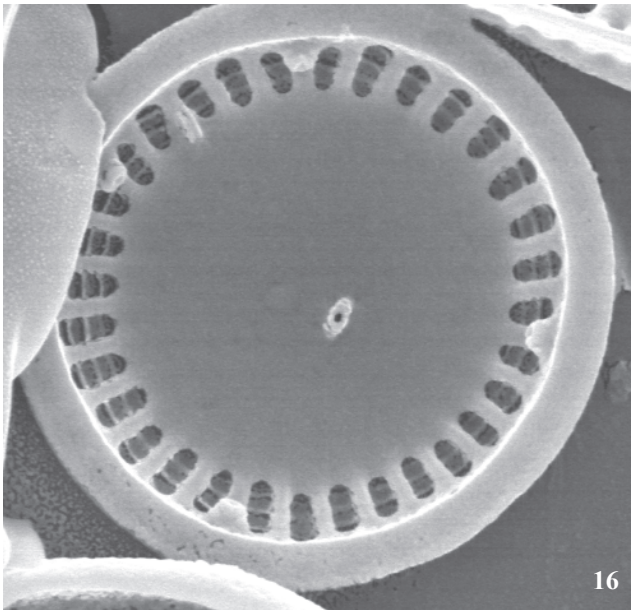
16

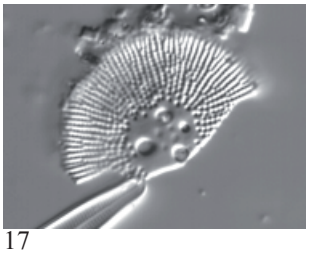
17


18


19


20

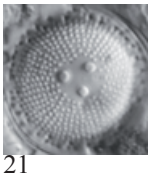
21


22

Plate 6 LM: x1500
SEM: x11000

Fig. 1 *Cyclotella* sp. No. 2 Llong

Figs. 2-16 *Discotella* sp. No. 1 Gerber

Figs. 17-25 *Discostella stelligera* (Cleve & Grunow) Houk & Klee

Fig. 1	Lake Llong, sediment PYR51
Fig. 3	Lake Llebreta, sediment PYR58
Figs. 4-13	Lake Gerber, sediment PYR63
Figs. 14-16	Lake Redon, sediment REDOM
Figs 17-24	Lake Port Bielh, sediment PYR28
Fig. 25	Lake Gros de Camporrells, sediment PYR110


1


2


3


4


5


6


7


8


9


10


11


12


13


14

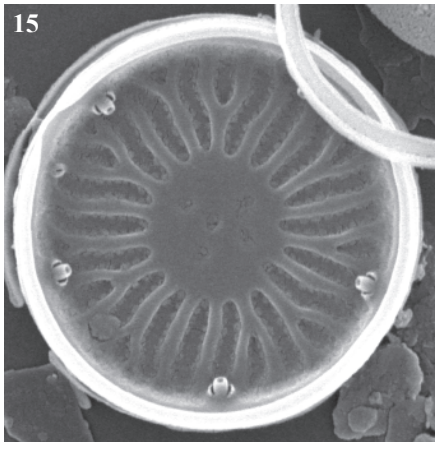
15

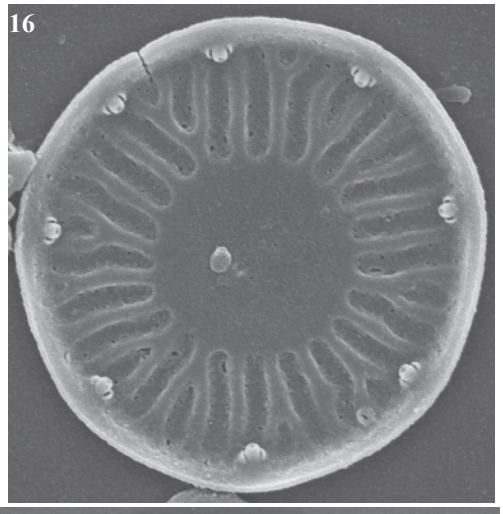
16


17


18


19


20


21


22


23


24

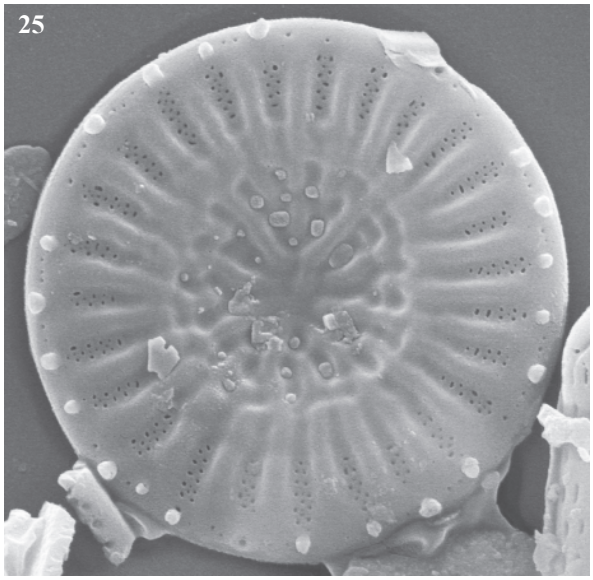
25

Plate 7 LM: x1500
SEM: x4000

Figs. 1-11 *Aulacoseira pfaffiana* (Reinsch) Krammer

Figs. 1-5 Lake Bleu de Rabassoles, sediment PYR112

Figs. 6, 7, 9 Lake Illa, sediment PYR66

Figs. 8, 10, 11 Lake Senó, sediment PYR84

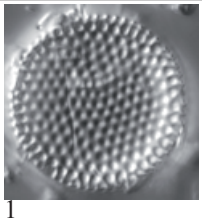
1

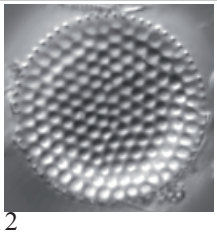
2

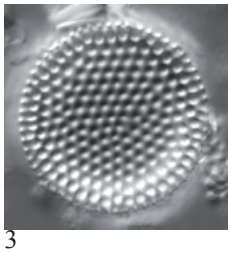
3

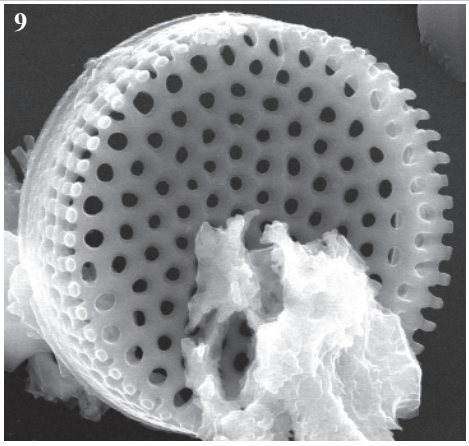
9


4

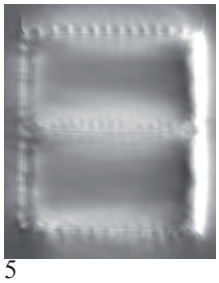
5

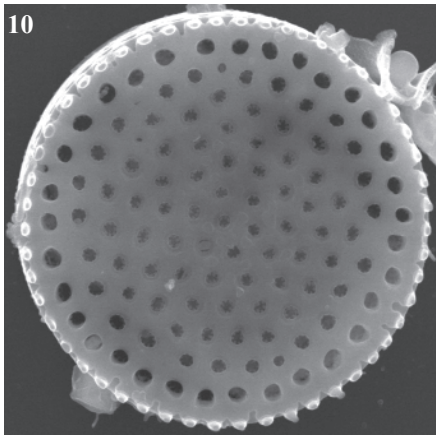
10


6


7

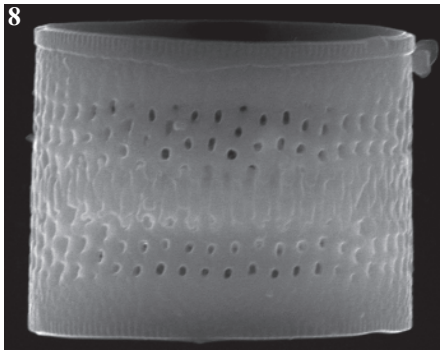
8

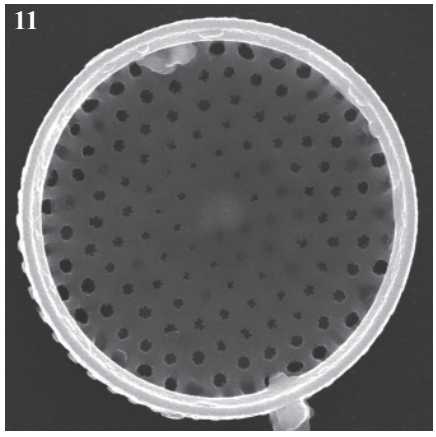
11

Plate 8 LM: x1500

Fig. 1	*Aulacoseira granulata* (Ehrenberg) Simonsen
Figs. 2-4	*Aulacoseira crenulata* (Ehrenberg) Thwaites
Figs. 5-6	*Aulacoseira valida* (Grunow) Krammer
Figs. 7-11	*Aulacoseira* cf. *valida* (Grunow) Krammer
Figs. 12-15	*Aulacoseira* cf. *subarctica* (O. Müller) Haworth
Figs. 16-20	*Aulacoseira perglabra* (Østrup) Haworth

Fig. 1	Lake Forcat Inferior, sediment PYR77
Figs. 2-6, 18-22	Lake Albe, sediment PYR96
Figs. 7-8	Lake Siscar, sediment PYR126
Figs. 9-15	Lake Ensangents Superior, sediment PYR106
Figs. 16-17	Lake Llong, sediment PYR59

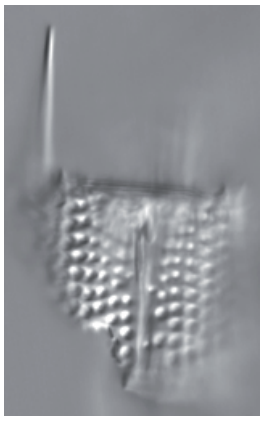
1

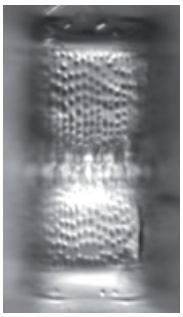
2

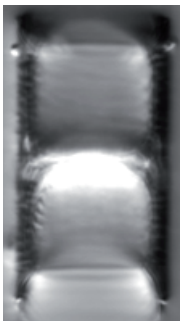
3


4


5


6


7

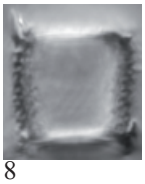
8


9

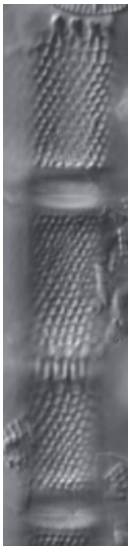
10

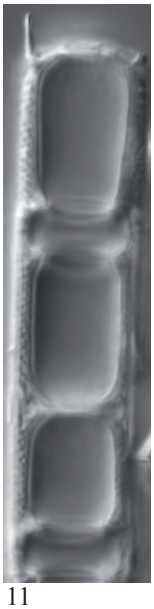
11


12


13


14


15


16

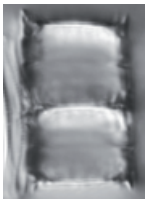
17


18

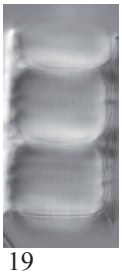
19

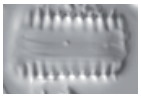
20

Plate 9 LM: x1500
SEM: Figs. 8-10 x4000, Fig. 11 x10000

Figs. 1-11 *Aulacoseira lirata* (Ehrenberg) Ross

Figs. 1-2, 8-11	Lake Redon, sediment REDOM
Figs. 3-4, 7	Lake Albe, sediment PYR96
Figs. 5-6	Lake Posets, sediment PYR42


1

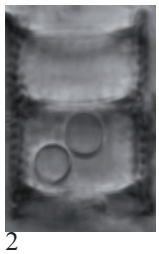
2


3


4

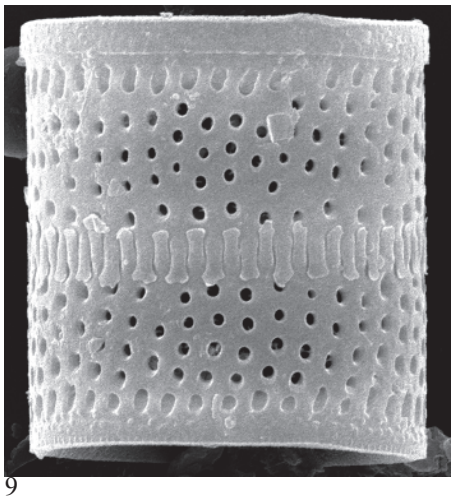
9

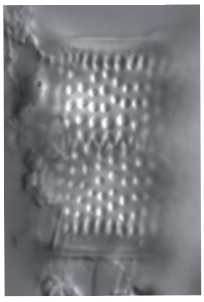
5


6

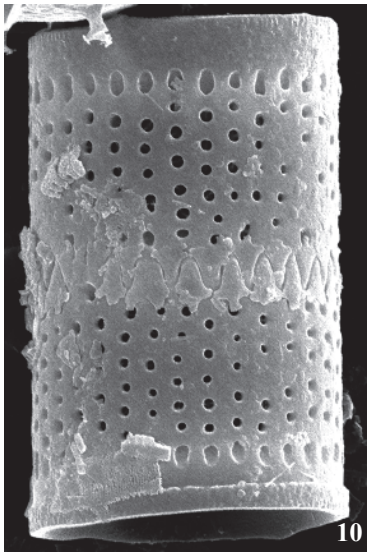
10


7

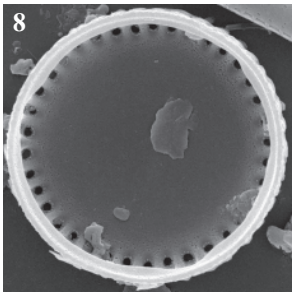
8

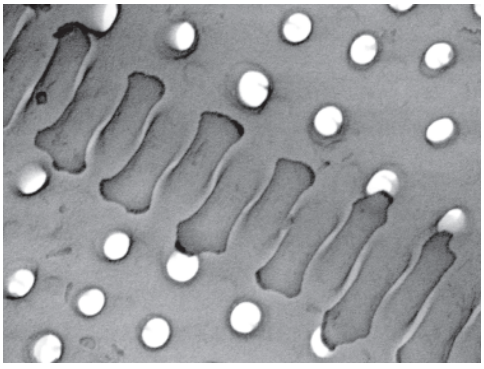
11

Plate 10 LM: x1500

Figs. 1-2	*Aulacoseira* cf. *lirata* var. *biseriata* (Grunow) Haworth
Figs. 3-6	*Aulacoseira* cf. *ambigua* (Grunow) Simonsen
Figs. 7-22	*Aulacoseira* sp. No. 1 Gerber
Figs. 23-44	*Aulacoseira* cf. *alpigena* (Grunow) Krammer

Figs. 1-4	Lake Redón, sediment REDOM
Figs. 5-6	Lake Cregueña, sediment PYR49
Figs. 7-22	Lake Gerber, sediment PYR63
Figs. 23-24	Lake Les Laquettes 1, sediment PYR27
Figs. 25-28	Lake Forcat Inferior, sediment PYR77
Figs. 29-32	Lake Pica, sediment PYR100
Figs. 33-40	Lake Bleu de Rabassoles, sediment PYR112
Figs. 41-44	Lake Negre, sediment PYR79

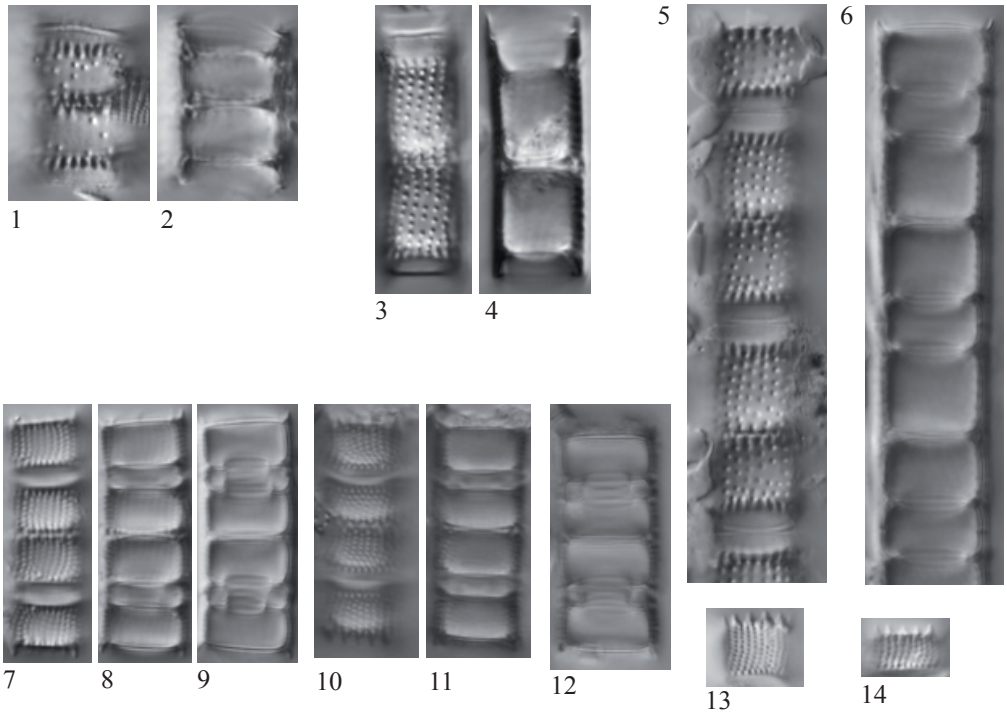
1
2
3
4
5
6
7
8
9
10
11
12
13
14
15
16
17
18
19
20
21
22
23
24
25
26
27
28
29
30
31
32
33
34
35
36
37
38
39
40
41
42
43
44

Plate 11 LM: x1500
SEM: x4000

Figs. 1-5	*Aulacoseira distans* (Ehrenberg) Simonsen
Fig. 6	*?Aulacoseira distans* (Ehrenberg) Simonsen
Figs. 7-9	*Aulacoseira humilis* (Cleve-Euler) Genkal & Trifonova in Trifonova & Genkal
Figs. 10-16	*Aulacoseira* sp.
Figs. 17-19	*Aulacoseira* cf. *nygaardii* (Camburn) Camburn & Charles

Figs. 1-5	Lake Negre, sediment PYR79
Fig. 6	Lake Redon, sediment REDOM
Figs. 7-10, 14-16	Lake Albe, sediment PYR96
Figs. 11-13	Lake Llong, sediment PYR59
Figs. 17-19	Lake Sotllo, sediment PYR89


1


2

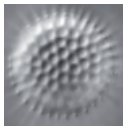
3


4


5

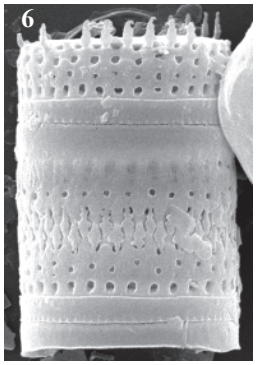


7


8


9


10


11


12


13


14


15


16


17


18


19

Plate 12 LM: x1500
SEM: x6000

Fig. 1	*Diatoma vulgaris* Bory
Figs. 2-8	*Diatoma mesodon* Kützing
Figs. 9-14	*Diatoma hyemalis* (Roth) Heiberg sensu Krammer & Lange-Bertalot 1991
Fig. 15	*Diatoma* sp. No. 1 Estom
Figs. 16-17	*Meridion circulare* var. *constrictum* (Ralfs) Van Heurck sensu Krammer & Lange-Bertalot 1991
Figs. 18-22	*Meridion circulare* (Greville) Agardh

Fig. 1	Lake Roumassot, sediment PYR04
Figs. 2, 7, 18	Lake Arratille, sediment PYR11
Fig. 3	Lake Posets, sediment PYR42
Figs. 4, 5, 8, 12	Lake Llebreta, sediment PYR58
Figs. 6, 19, 22	Lake Laurenti, sediment PYR111
Figs. 9-11, 13-15	Lake Estom, sediment PYR15
Fig. 16	Lake Labas, sediment PYR63
Fig. 17	Lake Estelat, sediment PYR120
Fig. 20	Lake Baiau Superior, sediment PYR76
Fig. 21	Lake Burg, sediment BURG1210


1


2


3


4


5

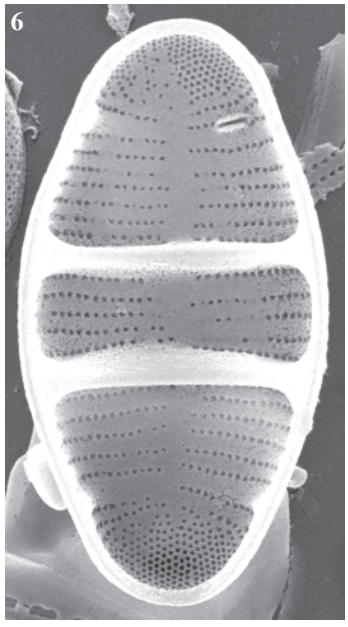
6


7


8


9


10


11


12


13


14

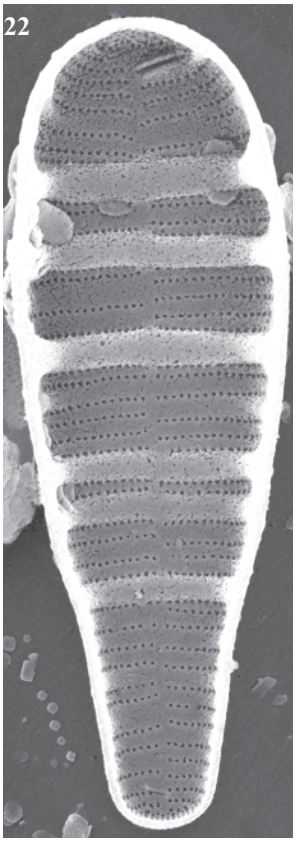
22


21


18


19


20


15


16


17

Plate 13 LM: x1500

Figs. 1-23	*Tabellaria flocculosa* (Roth) Kützing
Figs. 23-25	*Tabellaria ventricosa* Kützing
Fig. 27	*Tabellaria fenestrata* (Lyngbye) Kützing
Figs. 28-29	*Asterionella formosa* Hassall

Figs. 1-4	Lake Pica, epilithic EpiPYR100
Figs. 5-8, 11-16	Lake Senó, epilithic EpiPYR84
Figs. 9-10	Lake Bleu de Rabassoles, epilithic EpiPYR112
Figs. 17, 19, 21	Lake L`Estagnol, epilithic EpiPYR119
Fig. 18	Lake L`Estagnol, sediment PYR119
Figs. 22, 27	Lake Llebreta, sediment PYR58
Figs. 23, 24, 26	Lake Senó, sediment PYR84
Fig. 25	Lake Senó, epilithic EpiPYR84
Fig. 28	Lake Bersau, sediment PYR03
Fig. 29	Lake Airoto, sediment PYR73

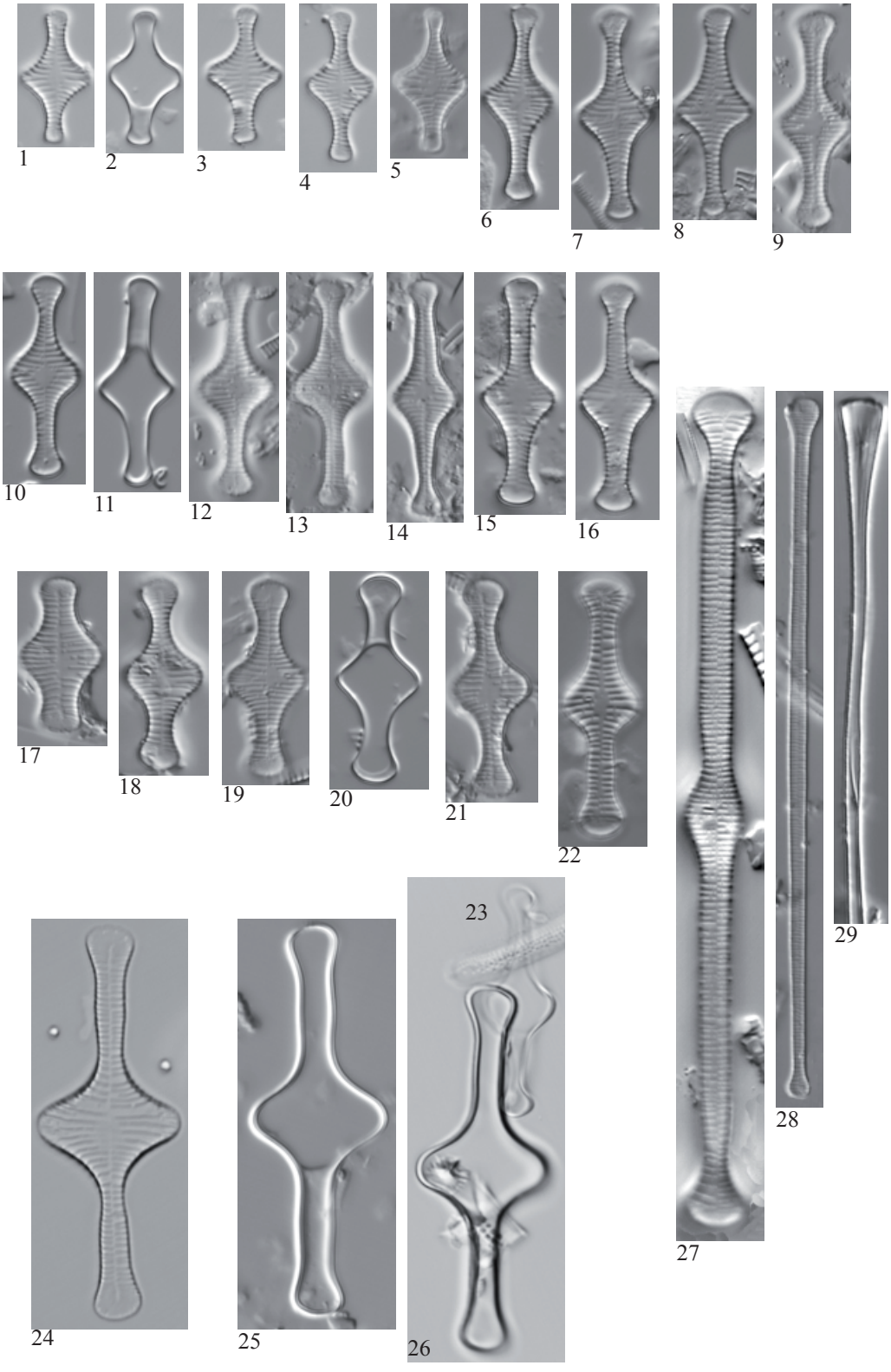
1
2
3
4
5
6
7
8
9
10
11
12
13
14
15
16
17
18
19
20
21
22
23
24
25
26
27
28
29

Plate 14 LM: x1500
SEM: Figs. 4-5 x2000, Fig. 22 x6000, Fig. 25 x9000, Figs. 23-24, 26-27 x10000

Fig. 1-2	*Fragila* sp. No. 1 Airoto
Figs. 3-5, 23-28	*Fragilaria delicatissima* (Smith) Lange-Bertalot
Figs. 6-13	*Fragilaria sp. (*?nanoides)
Figs. 14-17	*Fragilaria* cf. *gracilis* Østrup
Figs. 18-19	*Fragilaria* cf. *tenera (Smith) Lange-Bertalot*
Fig. 20	*Fragilaria saxoplanctonica* nom. prov.
Fig. 21	*Fragilaria* cf. *nanana* Lange-Bertalot
Fig. 22	*Fragilaria* cf. *nanoides* Lange-Bertalot

Figs. 1, 10-13	Lake Airoto, sediment PYR73
Fig. 2	Lake Les Laquettes, sediment PYR27
Figs. 3-5, 23-28	Lake Redón, sediment REDOM
Figs. 6-9	Lake Sen, sediment PYR40
Figs. 14, 18, 20	Lake Bersau, sediment PYR03
Fig. 19	Lake Posets, sediment PYR42
Fig. 21	Lake Tourrat, sediment PYR23
Fig. 22	Lake Monges, sediment PYR57

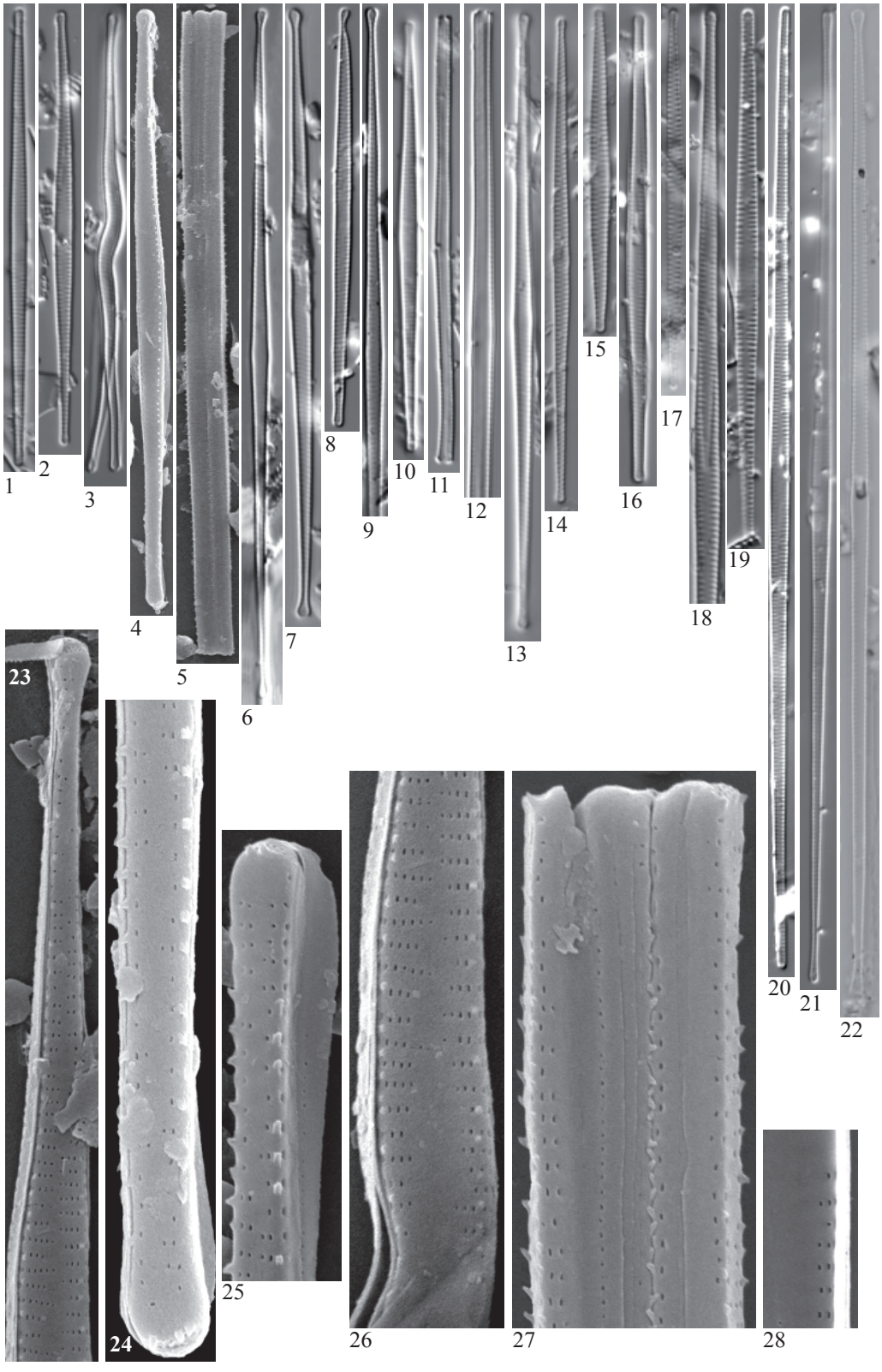
1
2
3
4
5
6
7
8
9
10
11
12
13
14
15
16
17
18
19
20
21
22
23
24
25
26
27
28

Plate 15 LM: x1500

Figs. 1-27	*Fragilaria* cf. *pararumpens* Lange-Bertalot, Hofmann & Werum
Figs. 28-31	*Fragilaria* spp.
Fig. 32	*Fragilaria* sp.
Fig. 33-41	*Fragilaria* sp. No. 2 Bersau
Fig. 42	*Fragilaria* sp. No. 3 Airoto
Fig. 43	*Fragilaria* cf. *rumpens* (Kützing) Carlson
Figs. 44-46	*Fragilaria* cf. *perminuta* (Grunow) Lange-Bertalot
Figs. 47-48	*Fragilaria* cf. *vaucheriae* (Kützing) Petersen
Fig. 49	*Fragilaria* cf. *recapitellata* Lange-Bertalot & Metzeltin
Fig. 50	*Fragilaria* sp. No. 4 Laquettes

Figs. 1-15, 18-28, 32-41	Lake Bersau, sediment PYR03
Figs. 16-17	Lake Burg, sediment BURG1007
Figs. 29-31	Lake Sen, sediment PYR40
Figs. 42	Lake Airoto, sediment PYR73
Fig. 43	Lake Eriste, sediment PYR43
Figs. 44-45	Lake Inferior de la Gallina, sediment PYR87
Fig. 46	Lake Bleu de Rabassoles, sediment PYR112
Fig. 47-49	Lake Llebreta, sediment PYR58
Fig. 50	Lake Les Laquettes, sediment PYR27

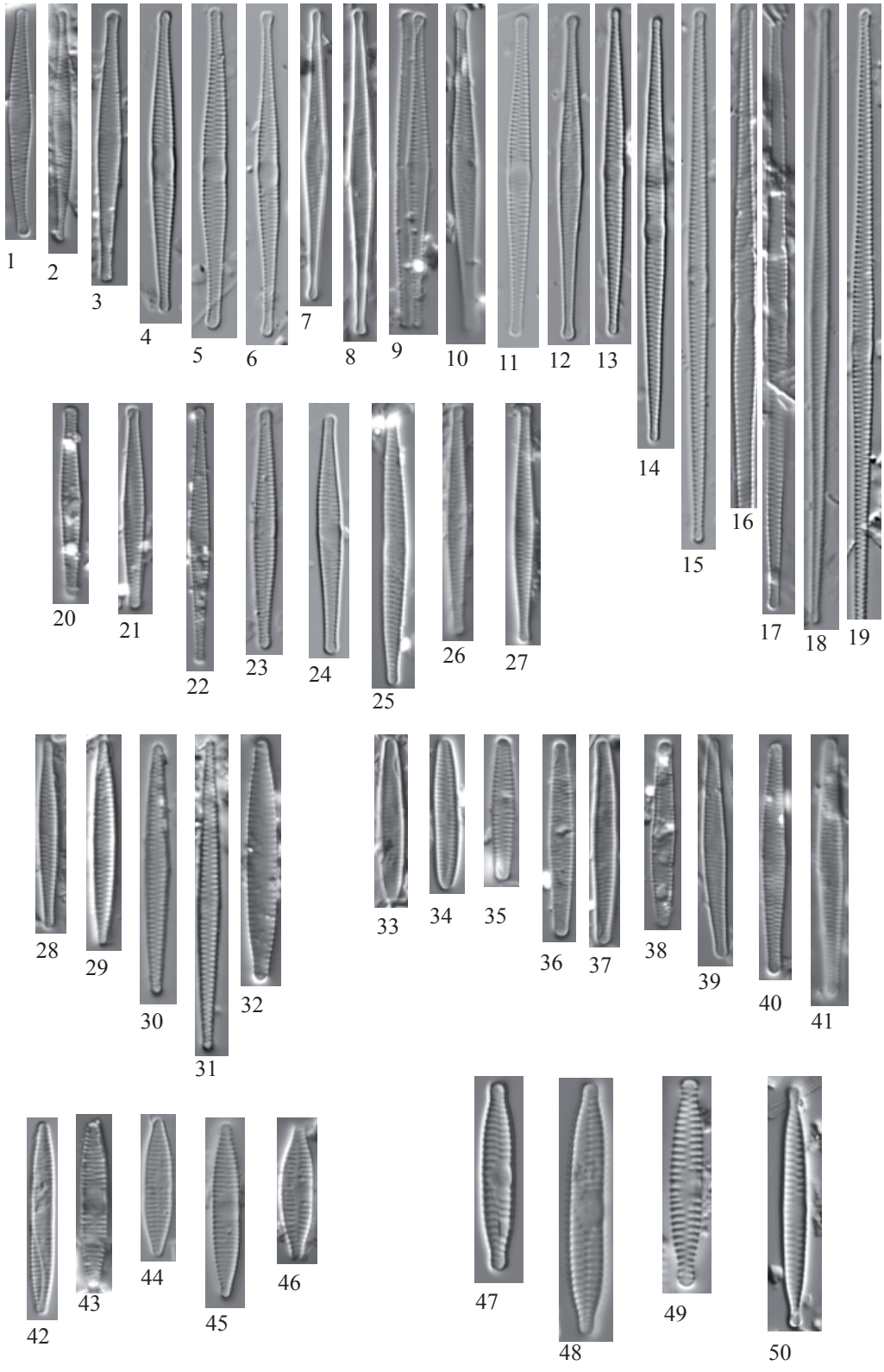
1
2
3
4
5
6
7
8
9
10
11
12
13
14
15
16
17
18
19
20
21
22
23
24
25
26
27
28
29
30
31
32
33
34
35
36
37
38
39
40
41
42
43
44
45
46
47
48
49
50

Plate 16 LM: x1500
SEM: Fig. 11 x3500, Fig. 12 x3000

Fig. 1	*Fragilaria* sp. No. 5 Aube, aff. *F. nevadensis* Linares-Cuesta & Sanchez-Castillo
Figs. 2-8	*Fragilaria alpestris* Krasske
Figs. 9-11	*Fragilaria* sp. No. 6 Blaou
Figs. 12-14	*Stauroforma* cf. *exiguiformis* (Lange-Bertalot) Flower, Jones & Round
Fig. 15	*Fragilaria* cf. *mesolepta* Rabenhorst
Figs. 16-17	*Fragilaria* sp. No. 7 Arratille
Figs. 18-19	*Staurosira parasitoides* Lange-Bertalot, Schmidt & Klee
Fig. 20	*Pseudostaurosira* cf. *microstriata* (Marciniak) Flower
Figs 21-22	*Pseudostaurosira parasitica* (Smith) Morales
Fig. 23	*Pseudostaurosira parasitica* var. *subconstricta* (Grunow) Morales

Fig. 1	Lake Senó, sediment PYR84
Figs. 2-8	Lake Helado del Monte Perdido, sediment PYR19
Figs. 9-10	Lake Blaou, epilithic EpiPYR94
Fig. 11	Lake Port Bielh, sediment PYR28
Fig. 12	Lake Redon, sediment REDOM
Fig. 13	Lake Plan, sediment PYR69
Fig. 14	Lake Romedo de Dalt, sediment PYR85
Fig. 15	Lake Burg, sediment BURG1169
Figs. 16-17, 20	Lake Arratille, sediment PYR11
Figs. 18-19, 21	Lake Acherito, sediment PYR01
Fig. 22	Lake Sen, sediment PYR40
Fig. 23	Lake Posets, sediment PYR42

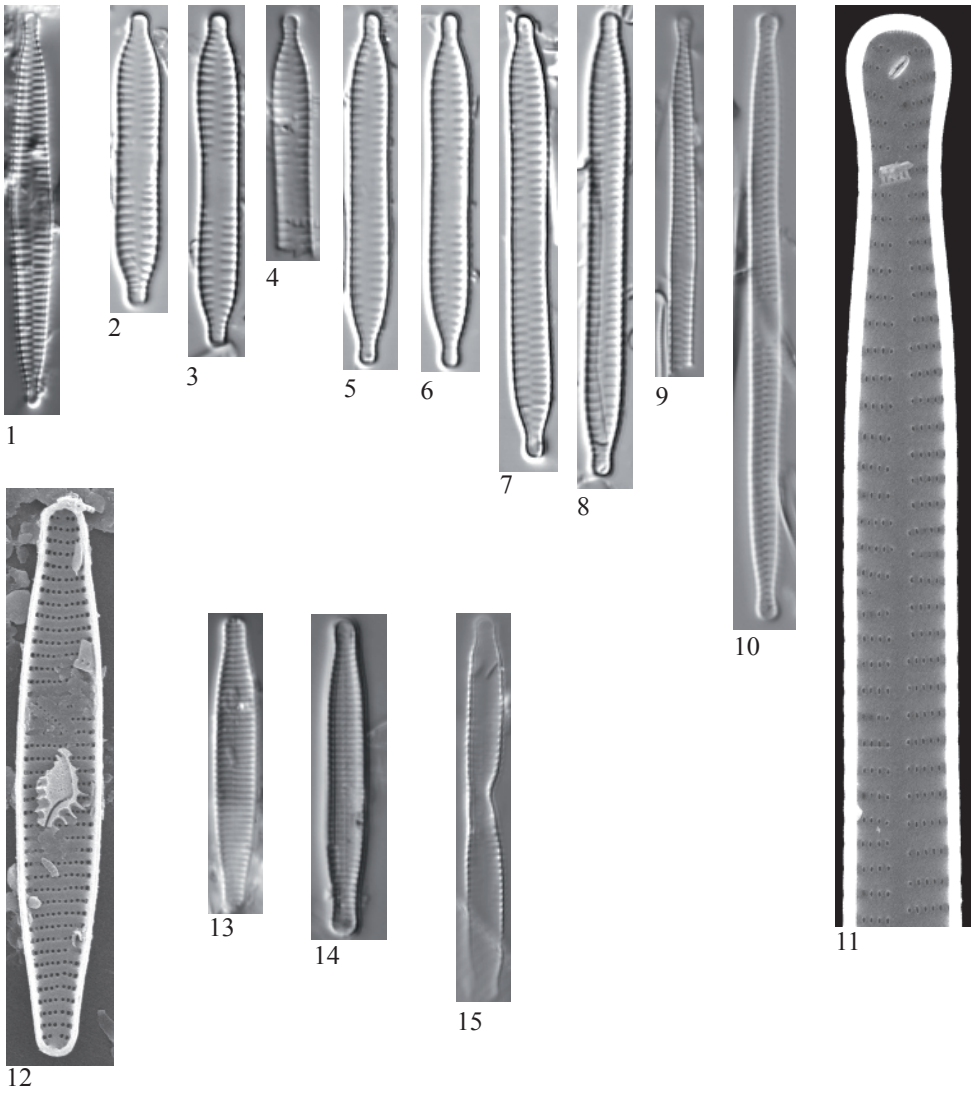
1
2
3
4
5
6
7
8
9
10
11
12
13
14
15
16
17
18
19
20
21
22
23

Plate 17 LM: x1500
SEM: Figs. 9-10,13 x10000, Figs.21-22 x6000

Figs. 1-10 *Pseudostaurosira microstriata* (Marciniak) Flower

Figs. 11-12 *Pseudostaurosira* cf. *brevistriata* (Grunow) Williams & Round

Fig. 13 *Pseudostaurosira* sp.

Fig. 14 *Pseudostaurosira* sp.

Figs. 15-22 *Fragilaria* cf. *opacolineata* Lange-Bertalot

Figs. 1-4, 9-10	Lake Posets, sediment PYR42
Figs. 5-7, 11-12	Lake Arratille, sediment PYR11
Figs. 8, 14	Lake Sen, sediment PYR40
Fig. 13	Lake Port Bielh, sediment PYR28
Figs. 15, 17-18	Lake Siscar, sediment PYR126
Fig. 16	Lake Ensangents Superior, sediment PYR106
Fig. 19	Lake Canals Roges, sediment PYR124
Fig. 20	Lake Basa de la Mora, sediment PYR32
Figs. 21-22	Lake Argonella de Mes Amunt, sediment PYR78

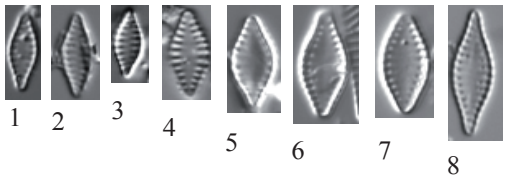
1 2 3 4 5 6 7 8

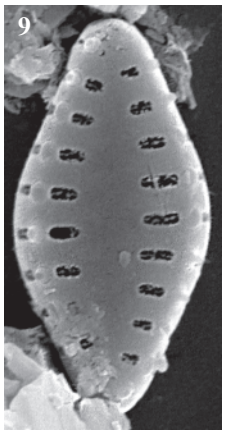
9


10

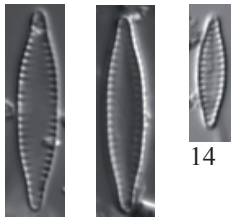
11 12 14

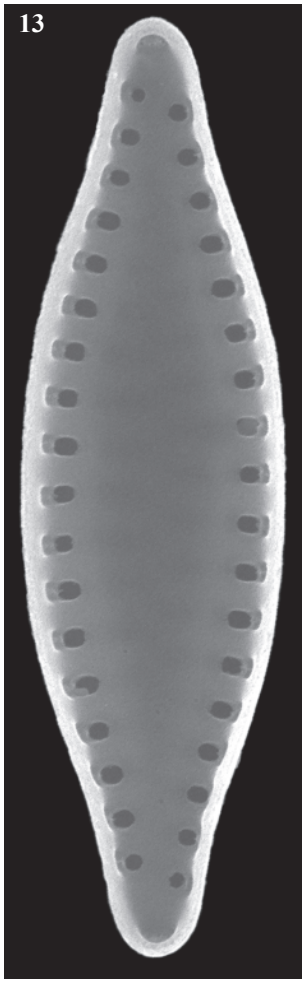
13


15 16 17 18 19 20


21

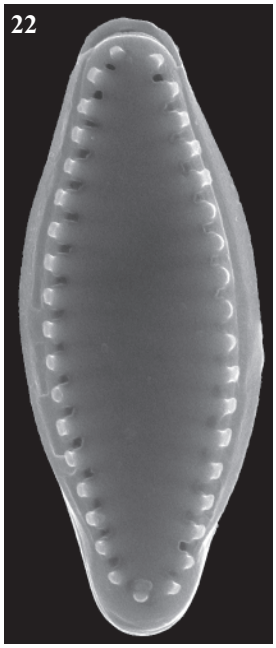
22

Plate 18 LM: x1500
SEM: x6000

Figs. 1-6	*Pseudostaurosira pseudoconstruens* (Marciniak) Williams & Round
Figs. 7-8	*Pseudostaurosira* cf. *robusta* (Fusey) Williams & Round
Figs. 9-11	*Pseudostaurosira robusta (Fusey) Williams & Round*
Figs. 12-38	*Pseudostaurosira* sp. No. 1 Arratille
Figs. 39-41	*Pseudostaurosira* sp. No. 2 Acherito
Fig. 42-43	*Tabularia fasciculata* (Agardh) Williams & Round

Fig. 1	Lake Burg, sediment
Figs. 2, 11	Lake Estom, sediment PYR15
Figs. 3, 13, 15, 31-32	Lake Sen, sediment PYR40
Figs. 4-6, 12, 14, 16-21, 23-30, 33-35	Lake Arratille, sediment PYR11
Fig. 7	Lake Siscar, sediment PYR126
Fig. 8	Lake Posets, sediment PYR42
Fig. 9	Lake Burg, sediment BURG1136
Fig. 10	Lake Burg, sediment BURG1132
Figs. 22, 37-38, 42	Lake Laurenti, sediment PYR111
Fig. 36	Lake Arnales, sediment PYR09
Figs. 39-41, 43	Lake Acherito, sediment PYR01

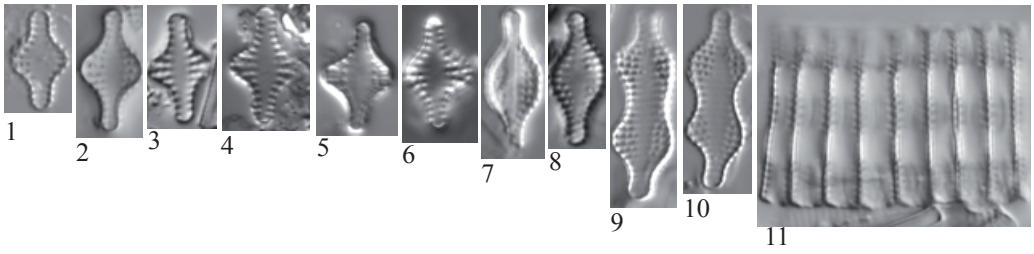
1
2
3
4
5
6
7
8
9
10
11

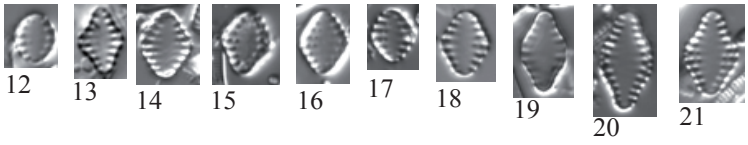
12
13
14
15
16
17
18
19
20
21

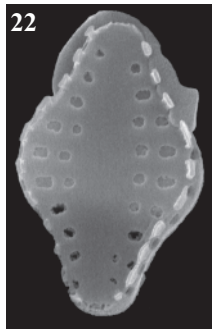
22

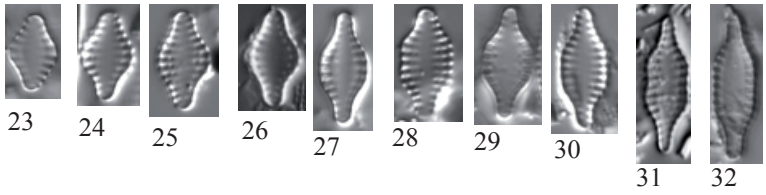
23
24
25
26
27
28
29
30
31
32

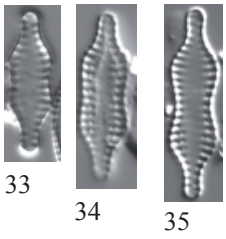
33
34
35

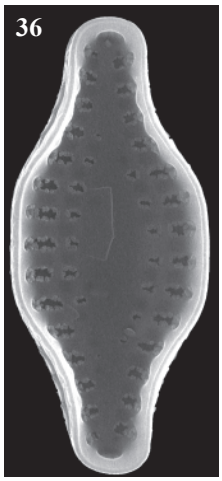
36


37


38


39


40

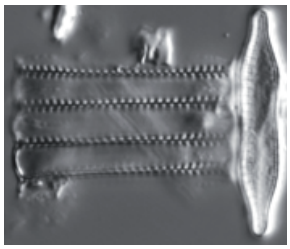
41


42


43

Plate 19 LM: x1500
SEM: Fig. 3 x 20000, Fig. 4x6000

Figs. 1-4	?*Pseudostaurosira robusta (Fusey) Williams & Round*
Figs. 5-22	*Staurosirella pinnata* (Ehrenberg) Williams & Round sensu lato
Figs. 23-31	*Staurosirella* cf. *confusa* Morales
Fig. 32	*Staurosirella oldenburgiana* (Hustedt) Morales
Figs. 33-51	*Staurosirella pinnata* (Ehrenberg) Williams & Round sensu lato
Figs. 52-55	*Punctastriata* cf. *lancettula* (Schumann) Hamilton & Siver M3
Figs. 56-57	*Staurosirella leptostauron* (Ehrenberg) Williams & Round

Figs. 1, 5-8, 19-25 28-30, 33-36 41-46, 48-51	Lake Arratille, sediment PYR11
Fig. 2	Lake Posets, sediment PYR42
Figs. 3-4	Lake Roumassot, sediment PYR04
Figs. 9-12, 26-27	Lake Burg, sediment BURG 953
Fig. 13-14	Lake Sen, sediment PYR40
Figs. 15-18	Lake Posets, sediment PYR42
Fig. 31	Lake Burg, sediment BURG 857
Fig. 32	Lake Arnales, sediment PYR09
Figs. 37, 39, 40, 47 52-54	Lake Burg, sediment BURG 543
Fig. 38	Lake Burg, sediment BURG 1192
Fig. 55	Lake Burg, sediment BURG 694
Fig. 56	Lake Acherito, sediment PYR01
Fig. 57	Lake Laurenti, sediment PYR111


1


2

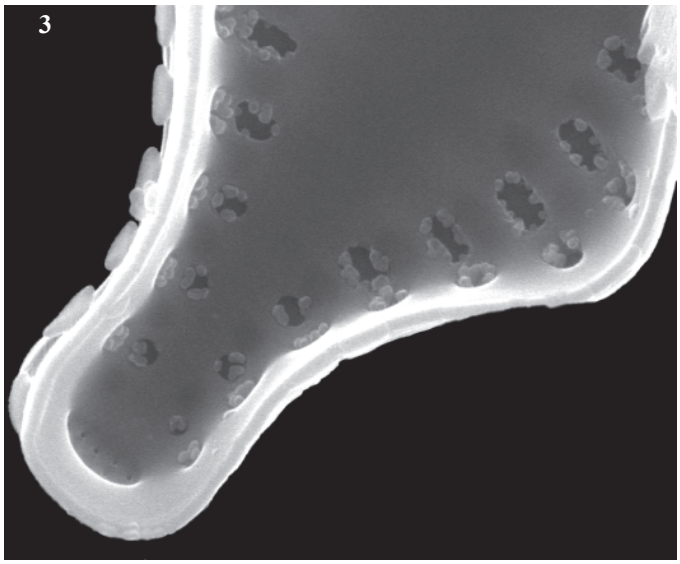
3

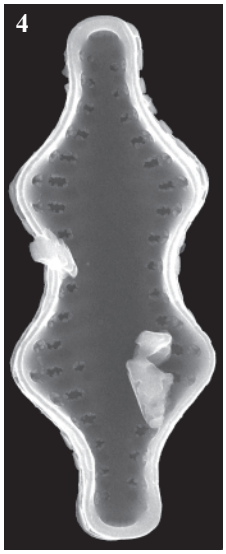
4


5-18

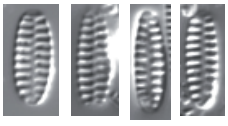
19-22

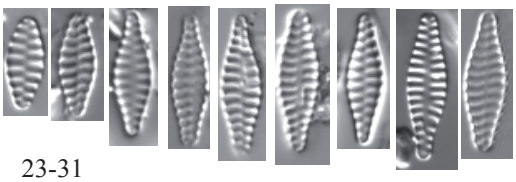
23-31


32

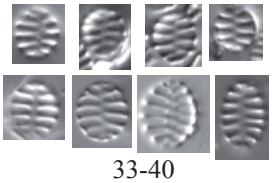
33-40

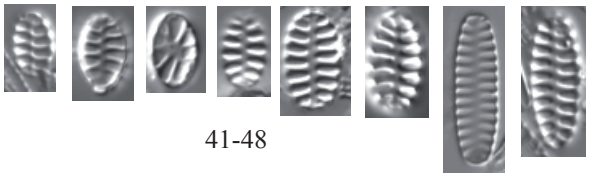
41-48


49


50


51


52


53


54


55


56


57

Plate 20 LM: x1500
SEM: Figs. 1-5,9 x5000, 7-8 x10000

Figs. 1-4, 7 *Staurosirella pinnata* (Ehrenberg) Williams & Round

Figs. 5-6 *Staurosirella* cf. *confusa* Morales

Figs. 8-9 *Punctastriata lancettula* (Schumann) Hamilton & Siver

Fig. 1	Lake Gran de Mainera, sediment PYR70
Figs. 2, 5-6, 9	Lake Laurenti, sediment PYR111
Fig. 3	Lake Gors de Camporrells, sediment PYR110
Fig. 4	Lake Posets, sediment PYR42
Figs. 7-8	Lake Burg, sediment BURG 930

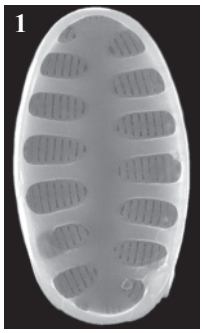
1

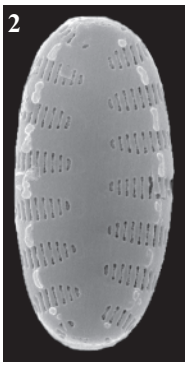
2

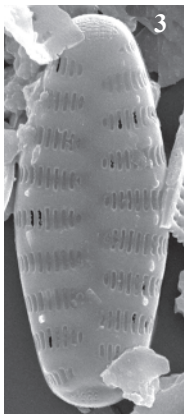
3

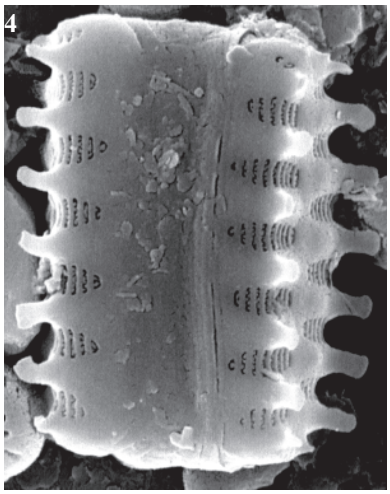
4

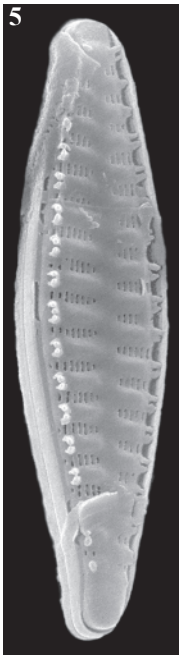
5

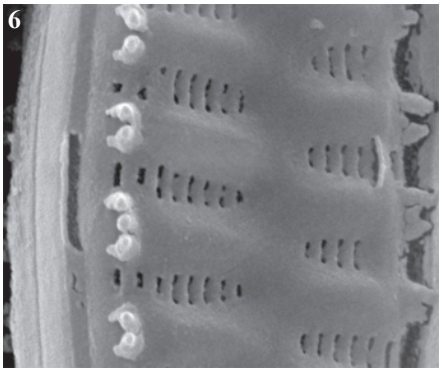
6


7

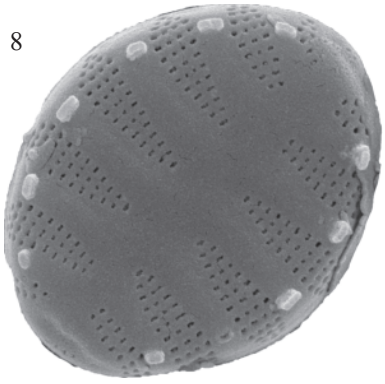
8


9

Plate 21 LM: Figs. 1.5, 7-8 x1500, Fig. 9 x750
SEM: x6000

Figs. 1-6 *Hannaea arcus* (Ehrenberg) Patrick
Figs. 7-9 *Ulnaria biceps* (Kützing) Compère *sensu lato*

Fig. 1	Lake Llebreta sediment PYR58
Figs. 2, 7-9	Lake Arratille, sediment PYR11
Fig. 3	Lake Redon, sediment REDOM
Fig. 4	Lake Les Laquettes 1, sediment PYR27
Fig. 5	Lake Inferior de la Gallina, sediment PYR87
Fig. 6	Lake Laurenti, sediment PYR111

1

2

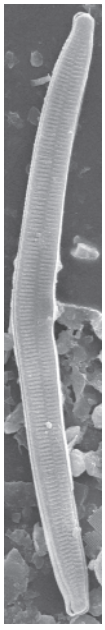

3

4

5

9

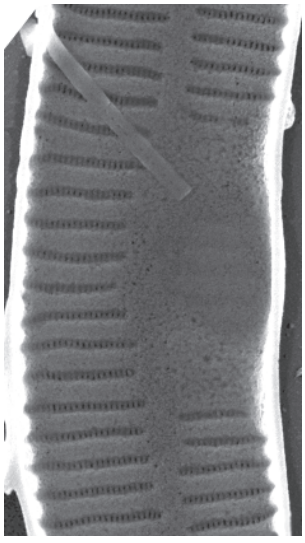

6

7

8

Plate 22 LM: x1500
SEM: Figs. 43-47 x10000, Figs. 48-49 x8000

Figs. 1-7	*Staurosira construens* Ehrenberg *sensu lato*
Figs. 8-32 43-48	*Staurosira construens* var. *venter* (Ehrenberg) Hamilton
Figs. 33-36	*Staurosira construens* aff. f. *subsalina* (Hustedt) Bukhtiyarova
Figs. 37-39	*Staurosira construens* var. *binodis* (Ehrenberg) Hamilton
Figs. 40-42, 49	*Staurosira construens* aff. var. *venter* (Ehrenberg) Hamilton

Figs. 1-2, 4-7, 8, 10	Lake Burg, sediment BURG 543
Figs. 3, 22, 31-32	Lake Burg, sediment BURG 1136
Fig. 11	Lake Burg, sediment BURG 853
Fig. 12	Lake Burg, sediment BURG 844
Figs. 13-14	Lake Burg, sediment BURG 831
Fig. 15	Lake Estom, sediment PYR15
Figs. 16-17	Lake Sen, sediment PYR40
Figs. 19-24, 30	Lake Arratille, sediment PYR11
Figs. 26-29, 39	Lake Ormiélas, sediment PYR05
Figs. 33-35	Lake Burg, sediment BURG 513
Fig. 36	Lake Les Laquettes 1, sediment PYR27
Fig. 37	Lake Burg, sediment BURG 420
Fig. 38	Lake Burg, sediment BURG 1181
Fig. 39	Lake Asnos, sediment PYR14
Figs. 41-42	Lake Acherito, sediment PYR01
Figs. 43-47	Lake Burg, sediment BURG 930
Fig. 48	Lake Mariola, sediment PYR80
Fig. 49	Lake Port Bielh, sediment PYR28


1


2


3


4


5


6


7

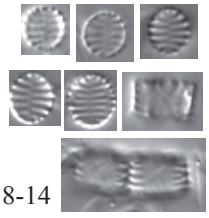
8-14


15


16


17


18


19


20


21


22


23


24


25


26


27


28


29


30


31


32


33


34


35


36


37


38


39


40


41


42

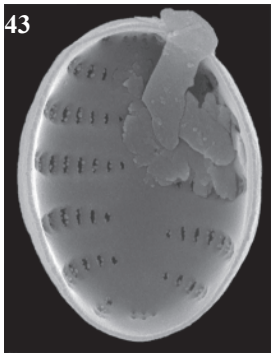
43

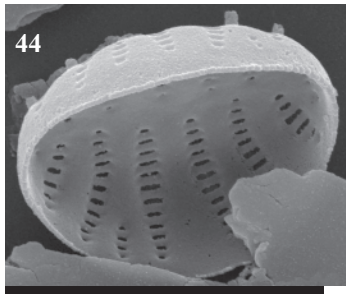
44

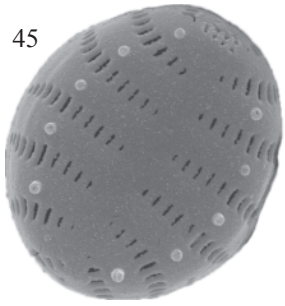
45

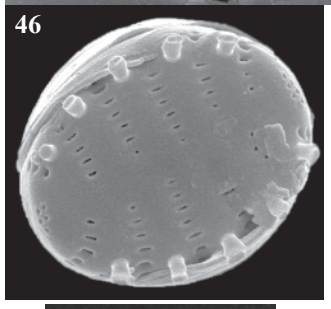
46

47

48

49

Plate 23 LM: x1500
SEM: x7500

Figs. 1-13 *Eunotia palatina* Lange-Bertalot & Krüger

Fig. 14 *Eunotia* cf. *palatina* Lange-Bertalot & Krüger

Fig. 1 Lake Airoto, sediment PYR73

Figs. 2-13 Lake Pica, sediment PYR100

Fig. 14 Lake Monges, sediment PYR57

Fig. 13 Manfred Ruppel photo


1


2


3


4


5


6


7


8


9


10


11


12

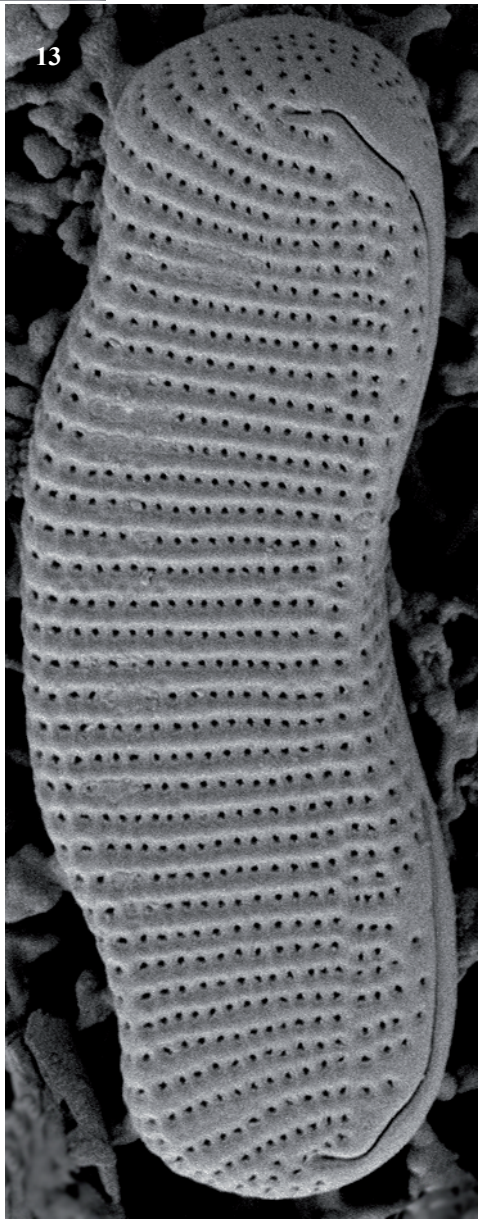
13


14

Plate 24	LM: x1500 SEM: Figs. 4-5 x2000, Fig. 22 x6000, Fig. 25 x9000, Figs. 23-24, 26-27 x 10000

Figs. 1-11	*Eunotia catalana* Lange-Bertalot & Rivera-Rondón
Fig. 12	*Eunotia lapponica* Grunow ex Cleve

Fig. 1	Lake Sotllo, epilithic EpiPYR89
Figs. 2-4, 9-12	Lake Baiau Superior, sediment PYR76
Figs. 5-6	Lake Negre, sediment PYR79
Figs. 7-8	Lake Pica Palòmera, sediment PYR52

Figs. 9-11	Manfred Ruppel photos

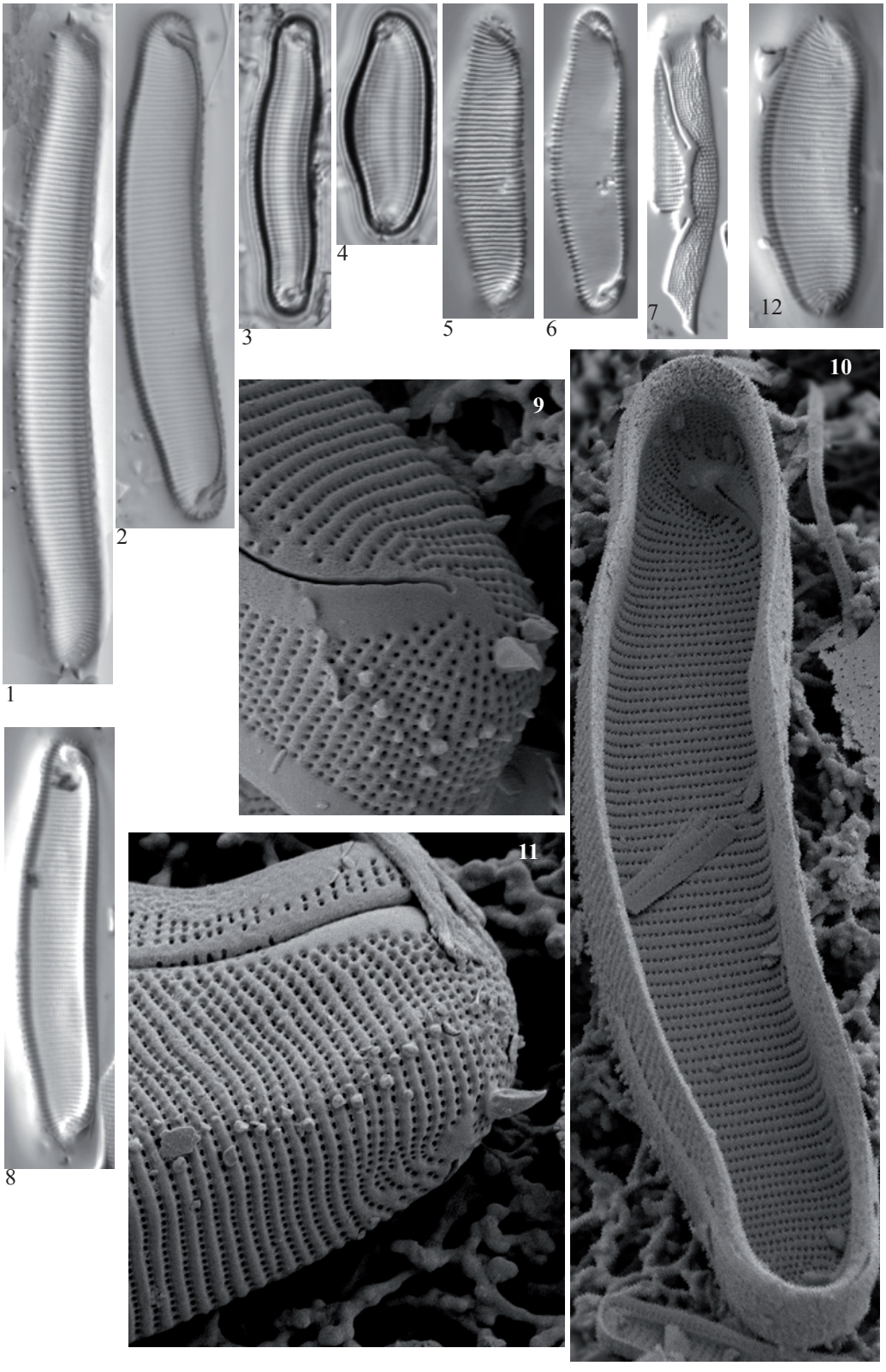
1
2
3
4
5
6
7
12
9
10
8
11

Plate 25 LM: x1500
SEM x3500

Fig. 1	*Eunotia suecica* A. Cleve
Fig. 2-3	*Eunotia diadema* Ehrenberg
Fig. 4	*Eunotia praerupta* Ehrenberg
Figs. 5-6	?*Eunotia circumborealis* Lange-Bertalot & Nörpel
Figs. 7-9	*Eunotia* cf. *dorofeyukae* Lange-Bertalot & Kulikovskiy
Figs. 10-11	*Eunotia* cf. *circumborealis* Lange-Bertalot & Nörpel
Fig. 12	*Eunotia* aff. *minor* (Kützing) Grunow
Figs. 13-14	*Eunotia curtagrunowii* Nörpel-Schempp & Lange-Bertalot
Fig. 15	*?Eunotia meridionalis* Lange-Bertalot & Tagliaventi
	? Eunotia islandica Østrup
Figs. 16-17	*Eunotia cisalpina* Lange-Bertalot & Cantonati
Figs. 18-19	*Eunotia* sp.

Fig. 1	Lake Forcat Inferior, epilithic PYR77
Fig. 2	Lake Baiau Superior, sediment PYR69
Fig. 3	Lake Redon, sediment REDOM
Fig. 4	Lake Estelat, sediment PYR120
Figs. 5-6	Lake Mariola, sediment PYR80
Fig. 7	Lake Burg, sediment BURG830
Fig. 8	Lake Acherito, epilithic EpiPYR01
Figs. 9-11	Lake Acherito, sediment PYR01
Fig. 12	Lake Burg, sediment BURG506
Figs. 13-15	Lake Senó, sediment PYR84
Fig. 16	Lake Monges, sediment PYR57
Fig. 17	Lake Llosás, sediment PYR46
Figs. 18-19	Lake PYR127, sediment sample


1

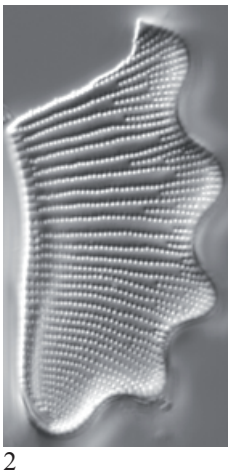
2

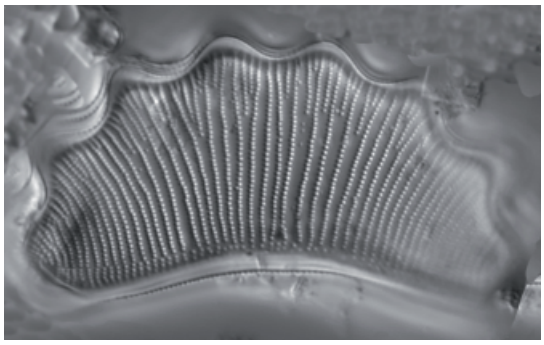
3


4

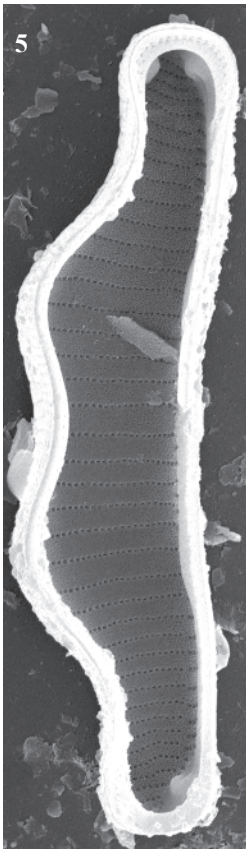
5


6


7


8


9


10


11


12


13


14


15


16


17


18

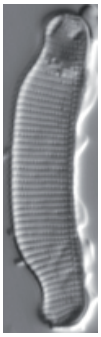
19

Plate 26 LM: x1500

Figs. 1-3	*Eunotia glacialis* Meister
Figs. 4-5	*Eunotia valida* Hustedt
Fig. 6	*Eunotia minor* (Kützing) Grunow
Fig. 7	*?Eunotia minor.* primary cell?
Fig. 8	*Eunotia pectinalis* (Kützing) Rabenhorst

Figs. 1, 6	Lake Mariola, sediment PYR80
Fig. 2	Lake Illa, sediment PYR66
Fig. 3	Lake Senó, sediment PYR84
Fig. 4	Lake Blaou, epilithic EpiPYR94
Fig. 5	Lake Angonella, sediment PYR78
Fig. 7	Lake Long de Liat, sediment PYR55
Fig. 8	Lake Blaou, sediment PYR94

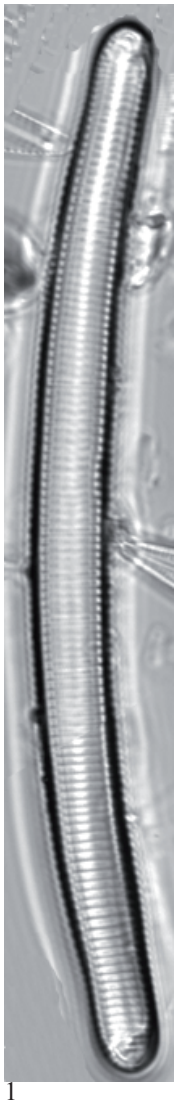
1

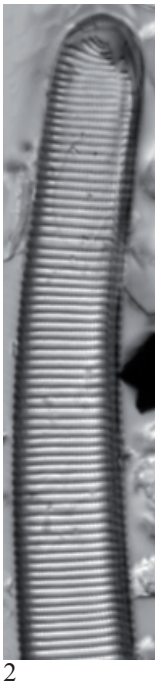
2

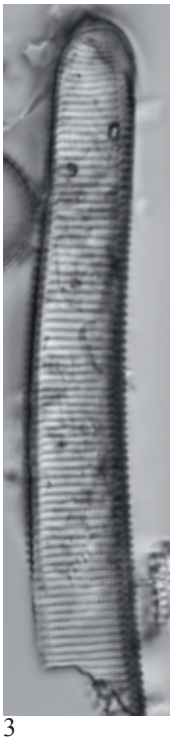
3


4


5


6

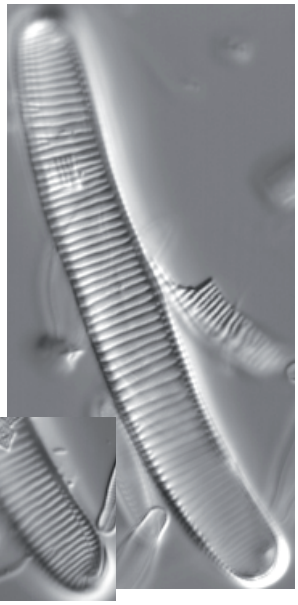
7


8

Plate 27 LM: x1500
SEM: Figs. 4 x2000, Figs.5-6 x3000, Fig. 7 x8000

Eunotia arcus Ehrenberg sensu lato

Fig. 1	Lake Port Bielh, sediment PYR28
Fig. 2	Lake Senó, epilithic EpiPYR84
Figs. 3-4	Lake Redon, sediment REDOM
Fig. 5	Lake Laurenti, sediment PYR111
Figs. 6-7	Lake Angonella, epilithic EpiPYR78

1

2

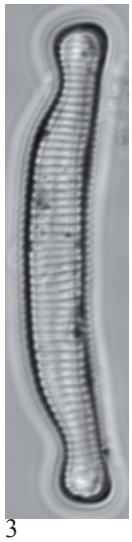

3

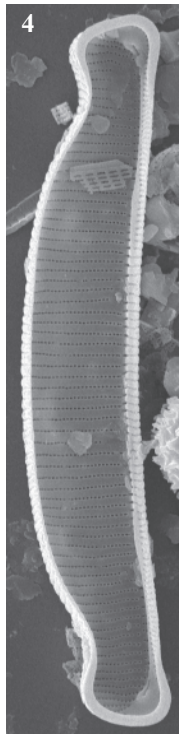

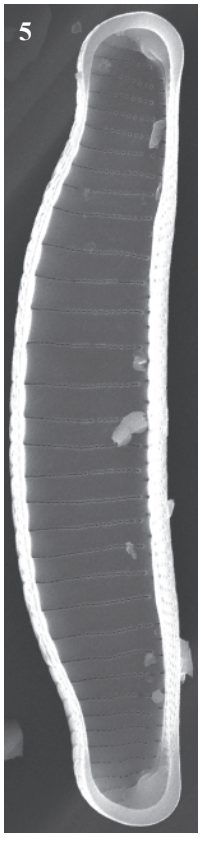

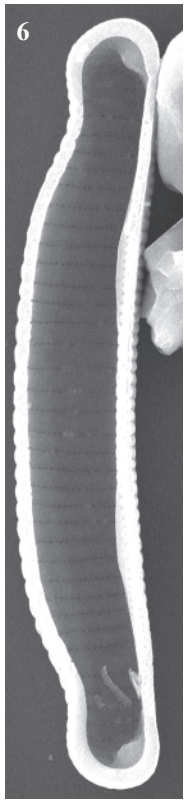

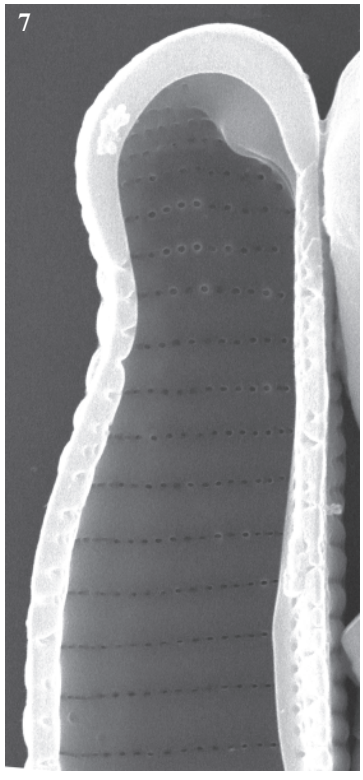

Plate 28 LM: x1500
SEM: x6000

Figs. 1-3	*Eunotia* aff. *soleirolii* (Kützing) Rabenhorst
Figs. 4-5	*Eunotia novaisiae* Lange-Bertalot & Luc Ector
Figs. 6-9	*Eunotia* aff. *soleirolii* (Kützing) Rabenhorst
Fig. 10	*Eunotia sudetica* O. Müller
Figs. 11-12	*Eunotia boreoalpina* Lange-Bertalot & Nörpel-Schempp
Figs. 13-17	*Eunotia incisa* Gregory
Fig. 18	*Eunotia* cf. *faba* Ehrenberg
Fig. 19	*Eunotia* sp
Figs. 20-22	*Eunotia intermedia* (Krasske) Nörpel & Lange-Bertalot
Figs. 23-25	*?Eunotia implicata* Norpel, Alles & Lange-Bertalot
Figs. 26-29	*Peronia fibula* (Brébisson in Kützing) Ross

Figs. 1-2	Lake Gelat Bergús, sediment PYR65
Figs. 3-5	Lake Monges, sediment PYR57
Fig. 6	Lake Mariola, sediment PYR80
Figs. 7-9	Lake Illa, sediment PYR66
Fig. 10	Lake Negre, sediment PYR79
Figs. 11, 16-17, 24-26	Lake Senó, sediment PYR84
Figs. 12, 27	Lake Inferior de la Gallina, sediment PYR87
Figs. 13, 20	Lake Romedo de Dalt, sediment PYR85
Figs. 14, 15	Lake Aixeus, epilithic PYR92
Figs. 18-19, 27	Lake Senó, epilithic EpiPYR84
Figs. 21, 23	Lake Sotllo, sediment PYR89
Fig. 22	Lake Baiau superior, sediment PYR76

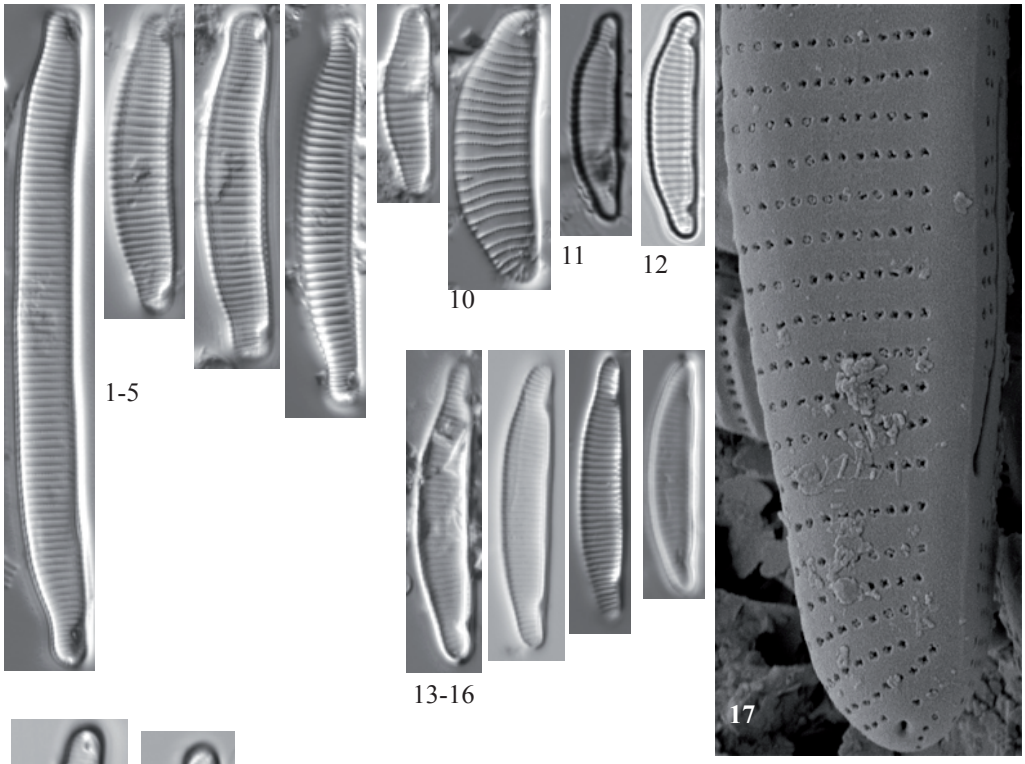
1-5
10
11
12
13-16
17

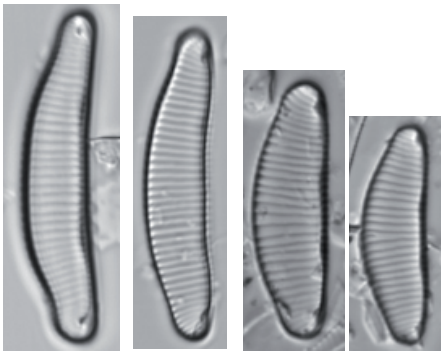
6-9

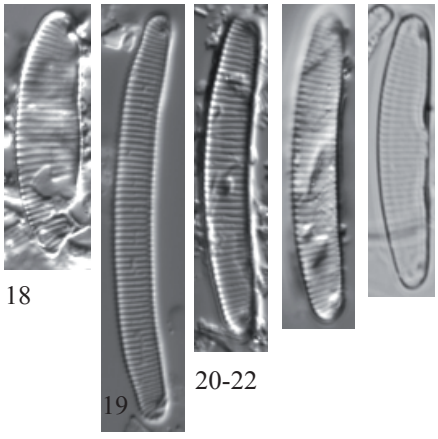
18
19
20-22

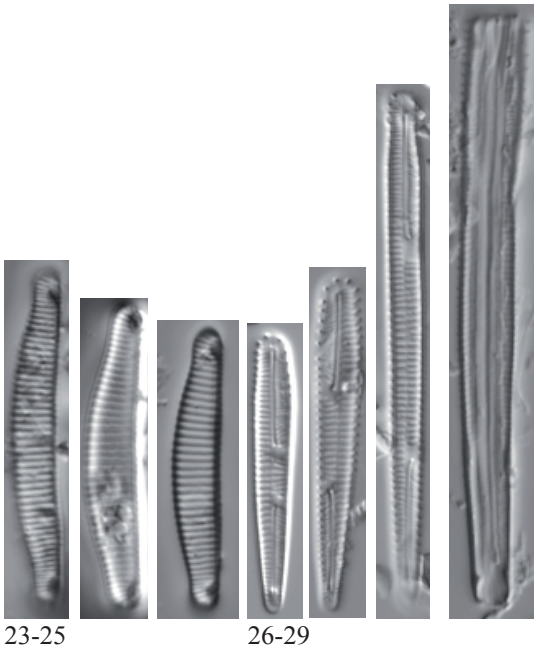
23-25
26-29

Plate 29 SEM: x6000

Fig. 1 *Eunotia intermedia* (Krasske) Nörpel & Lange-Bertalot

Fig. 2 *Eunotia* cf. *botuliformis* Wild, Nörpel & Lange-Bertalot

Figs. 3-5 *Eunotia minor* (Kützing) Grunow sensu lato

Figs. 1, 5 Lake Pica Palòmera, sediment PYR52

Fig. 2 Lake Illa, sediment PYR66

Figs. 3-4 Lake Senó, sediment PYR84

Figs. 1-5 Manfred Ruppel photos

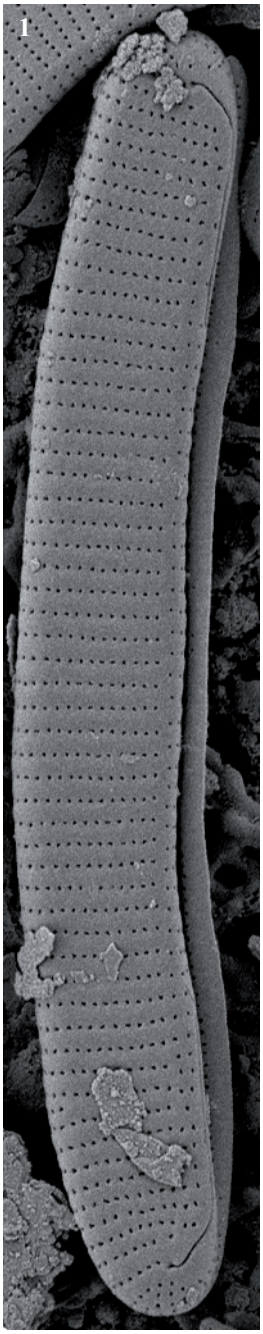
1

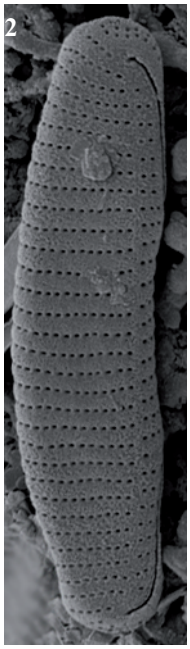
2

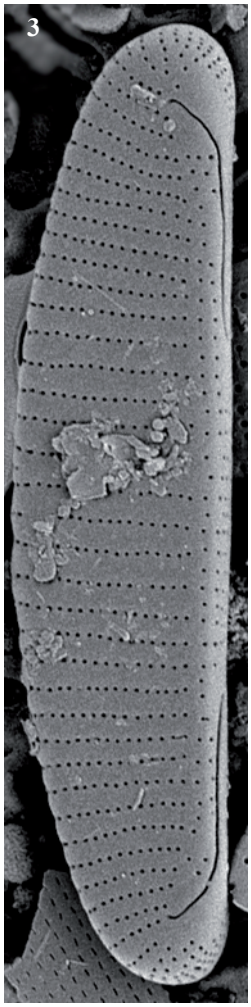
3

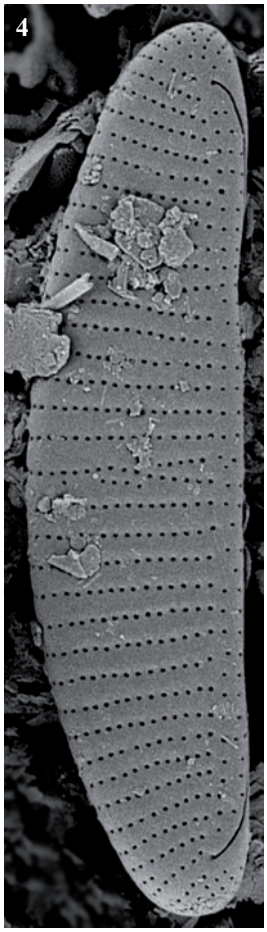
4

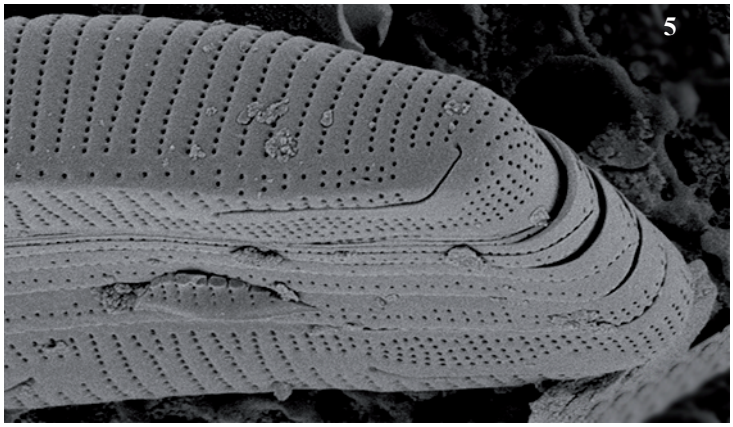
5

Plate 30 LM: x1500

Figs. 1-10	*Eunotia novaisiae* Lange-Bertalot & Luc Ector
Fig. 11	*?Eunotia implicata* Norpel, Alles & Lange-Bertalot
Figs. 12-39	Eunotia *novaisiae* var. *altopyrenaica* Lange-Bertalot & Rivera -Rondón

Figs. 1, 3-8, 10, 31, 37 39	Lake Senó, sediment PYR84
Figs. 2, 9, 15, 24, 27, 34	Lake Pica Palòmera, sediment PYR52
Fig. 11	Lake Sotllo, sediment PYR89
Figs. 12-14, 17-23	Lake Baiau superior, sediment PYR76
Figs. 16, 26, 29-30, 32-22, 35-36, 38	Lake Illa, sediment PYR66
Fig. 25	Lake Mariola, sediment PYR80
Figs. 28	Lake Aixeus, sediment PYR92

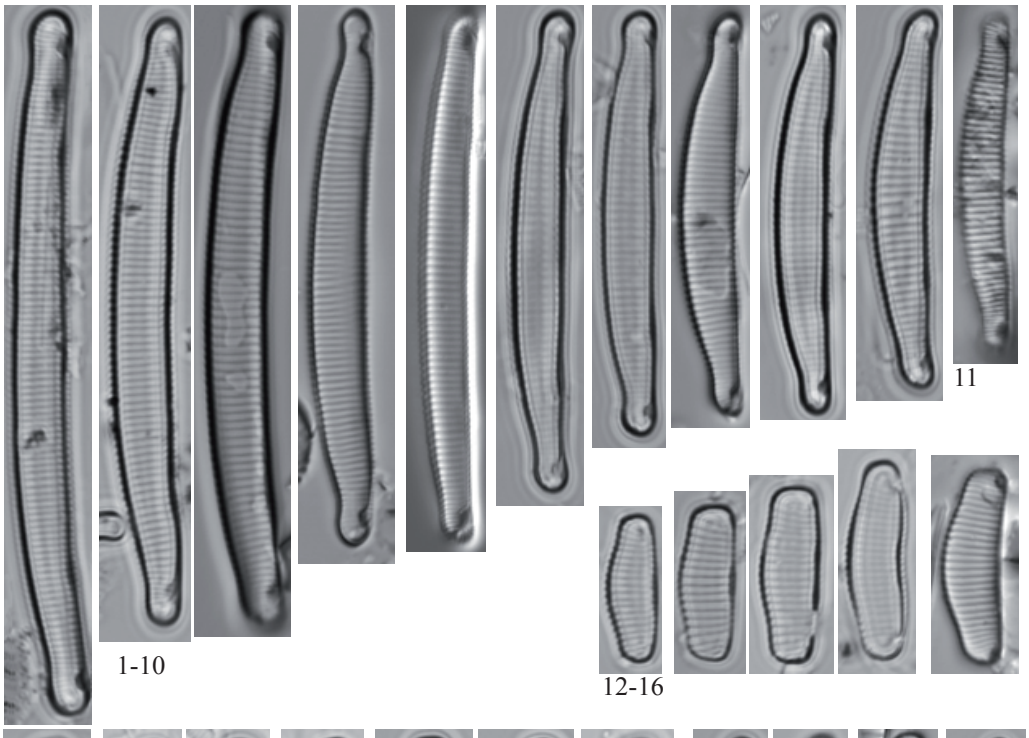
1-10
11
12-16

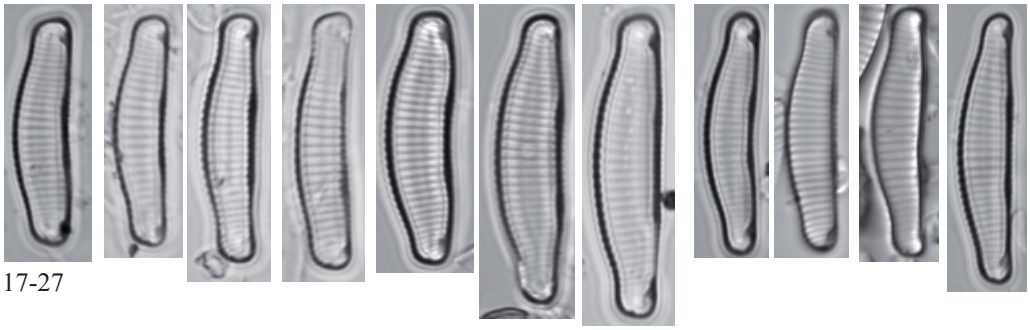
17-27

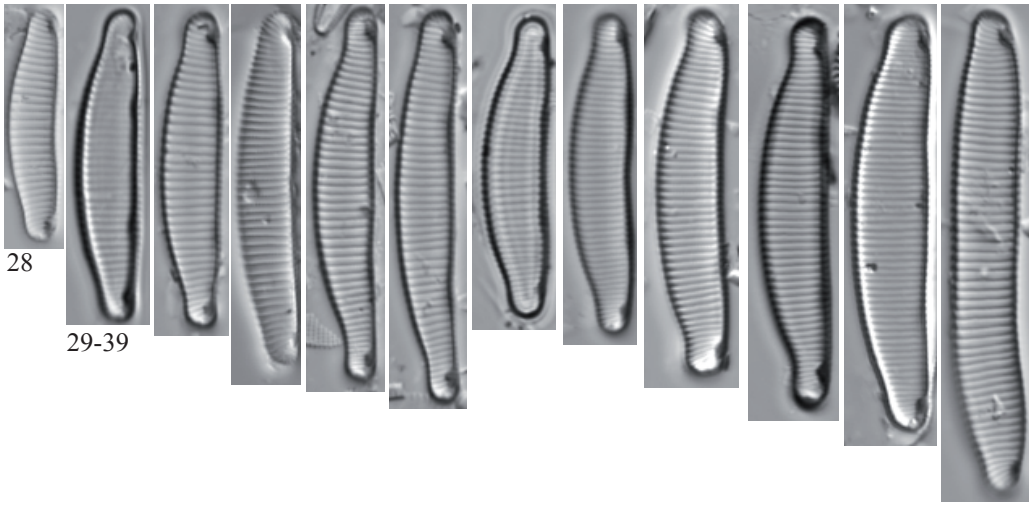
28
29-39

Plate 31 LM: x1500

Figs. 1-16, 26-29	*Eunotia subarcuatoides* Alles, Norpel & Lange-Bertalot
Figs. 17-22, 24-25	*Eunotia* cf. *seminulum* Norpel-Schempp & Lange-Bertalot
Fig. 23	*Eunotia seminulum* Norpel-Schempp & Lange-Bertalot
Figs. 30-31	*Eunotia* cf. *intermedia* (Krasske) Nörpel & Lange-Bertalot
Figs. 32-71	Eunotia sp ?aff. *E. pseudogroenlandica* Lange-Bertalot & Tagliaventi ?aff. *E. botuliformis* Wild, Nörpel & Lange-Bertalot
Figs. 72-77	Eunotia spp.

Figs. 1-2, 5-7, 9-16 27, 29, 70-71, 77	Lake Pica Palòmera, epilithic EpiPYR52
Figs. 3-4, 17-18, 26, 28, 64-65, 76	Lake Nere de Güèri, epilithic EpiPYR53
Fig. 8	Lake Garbet, sediment PYR81
Figs. 19-22, 61-63, 74-75	Lake Aixeus, epilithic EpiPYR92
Figs. 23, 45-48	Lake Negre, sediment PYR79
Fig. 24, 31, 49-60, 72-73	Lake Sotllo, sediment PYR89
Figs. 25, 32-44	Lake Baiau superior, sediment PYR76
Fig. 30	Lake Les Laquettes, sediment PYR27
Figs. 66-67	Lake Senó, sediment PYR84
Figs. 68-69	Lake Pica Palòmera, sediment PYR52

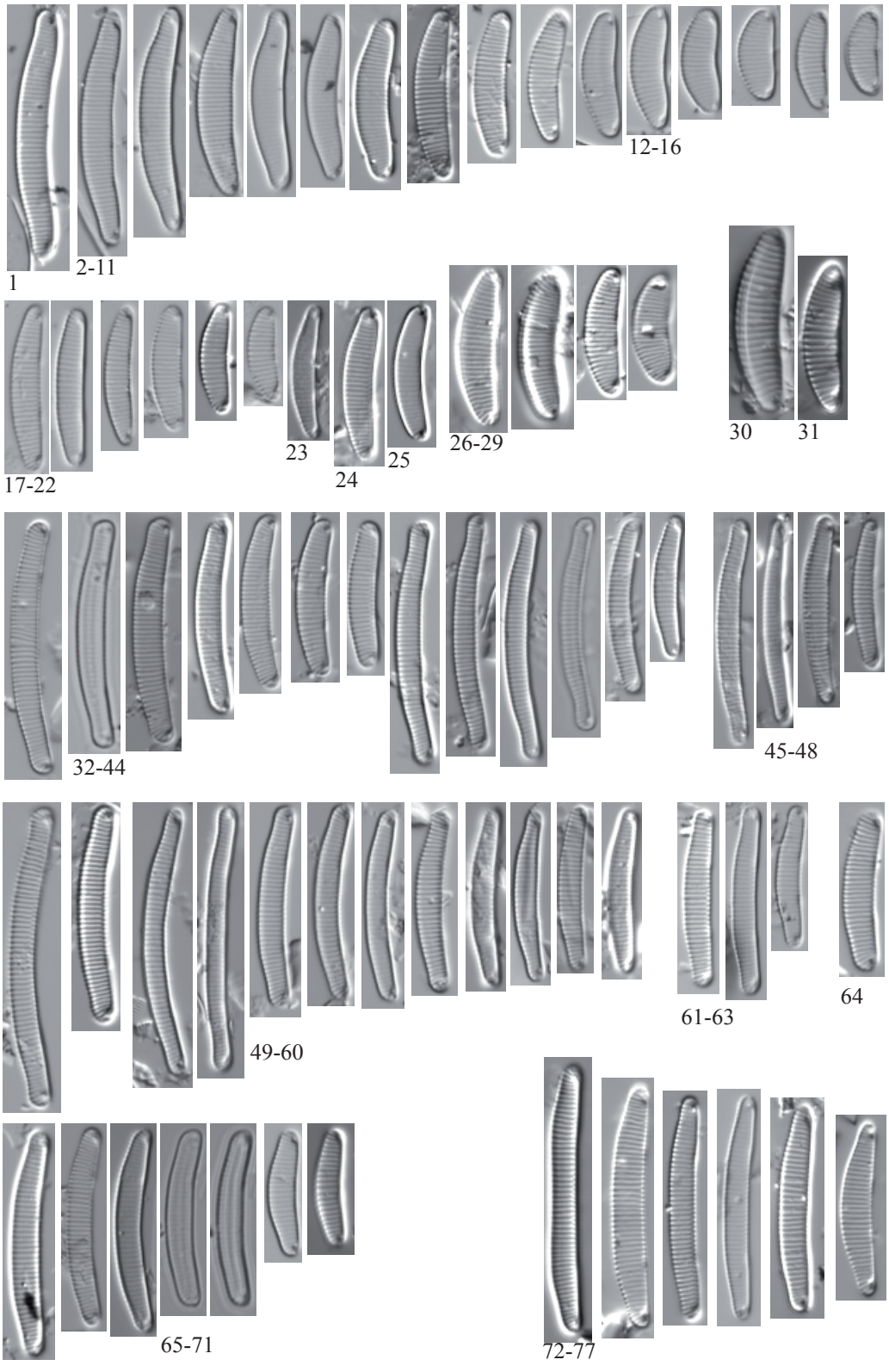
1
2-11
12-16
17-22
23
24
25
26-29
30
31
32-44
45-48
49-60
61-63
64
65-71
72-77

Plate 32	LM: x1500 SEM: Fig. 3 x 20000, Fig. 4x6000
Figs. 1-2	Eunotia *novaisiae* var. *altopyrenaica* Lange-Bertalot & Rivera-Rondón
Figs. 3-4	Eunotia sp ?aff. *E. pseudogroenlandica* Lange-Bertalot & Tagliaventi ?aff. *E. botuliformis* Wild, Nörpel & Lange-Bertalot
Figs. 5-6	*Eunotia subarcuatoides* Alles, Norpel & Lange-Bertalot

Figs. 1, 4, 6	Lake Senó, sediment PYR84
Fig. 2	Lake Baiau superior, sediment PYR76
Fig. 3	Lake Pica, sediment PYR100
Fig. 5	Lake Pica Palòmera, sediment PYR52

Figs. 1-6 Manfred Ruppel photos

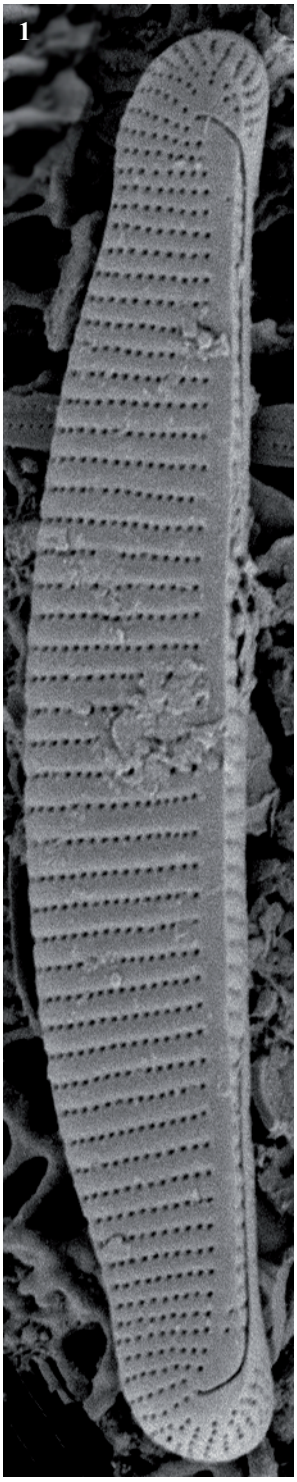
1

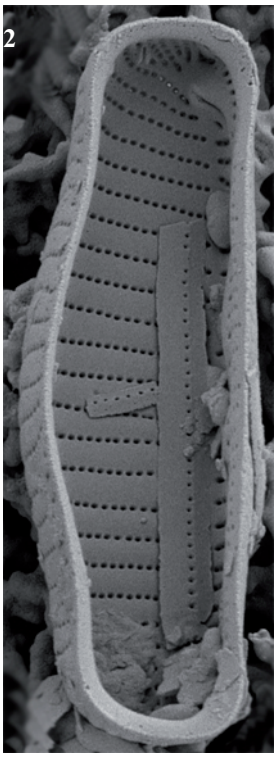
2

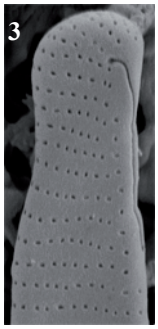
3

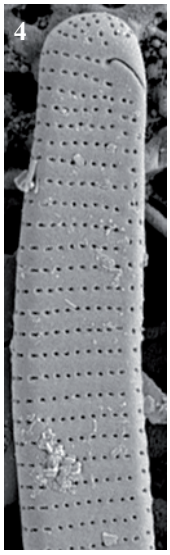
4

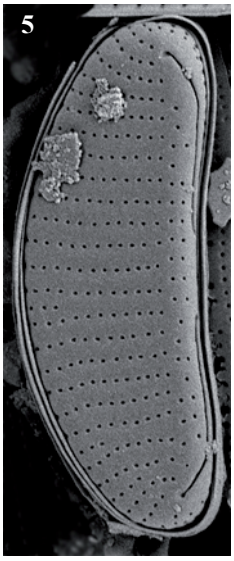
5

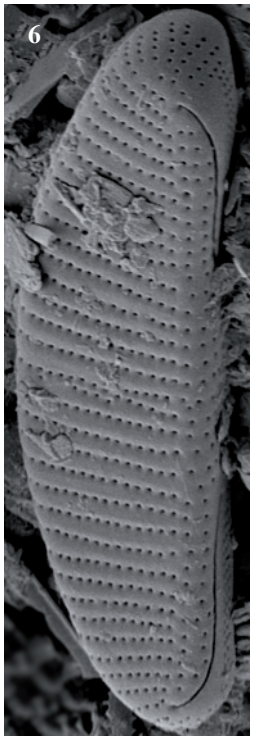
6

Plate 33 LM: x1500

Fig. 1	*Eunotia ambivalens* Lange-Bertalot & Tagliaventi
Figs. 2-7	*Eunotia bilunaris* (Ehrenberg) Schaarschmidt
Figs. 8-13	*Eunotia mucophila* (Lange-Bertalot & Nörpel-Schempp) Lange-Bertalot
Fig. 14	*Eunotia naegelii* Migula
Figs. 15-19	*Eunotia neocompacta* var. *vixcompacta* Lange-Bertalot

Figs. 1, 4	Lake Sen, sediment PYR40
Fig. 2	Lake Inferior de la Gallina, sediment PYR87
Fig. 3	Lake Forcat inferior, sediment PYR77
Figs. 5, 6, 7	Lake Posets, sediment PYR42
Figs. 8-10, 12-13	Lake Senó, epilithic EpiPYR84
Figs. 11, 15, 17, 19	Lake Monges, sediment PYR57
Fig. 14	Lake Mariola, sediment PYR80
Fig. 16	Lake Baiau superior, sediment PYR76
Fig. 18	Lake Senó, sediment PYR84

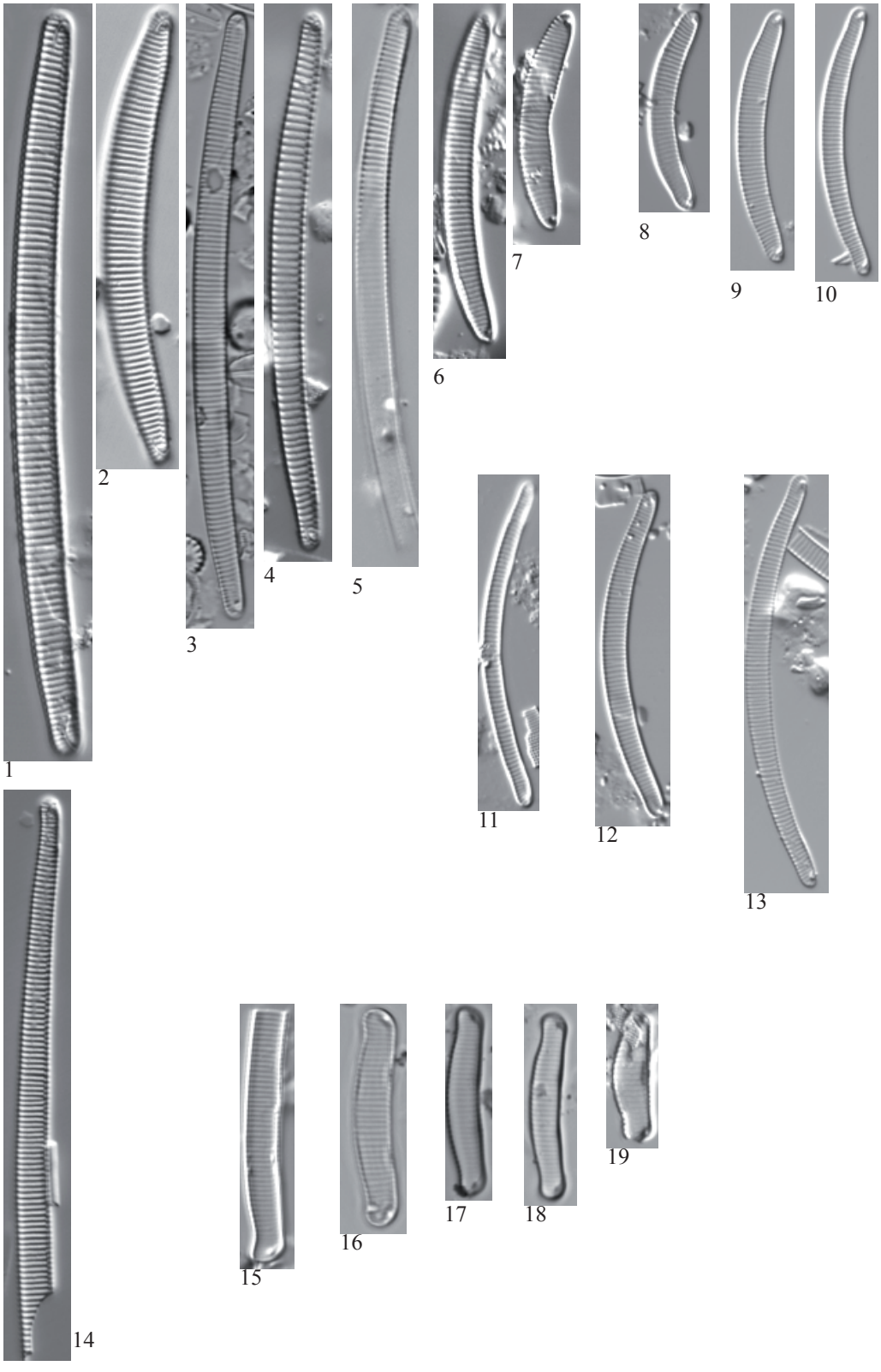
1
2
3
4
5
6
7
8
9
10
11
12
13
14
15
16
17
18
19

Plate 34 LM: x1500
SEM: x6000

Figs. 1-19, 25	*Eunotia nymanniana* Grunow
Fig. 20	*Eunotia* cf. *nymanniana* Grunow
Fig. 21	*Eunotia* cf. *exigua* (Brébisson Kutzing) Rabenhorst
Figs. 22-23, 26	*Eunotia exigua* (Brébisson Kutzing) Rabenhorst
Fig. 24	*Eunotia tenella* (Grunow) Hustedt
Fig. 27	*Eunotia* cf. *exigua* (Brébisson Kutzing) Rabenhorst

Figs. 1, 3-6, 8-20, 22, 25-27	Lake Pica Palòmera, epilithic EpiPYR52
Fig. 2	Lake Aixeus, sediment PYR92
Fig. 7	Lake Negre, sediment PYR79
Fig. 21	Lake Baiau superior, sediment PYR76
Fig. 23	Lake Eriste, sediment PYR43
Fig. 24	Lake Estelat, sediment PYR120

Figs. 25-27 Manfred Ruppel photos

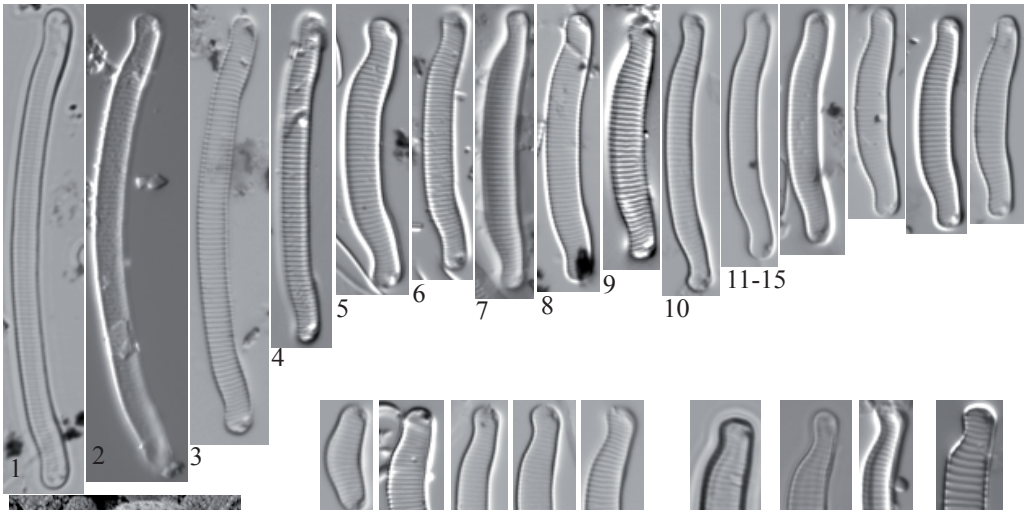
1
2
3
4
5
6
7
8
9
10
11-15

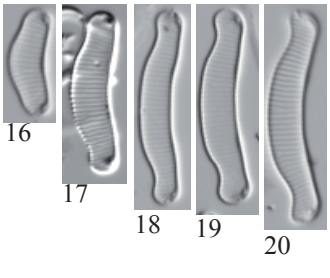
16
17
18
19
20

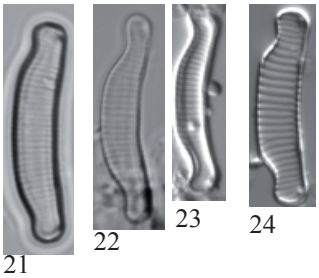
21
22
23
24

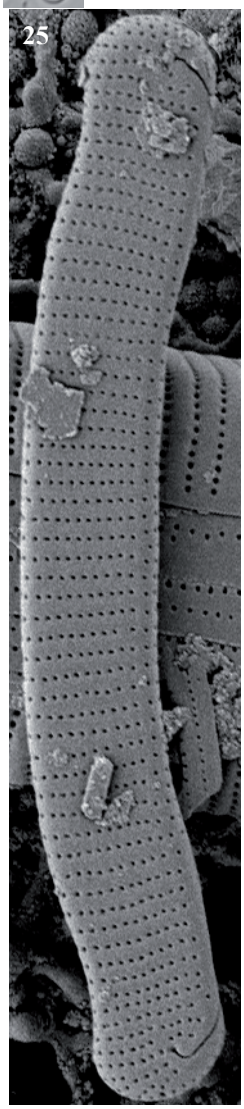
25


26

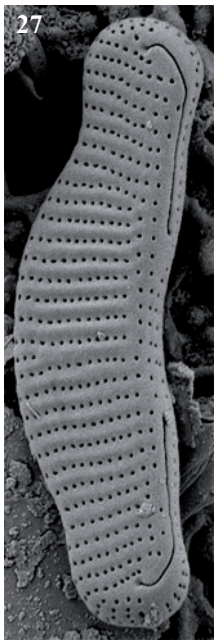
27

Plate 35 LM: x1500
SEM: Fig. 1 x 6000, Fig. 2x2000

Figs. 1-3 *Eunotia paludosa* Grunow
Figs. 4-5 *Eunotia neofallax* Nörpel-Schempp & Lange-Bertalot
Fig. 6 *Eunotia groenlandica* (Grunow) Norpel-Schempp & Lange-Bertalot
Fig. 7 *Eunotia* cf. *groenlandica* (Grunow) Norpel-Schempp & Lange-Bertalot
Fig. 8-10 *Eunotia fallax* A. Cleve
Fig. 11 *Eunotia fallacoides* Lange-Bertalot & Cantonati
Fig. 12 *Eunotia microcephala* Krasske

Figs. 1-2	Lake Senó, sediment PYR84
Fig. 3	Lake Aubé, sediment PYR82
Figs. 4-5	Lake Cregüeña, sediment PYR49
Figs. 6, 10	Lake Aixeus, sediment PYR92
Fig. 7	Lake Pica Palòmera, sediment PYR52
Fig. 8	Lake Baiau superior, sediment PYR76
Fig. 9	Lake Romedo de Dalt, epilithic EpiPYR85
Fig. 11	Lake Illa, sediment PYR66
Fig. 12	Lake Monges, sediment PYR57

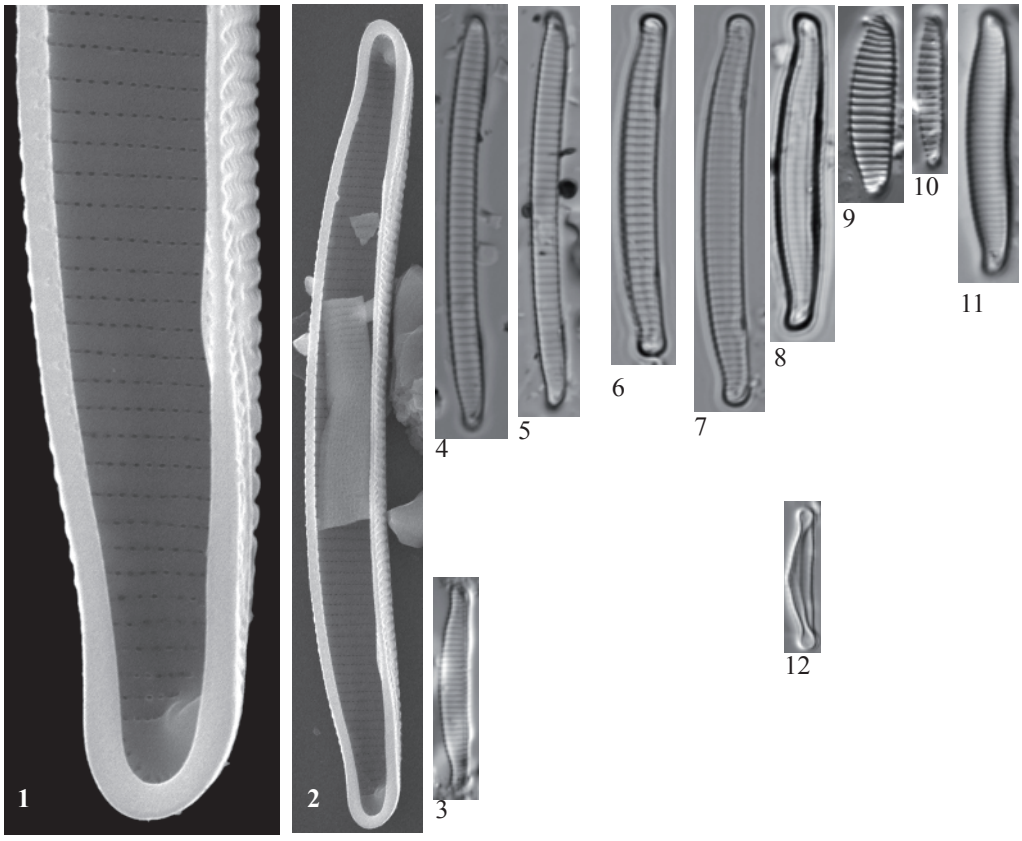
1
2
3
4
5
6
7
8
9
10
11
12

Plate 36 LM: x1500
SEM: Figs. 11,25,26 x 5000, Fig. 24 x8000

Figs. 1-2	*Eucocconeis coarctata* (Brébisson) Lange-Bertalot
Figs. 3-4	*Eucocconeis flexella* (Kützing) Meister
Figs. 5-6	*Eucocconeis alpestris* (Brun) Lange-Bertalot
Figs. 7-11	*Eucocconeis laevis* (Østrup) Lange-Bertalot
Fig. 12	*Psammothidium altaicum* (Poretzky) Bukhtiyarova
Fig. 13	*Karayevia carissima* (Lange-Bertalot) Bukhtiyarova
Figs. 14-15	*Karayevia oblongella* (Østrup) Aboal
Figs. 16-17	*Karayevia laterostrata* (Hustedt) Bukhtiyarova
Fig. 18	*?Achnanthes punctulata* Simonsen
Figs. 19-26	*Karayevia suchlandtii* (Hustedt) Bukhtiyarova

Figs. 1-2, 13, 18-23, 23-26	Lake Posets, sediment PYR42
Figs. 3-4	Lake Ormiélas, sediment PYR05
Figs. 5-9	Lake Llebreta, sediment PYR58
Fig. 10	Lake Acherito, sediment PYR01
Fig. 11	Lake Roumassot, epilithic EpiPYR04
Fig. 12	Lake Romedo de Dalt, sediment PYR85
Figs. 14-15	Lake Forcat Inf., sediment PYR77
Figs. 16-17	Lake Tourrat, sediment PYR23

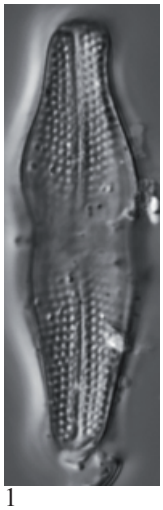
1


2


3


4


5


6


7


8


9


10

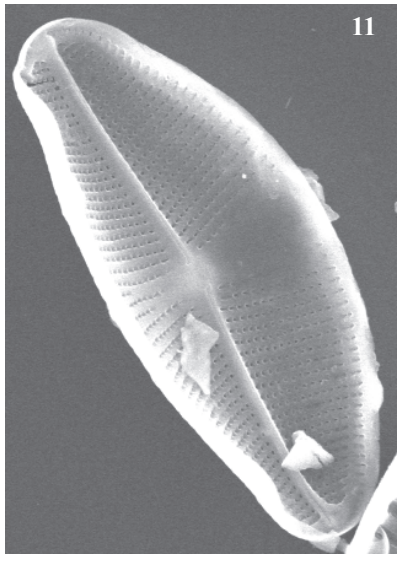
11


12


13


14


15


16


17


18

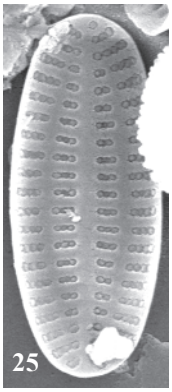
25

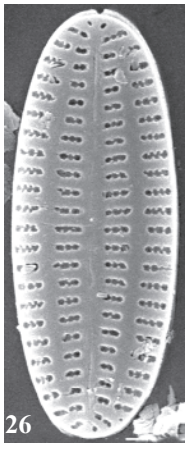
26


19


20

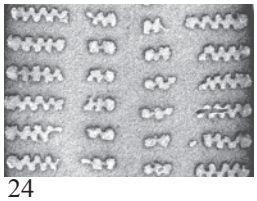
24


21


22


23

Plate 37 LM: x1500
SEM: Figs. 12 x 4500, Fig. 14 x10000

Figs. 1-4 *Nupela* cf. *impexiformis* (Lange-Bertalot) Lange-Bertalot
Figs. 5-8 *Nupela* cf. *gracillima* (Hustedt) Lange-Bertalot
Figs. 9-12 *Nupela lapidosa* (Krasske) Lange-Bertalot
Fig. 13-14 *Nupela silvahercynia* (Lange-Bertalot) Lange-Bertalot

Figs. 1-2	Lake Compte, sediment PYR97
Figs. 3-4, 10, 12	Lake Garbet, sediment PYR81
Figs. 5-7	Lake Helado de Marboré, sediment PYR18
Fig. 8	Lake Long de Liat, sediment PYR55
Fig. 9	Lake Coronas, epilithic EpiPYR47
Fig. 11	Lake Posets, epilithic EpiPYR42
Fig. 13	Lake Cregüeña, epilithic EpiPYR49
Fig. 14	Lake Port Bielh, epilithic EpiPYR28

1

2

3

4

5

6

7

8

9

10

11

13

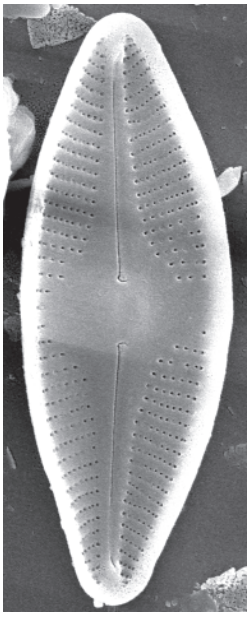

12

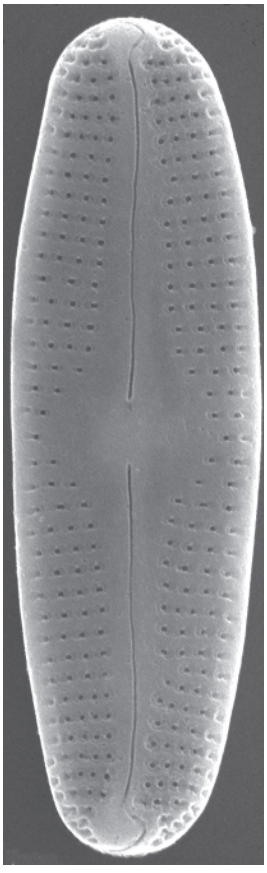

14

Plate 38 LM: x1500
SEM: Fig. 7 x 6000, Fig. 12 x 4500, Fig. 22 x8000

Figs. 1-2	*Planothidium* cf. *stewartii* (Patrick) Lange-Bertalot
Figs. 3-7	*Planothidium distinctum* (Messikommer) Lange-Bertalot
Figs. 8-9	*?Planothidium distinctum* (Messikommer) Lange-Bertalot
Figs. 10-12	*Platessa* cf. *conspicua* (Mayer) Lange-Bertalot
Figs. 13-14	*Planothidium lanceolatum* (Brébisson ex Kützing) Lange-Bertalot
Figs. 15-18	*Planothidium frequentissimum* (Lange-Bertalot) Lange-Bertalot
Figs. 19-21	*Planothidium* sp. No. 1 Pondiellos
Fig. 22	*Planothidium frequentissimum* (Lange-Bertalot) Lange-Bertalot
Figs. 23-31	*Planothidium rostratum (*Østrup) Lange-Bertalot
Figs. 32-35	*Planothidium oestrupii* (Cleve-Euler) Edlund
Figs. 36-37	*Planothidium peragalli* (Brun & Héribaud) Round et Bukhtiyarova
Figs. 38-41	*Planothidium calcar* (Cleve) M.B. Edlund

Figs. 1-2	Lake Trebens, sediment PYR114
Figs. 3-9, 34-35	Lake Posets, sediment PYR42
Figs. 10-12, 22	Lake Laurenti, sediment PYR111
Figs. 13-14	Lake La Munia, sediment PYR20
Figs. 15-16, 40-41	Lake Estom, sediment PYR15
Figs. 17-18	Lake Arratille, sediment PYR11
Figs. 19-20	Lake Pondiellos, sediment PYR08
Fig. 21	Lake Cap Long, sediment PYR24
Figs. 23-31	Lake Burg
Figs. 32-33	Lake Sen, sediment PYR40
Figs. 36-37	Lake Sen, sediment PYR120
Fig. 38	Lake Barsau, sediment PYR03
Fig. 39	Lake Acherito, sediment PYR01

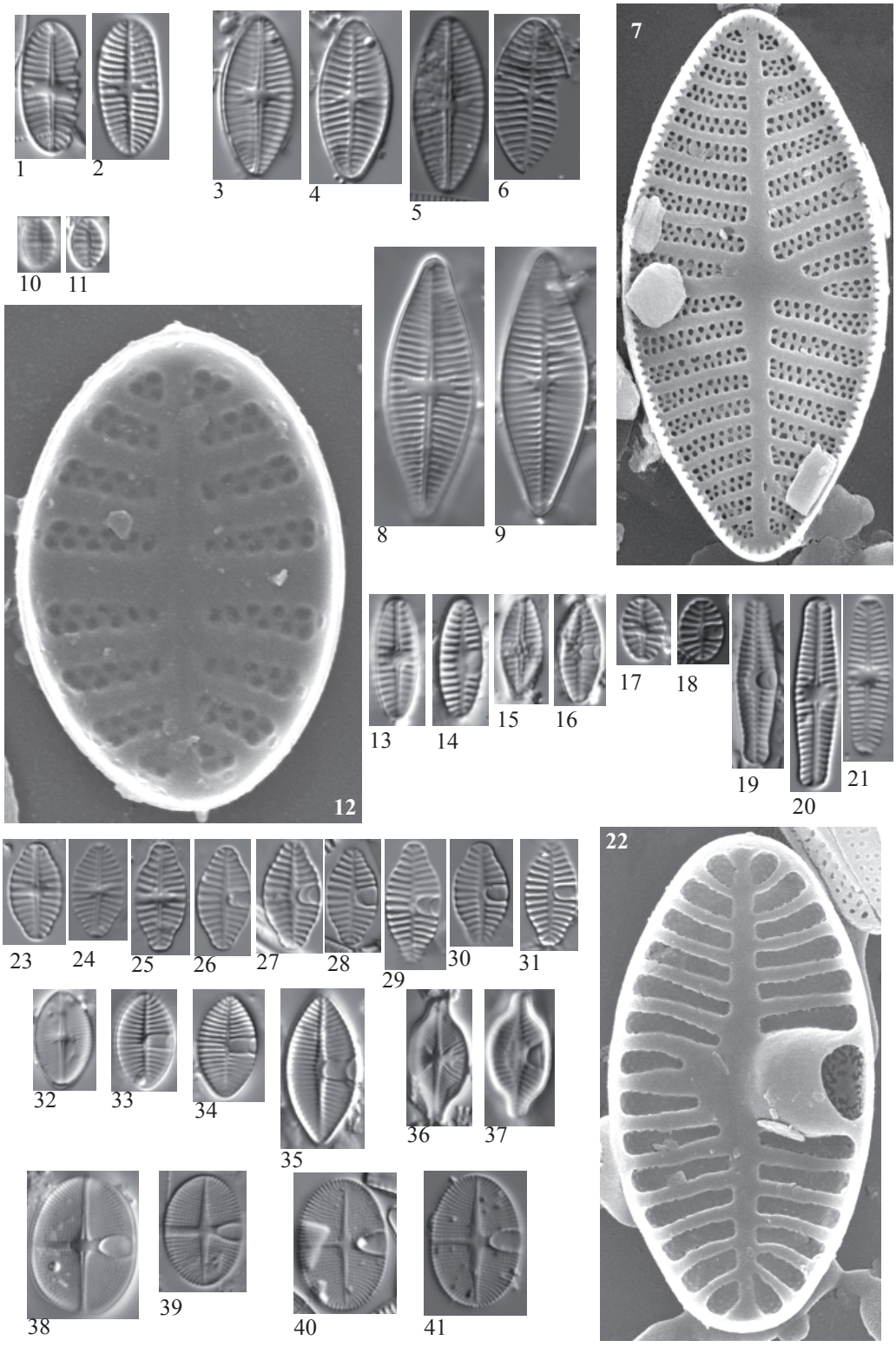
1
2
3
4
5
6
7
8
9
10
11
12
13
14
15
16
17
18
19
20
21
22
23
24
25
26
27
28
29
30
31
32
33
34
35
36
37
38
39
40
41

Plate 39	LM: x1500 SEM: x10000

Figs. 1-13, 18-21	*Achnanthes microscopica* (Cholnoky) Lange-Bertalot & Krammer
Figs. 14-17, 28-31	*?Achnanthes microscopica* (Cholnoky) Lange-Bertalot & Krammer
Figs. 22-27	*Achnanthes* sp. No. 2 Burg

Figs. 1-17, 19, 20-30	Lake Posets, sediment PYR42
Figs. 18, 20, 21, 28	Lake Redon, sediment REDOM
Figs. 23-27	Lake Burg, sediment BURG 953
Fig. 31	Lake Angonella, epilithic EpiPYR78

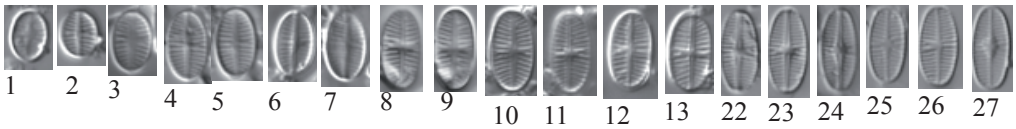
1
2
3
4
5
6
7
8
9
10
11
12
13
22
23
24
25
26
27

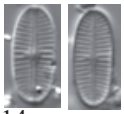
14
15

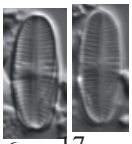
16
17

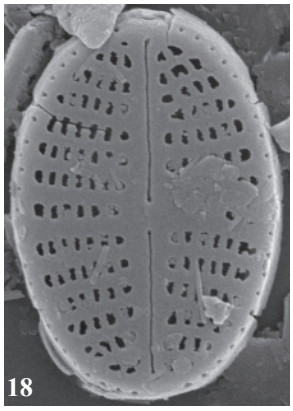
18

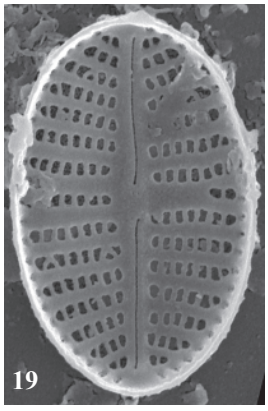
19

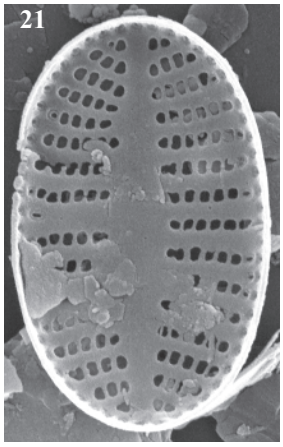
21

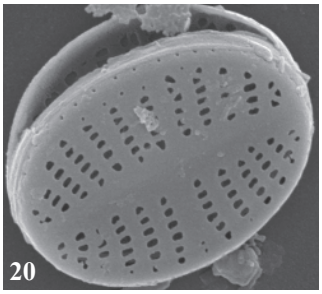
20

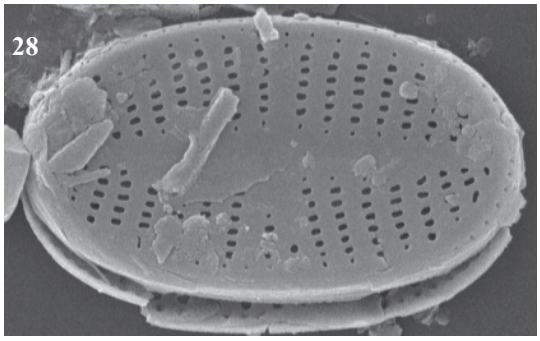
28

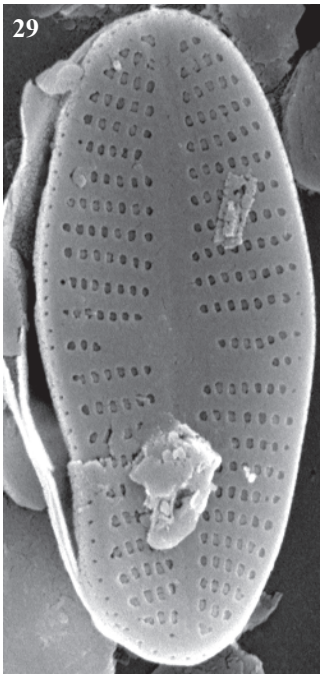
29

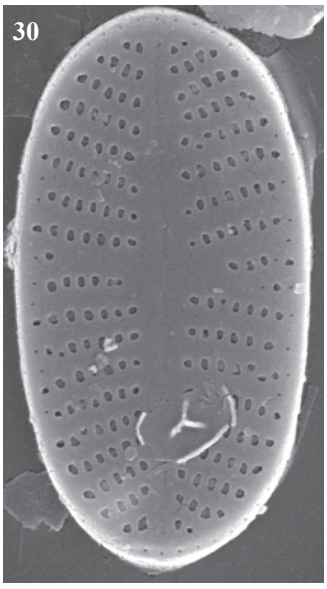
30


31

Plate 40 LM: x1500
SEM: x10000

Figs. 1-6 *Psammothidium didymum* (Hustedt) Bukhtiyarova & Round

Figs. 7-15 *Psammothidium subatomoides (*Hustedt) Bukhtiyarova et Round

Figs. 16-26 *Psammothidium levanderi* (Hustedt) Bukhtiyarova & Round

Fig. 27 *?Psammothidium levanderi* (Hustedt) Bukhtiyarova & Round

Figs. 1-2, 5-6	Lake Les Laquettes, sediment PYR27
Figs. 3-4, 7-12, 16-21 25-26	Lake Posets, sediment PYR42
Figs. 14-15	Lake Mariola, sediment PYR80
Figs. 22-24	Lake Sen, sediment PYR40
Fig. 27	Lake Urdiceto, sediment PYR125

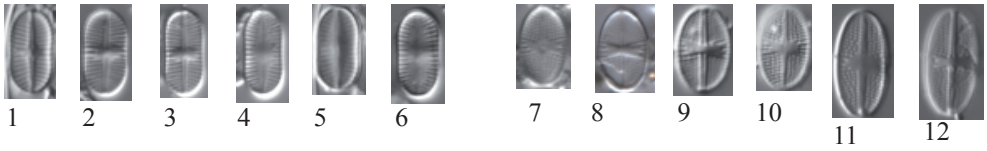
1
2
3
4
5
6
7
8
9
10
11
12

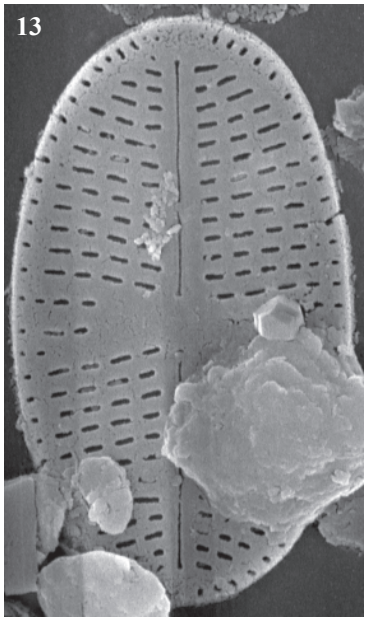
13

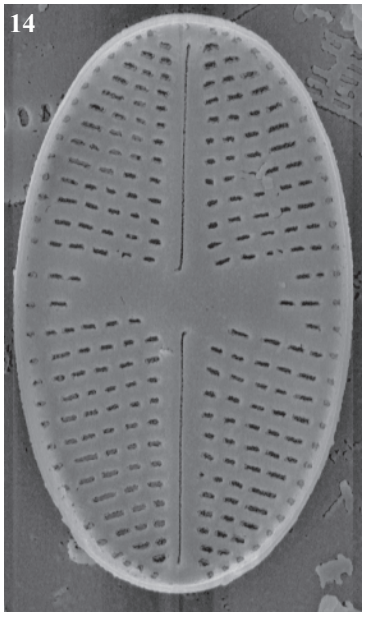
14

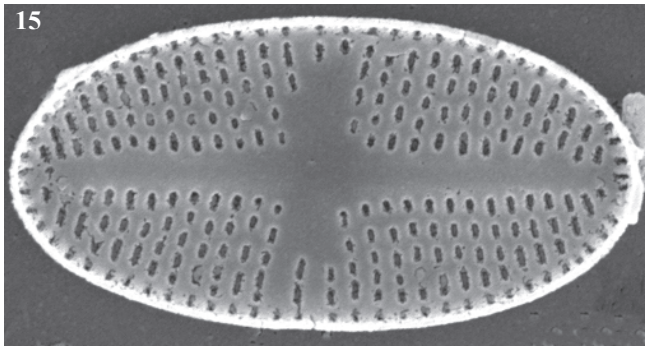
15

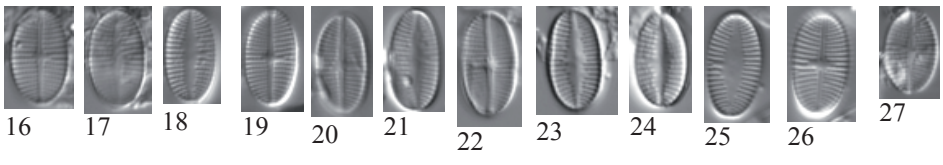
16
17
18
19
20
21
22
23
24
25
26
27

Plate 41 LM: x1500
SEM: Fig. 8 x10000 Figs. 18,19, 24 x9000

Figs. 1-8	*Achnanthidium* sp. No. 1 Posets
Figs. 9-19	*?Achnanthidium minutissimum* (Kützing) Czarnecki sensu lato
Figs. 20-21	*Achnanthidium* cf. *kranzii* (Lange-Bertalot) Round & Bukhtiyarova
Figs. 22-24	*Psammothidium rosenstockii* (Lange-Bertalot) Lange-Bertalot
Fig. 25	*Achnanthes* sp. No. 6 Pessó
Figs. 26-32	cf. *Achnanthidium atomus* (Hustedt) Monnier, Lange-Bertalot & Ector
Figs. 33-36	*Achnanthes* sp. No. 5 Posets

Figs. 1-7, 8, 33-35	Lake Posets, sediment PYR42
Figs. 9-12	Lake Les Laquettes, sediment PYR27
Figs. 13-15, 26-27	Lake Llebreta, sediment PYR58
Figs. 16-17	Lake Gerber, sediment PYR63
Figs. 18-19	Lake Laurenti, sediment PYR111
Figs. 20-21	Lake Eriste, sediment PYR43
Figs. 22-23	Lake Arratille, sediment PYR11
Fig. 24	Lake Gran de Mainera, sediment PYR70
Fig. 25	Lake Gran del Pessó, sediment PYR56
Figs. 28-29	Lake La Munia Superior, sediment PYR20
Figs. 30-32	Lake Glacé, sediment PYR17
Fig. 36	Lake Garbet, sediment PYR81

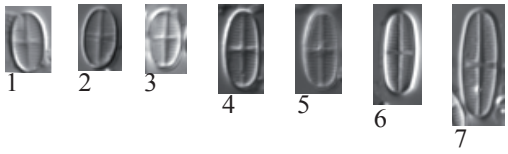
1
2
3
4
5
6
7

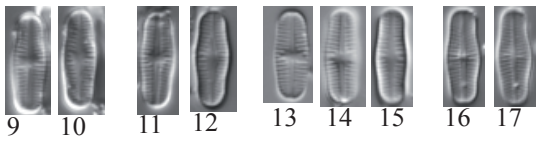
9
10
11
12
13
14
15
16
17

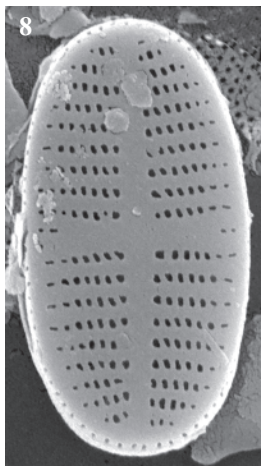
8

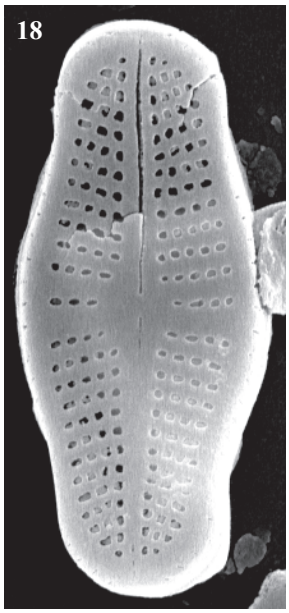
18

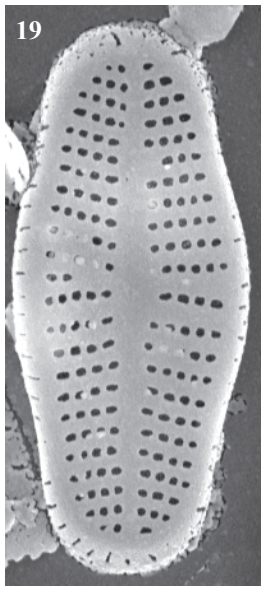
19

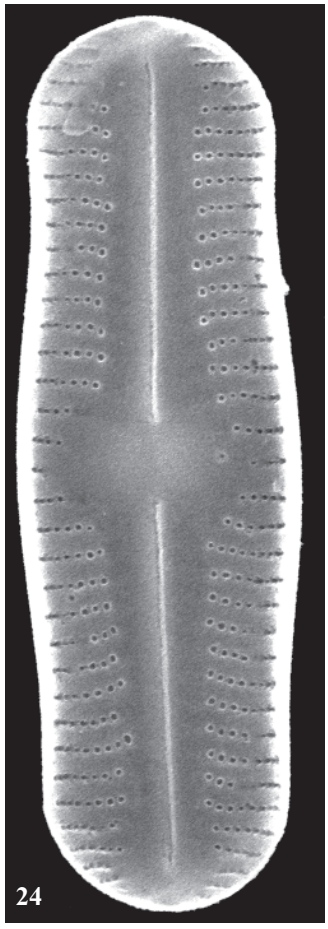
24

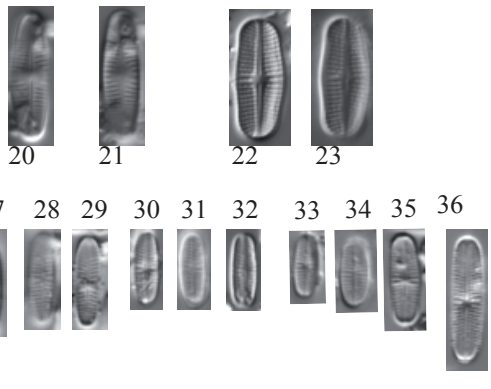
20
21
22
23
25
26
27
28
29
30
31
32
33
34
35
36

Plate 42 LM: x1500
SEM: Figs. 3-8 x 9000 Fig. 9 x20000

Figs. 1-9 *Achnanthidium minutissimum* (Kützing) Czarnecki sensu lato

Figs. 10-20 *Achnanthidium minutissimum* (Kützing) Czarnecki sensu lato

Figs. 21-24 *?Achnanthidium minutissimum* (Kützing) Czarnecki

Fig. 25 *Achnanthidium* sp

Figs. 1-2	Lake Llebreta, sediment PYR58
Figs. 3-5, 9	Lake Roumassot, sediment PYR04
Figs. 6-8	Lake Roumassot, epilithic EpiPYR04
Figs. 10.12	Lake Chelau Sup., sediment PYR41
Fig. 13	Lake Burg
Figs. 14-24	Lake Les Laquettes, sediment PYR27
Fig. 25	Lake Pixón, sediment PYR44

1 2

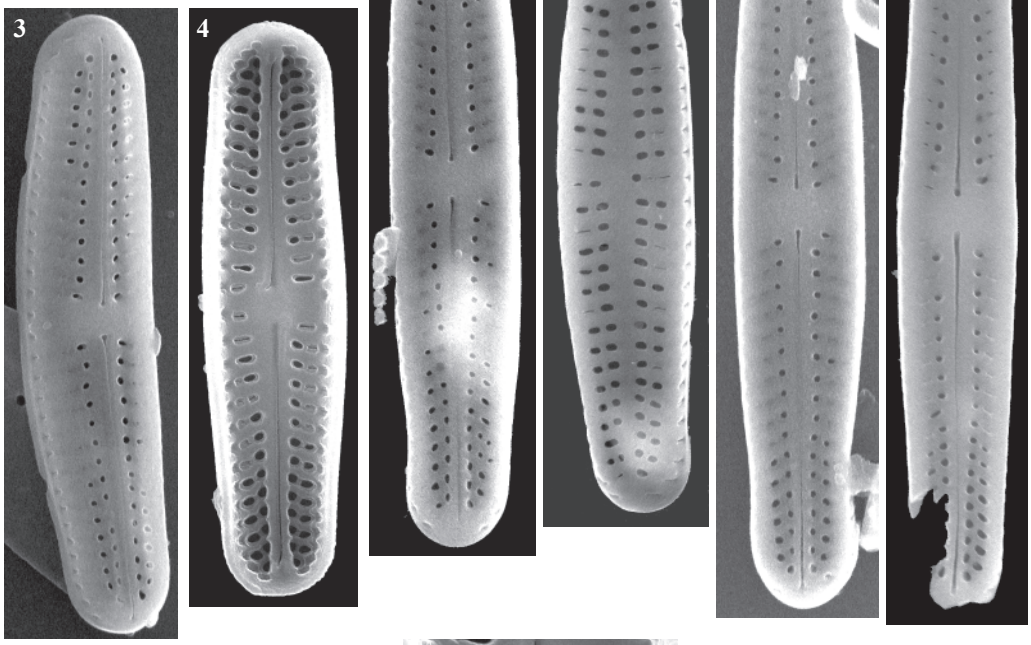

3 4 5 6 7 8

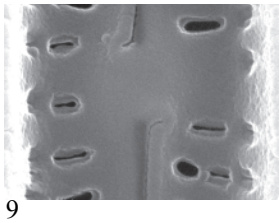

9

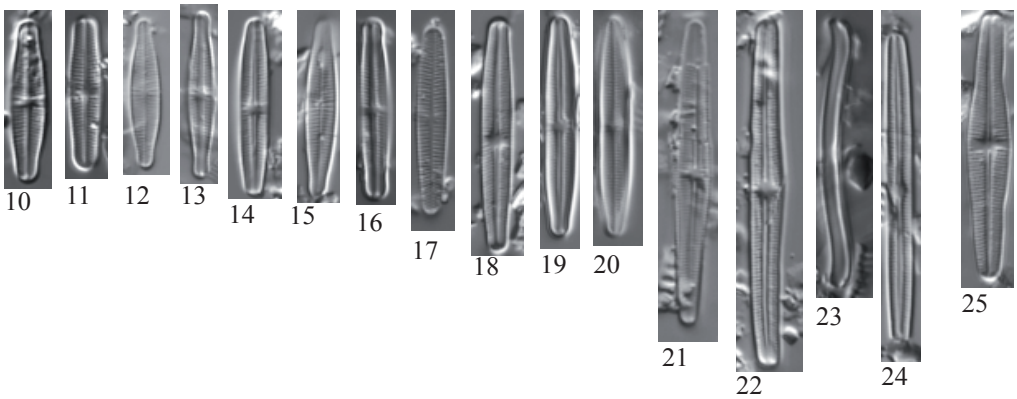

10 11 12 13 14 15 16 17 18 19 20 21 22 23 24 25

Plate 43 LM: x1500
SEM: x9000

Figs. 1-27 *Achnanthidium minutissimum* (Kützing) Czarnecki

Figs. 1-2, 11-20	Lake Posets, sediment PYR42
Figs. 3, 8	Lake Port Bielh, epilithic EpiPYR28
Figs. 4, 6	Lake Roumassot, epilithic EpiPYR04
Figs. 5, 7	Lake Pondiellos, epilithic EpiPYR08
Fig. 9	Lake Acherito, epilithic EpiPYR01
Fig. 10	Lake Mariola, epilithic EpiPYR80
Figs. 21-22	Lake Aubé, sediment PYR82
Fig. 23	Lake Burg, sediment BURG 932
Fig. 24	Lake Burg, sediment BURG 1007
Figs- 25-27	Lake Burg, sediment BURG 831

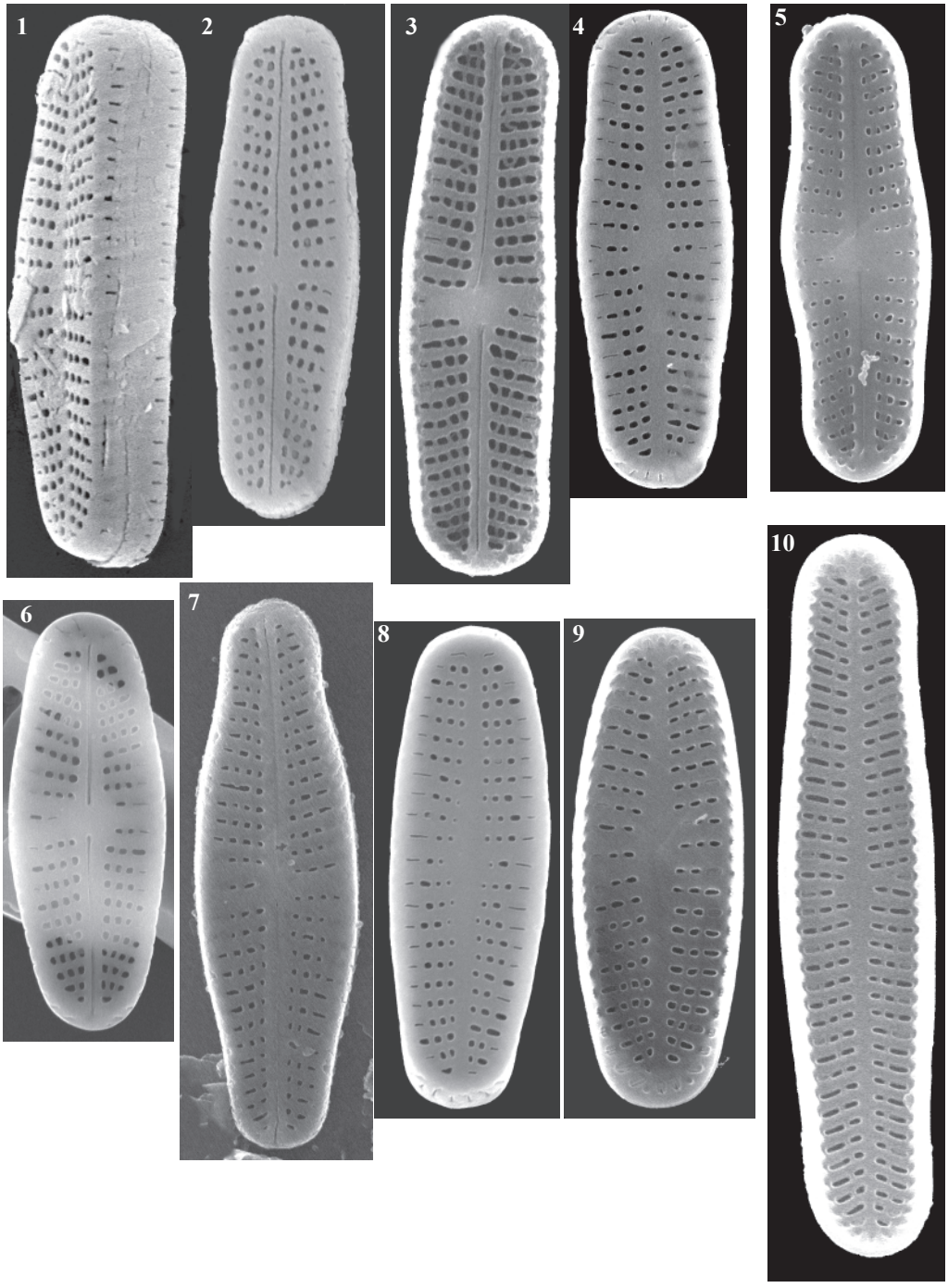
1
2
3
4
5
6
7
8
9
10
11
12
13
14
15
16
17
18
19
20
21
22
23
24
25
26
27

Plate 44 LM: x1500
SEM: x9000

Figs. 1-16 *Achnanthidium minutissimum* (Kützing) Czarnecki sensu lato

Figs. 17-24 cf. *Achnanthidium catenatum* (Bily & Marvan) H. Lange-Bertalot

Figs. 1-2, 5-9	Lake Llebreta, sediment PYR58
Figs. 3-4, 23-24	Lake Bersau, sediment PYR03
Figs. 10, 12	Lake Estom, sediment PYR15
Fig. 13	Lake Arratille, epilithic EpiPYR11
Figs. 14-15, 19-22	Lake Posets, sediment PYR42
Figs. 16, 18	Lake Port Bielh, epilithic EpiPYR28
Figs. 17	Lake Laurenti, sediment PYR111

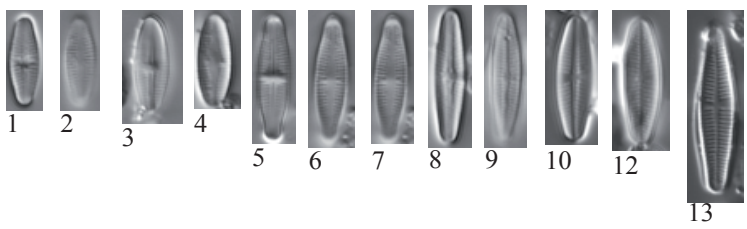
1
2
3
4
5
6
7
8
9
10
12
13

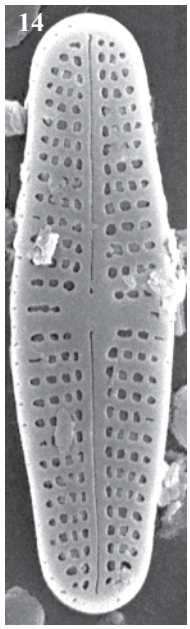
14

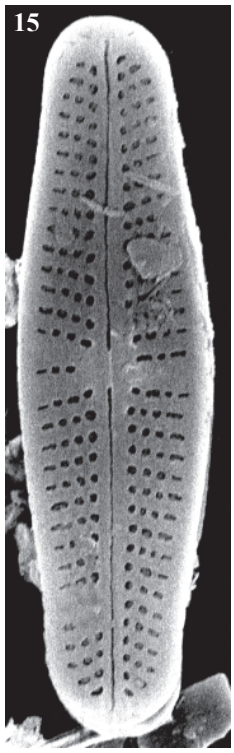
15

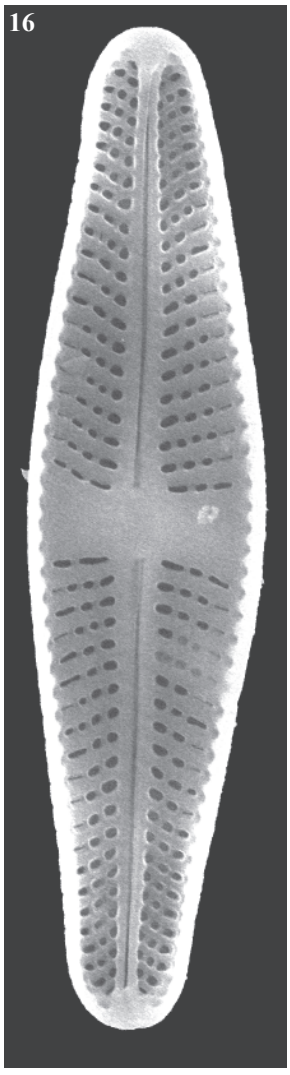
16

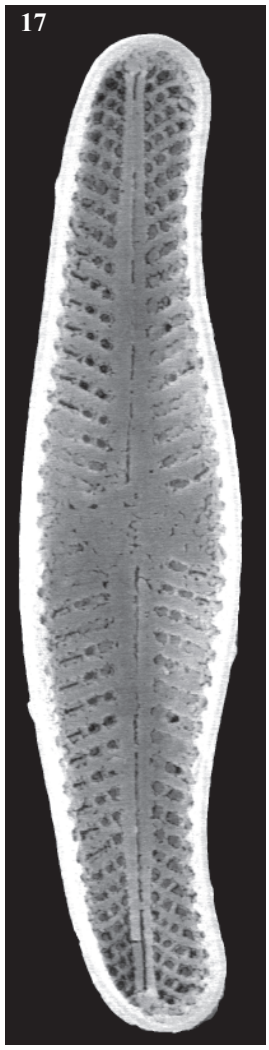
17

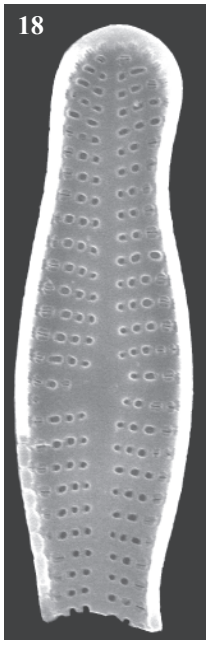
18

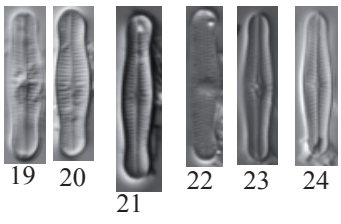
19
20
21
22
23
24

Plate 45 LM: x1500
SEM: x9000

Figs. 1-5 *Achnanthidium minutissimum* (Kützing) Czarnecki

Fig. 1 Lake, sediment BURG 939

Figs. 2-5 Lake Redon, sediment REDOM

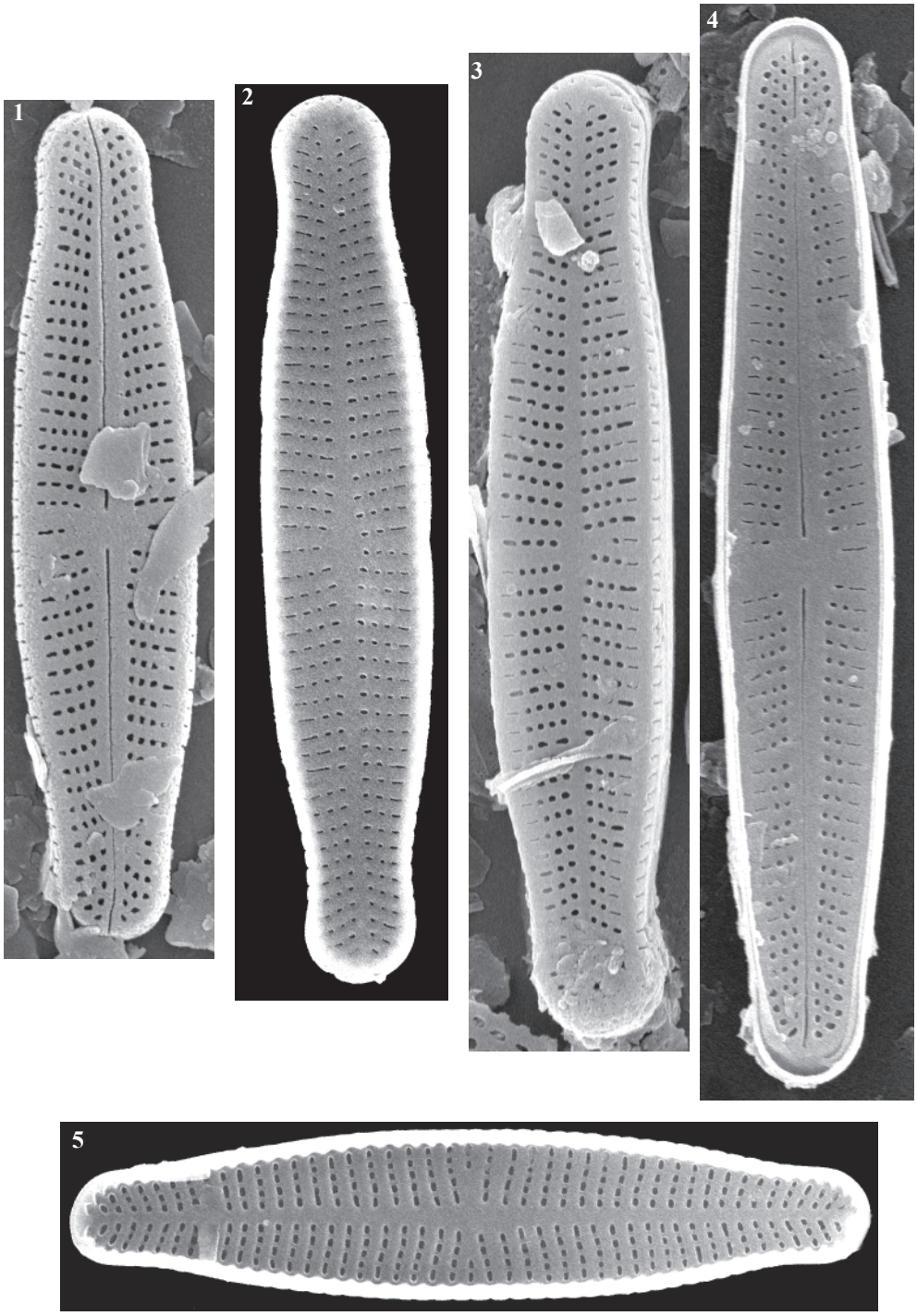
1
2
3
4
5

Plate 46 LM: x1500
SEM: 1-4 x9000, 5 x15000

Figs. 1-3, 5-10 *Achnanthidium minutissimum* (Kützing) Czarnecki

Fig. 4 *Achnanthidium caledonicum* (Lange-Bertalot) Lange-Bertalot

Fig. 1	Lake Roumassot, sediment PYR04
Figs. 2, 4-5	Lake Port Bielh, epilithic EpiPYR28
Fig. 3	Lake Angonella, epilithic EpiPYR78
Figs. 6, 9-10	Lake Les Laquettes, sediment PYR27
Figs. 7-8	Lake Posets, sediment PYR42

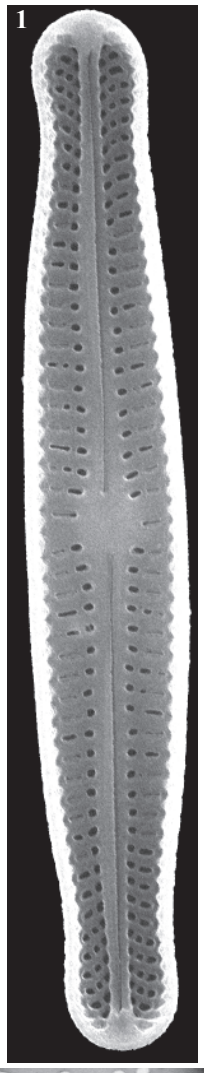
1

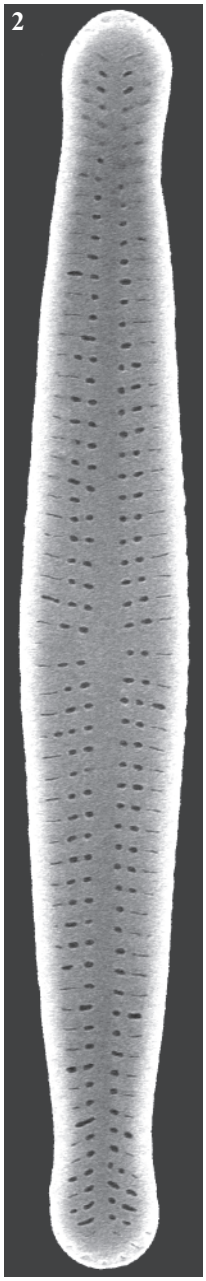
2

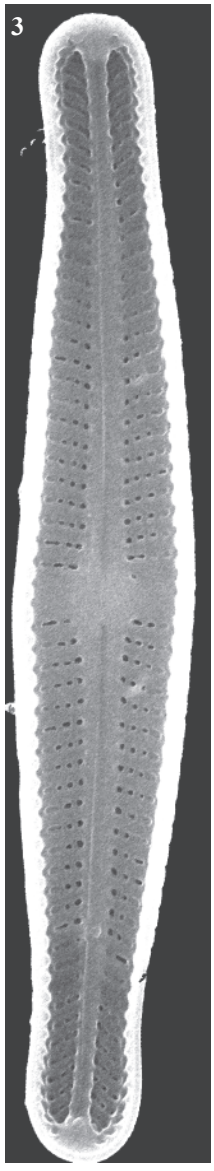
3

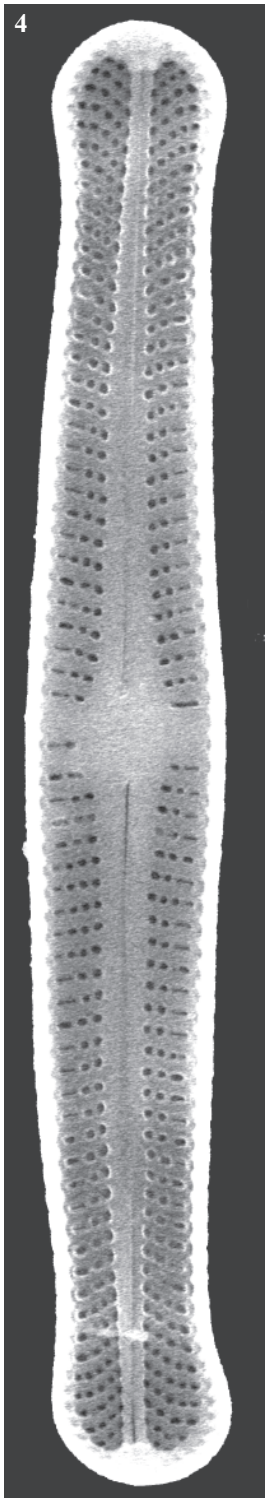
4

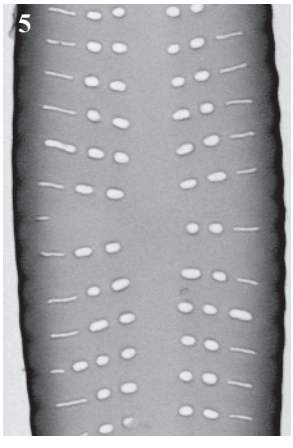
5


6


7


8


9


10

Plate 47 LM: x1500
SEM: x9000

Figs. 1-3 *Achnanthidium minutissimum* (Kützing) Czarnecki

Fig. 4-11, 21-24 ? *Achnanthidium minutissimum* (Kützing) Czarnecki

Figs. 12-18 *Achnanthes* sp. No. 8 Angonella

Fig. 25 *Achnanthidium* sp.

Fig. 1	Lake Les Laquettes, sediment PYR27
Figs. 2-3	Lake Posets, epilithic EpiPYR42
Figs. 4-11, 21-24	Lake Burg
Figs. 12-13	Lake Siscar, epilithic EpiPYR98
Figs. 14-16	Lake Angonella, epilithic EpiPYR78
Figs. 17-18	Lake Basa de la Mora, epilithic EpiPYR32
Figs. 19-20	Lake Eriste, epilithc EpiPYR43
Fig. 25	Lake Port Bielh, epilithic EpiPYR28

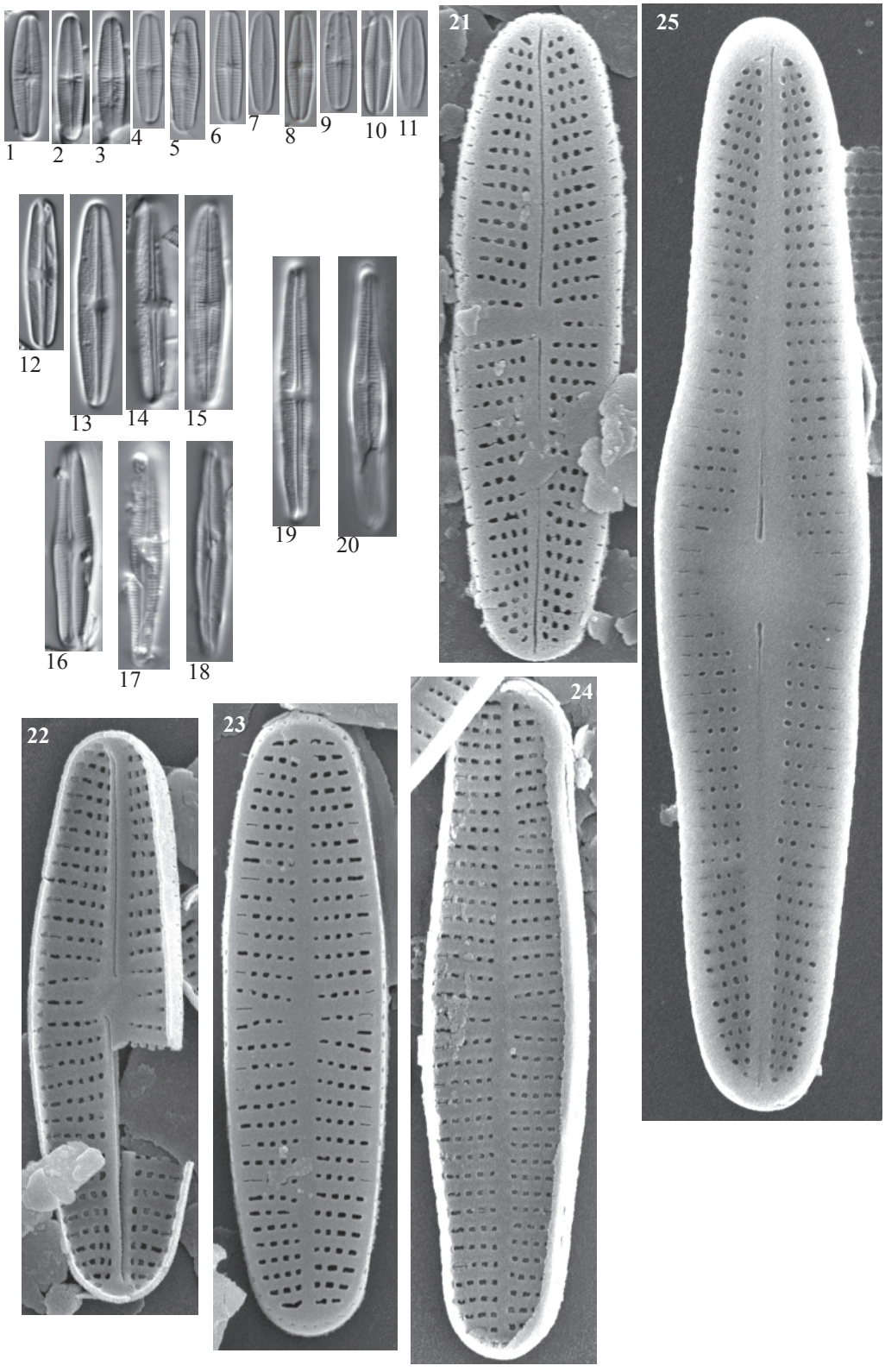
1
2
3
4
5
6
7
8
9
10
11
12
13
14
15
16
17
18
19
20
21
22
23
24
25

Plate 48 LM: x1500
SEM: x10000

Figs. 1-9 *Achnanthidium pfisteri* Lange-Bertalot

Figs. 10-11 *?Achnanthidium pfisteri* Lange-Bertalot
Figs. 12-42 *Achnanthidium pyrenaicum* (Hustedt) Kobayasi
Figs. 43-46 *Rossithidium pusillum* (Grunow) Round et Bukhtiyarova
Figs. 47-50 *Rossithidium linearis* (Smith) Round et Bukhtiyarova
Fig 51 *Rossithidium petersenii* (Hustedt) Round et Bukhtiyarova

Figs. 1-9	Lake Helado de Marboré, sediment PYR18
Figs. 10-11	Lake Filià, epilithic EpiPYR71
Figs. 12-13	Lake Negre, sediment PYR11
Figs. 14-15, 43-45	Lake Les Laquettes, sediment PYR27
Figs. 16, 17-30, 32-42, 51	Lake Llebreta, sediment PYR58
Fig. 31	Lake Estom, sediment PYR15
Fig. 36	Lake Roumassot, epilithic EpiPYR04
Fig. 46	Lake Posets, Sediment PYR42
Fig. 56	Lake Coronas, sediment PYR47
Figs. 48-50	Lake L`Estagnol, sediment PYR119

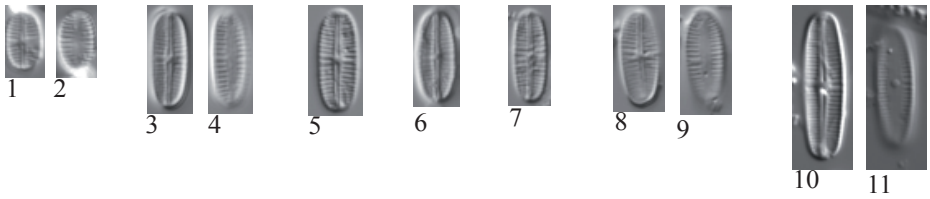
1
2
3
4
5
6
7
8
9
10
11

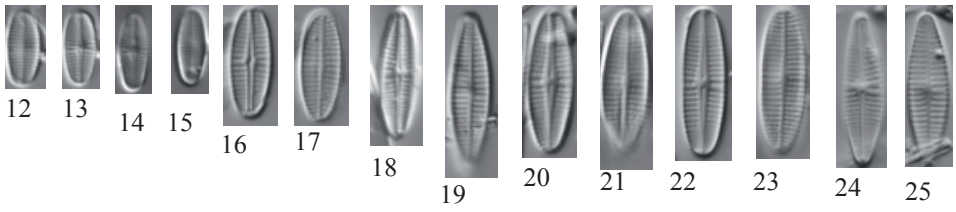
12
13
14
15
16
17
18
19
20
21
22
23
24
25

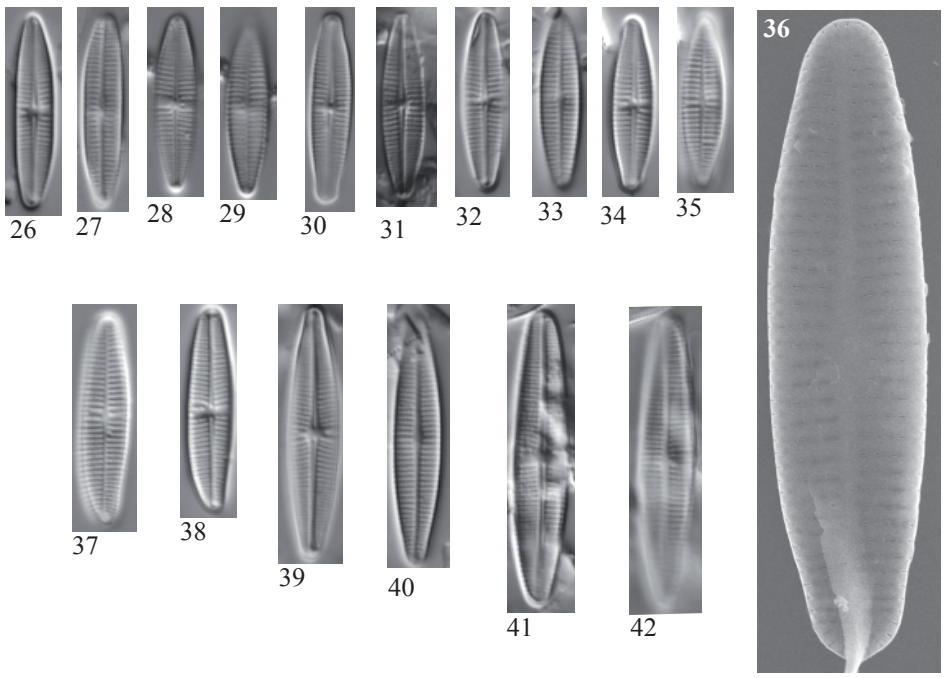
26
27
28
29
30
31
32
33
34
35
36
37
38
39
40
41
42

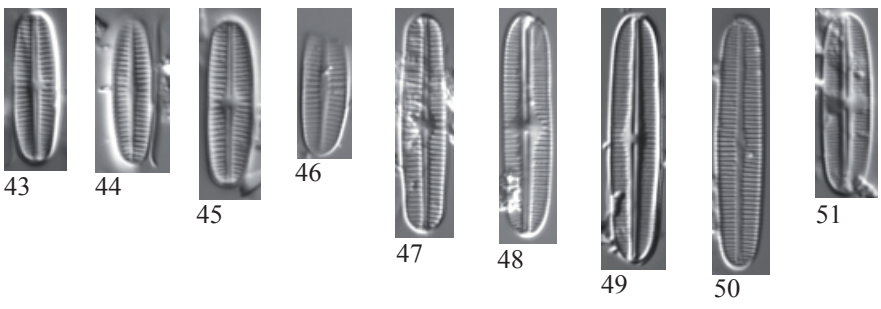
43
44
45
46
47
48
49
50
51

Plate 49 LM: x1500
SEM: Fig. 25 x11000, Fig. 26 x4000, Fig. 27-28 x 7000

Figs. 1-12 *Psammothidium helveticum* (Hustedt) Bukhtiyarova et Round

Figs. 13-27 *Achnanthes helvetica* var. *minor* Flower & Jones

Figs. 28-29 *Psammothidium helveticum* (Hustedt) Bukhtiyarova et Round

Fig. 30 *Psammothidium* sp

Figs. 1-2	Lake Blaou, sediment PYR94
Figs. 3-5	Lake Posets, sediment PYR42
Figs. 6-7	Lake Llosás, sediment PYR46
Figs. 8, 29	Lake Mariola, sediment PYR80
Figs. 9-10	Lake Forcat Inf., sediment PYR77
Figs. 11-12	Lake Bleu de Rabassoles, sediment PYR112
Figs. 13-22, 25-26	Lake Negre, sediment PYR79
Figs. 23-24	Lake Cregüeña, Sediment PYR49
Fig. 27	Lake Garbet, sediment PYR81
Fig. 28	Lake Redon, sediment REDOM
Fig. 30	Lake Illa, sediment PYR66

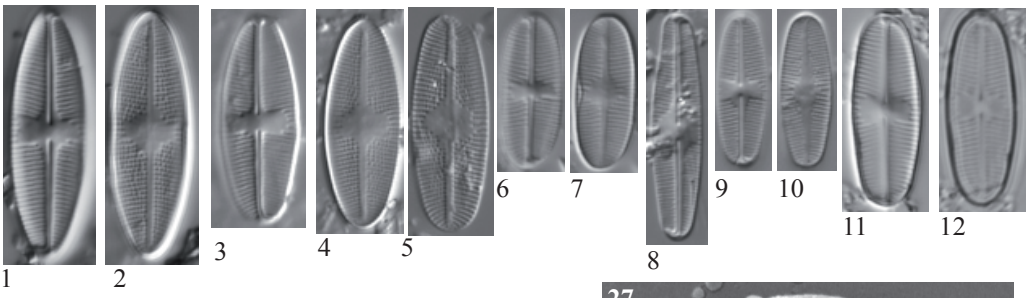
1
2
3
4
5
6
7
8
9
10
11
12

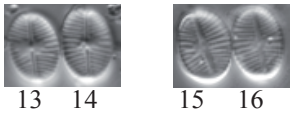
13
14
15
16

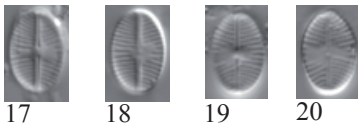
17
18
19
20

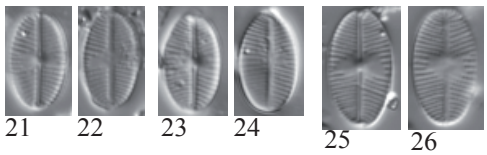
21
22
23
24
25
26

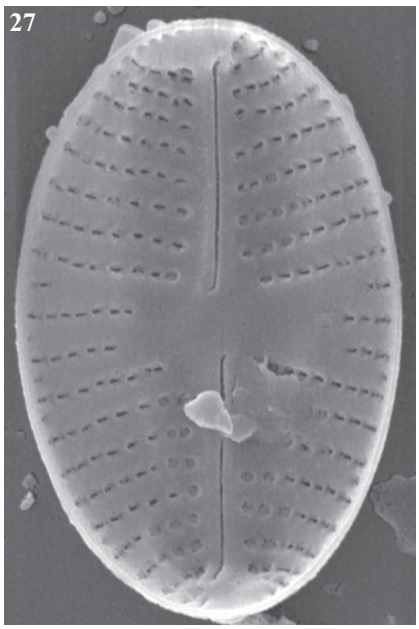
27

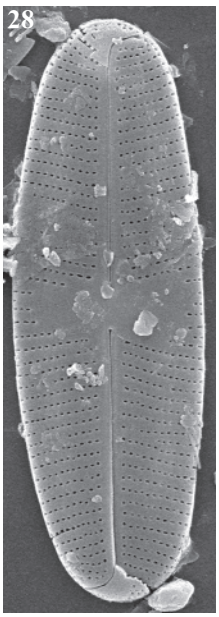
28

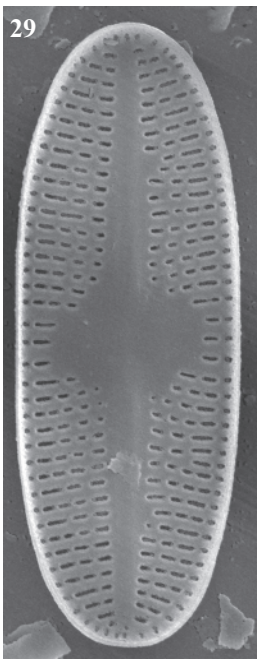
29

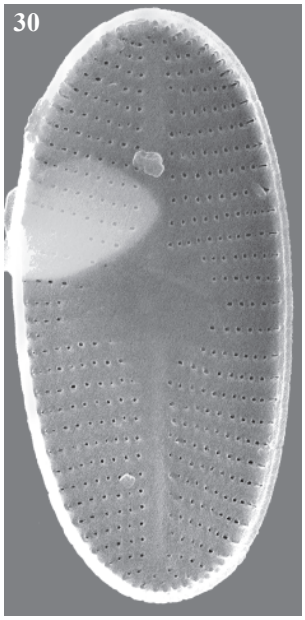
30

Plate 50 LM: x1500
SEM: x 9000

Figs. 1-10 *Psammothidium scoticum* (Flower et Jones) Bukhtiyarova & Round

Figs. 1-3	Lake Posets, sediment PYR42
Fig. 4	Lake Monges, sediment PYR57
Fig. 5	Lake Eriste, sediment PYR43
Figs. 6-10	Lake Redon, sediment REDOM
Fig. 11	Lake Garbet, sediment PYR81

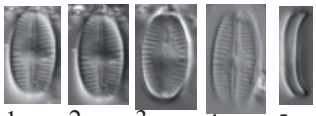
1
2
3
4
5

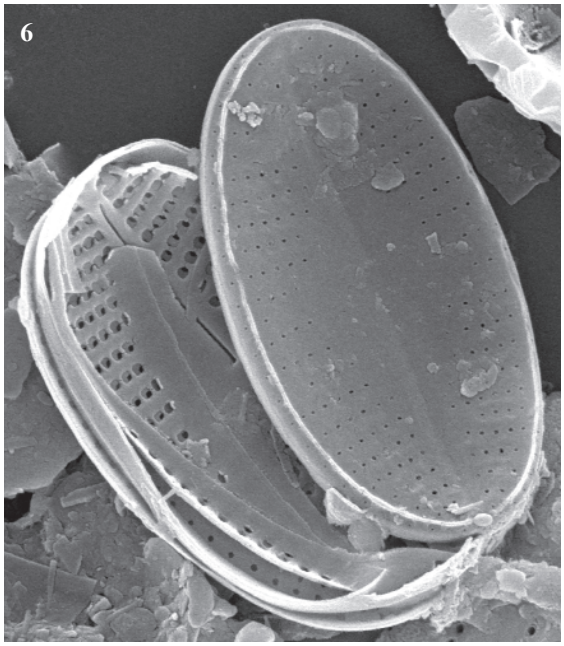
6

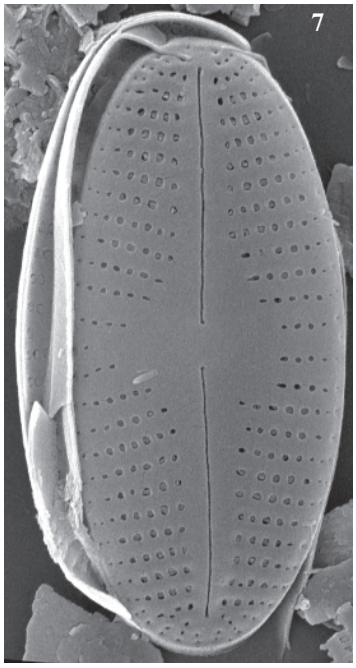
7

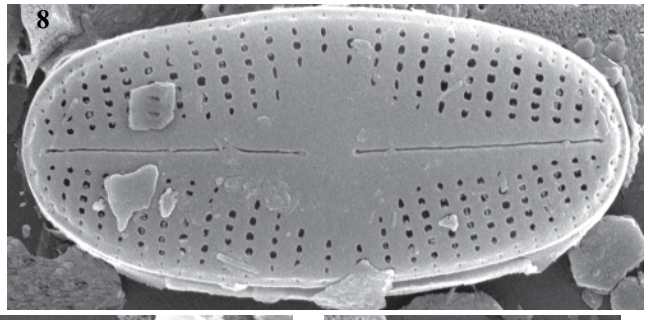
8


9

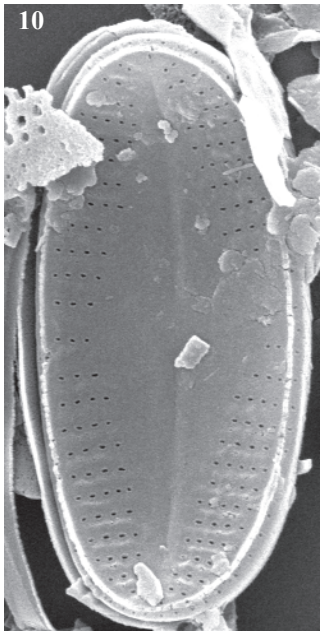
10

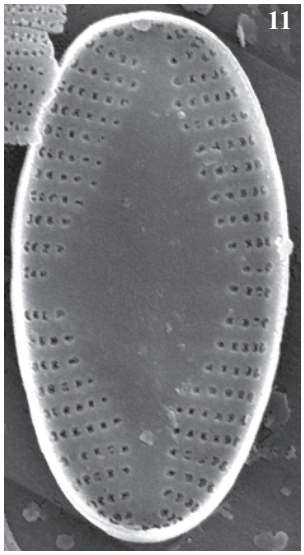
11

Plate 51 LM: x1500
SEM: x7000

Figs. 1-3	*Psammothidium bioretii* (Germain) Bukhtiyarova & Round
Figs. 4-6	*Psammothidium chlidanos* (Hohn & Hellerman) Lange-Bertalot
Figs. 7-9	*Psammothidium daonense* (Lange-Bertalot) Lange-Bertalot
Figs. 10-22	*Achnanthes* sp. No. 3 Posets
Figs. 23-24	P*sammothidium marginulatum* (Grunow) Bukhtiyarova et Round
Figs. 25-31	*Psammothidium acidoclinatum* (Lange-Bertalot) Lange-Bertalot
Figs. 32-36	*Psammothidium rossii* (Hustedt) Bukhtiyarova et Round
Figs. 37-41	*Achnanthes* sp. 7 Pixón
Figs. 42-43	*Psammothidium* cf. *daonense* (Lange-Bertalot) Lange-Bertalot
Figs. 44-49	*Psammothidium ventralis* (Krasske) Bukhtiyarova et Round
Figs. 50-53	*Achnanthes ziegleri* Lange-Bertalot

Figs. 1-2, 23-24	Lake Llebreta, sediment PYR58
Figs. 3, 6, 20-22	Lake Posets, sediment PYR42
Figs. 4-5	Lake Urdiceto, sediment PYR125
Figs. 7-9, 44-49	Lake Les Laquettes, sediment PYR27
Figs. 10-11, 32-34	Lake Siscar, sediment PYR126
Figs. 12-15, 18-19	Lake Monges, sediment PYR57
Figs. 16-17	Lake Cap Long, sediment PYR24
Figs. 25-30	Lake Bleu de Rabassoles, sediment PYR112
Fig. 31	Lake Senó, epilithic EpiPYR84
Figs. 35-36	Lake Estelat, sediment PYR120
Figs. 37-39	Lake Pixón, sediment PYR44
Figs. 40-41	Lake Blaou, sediment PYR94
Figs. 42-43	Lake Lliterola, epilithic EpiPYR33
Fig. 50	Lake Laurenti, sediment PYR111
Figs. 51-53	Lake Acherito, sediment PYR01


1


2


3


4


5


6


7


8


9


10


11


12


13


14


15


16


17


18


19


20


21


22


23


24


25


26


27


28


29


30

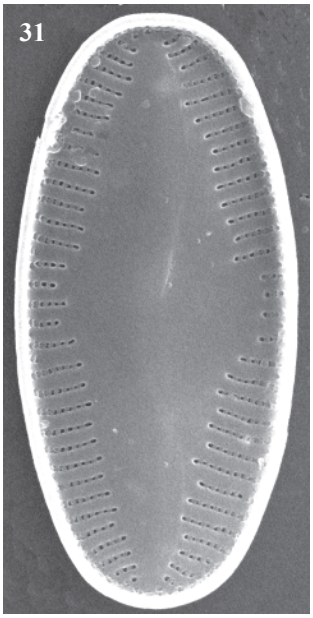
31


32


33


34


35


36


37


38


39


40

41

42

43

44

45

46

47

48

49

50

51

52

53

Plate 52 LM: x1500
SEM: x4500

Figs. 1-3, 7-9 *Cocconeis euglyptoides* (Geitler) Lange-Bertalot
Fig. 4 *?Cocconeis neothumensis* Krammer
Fig. 5-6 *Cocconeis neodiminuta* Krammer

Figs. 1-2	Lake Sen, sediment PYR40
Fig. 3	Lake Estom, sediment PYR15
Figs. 4-5	Lake Laurenti, epilithic EpiPYR111
Fig. 6	Lake Acherito, sediment PYR01
Fig. 7	Lake Roumassot, epilithic EpiPYR04
Fig. 8	Lake Arnales, epilithic EpiPYR09
Fig. 9	Lake Roumassot, sediment PYR04


1


2


3

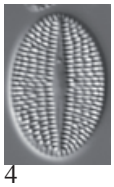
4


5


6

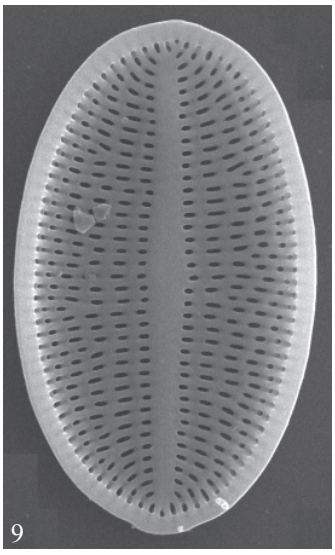
9

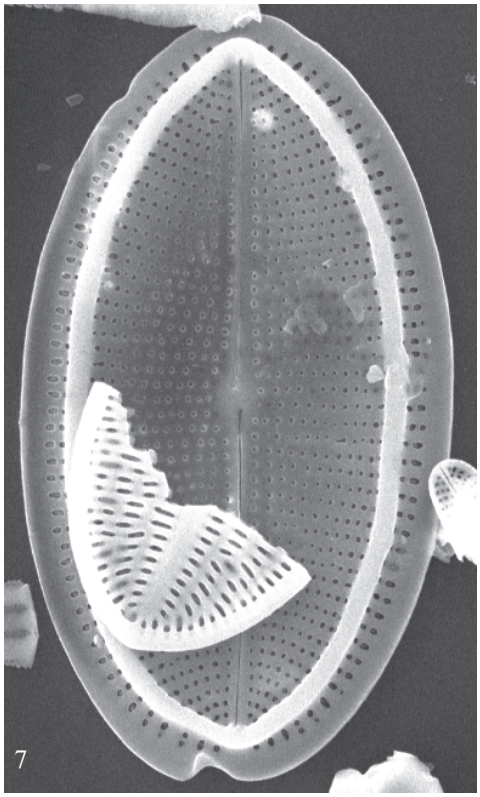
7

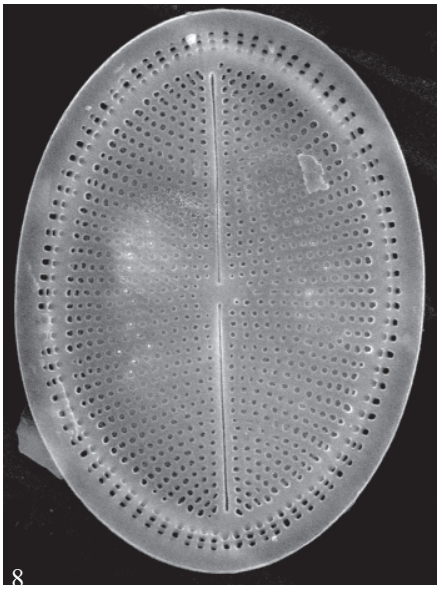
8

Plate 53 LM: x1500
SEM: x4000

Figs. 1-6	*Navicula caterva* Hohn & Hellerman
Figs. 7-8	*Navicula* cf. *caterva* Hohn & Hellerman
Figs. 9-19	*Navicula cryptocephala* Kützing
Figs. 20-23	*Navicula* cf. *cryptocephala* Kützing
Figs. 24-31	*Navicula wildii* Lange-Bertalot
Figs. 32-33	*Navicula* cf. *moskalii* Metzeltin, Witkowski & Lange-Bertalot
Figs. 34-36	*Navicula* cf. *cryptocephala* Kützing

Figs. 1-2, 5-6	Lake Sen, sediment PYR40
Figs. 3, 7-9	Lake Arnales, sediment PYR09
Figs. 4, 10-13, 19 35-36	Lake Posets, sediment PYR42
Figs. 14, 20-22, 24-31	Lake Arratille, sediment PYR11
Figs. 15, 17-18	Lake Acherito, sediment PYR01
Fig. 16	Lake Col d`Arratille, sediment PYR12
Fig. 23	Lake Mes Amunt de Tristaina, sediment PYR86
Fig. 32	Lake Helado del Monte Perdido, sediment PYR19
Fig. 33	Lake Tourrat, sediment PYR23
Fig. 34	Lake Arnales, epilithic EpiPYR09

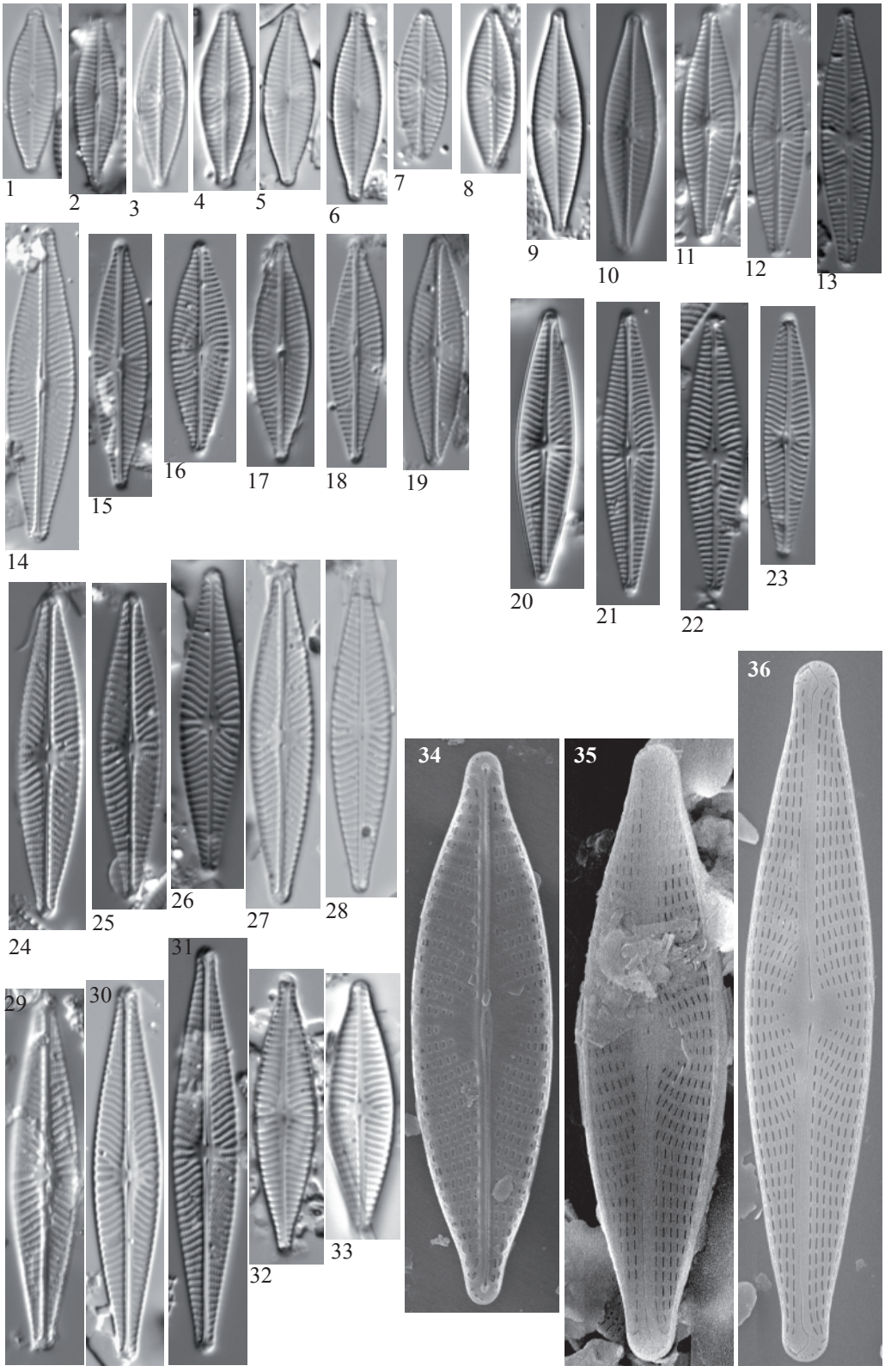
1
2
3
4
5
6
7
8
9
10
11
12
13
14
15
16
17
18
19
20
21
22
23
24
25
26
27
28
29
30
31
32
33
34
35
36

Plate 54 LM: x1500
SEM: x5000

Figs. 1-15 *Navicula cryptotenella* Lange-Bertalot
Figs. 16-19 *Navicula heimansioides* Lange-Bertalot
Figs. 20-22 *Navicula exilis* Kützing
Figs. 23-24 *Navicula notha* Wallace
Figs. 25-27 *Navicula cryptofallax* Lange-Bertalot & Hofmann

Figs. 1-6, 8-10, 12, 15	Lake Arratille , sediment PYR11
Fig. 7	Lake Sen, sediment PYR40
Figs. 13-14	Lake Col d`Arretille, sediment PYR12
Fig. 16	Lake Gelat Bergús, sediment PYR65
Figs. 17-19	Lake Bleu de Rabassoles, sediment PYR112
Fig. 20	Lake Llosás, sediment PYR46
Fig. 11	Lake Port Bielh, sediment EpiPYR28
Fig. 21	Lake Baiau Superior, sediment PYR76
Fig. 22	Lake Trebens, sediment PYR114
Fig. 23	Lake Argonella, sediment PYR78
Fig. 24	Lake Mes Amunt de Tristaina, sediment PYR86
Fig. 25	Lake Burg
Figs. 26-27	Lake Acherito, sediment PYR01

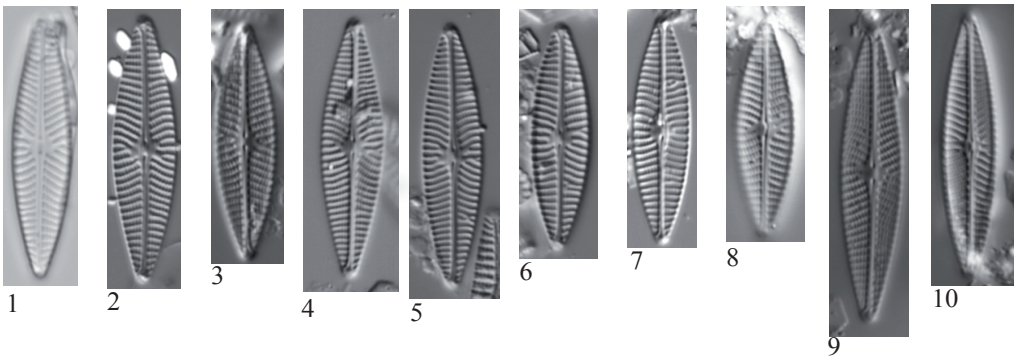
1
2
3
4
5
6
7
8
9
10

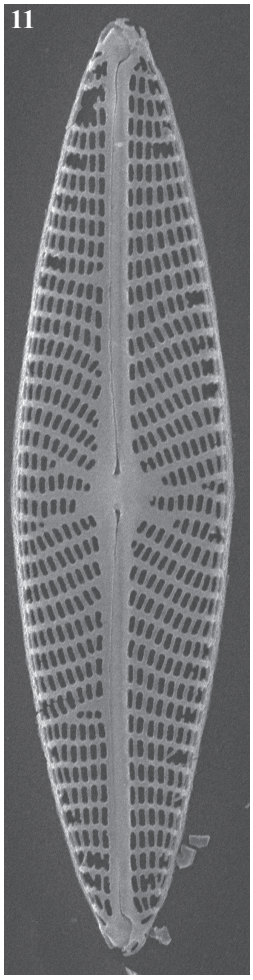
11

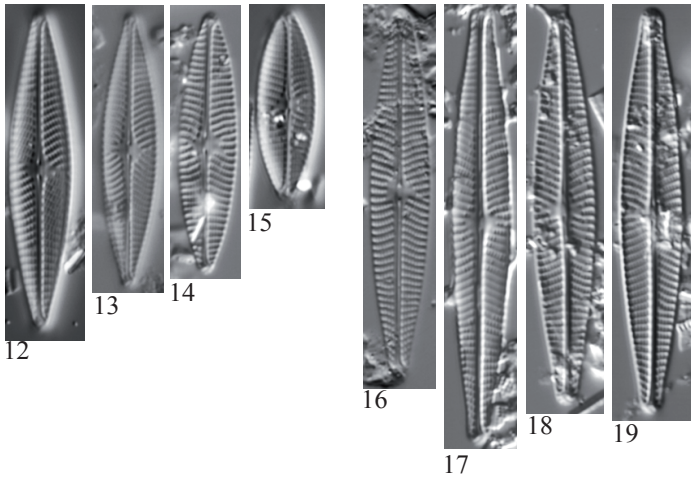
12
13
14
15
16
17
18
19

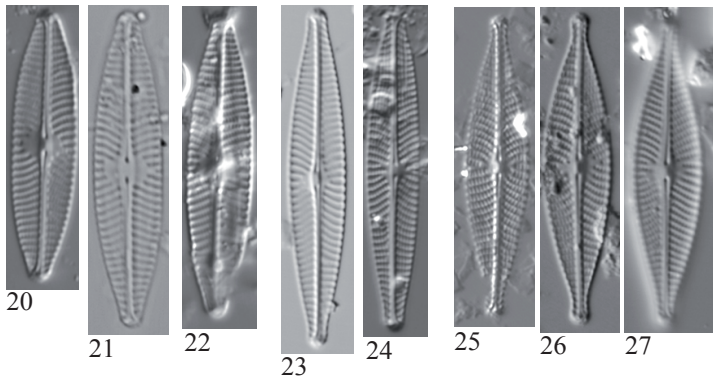
20
21
22
23
24
25
26
27

Plate 55 LM: x1500
SEM: x4000

Figs. 1, 8-13	*Navicula catalanogermanica* Lange-Bertalot & Hofmann
Figs. 2-6	*Navicula* cf. *antonii* Lange-Bertalot & Rumrich
Fig. 7	*Navicula* cf. *upsaliensis* (Grunow) Peragallo
Figs. 14-22	*Navicula pseudolanceolata* Lange-Bertalot
Figs. 23-26	*Navicula trophicatrix* Lange-Bertalot
Figs. 27-28	*Navicula subalpina* Reichardt
Fig. 29	*Navicula* cf. *libonensis* Schoeman
Figs. 30-31	*Navicula* sp. No. 9 Arratille

Fig. 1	Lake Laurenti , sediment PYR111
Figs. 2, 6	Lake Tourrat, sediment PYR23
Fig. 3	Lake Cap Long, sediment PYR24
Figs. 4-5, 12	Lake Acherito, sediment PYR01
Figs. 7, 13	Lake Barroude Inf., sediment PYR29
Figs. 8, 10-11, 24-26	Lake Col d`Arratille, sediment PYR12
Fig. 9	Lake Helado del Monte Perdido, epilithic EpiPYR19
Figs. 14-16, 23, 27-28	Lake Arratille, sediment PYR11
Fig. 17	Lake Montagnon, sediment PYR121
Figs. 18-20	Lake Arnales, sediment PYR09
Figs. 21-22	Lake Roumassot, sediment PYR04
Fig. 29	Lake Burg, sediment BURG 1195
Figs. 30-31	Lake Arratille, epilithic EpiPYR11

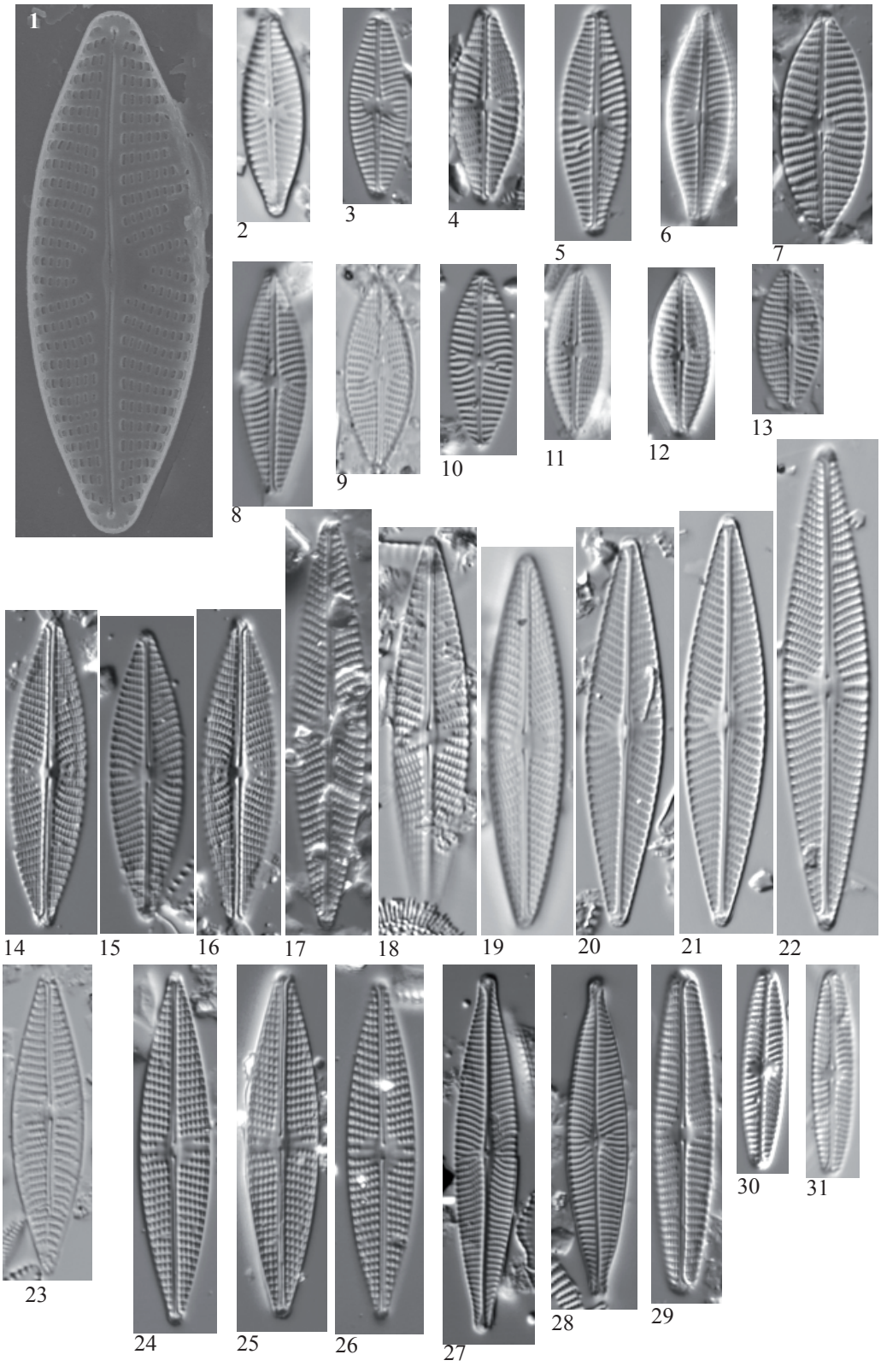
1
2
3
4
5
6
7
8
9
10
11
12
13
14
15
16
17
18
19
20
21
22
23
24
25
26
27
28
29
30
31

Plate 56 LM: x1500
SEM: x3000

Figs. 1-4 *Navicula* cf. *oligotraphenta* Lange-Bertalot & Hofmann
Figs. 5-6 *Navicula* cf. *trivialis* Lange-Bertalot
Figs. 7-8 *Navicula* sp.
Figs. 9-10 *Navicula viridula* Kützing

Fig. 1	Lake Burg, BURG 1195 cm
Fig. 2	Lake Basa de la Mora, sediment PYR32
Figs. 3-4	Lake Laurenti, sediment PYR111
Figs. 5-6	Lake Burg, sediment BURG 1068
Fig. 7	Lake Burg, sediment BURG 1072
Fig. 8	Lake Burg, sediment BURG 913
Figs. 9-10	Lake Burg, sediment BURG 843


1


2

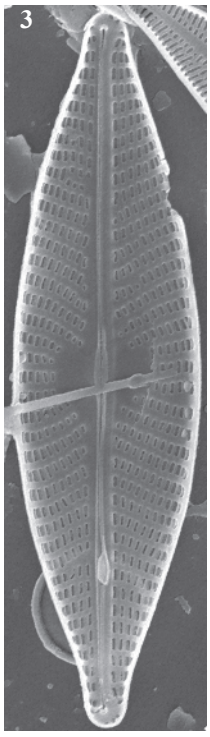
3

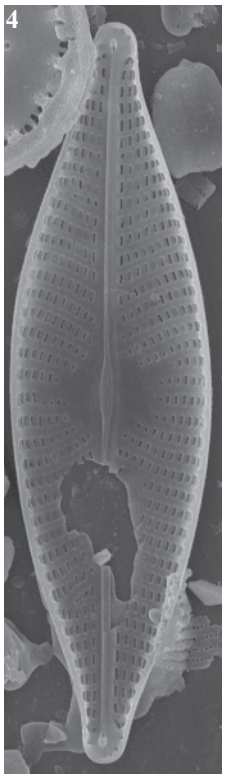
4

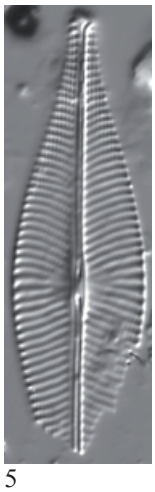
5

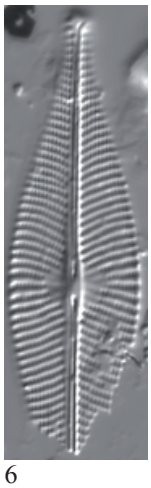
6


7


8


9


10

Plate 57 LM: x1500
SEM: x2500

Figs. 1-2 *Navicula vulpina* Kützing

Figs. 3-7 *Navicula radiosa* Kützing

Figs. 1-2, 7	Lake Arratille, sediment PYR11
Fig. 3	Lake Gran de la Pera, sediment PYR102
Fig. 4	Lake Plan, sediment PYR69
Fig. 5	Lake Sen, sediment PYR40
Fig. 6	Lake Posets, sediment PYR42

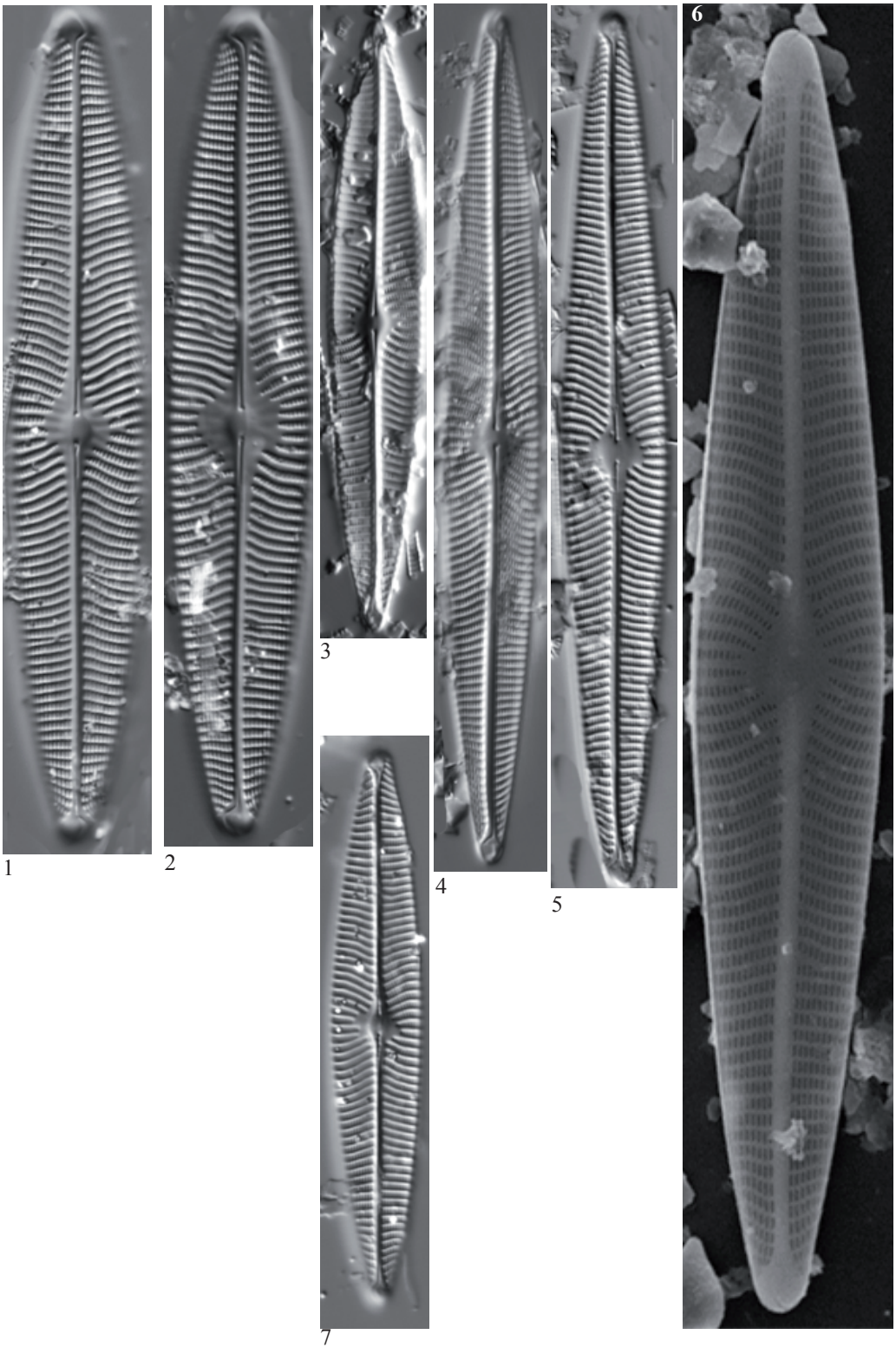
1
2
3
4
5
6
7

Plate 58 LM: x1500
SEM: x10000

Figs. 1-2 *Navicula venerablis* Hohn & Hellerman
Figs. 3-7 *Navicula angusta* Grunow

Fig. 1	Lake Coronas, sediment PYR47
Figs. 2-3	Lake Redon, sediment REDOM
Figs. 4-5, 7	Lake Mariola, sediment PYR80
Fig. 6	Lake Angonella, epilithic EpiPYR78


1


2


3


4

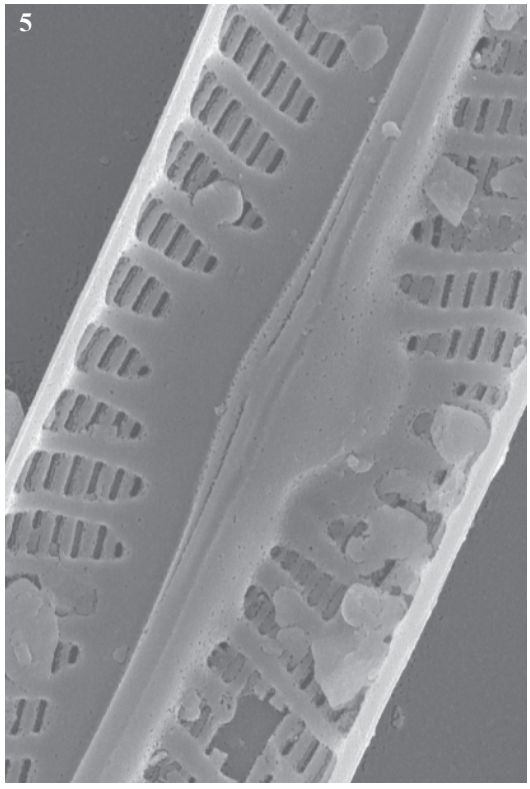
5


6

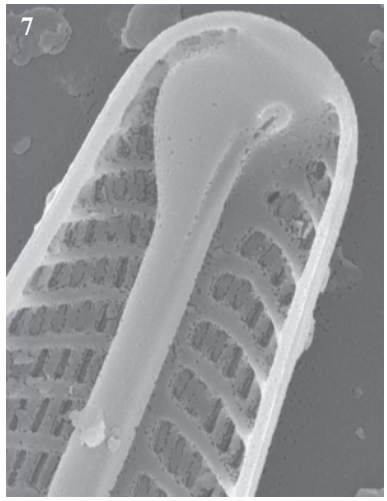
7

Plate 59 LM: x1500
SEM: Figs. 10-11 x5000, Figs. 19-20 x10000, Figs. 21-22 x4000

Figs. 1-11 *Sellaphora disjuncta* (Hustedt) D. G. Mann

Figs. 12-22 *Sellaphora laevissima* (Kützing) D. G. Mann

Figs. 1, 5, 7, 13, 18	Lake Posets, sediment PYR42
Fig. 2	Lake Burg, sediment BURG 1062
Figs. 3-4, 6	Lake Inferior de la Gallina, sediment PYR87
Figs. 8-9	Lake Llebreta, sediment PYR58
Figs.10-11, 14	Lake Burg
Fig. 12	Lake Arratille, sediment PYR11
Fig. 15	Lake Burg, sediment BURG 953
Fig. 16	Lake Burg, sediment BURG 543
Fig. 17	Lake Col d`Arratille, sediment PYR12

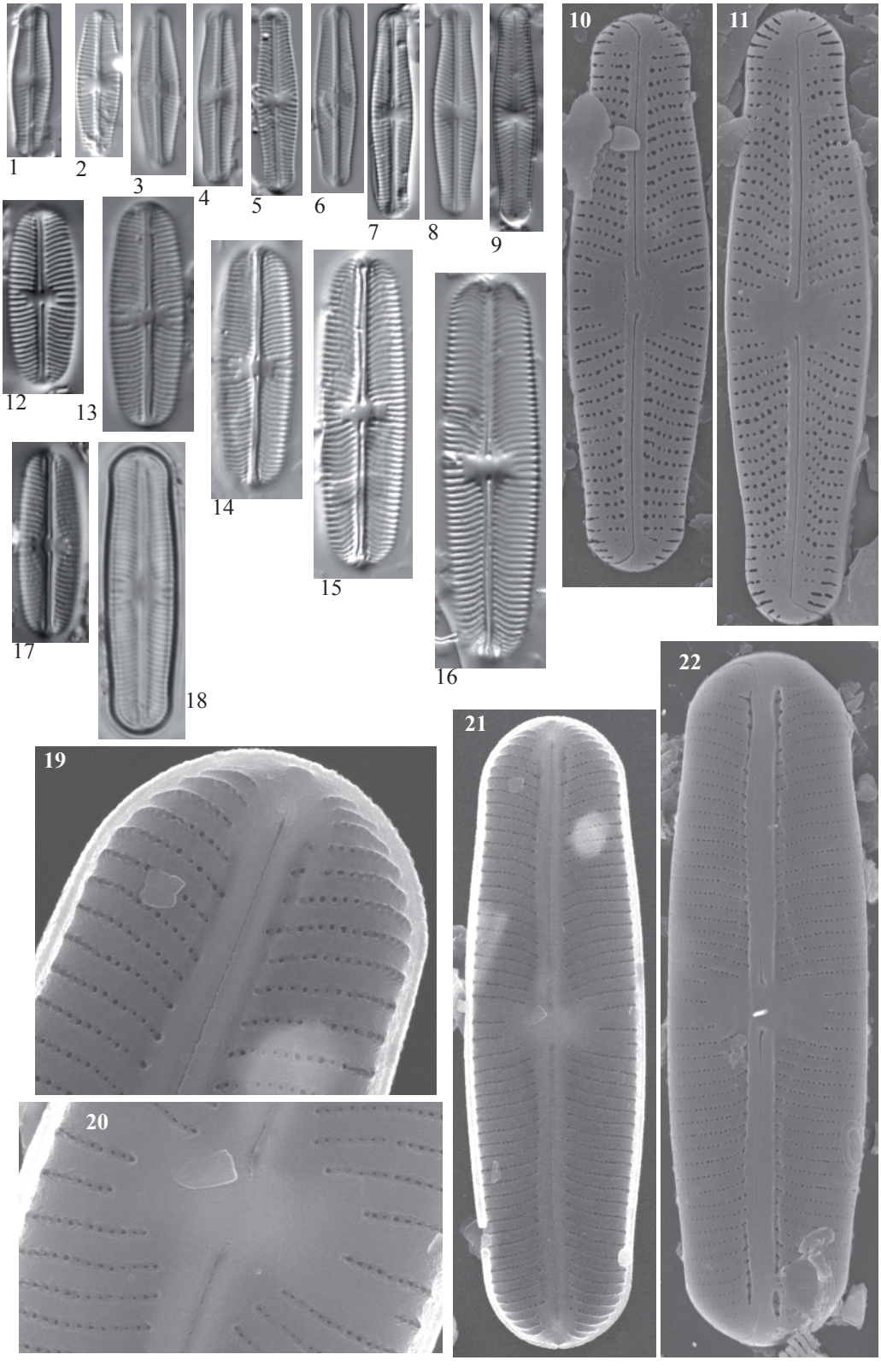
1
2
3
4
5
6
7
8
9
10
11
12
13
14
15
16
17
18
19
20
21
22

Plate 60 LM: x1500
SEM: Fig. 3 x9000, Fig. 4 x4000, Fig. 5 x3500, Fig. 6 x10000

Figs- 1-6 *Sellaphora bacillum* (Ehrenberg) D. G. Mann

Fig. 1 Lake Arratille, sediment PYR11

Figs. 2, 3-6 Lake Laurenti, sediment PYR111

1

2

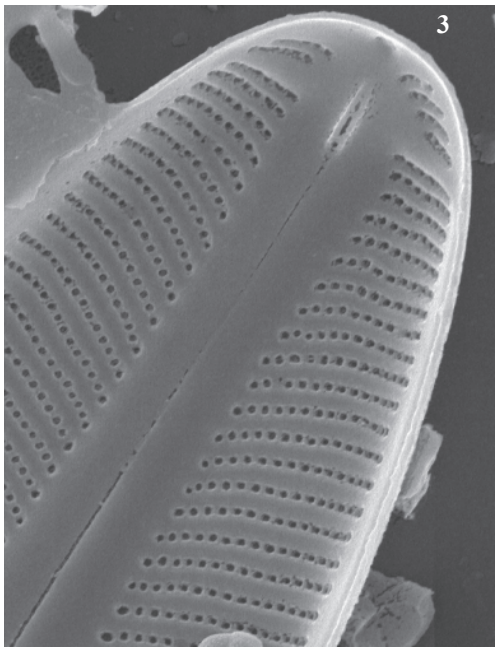

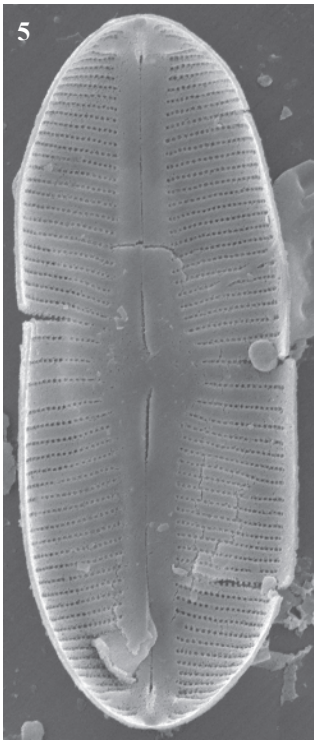

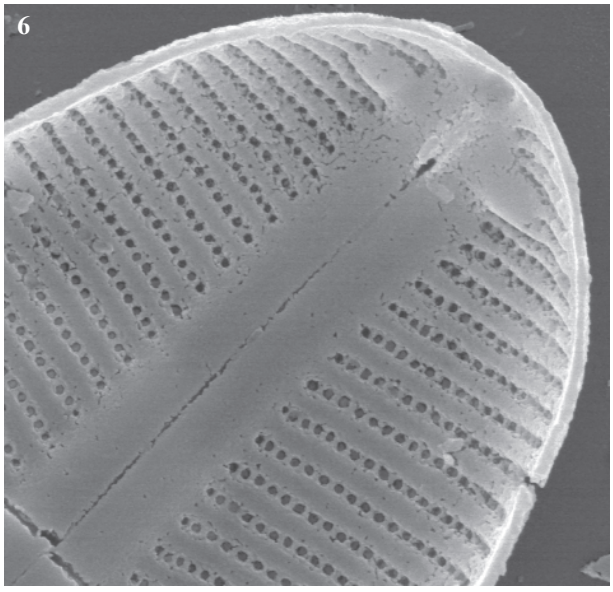

Plate 61 LM: x1500
SEM: x6000

Fig. 1 *Sellaphora pupula* (Kützing) Mereschkowsky sensu lato
cf. *Sellaphora blackfordensis* Mann & Droop
Figs. 2-11 *Sellaphora pseudopupula* (Krasske) Lange-Bertalot
12-14
Fig. 15 *Sellaphora pupula* (Kützing) Mereschkowsky sensu lato

Fig. 1	Lake Burg
Figs. 2, 6-7, 9-11	Lake Posets, sediment PYR42
Figs. 3, 5	Lake Albe, sediment PYR96
Fig. 4	Lake Arratille, sediment PYR11
Fig. 8	Lake Burg, sediment BURG 973
Fig. 12	Lake Angonella, epilithic EpiPYR78
Fig. 13	Lake Garbet, sediment PYR81
Fig. 14	Lake Laurenti, sediment PYR111
Fig. 15	Lake Acherito, sediment PYR01

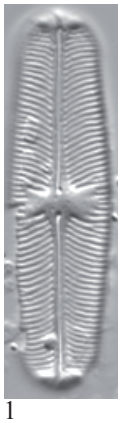
1


2


3


4


5


6


7


8


9


10


11


15

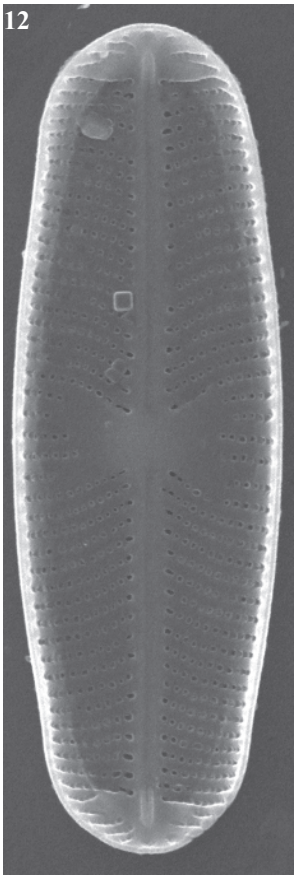
12

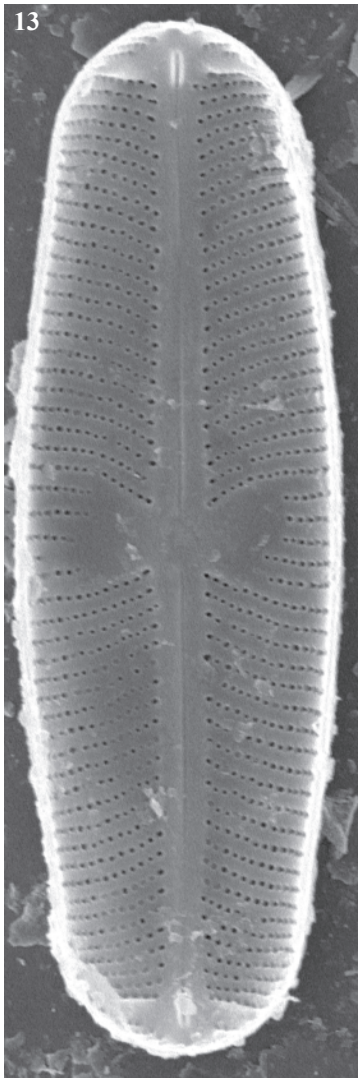
13

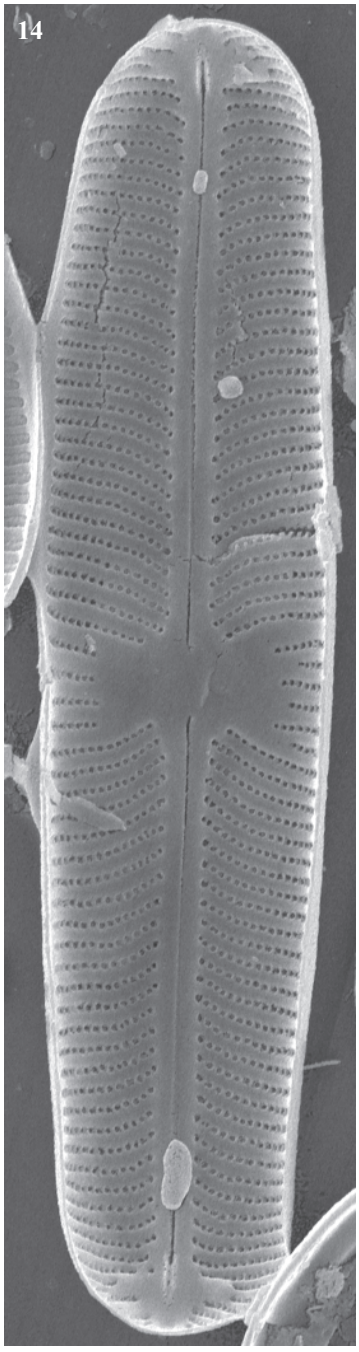
14

Plate 62 LM: x1500
SEM: Figs. 3, 10 x5000, Fig. 11 x4000, Fig. 12 x6000

Figs. 1-3	*Sellaphora stroemii* (Hustedt) Kobayasi
Figs. 4-6, 10	*Sellaphora pupula* (Kützing) Mereschkowsky sensu lato cf. *Sellaphora auldreekie* Mann & McDonald
Figs. 7-8	*Sellaphora pupula* (Kützing) Mereschkowsky sensu lato cf. *Sellaphora capitata* Mann & McDonald
Fig. 9	*Sellaphora* sp. No. 1 Ensangents
Fig. 11	*Sellaphora pupula* (Kützing) Mereschkowsky
Fig. 12	*Sellaphora* aff. *nanoides* Lange-Bertalot, Cavacini, Tagliaventi & Alfinito

Fig. 1	Lake Basa de la Mora, sediment PYR32
Fig. 2	Lake Gran de Mainera, sediment PYR70
Fig. 3	Lake Port Bielh, epilithic EpiPYR28
Fig. 4	Lake Burg, sediment BURG 927
Fig. 5	Lake Burg, sediment BURG 926
Fig. 6	Lake Arratille, sediment PYR11
Fig. 7	Lake Burg, sediment BURG 774
Fig. 8	Lake Burg, sediment BURG 782
Fig. 9	Lake Ensangents Sup., sediment PYR106
Figs. 10-11	Lake Laurenti, sediment PYR111
Fig. 12	Lake Gros de Camporrells, sediment PYR110

1

2

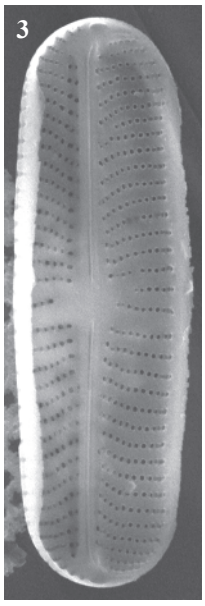

3

4

5

6

7

8

9

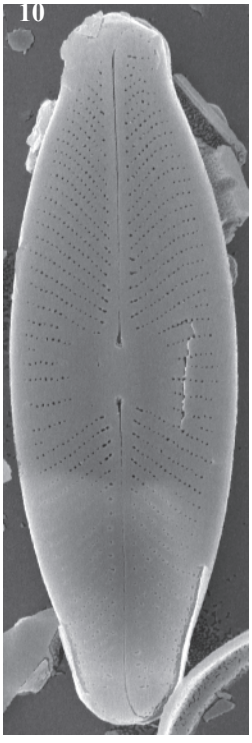

10

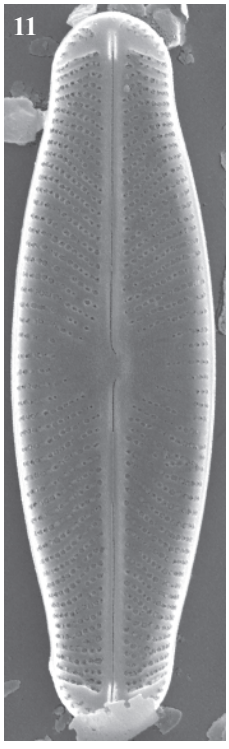

11

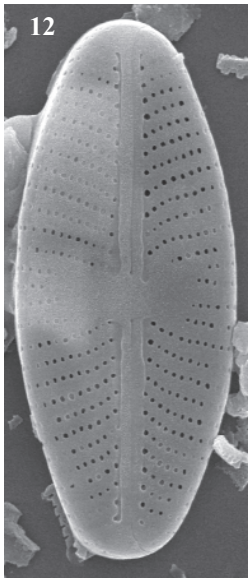

12

Plate 63 LM: x1500
SEM: Fig. 18 x6000, Fig. 19 x8000

Figs. 1-2 *Cavinula mollicula* (Hustedt) Lange-Bertalot

Figs. 3-10 *Cavinula cocconeiformis* (Gregory ex Greville) Mann & Stickle sensu lato

Figs. 11-19 *Cavinula pseudoscutiformis* (Hustedt) Mann & Stickle

Fig. 20 *Navicula* sp. No. 8 Sotllo

Figs. 1-2	Lake Negre, sediment PYR108
Fig. 3	Lake Laurenti, sediment PYR111
Figs. 4, 6-7, 11-12	Lake Inferior de la Gallina, sediment PYR87
Fig. 5	Lake Garbet, sediment PYR81
Figs. 8-10	Lake Blaou, sediment PYR94
Fig. 13	Lake Port Bielh, sediment PYR28
Fig. 14	Lake Arratille, sediment PYR11
Fig. 15	Lake Llebreta, sediment PYR58
Fig. 16	Lake Les Laquettes, sediment PYR27
Fig. 17	Lake Burg, sediment BURG 1187
Fig. 18	Lake Burg
Fig. 19	Lake Gros de Camporrells, sediment PYR110
Fig. 20	Lake Sotllo, epilithic PYR89


1


2


3


4


5


6


7

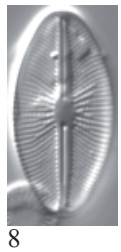
8


20

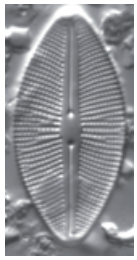
9

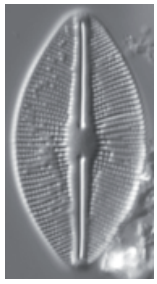
10

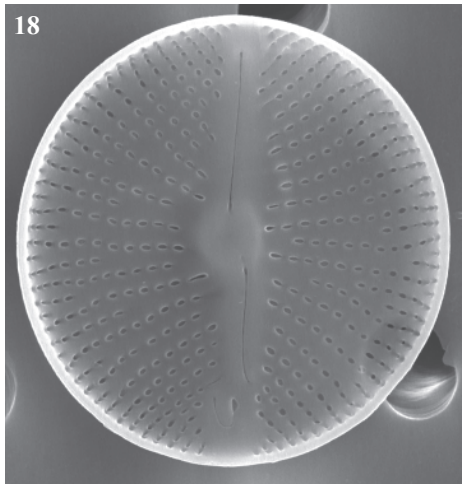
18


11


12


13


14


15

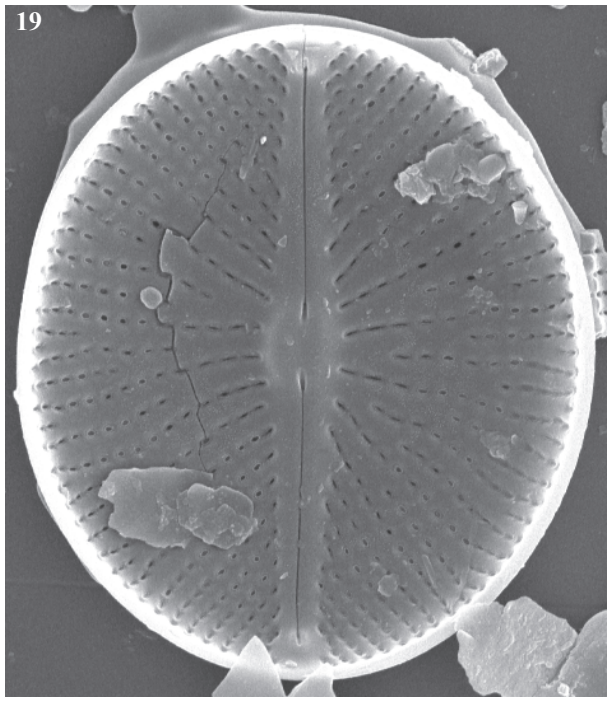
19


16


17

Plate 64 LM: x1500
SEM: Fig. 7 x4000, Fig. 17 x7000

Figs. 1-4	*Placoneis ignorata* (Schimanski) Lange-Bertalot
Figs. 5-7,9	*Placoneis explanata* (Hustedt) Lange-Bertalot
Fig. 8	*Placoneis symmetrica* (Hustedt) Lange-Bertalot
Fig. 10	*Placoneis* sp. No. 1 Acherito
Figs. 11-13	*Placoneis elginensis* (Gregory) Cox sensu lato
Figs. 14-15	*Placoneis* sp. No. 3 Burg
Fig. 16	*Placoneis* cf. *abiskoensis* (Hustedt) Lange-Bertalot et Metzeltin
Fig. 17	*Placoneis paraelginensis* Lange-Bertalot

Figs. 1, 3	Lake Negre, sediment PYR96
Fig. 2	Lake Burg, sediment BURG 480
Fig. 4	Lake Burg
Fig. 5-6	Lake Burg, sediment BURG 543
Fig. 7	Lake Blaou, sediment PYR27
Figs. 8, 10	Lake Port Bielh, sediment PYR01
Fig. 11	Lake Burg, sediment BURG 1053
Fig. 12	Lake Burg, sediment BURG 1007
Fig. 13	Lake Burg, sediment BURG 845
Fig. 14	Lake Burg, sediment BURG 1031
Fig. 15	Lake Burg, sediment BURG 848
Fig. 16	Lake Burg, sediment BURG 1104
Fig. 17	Lake Burg, sediment BURG 425


1


2


3


4

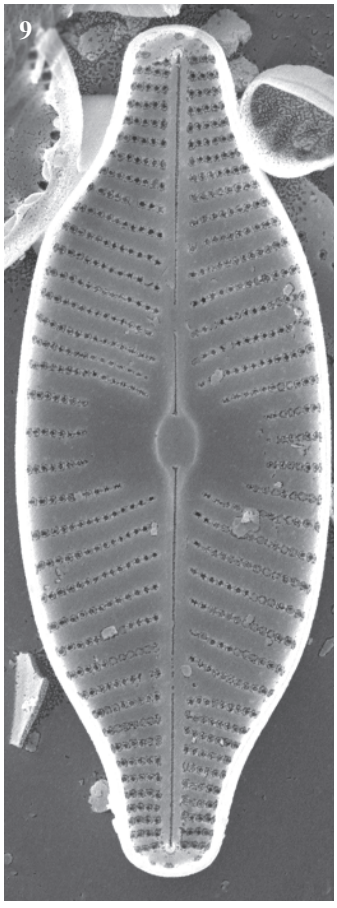
9


5


6


7


8


10


11


12


13

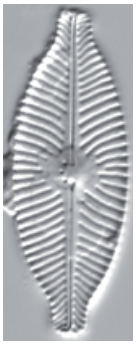
14


15


16


17

Plate 65 LM: x1500
SEM: Fig. 17 x7000

Fig. 1-4, 8 *Navicula* sp. No. 2 Liat
?5-7

Figs. 9-16 *Navicula detenta* Hustedt

Figs. 1, 3-5, 10-13	Lake Negre, sediment PYR42
Fig. 2	Lake Negre, sediment PYR55
Figs. 6-9	Lake Negre, sediment PYR40
Fig. 8	Lake Negre, sediment PYR80
Figs. 14-16	Lake Negre, epilithic EpiPYR78


1


2


3


4


5


6


7

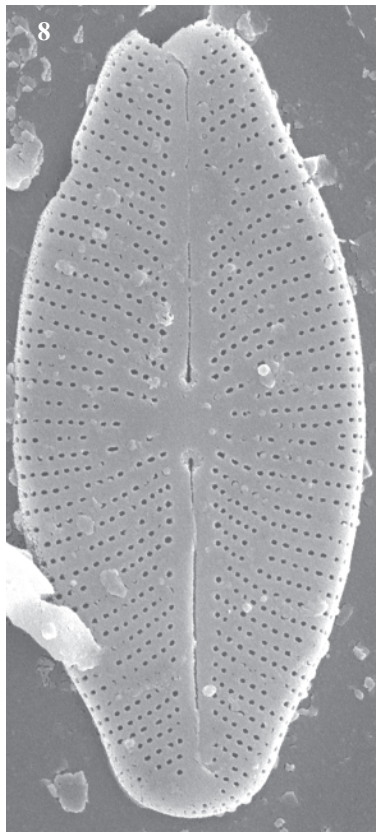
8


9


10


11


12

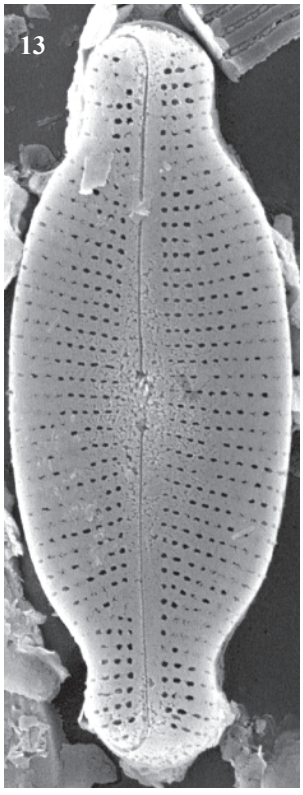
13


14

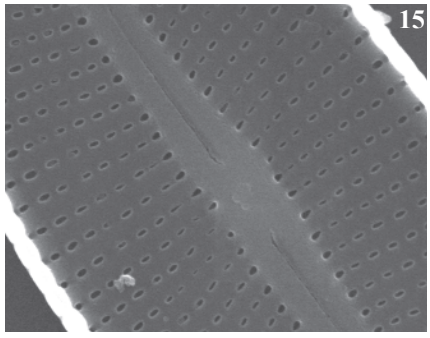
15

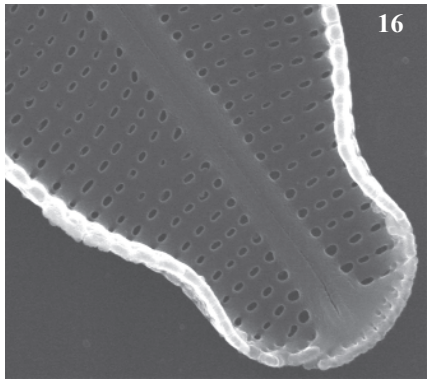
16

Plate 66 LM: x1500
SEM: Fig. 11 x15000, Figs. 12-13 x30000

Figs. 1-2	*Geissleria* cf. *paludosa* (Hustedt) Lange-Bertalot & Metzeltin
Fig. 3	*Geissleria* sp.
Figs. 4-5	*Geissleria* cf. *moseri* Metzeltin, Witkowski & Lange-Bertalot
Figs. 6-7, 11-13	*Geissleria acceptata* (Hustedt) Lange-Bertalot & Metzeltin
Figs. 8-10	*Geissleria similis* (Krasske) Lange-Bertalot & Metzeltin

Figs. 1, 2	Lake Burg, sediment BURG 1129
Fig. 3-4	Lake Posets, sediment PYR42
Fig. 5, 8-10	Lake Sen, sediment PYR40
Fig. 11-13	LLake Roumassot, sediment PYR04
Figs. 6-7	Lake Tourrat, sediment PYR23

Sample information of Plate 67

Figs. 1, 3, 26, 46	Lake Posets, sediment PYR42	Fig. 31	Burg, sediment BURG 1168
Figs. 2, 4, 45	Lake Llebreta, sediment PYR58	Fig. 32	Lake Chelau, epilithic EpiPYR41
Fig. 5	Lake Inf. Gallina, sediment PYR87	Fig. 33	Lake Estelat, sediment PYR120
Fig. 6	Lake Forcat Inf, sediment PYR77	Figs. 34-36, 38-40, 49	L. Cregüeña, sediment PYR49
Figs. 7-8, 10-11	Lake Monges, sediment EpiPYR57	Fig. 37	Lake Blau, sediment PYR113
Figs. 9, 27-28	Lake Burg	Figs. 41-42	Lake Sen, sediment PYR40
Fig. 12	Lake Pondiellos, sediment PYR08	Figs. 43-44	Lake Acherito, sediment PYR01
Fig. 13	Lake Sotllo, sediment EpiPYR89	Fig. 47	Lake Albe, sediment PYR96
Fig. 14	Burg, sediment BURG1093	Fig. 48	L. Les Laquettes, sed. PYR27
Figs. 15-18	L. Bleu de Rabassoles, sed. PYR112	Fig. 50	Burg, sediment BURG 1062
Fig. 19	Lake Plan, sediment PYR69	Fig. 51	Burg, sediment BURG 1192
Fig. 20	Lake Negre, sediment PYR79	Figs. 52, 59-62	Burg, sediment BURG 543
Fig. 21	Lake Laurenti, sediment PYR111	Figs. 53-55	Lake Arnales, sediment PYR09
Fig. 22	Lake Mariola, sediment PYR80	Fig. 56	Burg, sediment BURG 853
Fig. 23	Lake Illa, sediment PYR66	Fig. 57	Burg, sediment BURG 953
Fig. 24	Lake Llebreta, epilithic EpiPYR58	Fig. 58	Burg, sediment BURG 1069
Fig. 25	Lake Pica, epilithic EpiPYR100		
Fig. 29	Lake Cap Long, sediment PYR24		
Fig. 30	Lake Coronas, sediment PYR47		

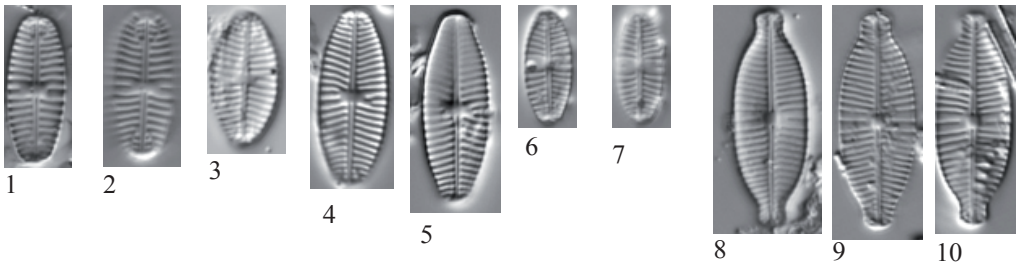
1
2
3
4
5
6
7
8
9
10

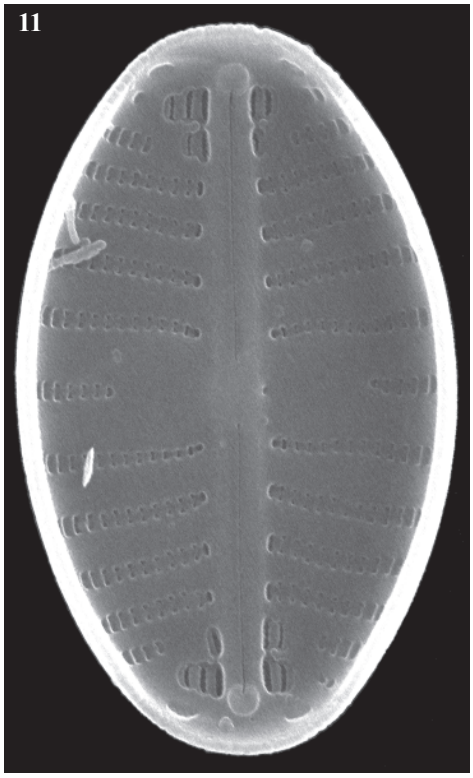
11

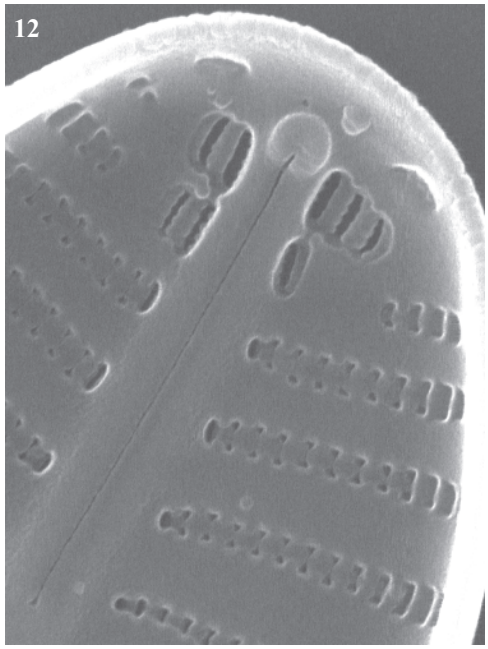
12

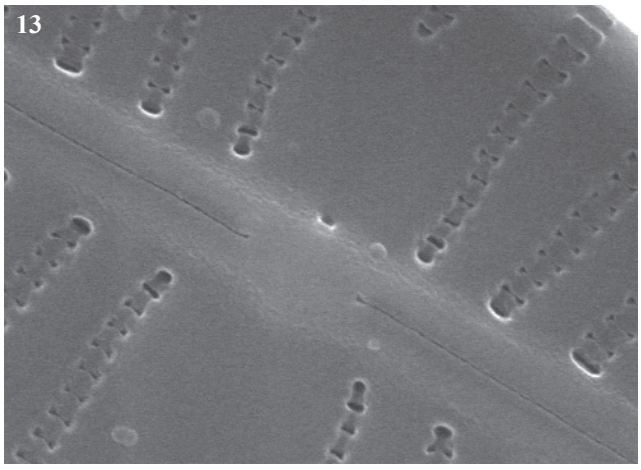
13

Plate 67 LM: x1500, SEM: x3000

Figs. 1-5 *Diadesmis perpusilla* (Grunow) Mann
Fig. 6 *Diadesmis fukushimae* Lange-Bertalot, Werum & Broszinski
Figs. 7-9 *Krasskella kriegerana* (Krasske) Ross & Sims
Figs. 10-11 *Microcostatus krasskei* (Hustedt) J.R. Johansen & J.C. Sray
Fig. 12 *Fallacia* sp. No. 1 Pondiellos
Fig. 13 *Fallacia vitrea* (Østrup) Mann
Fig. 14 *Fallacia* cf. *insociabilis (Krasske) Mann*
Figs. 15-19 *Chamaepinnularia mediocris* (Krasske) Lange-Bertalot
Fig. 20 *Chamaepinnularia* sp. No. 1 Negre
Fig. 21 *Chamaepinnularia hassiaca* (Krasske) Cantonati & Lange-Bertalot
Fig. 22 *Chamaepinnularia* sp. No. 3 Mariola
Fig. 23 *Chamaepinnularia* sp. No. 2 Illa
Fig. 24 *Chamaepinnularia* sp 3 Julma Olkky
Fig. 25 *Luticola* sp. No. 1 Pica
Fig. 26 *Luticola* sp. No. 2 Posets
Fig. 27 *Luticola* cf. *nivalis* (Ehrenberg) Mann
Fig. 28 *Luticola* sp. No. 7 Burg
Fig. 29 *Luticola* cf. *mutica* (Kützing) Mann
Fig. 30 *Luticola* sp. No. 5 Coronas
Fig. 31 *Luticola* sp. No. 6 Burg
Fig. 32 *Luticola* sp. No. 3 Chelau
Fig. 33 *Luticola* sp. No. 4 Estelat
Figs. 34-40 *Luticola* cf. *goeppertiana* (Bleisch in Rabenhorst) Mann
Figs. 41-42 *Hippodonta costulata* (Grunow) Lange-Bertalot, Metzeltin & Witkowski
Figs. 43-44 *Hippodonta* cf. *neglecta* Lange-Bertalot, Metzeltin & Witkowski
Figs. 45-48 *Navicula medioconvexa* Hustedt
Figs. 49 *Naviculadicta multiconfusa* Lange-Bertalot
Figs. 50-52 *Navicula glomus* Carter
Figs. 53-55 *Navicula opportuna* Hustedt
Figs. 56-62 *Navicula pseudoventralis* Hustedt sensu Krammer & Lange-Bertalot 1986

See sample information in the previous page

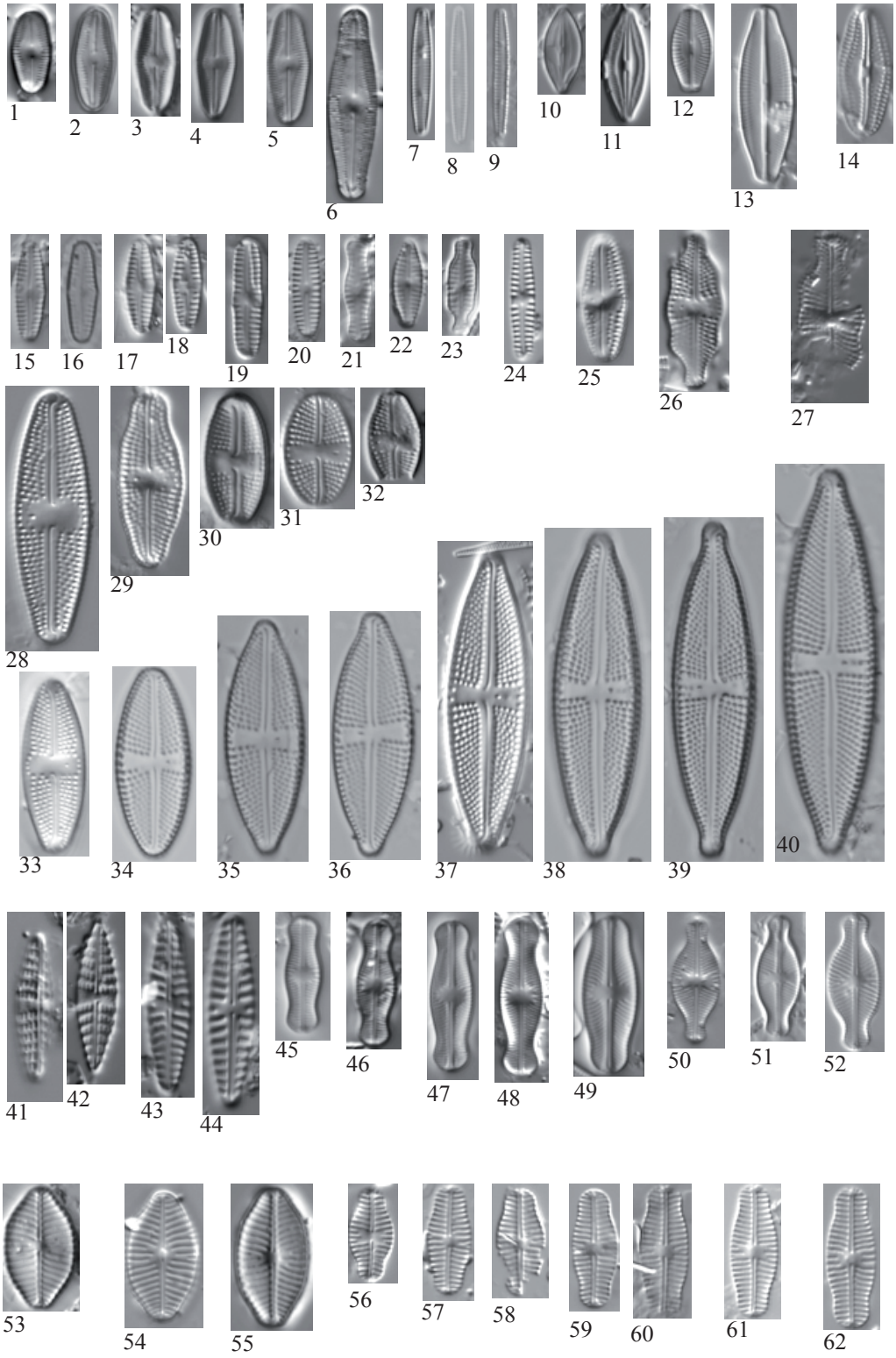
1
2
3
4
5
6
7
8
9
10
11
12
13
14
15
16
17
18
19
20
21
22
23
24
25
26
27
28
29
30
31
32
33
34
35
36
37
38
39
40
41
42
43
44
45
46
47
48
49
50
51
52
53
54
55
56
57
58
59
60
61
62

Plate 68 LM: x1500
SEM: Figs. 12-13 x10000, Fig. 26, 32, 35-37 x6000

Figs. 1-6	*Achnanthes carissima* Lange-Bertalot
Figs. 7-13	*Navicula schmassmanni* Hustedt
Figs. 14-17, 26	*Naviculadicta* sp. No. 3 Arratille
Figs. 18-21	*? Naviculadicta digitulus* (Hustedt) Lange-Bertalot
Figs. 22-25, 32	*Naviculadicta digitulus* (Hustedt) Lange-Bertalot aff. *Navicula fluens* Hustedt sensu Krammer & Lange-Bertalot 1986
Figs. 27-29	aff. *Navicula fluens*, *Naviculadicta* sp. No. 4 Arratille
Figs. 30-31	*Naviculadicta* sp. No. 5 Arratille
Figs. 33-37	*Naviculadicta digituloides* Lange-Bertalot
Fig. 38	cf. *Mayamaea atomus* (Kützing) Lange-Bertalot

Fig. 1	Lake Coronas, sediment PYR47
Figs. 2, 3-4	Lake Blaou, sediment PYR94
Figs. 5-9, 11-12, 18, 20, 22-25, 33-35	Lake Posets, sediment PYR42
Figs. 10, 19	Lake Sen, sediment PYR40
Figs. 13, 32, 36-37	Lake Redon, sediment REDOM
Figs. 14-17, 28-29, 31	Lake Arratille, sediment PYR11
Fig. 21	Lake Forcat Inf., sediment PYR77
Fig. 26	Lake Burg
Fig. 27	Lake Burg, sediment BURG 1198
Fig. 30	Lake Pondiellos, sediment PYR09
Fig. 38	Lake Burg, sediment BURG 760

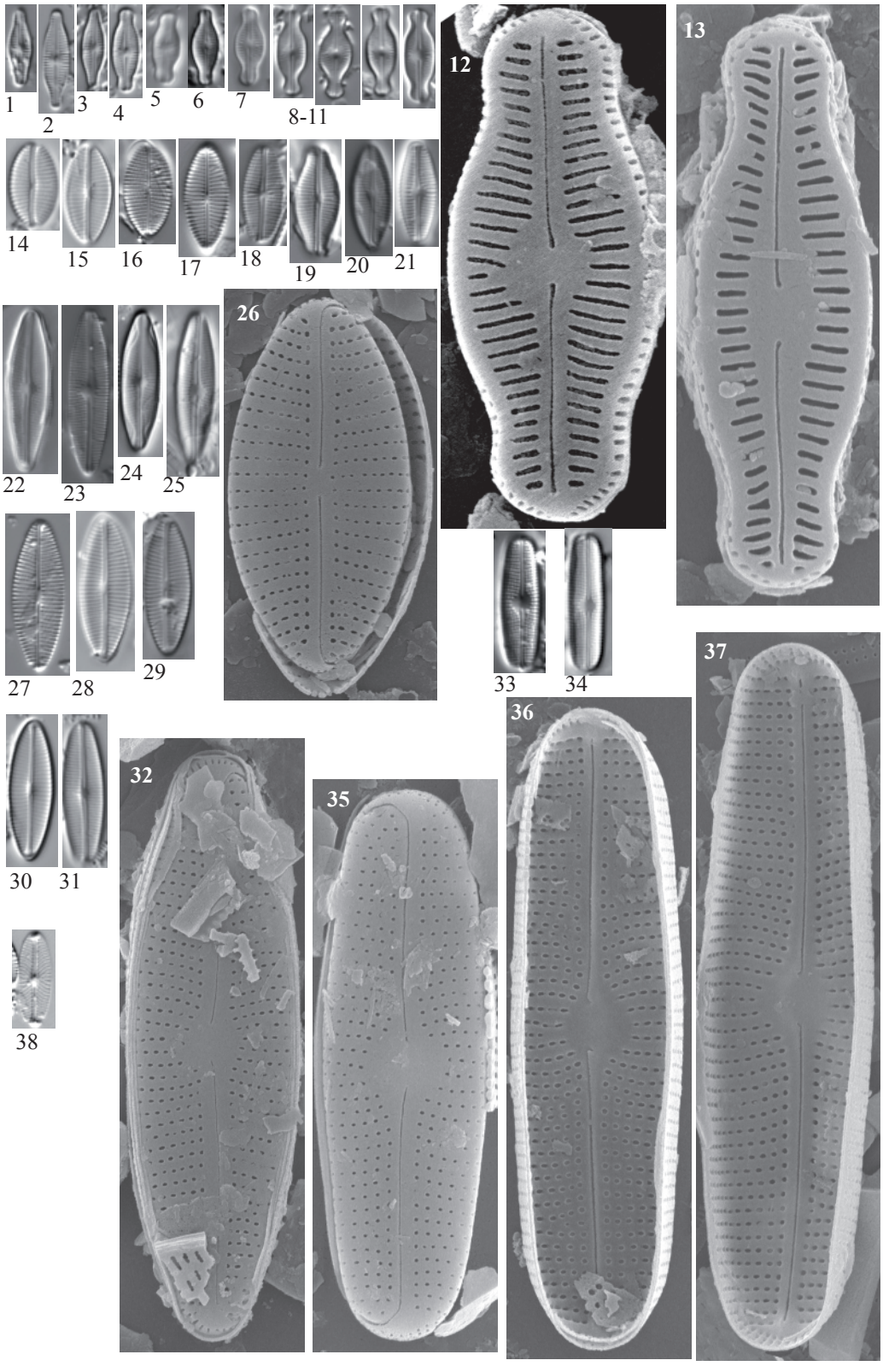
1
2
3
4
5
6
7
8-11
12
13
14
15
16
17
18
19
20
21
22
23
24
25
26
27
28
29
30
31
32
33
34
35
36
37
38

Plate 69 LM: x1500
SEM: Fig. 50 x10000, Figs. 51-52 x13000

Fig. 1, 50 *Naviculadicta* sp. No. 1 Ensangents
Fig. 2 *Naviculadicta* sp. No. 2 Bersau
Figs. 3-8 15-21 *Eolimna* sp. No. 5 Arnales
Figs. 9-14 *Eolimna* sp. No. 6 Marbore
Figs. 22 *Eolimna* spp.
Fig. 23-26 *Navicula* sp. No. 3 Laurenti
Fig. 27 *Navicula* sp. No. 4 Laquettes
Figs. 29-34 *Navicula* cf. *seminulum* Grunow
Figs. 35-40 *Navicula* cf. *seminulum* Grunow
Figs. 41-43 *Navicula utermoehli* Hustedt
Fig. 44 *Navicula* cf. *submuralis* Hustedt
Figs. 45-49 *Navicula* sp. No. 7 Bergus
Figs. 51-52 *Navicula* spp.

Figs. 1, 5	Lake Ensangents, sediment PYR106	Fig. 33, 35	L. Inf. de la Gallina, sed. PYR87
Fig. 2	Lake Bersau, epilithic EpiPYR03	Fig. 34	PYR127
Figs. 3-4, 45	Lake Port Bielh, sediment PYR28	Fig. 37	L. Burg, sediment BURG 848
Figs. 6-7, 14, 20, 49	Lake Siscar, sediment PYR126	Fig. 38	L. Burg, sediment BURG 851
Fig. 8	L. Burg, sediment BURG 932	Fig. 39	L. Burg, sediment BURG 932
Figs. 9, 11	L. Helado de Marboré, sed. PYR18	Fig. 40	L. Burg, sediment BURG 853
Figs. 10-13,18, 23, 26	L. Burg	Fig. 41	L. Burg, sediment BURG 831
Figs. 12, 27	Lake Laurenti, sediment PYR111	Fig. 42-44	Lake Arratille, sediment PYR11
Fig. 15	Lake Arnales, sediment PYR09	Fig. 46	L. Burg, sediment BURG 698
Fig. 16	L. Burg, sediment BURG 906	Fig. 47-48	L. Gelat Bergús, sediment PYR65
Fig. 17	L. Burg, sediment BURG 1007		
Figs. 19, 25, 28	Lake Les Laquettes, sediment PYR27		
Fig. 22	L. Burg, sediment BURG 837		
Fig. 24	L. Burg, sediment BURG 1153		
Fig. 26	L. Burg, sediment BURG 1053		
Fig. 32	Lake Sen, sediment PYR40		

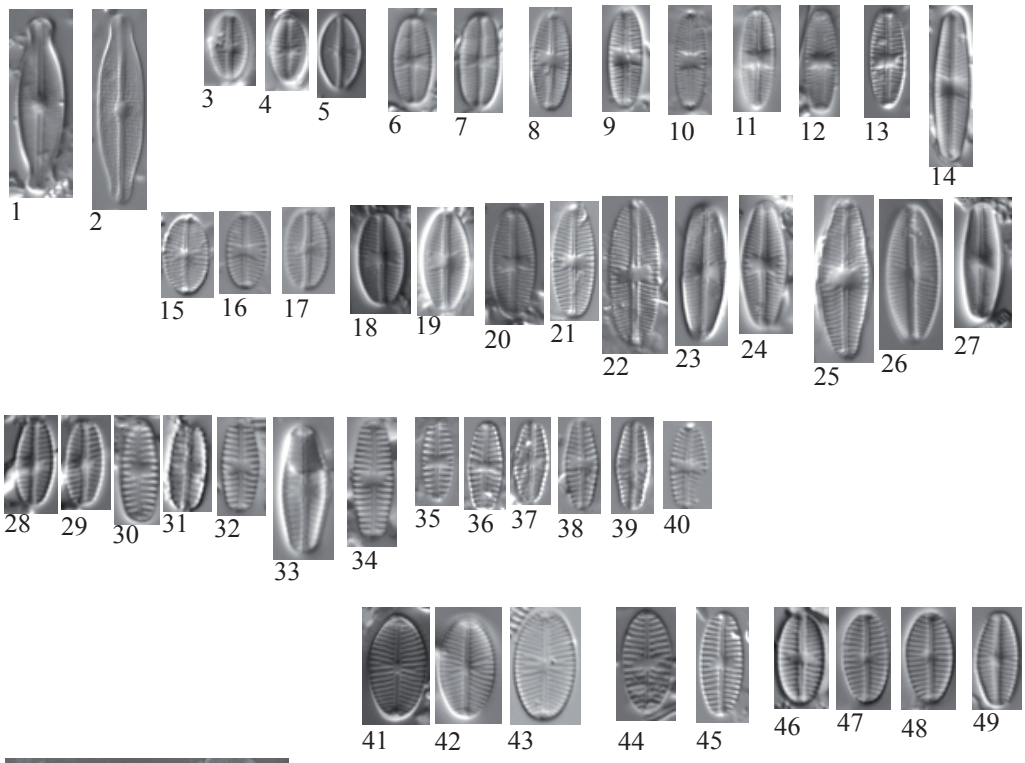
1
2
3
4
5
6
7
8
9
10
11
12
13
14
15
16
17
18
19
20
21
22
23
24
25
26
27
28
29
30
31
32
33
34
35
36
37
38
39
40
41
42
43
44
45
46
47
48
49

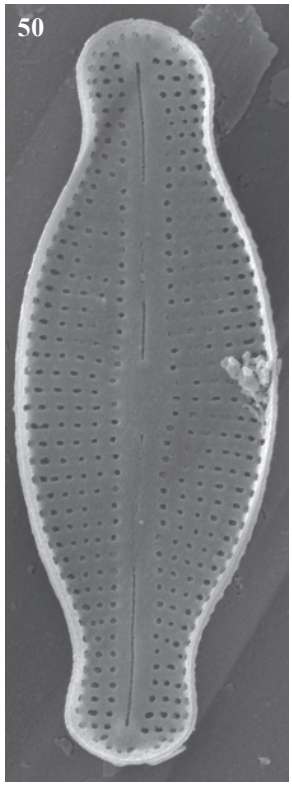
50

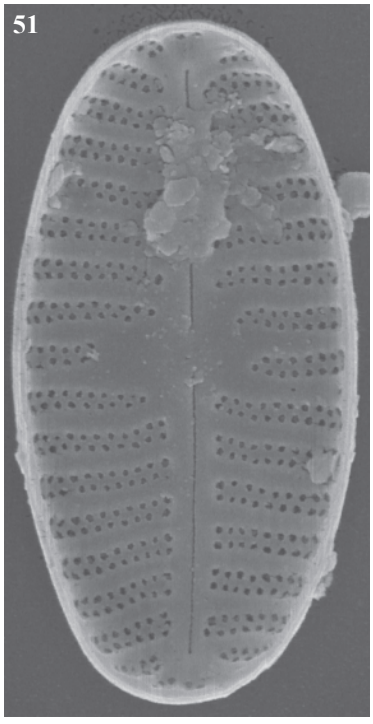
51

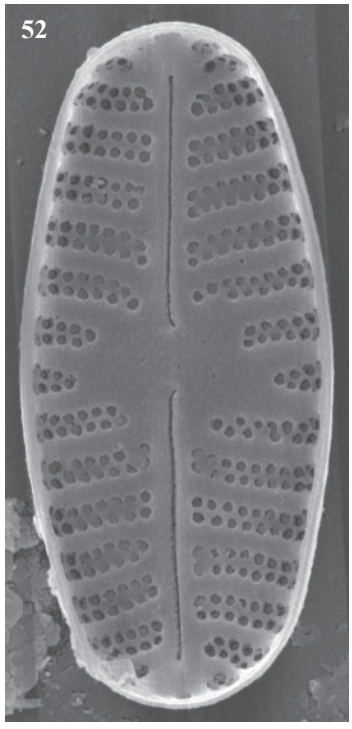
52

Plate 70 LM: x1500

Fig. 1	*Adlafia* cf. *suchlandtii* (Hustedt) Lange-Bertalot
Fig. 2	*Adlafia bryophila* (Petersen) Lange-Bertalot
Figs. 3-4	*Adlafia aquaeductae* (Krasske) Moser, Lange-Bertalot & Metzeltin
Fig. 5	*Adlafia* sp. No. 1 Barroude
Fig. 6	*Kobayasiella parasubtilissima* (Kobayasi & Nagumo) Lange-Bertalot
Figs. 7-8	*Kobayasiella subtilissima* (Cleve) Lange-Bertalot
Figs. 9-11	*Navicula brockmanni* Hustedt
Fig. 12	*Adlafia bryophila* (Petersen) Lange-Bertalot sensu lato
Fig. 13	*Adlafia* cf. *minuscula* (Grunow) H. Lange-Bertalot
Figs. 14-16	*Adlafia minuscula* (Grunow) H. Lange-Bertalot
Figs. 17-19	*Adlafia* cf. *suchlandtii* (Hustedt) Lange-Bertalot
Fig. 20	*Sellaphora* cf. *nanoides* Lange-Bertalot, Cavacini, Tagliaventi & Alfinito
Fig. 21	*Navicula* sp. No. 1 Laurenti
Figs. 22, 25	*Naviculadicta* cf. *difficillima* Hustedt
Figs. 23-24	*Naviculadicta* cf. *stauroneioides* Lange-Bertalot
Figs. 26-29	*Navicula absoluta* Hustedt sensu lato
Fig. 30	? *Placoneis* sp
Fig. 31	cf. *Navicula gerloffii* Schimanski
Figs. 32-38	*Navicula laterostrata* Hustedt
Figs. 39-40	*Kobayasiella* sp. 1 Seno *?Nupela tenuicephala* (Hustedt) Lange-Bertalot
Fig. 41	*Kobayasiella* sp. 2 Bleu

Fig. 1	Lake Coronas, sediment PYR70
Fig. 2	Lake Blaou, epilithic EpiPYR43
Fig. 3	Lake Posets, sediment PYR01
Fig. 4	Lake Sen, sediment PYR43
Fig. 5	Lake Blaou, epilithic EpiPYR29
Figs. 6, 40	Lake Sen, sediment PYR57
Fig. 7	Lake Sen, sediment PYR85
Fig. 8	Lake Sen, sediment PYR84

See next page for the others samples

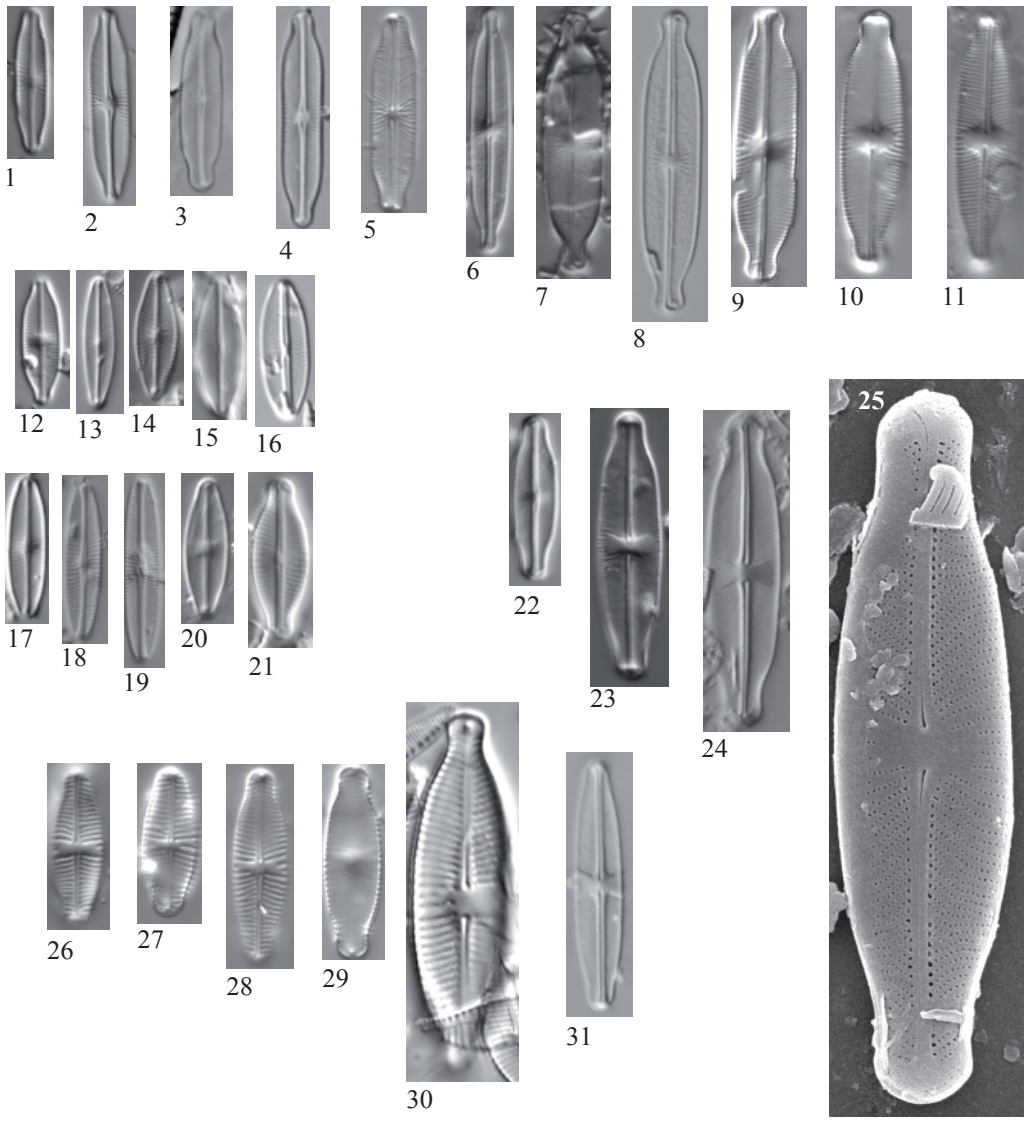
1
2
3
4
5
6
7
8
9
10
11
12
13
14
15
16
17
18
19
20
21
22
23
24
25
26
27
28
29
30
31
32
33
34
35
36
37
38
39
40
41

Plate 71 LM: x1500
SEM: x4500

Figs. 1-6 *Naviculadicta vitabunda* (Hustedt) Lange-Bertalot
Fig. 7 *Craticula molestiformis* (Hustedt) Mayama
Figs. 8-9 *Craticula submolesta* (Hustedt) Lange-Bertalot
Fig. 10 *Craticula* cf. *vixnegligenda* Lange-Bertalot
Fig. 11 *Craticula* sp. No. 1 Burg
Fig. 12 *Craticula cuspidata* (Kützing) Mann

Fig. 1	Lake Burg, sediment BURG 760
Figs. 2-3	Lake Port Bielh, sediment PYR28
Fig. 4	Lake Canals Roges, sediment PYR124
Figs. 5-6	Lake Burg, sediment BURG 543
Fig. 7	Lake Siscar, sediment PYR126
Fig. 8	Lake Coronas, sediment PYR47
Fig. 9	Lake Redon, sediment REDOM
Fig. 10	Lake Llosás, sediment PYR46
Fig. 11	L. Burg, sediment BURG 1070

Sample information of Plate 70

Fig. 9	L. Burg, sediment BURG 880
Figs. 10-11	Lake Burg, sediment BURG 987
Figs. 12	Lake Mariola, epilithic EpiPYR80
Fig. 13	Lake Arratille, sediment PYR11
Figs. 14, 20	Lake Cap Long, sediment PYR24
Figs. 15, 17	Lake Siscar, sediment PYR126
Figs. 16	Lake Bleu, epilithic EpiPYR22
Figs. 18-19	Lake Inf. de la Gallina, sediment PYR87
Fig. 21	Lake Laurenti, sediment PYR111
Figs. 22-23	Lake Coronas, sediment PYR47
Fig. 24	Lake Albe, sediment PYR96
Fig. 26	Lake Negre, epilithic EpiPYR108
Fig. 27	Lake Burg, sediment BURG 1080
Fig. 28-29	Lake Burg, sediment BURG 543
Fig. 30	L. Helado Monte Perdido, sediment PYR19
Fig. 31	Lake Mariola, sediment PYR80
Figs. 32-34, 36-38	Lake Burg, sediment BURG 543
Fig. 35	Lake Burg, sediment BURG 694
Figs. 39	LLake Senó, epilithic EpiPYR84
Fig. 41	L. Bleu de Rabassoles, EpiPYR112

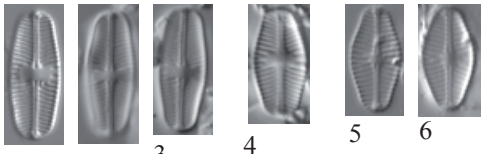

1 2 3 4 5 6

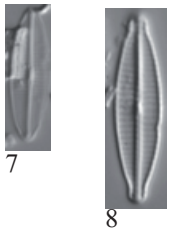

7 8

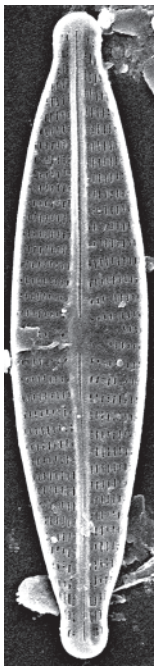

9

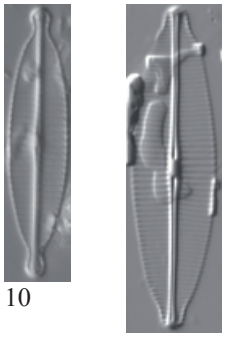

10 11

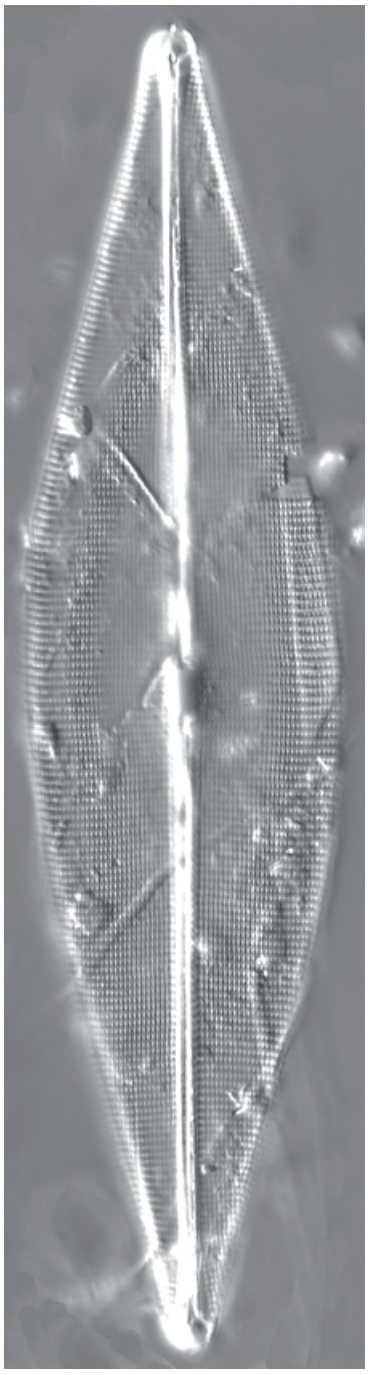

12

Plate 72 LM: x1500
SEM: Fig. 4 x1100, Fig. 5 x4000, Fig. 11 x10000

Fig. 1 *Gyrosigma* sp. No. 2 Mora

Figs. 2-9 *Gyrosigma* sp. No. 1 Sen

Fig. 1	Lake Basa de la Mora, sediment PYR32
Figs. 2-3	Lake Sen, sediment PYR40
Figs. 6-7	Lake Arratille, sediment PYR11
Figs. 4-5, 9	Lake Laurenti, sediment PYR111

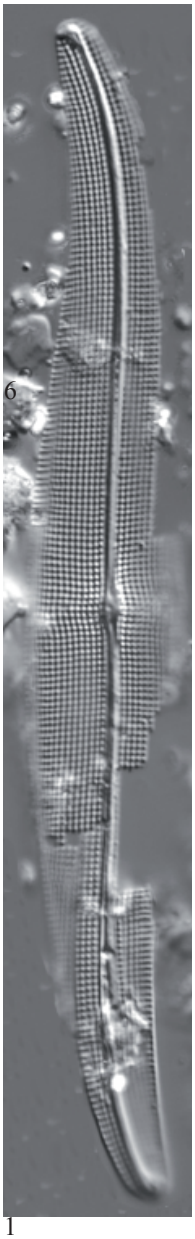
6

1

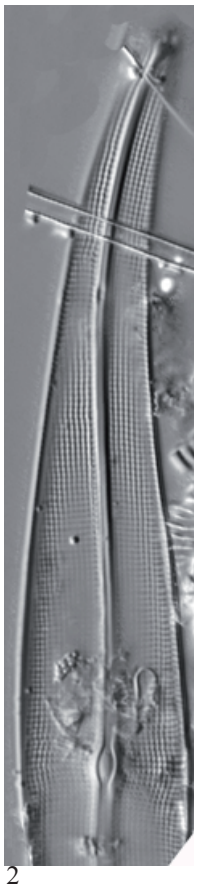
2

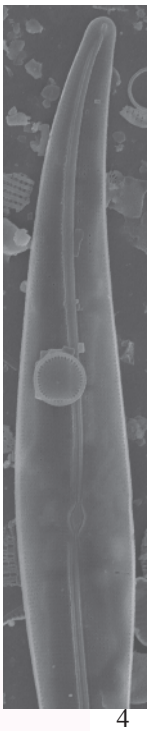
4

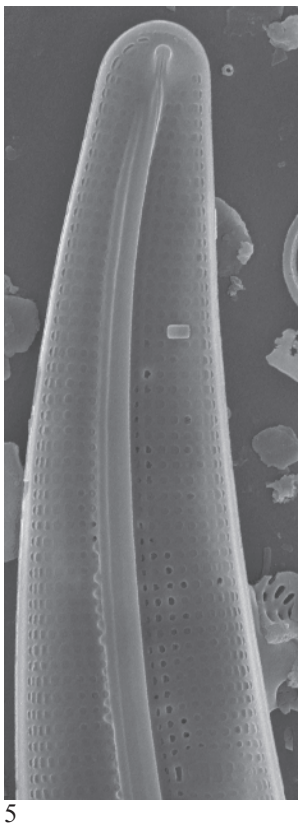
5

3


6


7

9

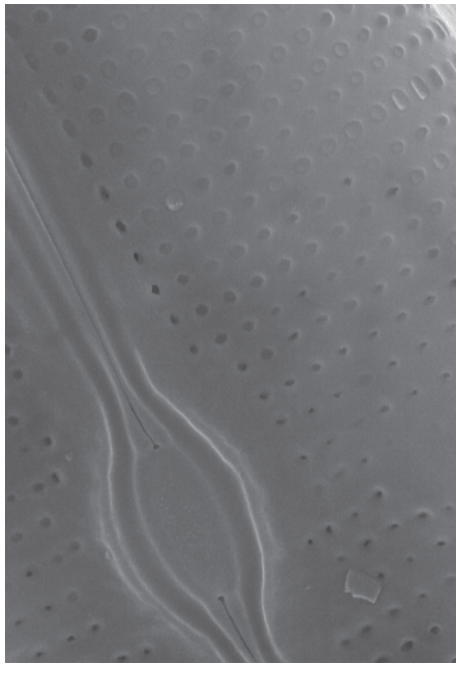

Plate 73 LM: x1500
SEM: Fig. 9 x5000, Fig. 17x2500

Figs. 1-9	*Neidium alpinum* Hustedt
Figs. 10-13	*Neidium affine* (Ehrenberg) Pfitzer sensu lato
Figs. 14-15	*Neidium longiceps* (Gregory) Ross
Fig. 16	*Neidiopsis* cf. *levanderi* (Hustedt) Lange-Bertalot & Metzeltin
Fig. 17	*Neidium* sp.
Fig. 18	*Neidium* cf. *dubium* (Ehrenberg) Cleve
Fig. 19-20	*Neidium* sp. No. 1 Illa

Figs. 1, 6, 15	Lake Gelat Bergús, sediment PYR65
Fig. 2	Lake Monges, sediment PYR57
Figs. 3, 5, 19	Lake Illa, sediment PYR66
Fig. 4	Lake Angonella, sediment PYR78
Fig. 7	Lake Negre, sediment PYR79
Fig. 8	Lake Bleu de Rabassoles, sediment PYR112
Fig. 9	Lake Bersau, sediment PYR03
Fig. 10	Lake Sen, sediment PYR40
Fig. 11	Lake Posets, sediment PYR42
Fig. 12	Lake Aixeus, sediment PYR92
Fig. 13	Lake Forcat Inf., sediment PYR77
Fig. 14	Lake Bachimala, sediment PYR31
Fig. 16	Lake Port Bielh, sediment PYR28
Fig. 17	Lake Arnales, epilithic EpiPYR09
Fig. 18	Lake Acherito, sediment PYR01
Fig. 20	Lake Senó, sediment PYR84

Fig. 9 Manfred Ruppel photo


1


2


3


4


5


6


7


8

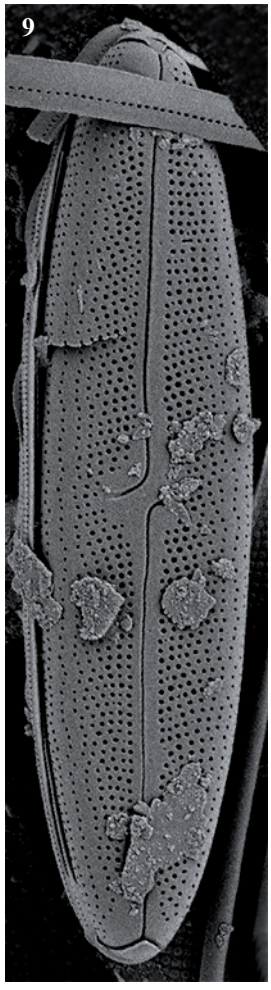
9


10


11


12


13


14


15

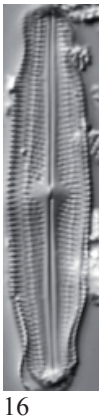
16

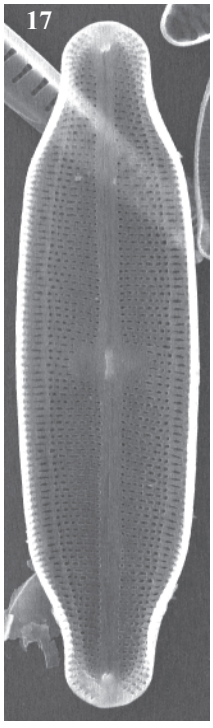
17


18


19


20

Plate 74 LM: x1500
SEM: x3000

Figs. 1-2	*Neidium* sp. No. 2 Illa ?Julma 1
Fig. 3	*Neidium* sp. No. 3 ?Julma 5
Fig. 4	*Neidium* cf. *ampliatum* (Ehrenberg) Krammer
Fig. 5	*Neidium* sp. No. 4 ?Julma 2
Fig. 6	*Neidium bisulcatum* (Lagerstedt) Cleve sensu Krammer

Figs. 1, 3, 5	Lake Illa, sediment PYR66
Fig. 2	Lake Garbet, sediment PYR81
Fig. 4	Lake Arratille, sediment PYR11
Fig. 6	Lake Port Bielh, sediment PYR28

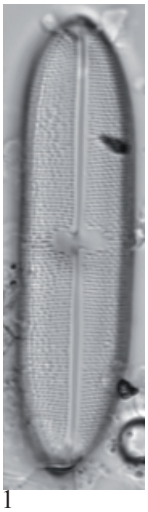

1

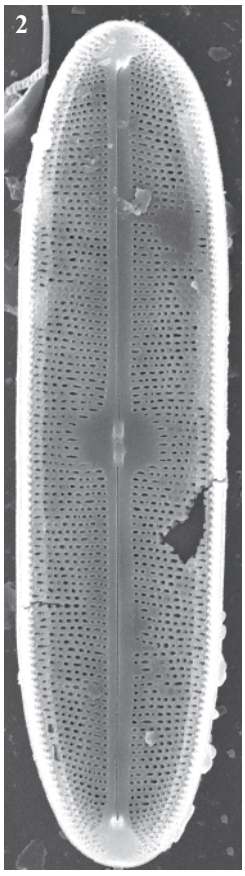

3

4

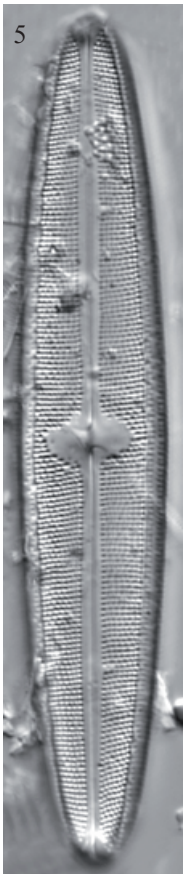

6

Plate 75 LM: x1500
SEM: x2500

Figs. 1, 8	*Stauroneis* sp. No. 8 Illa ? *Stauroneis acidoclinata* Lange-Bertalot & Werum
Figs. 2-7	*Stauroneis* cf. *acidoclinata* Lange-Bertalot & Werum
Figs. 9-10	*Stauroneis* cf. *reichardtii* Lange-Bertalot, Cavacini, Tagliaventi & Alfinito
Figs. 11-13	*Stauroneis smithii* Grunow
Figs. 14-18	*Stauroneis neohyalina* Lange-Bertalot & Kramme
Figs. 19-21	*Stauroneis* sp. No. 9 Forcat

Figs. 1, 3	Lake Illa, sediment PYR66
Figs. 2, 4, 6	Lake Posets, sediment PYR42
Figs. 5, 7, 18-19	Lake Forcat Inf., sediment PYR77
Fig. 8	Lake Baiao Superior, sediment PYR76
Figs. 9-12	Palaeolake Burg
Fig. 13	Lake Helado de Marboré, sediment PYR18
Figs. 14-16	Lake Inf. de la Gallina, sediment PYR87
Fig. 17	Lake Pixón, sediment PYR44
Figs. 20-21	Lake Redon, sediment REDOM

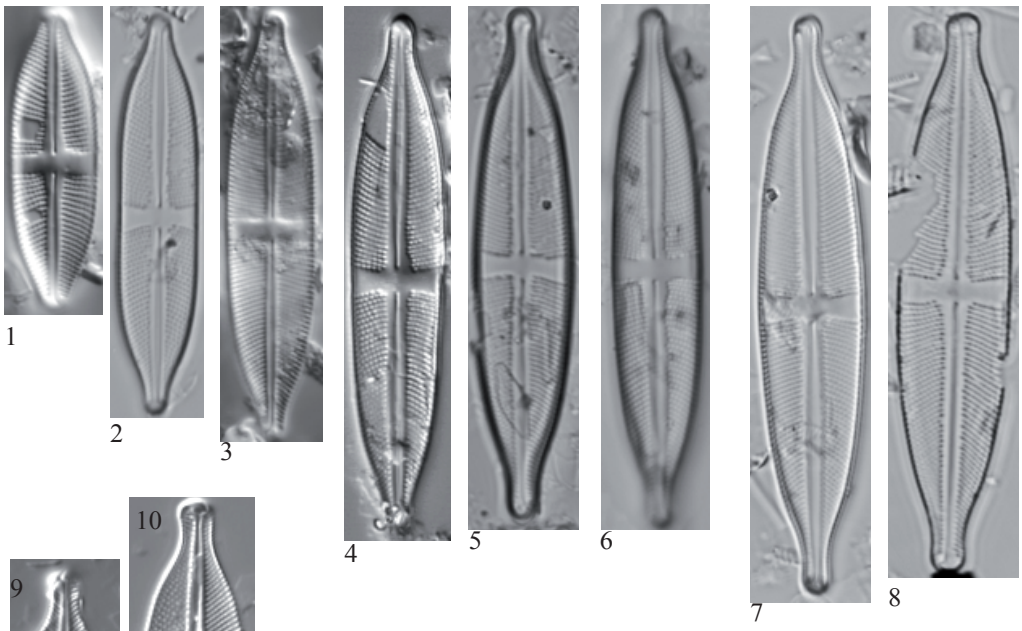
1
2
3
4
5
6
7
8
9
10
11
12
13

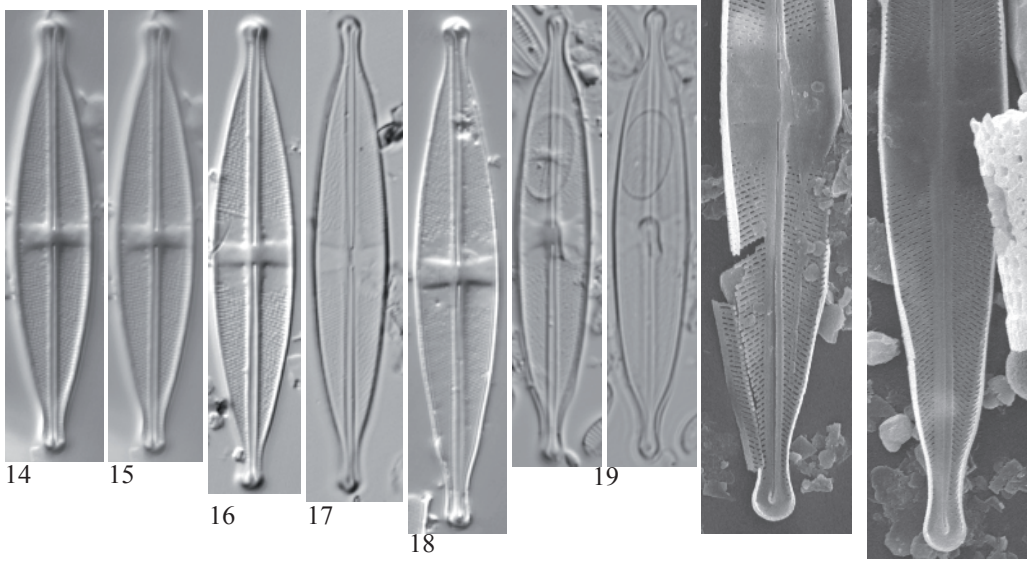
14
15
16
17
18
19
20
21

Plate 76 LM: x1500

Fig. 1	*Stauroneis* sp. No. 1 Tristaina
Figs. 2-3	*Stauroneis* sp. aff. *borrichii* Lund, No. 2 Illa
Fig. 4	*Stauroneis* sp. No. 3 Negre
Figs. 5-6	*Stauroneis siberica* (Grunow) Lange-Bertalot & Krammer
Figs. 7-8	*Stauroneis* sp. No. 4 Burg
Figs. 9-10	*Stauroneis gracilis* Ehrenberg
Fig. 11	*Stauroneis* sp. No. 5 Illa
Figs. 12-13	*Stauroneis* sp. No. 6 Burg
Fig. 14	*Stauroneis* sp. aff. *borrichii* Lund, No. 7 Burg

Fig. 1	Lake Mes Amunt de Tristaina, sediment PYR86
Figs. 2, 11	Lake Illa, sediment PYR66
Fig. 3	Lake Cregüeña, sediment PYR49
Fig. 4	Lake Negre, sediment PYR79
Fig. 5	Lake Arratille, sediment PYR11
Fig. 6	Lake Port Bielh, sediment PYR28
Fig. 7	Lake Burg, sediment BURG 616
Fig. 8	Lake Burg, sediment BURG 729
Fig. 9	Lake Posets, sediment PYR42
Fig. 10	Lake Les Laquettes, sediment PYR27
Figs. 12-13	Lake Burg, sediment BURG 755
Fig. 14	Lake Burg

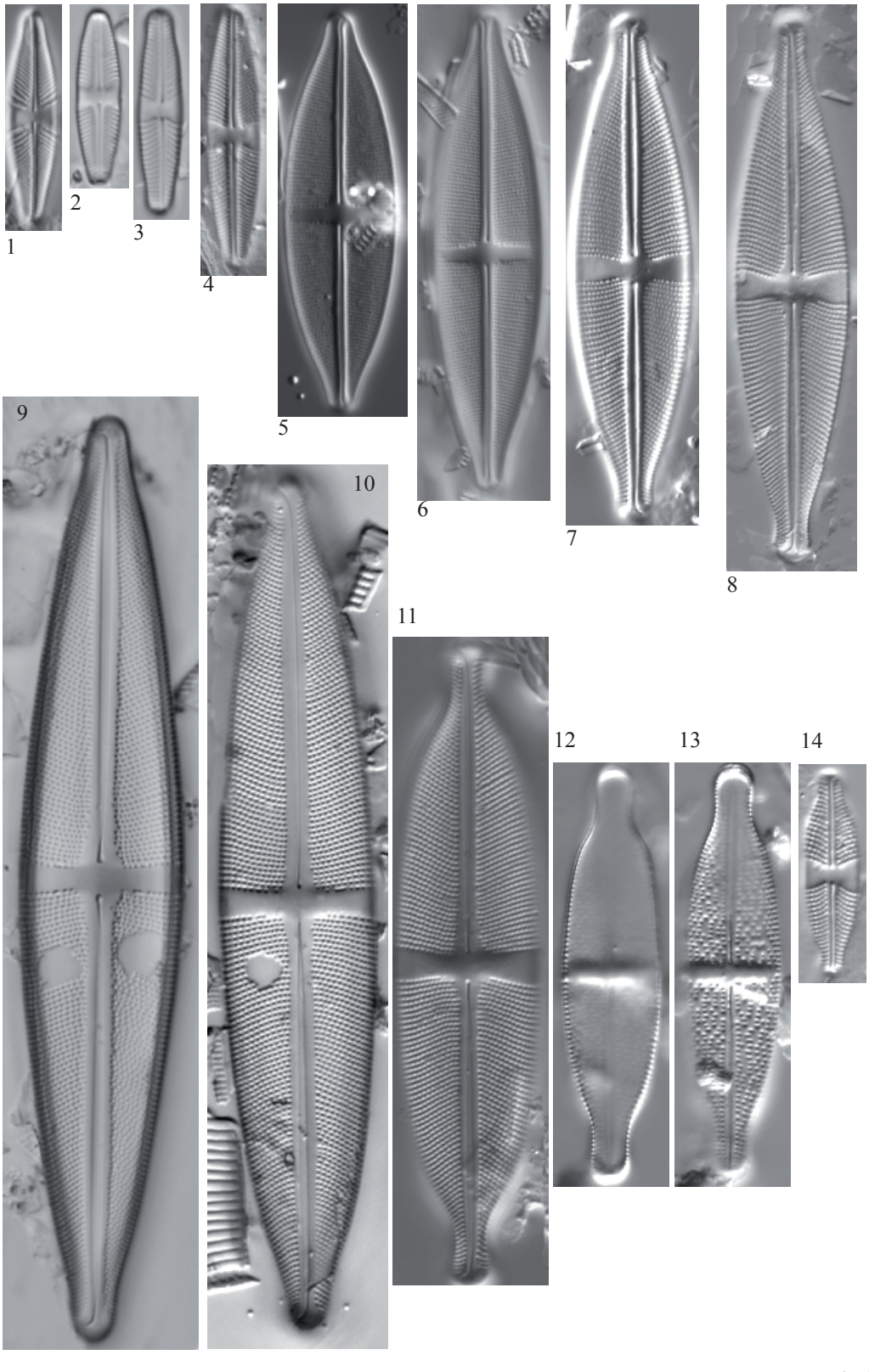
1
2
3
4
5
6
7
8
9
10
11
12
13
14

Plate 77 LM: x1500
SEM: 11-14 x4000, 15 x25000

Fig. 1 *Brachysira zellensis* (Grunow) Round & Mann

Figs. 2-6, 10 *Brachysira brebissonii* Ross

Figs. 7-8 11-13 *Brachysira intermedia* (Østrup) Lange-Bertalot

Fig. 9 *Brachysira* cf. *brebissonii* Ross

Fig. 1	Lake Arratille, sediment PYR11
Fig. 2	Lake Baiao Superior, sediment PYR76
Figs. 3, 7-9	Lake Seno, sediment PYR84
Fig. 4	Lake Aixeus, sediment PYR92
Figs. 5-6, 13	Lake Posets, sediment PYR42
Figs. 10-11	Lake Redon, sediment REDOM
Fig. 12	Lake Port Bielh, epilithic PYR28


1


2


3


4


5


6


7


8


9

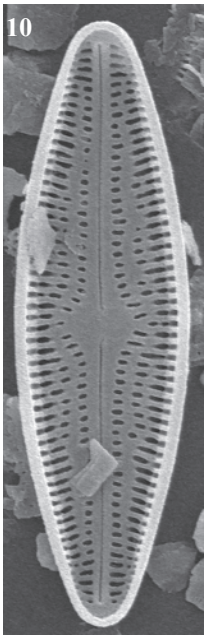

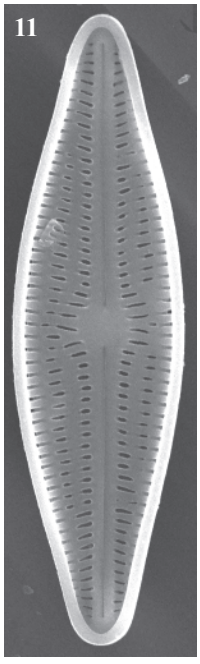

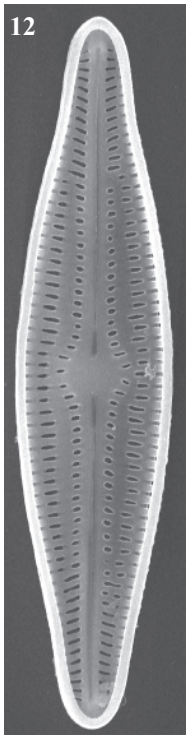

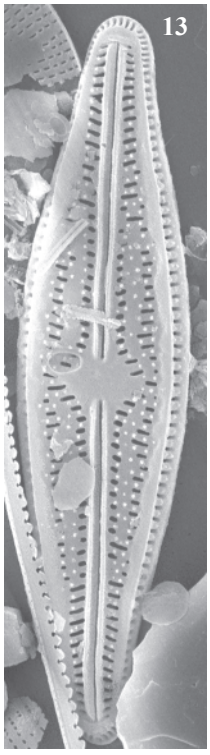

Plate 78 LM: x1500
SEM: x4000

Figs. 1-12, 15-16 18-22 *Brachysira neoexilis* Lange-Bertalot

Figs. 13-14 *Brachysira* cf. *procera* Lange-Bertalot

Fig. 17 *Brachysira* cf. *neglectissima* Lange-Bertalot

Figs. 1, 10, 12	Lake Les Laquettes, sediment PYR27
Figs. 2-3, 15	Lake Posets, sediment PYR42
Fig. 4	Lake Sen, sediment PYR40
Figs. 5, 11	Lake Long de Liat, sediment PYR55
Figs. 7-9, 13-14	Lake Llebreta, sediment PYR58
Fig. 16	Lake Bachimala Sup., sediment PYR31
Fig. 17	Lake Arratille, sediment PYR11
Figs. 6, 18-21	Lake Port Bielh, epilithic EpiPYR28
Fig. 22	Lake Redon, sediment REDOM

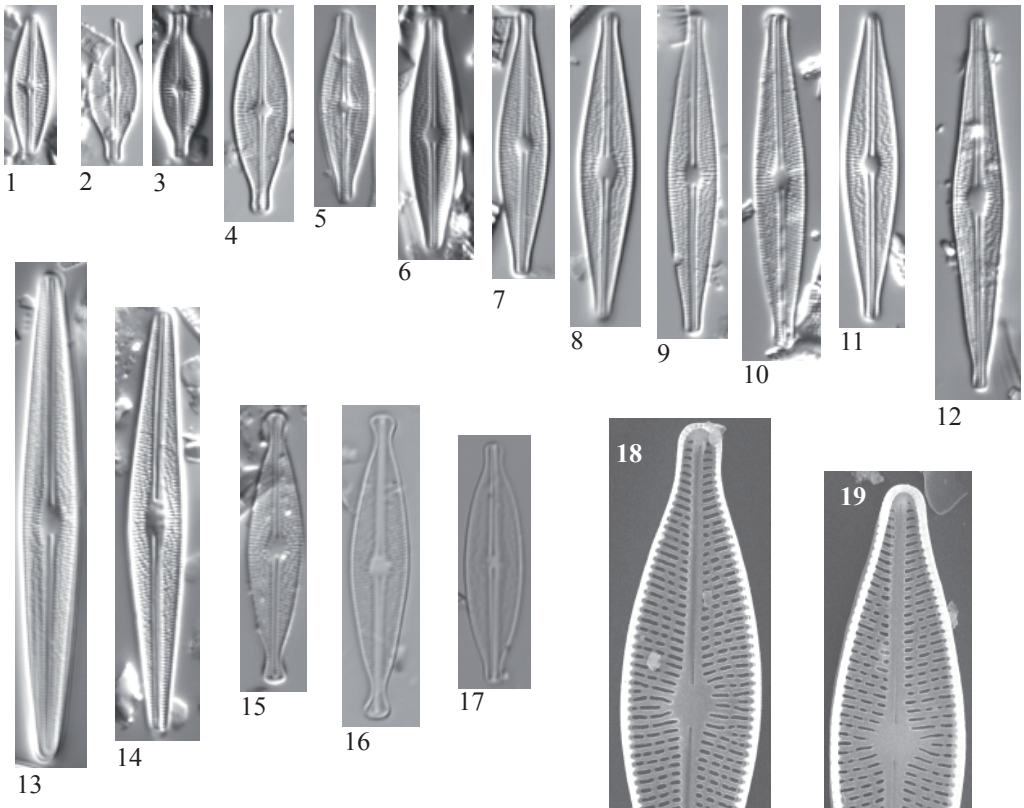
1
2
3
4
5
6
7
8
9
10
11
12
13
14
15
16
17
18
19
20
21
22

Plate 79 LM: x1500
SEM: x4000

Figs. 1-6 *Brachysira neoexilis* Lange-Bertalot

Fig. 7 *Brachysira* cf. *vitrea* (Grunow) Ross

Figs. 1, 2, 5 Lake Redon, sediment REDOM

Fig. 7 Lake Arnales, sediment PYR09

Figs. 3-4, 6 Lake Sen, sediment EpiPYR28

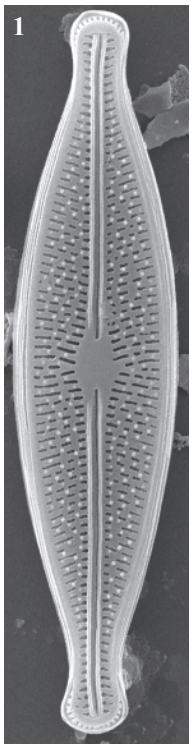
1

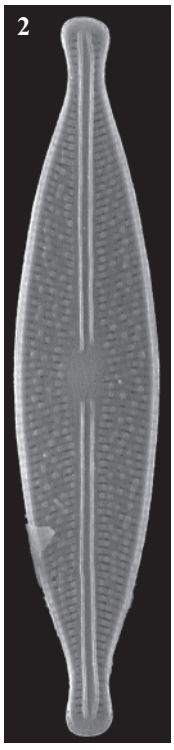
2

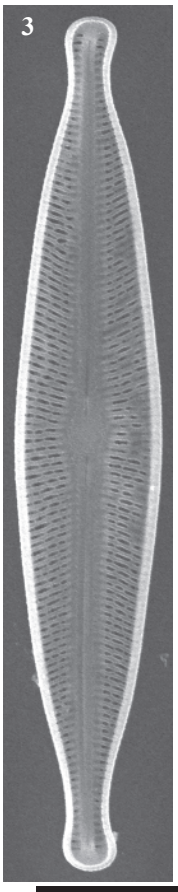
3

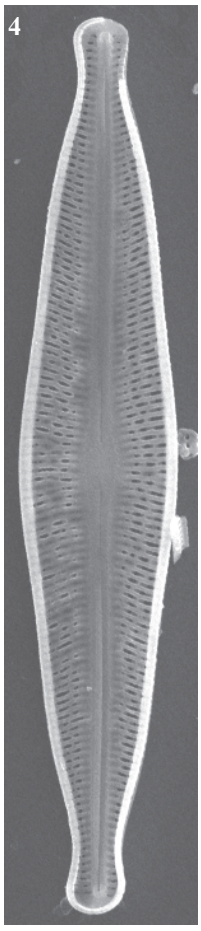
4

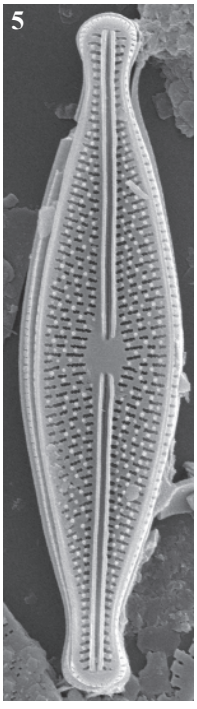
5

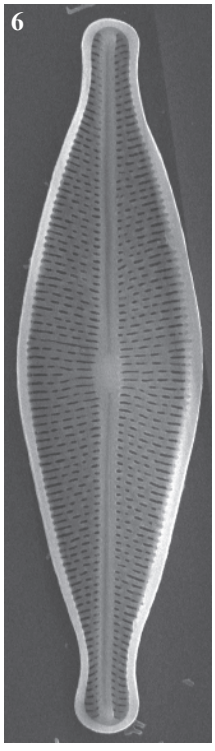
6

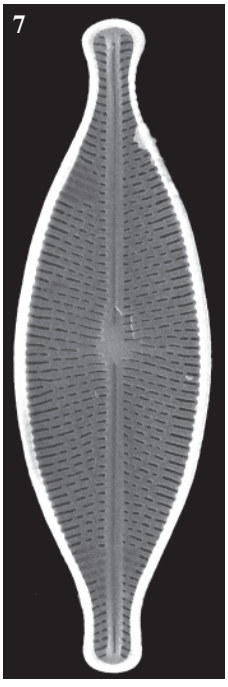
7

Plate 80 LM: x1500
SEM: Figs. 3,6 x15000, Fig. 5 x2000

Figs. 1-6 *Frustulia crassinervia* (Brébisson) Lange-Bertalot et Krammer

Figs. 1, 2 Lake Gelat Bergús, sediment PYR65

Figs. 3, 5-6 Lake Redon, sediment REDOM

Fig. 4 Lake Pica Palomera, sediment PYR52

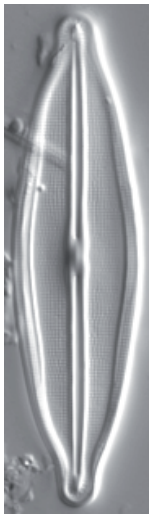

1

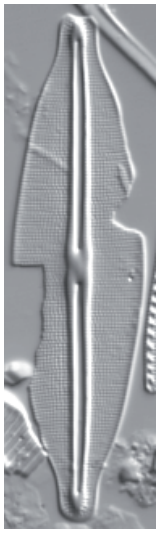

2

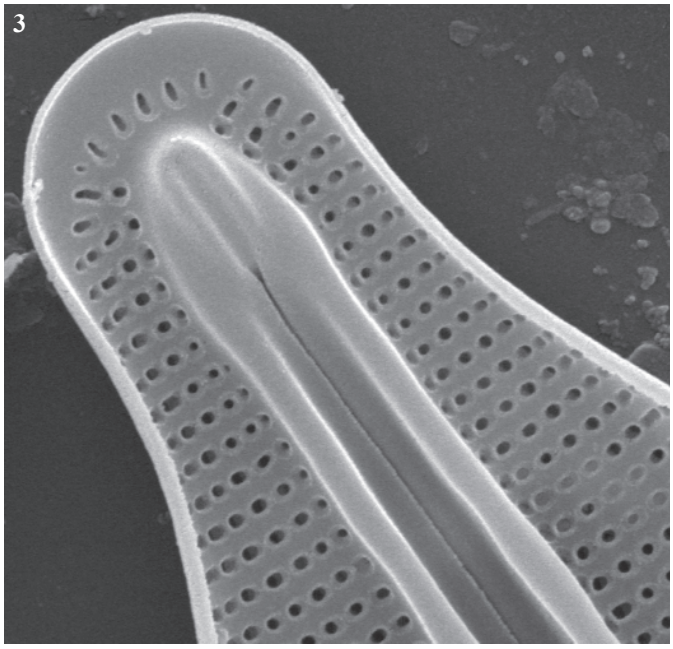

3

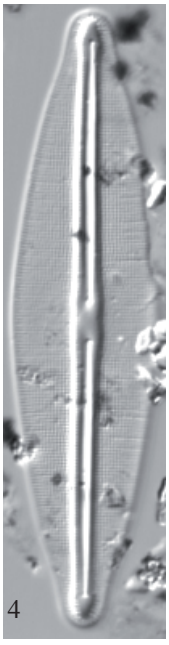

4

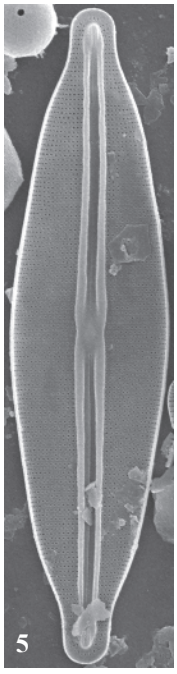

5

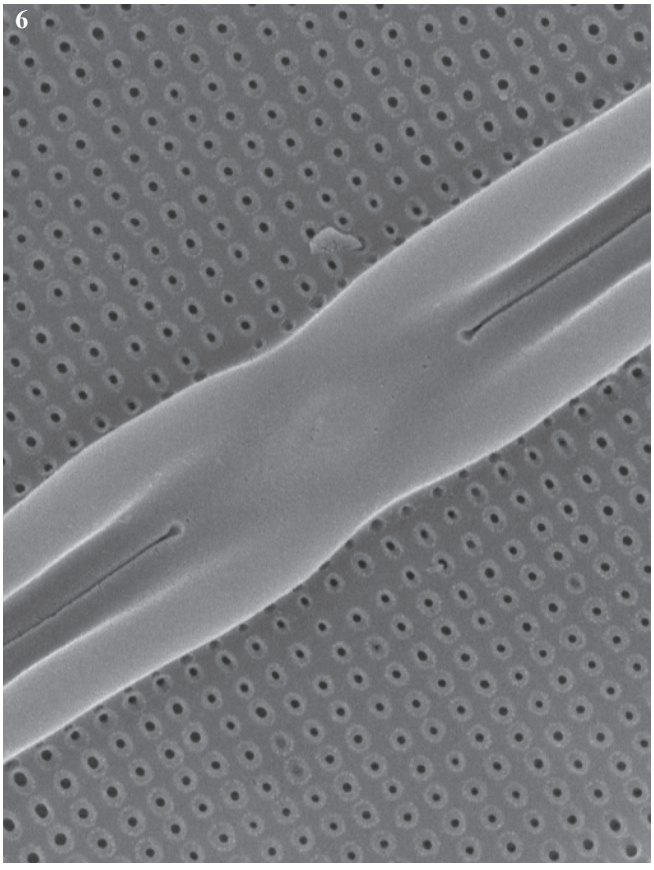

6

Plate 81 LM: x1500
SEM: Fig. 2 x1500, Figs. 3-4 x10000

Figs. 1-4 *?Frustulia crassinervia* (Brébisson) Lange-Bertalot et Krammer

Fig. 1 Lake Pica Palomera, sediment PYR52

Figs. 2-4 Lake Mariola, epilithic EpiPYR80

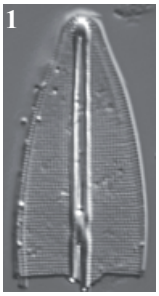
1

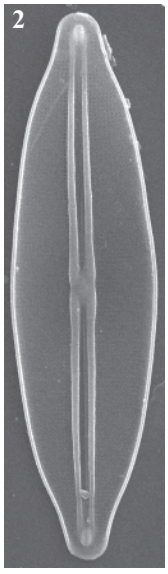
2


3

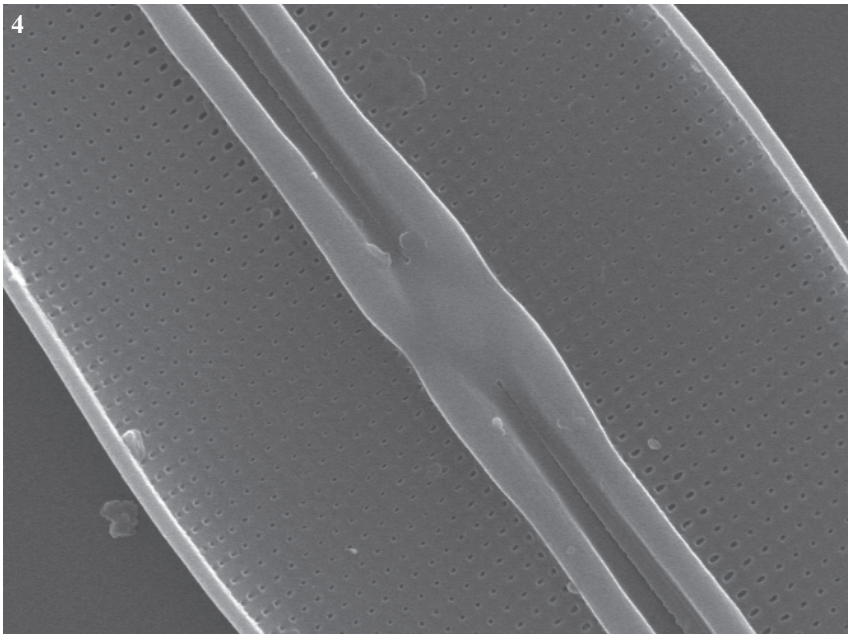
4

Plate 82 LM: x1500
SEM: Fig. 2 x2000, Figs. 3-4 x5000

Figs. 1-6 *Frustulia* cf. *saxonica* Rabenhorst

Figs. 1, 3-5 Lake Senó, epilithic EpiPYR84

Fig. 2 Lake Monges, sediment PYR57

Fig. 6 Lake Bleu de Rabassoles, epilithic EpiPYR112

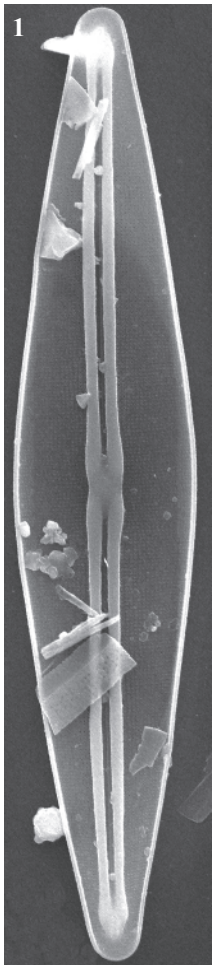
1

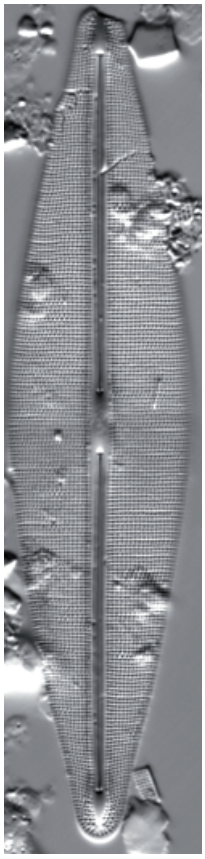
2

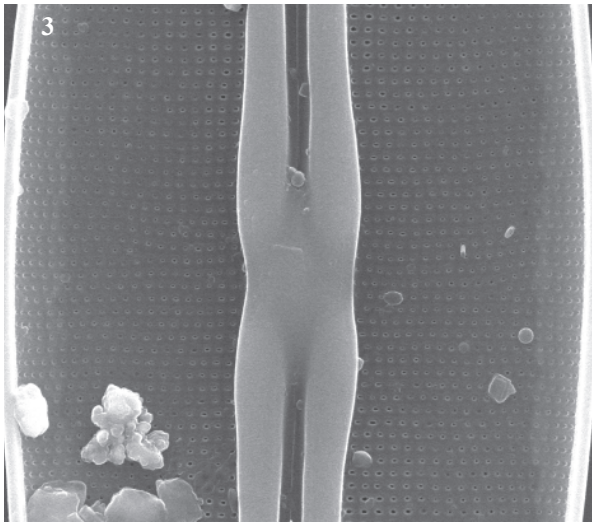
3

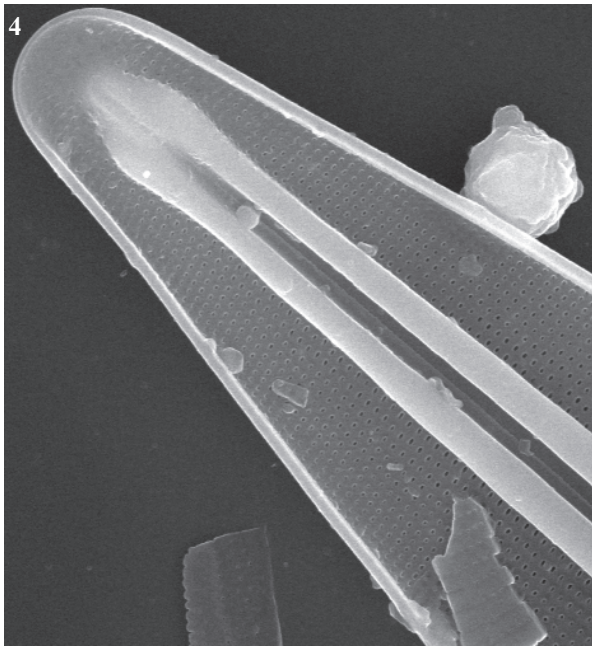
4

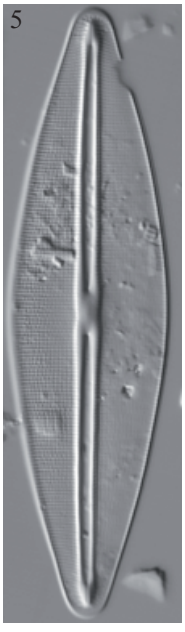
5

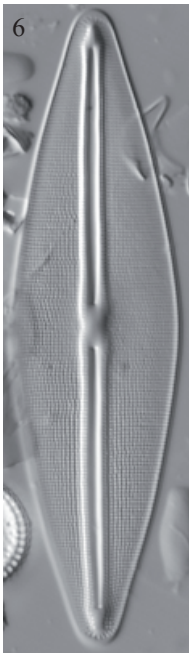
6

Plate 83 LM: x1500
SEM: Fig. 2 x1500, Figs. 3-4 x5000

Figs. 1-4 *Frustulia erifuga* Lange-Bertalot et Krammer

Fig. 5 *Amphipleura pellucida* (Kützing) Kützing

Fig. 1 Lake Senó, sediment PYR84

Figs. 2-4 Lake Redon, sediment REDOM

Fig. 5 Lake Burg, sediment BURG 1054

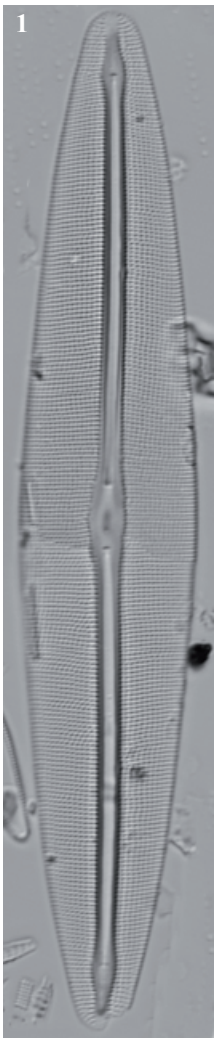
1

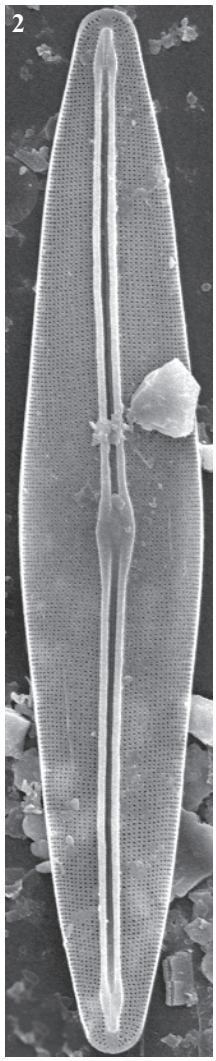
2

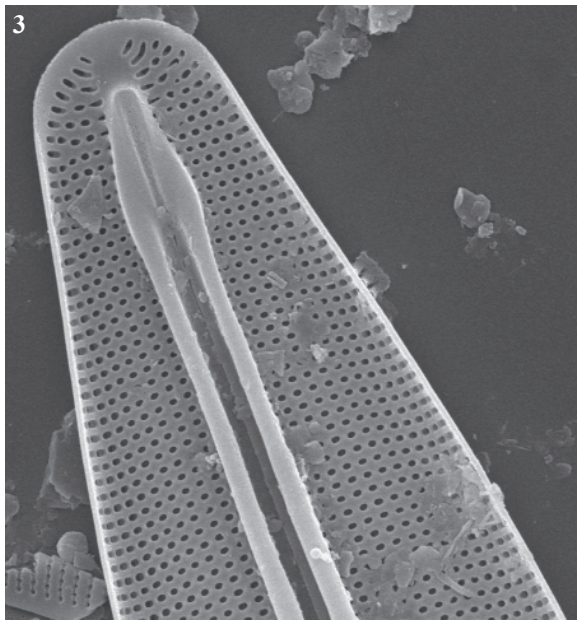
3

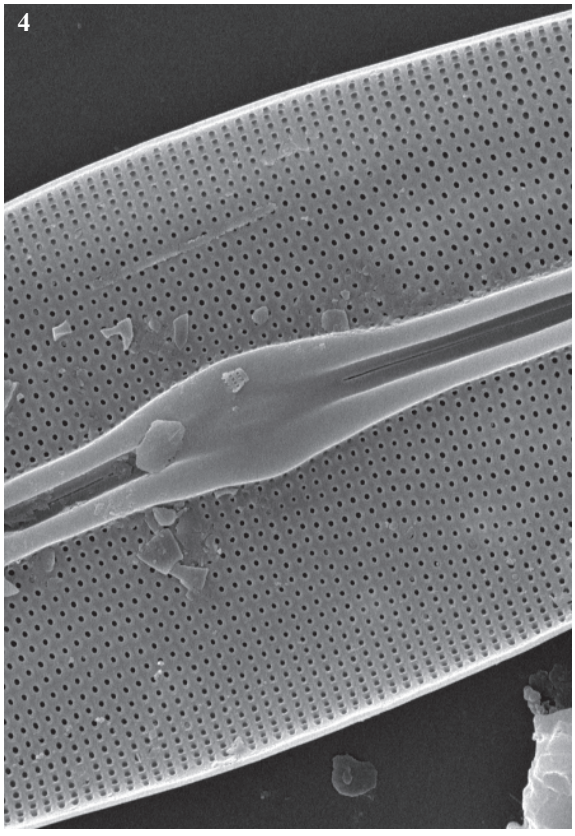
4


5

Plate 84	LM: x1500 SEM: x3000
Fig. 1	*Diploneis* cf. *oculata* (Brébisson) Cleve
Fig. 2	*Diploneis* cf. *peterseni* (petersenii) Hustedt
Figs. 3, 10	*Diploneis* cf. *modica* Hustedt
Fig. 4	*Diploneis* sp. No. 1 Pica Palomera
Figs. 5-6	*Diploneis* cf. *puella* (Schumann) Cleve
Fig. 7	*Diploneis* cf. *parma* Cleve sensu auct nonnull.
Figs. 8-9,11	*Diploneis* cf. *subovalis* Cleve

Fig. 1	Lake Basa de la Mora, sediment PYR32
Figs. 2, 6-7	Lake Sen, sediment PYR40
Fig. 3	Lake Acherito, sediment PYR01
Fig. 4	Lake Pica Palomera, sediment PYR52
Fig. 5	Lake Arnales, sediment PYR09
Fig. 8	Lake Eriste, sediment PYR43
Fig. 9	Lake Arratille, sediment PYR11
Figs. 10-11	Lake Laurenti, sediment PYR111

1

2

3

4

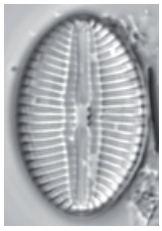

5

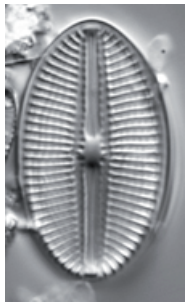

6

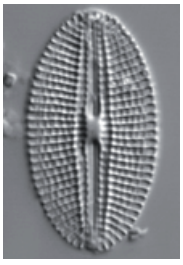

7

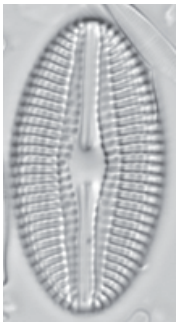

8

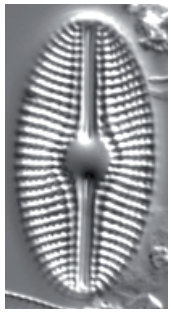

9

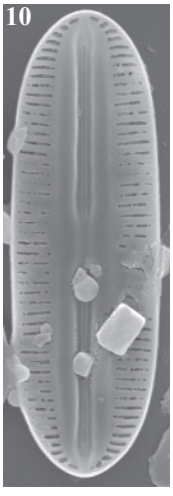

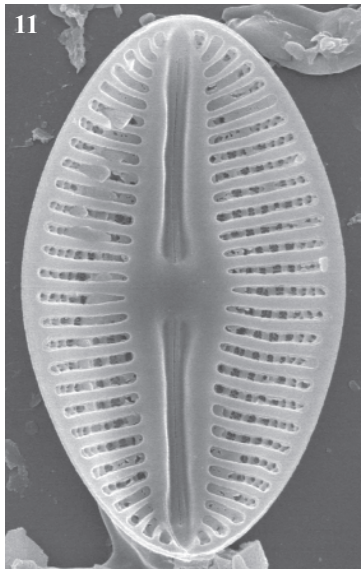

Plate 85 LM: x1500

Figs. 1-2	*Caloneis* sp. No. 1 Munia
Figs. 3-4	*Caloneis* cf. *lancettula* (Schulz) Lange-Bertalot & Witkowski
Fig. 5	*Caloneis* cf. *vasilyevae* Lange-Bertalot, Genkal & Vechov
Figs. 6-11, 17,18	*Caloneis* sp. No. 2 Posets
Figs. 12-15	*Caloneis silicula* (Ehrenberg) Cleve sensu lato
Fig. 16	*Caloneis* sp. No. 3 Posets
Fig. 19	*Caloneis alpestris* (Grunow) Cleve
Fig. 20	*Caloneis* sp. No. 4 Burg
Figs. 21-23	*Caloneis* sp. No. 5 Acherito
Fig. 24	*Caloneis* cf. *tenuis* (Gregory) Krammer
Figs. 25-27	*Caloneis* cf. *undulata* (Gregory) Krammer
Fig. 28	*Caloneis* cf. *lauta* Carter

Figs. 1, 2	Lake La Munia Sup., sediment PYR20
Fig. 3	Lake Burg, sediment BURG 616
Figs. 4, 21-23	Lake Acherito, sediment PYR01
Fig. 5	Lake Pica Palomera, sediment PYR52
Figs. 6-11, 17-18, 28	Lake Posets, sediment PYR42
Fig. 12	Lake Burg, sediment BURG 1216
Fig. 13	Lake Estom, sediment PYR15
Fig. 14	Lake Col d`Arratille, sediment PYR12
Fig. 15	Lake Burg, sediment BURG 703
Fig. 16	Lake Pixón, sediment PYR44
Fig. 19	Lake Arratille, sediment PYR11
Fig. 20	Lake Burg
Figs. 24-25	Lake Montoliu, epilithic EpiPYR54
Figs. 26-27	Lake Long de Liat, sediment PYR55

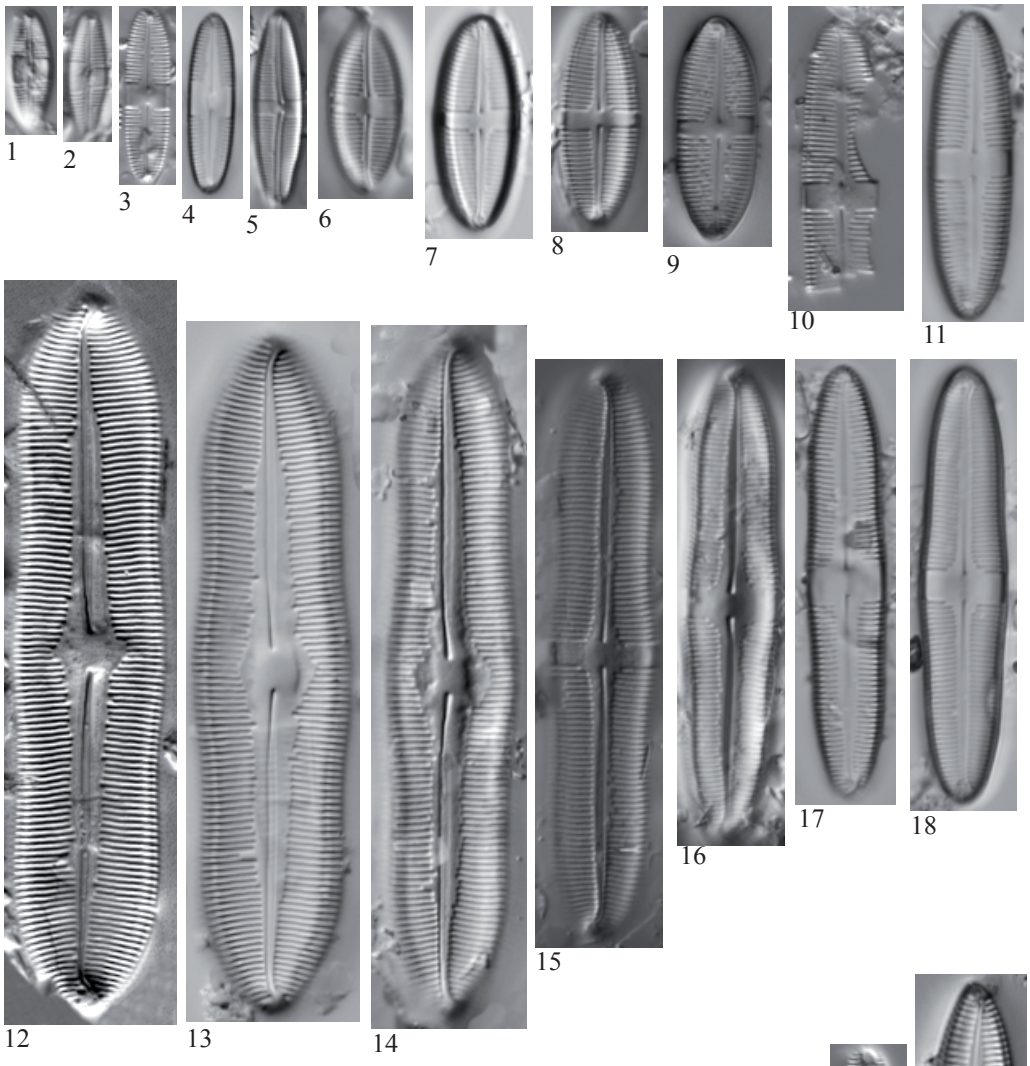
1
2
3
4
5
6
7
8
9
10
11
12
13
14
15
16
17
18
19
20
21
22
23
24
25
26
27
28

Plate 86 LM: x1500
SEM: Figs. 14,16 x3000, Fig. 18 x10000, Fig. 19 x15000

Fig. 1 *Pinnularia sinistra* Krammer

Figs. 2-10, 15 18-19 *Pinnularia subcapitata* Gregory

Fig. 11 *Pinnularia* sp. No. 1 Posets

Figs. 12-14 *Pinnularia* cf. *subanglica* Krammer

Figs. 16-17 *Pinnularia* cf. *rumrichae* Krammer

Fig. 1	Lake Llosás, sediment PYR46
Fig. 2	Lake Burg
Figs. 3, 11-12, 17	Lake Posets, sediment PYR42
Fig. 4	Lake Senó, epilithic EpiPYR84
Figs. 5, 10	Lake Senó, sediment PYR84
Fig. 6	Lake Burg, sediment BURG 958
Fig. 7	Lake Burg, sediment BURG 968
Fig. 9	Lake Redon, sediment REDOM
Fig. 13	Lake Arnales, sediment PYR09
Fig. 14	Lake Garbet, sediment PYR81
Figs. 16, 19-20	Lake Mariola, epilithic EpiPYR80

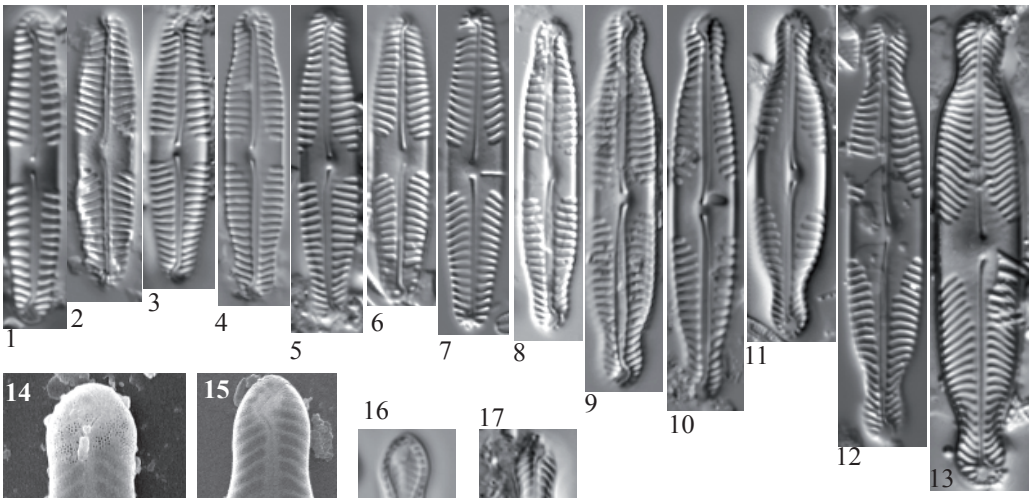
1
2
3
4
5
6
7
8
9
10
11
12
13

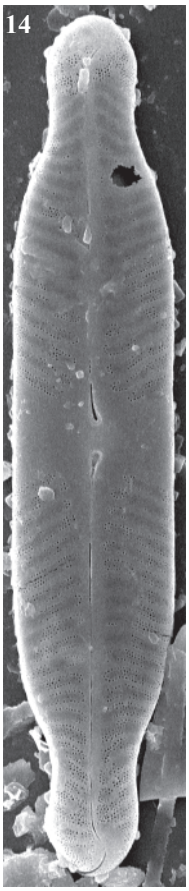
14

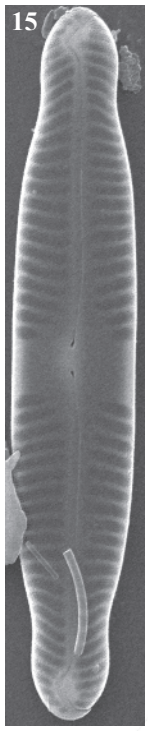
15


16


17

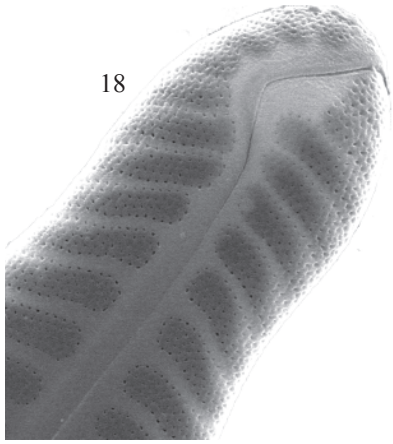
18

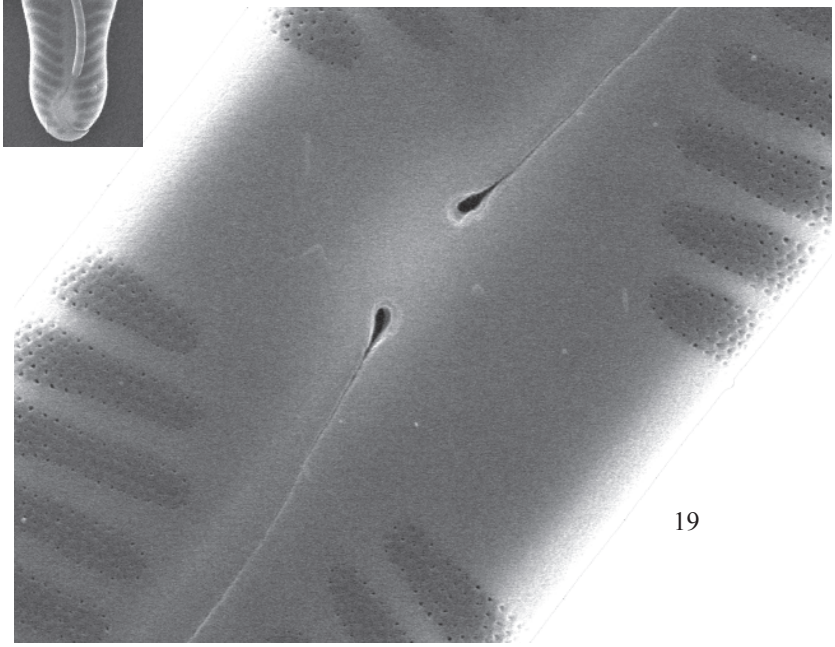
19

Plate 87 LM: x1500
SEM: Fig. 13 x10000, Fig. 14 x300, Figs. 16-18 x4500

Figs. 1-2	*Pinnularia* sp.
Fig. 3	*Pinnularia* sp.
Figs. 4-10 17-18	*Pinnularia* cf. *brebissonii* var. *minuta* Krammer
Fig. 11	*Pinnularia* sp. No. 3 Plan
Figs. 12-14	*Pinnularia* sp. No. 4 Mariola
Figs. 15-16	*Pinnularia* sp. No. 6 Estelat

Figs. 1-3, 5	Lake Posets, sediment PYR42
Fig. 4	Lake Baiau Superior, sediment PYR77
Fig. 6	Lake Arratille, sediment PYR11
Fig. 7	Lake Illa, sediment PYR66
Fig. 8	Lake Ensangents Sup., sediment PYR106
Fig. 9	Lake Burg
Fig. 10	Lake Burg, sediment BURG 1187
Fig. 11	Lake Plan, sediment PYR69
Fig. 12-14, 16	Lake Mariola, sediment PYR80
Fig. 15	Lake Estelat, sediment PYR120
Figs. 17-18	Lake Redon, sediment REDOM

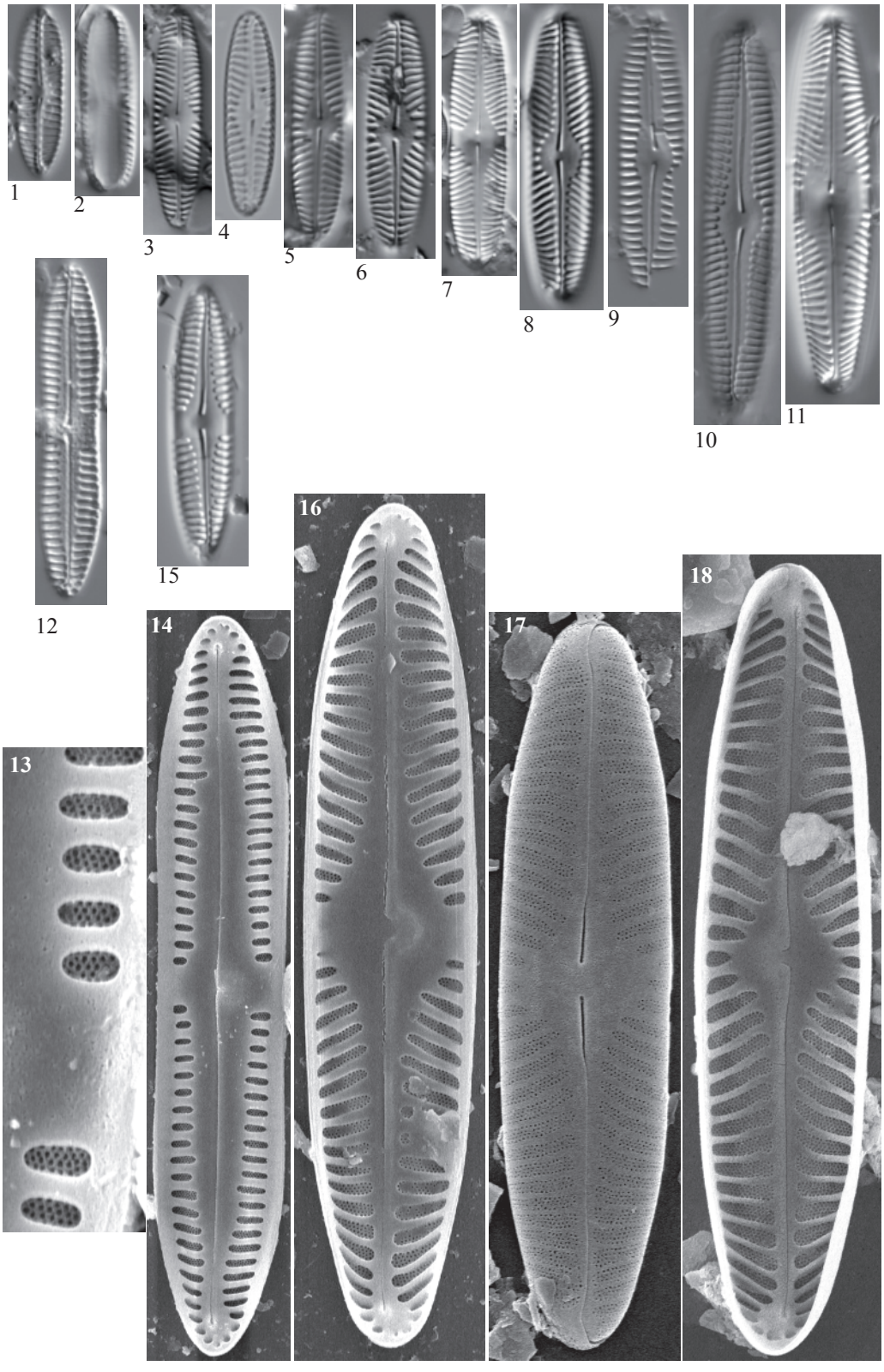
1
2
3
4
5
6
7
8
9
10
11
12
15
16
14
17
18
13

Plate 88 LM: x1500
SEM: Fig. 15 x3000, Fig. 23 x7500, Fig. 24 x10000

Fig. 1	*Hygropetra balfourianaa* (Grunow ex Cleve) Krammer & Lange Bertalot
Figs. 2-3	*Pinnularia* cf. *laucensis* Lange-Bertalot, Rumrich & Krammer
Figs. 4-6	*Pinnularia* sp. No. 12 Estelat, aff. perirrorata
Fig. 7	*Pinnularia* cf. *kuetzingii* Krammer
Fig. 8	*Pinnularia* sp. No. 7 Romedo
Fig. 9	*Pinnularia* sp. No. 8 Burg
Fig. 10	*Pinnularia subinterrupta* Krammer & Schroeter
Figs. 11-12	*Pinnularia* sp. No. 2 Illa
Fig. 13	*Pinnularia* sp
Fig. 14	*Pinnularia* sp. 15 Burg
Figs. 15-20 23-24	*Pinnularia microstauron* var. *nonfasciata* Krammer
Fig. 21	*Pinnularia* sp. No. 5 Mora
Fig. 22	*Pinnularia* sp. No. 14 Burg, aff. *Pinnularia divergens* Smith

Fig. 1	Lake Eriste, sediment PYR43
Figs. 2-3, 20	Lake Negre, sediment PYR79
Fig. 4	Lake Inf. de la Gallina, sediment PYR87
Figs. 5, 18, 23-24	Lake Mariola, epilithic EpiPYR80
Fig. 6	Lake Estelat, sediment PYR120
Fig. 7	Lake Inf. de la Gallina, epilithic EpiPYR87
Fig. 8	Lake Romedo de Dalt, epilithic EpiPYR85
Fig. 9	Lake Burg, sediment BURG 985
Fig. 10	Lake Illa, epilithic EpiPYR66
Figs. 11-12, 16-18	Lake Illa, sediment PYR66
Figs. 13-14	Lake Burg, sediment BURG 918
Fig. 19	Lake Posets, sediment PYR42
Fig. 21	Lake Basa de la Mora, sediment PYR32
Fig. 22	Lake Burg, sediment BURG 960

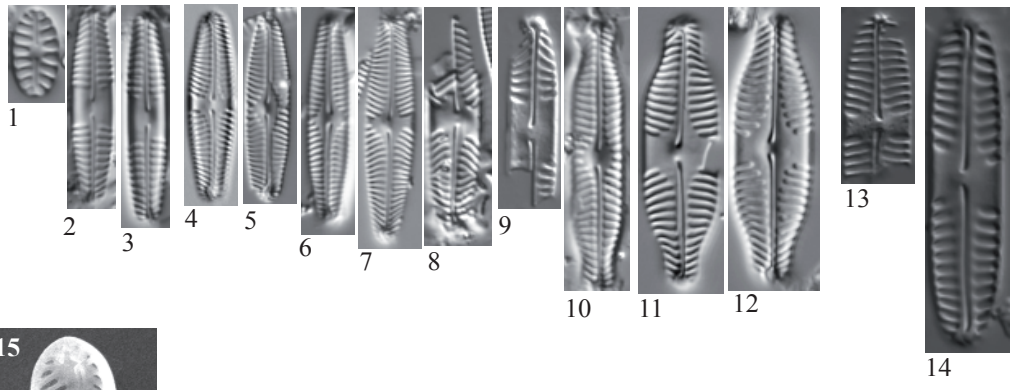
1
2
3
4
5
6
7
8
9
10
11
12
13
14

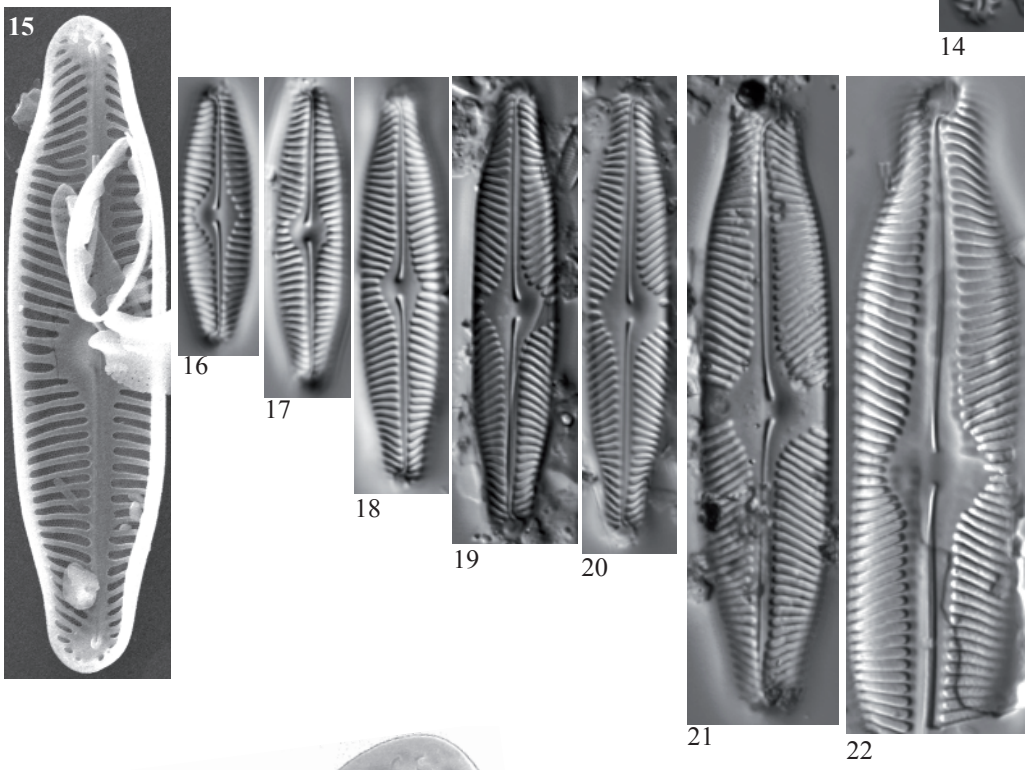
15
16
17
18
19
20
21
22

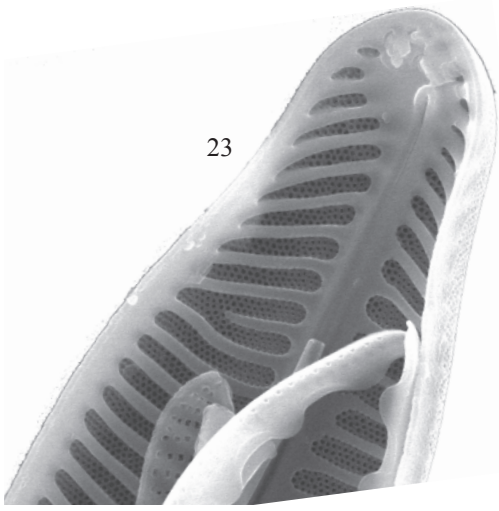
23

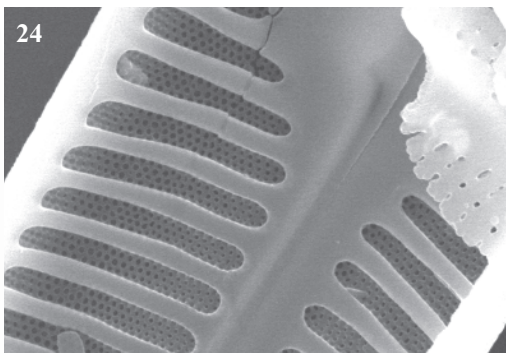
24

Plate 89 LM: x1500
SEM: Fig. 7 x8000, Fig. 8 x2000

Figs. 1-3 *Pinnularia grunowii* Krammer

Fig. 4 *Pinnularia* sp. No. 13 Albe

Figs. 5-8 *Pinnularia septentrionalis* Krammer

Fig. 1	Lake Burg
Fig. 2	Lake Burg, sediment BURG 917
Fig. 3	Lake Burg, sediment BURG 796
Fig. 4	Lake Albe, sediment PYR96
Fig. 5	Lake Sen, sediment PYR40
Fig. 6	Lake Posets, sediment PYR42
Figs. 7-8	Lake Laurenti, sediment PYR111

1

2

3

4

5

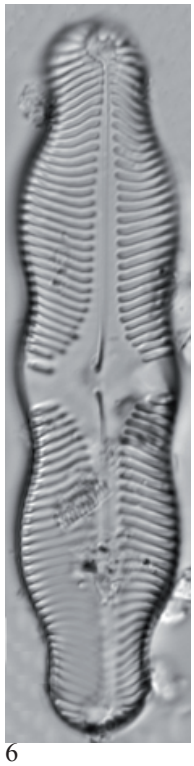

6

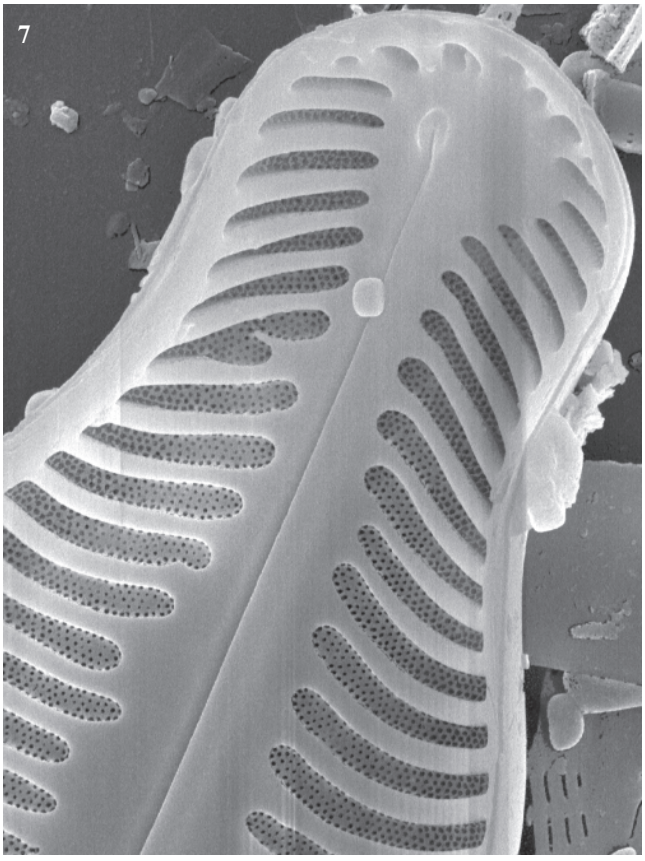

7

8

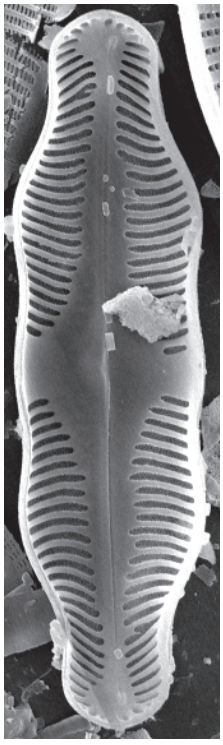

Plate 90 LM: x1500

Figs. 1-4	*Pinnularia borealis* Ehrenberg
Fig. 5	*Pinnularia* cf. *lata* (Brébisson) Smith
Fig. 6	*Pinnularia* sp. No. 9 Laquettes, aff. *subgibba* Krammer
Fig. 7	*Pinnularia* cf. *subgibba* Krammer
Figs. 8-9	*Pinnularia* sp. No. 10 Pica Palomera, aff. *pseudogibba* Krammer
Fig. 10	*Pinnularia* sp. No. 11 Trebens, aff. *tirolensis* (Metzeltin & Krammer) Krammer

Fig. 1	Lake Burg
Fig. 2	Lake Negre, sediment PYR79
Fig. 3	Lake Sotllo, epilithic EpiPYR89
Fig. 4	Lake Burg, sediment BURG 1057
Fig. 5	Lake Burg, sediment BURG 1195
Fig. 6	Lake Cap Long, sediment PYR27
Fig. 7	Lake Burg, sediment BURG 807
Fig. 8	Lake Pica Palomera, sediment PYR52
Fig. 9	Lake Senó, sediment PYR84
Fig. 10	Lake Trebens, sediment PYR114

1

2

3

4

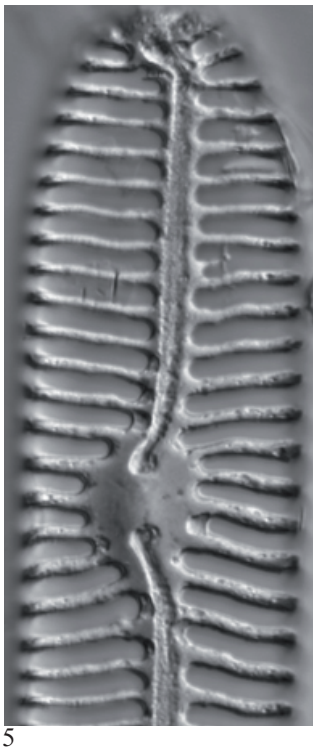

5

6

7

8

9

10

Plate 91 LM: Figs. 1-3 x1500, Fig. 4 x800

Fig. 1 *Pinnularia* sp.

Figs. 2-3 *Pinnularia* cf. *viridis* (Nitzsch) Ehrenberg

Fig. 4 *Pinnularia* cf. *latevittata* Cleve

Fig. 1 Lake Gelat Bergús, sediment PYR65

Fig. 2 Lake Senó, sediment PYR84

Fig. 3 Lake Burg

Fig. 4 Lake Bersau, sediment PYR03

1

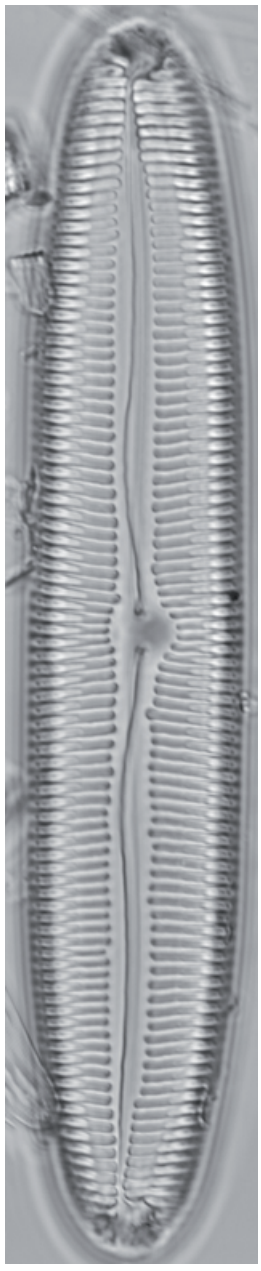

2

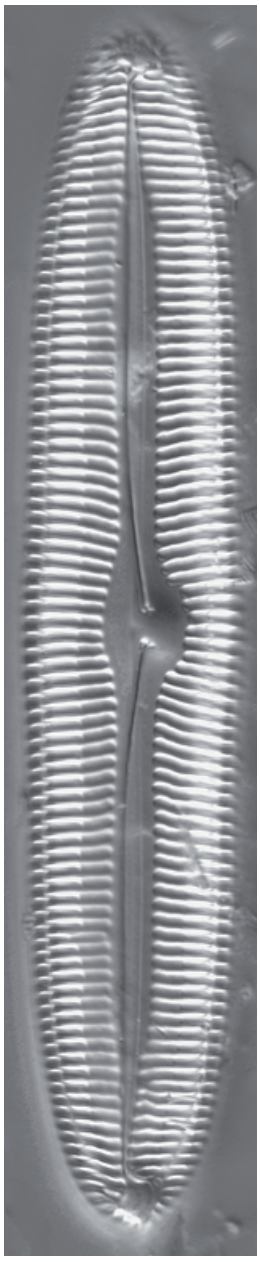

3

4

Plate 92 LM: x1500

Fig. 1	*Pinnularia* cf. *complexa* Krammer
Fig. 2	*Pinnularia* cf. *brebissonii* var. *acuta* Cleve-Euler
Fig. 3	*Pinnularia* cf. *divergens* var. *sublinearis* Cleve
Fig. 4	*Pinnularia platycephala* (Ehrenberg) Cleve
Figs. 5-6	*Pinnularia acuminata* Smith
Figs. 7-9	*Pinnula* sp. 16 Burg, aff. *P. divergens*

Fig. 1	Lake Bersau, epilithic EpiPYR03
Fig. 2	Lake Pondiellos Sup., sediment PYR08
Fig. 3	Lake Plan, sediment PYR69
Fig. 4	Lake PYR128
Figs. 5-6	Lake Illa, sediment PYR66
Fig. 7	Lake Burg, sediment BURG 838
Figs. 8-9	Lake Burg, sediment BURG 869

1

2

3

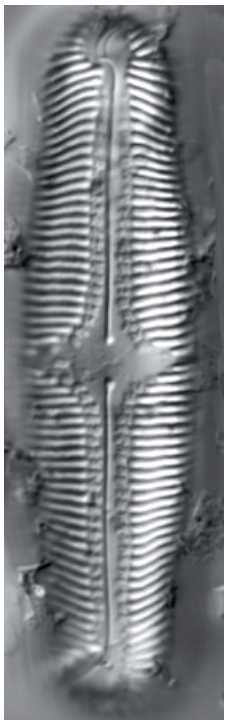

4

5

6

7

8

9

Plate 93 LM: x1500
Fig. 9 x5000, Fig. 10 x4000, Figs. 11,13 x10000, Fig. 12 x6000

Fig. 1 *?Cymbella parva* (Smith) Kirchner

Figs. 2-13 *Cymbella parva* (Smith) Kirchner

Figs. 1, 5, 7	Lake Sen, sediment PYR40
Fig. 2	Lake Acherito, sediment PYR01
Figs. 3, 6, 8	Lake Arratille, sediment PYR11
Figs. 4, 9-13	Lake Roumassot, epilithic EpiPYR04


1


2


3


4


5


6


7


8

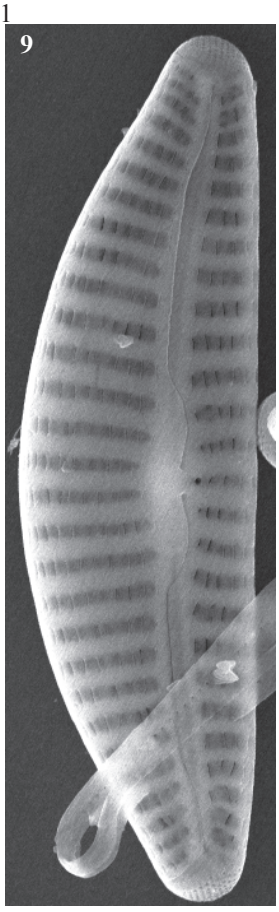
9

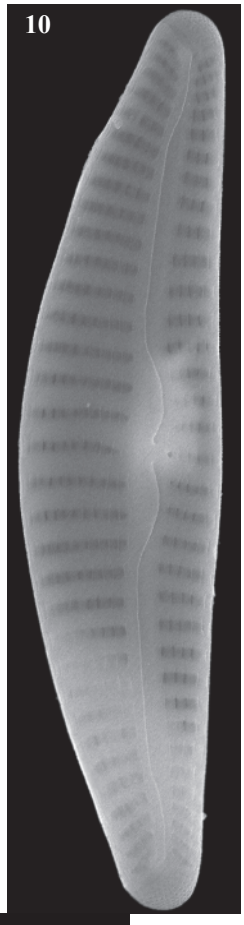
10

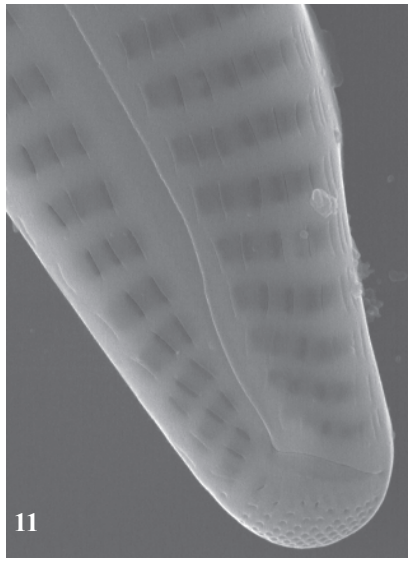
11

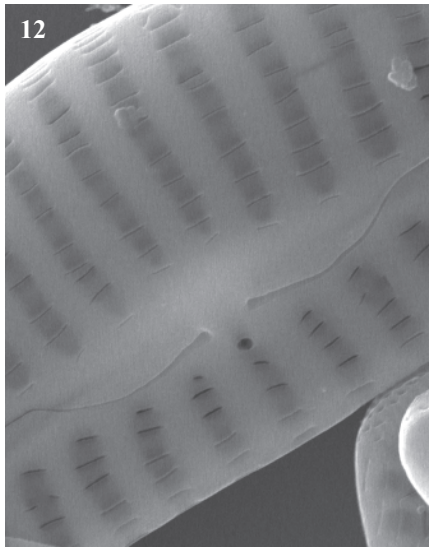
12

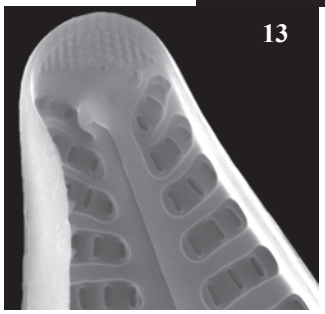
13

Plate 94 LM: x1500
SEM: Figs. 1-2,13 x3000, Fig. 3 x10000, Figs. 4-5 x6000

Cymbella parva (Smith) Kirchner

Figs. 1, 3, 5 Lake Gran de Mainera, epilithic EpiPYR70

Figs. 2, 4 Lake Roumassot, sediment PYR04

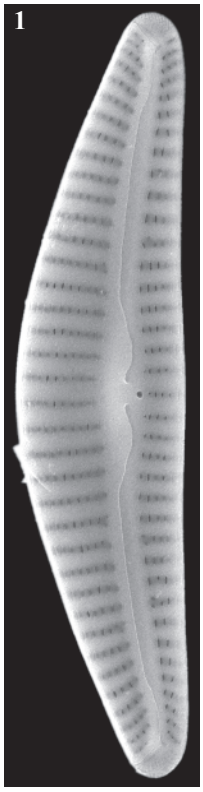
1

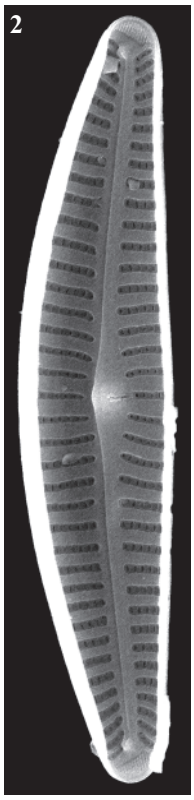
2

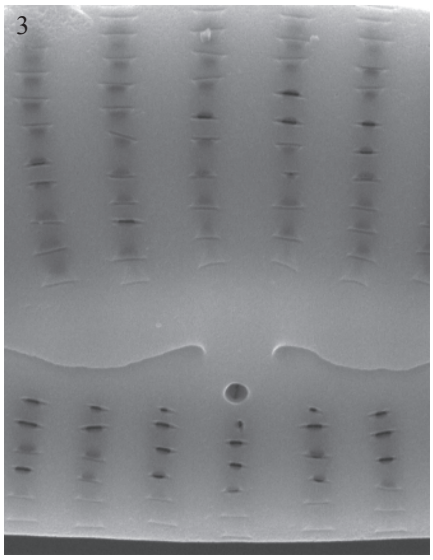
3

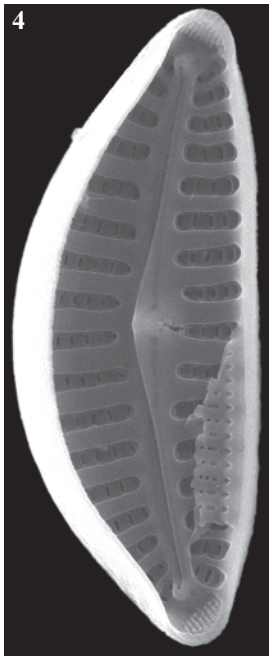
4

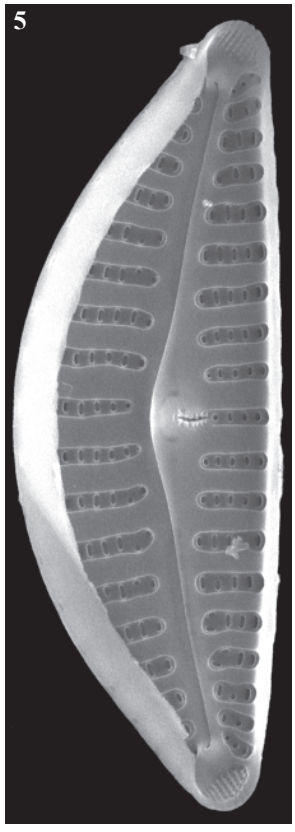
5

Plate 95 LM: x1500
SEM: Figs. 2,5 x2000, Figs. 3-4 x4000, Fig. 6 x5000

Cymbella lange-bertalotii Krammer

Fig. 1 Lake Arratille, sediment PYR11

Figs. 2-6 Lake Port Bielh, sediment EpiPYR28


1

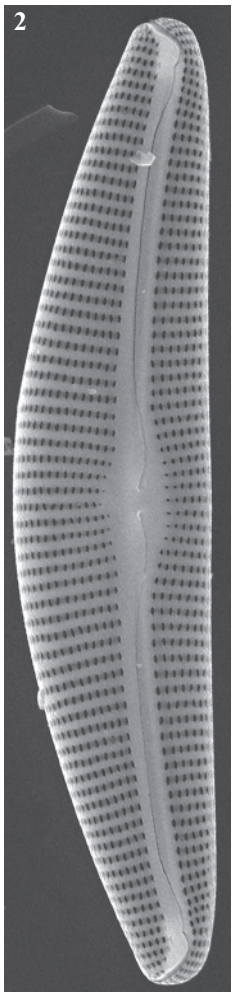
2

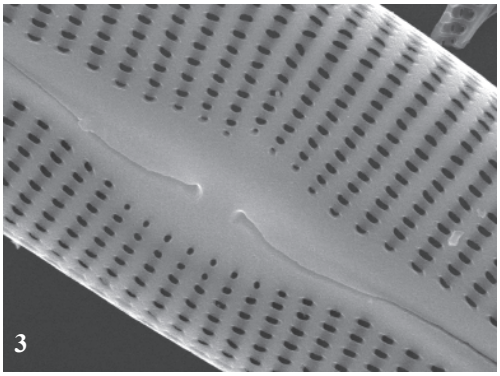
3

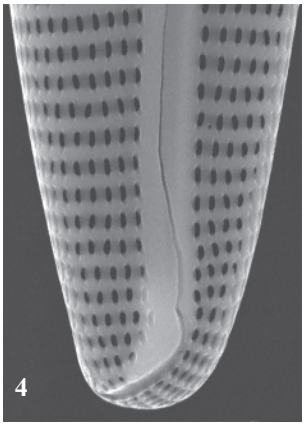
4

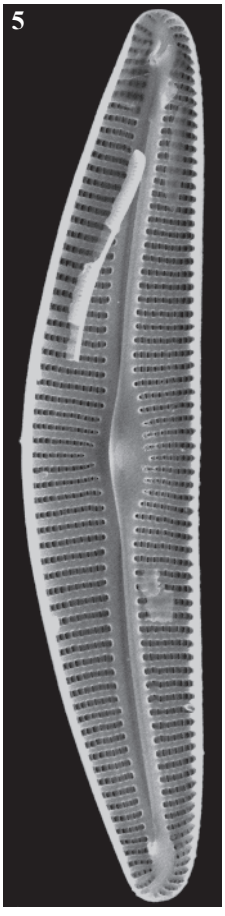
5

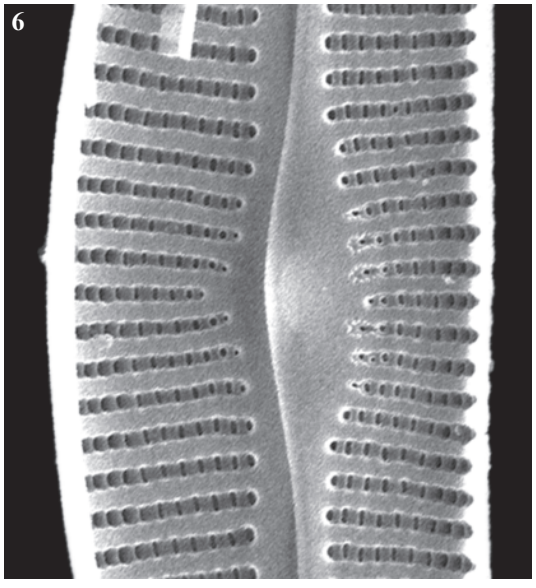
6

Plate 96 LM: x1500
SEM: Fig. 3,6 x6000, Fig. 5 x1500, Fig. 7 x10000

Figs. 1-2 *Cymbella* cf. *cymbiformis* Agardh
Figs. 3-7 *Cymbella cymbiformis* Agardh

Fig. 1	Lake Arratille, sediment PYR11
Fig. 2	Lake Sen, sediment PYR40
Figs. 3-7	Lake Roumassot, sediment PYR04
Fig. 4	Lake Posets, sediment PYR42

1

2

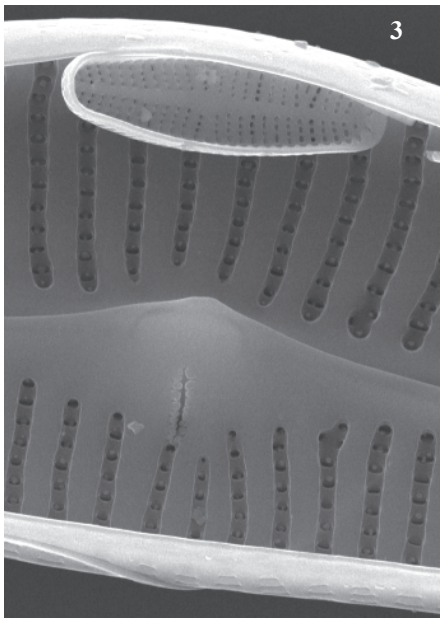

3

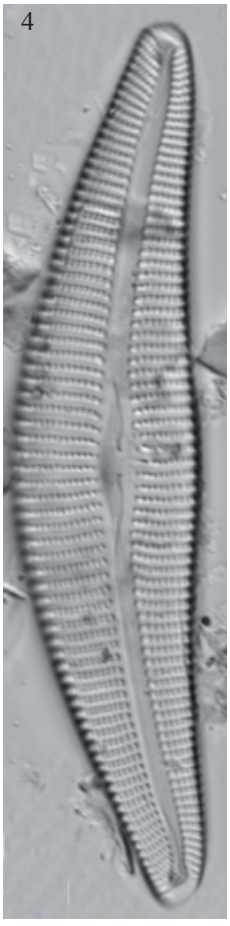

4

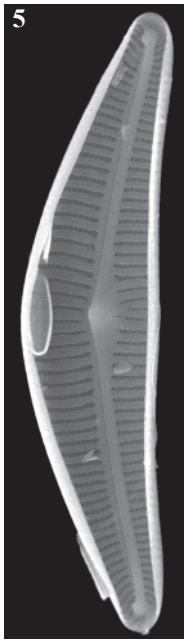

5

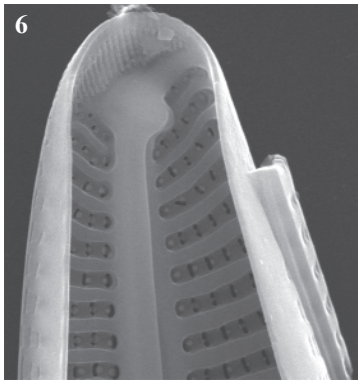

6

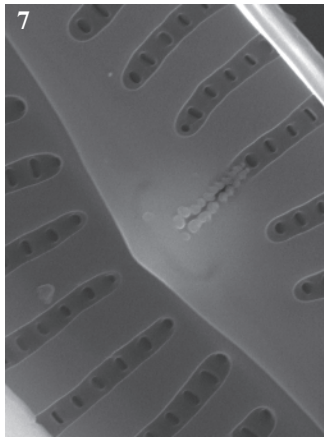

7

Plate 97 LM: x1500
SEM: Fig. 2 x1500, Figs. 3-4 x6000

Cymbella cf. *cymbiformis* Agardh

Fig. 1	Lake Gran de Mainera, sediment PYR70
Figs. 2-4	Lake Burg, sediment BURG 939
Fig. 5	Lake Burg

1

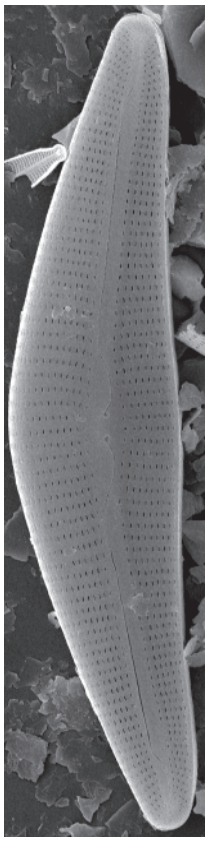

2

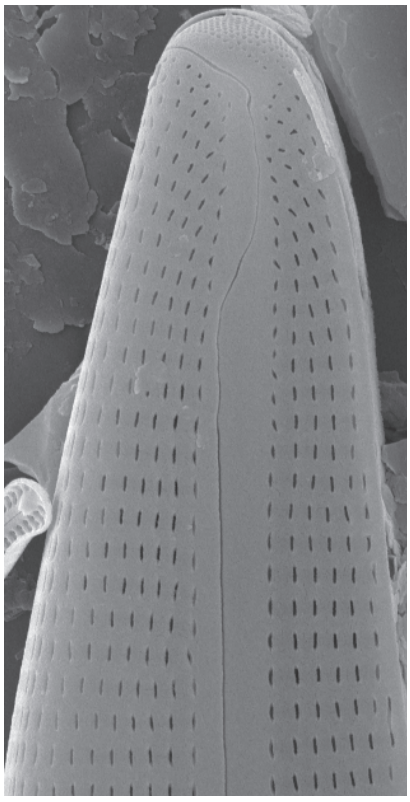

3

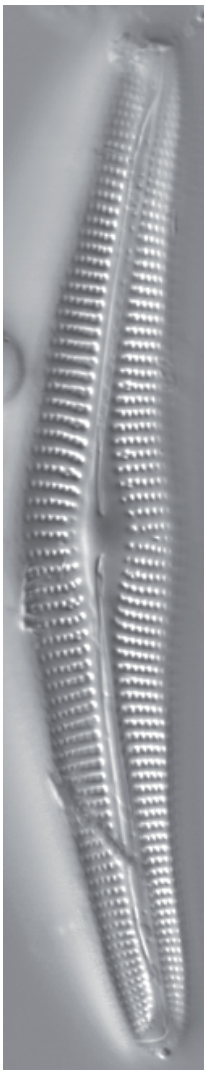

5

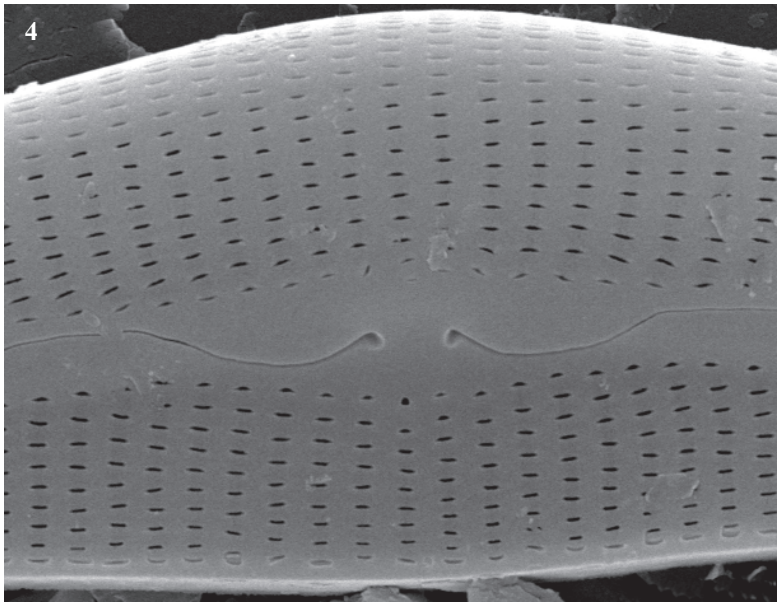

Plate 98 LM: x1500
SEM: x6000

Figs. 1-4 *Cymbella dorsenotata* Østrup

Fig. 1 Lake Arratille, sediment PYR11

Fig. 2 Lake Arnales, sediment PYR09

Figs. 3-4 Lake Roumassot, sediment PYR04

1

2

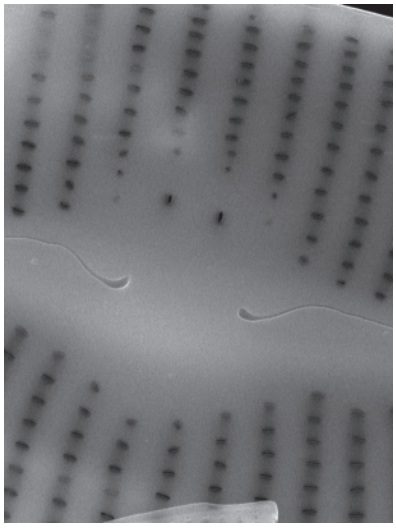

3

4

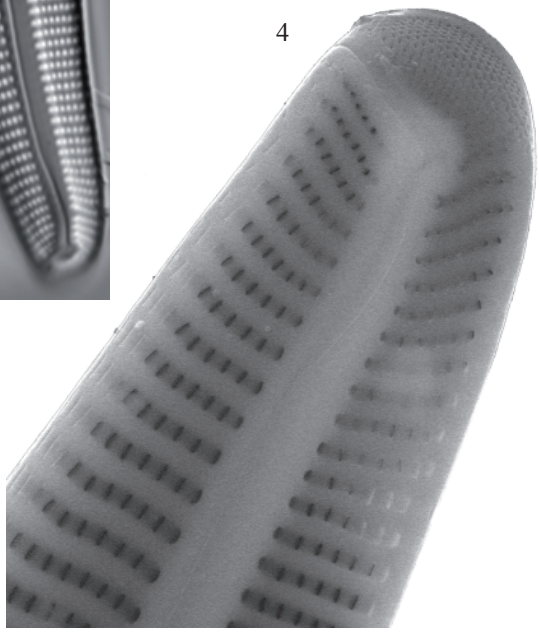

Plate 99 LM: x1500

Figs. 1-2 *Cymbella neoleptoceros* var. *tenuistriata* Krammer
Figs. 3-5 *Cymbella* cf. *neocistula* Krammer
Figs. 6-7 *Cymbella excisa* Kützing
Figs. 8-11 *Cymbella* cf. *subcistula* Krammer
Figs. 12-13 *Cymbella* cf. *proxima* Reimer

Figs. 1-2	Lake Acherito, sediment PYR01
Figs. 3, 5-7	Lake Posets, sediment PYR42
Figs. 4, 9-11, 13	Lake Gros de Camporrells, sediment PYR110
Fig. 8	Lake Angonella de Mes Amunt, sediment PYR78
Fig. 12	Lake Arnales, sediment PYR09


1


2


3

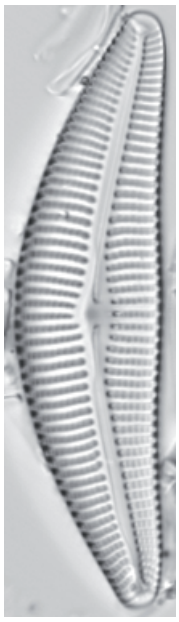
4


5


6


7

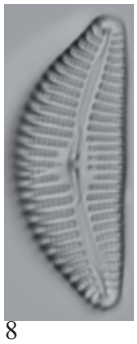
8


9


10

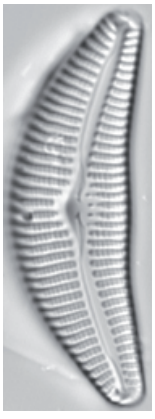
11

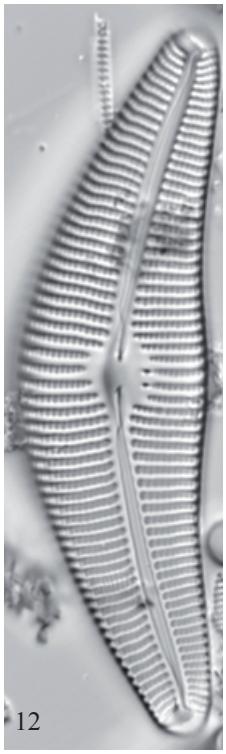
12

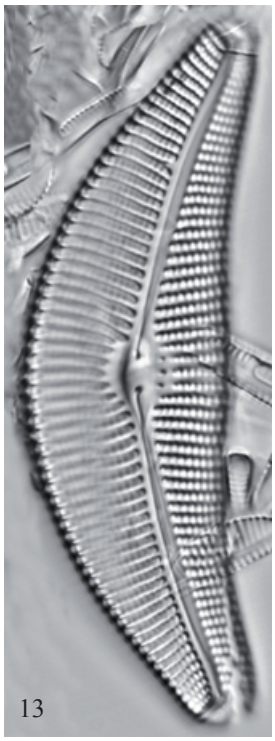
13

Plate 100 LM: x1500

Figs. 1-4	*Cymbopleura acuta* var. *angusta* Krammer
Fig. 5	*Cymbella subcuspidata* Krammer
Fig. 6	*Cymbopleura apiculata* Krammer
Figs. 7-8	*Cymbopleura* cf. *hercynica* (Schmidt) Krammer
Fig. 9	*Cymbopleura* sp. No. 2 Burg
Fig. 10	*Cymbopleura* sp
Fig. 11	*Cymbopleura anglica* (Lagerstedt) Krammer
Figs. 12-13	*Cymbopleura naviculiformis* (Auerswald) Krammer

Fig. 1	Lake Forcat Inf., sediment PYR77
Fig. 2	Lake Bleu de Rabassoles, sediment PYR112
Figs. 3-4	Lake Sotllo, sediment PYR89
Fig. 5	Lake Les Laquettes, sediment PYR27
Fig. 6	Lake Plan, sediment PYR69
Fig. 7	Lake Posets, sediment PYR42
Fig. 8	Lake Eriste, sediment PYR43
Fig. 9	Lake Burg, sediment BURG 1021
Fig. 10	Lake Burg, sediment BURG 833
Fig. 11	Lake Arratille, sediment PYR11
Fig. 12	Lake Pixón, sediment PYR44
Fig. 13	Lake Burg

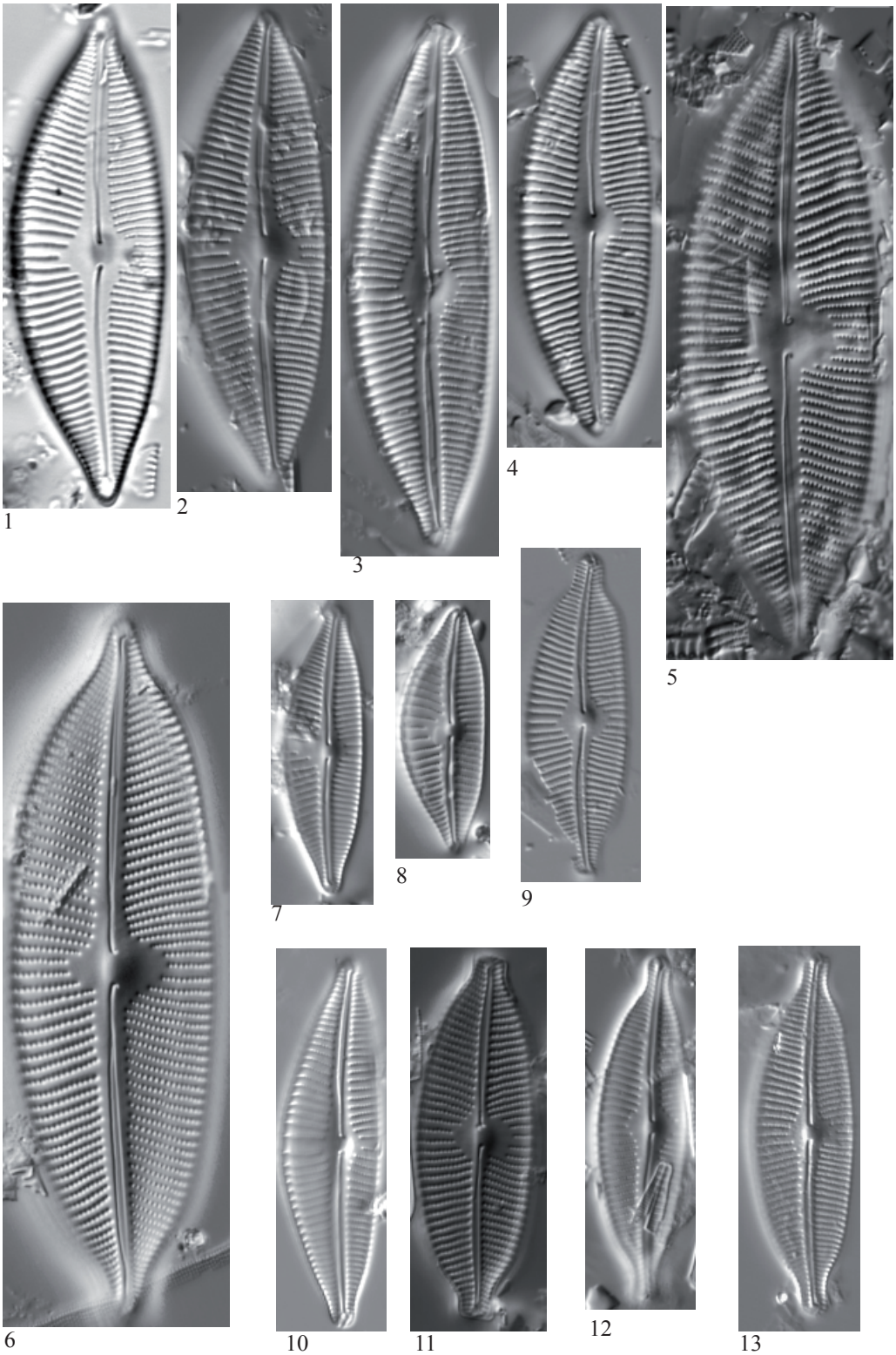
1
2
3
4
5
6
7
8
9
10
11
12
13

Plate 101 LM: x1500

Figs. 1-2	*Cymbopleura inaequalis* (Ehrenberg) Krammer
Fig. 3	*Cymbopleura subaequalis* var. *truncata* Krammer
Fig. 4	*Cymbopleura subaequalis* (Grunow) Krammer
Figs. 5-6	*Cymbopleura* cf. *subaequalis* (Grunow) Krammer

Figs. 1, 4	Lake Arratille, sediment PYR11
Fig. 2	Lake Ormiélas, sediment PYR05
Fig. 3	Lake Urdiceto, sediment PYR125
Figs. 5-6	Lake Monges, sediment PYR57

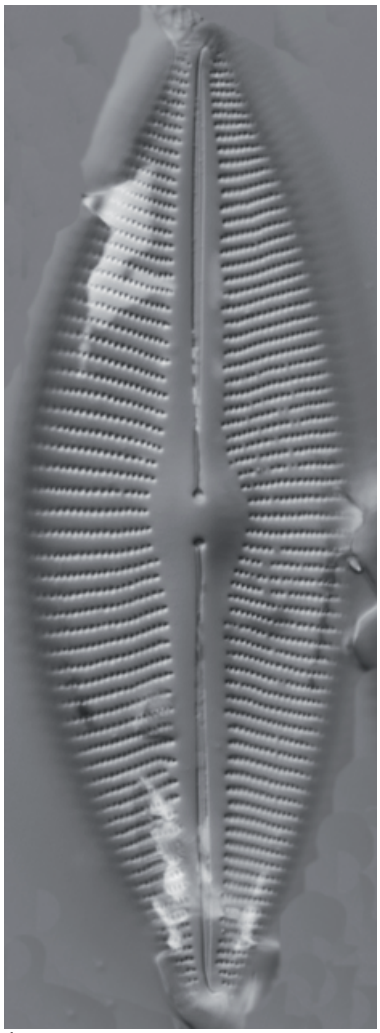

1

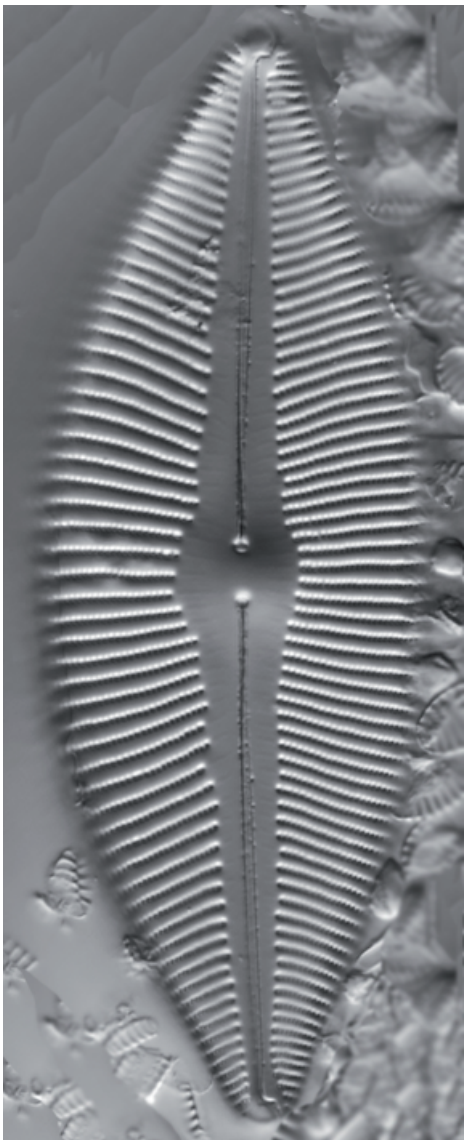

2

3

4

5

6

Plate 102 LM: x1500
SEM: x10000

Figs. 1-4	*Delicata delicatula* (Kützing) Krammer
Fig. 5	*Cymbella* sp cf. *lancettula* (Krammer) Krammer
Figs. 6-8	*Cymbopleura* cf. *pyrenaica* Le Cohu & Lange-Bertalot
Fig. 9	*Cymbella* sp.
Figs. 10-16	*Encyonopsis aequalis* (Smith) Krammer
Figs. 17-23	*?Encyonopsis aequalis* (Smith) Krammer ?*Encyonopsis kriegeri* (Krasske) Krammer

Fig. 1	Lake Arratille, sediment PYR11
Fig. 2	Lake Posets, sediment PYR42
Figs. 3-4	Lake Gran de Mainera, epilithic EpiPYR70
Fig. 5	Lake Bachimala Sup., sediment PYR31
Fig. 6	Lake Estom, sediment PYR15
Figs. 7-8	Lake Rond, sediment PYR72
Figs. 9, 19-20	Lake Senó, sediment PYR84
Figs. 10-11, 13-18, 21-23	Lake Sotllo, sediment PYR89
Fig. 12	Lake Negre, sediment PYR79

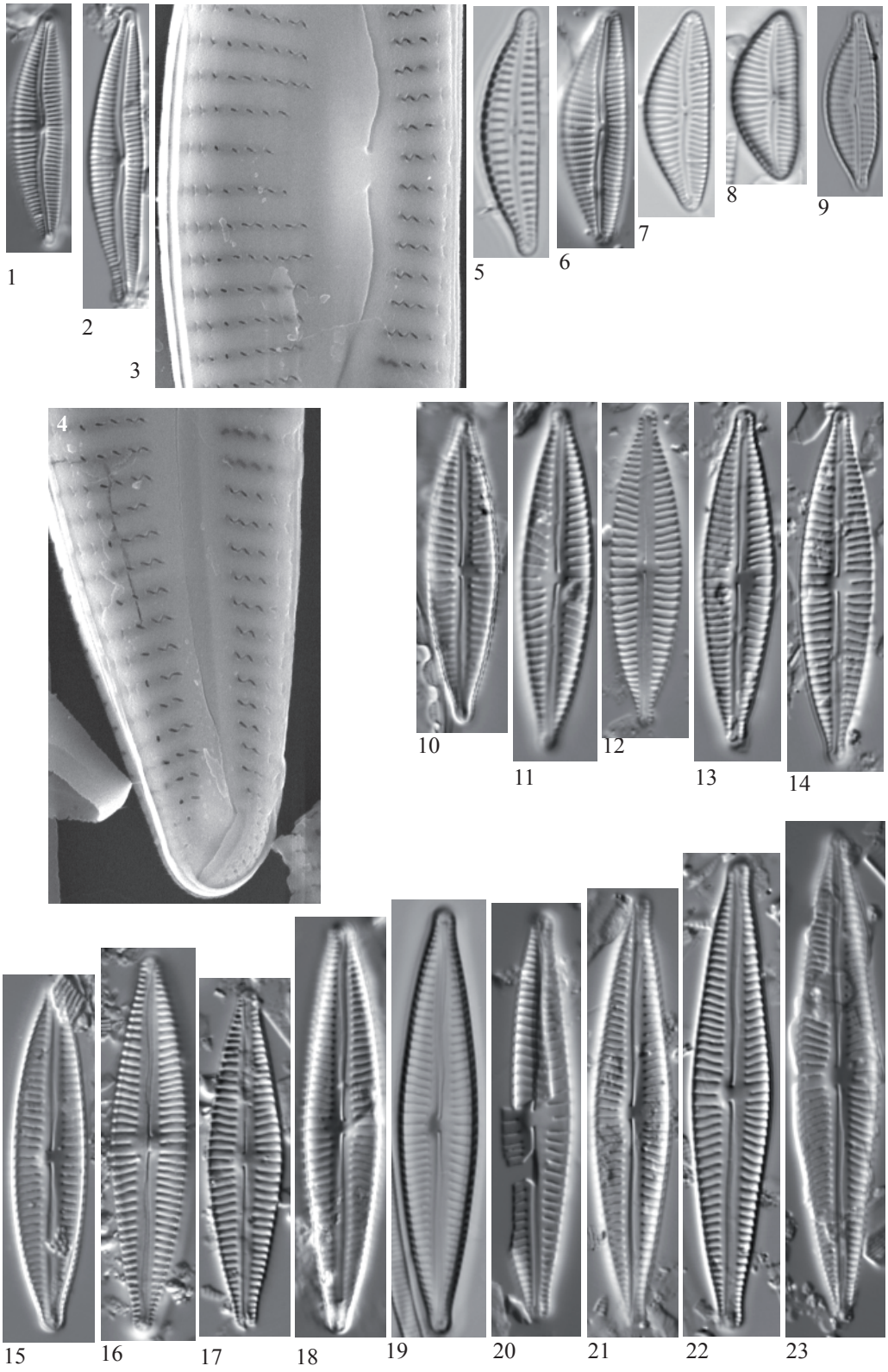
1
2
3
4
5
6
7
8
9
10
11
12
13
14
15
16
17
18
19
20
21
22
23

Plate 103 LM: Figs. 1.5, 7-8 x1500, Fig. 9 x750
SEM: Fig. 16 x10000, Figs. 17-19 x5000

Figs. 1-2	*Encyonopsis grunowii* Krammer
Figs. 3-5	*Encyonopsis cesatii* (Rabenhorst) Krammer
Figs. 6-7	*Encyonopsis* cf. *falaisensis* (Grunow) Krammer
Fig. 8	*Encyonopsis descripta* (Hustedt) Krammer
Fig. 9	*Encyonopsis* cf. *lanceola* (Grunow) Krammer
Figs. 10-19	*Encyonopsis subminuta* Krammer & Reichardt
Figs. 20-22	*Encyonopsis microcephala* (Grunow) Krammer
Figs. 23-24	*Encyonopsis minuta* Krammer et Reichardt
Figs. 25-26	*Encyonopsis* sp. No.1 Nere
Figs. 27-34	*Encyonopsis* cf. *krammeri* Reichardt

Fig. 1	Lake Llosás, sediment PYR46
Fig. 2	Lake Senó, sediment PYR84
Figs. 3-5, 8, 10, 19, 23	Lake Posets, sediment PYR42
Figs. 6-7	Lake Basa de la Mora, sediment PYR32
Fig. 9	Lake Filià, sediment PYR71
Fig. 11	Lake Bersau, sediment PYR03
Figs. 12-13	Lake Burg, sediment BURG 831
Fig. 14	Lake Arretille, sediment PYR11
Fig. 15	Lake Burg, sediment BURG 1127
Fig. 20	Lake Helado de Marboré, sediment PYR18
Figs. 21-22, 27-34	Lake Acherito, epilithic EpiPYR01
Fig. 24	Lake Col d`Arratille, sediment PYR12
Fig. 25	Lake Col d`Arratille, epilithic EpiPYR12
Fig. 26	Lake Nere de Güèri, epilithic EpiPYR53


1


2


3


4


5


6


7


8


9


10


11


12


13


14


15

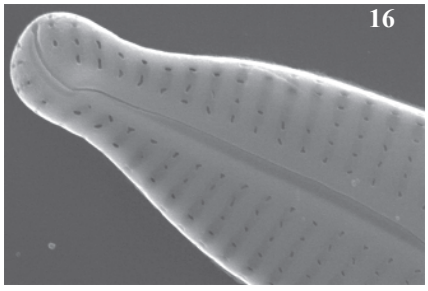
16


20


21


22


23


24


25


26


27


28


29


30


31


32


33


34

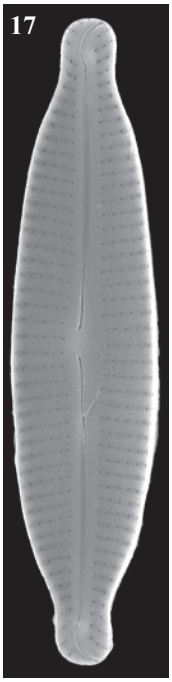
17

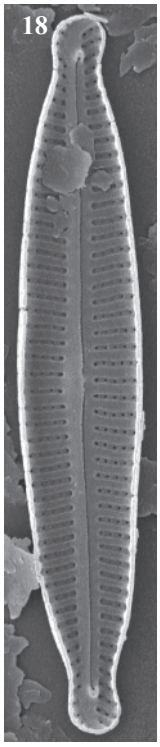
18

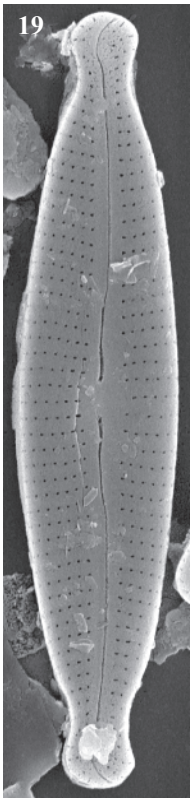
19

Plate 104 LM: x1500
SEM Figs 11,15 x4000, Fig. 16 x10000

Figs. 1-2 *Encyonema vulgare* Krammer

Figs. 3-16 *Encyonema silesiacum* (Bleisch) Mann

Figs. 17-19 *Encyonema lange-bertalotii* Krammer

Figs. 1-2	Lake Angonella, sediment PYR78
Figs. 3-5, 10, 19	Lake La Munia Sup., sediment PYR20
Figs. 6, 12	Lake Arratille, sediment PYR11
Fig. 7	Lake Sen, sediment PYR40
Figs. 8-9, 13-14	Lake Posets, sediment PYR42
Fig. 17	Lake Arnales, sediment PYR09
Fig. 18	Lake Rond, sediment PYR72
Fig. 11, 15-16	Lake Port Bielh, epilithic EpiPYR28

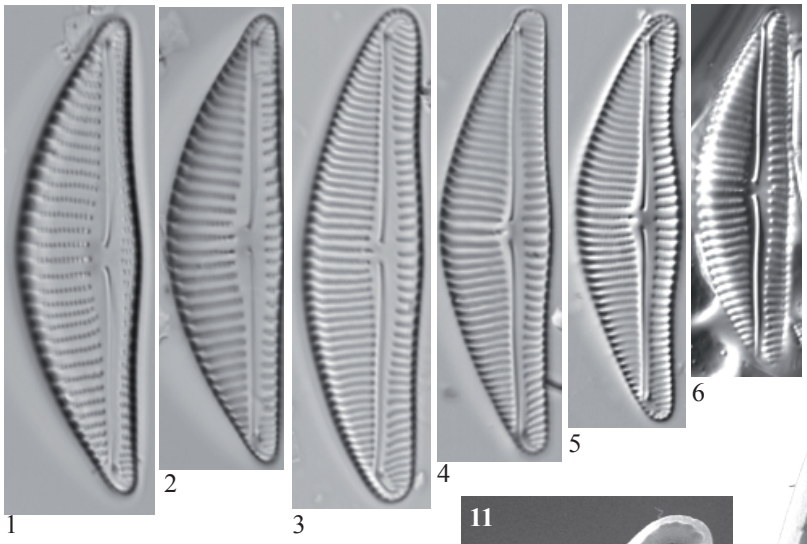
1
2
3
4
5
6

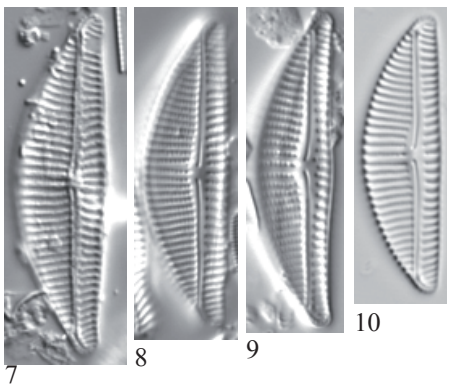
7
8
9
10

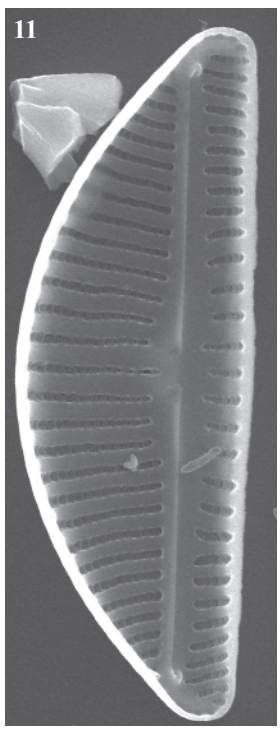
11


15

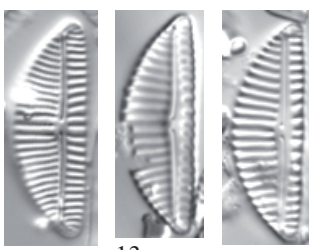
12
13
14

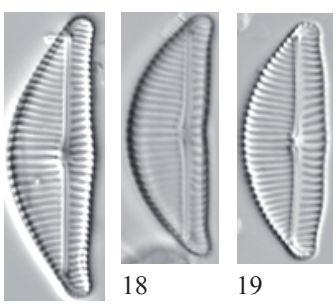
17
18
19

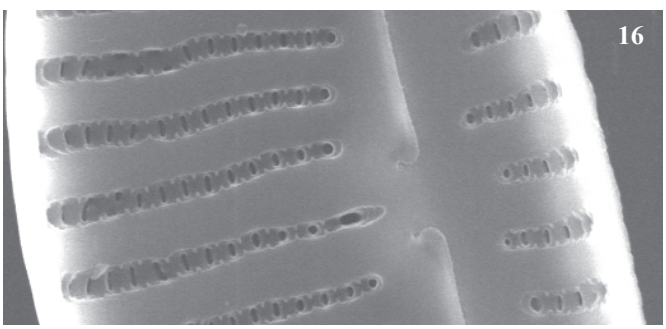
16

Plate 105 LM: x1500
SEM: Figs. 45,46,48 x6000, Fig. 47 x10000

Fig. 1	*Encyonema* sp. No. 9 Gerber
Figs. 2-7	*Encyonema* sp. No. 10 Burg, aff. *minutum* (Hilse) Mann
Figs. 8-10	*Encyonema* sp. No. 1 Mora
Fig. 11	*Encyonema* sp. No. 8 Filia
Fig. 12	*Encyonema* sp. No. 2 Sen
Fig. 13	*Encyonema* sp.
Figs. 14-31,45	complex *Encyonema minutum* (Hilse) Mann *Encyonema ventricosum* (Kützing) Grunow
Figs. 32-34	*Encyonema* sp.
Figs. 35-40	*Encyonema ventricosum* (Kützing) Grunow
Fig. 41	*Encyonema* sp. No. 7 Barroude
Figs. 42-44,48	*Encyonema reichardtii* (Krammer) Mann
Figs. 46-47	*Encyonema minutum* (Hilse) Mann

Fig. 1	Lake Gerber, sediment PYR63
Figs. 2-4, 7, 14	Lake Burg
Fig. 5	Lake Burg, sediment BURG 831
Fig. 6	L. Burg, sediment BURG 1007
Fig. 8	L. Col d`Arratille, sed. PYR12
Fig. 9	L. Basa de la Mora, sed. PYR32
Fig. 10	Lake Glacé, sediment PYR17
Fig. 11	Lake Filià, sediment PYR71
Figs. 12, 18-19, 22, 25, 27	Lake Sen, sediment PYR40
Figs. 13, 15-16, 20-21, 23, 26, 35-36	Lake Posets, sediment PYR42
Fig. 24	Lake Bersau, sediment PYR03
Fig. 29	L. H. Monte Perdido, sed. PYR19
Fig. 30	L. Bleu de Rabass., sed. PYR112
Figs. 17, 28, 31	L. Arratille, sediment PYR11
Figs. 32-34	L. Ormiélas, sediment PYR05
Fig. 40	Lake Eriste, sediment PYR43
Fig. 41	L. Barroude Inf., sediment PYR29
Figs. 42-43	Lake Cap Long, sediment PYR24
Fig. 18	Lake Pixón, sediment PYR44
Fig. 45	L. Roumassot, sediment EpiPYR04
Figs. 46-47	Lake Roumassot, sediment PYR04
Fig. 48	L. Pondiellos Sup., sed. EpiPYR08

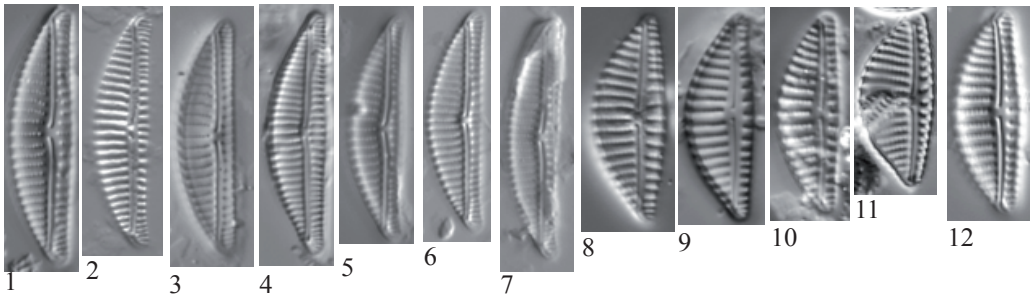
1
2
3
4
5
6
7
8
9
10
11
12

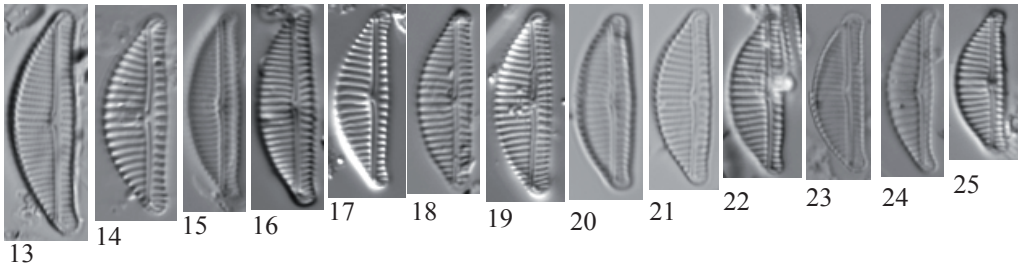
13
14
15
16
17
18
19
20
21
22
23
24
25

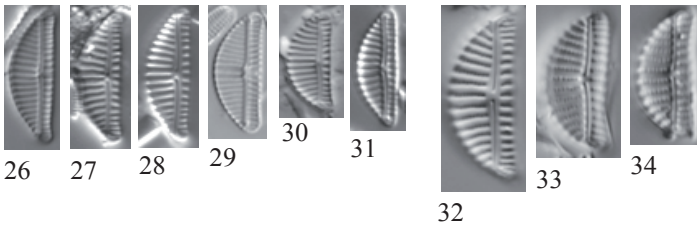
26
27
28
29
30
31
32
33
34

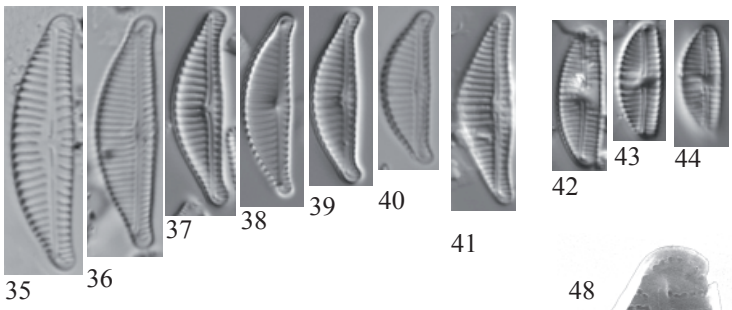
35
36
37
38
39
40
41
42
43
44

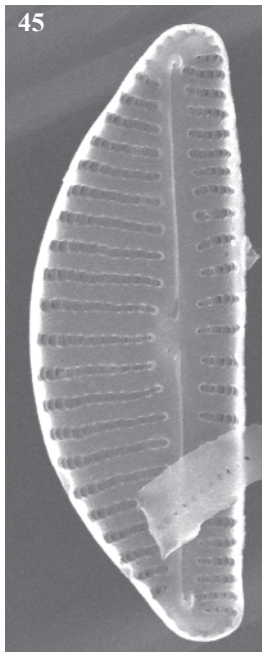
45

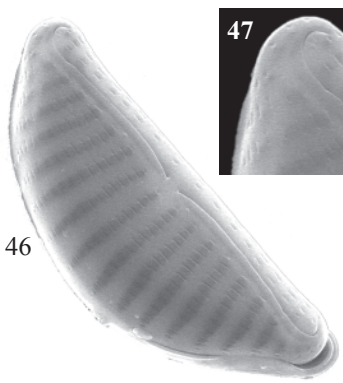
46
47

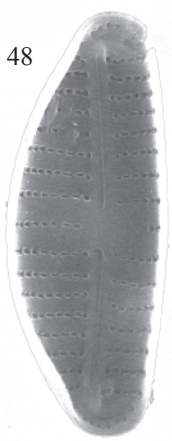
48

Plate 106 LM: x1500
SEM: Figs. 1, 3, 4 x10000, Figs. 5,6 x4000, Fig. 7 x2000

Figs. 1-2 *Encyonema minutum* (Hilse) Mann
Figs. 3-7 *Encyonema ventricosum* (Kützing) Grunow

Figs. 1-2	Lake Laurenti, sediment PYR111
Figs. 4-5	Lake Redon, sediment REDOM
Figs. 6-7	Lake Pondiellos, epilithic EpiPYR08
Fig. 3	Lake Posets, sediment PYR42

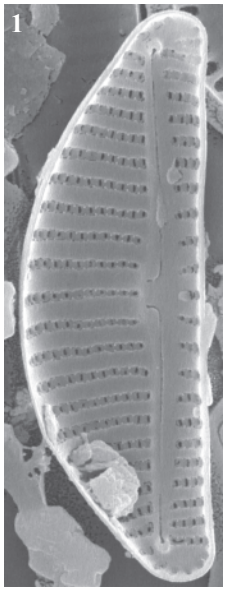
1

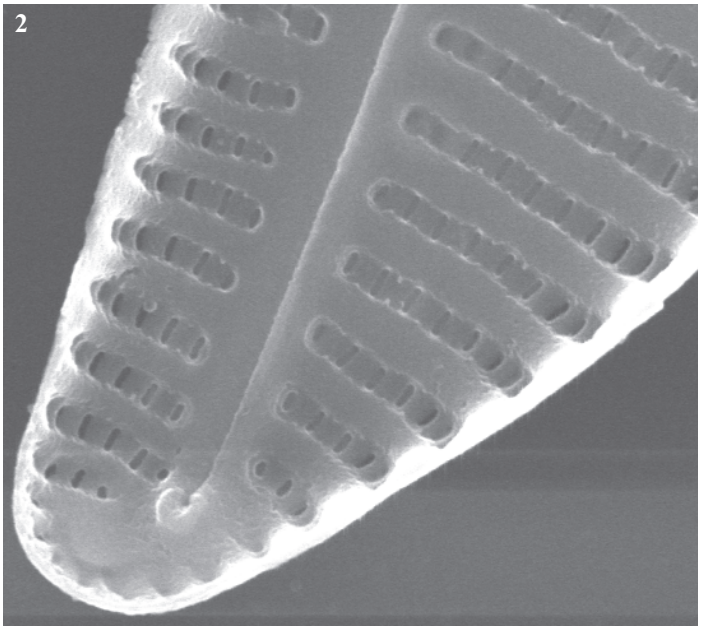
2

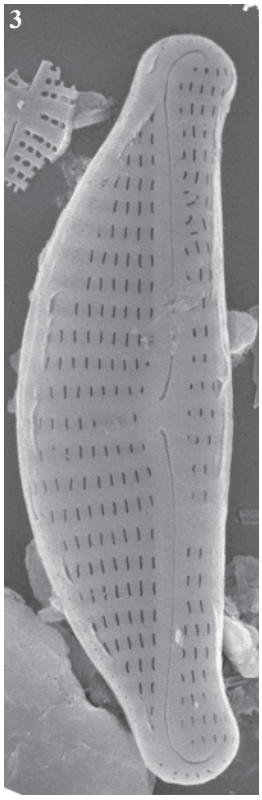
3


4

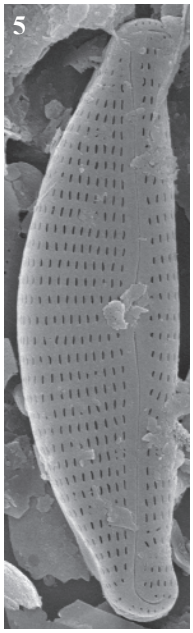
5

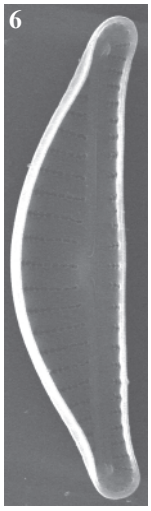
6

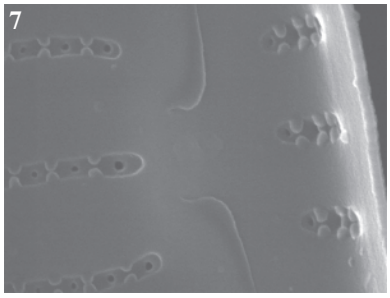
7

Plate 107 LM: x1500
SEM: Figs. 14-16 x6000, Figs. 17-18 x4000

Figs. 1-4, 14 *Encyonema perpusillum* (Cleve) Mann
Figs. 5-9, 15-16 *Encyonema gaeumannii* (Meister) Krammer
Figs. 10-13 17-18 *Encyonema neogracile* Krammer

Figs. 1-2	Lake Aubé, sediment PYR82
Figs. 3-4	Lake Monges, sediment PYR57
Figs. 5-7	Lake Blaou, sediment PYR94
Fig. 8	Lake Posets, sediment PYR42
Fig. 9	Lake Les Laquettes, sediment PYR27
Figs. 10-13	Lake Bleu de Rabassoles, epilithic EpiPYR112
Fig. 14	Lake Illa, sediment PYR66
Fig. 15	Lake Mariola, sediment PYR80
Figs. 16-18	Lake Redon, sediment REDOM

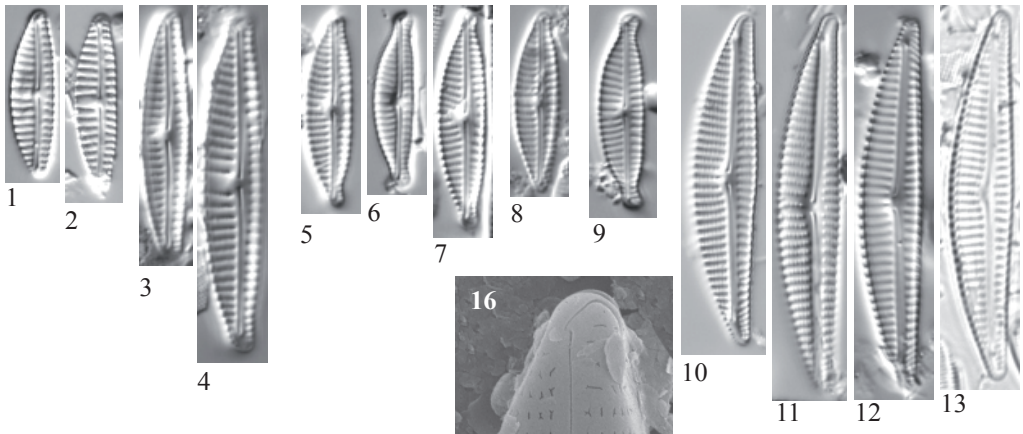
1
2
3
4
5
6
7
8
9
10
11
12
13

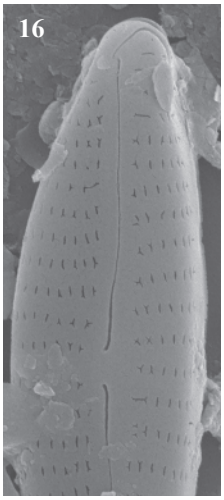
16

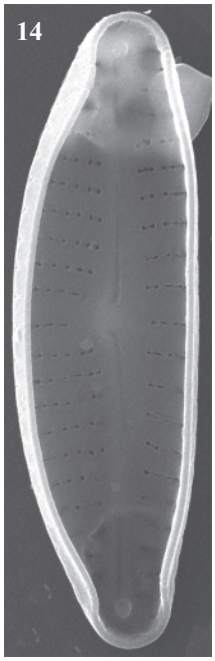
14

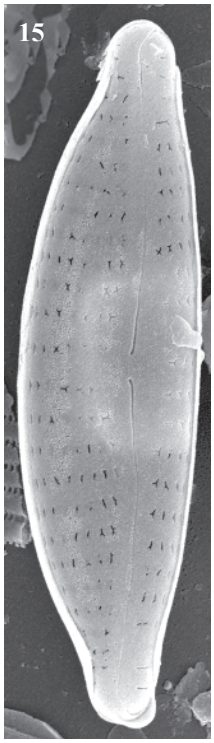
15

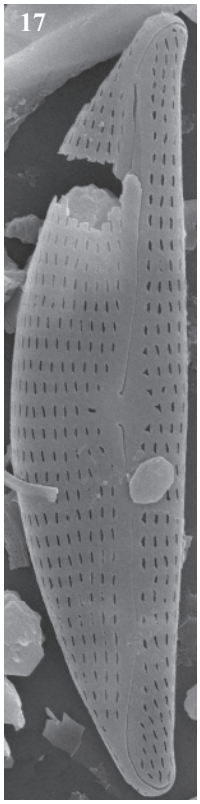
17

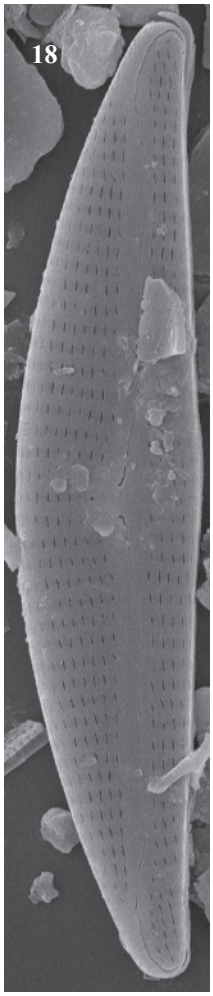
18

Plate 108 LM: x1500
SEM: x3000

Figs. 1-3	*Encyonema cespitosum* Kützing
Figs. 4-6	*Encyonema* cf. *obscurum* var. *alpina* Krammer
Fig. 7	*Encyonema* sp. No. 3 Sen
Fig. 8	*Encyonema silesiacum* (Bleisch) Mann
Figs. 9-10	? Primary cells
Figs. 11-14	*Encyonema* sp. No. 5 Pica Palomera
Figs. 15-16	*Encyonema* sp. No. 6 Seno
Figs. 17-22	*Encyonema hebridicum* Grunow ex Cleve
Figs. 23-27	*Reimeria sinuata* (Gregory) Kociolek & Stoermer emend Sala, Guerrero & Ferrario

Figs. 1-3, 27	Lake Estom, sediment PYR15
Figs. 4-5, 7	Lake Basa de la Mora, sediment PYR32
Fig. 6	Lake Arnales, sediment PYR09
Figs. 8, 21-22	Lake Arratile, sediment PYR76
Figs. 9-10	Lake Posets, sediment PYR11
Figs. 11, 13	Lake Pica Palomera, sediment PYR52
Fig. 12	Lake Mes Amunt de Tristaina, sediment PYR86
Fig. 14	Lake Burg
Fig. 15	Lake Senó, sediment PYR84
Fig. 16	Lake La Munia Sup., sediment PYR20
Fig. 17	Lake Mariola, sediment PYR80
Figs. 18, 20	Lake Negre, sediment PYR79
Fig. 19	Lake Monges, sediment PYR57
Fig. 23	Lake Laurenti, sediment PYR111
Fig. 24	Lake Les Laquettes, sediment PYR27
Fig. 25	Lake Llebreta, sediment PYR58
Fig. 26	Lake Helado del Monte perdido, epilithic EpiPYR19

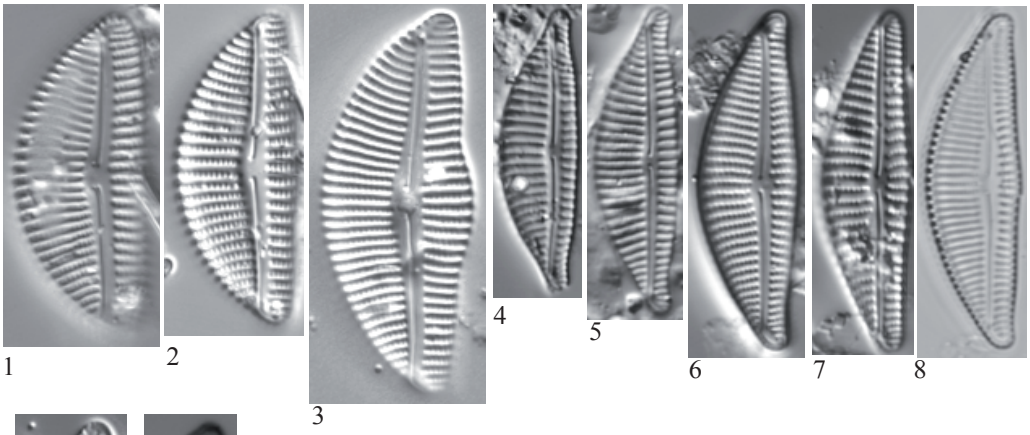
1
2
3
4
5
6
7
8

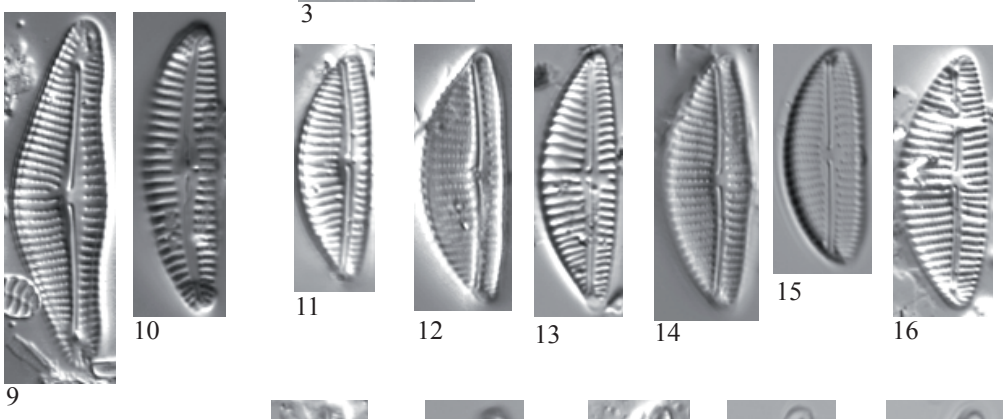
9
10
11
12
13
14
15
16

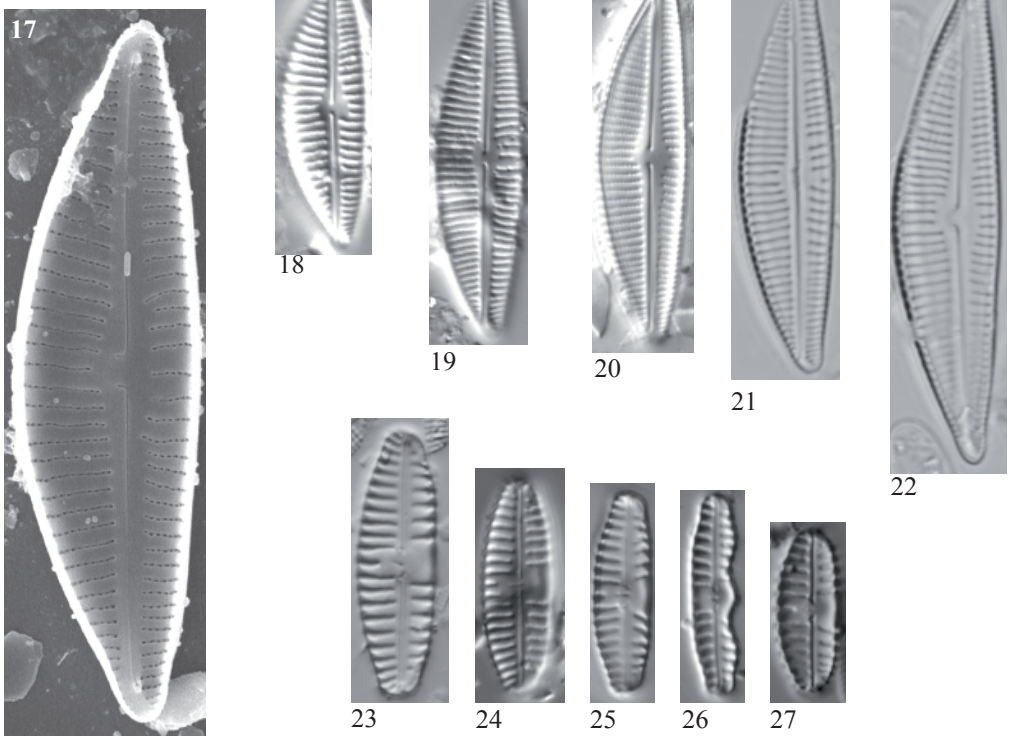
17
18
19
20
21
22
23
24
25
26
27

Plate 109	LM: x1500 SEM: Fig. 14 x8000, Fig. 15 x6000, Figs. 22-24 x3000
Figs. 1-2, 14	*Amphora pediculus* (Kützing) Grunow
Figs. 3-4	*Amphora neglecta* f. *densestriata* Foged
Figs. 5,15	*Amphora* cf. *inariensis* Krammer
Fig. 6	*Amphora* sp.
Figs. 7-11	*Amphora* cf. *eximia* Carter
Figs. 12-13	*Amphora* sp. No. 1 Sen
Fig. 16	*Amphora oligotraphenta* Lange-Bertalot
Fig. 17, 22	*Amphora* cf. *affinis* Kützing
Figs. 18-20, 23-24	*Amphora copulata* (Kützing) Schoeman & Archibald
Fig. 21	*Amphora lange-bertalotii* Z. Levkov & D. Metzeltin

Fig. 1	Lake Llebreta, sediment PYR58
Fig. 2	Lake Estanés, sediment PYR02
Figs. 3, 7, 8, 9, 13, 16	Lake Sen, sediment PYR40
Figs. 4, 10-12, 19, 21	Lake Posets, sediment PYR42
Figs. 5-6	Lake Pondiellos Sup., sediment PYR08
Fig. 17	Lake Basa de la Mora, sediment PYR32
Fig. 14-15, 22, 24	Lake Laurenti, sediment PYR111
Fig. 18	Lake Arratille, sediment PYR11
Fig. 20	Lake Pixón, sediment PYR44
Fig. 23	Lake Arnales, epilithic EpiPYR09

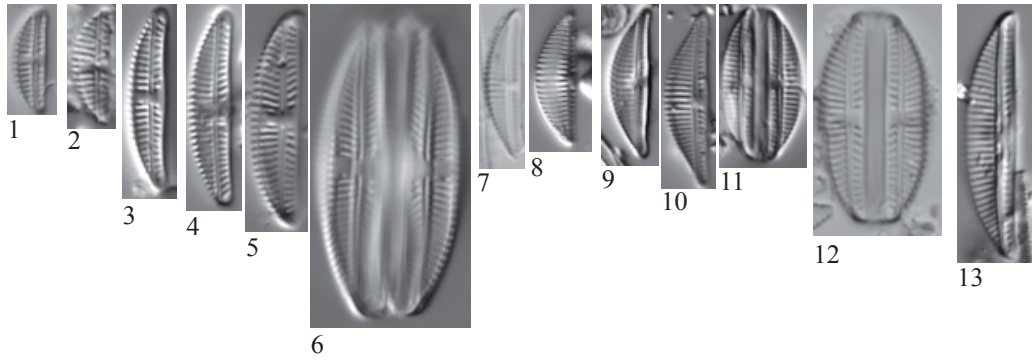
1
2
3
4
5
6
7
8
9
10
11
12
13

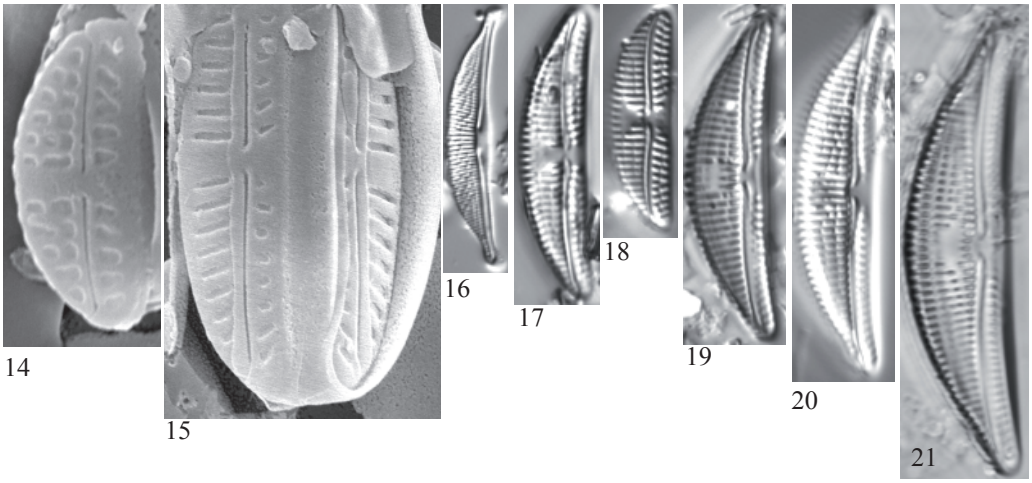
14
15
16
17
18
19
20
21

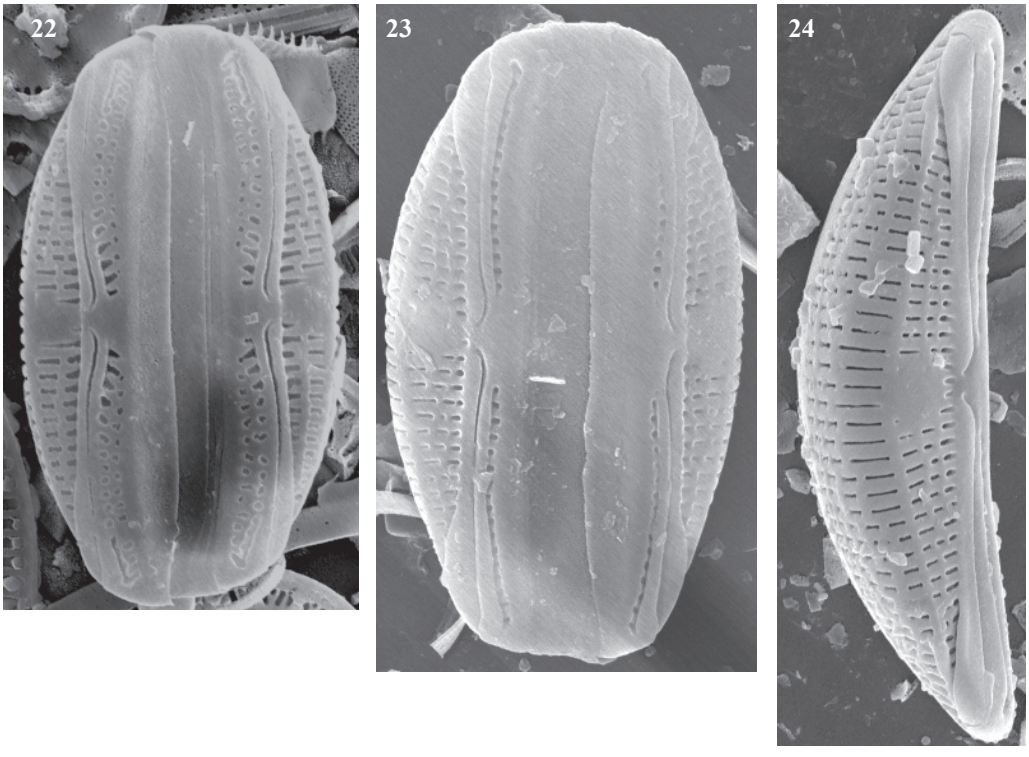
22
23
24

Plate 110 LM: x1500
SEM: Fig. 10 x10000 Fig. 11 x2000

Fig. 1	*Gomphonema coronatum* Ehrenberg
Fig. 2	*Gomphonema* cf. *acuminatum* Ehrenberg
Figs. 3-4	*Gomphonema acuminatum* Ehrenberg
Figs. 5-6, 10-11	*Gomphonema capitatum* Ehrenberg
Fig. 7	*Gomphonema* cf. *truncatum* Ehrenberg
Figs. 8-9	*Gomphonema truncatum* Ehrenberg

Fig. 1	Lake Llebreta, sediment PYR58
Figs. 2, 5-6	Lake Posets, sediment PYR42
Figs. 3-4	Lake Burg
Fig. 7	Lake Burg, sediment BURG 1176
Figs. 8-9	Lake Angonella de Més Amunt, sediment PYR78
Figs. 10-11	Lake Gran de Mainera, epilithic EpiPYR70

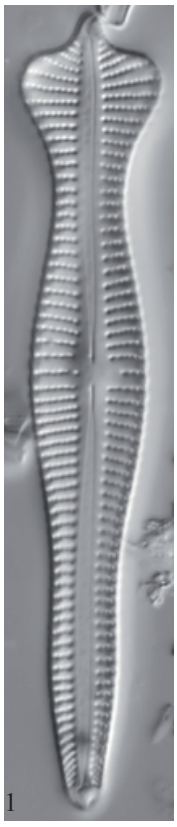
1


2

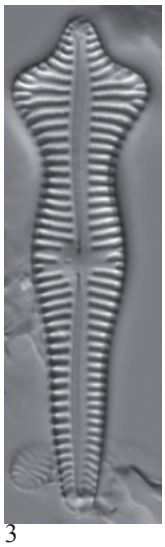
3


4


5


6


7


8

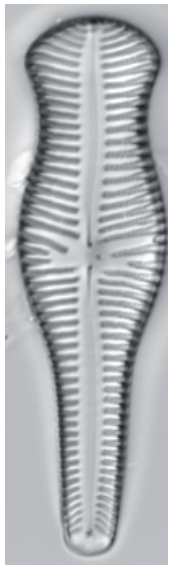
9

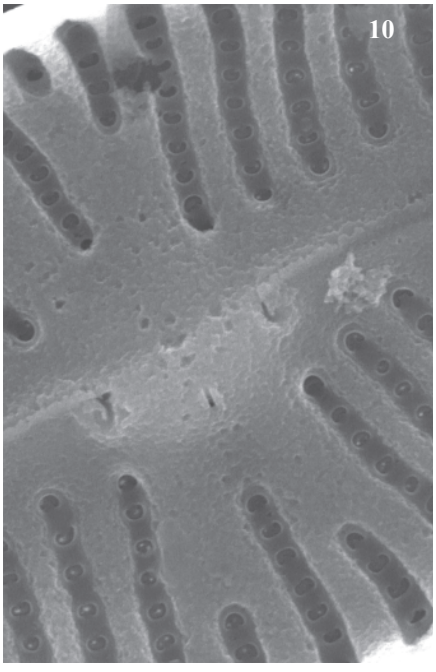
10

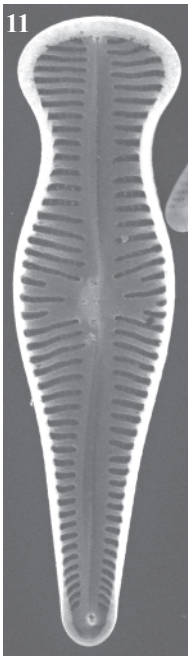
11

Plate 111 LM: x1500

Figs. 1-2	*Gomphonema brebissonii* Kützing
Figs. 3-5	*Gomphonema montanum* Schumann
Figs. 6	*Gomphonema clavatum* Ehrenberg
Figs. 7-8	*Gomphonema subclavatum* (Grunow) Grunow
Fig. 9-10	*Gomphonema* cf. *subclavatum* (Grunow) Grunow
Fig. 11	*Gomphonema* sp. No. 1 Acherito
Fig. 12	*Gomphonema* sp. No. 2 Laquettes
Figs. 13-25	*Gomphonema lateripunctatum* Reichardt & Lange-Bertalot
Fig. 26-27	*Gomphonema vibrio* Ehrenberg

Fig. 1	Lake PYR128
Fig. 2	Lake Gran del Pessó, sediment PYR56
Figs. 3-4	Lake Cregüeña, sediment PYR49
Fig. 5	Lake Més Amunt de Tristaina, epilithic EpiPYR86
Fig. 6	Lake Compte, sediment PYR97
Fig. 7	Lake Forcat Inf., sediment PYR77
Fig. 8	Lake Siscar, sediment PYR126
Fig. 9	Lake Romedo de Dalt, sediment PYR85
Fig. 10	Lake Inferior de la Gallina, sediment PYR87
Figs. 11, 24, 26-27	Lake Acherito, sediment PYR01
Figs. 12, 15-19, 21-22	Lake Les Laquettes, sediment PYR27
Fig. 13	Lake Arratille, sediment PYR11
Fig. 14	Lake Asnos, sediment PYR14
Figs. 20, 25	Lake Rond, sediment PYR72
Fig. 23	Lake Gros de Camporrells, sediment PYR110

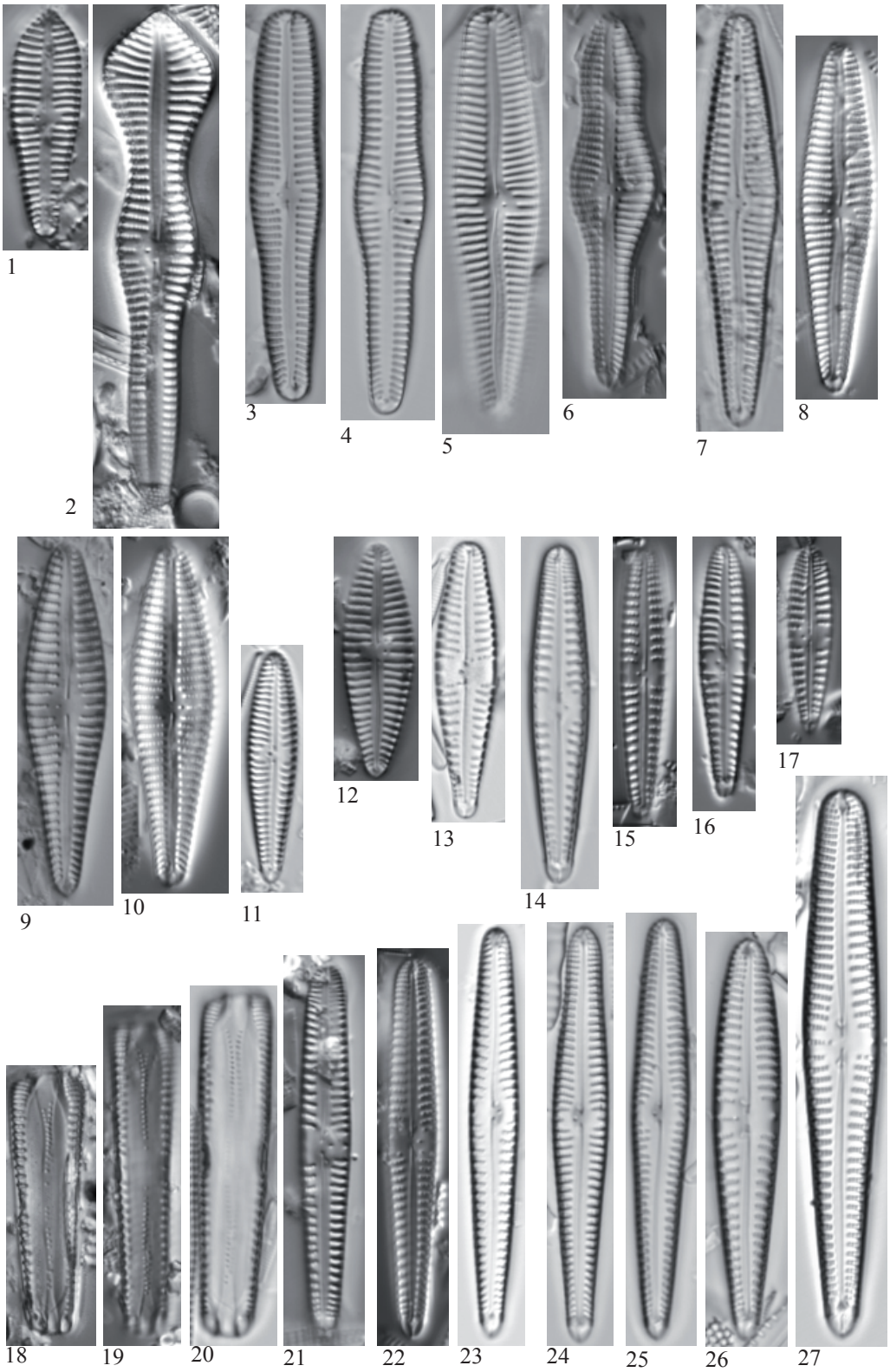
1
2
3
4
5
6
7
8
9
10
11
12
13
14
15
16
17
18
19
20
21
22
23
24
25
26
27

Plate 112 LM: x1500
SEM: Figs. 4-5 x5000, Figs. 6-7 x15000, Fig. 8 x10000

Figs. 1-8 *Gomphonema lateripunctatum* Reichardt & Lange-Bertalot

Figs. 1, 4, 6-7	Lake Roumassot, epilithic EpiPYR04
Fig. 2	Lake Les Laquettes, sediment PYR27
Figs. 5, 8	Lake Port Bielh, epilithic EpiPYR28


1


2


3

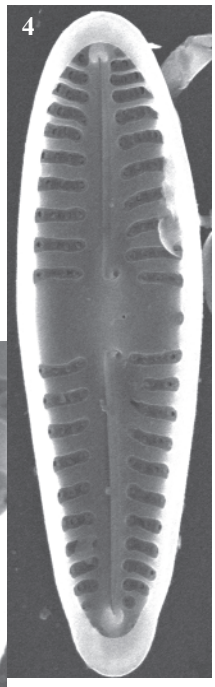
4


5

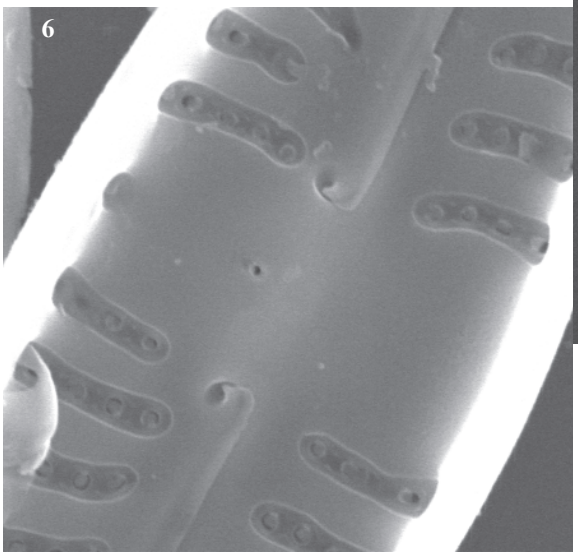
6

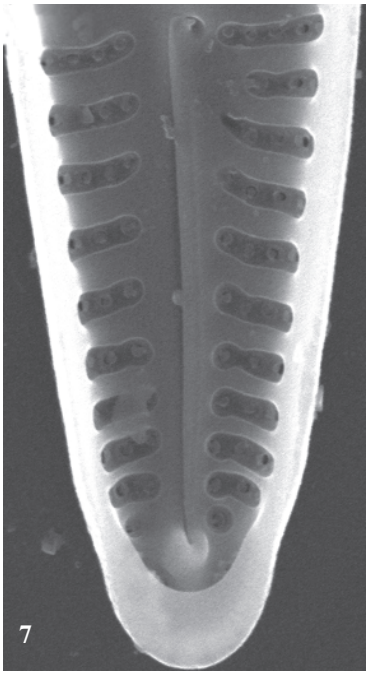
7

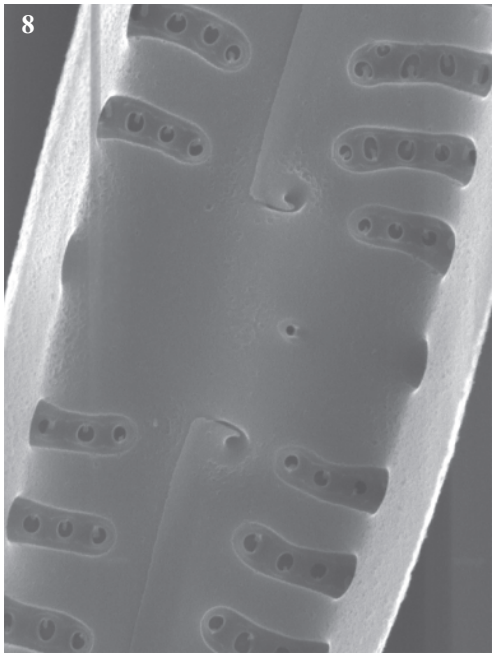
8

Plate 113 LM: x1500
SEM: Fig. 42 x5000

Fig. 1-2	*Gomphonema* cf. *designatum* Reichardt
Fig. 3	*?Gomphonema minusculum* Krasske
Figs. 4-7	*Gomphonema* cf. *pumilum* (Grunow) Reichardt & Lange-Bertalot
Figs. 8-10	*Gomphonema* cf. *elegantissimum* Reichardt & Lange-Bertalot
Figs. 11-12	*Gomphonema* cf. *pseudotenellum* Lange-Bertalot
Figs. 13-17	*Gomphonema* cf. *minusculum* Krasske
Fig. 18	*Gomphonema* sp. No. 4 Posets
Figs. 19-20	G*omphonema* cf. *lacus-vulcani* Reichardt & Lange-Bertalot
Fig. 21	*Gomphonema* sp. No. 5 Chelau
Figs. 22-30	*Gomphonema* sp. No. 6 Inferior
Fig. 31	*Gomphonema* sp. No. 7 Burg
Fig. 32	*Gomphonema* sp. No. 8 Laquettes
Fig. 33	*Gomphonema occultum* Reichardt & Lange-Bertalot
Figs. 34-35	*Gomphonema tergestinum* (Grunow) Fricke
Fig. 36	cf. G*omphonemopsis* sp. No. 1 Compte
Figs. 37-42	*Gomphonema* sp. No. 9 Posets
Figs. 43-48	*Gomphoneis* cf. *olivaceoides* (Hustedt) Carter
Figs. 49-50	*Gomphonema* sp. No. 10 Inferior
Fig. 51	*Gomphonema* cf. *rhombicum* Fricke
Fig. 52	*Gomphonema* sp. No. 11 Ormiélas aff. *G. tenue*

Fig. 1	Lake Helado de Marboré, sediment PYR18
Fig. 2	Lake Pondiellos Sup., epilithic EpiPYR08
Fig. 3	Palaelake Burg, sediment BURG 804
Figs. 4, 45	Lake Arratille, sediment PYR11
Fig. 5	Lake Tourrat, sediment PYR23
Figs. 6, 8-9, 12-13, 30	Lake Acherito, sediment PYR01
Fig. 7	Lake Compte, sediment PYR97
Fig. 10	Lake Gran de Mainera, sediment PYR70
Figs. 11, 32	Lake Les Laquettes, sediment PYR27
Fig. 14	Lake Roumassot, sediment PYR04
Fig. 15	Lake Acherito, epilithic EpiPYR01

Sample information continued on the next page

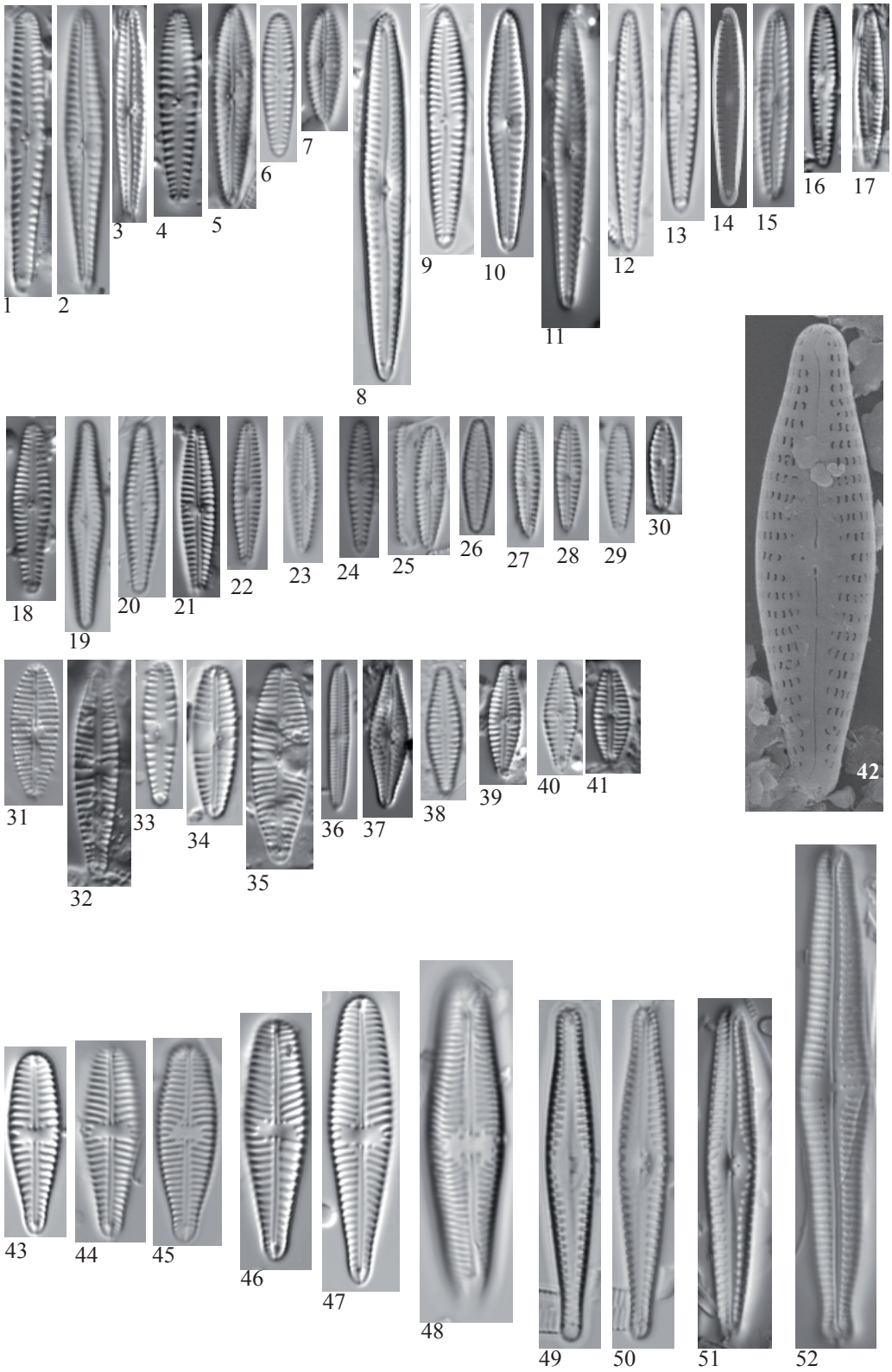
1
2
3
4
5
6
7
8
9
10
11
12
13
14
15
16
17
18
19
20
21
22
23
24
25
26
27
28
29
30
31
32
33
34
35
36
37
38
39
40
41
42
43
44
45
46
47
48
49
50
51
52

Plate 114 SEM: Fig. 1 x6000, Figs. 2-3, 5-7 x15000 Fig. 4 x4000

Figs. 1-3 *Gomphonema* cf. *minusculum* Krasske
Figs. 4-7 *Gomphonema* sp.

Figs. 1-7 Lake Roumassot, sediment PYR04

Sample information of Plate 113

Figs. 16-17	Lake Port Bielh, sediment PYR28
Figs. 18-20, 37, 42	Lake Posets, sediment PYR42
Fig. 21	Lake Chelau Sup., sediment PYR41
Figs. 22-29, 49-50	Lake Inf. de la Gallina, sediment PYR87
Fig. 31	Lake Burg
Fig. 33	Lake Bleu epilithic EpiPYR22
Figs. 34, 43-44, 46-48	Lake La Munia Sup., sediment PYR20
Fig. 35	Lake Cap Long, sediment PYR24
Figs. 36-41	Lake Compte epilithic EpiPYR97
Fig. 51	Lake Trebens, sediment PYR114
Fig. 52	Lake Pica Palomera epilithic EpiPYR52


1

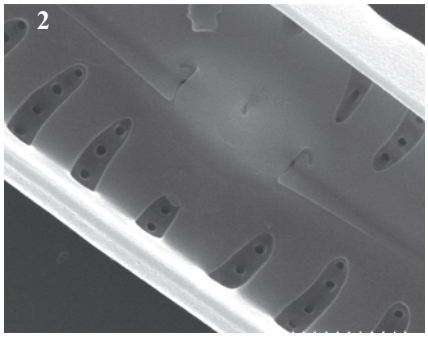
2

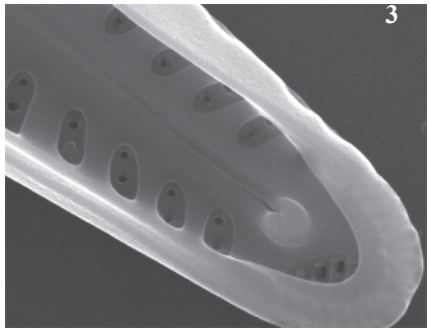
3


4

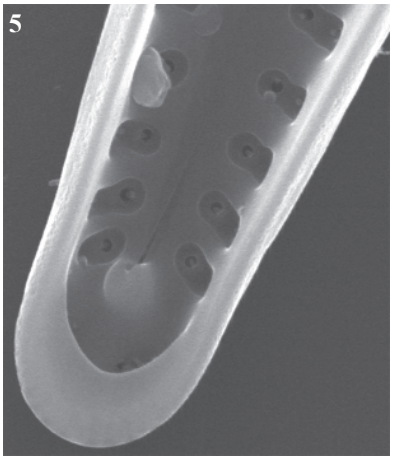
5

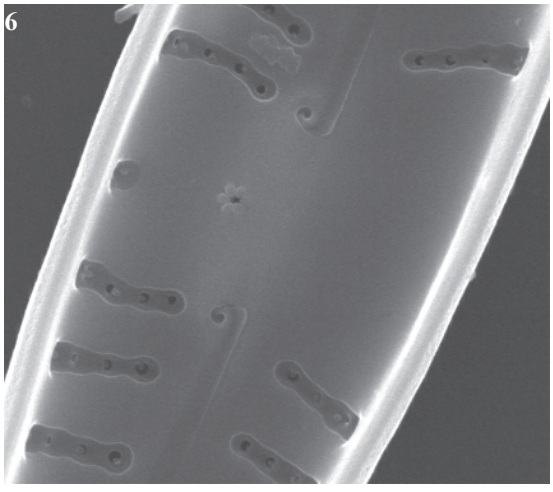
6

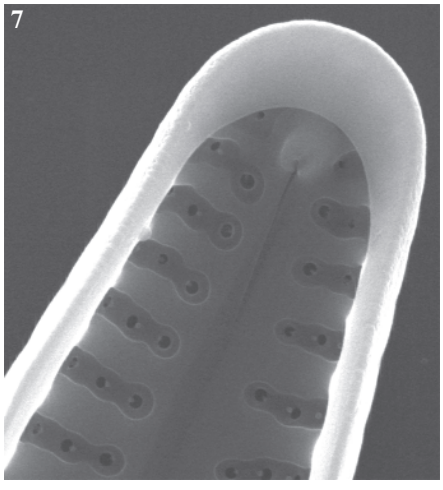
7

Plate 115 LM: x1500

Fig. 1	*Gomphonema sarcophagus* Gregory
Fig. 2	*Gomphonema* sp. No. 12 Burg
Fig. 3	*Gomphonema lapponicum* (Cleve) Cleve-Euler
Fig. 4	*Gomphonema micropus* Kützing
Fig. 5	*Gomphonema* sp. No. 13 Gerber
Fig. 6	*Gomphonema* sp. No. 14 Cap Long
Figs. 7-10	*Gomphonema* sp. No. 15 Coronas
Figs. 11-13	*Gomphonema* cf. *cymbelliclinum* Reichardt & Lange-Bertalot
Figs. 14-15	*Gomphonema parvulum* (Kützing) Kützing sensu lato
Fig. 16	*Gomphonema parvulum* (Kützing) Kützing sensu lato
Fig. 17-21	*Gomphonema* sp. No. 16 Estagnol
Figs. 22-24	*Gomphonema* sp. No. 17 Gerber
Fig. 25	*Gomphonema* cf. *gracile* Ehrenberg
Figs. 26-31	*Gomphonema* cf. *hebridense* Gregory
Figs. 32-33	*Gomphonema auritum* Braun
Figs. 34-37	*Gomphonema* sp. No. 20 Laquettes
Figs. 38-44	*Gomphonema* spp aff. *Gomphonema parvulum* (Kützing) Kützing sensu lato
Fig. 45-47	*Gomphonema* cf. *acidoclinatum* Lange-Bertalot & Reichardt
Fig. 48-50	*Gomphonema* sp. No. 18 Laquettes
Fig. 51	*Gomphonema* sp. No. 19 Laquettes

Fig. 1	Lake Burg, sediment 970
Fig. 2	Lake Burg, sediment 473
Figs. 3, 11-12, 15, 28	Lake Cregüeña, sediment PYR49
Fig. 4	Lake Rond, sediment PYR72
Figs. 5, 22-23	Lake Gerber, sediment PYR63
Fig. 6	Lake Cap Long, epilithic EpiPYR24
Fig. 7	Lake Coronas, sediment PYR47
Figs. 8-9, 18, 20-21	Lake L´Estagnol, sediment PYR119
Figs. 10, 13, 19, 24	Lake Inf. de la Gallina, sediment PYR87
Figs. 14, 27	Lake Bachimala Sup., sediment PYR31
Figs. 16, 25	Lake Mariola, sediment PYR80

Sample information continued on the next page

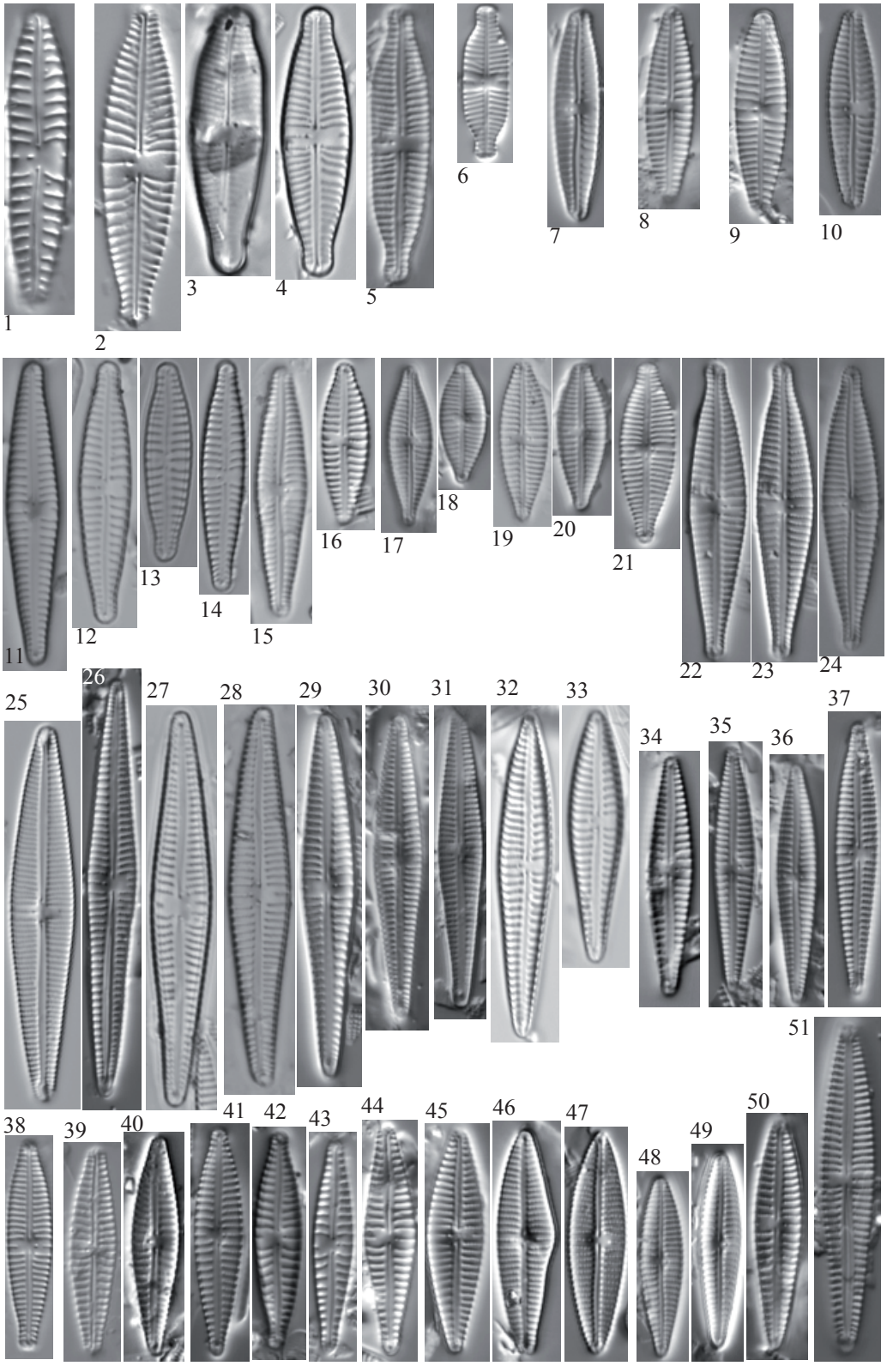
1
2
3
4
5
6
7
8
9
10
11
12
13
14
15
16
17
18
19
20
21
22
23
24
25
26
27
28
29
30
31
32
33
34
35
36
37
38
39
40
41
42
43
44
45
46
47
48
49
50
51

Plate 116 SEM: Fig. 1 x1800, Figs. 2, 4 x15000, Fig. 3 x9000

Figs. 1-4 *Gomphonema hebridense* Gregory

Figs. 1-4	Lake Port Bielh, sediment EpiPYR28

Sample information of Plate 115

Figs. 17, 38-39	Lake Burg
Figs. 26, 29-31, 35-37, 41-43, 48-51	Lake Les Laquettes, sediment PYR27
Fig. 32	Lake Arratille, sediment PYR11
Fig. 33	Lake Acherito, sediment PYR01
Figs. 34, 40	Lake Sen, sediment PYR40
Fig. 44	Lake Eriste, sediment PYR43
Fig. 45	Lake Pixón, sediment PYR44
Figs. 46-47	Lake Pica, sediment PYR100

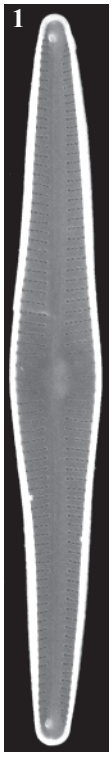
1

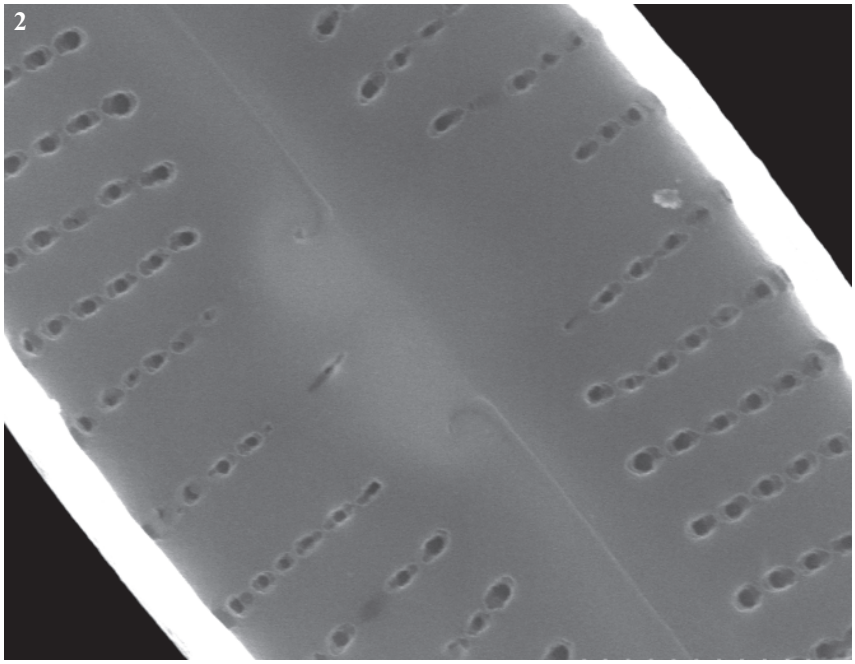
2

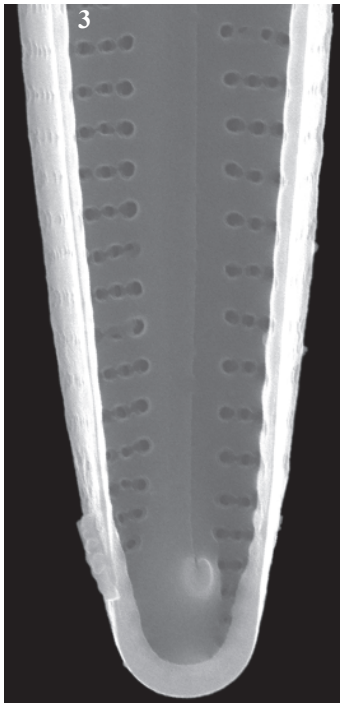
3

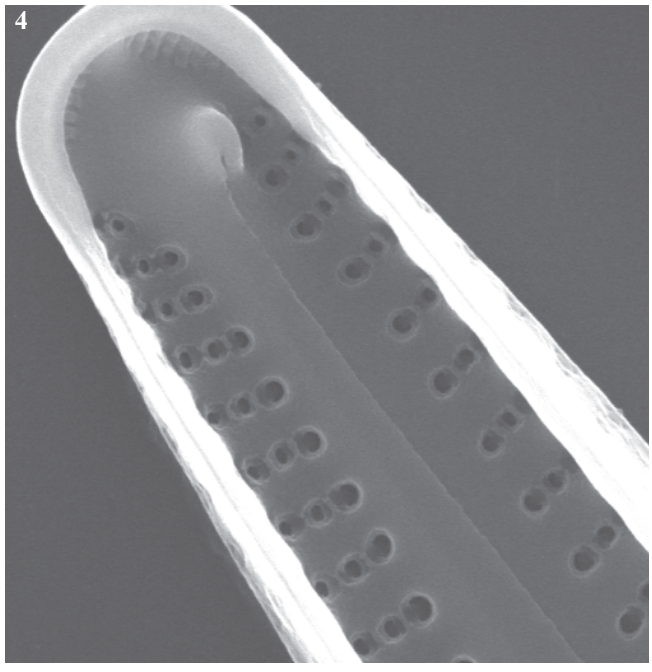
4

Plate 117 LM: x1500
SEM: 4-7, 8, 13, 14 x8000 20 x5000

Figs. 1-6 *Nitzschia* sp. No. 4 Airoto

Figs. 7-15 *Nitzschia* spp
Fig. 9-10, 12 *Nitzschia* sp. No. 6 Sen
Fig. 11 *Nitzschia* sp. No. 5 Arratille

Figs. 16-20 *Nitzschia* sp. No. 1 Sen

Figs. 1, 3, 19-20	Lake Posets, sediment PYR42
Fig. 2	Lake Illa, sediment PYR66
Fig. 4	Lake Redon, sediment REDOM
Fig. 5	Lake Roumassot, epilithic EpiPYR04
Fig. 6	Lake Roumassot, sediment PYR04
Fig. 7	Lake Port Bielh, epilithic EpiPYR28
Fig. 8	Lake Garbet, sediment PYR81
Figs. 9, 15	Lake Gran de Mainera, sediment PYR70
Fig. 10	Lake Rond, sediment PYR72
Fig. 11	Lake Arratille, sediment PYR11
Figs. 12, 16-18	Lake Sen, sediment PYR40
Fig. 13	Lake Laurenti, sediment PYR111
Fig. 14	Lake Arnales, epilithic EpiPYR09


1-3

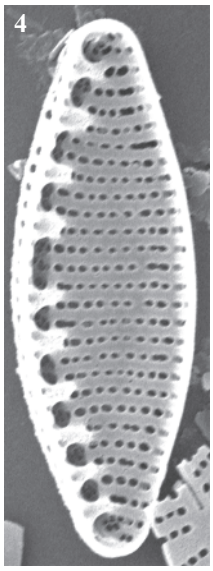
4

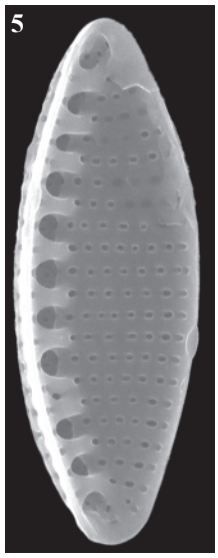
5

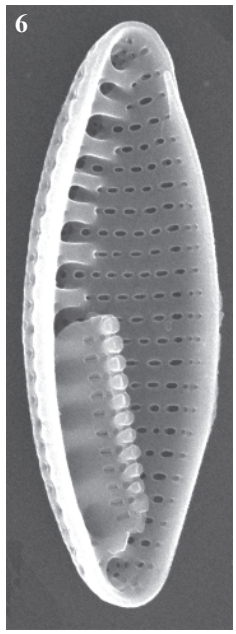
6

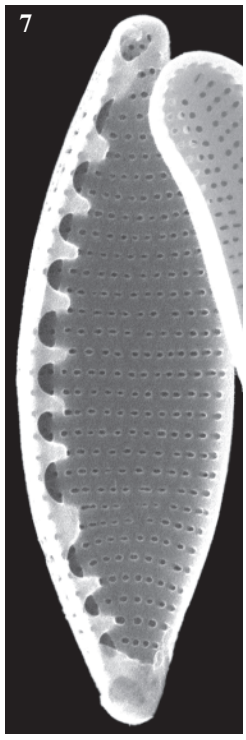
7

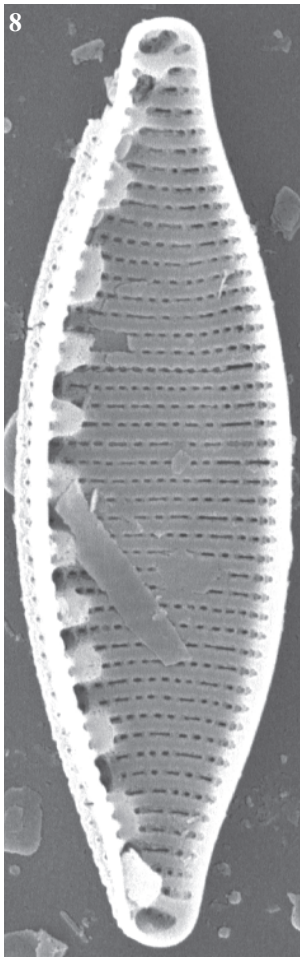
8


9


10


11


12

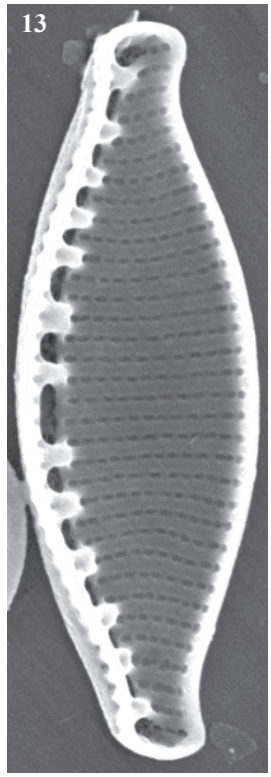
13


15


16


17


18


19

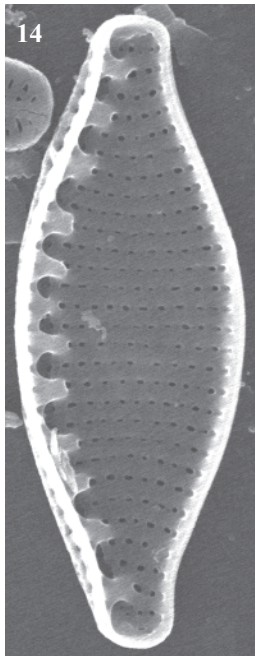
14

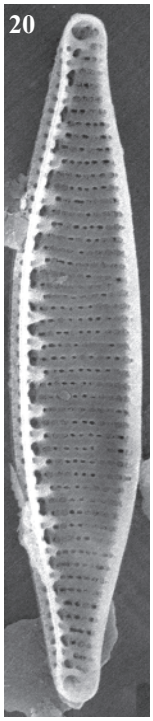
20

Plate 118 LM: x1500
SEM: x8000

Figs. 1-4	*Nitzschia* cf. *frustulum* (Kützing) Grunow
Figs. 5-6	*Nitzschia* cf. *inconspicua* Grunow
Figs. 7-13	*Nitzschia* cf. *alpina* Hustedt
Figs. 14, 27-30	*Nitzschia* sp
Figs. 15-18	*Nitzschia acidoclinata* Lange-Bertalot
Fig. 19-22	*Nitzschia* cf. *perminuta* (Grunow) Peragallo M1
Figs. 23-26, 31	*Nitzschia* cf. *perminuta* (Grunow) Peragallo M2

Fig. 1	Lake Roumassot, epilithic EpiPYR04
Fig. 2	Lake Etriste, sediment PYR43
Fig. 3	Lake Estom, sediment PYR15
Figs. 4-6, 16	Lake Burg
Fig. 7	Lake Filià, sediment PYR71
Fig. 8	Lake Llebreta, sediment PYR58
Figs. 9-13, 14, 28-30	Lake Posets, sediment PYR42
Figs. 15, 17	Lake Bersau, sediment PYR03
Figs. 18, 20-22	Lake Inf. de la Gallina, sediment PYR87
Fig. 19	Lake Arratille, sediment PYR11
Fig. 23	Lake Sen, sediment PYR40
Fig. 24	Lake Gelat Bergús, sediment PYR65
Figs. 25-26	Lake Basa de la Mora, sediment PYR32
Fig. 27	Lake Redon, sediment REDOM
Fig. 31	Lake Port Bielh, epilithic EpiPYR28

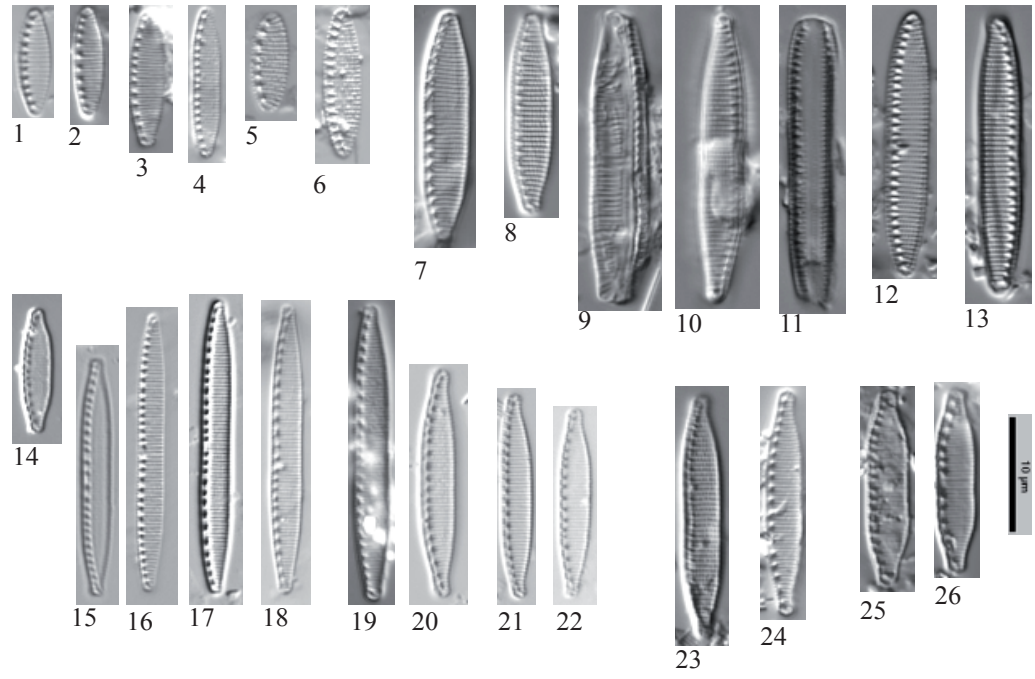
1
2
3
4
5
6
7
8
9
10
11
12
13
14
15
16
17
18
19
20
21
22
23
24
25
26
10 µm

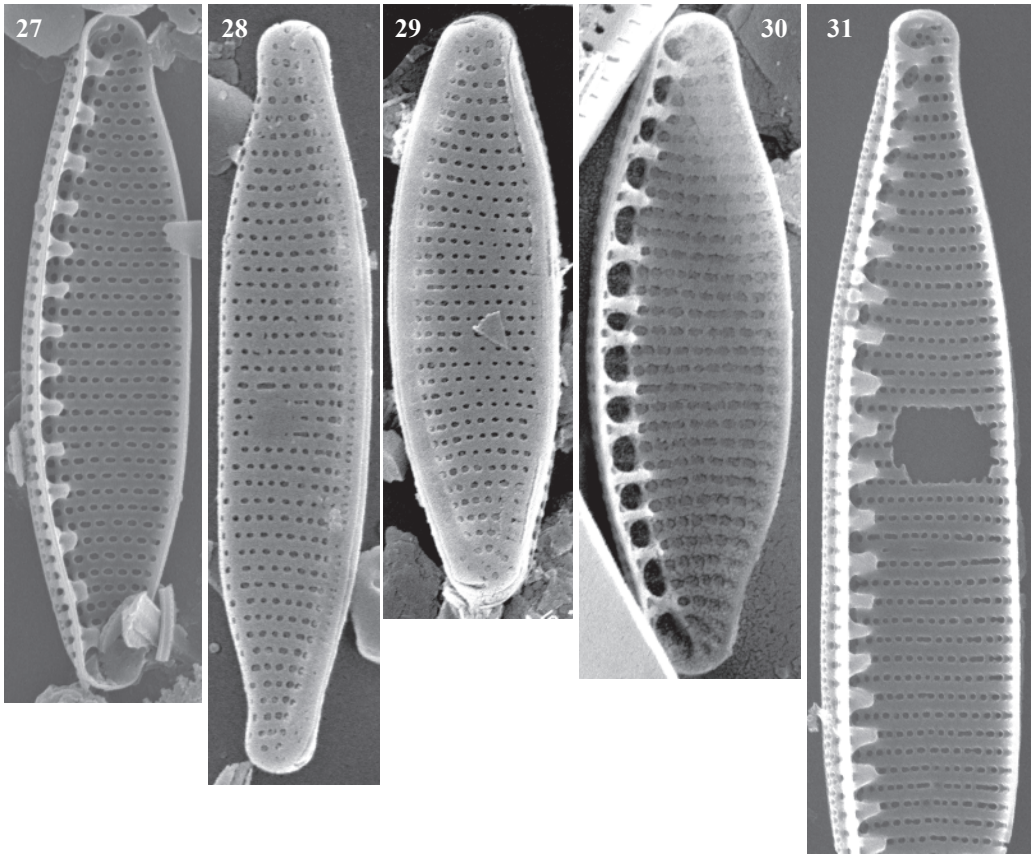
27
28
29
30
31

Plate 119 LM: x1500
SEM: Figs. 8-9 x6000, Fig. 10 x4500

Fig. 1	*Nitzschia* sp. No. 16 Mora
Figs. 2-3	*Nitzschia* cf. *pumila* Hustedt
Figs. 4-5, 10	*Nitzschia* cf. *pumila* Hustedt
Figs. 6-9	*Nitzschia* sp. No. 2 Posets
Figs. 11-17	*Nitzschia* cf. *bryophila* (Hustedt) Hustedt
Figs. 18-23	*Nitzschia* sp. No. 15 Burg, aff. *bryophila* (Hustedt) Hustedt
Figs. 24-28	*Nitzschia* cf. *bryophila* (Hustedt) Hustedt
Fig. 29	*Nitzschia* sp.
Fig. 30	*Nitzschia* sp. No. 13 Coronas
Fig. 31	*Nitzschia* sp. No. 3 Airoto
Figs. 32-33	*Nitzschia palea* var. *debilis* (Kützing) Grunow

Fig. 1	Lake Basa de la Mora, sediment PYR32
Fig. 2	Lake Arnales, sediment PYR09
Fig. 3	Lake Burg, sediment BURG 1116
Figs. 4-8, 29	Lake Posets, sediment PYR42
Fig. 9	Lake Pondiellos Sup., epilithic EpiPYR08
Fig. 10	Lake Port Bielh, epilithic EpiPYR28
Fig. 11	Lake Inf. de la Gallina, sediment PYR87
Fig. 12	Lake Illa, epilithic EpiPYR66
Figs. 18-23	Lake Burg
Figs. 24-26	Lake Sen, sediment PYR40
Fig. 27	Lake Més Amunt de Tristaina, sediment PYR86
Fig. 28	Lake Pixón, sediment PYR44
Fig. 30	Lake Coronas, epilithic EpiPYR47
Fig. 31	Lake Airoto, sediment PYR73
Fig. 32	Lake Pondiellos Sup., sediment PYR08
Fig. 33	Lake Lliterola, sediment PYR33

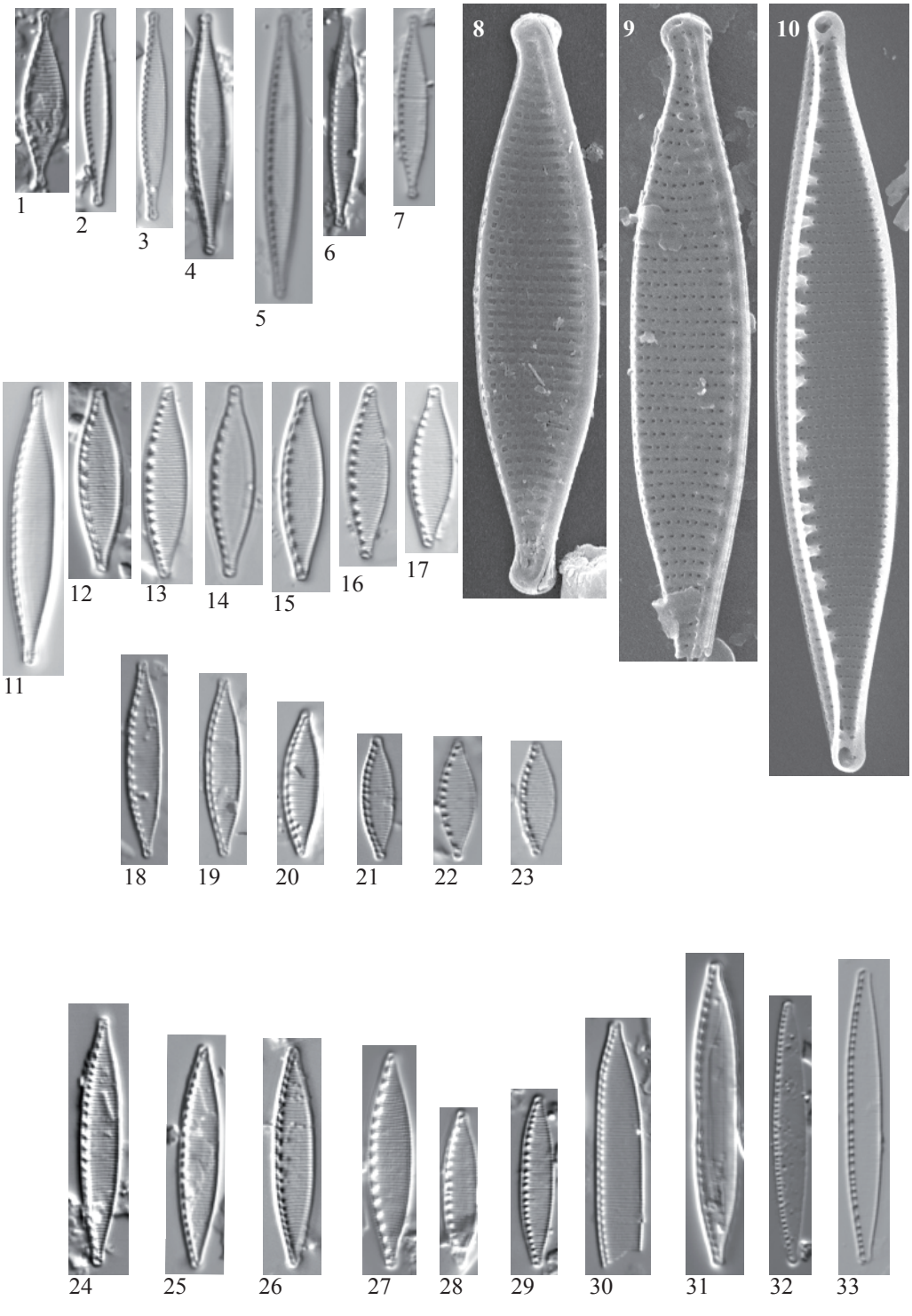
1
2
3
4
5
6
7
8
9
10
11
12
13
14
15
16
17
18
19
20
21
22
23
24
25
26
27
28
29
30
31
32
33

Plate 120 LM: x1500
SEM x3000

Figs. 1-3 *Nitzschia* sp. No. 7 Posets
Figs. 4-6 *Nitzschia* cf. *paleacea* (palacea) Grunow
Figs. 7-8 *Nitzschia* sp. No. 11 Burg
Figs. 9-10 *Nitzschia* sp. No. 12 Burg
Figs. 11-12 *Nitzschia* sp. No. 8 Bergeus
Figs. 13-16 *Nitzschia gracilis* Hantzsch
Fig. 17 *Nitzschia* cf. *linearis* var. *subtilis* Hustedt
Figs. 18-19 *Nitzschia pura* Hustedt
Figs. 20-22 *Nitzschia* cf. *dissipata* (Kützing) Grunow
Fig. 23 *Nitzschia garrensis* Hustedt
Fig. 24 *Nitzschia* sp. No.10 Mora
Fig. 25 *Nitzschia rectiformis* Hustedt
Fig. 26 *Nitzschia* sp. No. 9 Mora
Fig. 27 *Nitzschia* sp. No. 14 Burg
Fig. 28 cf. *Nitzschia amphibia* var. *fossilis* Grunow
Figs. 29-30 *Hantzschia* cf. *amphioxys* (Ehrenberg) Grunow
Figs. 31-32 *Hantzschia* cf. *rhaetica* Meister

Figs. 1-3, 18, 21, 28-29	Lake Posets, sediment PYR42	Fig. 20	Lake Sen, sediment PYR40
Figs. 4-6	Lake Compte, sediment PYR97	Fig. 22	Lake Albe, sediment PYR96
Fig. 7	L. Burg, sediment BURG 1006	Fig. 23	Lake Acherito, sediment PYR01
Fig. 8	L. Burg, sediment BURG 1007	Figs. 24, 26	L. Basa de la Mora, sediment PYR32
Figs. 9-10	Lake Burg	Fig. 25	L. Més Amunt de Tristaina, sediment PYR86
Fig. 11	Lake Eriste, sediment PYR43	Fig. 27	L. Burg, sediment BURG 755
Figs. 12, 30	L. Gelat Bergús, sed. PYR65	Figs. 31-32	L. Burg, sediment BURG 1195
Fig. 13	L. Inf. Gallina, epilit. EpiPYR87		
Fig. 14	L. Urdiceto, sediment PYR125		
Fig. 15	Lake Illa, sediment PYR66		
Fig. 16	L. L`Estagnol, epil. EpiPYR119		
Fig. 17	L. Pondiellos Sup., epil. EpiPYR08		
Fig. 19	Lake Mariola, sediment PYR80		

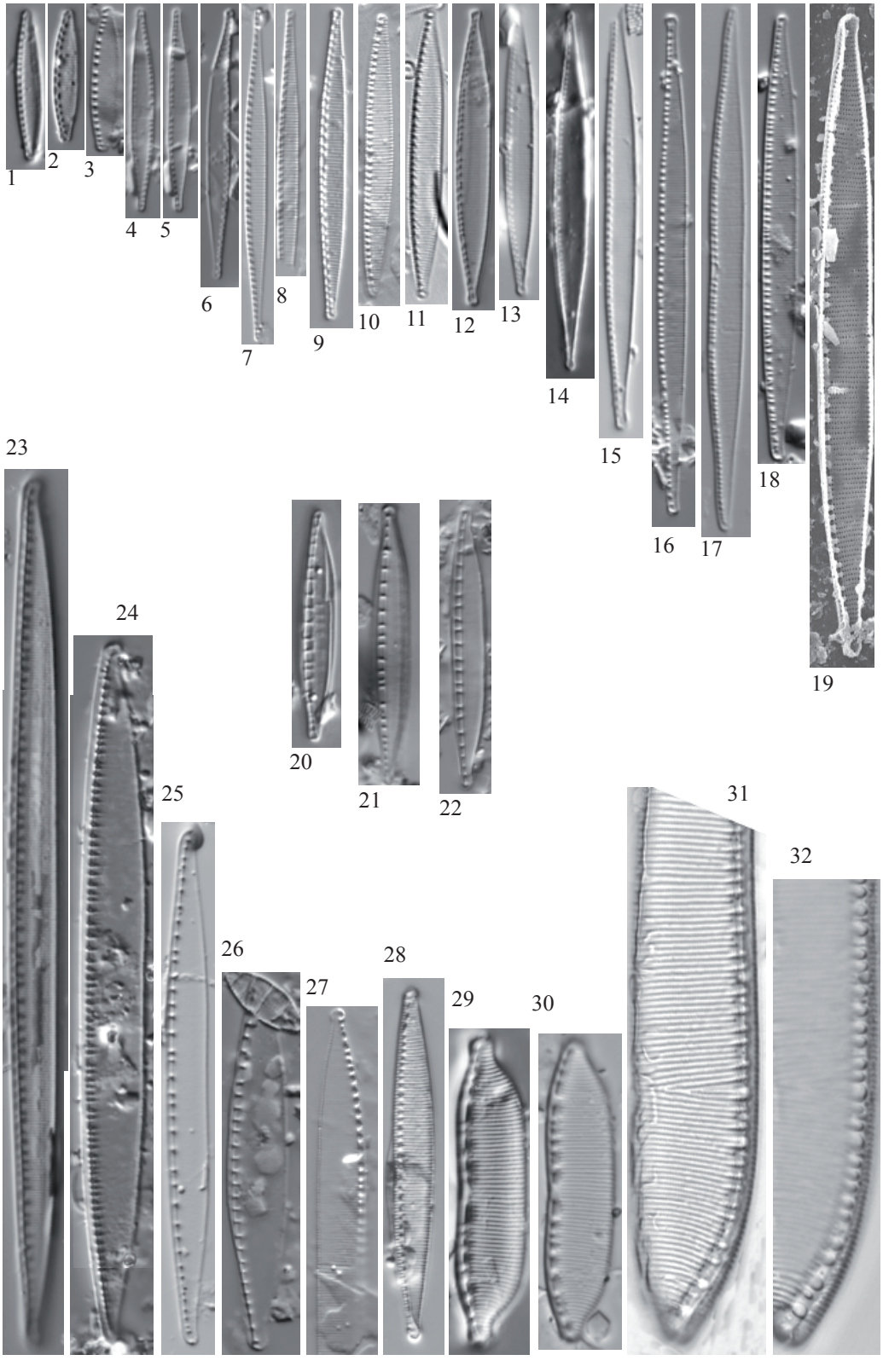
1
2
3
4
5
6
7
8
9
10
11
12
13
14
15
16
17
18
19
20
21
22
23
24
25
26
27
28
29
30
31
32

Plate 121 LM: x 1500
SEM: Figs. 6, 7 x3000, Fig. 8 x400, Fig. 9 x2000, Fig. 10 x10000

Figs. 1-7 *Nitzschia angustata* (W. Smith) Grunow
Figs. 8-10 *Nitzschia rectiformis* Hustedt

Figs. 1, 3-5	Lake Estom, sediment PYR15
Fig. 2	Lake Posets, sediment PYR42
Figs. 6-7	Lake Port Bielh, epilithic EpiPYR28
Figs. 8-10	Lake Redon, sediment REDOM

1

2

3

4

5

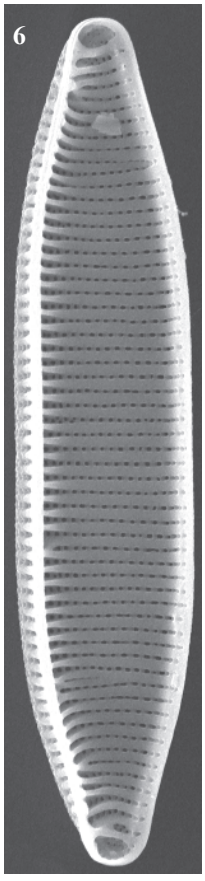

6

7

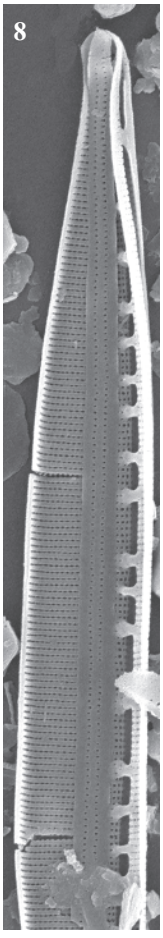

8

9

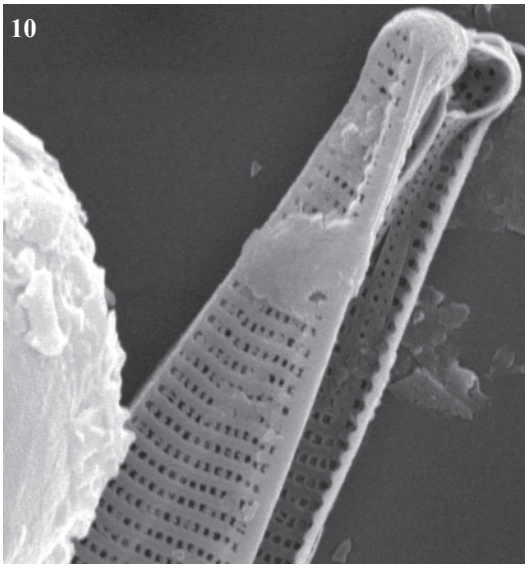

10

Plate 122 LM: x1500
SEM: Figs. 6,7,12 x10000, Figs. 13-15 x5000

Figs. 1-15 *Denticula tenuis* Kützing

Figs. 1-2, 5, 8-9, 12, 14	Lake Posets, sediment PYR42
Figs. 3-4, 10-11	Lake Sen, sediment PYR40
Figs. 6, 7	Lake Roumassot, sediment PYR04
Figs. 12, 15	Lake Pondiellos Sup., epilithic EpiPYR08
Fig. 13	Lake Port Bielh, epilithic EpiPYR28


1


2


3


4


5

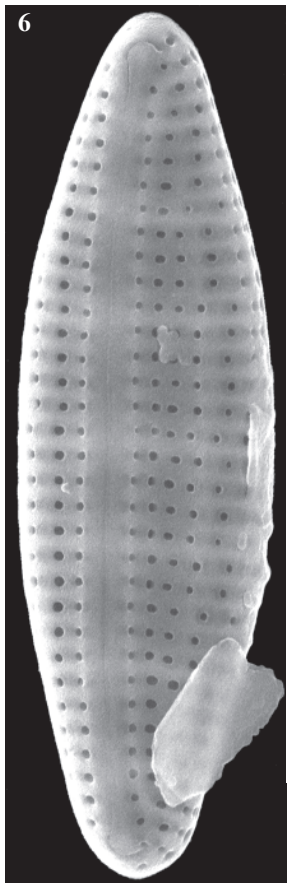
6

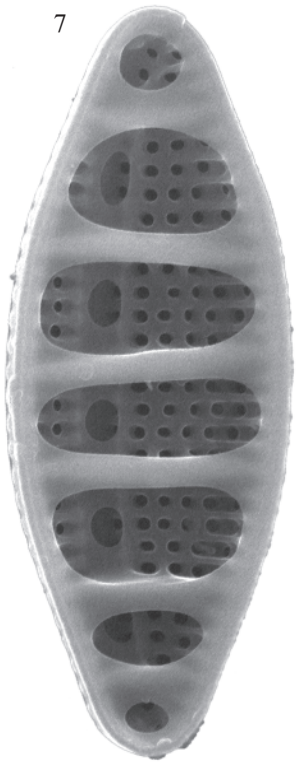
7


8


9


10


11

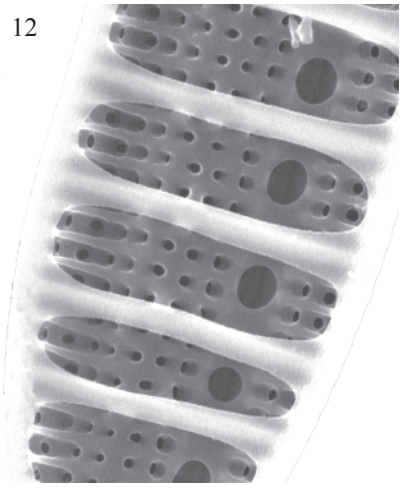
12

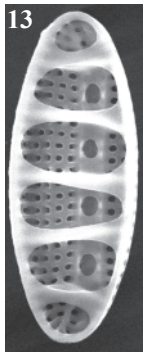
13

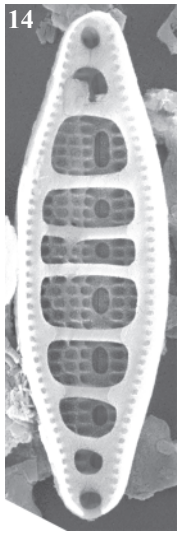
14

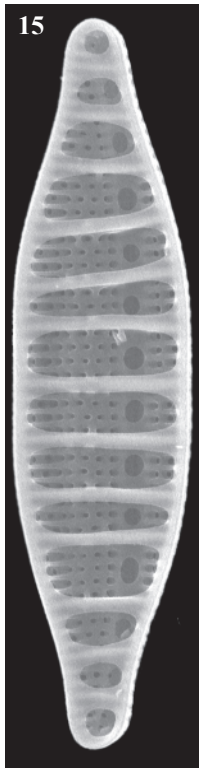
15

Plate 123 LM: x1500
SEM: x3000

Figs. 1-6 *Epithemia turgida* (Ehrenberg) Kützing
Figs. 7-10 *Epithemia* cf. *adnata* (Kützing) Brébisson
Figs. 11-17 *Epithemia sorex* Kützing

Figs. 1-9, 11 Lake Burg, sediment BURG 1115
Figs. 10, 15-16 Lake Burg, sediment BURG 1104
Fig. 12 Lake Burg, sediment BURG 1116
Fig. 17 Lake Roumassot, sediment PYR04

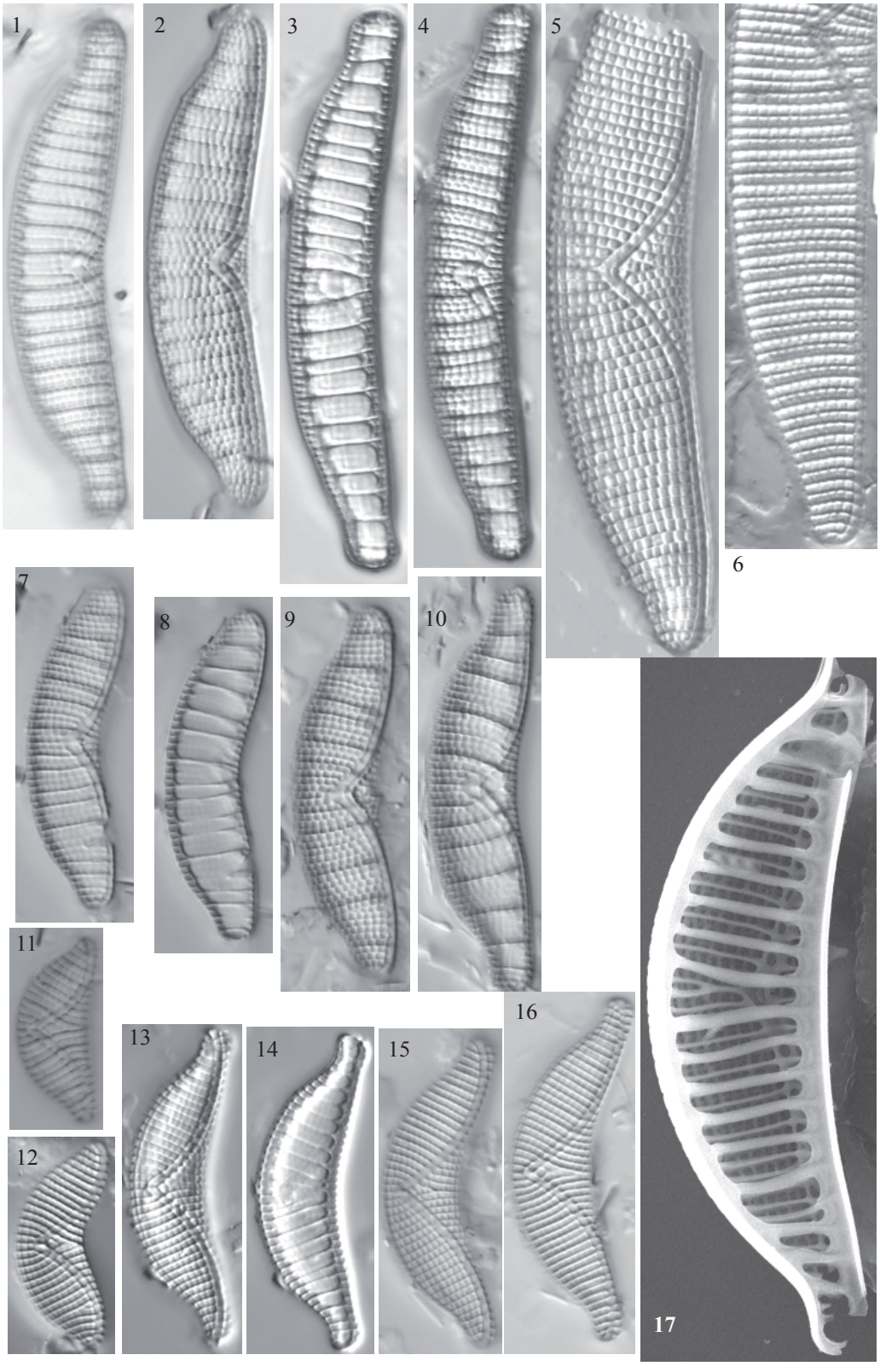
1
2
3
4
5
6
7
8
9
10
11
12
13
14
15
16
17

Plate 124 LM: x1500

Figs. 1-2, 7-8	*Epithemia goeppertiana* Hilse
Fig. 3	*Epithemia* cf. *goeppertiana* Hilse
Figs. 4-6	*Rhopalodia gibba* (Ehrenberg) Müller
Fig. 9	*Epithemia cistula* (Ehrenberg) Ralfs

Figs, 1-2, 7-8	Lake Estom, sediment PYR15
Fig. 3	Lake Burg, sediment sample
Figs. 4-6	Lake Burg, sediment BURG 519
Fig. 9	Lake Acherito, sediment PYR01

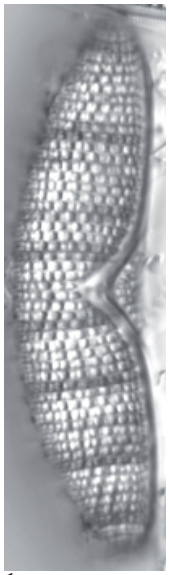

1

2

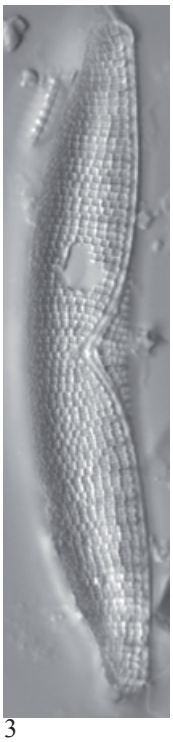

3

4

5

6

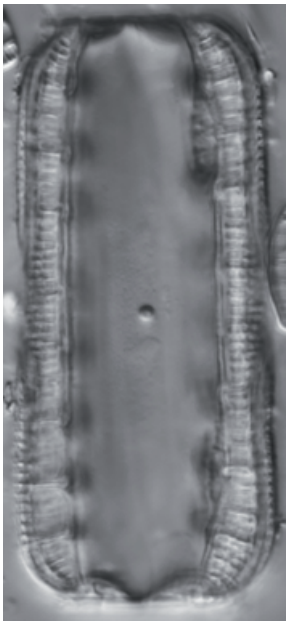

7

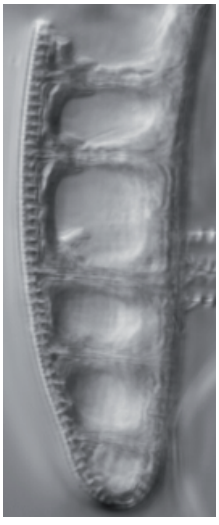

8

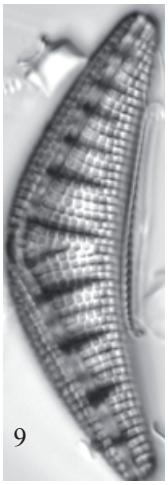

9

Plate 125 LM: x1500
SEM: Fig. 2 x8000, Fig. 3 x4000

Figs. 1-3 *Surirella cf. roba* Leclercq
Figs. 4-5 *Surirella cf. bohemica* Maly
Figs. 6-7 *Surirella angusta* Kützing
Fig. 8 *Surirella helvetica* Brun

Figs. 1-2 Lake Posets, sediment PYR42
Fig. 3 Lake Redon, sediment REDOM
Figs. 4-5 Lake Forcat Inf., sediment PYR77
Fig. 6 Lake Coronas, sediment PYR47
Fig. 7 Lake Les Laquettes, sediment PYR27
Fig. 8 Lake Tourrat, sediment PYR23

1

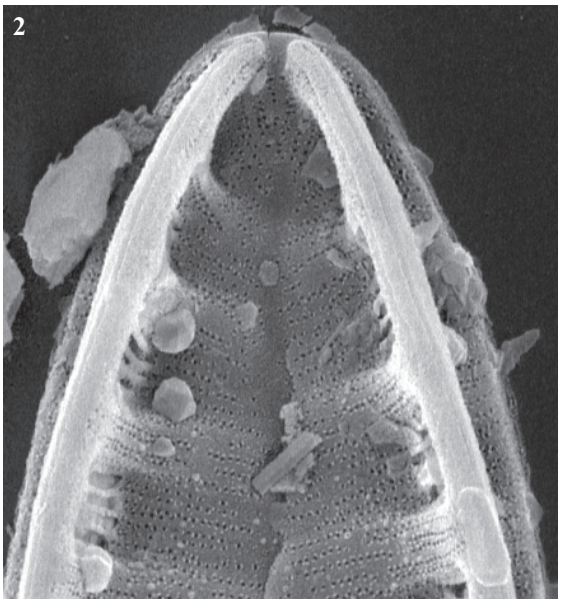

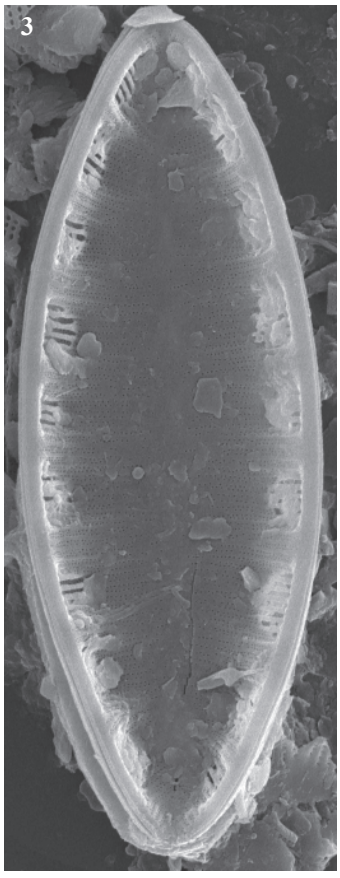

4

5

6

7

8

Plate 126 LM: x1500

Fig. 1	*Surirella* aff. *robusta* Ehrenberg
Fig. 2	*Surirella* cf. *linearis* Smith
Figs. 3-5	*Stenopterobia densestriata* (Hustedt) Krammer
Figs. 6-11	*Stenopterobia delicatissima* (Lewis) Van Heurck

Figs. 1, 7	Lake Les Laquettes, sediment PYR27
Fig. 2	Lake Gran de Mainera, sediment PYR70
Figs. 3-6	Lake Romedo de Dalt, sediment PYR85
Figs. 8-11	Lake Bleu de Rabassoles, sediment PYR112

1

2

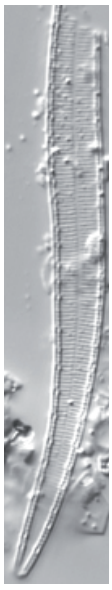

3

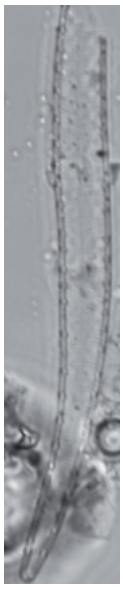

4

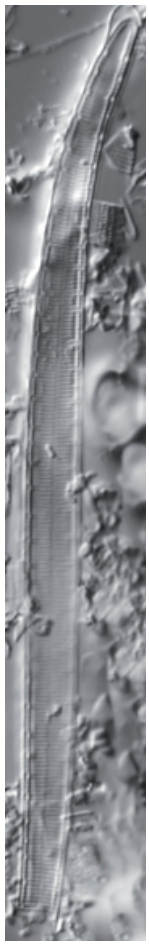

5

6

7

8

9

10

11

Plate 127 LM: x900
SEM: Fig. 1 x900, Fig. 3 x4500

Figs. 1-3 *Cymatopleura elliptica* (Brebisson) Smith

Figs. 1, 3 Lake Laurenti, sediment PYR111

Fig. 2 Lake Col d`Arretille, sediment PYR12

1

2

3

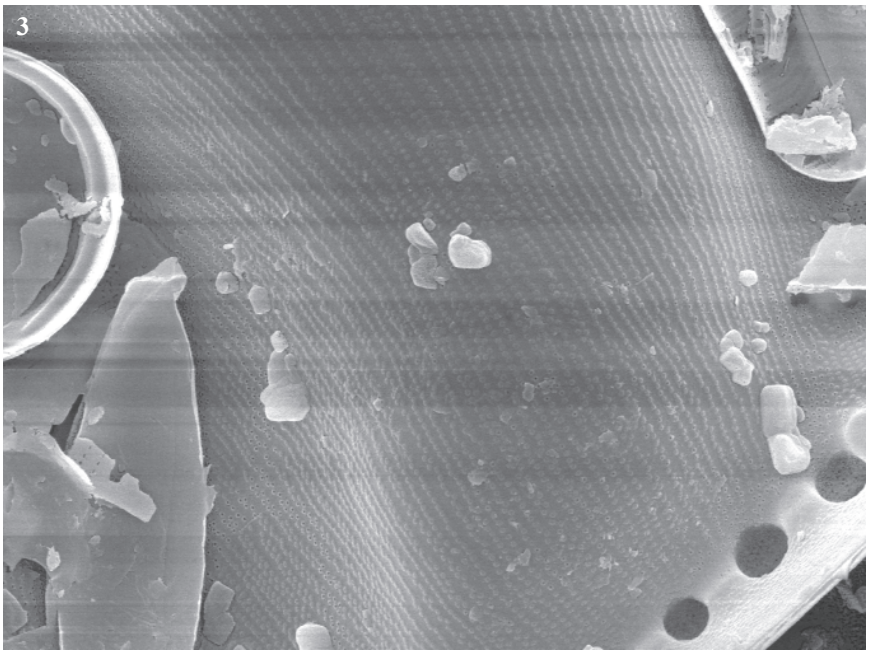

Appendix 2

Summary of the indicator analyses showing the significant indicator species of the sediment training-set. I_{sb}: irradiance at the bottom (µE/m^2/s), ADBB: active diatom biofilm at the bottom, ICD: ice cover duration (days), Temp.: temperature (ºC), TN: total nitrogen, TP: total phosphorous (µg/L), DIN: dissolved inorganic nitrogen (µg/L). SO_4^{2-} and Si units are µeq/L and mol/L, respectively. Details of the habitat indicators are explained in chapters 8 and 9.

[Rivera Rondón, C.A. 2013. Diatom-based reconstruction of Late Glacial and Early Holocene environment in the Pyrenees. Ph.D. Thesis, Universitat de Barcelona. 584pp]

		Group of indicators			
Type	Species	pH-ANC	Nutrients	Physical	Habitat
Araphid	Asterionella formosa Hassall		Si:P <100:1, TN:TP <50:1, DIN<100 TP>10		
	Fragilaria sp. No. 9 Redon			Isb <10	
	Fragilaria delicatissima (Smith) Lange-Bertalot		TN:TP <50:1, DIN <100 TP >4	Isb <120	
	Stauroforma cf. exiguiformis (Lange-Bertalot) Flower, Jones & Round	SO4 <50 pH 5.5-6.5		Temp. >15	ADBB
	Fragilaria pararumpens Lange-Bertalot, Hofmann & Werum			Isb <10	non-Potamids, psam-deep
	Fragilaria cf. vaucheriae (Kützing) Petersen			ICD <180	
	Meridion circulare (Greville) Agardh		TN:TP <110:1, DIN<100 TP>10	ICD <180	
	Pseudostaurosira sp. No. 2 Acherito				Macroph., ADBB
	Pseudostaurosira cf. brevistriata (Grunow) Williams & Round			Temp. >10	Macroph., Potamids, psam-shallow
	Pseudostaurosira microstriata (Marciniak) Flower	pH >5.5			
	Fragilaria cf. opacolineata Lange-Bertalot		TN:TP <50:1, DIN <100 TP >4	Temp. >15	Macroph., ADBB
	Pseudostaurosira parasitica var. subconstricta (Grunow) Morales			ICD <160	
	Pseudostaurosira pseudoconstruens (Marciniak) Williams & Round		TN:TP <110:1		ADBB
	Punctastriata lancettula (Schumann) Hamilton & Siver			ICD <180	psam-shallow, ADBB
	Staurosirella leptostauron (Ehrenberg) Williams & Round				Macroph., psam-shallow
	Staurosirella oldenburgiana (Hustedt) Morales			Isb >120, Temp. >15	Macroph., Potamids, psam-shallow, ADBB
	Staurosirella pinnata (Ehrenberg) Williams & Round	pH >5.5			
	Punctastriata cf. lancettula (Schumann) Hamilton & Siver M1	SO4 >50 pH >7.25			Macroph., psam-shallow, ADBB
	Staurosira construens Ehrenberg			ICD <195, Temp. >10	
	Diatoma mesodon Kützing				plankton
	Ulnaria biceps (Kützing) Compère sensu lato		TN:TP <110:1	ICD <180	Macroph.
Centric	Aulacoseira sp. No. 1 Gerber			ICD 160-180	
	Aulacoseira cf. alpigena (Grunow) Krammer	pH 5.5-7.25			non-macroph.
	Aulacoseira cf. nygaardii (Camburn) Camburn & Charles	SO4 >50 pH <5.5			
	Aulacoseira perglabra (Østrup) Haworth		TN:TP <50:1		
	Aulacoseira pfaffiana (Reinsch) Krammer	pH <6.5			

		Group of indicators			
Type	Species	pH-ANC	Nutrients	Physical	Habitat
	Aulacoseira cf. subarctica (O. Müller) Haworth				ADBB
	Aulacoseira cf. valida (Grunow) Krammer		TN:TP <50:1, DIN<100 TP>10	Temp. >15	Macroph., ADBB
	Cyclotella sp. No. 1 Llebreta			ICD <160	
	Cyclotella sp. No. 2 Llong				Macroph.
	Cyclotella sp. No. 3 Laurenti			ICD <160	Macroph.
	Cyclotella praetermissa Lund			ICD <195	
	Discostella stelligera (Cleve & Grunow) Houk & Klee			Isb <120, Temp. >10	
Cymbelloid	Amphora copulata (Kützing) Schoeman & Archibald	pH >7.25	Si:N<1		
	Amphora cf. eximia Carter	pH >7.25	Si:N<1	Temp. <15	
	Amphora neglecta f. densestriata Foged	pH >7.25			
	Cymbopleura inaequalis (Ehrenberg) Krammer				ADBB
	Cymbella lange-bertalotii Krammer			Isb >120	Potamids
	Cymbopleura naviculiformis (Auerswald) Krammer		Si<10, Si:N<1		
	Cymbella parva (Smith) Kirchner				Macroph., Potamids, psammon
	Cymbopleura cf. pyrenaica Le Cohu & Lange-Bertalot		Si:N<1		Potamids
	Cymbopleura subaequalis (Grunow) Krammer		Si<10, Si:N<1		
	Delicata delicatula (Kützing) Krammer	SO4 >50 pH >7.25			Macroph., Potamids, psam-shallow, ADBB
	Denticula tenuis Kützing	pH >7.25	Si:N<1, TN:TP >50:1, TP< 10		
	Encyonema sp. No. 1 Mora		Si:N<1, DIN>100 TP4-10	Isb >120	Macroph., Potamids
	Encyonema sp. No. 2 Sen				plankton
	Encyonema gaeumannii (Meister) Krammer	pH <6.5		Isb <120	
	Encyonema hebridicum Grunow ex Cleve	pH <6.5			
	Encyonema minutum (Hilse) Mann	pH >5.5			
	Encyonema neogracile Krammer		Si<10		
	Encyonema obscurum var. alpina Krammer		Si:N<1, DIN>100 TP4-10	Isb >120	
	Encyonema perpusillum (Cleve) Mann	pH <6.5	DIN<100 TP<4		psam-deep
	Encyonema reichardtii (Krammer) Mann			Temp. <10	
	Encyonema silesiacum (Bleisch) Mann	pH >5.5			
	Encyonopsis aequalis (Smith) Krammer	SO4 >50 pH <6.5			

		Group of indicators			
Type	Species	pH-ANC	Nutrients	Physical	Habitat
	Encyonopsis cesatii (Rabenhorst) Krammer		DIN>100 TP4-10		Potamids
	Encyonopsis descripta (Hustedt) Krammer			ICD <160	Macroph.
	Encyonopsis cf. falaisensis (Grunow) Krammer				Potamids
	Encyonopsis microcephala (Grunow) Krammer		TN:TP 50-110:1		
	Encyonopsis subminuta Krammer & Reichardt	pH >7.25	Si:N<1, TP 4-10	ICD <180	Macroph., Potamids
	Reimeria sinuata (Gregory) Kociolek & Stoermer emend Sala, Guerrero & Ferrario		Si:P <100:1		
Eunotioid	Eunotia bilunaris (Ehrenberg) Schaarschmidt	pH <6.5			plankton
	Eunotia boreoalpina Lange-Bertalot & Nörpel-Schempp	SO4 <50 pH 5.5-6.5			
	Eunotia catalana Lange-Bertalot & Rivera-Rondón	SO4 >50 pH <5.5			non-macroph.
	Eunotia exigua (Brébisson Kutzing) Rabenhorst	SO4 >50 pH <6.5	DIN<100 TP<4		
	Eunotia implicata Norpel, Alles & Lange-Bertalot	SO4 >50 pH <6.5			
	Eunotia incisa Gregory	SO4 <50 pH 5.5-6.5			
	Eunotia intermedia (Krasske) Nörpel & Lange-Bertalot	SO4 >50 pH <6.5			
	Eunotia cf. islandica Østrup	SO4 >50 pH <5.5			
	Eunotia mucophila (Lange-Bertalot & Nörpel-Schempp) Lange-Bertalot	SO4 <50 pH 5.5-6.5			
	Eunotia novaisiae Lange-Bertalot & Luc Ector		Si<10	Temp. <10	
	Eunotia nymanniana Grunow	SO4 >50 pH <5.5			
	Eunotia paludosa Grunow				psam-deep
	Eunotia cf. pseudogroenlandica Lange-Bertalot & Tagliaventi	SO4 >50 pH <6.5			
	Eunotia cf. soleirolii (Kützing) Rabenhorst	pH <6.5			
	Eunotia subarcuatoides Alles, Norpel & Lange-Bertalot	pH 5.5-6.5			
	Peronia fibula (Brébisson in Kützing) Ross	SO4 <50 pH 5.5-6.5	Si<10		
Gomphoid	Gomphonema sp. No. 15 Coronas		Si:N<1, Si:P <100:1		
	Gomphonema sp. No. 4 Posets		DIN>100 TP4-10		
	Gomphonema sp. No. 9 Posets				non-psam
	Gomphonema cf. acidoclinatum Lange-Bertalot & Reichardt		DIN<100 TP>10		
	Gomphonema acuminatum Ehrenberg		Si:P <100:1		
	Gomphonema auritum Braun		TN:TP <110:1		Macroph., Potamids
	Gomphonema brebissonii Kützing			Isb <10	
	Gomphonema lateripunctatum Reichardt & Lange-Bertalot				Macroph., Potamids, non-psam
	Gomphonema cf. minusculum Krasske			Temp. <10	

		Group of indicators			
Type	Species	pH-ANC	Nutrients	Physical	Habitat
	Gomphonema cf. parvulum (Kützing) Kützing sensu lato		Si<10, Si:P <100:1, DIN<100 TP>10	Temp. >15	Macroph.
	Gomphonema pumilum (Grunow) Reichardt & Lange-Bertalot		DIN>100 TP4-10		
	Gomphonema subclavatum (Grunow) Grunow	SO4 >50 pH 6.5-7.25			
	Gomphonema truncatum Ehrenberg				Macroph., Potamids
Monoraphid	Achnanthidium cf. minutissimum (Kützing) Czarnecki M4			Temp. <10	non-psam
	Achnanthes sp. No. 3 Posets		Si<10, Si:N<1		
	Achnanthidium atomus (Hustedt) Monnier, Lange-Bertalot & Ector		Si:N<1		
	Achnanthidium cf. minutissimum (Kützing) Czarnecki M1			ICD <160	
	Achnanthes microscopica (Cholnoky) Lange-Bertalot & Krammer	pH 5.5-6.5			
	Achnanthidium pfisteri Lange-Bertalot			Temp. <10	
	Achnanthidium pyrenaicum (Hustedt) Kobayasi				non-psam
	Cocconeis euglyptoides (Geitler) Lange-Bertalot				Macroph.
	Karayevia laterostrata (Hustedt) Bukhtiyarova			Isb <10	psam-deep
	Karayevia suchlandtii (Hustedt) Bukhtiyarova			ICD >160	
	Nupela cf. gracillima (Hustedt) Lange-Bertalot		Si<10, Si:N<1	Isb <10	
	Nupela cf. impexiformis (Lange-Bertalot) Lange-Bertalot			ICD <160	
	Nupela lapidosa (Krasske) Lange-Bertalot	SO4 <50 pH 5.5-6.5			plankton
	Planothidium distinctum (Messikommer) Lange-Bertalot		TN:TP >110:1		non-macroph.
	Planothidium frequentissimum (Lange-Bertalot) Lange-Bertalot			ICD <160	
	Planothidium peragallii (Brun & Héribaud) Round & Bukhtiyarova				ADBB
	Psammothidium acidoclinatum (Lange-Bertalot) Lange-Bertalot	SO4 >50 pH <6.5			non-macroph.
	Psammothidium bioretii (Germain) Bukhtiyarova & Round				non-psam
	Psammothidium helveticum (Hustedt) Bukhtiyarova et Round	pH <7.25	TP <4		non-Potamids
	Psammothidium levanderi (Hustedt) Bukhtiyarova & Round			Temp. >10	
	Psammothidium marginulatum (Grunow) Bukhtiyarova et Round	SO4 <50 pH 5.5-6.5	Si:P >100:1	Isb <120	
	Psammothidium rossii (Hustedt) Bukhtiyarova et Round		TN:TP <50:1, DIN <100 TP >4	Isb >120, Temp. >15	Macroph., Potamids, ADBB
	Psammothidium scoticum (Flower et Jones) Bukhtiyarova & Round	pH 5.5-7.25			non-macroph.
	Psammothidium subatomoides (Hustedt) Bukhtiyarova et Round	pH 5.5-6.5			
	Psammothidium ventrale (Krasske) Bukhtiyarova et Round			Isb 10-120	non-psam

		Group of indicators			
Type	Species	pH-ANC	Nutrients	Physical	Habitat
	Rossithidium linearis (Smith) Round et Bukhtiyarova		DIN<100 TP>10	ICD 160-180	
	Rossithidium pusillum (Grunow) Round et Bukhtiyarova				Macroph.
Naviculoid	Adlafia cf. minuscula (Grunow) Lange-Bertalot		TN:TP <50:1	Isb >120	
	Brachysira brebissonii Ross	pH <6.5			
	Brachysira intermedia (Østrup) Lange-Bertalot		TN:TP <50:1		
	Brachysira neoexilis Lange-Bertalot				non-ADBB
	Chamaepinnularia No. 1 Negre	pH <6.5			
	Chamaepinnularia mediocris (Krasske) Lange-Bertalot	pH <6.5			
	Craticula submolesta (Hustedt) Lange-Bertalot				non-macroph.
	Diploneis cf. peterseni (petersenii) Hustedt	pH >7.25	Si:N<1, DIN>100 TP4-10		
	Diploneis cf. puella (Schumann) Cleve		Si:N<1		Macroph.
	Diploneis cf. subovalis Cleve				Macroph.
	Navicula spp. aff. N. minima		TN:TP <50:1	Temp. >15	Macroph.
	Frustulia crassinervia (Brébisson) Lange-Bertalot et Krammer	pH <6.5			
	Frustulia cf. saxonica Rabenhorst	SO4 >50 pH <6.5		ICD 180-195	non-macroph.
	Geissleria acceptata (Hustedt) Lange-Bertalot & Metzeltin			Temp. <10	
	Geissleria similis (Krasske) Lange-Bertalot & Metzeltin		Si<10, Si:N<1		
	Gyrosigma sp. No. 1 Sen				Macroph.
	Gyrosigma sp. No. 2 Mora		Si:N<1		
	Hippodonta costulata (Grunow) Lange-Bertalot, Metzeltin & Witkowski			Isb <10	psam-deep
	Hippodonta cf. neglecta Lange-Bertalot, Metzeltin & Witkowski		Si:N<1, Si:P <100:1		
	Kobayasiella parasubtilissima (Kobayasi & Nagumo) Lange-Bertalot	SO4 <50 pH 5.5-6.5			
	Kobayasiella subtilissima (Cleve) Lange-Bertalot	SO4 <50 pH 5.5-6.5			
	Luticola sp. No. 5 Coronas		Si:N<1, Si:P <100:1	Temp. <10	
	Naviculadicta sp. No. 1 Ensangents	SO4 <50 pH 5.5-6.5		Isb <10	
	Navicula sp. No. 1 Laurenti		DIN<100 TP>10	ICD <160	
	Navicula sp. No. 2 Liat		Si<10, Si:N<1		non-macroph.
	Navicula sp. No. 3 Laurenti		TN:TP <50:1		ADBB
	Navicula sp. No. 4 Laquettes		TN:TP <50:1	Temp. >15	Macroph., Potamids, psam-shallow, ADBB

		Group of indicators			
Type	Species	pH-ANC	Nutrients	Physical	Habitat
	Navicula sp. No. 7 Bergus	pH 5.5-6.5	Si:N>1, TN:TP <50:1		
	Navicula angusta Grunow	pH 5.5-7.25			
	Navicula catalanogermanica Lange-Bertalot & Hofmann	pH >7.25	Si:N<1, DIN>100 TP4-10		
	Navicula cryptotenella Lange-Bertalot	SO4 >50 pH >7.25	DIN>100 TP4-10	Isb >120	
	Navicula cryptofallax Lange-Bertalot & Hofmann			ICD <160	
	Naviculadicta digituloides Lange-Bertalot		Si:N<1		non-Potamids
	Navicula heimansioides Lange-Bertalot		TN:TP <50:1		
	Navicula krasskei Hustedt			Isb <10	psam-deep
	Adlafia aff. minuscula (Grunow) Lange-Bertalot		TN:TP <50:1	Isb >120, Temp. >15	Macroph.
	Navicula cf. oligotraphenta Lange-Bertalot & Hofmann		Si:N<1	ICD <160	
	Navicula pseudolanceolata Lange-Bertalot			Isb >120	Macroph., Potamids
	Navicula radiosa Kützing			ICD <195	Macroph.
	Navicula schmassmanni Hustedt	pH 5.5-6.5			
	Navicula cf. seminulum Grunow			Temp. >15	
	Sellaphora cf. stauroneioides (Lange-Bertalot) Vesela & Johansen		Si:P <100:1		
	Navicula cf. submuralis Hustedt		Si:P <100:1, TN:TP <50:1		
	Navicula cf. trivialis Lange-Bertalot			ICD <160	
	Navicula trophicatrix Lange-Bertalot		Si:N<1	ICD <160	
	Navicula venerablis Hohn & Hellerman		Si<10, TN:TP <50:1		
	Navicula wildii Lange-Bertalot			ICD <180	Macroph.
	Neidium affine (Ehrenberg) Pfitzer sensu lato	pH <6.5			non-macroph., non-Potamids
	Neidium alpinum Hustedt	pH <6.5			
	Neidium longiceps (Gregory) Ross		TN:TP <50:1		
	Sellaphora laevissima (Kützing) Mann			Temp. >10	
	Sellaphora cf. nanoides Lange-Bertalot, Cavacini, Tagliaventi & Alfinito			Temp. <10	
	Sellaphora pseudopupula (Krasske) Lange-Bertalot				
	Sellaphora pupula (Kützing) Mereschkowsky sensu lato		Si<10, Si:N<1, Si:P <100:1		
	Stauroneis gracilis Ehrenberg			Temp. >15	

		Group of indicators			
Type	Species	pH-ANC	Nutrients	Physical	Habitat
	Stauroneis smithii Grunow		Si<10, Si:N<1		
Nitzschioid	Hantzschia cf. amphioxys (Ehrenberg) Grunow		Si:P <100:1		
	Nitzschia sp. No.10 Mora				psam-deep
	Nitzschia sp. No. 1 Sen	pH >7.25	Si:N<1, TN:TP >50:1		
	Nitzschia sp. No. 2 Posets			Isb >120	ADBB
	Nitzschia sp. No. 5 Arratille		Si<10		
	Nitzschia sp. No. 9 Mora			Temp. >15	
	Nitzschia acidoclinata Lange-Bertalot		Si<10, DIN>100 TP4-10		
	Nitzschia gracilis Hantzsch		Si<10, Si:N<1		
	Nitzschia sp. No. 11 Burg		TN:TP <50:1	ICD <160	
	Nitzschia cf. perminuta (Grunow) Peragallo M2				non-macroph.
	Nitzschia palea var. debilis (Kützing) Grunow			Temp. <10	
Pinnulariid	Caloneis cf. Vasileyevae Lange-Bertalot, Genkal & Vekhov	SO4 >50 pH <5.5			
	Pinnularia sp. No. 10 Pica Palomera	SO4 >50 pH <5.5			
	Pinnularia sp. No. 4 Mariola	pH 5.5-7.25			
	Pinnularia acuminata Smith		Si<10		
	Pinnularia cf. brebissonii var. acuta Cleve-Euler			Temp. <10	
	Pinnularia cf. brebissonii var. minuta Krammer			ICD >160	
	Pinnularia cf. laucensis Lange-Bertalot, Rumrich & Krammer	SO4 >50 pH <5.5			
	Pinnularia microstauron var. nonfasciata Krammer	SO4 >50 pH <6.5	DIN<100	Temp. <10	non-macroph.
	Pinnularia cf. subanglica Krammer			Isb 10-120	
	Pinnularia subcapitata Gregory	SO4 <50 pH 5.5-6.5			
	Pinnularia septentrionalis Krammer		Si:N<1		
	Pinnularia sinistra Krammer				psam-deep
Surirelloid	Stenopterobia delicatissima (Lewis) Van Heurck	pH <6.5			
	Surirella angusta Kützing		Si:P <100:1, DIN>100 TP4-10	Temp. <10	non-macroph.
	Surirella cf. linearis Smith	pH <7.25			non-macroph.
	Surirella cf. roba Leclercq	pH <6.5		Isb <120	plankton
	Surirella cf. robusta Ehrenberg	pH <6.5			